

1
2
3
4
5
6
7
8
9
10
11
12
13

CCSP Synthesis and Assessment Product 1.2

Past Climate Variability and Change in the Arctic and at High Latitudes

Chapter 1 — Executive Summary

Chapter Lead Authors

Richard B. Alley, Pennsylvania State University, University Park, PA

Julie Brigham-Grette, University of Massachusetts, Amherst , MA

Gifford Miller, University of Colorado, Boulder, CO

Leonid Polyak, Ohio State University, Columbus, OH

James White, University of Colorado, Boulder, CO

13 **1.1 Introduction**

14

15 Paleoclimate records play a key role in our understanding of Earth’s past and present
16 climate system and in our confidence in predicting future climate changes. Paleoclimate data
17 help to elucidate past and present active mechanisms of climate change by placing the short
18 instrumental record into a longer term context and by permitting models to be tested beyond the
19 limited time that instrumental measurements have been available.

20 Recent observations in the Arctic have identified large ongoing changes and important
21 climate feedback mechanisms that multiply the effects of global-scale climate changes. Ice is
22 especially important in these “Arctic amplification” processes, which also involve the ocean, the
23 atmosphere, and the land surface (vegetation, soils, and water). As discussed in this report,
24 paleoclimate data show that land and sea ice have grown with cooling temperatures and have
25 shrunk with warming ones, amplifying temperature changes while causing and responding to
26 ecosystem shifts and sea-level changes.

27

28 **1.2 Major Questions and Related Findings**

29

30 *How have temperature and precipitation changed in the Arctic in the past? What does this tell*
31 *us about Arctic climate that can inform projections of future changes?*

32 The Arctic has undergone dramatic changes in temperature and precipitation during the
33 past 65 million years (m.y.) (the Cenozoic Era) of Earth history. Arctic temperature changes
34 during this time exceeded global average temperature changes during both warm times and cold
35 times, supporting the concept of Arctic amplification.

36 At the beginning of the Cenozoic Era, 65 million years ago (Ma), there was no sea ice on
37 the Arctic Ocean, and neither Greenland nor Antarctica supported an ice sheet. General cooling
38 since that time is attributed mainly to a slow decrease in greenhouse gases, especially carbon
39 dioxide, in the atmosphere. Ice developed during this slow, “bumpy” cooling, first as mountain
40 glaciers and as seasonal sea ice in the Arctic Ocean. Following a global warm period about 3.5
41 Ma in the middle Pliocene, when extensive deciduous forests grew in Arctic regions now
42 occupied by tundra, further cooling crossed a threshold about 2.6 Ma, allowing extensive ice to
43 develop on Arctic land areas and thus initiating the Quaternary ice ages. This ice has responded
44 to persistent features of Earth’s orbit over tens of thousands of years, growing when sunshine
45 shifted away from the Northern Hemisphere and melting when northern sunshine returned..
46 These changes were amplified by feedbacks such as greenhouse-gas concentrations that rose and
47 fell as the ice shrank and grew, and by the greater reflection of sunshine caused by more-
48 extensive ice. Human civilization developed during the most recent of the relatively warm
49 interglacials, the Holocene (about 11.5 thousand years ago (ka) to the present). The penultimate
50 warm interval, about 130–120 ka, received somewhat more Northern-Hemisphere summer
51 sunshine than the Holocene owing to differences in Earth’s orbital configuration. Because this
52 more abundant summer sunshine warmed the Arctic about 5°C above recent temperatures, the
53 Greenland ice sheet was substantially smaller than its current size and almost all glaciers melted
54 completely at that time.

55 The last glacial maximum peaked at about 20 ka when the Arctic was about 20°C colder
56 than at present. Ice recession was well underway by 16 ka, and most of the Northern Hemisphere
57 ice sheets melted by 7 ka. Summer sunshine rose steadily from 20 ka to a maximum (10% higher
58 than at present due to the Earth’s orbit) about 11 ka ago, and has been decreasing since then. The

59 extra energy received in summer in the early Holocene resulted in warmer summers throughout
60 the Arctic. Temperatures were 1°–3°C above 20th century averages, enough to completely melt
61 many small glaciers in the Arctic and to slightly shrink the ice sheet on Greenland. Summer sea-
62 ice limits were significantly less than their 20th century average. As summer sunshine decreased
63 in the second half of the Holocene, glaciers re-established or advanced, and sea ice became more
64 extensive. Late Holocene cooling reached its nadir during the Little Ice Age (about 1250–1850
65 AD), when most Arctic glaciers reached their maximum Holocene extent. Warming during the
66 19th century has resulted in Arctic-wide glacier recession, the northward advance of terrestrial
67 ecosystems, and the reduction of perennial (year-round) sea ice in the Arctic Ocean. These trends
68 will continue if greenhouse gas concentrations continue to increase into the future.

69 Paleoclimate reconstructions of Arctic temperatures compared with global temperature
70 changes during four key intervals during the past 4 m.y. allow a quantitative estimate of Arctic
71 amplification. These data suggest that Arctic temperature change is 3 to 4 times the global
72 average temperature change during both cold and warm departures.

73

74 ***How rapidly have temperature and precipitation changed in the Arctic in the past? What do***
75 ***these past rates of change tell us about Arctic climate that can inform projections of future***
76 ***changes?***

77 As discussed with the previous question, climate changes on numerous time scales for various
78 reasons, and it has always done so. In general, longer-lived changes are somewhat larger but
79 much slower than shorter-lived changes.

80

81 Processes linked to continental drift (plate tectonics) have affected atmospheric and oceanic
82 currents and the composition of the atmosphere over tens of millions of years; in the Arctic, a
83 global cooling trend has switched conditions from being ice-free year-round near sea level to icy
84 conditions more recently. Within the icy times, variations in Arctic sunshine in response to
85 features of Earth’s orbit have caused regular cycles of warming and cooling over tens of
86 thousands of years that were roughly half the size of the continental-drift-linked changes. This
87 “glacial-interglacial” cycling was amplified by colder times bringing reduced greenhouse gases
88 and greater reflection of sunlight, especially from expanded ice-covered regions. This glacial-
89 interglacial cycling has been punctuated by sharp-onset, sharp-end (in as little as 1–10 years)
90 millennial oscillations, which near the North Atlantic were roughly half as large as the glacial-
91 interglacial cycling but which were much smaller Arctic-wide and beyond. The current warm
92 period of the glacial-interglacial cycling has been influenced by cooling events from single
93 volcanic eruptions, slower but longer lasting changes from random fluctuations in frequency of
94 volcanic eruptions and from weak solar variability, and perhaps by other classes of events. Very
95 recently, human effects have become evident, not yet showing both size and duration that exceed
96 peak values of natural fluctuations further in the past, but with projections indicating that human
97 influences could become anomalous in size and duration and, hence, in speed.

98

99 ***What does the paleoclimate record tell us about the past size of the Greenland ice sheet and its***
100 ***implications for sea level changes?***

101 The paleo-record shows that the Greenland ice sheet has consistently lost mass when the
102 climate warmed and grown when the climate cooled, even at times of negligible sea-level
103 change. In contrast, no changes in the ice sheet have been documented independent of

104 temperature changes. Moreover, snowfall has increased when the climate warmed, but the ice
105 sheet lost mass nonetheless; increased accumulation in the ice sheet center was not sufficient to
106 counteract increased melt and flow near the edges. Most of the documented changes (of both ice
107 sheet and forcings) spanned multi-millennial periods, but limited data show rapid responses to
108 rapid forcings have also occurred. In particular, regions near the ice margin have been observed
109 to respond within a few decades. However, major changes of the ice sheet are thought to take
110 centuries to millennia, and this is supported by the limited data.

111 The paleo-record does not yet give any strong constraints on how rapidly a near-complete loss of
112 the ice sheet could occur, although the paleo-data indicate that onset of shrinkage will be
113 essentially immediate after forcings begin. The available evidence suggests such a loss requires
114 a sustained warming of at least 2-7°C above mean 20th century values, but this threshold is
115 poorly defined. The paleo-archives are sufficiently sketchy that temporary ice sheet growth in
116 response to warming, or changes induced by factors other than temperature, could have occurred
117 without being recorded.

118

119 ***What does the paleoclimate record tell us about past changes in Arctic sea ice cover, and what***
120 ***implications does this have for consideration of recent and potential future changes?***

121 Although incomplete, existing data outline the development of Arctic **sea-ice** cover from
122 the ice-free conditions of the early Cenozoic. Some data indicate that sea ice has consistently
123 covered at least part of the Arctic Ocean for the last 13–14 million years, and it has been most
124 extensive during the most recent approximately 2 m.y. Other data argue against the development
125 of perennial (year-round) sea ice until the most recent few million years. Nevertheless, episodes
126 of considerably reduced ice cover, or even a seasonally ice-free Arctic Ocean, probably

127 punctuated even this latter period. Warmer climates associated with the orbitally paced
128 interglacials promoted these episodes of diminished ice. The current sea ice reduction in the
129 Arctic began during the late 19th century and has accelerated during the last several decades. It is
130 the largest ice reduction during at least the last few thousand years, and it is progressing at a very
131 fast rate that appears to have no analogs in the past.

132

133 **1.3 Recommendations**

134

135 Paleoclimatic data on the Arctic are generated by numerous international investigators
136 who study a great range of archives throughout the vast reaches of the Arctic. The value of this
137 diversity is evident in this report. Many of the key results of this report rest especially on the
138 outcomes of community-based syntheses, including the CAPE Project, and multiply replicated,
139 heavily sampled archives such as the central Greenland deep ice cores. Results from the ACEX
140 deep coring in Arctic Ocean sediments were appearing as this report was being written. These
141 results are quite valuable and will become more so with synthesis and replication, including
142 comparison with land-based and marine records. The number of questions answered, and raised,
143 by this one new data set shows how sparse the data are on many aspects of Arctic paleoclimatic
144 change. *We recommend that future research maintain and expand the diversity of*
145 *investigators, techniques, archives, and geographic locations, while promoting development of*
146 *community-based syntheses and multiply replicated, heavily sampled archives. Only through*
147 *breadth and depth can the remaining uncertainties be reduced while confidence in the results*
148 *is improved.*

149

150 The questions asked of this study by the CCSP are relevant to public policy and require
151 answers. The answers provided here are, we hope, useful and informative. However, we
152 recognize that despite the contributions of many community members to this report, in many
153 cases a basis was not available in the refereed scientific literature to provide answers with the
154 accuracy and precision desired by policymakers. ***We recommend that members of the Arctic
155 paleoclimatic community formulate future research activities to address in greater detail the
156 policy-relevant questions motivating this report.***

157
158 Paleoclimatic data provide very clear evidence of past changes in important aspects of the
159 Arctic climate system. The ice of the Greenland ice sheet, smaller glaciers and ice caps, the
160 Arctic Ocean, and in soils is shown to be vulnerable to warming, and Arctic ecosystems are
161 strongly affected by changing ice and climate. National and international studies generally
162 project rapid warming in the future. If this warming occurs, the paleoclimatic data indicate that
163 ice will melt and associated impacts will follow, with implications for ecosystems and
164 economies. ***We recommend that policymakers and science managers use the results presented
165 here in design of monitoring, process, and model-projection studies of Arctic change and
166 linked global responses.***

CCSP Synthesis and Assessment Product 1.2

**Past Climate Variability and Change in the Arctic and at High
Latitudes**

Chapter 2 —

INTENTIONALLY BLANK

**This is a place holder in the event that an additional introductory
chapter is deemed desirable based on the public comments.**

1 **CCSP Synthesis and Assessment Product 1.2**
2 **Past Climate Variability and Change in the Arctic and at High Latitudes**

3
4 **Chapter 3 — Preface: Why and How to Use This Synthesis and Assessment**
5 **Report**

6
7 **Chapter Lead Author**

8 Joan Fitzpatrick, U.S. Geological Survey

9 **Contributing Authors**

- 10
11 **Richard B. Alley**, Pennsylvania State University, University Park, PA
12 **Julie Brigham-Grette**, University of Massachusetts, Amherst , MA
13 **Gifford Miller**, University of Colorado, Boulder, CO
14 **Leonid Polyak**, Ohio State University, Columbus, OH
15 **Mark Serreze**, University of Colorado, Boulder, CO

16

16 **3.1 Introduction**

17

18 The U.S. Climate Change Science Program (CCSP), a consortium of Federal agencies
19 that investigate climate, has established a Synthesis and Assessment Program as part of its
20 Strategic Plan. A primary objective of the CCSP is to provide the best science-based knowledge
21 possible to support public discussion and government- and private-sector decisions about the
22 risks and opportunities associated with changes in climate and in related environmental systems
23 (U.S. Climate Change Science Program, 2007). The CCSP has identified an initial set of 21
24 Synthesis and Assessment Products (SAPs) that address the highest-priority research,
25 observation, and information needed to support decisions about issues related to climate change.
26 This assessment, SAP 1.2, focuses on the evidence for and record of past climate change in the
27 Arctic. This SAP is one of 3 reports that address the climate-variability-and-change research
28 element and Goal 1 of the CCSP Strategic Plan to improve knowledge of the Earth’s past and
29 present climate and environment, including its natural variability, and improve understanding of
30 the causes of observed variability and change.

31

32 The development of an improved understanding of natural, long-term cycles in climate
33 is one of the primary goals of the climate research element and Goal 1 of the CCSP. The Arctic
34 region of Earth, by virtue of its sensitivity to the effects of climate change through strong climate
35 feedback mechanisms, has a particularly informative paleoclimate record. Because mechanisms
36 operating in the Arctic and at high northern latitudes are also linked to global climate
37 mechanisms, an examination of how Arctic climate has changed in the past is also globally
38 informative.

39

40 **3.2 Motivation for this Report**

41

42 **3.2.1 Why Does the Past Matter?**

43 Paleoclimate records play a key role in our understanding of Earth’s past and present
44 climate system and in predicting future climate changes. Paleoclimate data help to elucidate past
45 and present active mechanisms by permitting computer-based models to be tested beyond the
46 short period (less than 250 years) of instrumental records. Paleo-records also provide quantitative
47 estimates of the magnitude of the polar amplification of (more intense response to) climate
48 change. These estimates can also be used to evaluate polar amplification derived from model
49 simulations of past and future climate changes.

50 This important role of paleoclimate records is recognized, for example, by inclusion of
51 paleoclimate as Chapter 6 of the 11-chapter Fourth Assessment Report of Working Group I
52 (AR4-I) of the Intergovernmental Panel on Climate Change (IPCC), and by the extensive
53 references to paleoclimatic data in climate change reports of the U.S. National Research Council,
54 such as *Climate Change Science: An Analysis of Some Key Questions* (Cicerone et al., 2001).

55 The pre-instrumental context of Earth’s climate system provided by paleodata strengthens
56 the interlocking web of evidence that supports scientific results regarding climate change. For
57 example, in considering whether fossil-fuel burning is an important contributor to the recent rise
58 in atmospheric carbon-dioxide concentrations, researchers must determine and quantify global
59 sources and sinks of carbon in Earth’s overall carbon budget. But one can also ask whether the
60 change of atmospheric carbon-dioxide concentrations observed in the instrumental record for the
61 past 100 years falls inside or outside the range of natural variability as revealed in the paleo-

62 record and, if inside, whether the timing of changes in carbon dioxide levels matches any known
63 natural cycles that can explain them. Answers to such questions must come from paleoclimate
64 data, because the instrumental record is much too short to characterize the full range of natural
65 fluctuations.

66 Testing and validation of climate models requires the use of several techniques, as
67 described in Chapter 8 of IPCC AR4-I (2007) The specific role of paleoclimate information is
68 described there: “Simulations of climate states from the more distant past allow models to be
69 evaluated in regimes that are significantly different from the present. Such tests complement the
70 ‘present climate’ and ‘instrumental period climate’ evaluations, since 20th century climate
71 variations have been small compared with the anticipated future changes under forcing scenarios
72 derived from the IPCC *Special Report on Emission Scenarios* (SRES).”

73

74 **3.2.2 Why the Arctic?**

75 During the past century the planet has warmed, overall, by 0.74°C (0.56°–0.92°C)
76 (IPCC, 2007). Above land areas in the Arctic, air temperatures have warmed as much as 3°C
77 (exceeding 4°C in winter; Serreze and Francis, 2006) during the same period of time.
78 Instrumental records indicate that in the past 30 years, average temperatures in the Arctic have
79 increased at almost twice the rate of the planet as a whole. Attendant changes include reduced
80 sea ice, reduced glacier extent, increased coastal erosion, changes in vegetation and wildlife
81 habitats, and permafrost degradation. Global climate models incorporating the current trend of
82 increasing greenhouse gases project continued warming in the near future and a continued
83 amplification of global signals in the Arctic. . The sensitivity of the Arctic to changed forcing is

84 due to powerful positive feedbacks in the Arctic climate system. These feedbacks produce large
85 effects on Arctic climate while also having significant impacts on the global climate system.

86 This high degree of sensitivity makes the paleoclimate history of the Arctic especially
87 informative when one considers the issue of modern climate change. Summaries of recent
88 changes in the Arctic environment (e.g., Correll, 2004; Richter-Menge et al., 2006) are based
89 primarily on observations and instrumental records. This report uses paleoclimate records to
90 provide a longer-term context for recent Arctic warming; that context allows us to better
91 understand the potential for future climate changes. Paleoclimate records provide a way to

- 92 • define the range of past natural variability in the Arctic and the magnitude of polar
93 amplification,
- 94 • evaluate the past rates of Arctic climate change (and thereby provide a long-term context for
95 current rates of change),
- 96 • identify past Arctic warm states that are potential analogs of future conditions,
- 97 • quantify the effects of abrupt perturbations (such as large injections of volcanic ash into the
98 atmosphere) and threshold behaviors, and
- 99 • gain insights into how the Arctic has behaved during past warm times by identifying critical
100 feedbacks and their mechanisms.

101

102 **3.3 Focus and Scope of this Synthesis Report (Geographic and Temporal)**

103

104 The content of this report follows from the prospectus developed early in its planning
105 (this prospectus is available at the CCSP website, <http://www.climatescience.gov>), and it is
106 focused on four topical areas in which the paleo-record can most strongly inform discussions of

107 climate change. These topics, each addressed in a separate chapter of this synthesis report, are:

- 108 • The history of past changes in Arctic temperature and precipitation,
- 109 • Past rates of change in the Arctic,
- 110 • The paleo-history of the Greenland Ice Sheet, and
- 111 • The paleo-history of sea ice in the Arctic.

112 In general, the temporal scope of this report covers the past 65 million years (m.y.) from the
113 early Cenozoic (65 Ma, million years ago) to the recent Holocene (today). Each chapter presents
114 information in chronological sequence from oldest to youngest. The degree of detail in the report
115 generally increases as one moves forward in time because the amount and detail of the available
116 information increases as one approaches the present. The geographic scope of this report,
117 although focused on the Arctic, includes some sub-Arctic areas especially in and near the North
118 Atlantic Ocean in order to make use of many relevant paleo-records from these regions.

119

120 The specific questions posed in the report are as listed below:

121 *1) How have temperature and precipitation changed in the Arctic in the past? What does this*
122 *tell us about Arctic climate that can inform projections of future changes?*

123 This report documents what is known of high-latitude temperature and precipitation
124 during the past 65 million years at a variety of time scales, using sedimentary, biological, and
125 geochemical **proxies**—indirect recorders—obtained largely from ice cores, lake sediment, and
126 marine sediment but also from sediment found in river and coastal bluffs and elsewhere.
127 Sedimentary deposits do not record climate data in the same way that a modern scientific
128 observer does, but climatic conditions control characteristics of many sediments, so these
129 sedimentary characteristics can serve as proxies for the climate that produced them (e.g.,

130 Bradley, 1999). (See Chapter 4 for a discussion of proxies.) Some of the many proxies routinely
131 used are :

- 132 • the character of organic matter,
- 133 • the isotopic geochemistry of minerals or ice,
- 134 • the abundance and types of macrofossils and microfossils, and
- 135 • the occurrence and character of specific chemicals (biomarkers) that record the
136 presence or absence of certain species and of the conditions under which those
137 species grew.

138 Historical records taken from diaries, notebooks, and logbooks are also commonly used to link
139 modern data with paleoclimate reconstructions.

140 The proxy records document large changes in the Arctic. As described in Chapter 5,
141 comparison of Arctic paleoclimatic data with records from lower latitude sites for the same time
142 period shows that temperature changes in the Arctic were greater than temperature changes
143 elsewhere (changes were “amplified”). This Arctic amplification occurred for climate changes
144 with different causes. Physical understanding shows that this amplification is a natural
145 consequence of features of the Arctic climate system.

146

147 ***2) How rapidly have temperature and precipitation changed in the Arctic in the past? What do***
148 ***these past rates of change tell us about Arctic climate that can inform projections of future***
149 ***changes?***

150 The climate record of Earth shows changes that operate on many time scales—tens of
151 millions of years for continents to rearrange themselves, to weeks during which particles from a
152 major volcanic eruption spread in the stratosphere and block the sun. This report summarizes

153 paleoclimate data on past rates of change in the Arctic and subarctic on all relevant time scales,
154 and it characterizes in particular detail the records of past abrupt changes that have had
155 widespread effects. This section of the report has been coordinated with CCSP Synthesis and
156 Assessment Product 3.4, the complete focus of which is on global aspects of abrupt climate
157 change.

158 The data used to assess rates of change in chapter 6 are primarily the same as those used
159 to assess the magnitudes of change in chapter 5. However, as discussed in chapter 5, the
160 existence of high-time-resolution records that cannot always be synchronized exactly to other
161 records, and additional features of the paleoclimatic record, motivate separate treatment of these
162 closely related features of Arctic climate history.

163 Faster or less expected changes have larger effects on natural and human systems than do
164 slower, better anticipated changes (e.g., National Research Council, 2002). Comparison of
165 projected rates of change for the future (IPCC, 2007) with those experienced in the past can thus
166 provide insights to the level of impacts that may occur.. Chapter 6 summarizes rates of Arctic
167 change in the past, compares these with recent Arctic changes and to non-Arctic changes, and
168 assesses processes that contribute to the rapidity of some Arctic changes.

169

170 ***3) What does the paleoclimate record tell us about the past size of the Greenland ice sheet and***
171 ***its implications for sea level changes?***

172 Paleoclimate data allow us to reconstruct the size of the Greenland ice sheet at various
173 times in the past, and they provide insight to the climatic conditions that produced those changes.
174 This report summarizes those paleoclimate data and what they suggest about the mechanisms
175 that caused past changes and might contribute to future changes.

176 An ice sheet leaves tracks—evidence of its passage—on land and in the ocean; those
177 tracks show how far it extended and when it reached that extent, (e.g., Denton et al., 2005). On
178 land, moraines (primarily rock material), which were deposited in contact with the edges of the
179 ice, document past ice extents especially well. Beaches now raised out of the ocean following
180 retreat of ice that previously depressed the land surface, and other geomorphic indicators, also
181 preserve important information. Moraines and other ice-contact deposits in the ocean record
182 evidence of extended ice; isotopic ratios of shells that grew in the ocean may reveal input of
183 meltwater, and iceberg-rafted debris identified in sediment cores can be traced to source regions
184 supplying the icebergs (e.g., Hemming, 2004). The history of ice thickness can be traced by use
185 of moraines or other features on rock that projected above the level of the ice sheet, by the
186 history of land rebound following removal of ice weight, and by indications (especially total gas
187 content) in ice cores (Raynaud et al., 1997). Models can also be used to assimilate data from
188 coastal sites and help constrain inland conditions. This report integrates these and other sources
189 of information that describe past changes in the Greenland ice sheet.

190 Changes in glaciers and ice sheets, especially the Greenland ice sheet, have global
191 repercussions. Complete melting of the Greenland ice sheet would raise global sea level by 7
192 meters (m); even partial melting would flood the world’s coasts (Lemke et al., 2007). Freshwater
193 from melting ice-sheets delivered to the oceans in sensitive regions—the North Atlantic Ocean,
194 for example—could contribute to changes in extent of sea ice, ocean circulation, and climate and
195 could produce strong regional and possibly global effects (Meehl et al., 2007).

196

197 ***4) What does the paleoclimate record tell us about past changes in Arctic sea ice cover, and***
198 ***what implications does this have for consideration of recent and potential future changes?***

199 This report documents past periods when the extent of Arctic sea ice was reduced, and
200 evaluates the scope, causes, and effects of these reductions (e.g., CAPE, 2006). The extent of
201 past sea ice and patterns of sea-ice drift are recorded in sediments preserved on the sea floor.
202 Sea-ice extent can also be reconstructed from fossil assemblages preserved in ancient beach
203 deposits along many Arctic coasts (Brigham-Grette and Hopkins, 1995; Dyke et al., 1996).

204 Recent advances in tapping the Arctic paleoceanographic archives, notably the first deep-
205 sea drilling in the central Arctic Ocean (Shipboard Scientific Party, 2005) and the 2005 Trans-
206 Arctic Expedition (Darby et al., 2005), have provided new, high-quality material with which to
207 identify and characterize warm, reduced-ice events of the past, which may serve as analogs for
208 possible future conditions (e.g., Holland *et al.*, 2006). Sea ice fundamentally affects the climate
209 and oceanography of the Arctic (e.g., Seager et al., 2002), the ecosystems, and human use. The
210 implications of reduced sea ice extend throughout the Arctic and beyond, and they bear on such
211 issues as national security and search-and-rescue (National Research Council, 2007).

212

213 **3.4 Report and Chapter Structure**

214

215 This report is organized into five primary technical chapters. The first of these (Chapter
216 4) provides a conceptual framework for the information presented in the succeeding chapters,
217 each of which focuses on one of the topics described above. Chapter 4 also contains information
218 on the standardized use of time scales and geological terminology in this report.

219 Each of the topical chapters (Chapters 5 through 8) answers, in this order, the questions
220 “Why, how, what, and so what?” The “Why” or opening introductory segment for each chapter
221 outlines the relevance of the topic to the issue of modern climate change. The “How” segment

222 discusses the sources and types of data compiled to build the paleoclimate record and the
223 strengths and weaknesses of the information. The ““What”” segment is the paleo-record
224 information itself, presented in chronological order, oldest to most recent. The final “So what”
225 segment discusses the significance of the material contained in the chapter and its relevance to
226 current climate change. Each technical chapter is preceded by an abstract that outlines the
227 principal conclusions contained in the body of the chapter itself. Bolded words in the text
228 indicate entries in the technical glossary at the end of this report.

229

230 **3.5 The Synthesis and Assessment Product Team**

231

232 Four of the Lead Authors of this report were constituted as a Federal Advisory
233 Committee (FAC) that was charged with advising the U.S. Geological Survey and the CCSP on
234 the scientific and technical content related to the topic of the paleoclimate history of the Arctic as
235 described in the SAP 1.2 prospectus. (See Public Law 92-463 for more information on the
236 Federal Advisory Committee Act; see the GSA website <http://fido.gov/facadatabase/> for specific
237 information related to the SAP 1.2 Federal Advisory Committee.) The FAC for SAP 1.2 acquired
238 input from more than 30 contributing authors in five countries. These authors provided
239 substantial content to the report, but they did not participate in the Federal Advisory Committee
240 deliberations upon which this SAP was developed.

241

241 **Chapter 3 References Cited**

242

243 **Bradley, R.S.**, 1999: Paleoclimatology: Reconstructing Climates of the Quaternary. Academic
244 Press, San Diego, CA, 610 pp.

245

246 **Brigham-Grette, J.** and D.M. Hopkins, 1995: Emergent-Marine record and Paleoclimate of the
247 Last Interglaciation along the northwest Alaskan coast, *Quaternary Research*, **43**, 154-
248 173.

249

250 **CAPE-Last Interglacial Project Members**, 2006: Last Interglacial Arctic warmth confirms
251 polar amplification of climate change. *Quaternary Science Reviews*. **25**, 1383-1400.

252

253 **Cicerone, R.J.**, E.J. Barron, R.E. Dickinson, I.F. Fung, J.E. Hansen, T.R. Karl, R.S. Lindzen,
254 J.C. McWilliams, F.S. Rowland, and J.M. Wallace, 2001: *Climate change science: an*
255 *analysis of some key questions*. National Academy Press, Washington, DC.

256

257 **Correll, R.** et al., 2004: *Impacts of a Warming Arctic: Arctic Climate Impact Assessment*.
258 Cambridge University Press, 139 pp.

259

260 **Darby, D.**, M. Jakobsson, and L. Polyak, 2005: Icebreaker expedition collects key Arctic
261 seafloor and ice data. *EOS*, **86(52)**, 549-556

262

263 **Denton, G.H.**, R.B. Alley, G.C. Comer, and W.S. Broecker, 2005: The role of seasonality in
264 abrupt climate change. *Quaternary Science Reviews*, **24(10-11)**, 1159-1182.

265

266 **Dyke, A.S.**, J. Hooper, and J.M. Savelle, 1996: History of sea ice in the Canadian Arctic
267 archipelago based on postglacial remains of the bowhead whale. *Arctic*, **49(3)**, p. 235-
268 255.

269

270 **Hemming, S.R.**, 2004: Heinrich events: Massive late Pleistocene detritus layers of the North
271 Atlantic and their global climate imprint. *Reviews of Geophysics* **42(2)**, RG1005.

272

273 **Holland**, M.M., C.M. Bitz, and B. Tremblay, 2006: Future abrupt reductions in the summer
274 Arctic sea ice. *Geophysical Research Letters*, **33**, L23503.

275

276 **IPCC**, 2000: *Special Report on Emissions Scenarios*, [Nebojsa Nakicenovic and Robert Swart,
277 eds.]. Cambridge University Press, Cambridge, UK, 612 pp.

278

279 **IPCC**, 2007: Summary for Policymakers. In: *Climate Change 2007—The Physical Science*
280 *Basis. Contribution of Working Group I to the Fourth Assessment Report of the*
281 *Intergovernmental Panel on Climate Change*, [Solomon, S., D. Qin, M. Manning, Z.
282 Chen, M. Marquis, K.B. Averyt, M. Tignor and H.L. Miller (eds.)]. Cambridge
283 University Press, Cambridge, United Kingdom and New York.

284

285 **Lemke**, P., J. Ren, R.B. Alley, I. Allison, J. Carrasco, G. Flato, Y. Fujii, G. Kaser, P. Mote, R.H.
286 Thomas, and T. Zhang, 2007: Observations: Changes in Snow, Ice and Frozen Ground.
287 In: *Climate Change 2007—The Physical Science Basis. Contribution of Working Group I*
288 *to the Fourth Assessment Report of the Intergovernmental Panel on Climate Change*,
289 [Solomon, S., D. Qin, M. Manning, Z. Chen, M. Marquis, K.B. Averyt, M. Tignor and
290 H.L. Miller (eds.)]. Cambridge University Press, Cambridge, United Kingdom and New
291 York, 996 pp.

292

293 **Meehl**, G.A., T.F. Stocker, W.D. Collins, P. Friedlingstein, A.T. Gaye, J.M. Gregory, A. Kitoh,
294 R. Knutti, J.M. Murphy, A. Noda, S.C.B. Raper, I.G. Watterson, A.J. Weaver and Z.-C.
295 Zhao, 2007: Global Climate Projections. In: *Climate Change 2007—The Physical*
296 *Science Basis. Contribution of Working Group I to the Fourth Assessment Report of the*
297 *Intergovernmental Panel on Climate Change*, [Solomon, S., D. Qin, M. Manning, Z.
298 Chen, M. Marquis, K.B. Averyt, M. Tignor and H.L. Miller (eds.)]. Cambridge
299 University Press, Cambridge, United Kingdom and New York, pp. 747-845.

300

301 **National Research Council (NRC)**, 2002: *Abrupt Climate Change, Inevitable Surprises*.
302 National Academy Press, Washington, DC, 230 pp.

303
304
305
306
307
308
309
310
311
312
313
314
315
316
317
318
319
320
321
322
323
324
325
326
327
328

National Research Council (NRC) Committee on the Assessment of U.S. Coast Guard Polar Icebreaker Roles and Future Needs, 2007: *Polar Icebreakers in a Changing World: An Assessment of U.S. Needs*. National Academy of Sciences Press, 122 pp.

Raynaud, D., J. Chappellaz, C. Ritx, and P. Martinerie, 1997: Air content along the Greenland Ice Core Project core: A record of surface climatic parameters and elevation in central Greenland. *Journal of Geophysical Research*, **102(C12)**, 26607-26613.

Richter-Menge, J., J. Overland, A. Proshutinsky, V. Romanovsky, L. Bengtsson, L. Brigham, M. Dyrgerov, J.C. Gascard, S. Gerland, R. Graversen, C. Haas, M. Karcher, P. Kuhry, J. Maslanik, H. Melling, W. Maslowski, J. Morison, D. Perovich, R. Przybylak, V. Rachold, I. Rigor, A. Shiklomanov, J. Stroeve, D. Walker, and J. Walsh, 2006: State of the Arctic Report. NOAA OAR Special Report, NOAA/OAR/PMEL, Seattle, WA, 36 pp.

Seager, R., D.S. Battisti, J. Yin, N. Gordon, N. Naik, A.C. Clement, and M.A. Cane, 2002: Is the Gulf Stream responsible for Europe's mild winters? *Quarterly Journal of the Royal Meteorological Society*, **128B**, 2563–86.

Serreze, M.C., and J.A. Francis, 2006: The Arctic Amplification Debate: *Climatic Change*, **76(3-4)**, 241-264.

Shipboard Scientific Party, 2005: *Arctic Coring Expedition (ACEX): paleoceanographic and tectonic evolution of the central Arctic Ocean*. IODP Preliminary Report, 302, www.ecord.org/exp/acex/302PR.pdf.

1 **CCSP Synthesis and Assessment Product 1.2**
2 **Past Climate Variability and Change in the Arctic and at High Latitudes**

3

4 **Chapter 4 — Paleoclimate Concepts**

5

6 **Chapter Lead Authors**

7 **Richard B. Alley**, Pennsylvania State University, University Park, PA

8 **Joan Fitzpatrick**, U.S. Geological Survey, Denver, CO

9 **Contributing Authors**

10 **Julie Brigham-Grette**, University of Massachusetts, Amherst , MA

11 **Gifford Miller**, University of Colorado, Boulder, CO

12 **Daniel Muhs**, U.S. Geological Survey, Denver, O

13 **Leonid Polyak**, Ohio State University, Columbus, OH

14 **ABSTRACT**

15

16 Interpretation of paleoclimate records requires an understanding of Earth’s climate
17 system, the causes (forcings) of climate changes, and the processes that amplify (positive
18 feedback) or damp (negative feedback) these changes. Paleoclimatologists reconstruct the history
19 of climate from proxies, which are those characteristics of sedimentary deposits that preserve
20 paleoclimate information. A great range of physical, chemical, isotopic, and biological
21 characteristics of lake and ocean sediments, ice cores, cave formations, tree rings, the land
22 surface itself, and more are used to reconstruct past climate. Ages of climate events are obtained
23 by counting annual layers, measuring effects of the decay of radioactive atoms, assessing other
24 changes that accumulate through time at rates that can be assessed accurately, and using time-
25 markers to correlate sediments with others that have had their ages measured more accurately.
26 Not all questions about the history of Earth’s climate can be answered through paleoclimatology:
27 in some cases the necessary sediments are not preserved, or the climatic variable of interest is not
28 recorded in the sediments. Nonetheless, many questions can be answered from the available
29 information.

30 An overview of the history of Arctic climate over the past 65 million years (m.y.) shows
31 a long-term irregular cooling over tens of millions of years. As ice became established in the
32 Arctic, it grew and shrank over tens of thousands of years in regular cycles. During at least the
33 most recent of these cycles, shorter-lived large and rapid fluctuations occurred, especially around
34 the North Atlantic Ocean. The last 11,000 years or so have remained generally warm and
35 relatively stable, but with small climate changes of varying spacing and size. Assessment of the
36 causes of climate changes, and the records of those causes, shows that reduction in atmospheric
37 carbon-dioxide concentration and changes in continental positions were important in the cooling

38 trend over tens of millions of years. The cycling in ice extent was paced by features of Earth's
39 orbit and amplified by the effects of the ice itself, changes in carbon dioxide and other
40 greenhouse gases, and additional feedbacks. Abrupt climate changes were linked to changes in
41 the circulation of the ocean and the extent of sea ice. Changes in the sun's output and in Earth's
42 orbit, volcanic eruptions, and other factors have contributed to the natural climate changes since
43 the end of the last ice age.

44

44 **4.1 Introduction**

45 Most people notice the weather. Day to day, week to week, and even year to year,
46 changes in such parameters as minimum and maximum daily temperatures, precipitation
47 amounts, wind speeds, and flood levels are all details about the weather that nearly everyone
48 shares in daily conversations. When all else fails, most people can talk about the weather.

49 Evaluating longer-term trends in the weather (tens to hundreds of years or even longer) is
50 the realm of climate science. *Climate* is the average weather, usually defined as the average of
51 the past 30 years. *Climate change* is the long-term change of the average weather, and climate
52 change is the focus of this assessment report. While most people accept that the weather is
53 always changing on the time scale of recent memory, geologists reconstruct climate on longer
54 time scales and use these reconstructions to help understand why climate changes. This improved
55 understanding of Earth’s climate system informs our ability to predict future climate change.
56 Reconstructions of past climate also allow us to define the range of natural climate variability
57 throughout Earth’s history. This information helps scientists assess whether climate changes
58 observable now may be part of a natural cycle or whether human activity may play a role. The
59 relevance of climate science lies in the recognition that even small shifts in climate can and have
60 had sweeping economic and societal effects (Lamb, 1997; Ladorie, 1971).

61 Indications of past climate, called climate proxies, are preserved in geological records;
62 they tell us that Earth’s climate has rarely been static. For example, during the past 70 million
63 years (“m.y.”), of Earth history, large changes have occurred in average global temperature and
64 in temperature differences between tropical and polar regions, as well as ice-age cycles during
65 which more than 100 m of sea level was stored on land in the form of giant continental ice sheets
66 and then released back to the ocean by melting of that ice. Climate change includes long-term

67 trends lasting tens of millions of years, and abrupt shifts occurring in as little as a decade or less,
68 both of which have resulted in large-scale reorganizations of oceanic and atmospheric circulation
69 patterns. As we discuss in the following sections, these climate changes are understood to be
70 caused by combinations of the drifting of continents and mountain-building in response to plate-
71 tectonic forces that cause continental drift and mountain-building forces, variations in Earth's
72 orbit about the Sun, and changes in atmospheric greenhouse gases, solar irradiance, and
73 volcanism, all of which can be amplified by powerful positive feedback mechanisms, especially
74 in the Arctic. Documenting past climates and developing scientific explanations of the observed
75 changes (paleoclimatology) inform efforts to understand the climate, reveal features of
76 importance that must be included in predictive models, and allow testing of the models
77 developed.

78 An overview of key climate processes is provided here, followed by a summary of
79 techniques for reconstructing past climatic conditions. Additional details pertaining to specific
80 aspects of the Arctic climate system and its history are presented in the subsequent chapters.

81

82 **4.2 Forcings, Feedback, and Variability**

83 An observed change in climate may depend on more than one process. Tight linkages and
84 interactions exist between these processes, as described below, but it is commonly useful to
85 divide these processes into three categories: internal variability, forcings, and feedbacks. (For
86 additional information, see Hansen et al., 1984, Peixoto and Oort, 1992; or IPCC, 2007 among
87 other excellent sources.)

88 Internal variability is familiar to weather watchers: if you don't like the weather now,
89 wait for tomorrow and something different may arrive. Even though the Sun's energy, Earth's

90 orbit, the composition of the atmosphere, and many other important controls are the same as
91 yesterday, different weather arrives because complex systems exhibit fluctuations within
92 themselves. This variability tends to average out over longer time periods, so climate is less
93 variable than weather; however, even the 30-year averages typically used in defining the climate
94 vary internally. For example, without any external cause, a given 30-year period may have one
95 more El Niño event in the Pacific Ocean, and thus slightly warmer average temperatures, than
96 the previous 30-year period.

97 Forced changes are caused by an event outside the climate system. If the Sun puts out
98 more energy, Earth will warm in response. If fewer volcanoes than average erupt during a given
99 century, then less sunlight than normal will be blocked by particles from those volcanoes, and
100 Earth's surface will warm in response. If burning fossil fuel raises the carbon-dioxide
101 concentration of the atmosphere, then more of the planet's outgoing radiation will be absorbed
102 by that carbon dioxide, and Earth's surface will warm in response. Depending on often-random
103 processes, different forcings may combine to cause large climate swings or offset to cause
104 climate changes to be small.

105 When one aspect of climate changes, whether in response to some forcing or to internal
106 variability, other parts of the climate system respond, and these responses may affect the climate
107 further; if so, then these responses are called feedbacks. How much the temperature changes in
108 response to a forcing of a given magnitude (or in response to the net magnitude of a set of
109 forcings) depends on the sum of all of the feedbacks. Feedbacks can be characterized as positive,
110 serving to amplify the initial change, or negative, acting to partially offset the initial change.

111 As an example, some of the sunshine reaching Earth is reflected back to space by snow
112 without warming the planet. If warming (whether caused by an El Niño, increased output from

113 the Sun, increased carbon dioxide concentration in the atmosphere, or anything else) melts snow
114 and ice that otherwise would have reflected sunshine, then more of the Sun’s energy will be
115 absorbed, causing additional warming and the melting of more snow and ice. This additional
116 warming is a feedback (usually called the ice-albedo feedback). This ice-albedo feedback is
117 termed a positive feedback, because it amplifies the initial change.

118

119 **4.2.1 The Earth’s Heat Budget—A Balancing Act**

120 On time scales of hundreds to thousands of years, the energy received by the Earth from
121 the Sun and the energy returned to space balance almost exactly; imbalance between incoming
122 and outgoing energy is typically less than 1% over periods as short as years to decades. (Figure
123 4.1). This state of near-balance is maintained by the very strong negative feedback linked to
124 thermal radiation. All bodies “glow” (send out radiation), and warmer bodies glow more brightly
125 and send out more radiation than cooler ones. (Watching the glow of a burner on an electric
126 stove become visible as it warms shows this effect very clearly.) Some of the Sun’s energy
127 reaching Earth is reflected without causing warming, and the rest is absorbed to warm the planet.
128 The warmer the planet, the more energy it radiates back to space. A too-cold planet (that is, a
129 planet colder than the temperature at which it would be in equilibrium) will receive more energy
130 than is radiated, causing the planet to warm, thus increasing radiation from Earth until the
131 incoming and outgoing energy balance. Similarly, a too-warm planet will radiate more energy
132 than is received from the Sun, producing cooling to achieve balance. Greenhouse gases in the
133 atmosphere block some of the outgoing radiation, transferring some of the energy from the
134 blocked radiation to other air molecules to warm them, or radiating the energy up or down. The
135 net effect is to cause the lower part of the atmosphere (the troposphere) and the surface of the

136 planet to be warmer than they would have been in the absence of those greenhouse gases. The
137 global average temperature can be altered by changes in the energy from the sun reaching the top
138 of our atmosphere, in the reflectivity of the planet (the planet's albedo), or in strength of the
139 greenhouse effect..

140

141 **FIGURE 4.1 NEAR HERE**

142

143 Equatorial regions receive more energy from space than they emit to space, polar regions
144 emit more energy to space than they receive, and the atmosphere and ocean transfer sufficient
145 energy from the equatorial to the polar regions to maintain balance (for additional information
146 see Nakamura and Oort, 1988, Peixoto and Oort, 1992, and Serreze et al., 2007).

147 Important forcings described later in this section include changes in the Sun; cyclical
148 features of Earth's orbit (Milankovitch forcing); changes in greenhouse gas concentrations in
149 Earth's atmosphere; the shifting shape, size, and positions of the continents (plate tectonics);
150 biological processes; volcanic eruptions; and other features of the climate system. Other possible
151 forcings, such as changes in cosmic rays or in blocking of sunlight by space dust, cannot be ruled
152 out entirely but do not appear to be important.

153

154 **4.2.2 Solar Irradiance Forcing**

155 **4.2.2a Effects of the Aging of the Sun**

156 Energy emitted by the Sun is the primary driver of Earth's climate system. The Sun's
157 energy, or irradiance, is not constant, and changes in solar irradiance force changes in Earth's
158 climate. Our understanding of the physics of the Sun indicates that during Earth's 4.6-billion-

159 year history, the Sun’s energy output should have increased smoothly from about 70% of modern
160 output (see, for example, Walter and Barry, 1991). (Direct paleoclimatic evidence of this
161 increase in solar output is not available.) During the last 100 m.y., changes in solar irradiance are
162 calculated to have been less than 1%, or less than 0.000001% per century. Therefore, the effects
163 of the Sun’s aging have no bearing on climate change over time periods of millennia or less. For
164 reference, the 0.000001% per century change in output from aging of the Sun can be compared
165 with other changes, for example:

- 166 • maximum changes of slightly under 0.1% over 5 to 6 years as part of the sunspot cycle
167 (Foukal et al., 2006);
- 168 • the estimated increase from the year 1750 to 2005 in solar output averaged across sunspot
169 cycles, which also is slightly under 0.1% (Forster et al., 2007; see below); and
- 170 • the warming effect of carbon dioxide added to the atmosphere from 1750 to 2005.

171 This addition is estimated to have had the same warming effect globally as an increase in
172 solar output of ~0.7% (Forster et al., 2007), and thus it is much larger than changes in
173 solar irradiance during this same time interval.

174

175 **4.2.2b Effects of Short-Term Solar Variability**

176 Earth-based observations and, in recent years, more-accurate space-based observations
177 document an 11-year solar cycle that results from changes within the Sun. Changes in solar
178 output associated with this cycle cause peak solar output to exceed the minimum value by
179 slightly less than 0.1% (Beer et al., 2006; Foukal et al., 2006; Camp and Tung, 2007). A satellite
180 thus measures a change from maximum to minimum of about 0.9 W/m^2 , out of an average of
181 about 1365 W/m^2 . This value is usually recalculated as a “radiative forcing” for the lower

182 atmosphere. It is divided by 4 to account for spreading of the radiation around the spherical Earth
183 and multiplied by about 0.7 to allow for the radiation that is directly reflected without warming
184 the planet (Forster et al., 2007). The climate response to this sunspot cycling has been estimated
185 as less than 0.1°C (Stevens and North, 1996) to almost 0.2°C (Camp and Tung, 2007). As
186 discussed by Hegerl et al. (2007), the lack of any trend in solar output over longer times than this
187 sunspot cycling, as measured by satellites, excludes the Sun as an important contributor to the
188 strong warming during the interval of satellite observations, but the solar variability may have
189 contributed weakly to temperature trends in the early part of the 20th century.

190 Over longer time frames, indirect proxies of solar activity (historical sun-spot records,
191 tree-rings and ice-cores) also exhibit 11-year solar cycles as well as longer-term variability.
192 Common longer cycles are about 22, 88 and 205 years (e.g., Frohlich and Lean, 2004). The
193 historical climate record suggests that periods of low solar activity may be linked to climate
194 anomalies. For example, the solar minima known as the "Dalton Minimum" and the "Maunder
195 Minimum" (1790–1820 AD, and 1645–1715 AD, respectively) correspond with the relatively
196 cool conditions of the Little Ice Age. However, the magnitude of radiative forcing that can be
197 attributed to variations in solar irradiance remains debated (e.g., Baliunas and Jastrow, 1990;
198 Bard et al., 2000; Fleitmann, et al., 2003; Frolich and Lean, 2004; Amman et al., 2007;
199 Muscheler et al., 2007). An extensive summary of estimates of solar increase since the Maunder
200 Minimum is given by Forster et al. (2007), which lists a preferred value of a radiative forcing of
201 $\sim 0.2 \text{ W/m}^2$, although the report also lists older estimates of just less than 0.8 W/m^2 , still well
202 below the estimated radiative forcing of the human-caused increase in atmospheric carbon
203 dioxide ($\sim 1.7 \text{ W/m}^2$) (IPCC, 2007).

204

4.2.3 Orbital Forcing and Milankovitch Cycles

Irregularities in Earth’s orbital parameters, often referred to as “Milankovitch variations” or “Milankovitch cycles,” after the Serbian mathematician who suggested that these irregularities might control ice-age cycles, result in systematic changes in the seasonal and geographic distribution of incoming solar radiation (insolation) for the planet (Milankovitch, 1920, 1941). The Milankovitch cycles have almost no effect on total sunshine reaching the planet over time spans of years or decades; they have only a small effect on total sunshine reaching the planet over tens of thousands of years and longer; but they have large effects on north-south and summer-winter distribution of sunshine. These “Milankovitch variations” (Figure 4.2) are due to three types of changes: (1) the eccentricity (out-of-roundness) of Earth’s orbit around the Sun varies from nearly circular to more elliptical and back over about 100 thousand years (k.y.) (E in Figure 4.2); (2) the obliquity (how far the North Pole is tilted away from “straight up” out of the plane containing Earth’s orbit about the Sun) tilts more and then less over about 41 k.y. (T in Figure 4.2); and (3) the precession (the wobble of Earth’s rotational axis, moves Earth from its position closest to the Sun in the Northern-Hemisphere summer (the southern winter) to its position farthest from the Sun in the northern summer (the southern winter and back again in cycles of about 19–23 k.y. (P in Figure 4.2) (e.g., Loutre et al., 2004). These orbital features are linked to the influence of the gravity of Jupiter and the moon, among others, acting on Earth itself and on the bulge at the equator caused by Earth’s rotation. These features are relatively stable, and can be calculated for periods of millions of years with high accuracy. Paleoclimatic records show the influence of these changes very clearly (e.g., Imbrie et al., 1993).

226

227

FIGURE 4.2 NEAR HERE

228

229 The variations in eccentricity (orbital “out of roundness” or departure from circularity)
230 affect the total sunshine received by the planet in a year, but by less than 0.5% between extremes
231 (hence giving very small changes of less than 0.001% per century). The other orbital variations
232 have essentially no effect on the total solar energy received by the planet as a whole. However,
233 large variations do occur in energy received at a particular latitude and season (with offsetting
234 changes at other latitudes and in other seasons); changes have exceeded 20% in 10,000 years
235 (which is still only 0.2% per century, again with offsetting changes in other latitudes and seasons
236 so that the total energy received is virtually constant).

237 In the Arctic, the most important orbital controls are the tilt of Earth’s axis (T in Figure
238 4.2), where high tilt angles result in much more high-latitude insolation than do low tilt angles,
239 and the precession or wobble of Earth’s rotational axis (P in Figure 4.2). When Earth is closest to
240 the Sun at the summer solstice, insolation is significantly greater than when Earth is at its
241 greatest distance from the Sun at the summer solstice. For example, 11 thousand years ago (ka),
242 Earth was closest to the Sun at the Northern Hemisphere summer solstice, but the summer
243 solstice has been steadily moving toward the greatest distance from the Sun since then, such that
244 at present Northern Hemisphere summer occurs when Earth is almost the greatest distance from
245 the Sun, resulting in 9% less insolation in Arctic midsummers today than at 11 ka (Figure 4.3).
246 On the basis of this orbital consideration alone, Arctic summers should have been cooling during
247 this interval in response to the precession of the equinoxes.

248

249

FIGURE 4.3 NEAR HERE

250

251

252 **4.2.4 Greenhouse Gases in the Atmosphere**

253 Roughly 70% of the incoming solar radiation is absorbed by the planet, warming the
254 land, water, and air (Forster et al., 2007). Earth, in turn, radiates energy to balance what it
255 receives, but at a longer wavelength than that of the incoming solar radiation. Greenhouse gases
256 are those gases present in the atmosphere that allow incoming shortwave radiation to pass largely
257 unaffected, but that absorb some of Earth's outgoing longwave radiation band (Figure 4.1).
258 Greenhouse gases play a key role in keeping the planetary temperature within the range
259 conducive to life. In the absence of greenhouse gases in Earth's atmosphere, the planetary
260 temperature would be about -19°C (-2°F); with them, the average temperature is about 33°C
261 (about 57°F) higher (Hansen et al., 1984; Le Treut et al., 2007). The primary pre-industrial
262 greenhouse gases include, in order of importance, water vapor, carbon dioxide, methane, nitrous
263 oxide, and tropospheric ozone. Concentrations of these gases are directly affected by
264 anthropogenic (human) activities, with the exception of water vapor as discussed below. Purely
265 anthropogenic recent additions to greenhouse gases include a suite of halocarbons and
266 fluorinated sulfur compounds (Ehhalt et al., 2001).

267 Typically, carbon dioxide is a less important greenhouse gas than water vapor near
268 Earth's surface. Changing the carbon-dioxide concentration of the atmosphere is relatively easy,
269 but changing the atmospheric concentration of water vapor to any appreciable degree is difficult
270 except by changing the temperature. Natural fluxes of water vapor into and out of the atmosphere
271 are very large, equivalent to a layer of water across the entire surface of Earth of about 2
272 cm/week (e.g., Peixoto and Oort, 1992); human perturbations to these fluxes are relatively very
273 small (Forster et al., 2007). However, the large ocean surface and moisture from plants provide

274 important water sources that can yield more water vapor to warmer air; relative humidity tends to
275 remain nearly constant as climate changes, so warming for any reason introduces more water
276 vapor to the air and increases the greenhouse effect in a positive feedback (Hansen et al., 1984;
277 Pierrehumbert et al., 2007). Hence, discussions of forcing of changes in climate focus especially
278 on carbon dioxide, and to a lesser degree on methane and other greenhouse gases, rather than on
279 water vapor (Forster et al., 2007).

280 Carbon dioxide concentrations in the atmosphere are tied into an extensive natural system
281 of terrestrial, atmospheric, and oceanic sources and sinks called the global carbon cycle (see
282 Prentice et al. (2001) in the IPCC 3rd Assessment Report for a comprehensive discussion). The
283 possible effect of increasing CO₂ levels in the atmosphere was first recognized by Arrhenius
284 (1896). By the 1930s, mathematical models linking greenhouse gases and climate change
285 (Callendar, 1938) projected that a doubling of atmospheric CO₂ concentration would increase the
286 mean global temperature by 2°C and would warm the poles considerably more. (Le Treut et al.
287 (2007) provides a detailed historical perspective on the recognition of Earth's greenhouse effect.)
288 By the 1970s, CH₄, N₂O and CFCs were widely recognized as important additional
289 anthropogenic greenhouse gases (Ramanathan, 1975).

290 The direct relationship between climate change and greenhouse gases such as CO₂ and
291 methane is clearly described by the recent Intergovernmental Panel on Climate Change report
292 (IPCC, 2007). Information summarized there highlights the likelihood that changes in
293 concentrations of greenhouse gases will especially affect the Arctic (Figure 4.4) and focuses
294 attention on greenhouse gases as well as other influences on the Arctic, as discussed in this
295 report especially in Chapter 5 (temperature and precipitation history).

296

297 FIGURE 4.4 NEAR HERE

298

299

300 **4.2.5 Plate Tectonics**

301 The drifting of continents (explained by the theory of plate tectonics) moves land masses
302 from equator to pole or the reverse, opens and closes oceanic “gateways” between land masses
303 thus redirecting ocean currents, raises mountain ranges that redirect winds, and causes other
304 changes that may affect climate. These changes can have very large local to regional effects
305 (moving a continent from the pole to the equator obviously will greatly change the climate of
306 that continent). Moving continents around may have some effect on the average global
307 temperature, in part through changes in the planet’s albedo (Donnadiou et al., 2006).

308 Processes linked to continental rearrangement can strongly affect global climate by
309 altering the composition of the atmosphere and thus the strength of the greenhouse effect,
310 especially through control of the carbon-dioxide concentration of the atmosphere (e.g., Berner,
311 1991; Royer et al., 2007). Over millions of years, the atmospheric concentration of carbon
312 dioxide is controlled primarily by the balance between carbon-dioxide removal through chemical
313 reactions with rocks near the Earth’s surface, and carbon-dioxide release from volcanoes or other
314 pathways involving melting or heating of rocks that sequester carbon dioxide. Because higher
315 temperatures cause carbon dioxide to react more rapidly with Earth-surface rocks, atmospheric
316 warming tends to speed removal of carbon dioxide from the air and thus to limit further
317 warming, in a negative feedback (Walker et al., 1981). Because the tectonic processes causing
318 continental drift control the rate of volcanism, and can change over millions of years, changes in
319 atmospheric carbon-dioxide concentration can be forced by the planet beneath.

320

321 **4.2.6 Biological Processes**

322 Biological processes can both absorb and release carbon dioxide, such that evolutionary
323 changes have contributed to atmospheric changes. For example, some carbon dioxide taken from
324 the air by plants is released by their roots into the soil, by respiration while living and by decay
325 after death. Thus, plants speed the reaction of atmospheric carbon dioxide with rocks (Berner,
326 1991; Beerling and Berner, 2005). This process could not have occurred on the early Earth
327 before the evolution of plants with roots.

328 Plants are composed in part of carbon dioxide removed from the atmosphere, and burning
329 (oxidation) of plants releases most of this carbon dioxide back to the atmosphere (minus the
330 small fraction that reacts with rocks in the soil). When plants are buried without burning and
331 altered to form fossil fuels, the atmospheric carbon-dioxide level is reduced; later, natural
332 processes may bring the fossil fuels back to the surface to decompose and release the stored
333 carbon dioxide. (Humans are greatly accelerating these natural processes; fossil fuels that
334 required hundreds of millions of years to accumulate are being burned in hundreds of years.)
335 Rapid burial favors preservation of organic matter, whereas dead things left on the surface will
336 decompose. Thus, changes in rates of sediment deposition linked to continental rearrangement
337 are among the processes that may affect the formation and breakdown of fossil fuels and thus the
338 strength of the atmospheric greenhouse effect.

339 Continents move more or less as rapidly as fingernails grow, so that a major reshuffling
340 of the continents requires about 100 million years, and the opening or closing of an oceanic
341 gateway may require millions of years (e.g., Livermore et al., 2007). Major evolutionary changes
342 have required millions of years or longer (e.g., d'Hondt, 2005). Thus, those changes in the

343 greenhouse effect that modified Earth's climate or were linked to continental drift or biological
344 evolution have been highly influential over time spans of tens of millions of years, but they have
345 had essentially no effect over shorter intervals of centuries or millennia. (Note that if one
346 considers hundreds of thousands of years or longer, an increase in volcanic activity may notably
347 increase carbon dioxide in the atmosphere, causing warming. However, volcanic release of
348 carbon dioxide is small enough that in a few millennia or less the changes in volcanic release
349 have not notably affected the carbon-dioxide concentration of the atmosphere. The main short-
350 term effect of an increase in volcanic eruptions is to cool the planet by blocking the Sun, as
351 discussed next.)

352

353 **4.2.7 Volcanic Eruptions**

354 Volcanic eruptions are an important natural cause of climate change on seasonal to multi-
355 decadal time scales. Large explosive volcanic eruptions inject both particles and gases into the
356 atmosphere. Particles are removed by gravity in days to weeks. Sulfur gases, in contrast, are
357 converted rapidly to sulfate aerosols (tiny droplets of sulfuric acid) that have a residence time in
358 the stratosphere of about 3 years and are transported around the world and poleward by
359 circulation within the stratosphere. Tropical eruptions typically influence both hemispheres,
360 whereas eruptions at middle to high latitudes usually affect only the hemisphere of eruption
361 (Shindell et al., 2004; Fischer et al., 2007). Consequently, the Arctic is affected primarily by
362 tropical and Northern Hemisphere eruptions.

363 The radiative and chemical effects of the global volcanic aerosol cloud produce strong
364 responses in the climate system on short time scales (see Figure 6.5) (Briffa et al., 1998; deSilva
365 and Zielinski, 1998; Oppenheimer, 2003). By scattering and reflecting some solar radiation back

366 to space, the aerosols cool the planetary surface, but by absorbing both solar and terrestrial
367 radiation, the aerosol layer also heats the stratosphere. A tropical eruption produces more heating
368 in the tropics than in the high latitudes and thus a steeper temperature gradient between the pole
369 and the equator, especially in winter. In the Northern Hemisphere winter, this steeper gradient
370 produces a stronger jet stream and a characteristic stationary tropospheric wave pattern that
371 brings warm tropical air to Northern Hemisphere continents and warms winter temperatures.
372 Because little solar energy reaches the Arctic during winter months, the transfer of warm air
373 from tropical sources to high latitudes has more effect on winter temperatures than does the
374 radiative cooling effect from the aerosols. However, during the summer months, radiative
375 cooling dominates, resulting in anomalously cold summers across most of the Arctic. The 1991
376 Mt. Pinatubo eruption in the Philippines resulted in volcanic aerosols covering the entire planet,
377 producing global-average cooling, but winter warming over the Northern Hemisphere continents
378 in the subsequent two winters (Stenchikov et al., 2004, 2006).

379 Three large historical Northern Hemisphere eruptions have been studied in detail: the 939
380 AD Eldgjá (Iceland), 1783–1784 AD Laki (Iceland), and 1912 AD Novarupta (Katmai, Alaska)
381 eruptions. All caused cooling of the Arctic during summer but no winter warming (Thordarson et
382 al., 2001; Oman et al., 2005, 2006).

383 When widespread stratospheric volcanic aerosols settle out, some of the sulfate falls onto
384 the Antarctic and Greenland ice sheets (Figure 4.5). Measurements of those sulfates present in
385 ice cores can be used to estimate the Sun-blocking effect of the eruption. Large volcanic
386 eruptions, especially those within a few decades of each other, are thought to have promoted
387 cooling during the Little Ice Age (about 1280–1850 AD) (Anderson et al., 2008). A

388 comprehensive review of the effects of volcanic eruptions on climate and of records of past
389 volcanism is provided by Robock (2000, 2007).

390

391

FIGURE 4.5 NEAR HERE

392

393

394

395

396

397

398

399

400

401

402

403

404

405

FIGURE 4.6 NEAR HERE

406

407

4.2.8 Other influences

408

409

410

Paleoclimatic records discount some speculative mechanisms of climate change. For example, about 40,000 years ago natural fluctuations reduced the strength of Earth's magnetic field essentially to zero for about one millennium. The cosmic-ray flux into the Earth system

411 increased greatly, as recorded by a large peak in beryllium-10 in sedimentary records. However,
412 the climate record does not change in parallel with changes in beryllium-10, indicating that the
413 cosmic-ray increase had little or no effect on climate (Muscheler et al., 2005). Large changes in
414 concentration of extraterrestrial dust between Earth and Sun might lead to changes in solar
415 energy reaching Earth and thus to changes in climate; however, the available sedimentary
416 records show no no significant changes in the rate of infall of such extraterrestrial dust (Winckler
417 and Fischer, 2006).

418 The climate is a complex, integrated system, and it operates through strong linked
419 feedbacks, internal variability, and numerous forcings. On time scales of centuries or less,
420 however, many of the drivers of past climate change—such as drifting continents, biological
421 evolution, aging of the Sun, and features of Earth’s orbit—have no discernible influence on the
422 climate. Small variations in climate appear to have been caused by small variations in the Sun’s
423 output, occasional short-lived cooling caused by explosive volcanic eruptions, and greenhouse-
424 gas changes have affected the planet’s temperature.

425

426 **4.3 Reading the History of Climate Through Proxies**

427 A modern historian trying to understand our human story cannot go back in time and
428 replay an important event. Instead, the historian must rely on indirect evidence: eyewitness
429 accounts (which may not be highly accurate), artifacts, and more. It is as if the historical figures,
430 who cannot tell their tale directly, have given their proxies to other people and other things to
431 deliver the story to the modern historian.

432 Historians of climate—paleoclimatologists—are just like other historians: they read the
433 indirect evidence that the past sends by proxy. All historians are aware of the strengths and

434 weaknesses of proxy evidence, of the value of weaving multiple strands of evidence together to
435 form the complete fabric of the story, of the necessity of knowing when things happened as well
436 as what happened, and of the ultimate value of using history to inform understanding and guide
437 choices.

438 Some of the proxy evidence used by paleoclimatologists would be familiar to more-
439 traditional historians. Written accounts of many different activities often include notes on the
440 weather, on the presence or absence of ice on local water bodies, and on times of planting or
441 harvest and the crops that grew or failed. If care is taken to account for the tendency of people to
442 report the rare rather than the commonplace, and to include the effects of changes in husbandry
443 and other issues, written records can contribute to knowledge of climate back through written
444 history. However, human accounts are lacking for almost all of Earth's history. The
445 paleoclimatologist is forced to rely on evidence that is less familiar to most people than are
446 written records. Remarkably, these natural proxies may reveal even more than the written
447 records.

448

449 **4.3.1 Climate's Proxies**

450 Much of the history of a civilization can be reconstructed from the detritus its people left
451 behind. Similarly, paleoclimate records are typically developed through analysis of sediment,
452 broadly defined. "Sediment" may include the ice formed as years of snowfall pile up into an ice
453 sheet, the mud accumulating at the bottom of the sea or a lake, the annual layers of a tree, the
454 thin sheets of mineral laid one on top of another to form a stalagmite in a cave, the piles of rock
455 bulldozed by a glacier, the piles of desert sand shaped into dunes by the wind, the odd things
456 collected and stored by packrats, and more (e.g., Crowley and North, 1991; Bradley, 1999;

457 Cronin, 1999). For a sediment to be useful, it must do the following: (1) preserve a record of the
458 conditions when it formed (i.e., subsequent events cannot have erased the original story and
459 replaced it with something else); (2) be interpretable in terms of climate (the characteristics of
460 the deposit must uniquely relate to the climate at the time of formation); and (3) be “datable”
461 (i.e., there must be some way to determine the time when the sediment was deposited). Here, we
462 first present one well-known paleoclimatic indicator as an example, then discuss general issues
463 raised by that example, and follow with a discussion of many types of paleoclimatic indicators.

464 Long records of Earth’s climate are commonly reconstructed from climate proxies
465 preserved in deep-ocean sediments. One of the best-known proxy records of climate change is
466 that recorded by benthic (bottom-dwelling) foraminifers, microscopic organisms that live on the
467 sea floor and secrete calcium-carbonate shells in equilibrium with the sea water. The isotopes of
468 oxygen in the carbonate are a function of both the water temperature (which often does not
469 change very rapidly with time or very steeply with space in the deep ocean) and changes in
470 global ice volume. Global ice volume determines the relative abundances of the isotopes oxygen-
471 16 and oxygen-18 in seawater. Snow has relatively less of the heavy oxygen-18 than its seawater
472 source. Consequently, as ice sheets grow on land, the ocean becomes enriched in the heavy
473 oxygen-18, and this enrichment is recorded by the oxygen isotopic composition of foraminifer
474 shells. The proportion of the heavy and light isotopes of oxygen is usually expressed as $\delta^{18}\text{O}$;
475 positive $\delta^{18}\text{O}$ values represent extra amounts of the heavy isotope of oxygen, and negative values
476 represent samples with less of the heavy isotope than average seawater. Positive $\delta^{18}\text{O}$ reflects
477 glacial times (colder, more ice), whereas more negative $\delta^{18}\text{O}$ reflects interglacial (warmer, less
478 ice) times in Earth’s history. Although the $\delta^{18}\text{O}$ of foraminifer shells does not reveal where the
479 glacial ice was located, the record does provide a globally integrated value of the amount of

480 glacial ice on land, especially if appropriate corrections are made for temperature changes by use
481 of other indicators. In the absence of changes in global ice volume, changes in benthic
482 foraminifer $\delta^{18}\text{O}$ reflect changes in ocean temperatures: more positive $\delta^{18}\text{O}$ values indicate
483 colder water, and more negative $\delta^{18}\text{O}$ values indicate warmer water.

484 Written documents have sometimes been erased and rewritten, in a deliberate attempt to
485 distort history or because the paper was more valuable than the original words.

486 Paleoclimatologists are continually watching for any signs that a climate record has been
487 “erased” and “rewritten” by events since deposition of the sediment. Occasionally, this vigilance
488 proves to be important. For example, water may remove isotopes carrying paleoclimatic
489 information from shells and replace them with other isotopes telling a different story (e.g.,
490 Pearson et al., 2001). However, except for the very oldest deposits from early in Earth’s history,
491 it is usually possible to tell whether a record has been altered, and this problem should not affect
492 any of the conclusions presented in this report.

493 Finding the link between climate and some characteristic of the sediment is then required.
494 The climate is recorded in myriad ways by physical, biological, chemical, and isotopic
495 characteristics of sediments.

496 Physical indicators of past climate are often easy to read and understand. For example, a
497 sand dune can form only if dry sand is available to be blown around by the wind, without being
498 held down by plant roots. Except near beaches (where fluctuations in water level reveal bare
499 sand), a dry climate is needed to keep grass off the sand so the sand can blow around. Today in
500 northwestern Nebraska, the huge dune field of the Sand Hills is covered in grass (Figure 4.7).
501 The dunes formed during drier conditions in the past, but wetter conditions now allow grass to
502 grow on top (e.g., Muhs et al., 1997). Similarly, the sediments left by glaciers are readily

503 identified, and those sediments in areas that are ice free today attest to changing climate. A very
504 different physical indicator of past climate is the temperatures measured in boreholes. Just as a
505 Thanksgiving turkey placed in an oven takes a while to warm in the middle, the two-mile-thick
506 ice sheet of Greenland has not finished warming from the ice age, and the cold temperatures at
507 depth reveal how cold the ice age was (Cuffey and Clow, 1997).

508

509

FIGURE 4.7 NEAR HERE

510

511 Many paleoclimate records are based directly on living things. Tundra plants are quite
512 different from those living in temperate forests. If pollen, seeds, and twigs found in deep layers
513 of a sediment core came from tundra plants, and those found in shallow layers came from
514 temperate-forest plants, a formerly cold time that has warmed is indicated. Trees grow more
515 rapidly and add thicker rings when climatic conditions are more favorable. In very dry regions,
516 this feature allows trees to be used in reconstruction of rainfall; in cold regions, growth may be
517 more closely linked to temperature (Fritts, 1976; Cook and Kairiukstis, 1990)

518

519 Chemical analysis of sediments may reveal additional information about past climates.
520 As one example, some single-celled organisms in the ocean change the chemistry of their cell
521 walls in response to changing temperature: they use more-flexible molecules to offset the
522 increase in brittleness caused by colder temperatures. These molecules are sturdy and persist in
523 sediments after the organism dies, so the history of the ratio of stiffer to less-stiff molecules in a
524 sediment core provides a history of the temperature at which the organisms grew. (In this case,
525 the organisms are prymnesiophyte algae, the chemicals are alkenones, and the frequency of
carbon double bonds controls the stiffness (Muller et al., 1998); other such indicators exist.)

526 Isotopic ratios are among the most commonly used proxy indicators of past climates.
527 Consider just one example, providing one of the ways to determine the past concentration of
528 carbon dioxide. All carbon atoms have 6 protons in their nuclei, most have 6 neutrons (making
529 carbon-12), but some have 7 neutrons (carbon-13) and a few have 8 neutrons (radioactive
530 carbon-14). The only real difference between carbon-12 and carbon-13 is that carbon-13 is a bit
531 heavier. The lighter carbon-12 is “easier” for plants to use, so growing plants preferentially
532 incorporate carbon from carbon dioxide containing only carbon-12 rather than carbon-13.
533 However, if carbon dioxide is scarce in the environment, the plants cannot be picky and must use
534 what is available. Hence, the carbon-12:carbon-13 ratio in plants provides an indicator of the
535 availability of carbon dioxide in the environment. The sturdy cell-wall chemicals described in the
536 previous paragraph can be recovered and their carbon isotopes analyzed, providing an estimate
537 of the carbon-dioxide concentration at the time the algae grew (e.g., Pagani et al., 1999).

538 Much of the science of paleoclimatology is devoted to calibration and interpretation of
539 the relation between sediment characteristics and climate (see National Research Council, 2006).
540 The relationship of some indicators to climate is relatively straightforward, but other
541 relationships may be complex. The width of a tree ring, for example, is especially sensitive to
542 water availability in dry regions, but it may also be influenced by changes in shade from
543 neighboring trees, an attack of beetles or other pests that weaken a tree, the temperature of the
544 growing season, and more. Extensive efforts go into calibration of paleoclimatic indicators
545 against the climatic variables. Because paleoclimatic data cannot be collected everywhere,
546 additional work is devoted to determining which areas of the globe have climates that can be
547 reconstructed from the available paleoclimatic data. Wherever possible, multiple indicators are

548 used to reconstruct past climates and to assess agreement or disagreement (National Research
549 Council, 2006). Conclusions about climate typically rest on many lines of evidence.

550

551 **4.3.2 The Age of the Sediments**

552 History requires “when” as well as “what.” Many techniques reveal the “when” of
553 sediments, sometimes to the nearest year. In general, more-recent events can be dated more
554 precisely.

555 Climate records that have been developed from most trees, and from some ice cores and
556 sediment cores, can be dated to the nearest year by counting annual layers. The yearly nature of
557 tree rings from seasonal climates is well known. A lot of checking goes into demonstrating that
558 layers observed in ice cores and special sediment cores are annual, but in some cases the layering
559 clearly is annual (Alley et al., 1997), allowing quite accurate counts. The longest-lived trees may
560 be 5000 years old; use of overlapping living and dead wood has allowed extension of records to
561 more than 10,000 years (Friedrich et al., 2004); and the longest annually layered ice cores
562 recovered to date extend beyond 100,000 years (Meese et al., 1997). However, relatively few
563 records can be absolutely dated in this way.

564 Other techniques that have been used for dating include measuring the damage that
565 accumulates from cosmic rays striking things near Earth’s surface (those rays produce beryllium-
566 10 and other isotopes), observing the size of lichen colonies growing on rocks deposited by
567 glaciers, and identifying the fallout of particular volcanic eruptions that can be dated by
568 historical accounts or annual-layer counting.

569 Most paleoclimatic dating uses the decay of radioactive elements. Radiocarbon is
570 commonly used for samples containing carbon from the most recent 40,000 years or so (very

571 little of the original radiocarbon survives in older samples, causing measurements difficulties and
572 allowing even trace contamination by younger materials to cause large errors in estimated age, so
573 other techniques are preferred). Many other isotopes are used for various materials and time
574 intervals, extending back to the formation of Earth. Intercomparison with annual-layer counts,
575 with historical records, and between different techniques shows that quite high accuracy can be
576 obtained, so that it is often possible to have errors in age estimates of less than 1%. (That is, if an
577 event is said to be 100,000 years old, the event can be said with high confidence to have occurred
578 sometime between 99,000 years and 101,000 years ago.)

579

580 **4.4 Cenozoic Global History of Climate**

581 As emphasized in the Summary for Policymakers of IPCC (2007) and in the body of that
582 report, a paleoclimatic perspective is important for understanding Earth's climate system and its
583 forcings and feedbacks. Arctic records, and especially Arctic ice-core records, have provided key
584 insights. The discussion that follows briefly discusses selected features in the history of Earth's
585 climate and the forcings and feedbacks of those climate events. This discussion does not treat all
586 of the extensive literature on these topics, but it is provided here as a primer to help place the
587 main results of this report in context. (Kump et al. (2003) is a more-complete yet accessible
588 introduction to this topic.)

589 This report focuses on the Cenozoic Era, which began about 65 Ma with the demise of
590 the dinosaurs and continues today (see section 4.5 for a discussion of the chronology used in this
591 report). During most of this 65 m.y. interval, deep-sea records of foraminifer $\delta^{18}\text{O}$ (a powerful
592 paleoclimatic indicator, described above in section 4.4.1), which integrate the sedimentary record
593 in several ocean basins, show that Earth was warmer than at present and supported a smaller

594 volume of ice (Figure 4.8). Yet, following the peak warming of the early Eocene, about 50–55
595 Ma, global temperatures generally declined (Miller et al., 2005). Although this record is not
596 specific about Arctic climate change, the record indicates that the global gradient (or difference)
597 in temperature between polar regions and the tropics was smaller when global climate was
598 warmer, and that this gradient increased as the high latitudes progressively cooled (Barron and
599 Washington, 1982). Changes in the gradient cause changes in atmospheric and oceanic
600 circulation. The overall cooling trend of the past 55 m.y. was punctuated by intervals during
601 which the cooling was reversed and the oceans warmed, only to cool rapidly again at a later time.
602 Examples of such accelerated cooling include rapid decreases in foraminifer $\delta^{18}\text{O}$ about 34 Ma
603 and again about 23 Ma, which are thought to reflect the rapid buildup of ice in Antarctica in only
604 a few hundred thousand years (Zachos et al., 2001). The Paleocene-Eocene thermal maximum
605 (about 55 Ma) represents a major interval of global warming when CO_2 levels are estimated to
606 have risen abruptly (Shellito et al., 2003), perhaps owing to the rapid release of methane from
607 sea-floor sediments (Bralower et al., 1995).

608

609

FIGURE 4.8 NEAR HERE

610

611 The style and tempo of global climate change during the past 5.3 m.y. is depicted well by
612 the foraminifer $\delta^{18}\text{O}$ record of Lisiecki and Raymo (2005) (Figure 4.9; see section 4.4.1 for a
613 discussion of this proxy). This composite record provides a well-dated stratigraphic tool against
614 which other records from around world can be compared. The foraminifer $\delta^{18}\text{O}$ record reflects
615 changes in both global ice volume and ocean bottom-water temperature change, and with the
616 same sense—An increase in global ice or a decrease in ocean temperatures pushes the indicator

617 in the same direction. The foraminifer $\delta^{18}\text{O}$ record indicates low-magnitude climate changes
618 from 5.3 until about 2.7 Ma, when the amplitude of the foraminifer $\delta^{18}\text{O}$ signal increased
619 markedly. This shift in foraminifer $\delta^{18}\text{O}$ amplitude coincides with widespread indications of
620 onset of northern continental glaciation (see Chapter 5, temperature and precipitation history).
621 The oxygen isotope fluctuations since 2.7 Ma are commonly used as a global index of the
622 frequency and magnitude of glacial-interglacial cycles. In addition to the fluctuations, the data
623 show that within the past 3 m.y., average ocean temperatures have been dropping. Global
624 circulation models constrained by extensive paleoclimatic data targeting the late Pliocene
625 interval from 3.3 to 3.0 Ma suggest that global temperatures were warmer by as much as 2°C or
626 3°C at that time (see Jiang et al., 2005; IPCC, 2007).

627

628 **FIGURE 4.9 NEAR HERE**

629

630 The large fluctuations in foraminifer $\delta^{18}\text{O}$ beginning about 2.7 Ma exhibited clear
631 periodicities matching those of the Milankovitch forcing (those periodicities are also present in
632 smaller, older fluctuations). A 41 k.y. periodicity was especially apparent, as well as the 19–23
633 k.y. periodicity. More recently, within the last 0.9 m.y. or so, the variations in $\delta^{18}\text{O}$ became even
634 bigger, and while the 41 k.y. and 19–23 k.y. periodicities continued, a 100 k.y. periodicity
635 became dominant. The reasons for this shift remain unclear and are the focus of much research
636 (Clark et al., 2006; Ruddiman, 2006; Huybers, 2007; Lisiecki and Raymo, 2007).

637

638 Moving toward the present, the number of available records increases greatly, as does
639 typical time resolution of the records and the accuracy of dating (see section 4.4). The large ice-
age cycling of the last 0.9 m.y. produced growth and retreat of extensive ice sheets across broad

640 regions of North America and Eurasia, as well as smaller extensions of ice in Greenland,
641 Antarctica, and many mountainous areas. Ice in North America covered New York and Chicago,
642 for example. The water that composed those ice sheets had been removed from the oceans,
643 causing non-ice-covered coastlines typically to lie well beyond modern boundaries. Melting of
644 ice sheets exposed land that had been ice-covered and submerged coastal land, but with a
645 relatively small net effect (e.g., Kump and Alley, 1994). The ice-age cycling caused large
646 temperature changes, of many degrees to tens of degrees in some places (see Chapter 5,
647 temperature and precipitation history).

648 Climate changed in large abrupt jumps (see section 6.4.3) during the most recent of the
649 glacial intervals and probably during earlier ones. In records from near the North Atlantic such as
650 Greenland ice cores, roughly half of the total difference between glacial and interglacial
651 conditions was achieved (as recorded by many climate-change indicators) in time spans of
652 decades to years. Changes away from the North Atlantic were notably smaller, and in the far
653 south the changes appear to see-saw (southern warming with northern cooling). The “shape” of
654 the climate records is interesting: northern records typically show abrupt warming, gradual
655 cooling, abrupt cooling, near-stability or slight gradual warming, and then they repeat (see Figure
656 7.9).

657 The most recent interglacial interval has lasted slightly more than 10,000 years. Generally
658 warm conditions have prevailed compared with the average of the last 0.9 m.y. However,
659 important changes have been observed. These changes include broad warming and then cooling
660 in only millennia, abrupt events probably linked to the older abrupt changes, and additional
661 events with various spacings and sizes that have a range of causes, which will be described more
662 in Chapters 5 (temperature and precipitation history) and 6 (rates of Arctic climate change).

663

664 **4.5 Chronology**

665 In any discussion of past climate periods, we must use a time scale understandable to all
666 readers. Beyond the historical period, then, we must use time periods that are within the realm of
667 geology. In this report, we use two sets of terminology for prehistoric time periods, one for the
668 longer history of Earth and one for much more recent Earth history, approximately the past 2.6
669 m.y. (the Quaternary Period). For the longer period of Earth history, we use the terminology and
670 time scale adopted by the International Commission on Stratigraphy (Ogg, 2004). This time scale
671 is well established and has been widely accepted throughout the geologic community. The
672 Quaternary Period is the youngest geologic period in this time scale, and constitutes the past
673 approximately 2.6 m.y. (<http://www.stratigraphy.org/gssp.htm>; Jansen et al., 2007) (Figure 4.10).
674 The Quaternary Period is of particular interest in this report, because this time interval is
675 characterized by dramatic changes—between glacial and interglacial—in climate.

676

677

FIGURE 4.10 NEAR HERE

678

679 Some problems are associated with the use of time scales within the Quaternary Period.
680 These problems are common to all geologic dating, but they assume additional importance in the
681 Quaternary because the focus during this geologically short, recent period is on relatively short-
682 lived events. Very few geologic records for the Quaternary Period are continuous, well dated,
683 and applicable to all other records of climate change. Furthermore, many geologic deposits
684 preserve records of events that are time-transgressive or diachronous. That is, a particular
685 geologic event is recorded earlier at one geographic location and later at another.

686 A good example of time-transgression is the most recent deglaciation of mid-continent North
687 America, the retreat of the Laurentide ice sheet. Although this retreat marked a major shift in a
688 climate state, from a glacial period to an interglacial period, by its very nature it occurred at
689 different times in different places. In midcontinental North America, the Laurentide ice sheet had
690 begun to retreat from its southernmost position in central Illinois after about 22.6 ka, but it was
691 still present in what is now northern Illinois until after about 15.1 ka, and was still in Wisconsin
692 and Michigan until after about 12.9 ka (Johnson et al., 1997) (radiocarbon ages were converted
693 using the algorithm of Fairbanks et al., 2005), and in north-central Labrador until about 6 ka
694 (Dyke and Prest, 1987). Thus, the geologic record of when the present “interglacial” period
695 began is older in central Illinois than it is in northern Michigan, which in turn is older than it is in
696 southern Canada. Time transgression as a concept also applies to phenomena other than geologic
697 processes. Migration of plant communities (biomes) as a result of climate change is not an
698 instantaneous process throughout a wide geographic region. Thus, many records of climate
699 change that reflect changes in plant communities will take place at different times in a region as
700 taxa within that community migrate.

701 Another difficulty is not with the geologic records themselves but with the terms used in
702 different regions to describe them. For example, “Sangamon” is the name of the last interglacial
703 period in the mid-continent of North America (Johnson et al., 1997) and the term “Eemian” is
704 used for the last interglacial period in Europe. However, North American workers apply the term
705 Sangamon primarily to rock-stratigraphic records (tills deposited by glaciers and old soils called
706 paleosols). The Sangamon interglacial is considered to have lasted several tens of thousands of
707 years, because no glacial ice was present in the mid-continent between the last major glacial
708 event (“Illinoian”) and the most recent one (“Wisconsinan”). In contrast, the term Eemian, used

709 by European workers, is often applied to pollen records and is reserved for a period of time,
710 perhaps less than 10,000 years, when climate conditions were as warm or warmer than present.

711 Nevertheless, it is crucial that at least some terminology is used as a common basis for
712 discussion of geologic records of climate change during the Quaternary. In this report, we have
713 chosen to use the stages of the oxygen isotope record from foraminifers in deep-sea cores as our
714 terminology for discussing different intervals of time within the Quaternary Period. The
715 identification of glacial-interglacial changes in deep-sea cores, and the naming of stages for
716 them, began with a landmark report by Emiliani (1955). The oxygen isotope composition of
717 carbonate in foraminifer skeletons in the ocean shifts as climate shifts from glacial to interglacial
718 states (see section 4.4.1, above). These shifts are due both to changes in ocean temperature and
719 changes in the isotopic composition of seawater. The latter changes result from the shifts in
720 oxygen isotopic composition of seawater, in turn a function of ice volume on land. Because the
721 temperature and ice-volume influences on foraminiferal oxygen-isotope compositions are in the
722 same direction, the record of glacial-interglacial changes in deep-sea cores is particularly robust.

723 The oxygen isotope record of glacial-interglacial cycles has been studied and well
724 documented in hundreds of deep-sea cores. The same glacial-interglacial cycles are easily
725 identified in cores from all the world's oceans (Bassinot, 2007). It is, therefore, truly a
726 continuous and global record of climate change within the Quaternary Period. Furthermore, a
727 variety of geologic records of climate change show the same glacial-interglacial cycles that can
728 be compared and correlated with the deep-sea record. These geologic records include glacial
729 records (e.g., Booth et al., 2004; Andrews and Dyke, 2007), ice cores (e.g., NGRIP, 2004; Jouzel
730 et al., 2007), cave carbonates (e.g., Winograd et al., 1992, 1997), and eolian sediments (e.g., Sun
731 et al., 1999). Furthermore, deep-sea cores themselves sometimes contain, in addition to

732 foraminifers, other records of climate change such as pollen from past vegetation (e.g., Heusser
733 et al., 2000) or eolian (wind-deposited) sediments that record glacial and interglacial climates on
734 land (e.g., Hovan et al., 1991).

735 The time scales that have been developed for the oxygen isotope record are important to
736 understand. The mostly widely used time scales are those that have been developed by use of
737 “stacked” deep-sea core records (i.e., multiple core records, from more than one ocean) that are
738 in turn, “tuned” or “dated” by a combination of identification of dated paleomagnetic events and
739 an assumed forcing of climate change by changes in the parameters related to Earth-Sun orbital
740 geometry, precession, and obliquity.

741 Initially, dated paleomagnetic events were used with an assumed constant sedimentation
742 rate to provide a first estimate of the timing of the main variations in the climate. The timing
743 closely matched the known periodicities in Earth-Sun orbital geometry, to a degree that provided
744 very high confidence that those known periodicities were affecting the climate. Then, this result
745 was used to fine-tune the dating by adjusting the sedimentation rates to allow closer match
746 between the data and the orbital periodicities. The practice is often referred to as “astronomical”
747 or “orbital” tuning. The strategy behind “stacking” multiple records is to eliminate possible local
748 effects on a core and present a smoothed, global record. Several highly similar time scales have
749 been developed using this approach. The most commonly cited are the SPECMAP studies of
750 Imbrie et al. (1984) and Martinson et al. (1987) (Figure 4.11), and the more recent work of
751 Lisiecki and Raymo (2005).

752

753

FIGURE 4.11 NEAR HERE

754

755 However, there are disadvantages to using the astronomically tuned oxygen isotope records.
756 Very few deep-sea cores are dated directly, except in the upper parts that are within the range of
757 radiocarbon dating, or at widely spaced depths where paleomagnetic events are recorded. In
758 addition, after the initial tests, the astronomical tuning approach assumes that the orbital
759 parameters, particularly precession and obliquity, are the primary forcing mechanisms behind
760 climate change on glacial-interglacial time scales in the Quaternary Period. Challenges to this
761 assumption are based on directly dated cave calcite records (Winograd et al., 1992, 1997) and
762 emergent coral reef terraces (Szabo et al., 1994; Gallup et al., 2002; Muhs et al., 2002), although
763 in general the assumption appears to be more-or-less accurate. Additional assumptions, including
764 that response is proportional to forcing, are inherent in tuning.

765 Recognizing the assumptions inherent in the SPECMAP time scale, we use this time scale
766 and the marine oxygen isotope stage terminology in this report for four reasons:

- 767 1. the wide acceptance and use in the scientific community,
- 768 2. the continuous nature of the record,
- 769 3. the global aspect of the record, and
- 770 4. the ability to subdivide the periods of time under consideration.

771 Regarding the latter, for example, the marine record can accommodate the problem in the use of
772 “Sangamon,” as used in North America compared with “Eemian,” in Europe. The Sangamon
773 interglacial, as used by North Americans, includes all of marine isotope stage 5 (MIS 5), as well
774 as perhaps parts of MIS 4. However, the Eemian, as used by most European workers, would
775 include only MIS 5e or 5.5, an interval within the greater MIS 5.

776

777 **4.6 Synopsis**

778 Earth's climate is a complex, interrelated system of air, water, ice, land surface, and living
779 things responding to the Sun's energy. Scientific understanding of this system has been
780 increasing rapidly, and the broad outline is now quite well known, although many details remain
781 obscure and further discoveries are guaranteed.

782 The climate system can be forced to change, but it also varies internally without external
783 forcing. Both forced and unforced variations interact with various feedback processes that may
784 either amplify or reduce the resulting climate change, often with interesting patterns in space and
785 time.

786 Changes in the energy emitted by the Sun, the amount of that energy reaching Earth, the
787 amount of that energy reflected by Earth, and the greenhouse effect of the atmosphere are
788 important in controlling global climate. Changes in continental positions, ocean currents, wind
789 patterns, clouds, vegetation, ice, and more affect regional climates as well as contribute to the
790 global picture. The Sun has brightened slowly for billions of years, and its brightness shows very
791 small fluctuations measured in years to centuries. Features of Earth's orbit change the latitudinal
792 and seasonal distribution of sunshine, and they have a small effect on total sunshine reaching the
793 planet over tens of thousands of years. Great tectonic forces in the Earth rearrange continents and
794 promote or reduce volcanic activity and growth of mountain ranges. All three affect greenhouse-
795 gas concentrations and other features of the climate over millions of years or longer, and they
796 interact with changes in the biosphere in response to biological evolution. And, these general
797 statements omit many interesting and increasingly well-understood features of the system.

798 Many deposits of the Earth system—muds and cave formations and tree rings and ice layers
799 and many more—have characteristics that reflect the climate at the time of formation, that are
800 preserved after formation, and that reveal their age of formation. Careful consideration of these

801 deposits underlies paleoclimatology, the study of past climates. Varied investigative techniques
802 focus on physical, chemical, isotopic, and biological indicators, and they provide surprisingly
803 complete histories of changes in time and space.

804 This report especially focuses on the last tens of millions of years. This interval has been
805 characterized by slow cooling, leading from a largely ice-free world to ice-age cycling in
806 response to orbital changes. Both the cooling trend and the ice-age cycling were punctuated
807 occasionally by abrupt shifts. The last approximately 10,000 years have been a reduced-ice
808 interglacial during the ice-age cycling, but they have experienced a variety of climate changes
809 linked to changing volcanism, ocean currents, solar output, and—recently evident—human
810 perturbation.

811

811 FIGURE CAPTIONS

812

813 **Figure 4.1** Earth's energy budget is a balance between incoming and outgoing radiation.

814 [Numbers are in watts per square meter of the Earth's surface, and some estimates may be

815 uncertain by as much as 20%.] Incoming shortwave radiation from the sun entering Earth's

816 atmosphere [342 W/m^2] may be reflected by clouds, or absorbed or reflected as longwave

817 radiation by the Earth. The greenhouse effect involves the absorption and reradiation of energy

818 by atmospheric greenhouse gases and particles, resulting in a downward flux of infrared

819 radiation (longwave) from the atmosphere to the surface (back radiation) causing higher surface

820 temperatures. In this figure, Earth is in energy balance with the total rate of energy lost from

821 Earth (107 W/m^2 of reflected sunlight plus 235 W/m^2 of infrared [long-wave] radiation) equal to

822 the 342 W/m^2 of incident sunlight (Kiehl and Trenberth, 1997).

823

824 **Figure 4.2** Earth's orbital variations (Milankovitch cycles) control the amount of sunlight

825 received (insolation) at a given place on Earth's surface (Rahmstorf and Schellnhuber, 2006;

826 Jansen et al., 2007). E, variation in the eccentricity of the orbit (owing to variations in the minor

827 axis of the ellipse) with an approximate 100 k.y. periodicity; P, precession, changes in the

828 direction of the axis tilt at a given point of the orbit, which has an approximate 19 to 23 k.y.

829 periodicity; T, changes in the tilt (obliquity) of Earth's axis, which has an approximate 41 k.y.

830 periodicity.

831

832 **Figure 4.3.** Milankovitch-driven monthly insolation anomalies (deviations from present), 20–0

833 ka. at 60°N . Y axis, calendar months. Contours and numbers depict a history of insolation

834 values. Contours in watts per square meter (W/m^2) (data from Berger and Loutre, 1992).

835 Midsummer insolation values at 11 ka exceeded 40 W/m^2 , whereas current values are less than
836 10 W/m^2 .

837

838 **Figure 4.4** Mean surface temperature anomalies for Earth relative to 1951–1980. Panel A, the
839 global average. Panel B, temperature anomalies 2000–2005. High northern latitudes show the
840 largest anomalies for this time period (Hansen et al., 2006).

841

842 **Figure 4.5** Simulated spatial distribution of volcanic sulfate aerosols (kg/km^2) produced by the
843 Laki (1783), Katmai (1912), Tambora (1815), and Pinatubo (1991) eruptions in the Arctic (region
844 shown, $66^\circ\text{--}82^\circ\text{N}$. and $50^\circ\text{--}35^\circ\text{W}$.). Blue, smaller than average deposits; yellow, orange, and red,
845 increasingly larger than average deposits (from Gao et al., 2007). Volcanic evidence derived from
846 44 ice cores; analysis used the NASA Goddard Institute for Space Studies (GISS) ModelE
847 climate model.

848

849 **Figure 4.6** Isotopic record of temperature response in Greenland snow to large volcanic
850 eruptions reconstructed from the GISP2 ice core (modified from Stuiver et al., 1995).

851

852 **Figure 4.7** The Sand Hills of western Nebraska. The Sand Hills cover $51,400 \text{ km}^2$ (about a
853 quarter of the state) and are the largest sand-dune deposit in the United States. They derive from
854 Pleistocene glacial outwash eroded from the Rocky Mountains and now stabilized by vegetation.
855 The hills are characterized by crowded crescent-shaped (barchan) dunes, general absence of
856 drainage, and numerous tiny lakes filling the closed depressions between dunes. (Photo credit:
857 NASA/GSFC/METI/ERSDAC/JAROS, and U.S./Japan ASTER Science Team. This ASTER

858 simulated natural color image was acquired September 10, 2001, covers an area of about 57.9 x
859 61.6 km, and is centered near 42.1° N. and 102.2° W.)

860

861 **Figure. 4.8.** Global compilation of more than 40 deep sea benthic $\delta^{18}\text{O}$ isotopic records taken
862 from Zachos et al. (2001), updated with high-resolution Eocene through Miocene records from
863 Billups et al. (2002), Bohaty and Zachos (2003), and Lear et al. (2004). Dashed blue bars, times
864 when glaciers came and went or were smaller than now; solid blue bars, ice sheets of modern
865 size or larger. (Figure and text from IPCC Chapter 6, Paleoclimate, Jansen et al., 2007.)

866

867 **Figure. 4.9.** Composite stack of 57 benthic oxygen isotope records (a proxy for temperature)
868 from a globally distributed network of marine sediment cores. This foraminifer $\delta^{18}\text{O}$ record
869 indicates low-magnitude climate changes from about 5.3–2.7 Ma, when the amplitude of the
870 foraminifer $\delta^{18}\text{O}$ signal increased markedly (data from Lisiecki and Raymo (2005) and
871 associated website)

872

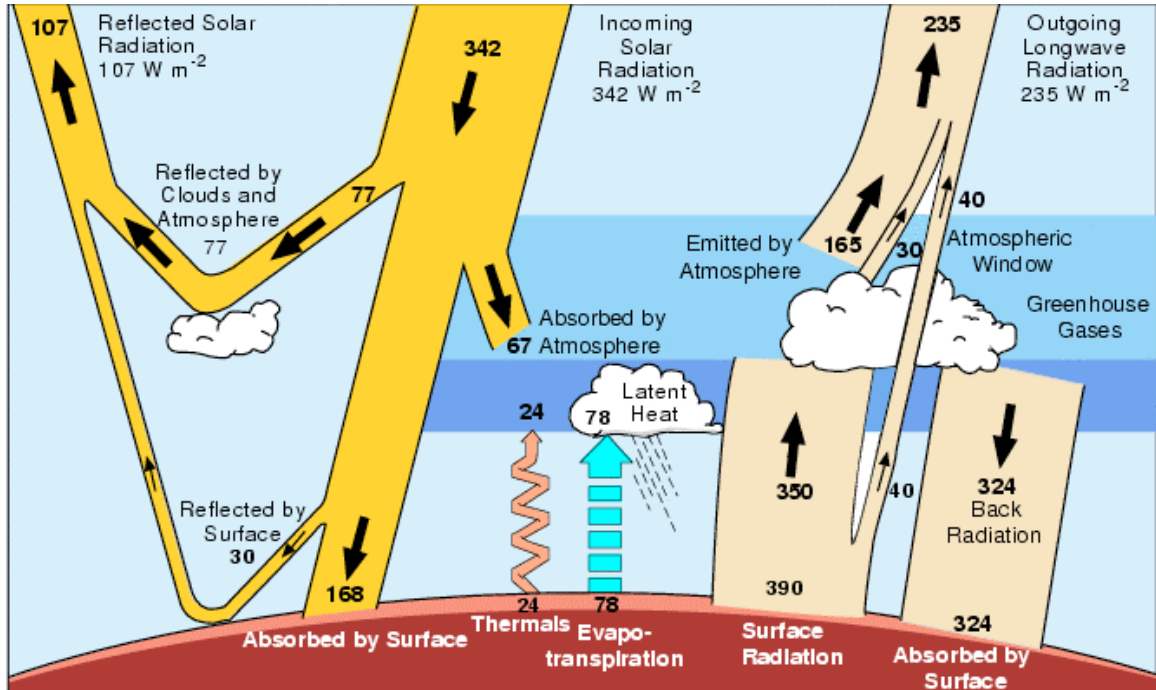
873 **Figure 4.10.** Cenozoic time periods as used in this report (modified from Ogg and 2004).

874

875 **Figure 4.11.** Marine isotope stage (MIS) nomenclature and chronology used in this report (after
876 Imbrie et al., 1984; Martinson et al., 1987). Red numbers, interglacial intervals; blue numbers,
877 glacial intervals.

878

878

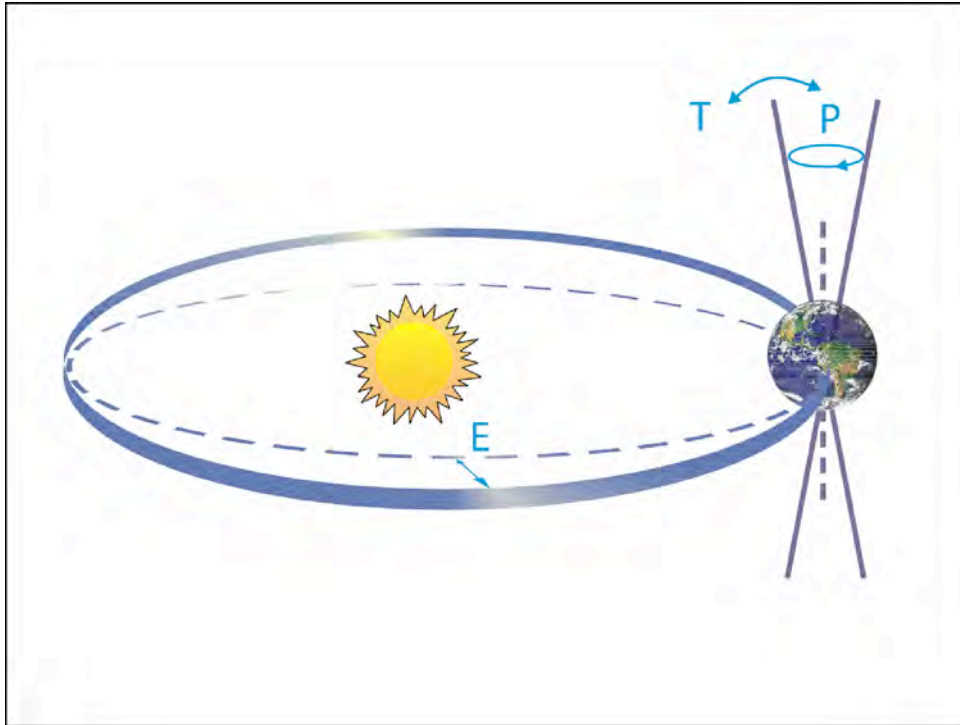


879

880 **Figure 4.1** Earth's energy budget is a balance between incoming and outgoing radiation.

881 [Numbers are in watts per square meter of the Earth's surface, and some estimates may be
 882 uncertain by as much as 20%.] Incoming shortwave radiation from the sun entering Earth's
 883 atmosphere [342 W/m^2] may be reflected by clouds, or absorbed or reflected as longwave
 884 radiation by the Earth. The greenhouse effect involves the absorption and reradiation of energy
 885 by atmospheric greenhouse gases and particles, resulting in a downward flux of infrared
 886 radiation (longwave) from the atmosphere to the surface (back radiation) causing higher surface
 887 temperatures. In this figure, Earth is in energy balance with the total rate of energy lost from
 888 Earth (107 W/m^2) of reflected sunlight plus 235 W/m^2 of infrared [long-wave] radiation) equal to
 889 the 342 W/m^2 of incident sunlight (Kiehl and Trenberth, 1997).

890

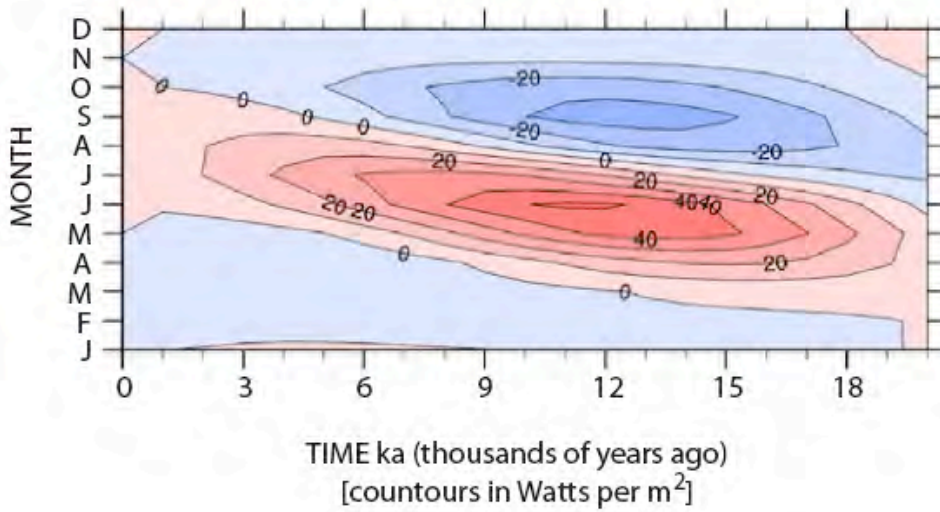


890

891

892 **Figure 4.2** Earth's orbital variations (Milankovitch cycles) control the amount of sunlight
893 received (insolation) at a given place on Earth's surface (Rahmstorf and Schellnhuber, 2006;
894 Jansen et al., 2007). E, variation in the eccentricity of the orbit (owing to variations in the minor
895 axis of the ellipse) with an approximate 100 k.y. periodicity; P, precession, changes in the
896 direction of the axis tilt at a given point of the orbit, which has an approximate 19 to 23 k.y.
897 periodicity; T, changes in the tilt (obliquity) of Earth's axis, which has and approximate 41 k.y.
898 periodicity.

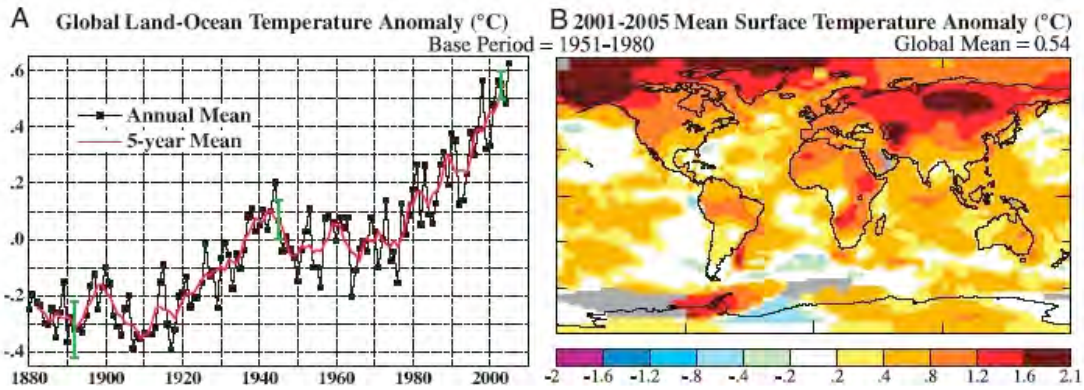
899



899

900 **Figure 4.3.** Milankovitch-driven monthly insolation anomalies (deviations from present), 20–0
 901 ka at 60°N. Y axis, calendar months. Contours and numbers depict a history of insolation values.
 902 Contours in watts per square meter (W/m^2) (data from Berger and Loutre, 1992). Midsummer
 903 insolation values at 11 ka exceeded $40 W/m^2$, whereas current values are less than $10 W/m^2$.
 904

904



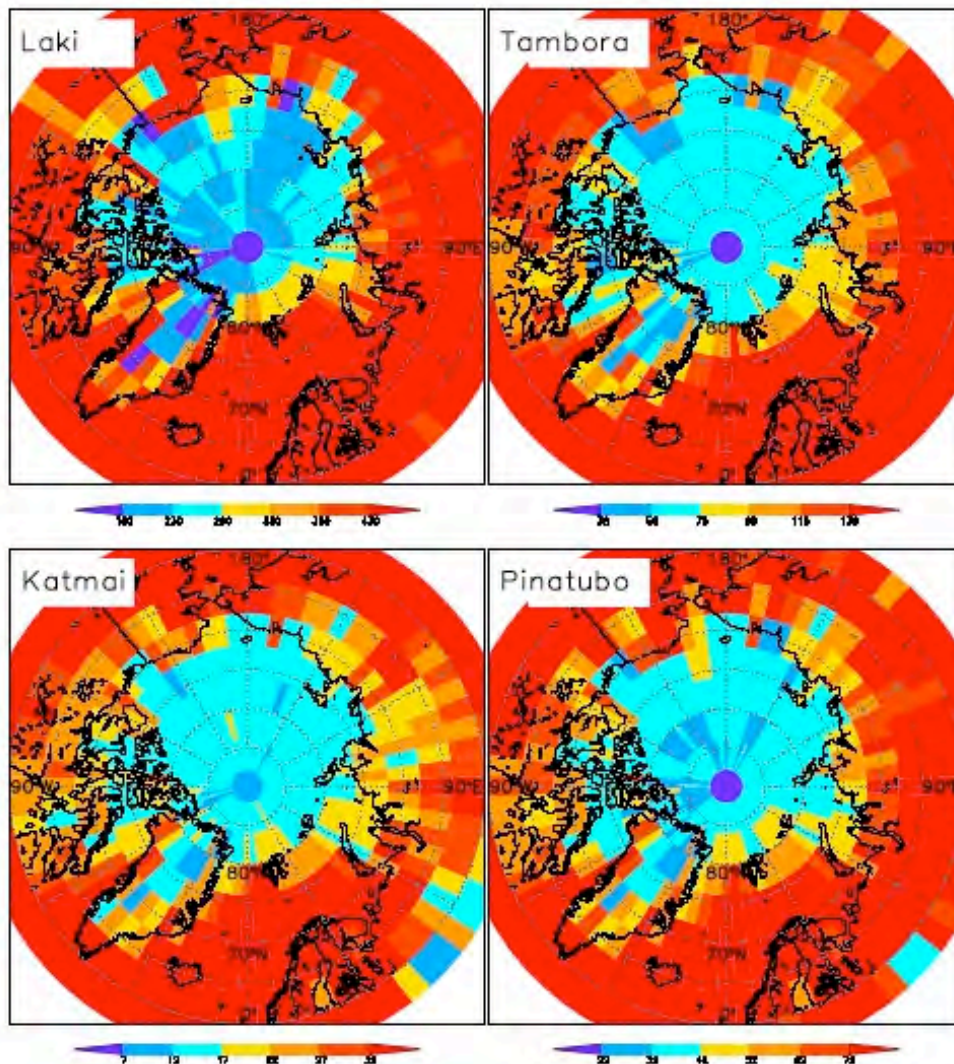
905

906 **Figure 4.4** Mean surface temperature anomalies for Earth relative to 1951–1980. Panel A, the
 907 global average. Panel B, temperature anomalies 2000–2005. High northern latitudes show the
 908 largest anomalies for this time period (Hansen et al., 2006).

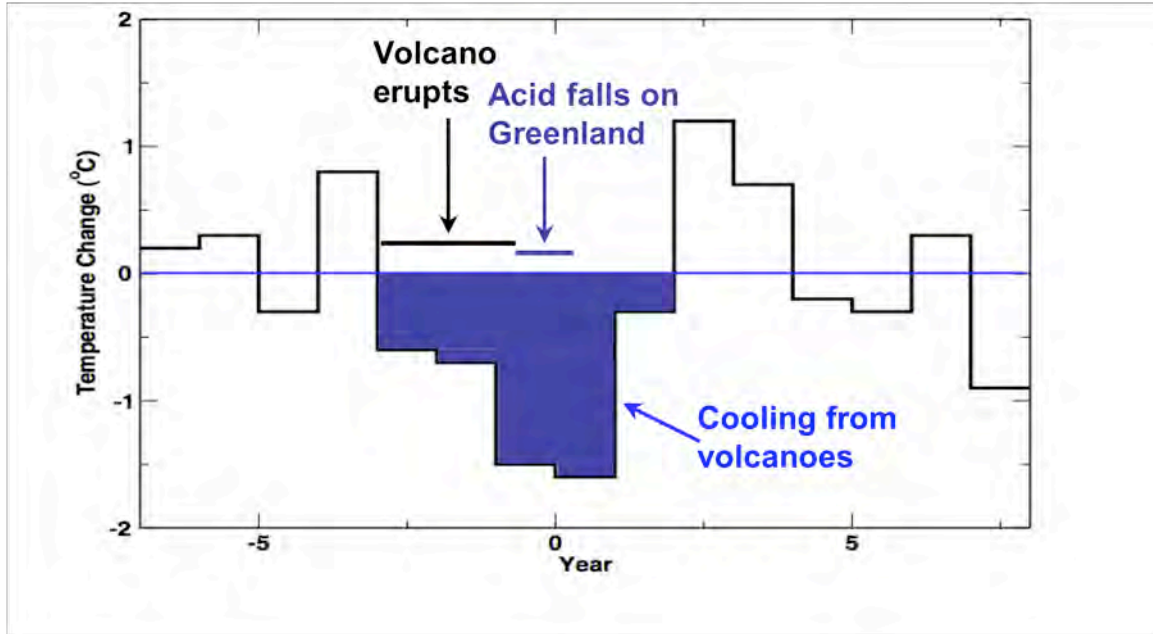
909

909

910



911 **Figure 4.5** Simulated spatial distribution of volcanic sulfate aerosols (kg/km^2) produced by the
 912 Laki (1783), Katmai (1912), Tambora (1815), and Pinatubo (1991) eruptions in the Arctic (region
 913 shown, $66^\circ\text{--}82^\circ\text{N}$. and $50^\circ\text{--}35^\circ\text{W}$.). Blue, smaller than average deposits; yellow, orange, and red,
 914 increasingly larger than average deposits (from Gao et al., 2007). Volcanic evidence derived from
 915 44 ice cores; analysis used the NASA Goddard Institute for Space Studies (GISS) ModelE
 916 climate model.

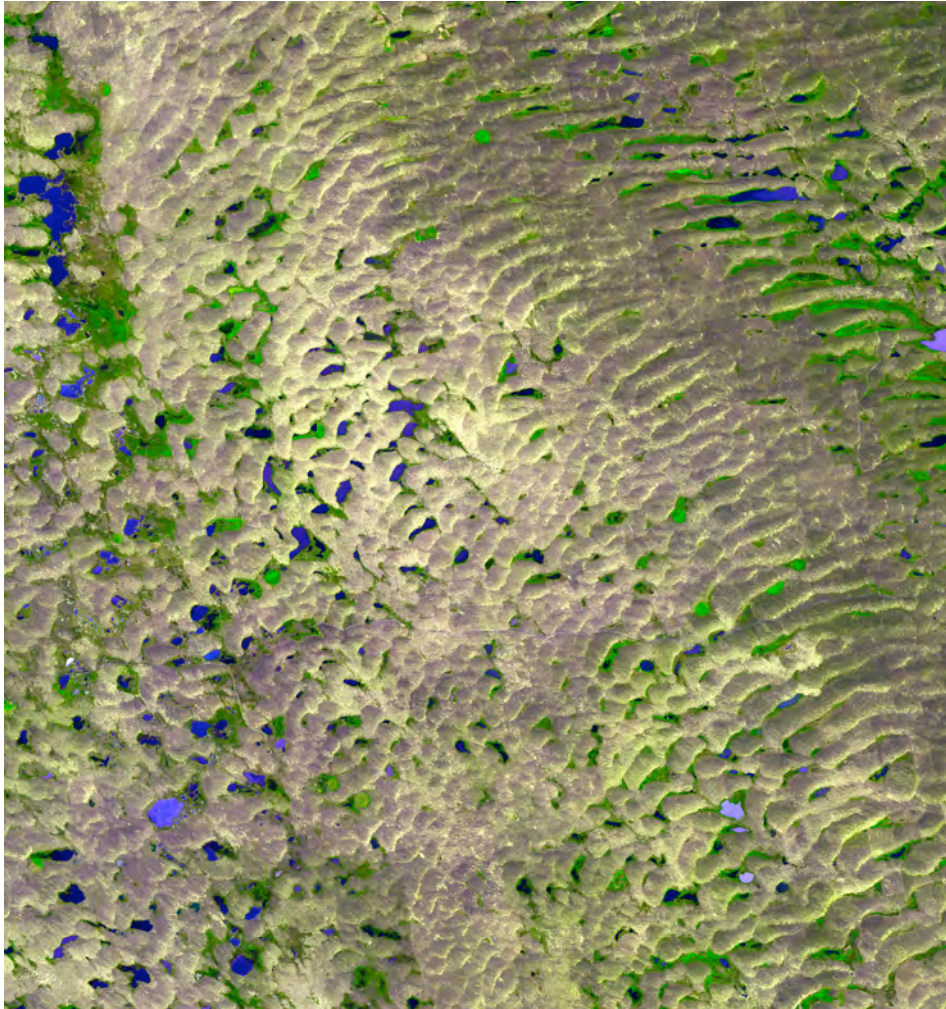


917

918 **Figure 4.6** Temperature response (derived from stable isotopes) in Greenland snow to large
919 volcanic eruptions reconstructed from the GISP2 ice core. (modified from Stuiver et al., 1995).

920

920

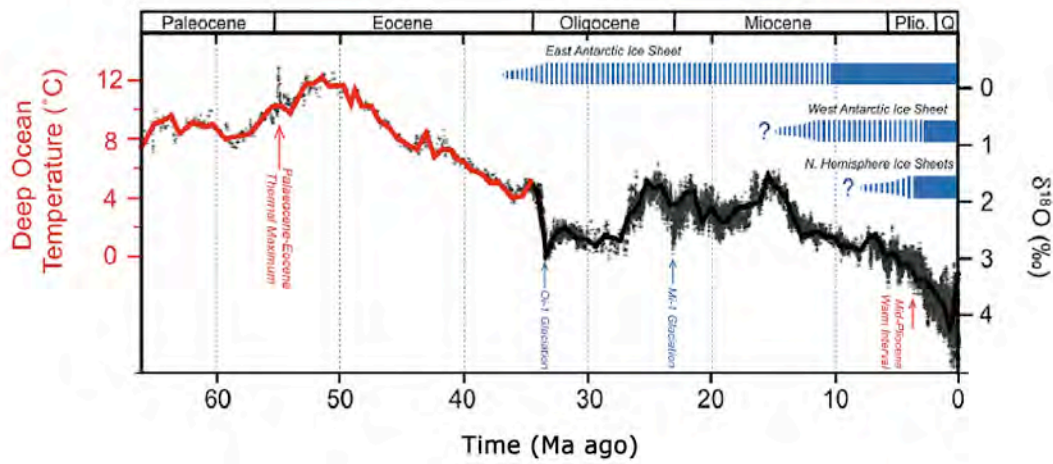


921

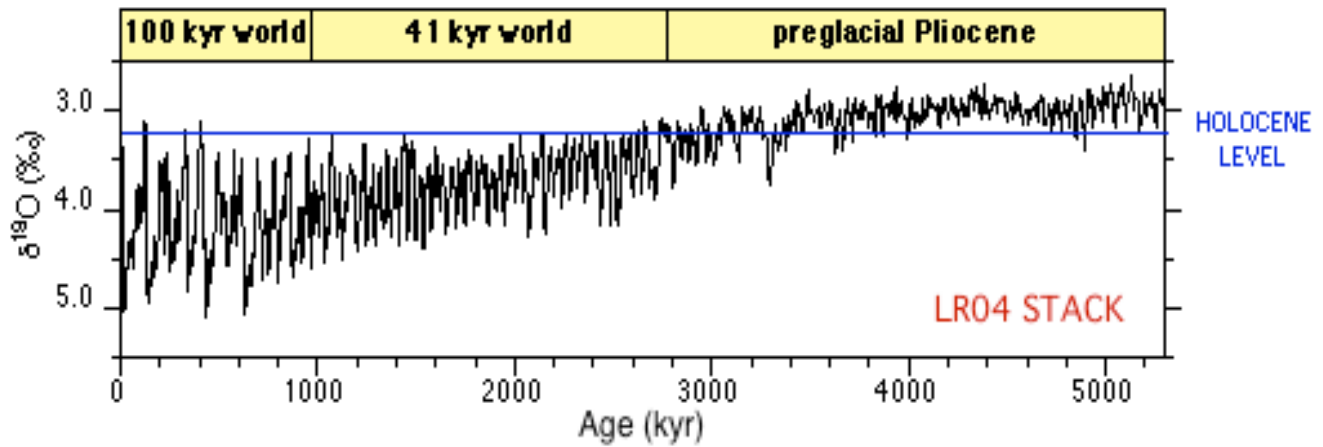
922 **Figure 4.7** The Sand Hills of western Nebraska. The Sand Hills cover 51,400 km² (about a
923 quarter of the state) and are the largest sand-dune deposit in the United States. They derive from
924 Pleistocene glacial outwash eroded from the Rocky Mountains and now stabilized by vegetation.
925 The hills are characterized by crowded crescent-shaped (barchan) dunes, general absence of
926 drainage, and numerous tiny lakes filling the closed depressions between dunes. (Photo credit:
927 NASA/GSFC/METI/ERSDAC/JAROS, and U.S./Japan ASTER Science Team. This ASTER
928 simulated natural color image was acquired September 10, 2001, covers an area of about 57.9 x
929 61.6 km, and is centered near 42.1° N. and 102.2° W.)

930

930



931 **Figure 4.8.** Global compilation of more than 40 deep sea benthic $\delta^{18}\text{O}$ isotopic records taken
 932 from Zachos et al. (2001), updated with high-resolution Eocene through Miocene records from
 933 Billups et al. (2002), Bohaty and Zachos (2003), and Lear et al. (2004). Dashed blue bars, times
 934 when glaciers came and went or were smaller than now; solid blue bars, ice sheets of modern
 935 size or larger. (Figure and text modified from IPCC Chapter 6, Paleoclimate, Jansen et al., 2007.)
 936



936

937

938 **Figure. 4.9.** Composite stack of 57 benthic oxygen isotope records (a proxy for temperature)
 939 from a globally distributed network of marine sediment cores. This foraminifer δ¹⁸O record
 940 indicates low-magnitude climate changes from about 5.3–2.7 Ma, when the amplitude of the
 941 foraminifer δ¹⁸O signal increased markedly (data from Lisiecki and Raymo (2005) and
 942 associated website)

943

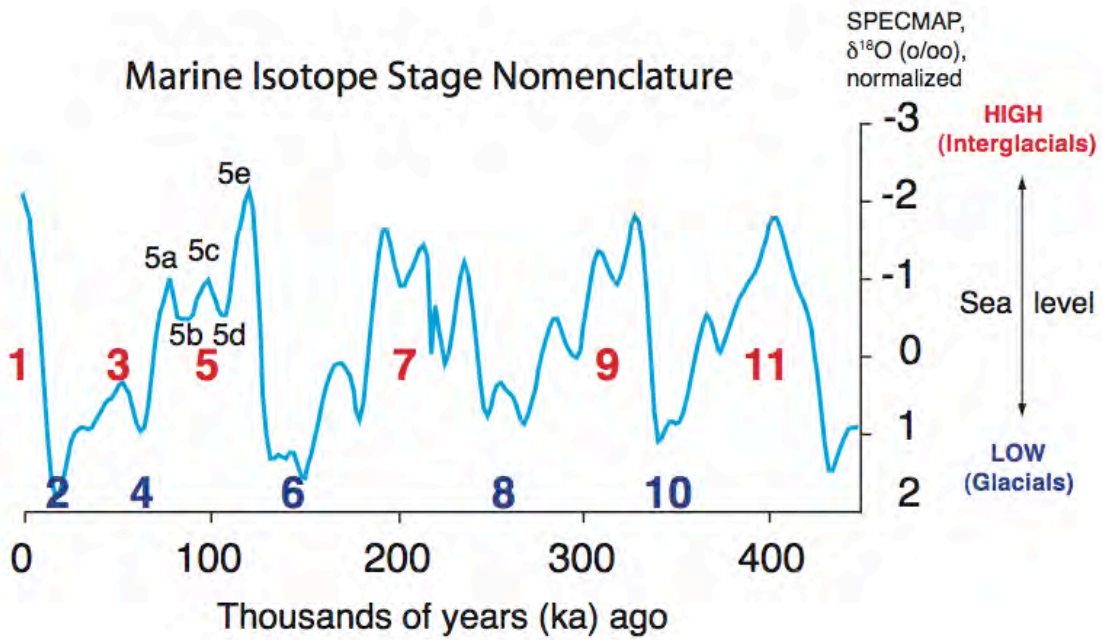
943

ERATHEM / ERA	SYSTEM, SUBSYSTEM PERIOD, SUBPERIOD	SERIES / EPOCH	Age estimate of Boundary	
Cenozoic	Quaternary	Holocene	11,477 yr	
		Pleistocene	2.588 Ma	
	Neogene	Pliocene	5.332 Ma	
		Miocene	23.03 Ma	
			Oligocene	33.9 Ma
	Paleogene	Eocene	55.8 Ma	
		Paleocene	65.5 Ma	

944 **Figure 4.10.** Cenozoic time periods as used in this report (modified from Ogg and 2004)

945

945



946 **Figure 4.11.** Marine isotope stage (MIS) nomenclature and chronology used in this report (after
 947 Imbrie et al., 1984; Martinson et al., 1987). Red numbers, interglacial intervals; blue numbers,
 948 glacial intervals.

949

950

950 **Chapter 4 References Cited**

951

952 **Alley, R.B., C.A. Shuman, D.A. Meese, A.J. Gow, K.C. Taylor, K.M. Cuffey, J.J. Fitzpatrick,**
953 **P.M. Grootes, G.A. Zielinski, M. Ram, G. Spinelli, and B. Elder, 1997: Visual-**
954 **stratigraphic dating of the GISP2 ice core—Basis, reproducibility, and application.**
955 ***Journal of Geophysical Research*, **102(C12)**, 26,367-26,381.**

956

957 **Ammann, C.M., F. Joos, D.S. Schimel, B.L. Otto-Bliesner, and R.A. Tomas, 2007: Solar**
958 **influence on climate during the past millennium—Results from transient simulations with**
959 **the NCAR Climate System Model. *Proceedings of the National Academy of Sciences of***
960 ***the United States*, **104**, 3713-3718.**

961

962 **Anderson, R.K., Miller, G.H., Briner, J.P., Lifton, N.A., DeVogel, S.B, 2008: A millennial**
963 **perspective on Arctic warming from ¹⁴C in quartz and plants emerging from beneath ice**
964 **caps. *Geophysical Research Letters*, **35**, L01502. doi:10.1029/2007GL032057**

965

966 **Andrews, J.T. and A.S. Dyke, 2007: Late Quaternary in North America. In: *The Encyclopedia of***
967 ***Quaternary Sciences* [Elias, S. (ed.)]. Elsevier, Amsterdam, pp. 1095-1101.**

968

969 **Arrhenius, S., 1896: On the influence of carbonic acid in the air upon the temperature on the**
970 **ground. *Philosophical Magazine*, **41**, 237-276**

971

972 **Baliunas, S. and Jastrow, R., 1990: Evidence for long-term brightness changes of solar-type**
973 **stars. *Nature* **348**:520 -522.**

974

975 **Bard, E., Raisbeck, G., Yiou, F., Jouzel, J., 2000: Solar irradiance during the last 1200 years**
976 **based on cosmogenic nuclides. *Tellus B* **52**:985-992.**

977

- 978 **Barron, E.J. and W.M. Washington, 1982:** Atmospheric circulation during warm geologic
979 periods—Is the equator-to-pole surface-temperature gradient the controlling factor?
980 *Geology*, **10**, 633-636.
981
- 982 **Bassinot, F.C., 2007:** Oxygen isotope stratigraphy of the oceans. In: *The Encyclopedia of*
983 *Quaternary Sciences* [Elias, S. (ed.)]. Elsevier, Amsterdam, pp. 1740-1748.
984
- 985 **Beer, J., M. Vonmoos, and R. Muscheler, 2006:** Solar variability over the past several millennia.
986 *Space Science Reviews*, **125(1-4)**, 67-79.
987
- 988 **Beerling, D.J. and R.A. Berner, 2005:** Feedbacks and the coevolution of plants and atmospheric
989 CO₂. *Proceedings of the National Academy of Sciences of the United States*, **102**, 1302-
990 1305.
991
- 992 **Berger, A., Loutre, M.F., 1992:** Astronomical solutions for paleoclimate studies over the last 3
993 million years. *Earth and Planetary Science Letters*, **111**, 369–382.
994
- 995 **Berner, R.A., 1991:** A model for atmospheric CO₂ over Phanerozoic time. *American Journal of*
996 *Science*, **291**, 339-376.
997
- 998 **Billups, K., J.E.T. Channell, and J. Zachos, 2002:** Late Oligocene to early Miocene
999 geochronology and paleoceanography from the subantarctic South Atlantic.
1000 *Paleoceanography*, **17(1)**, 1004, doi:10.1029/2000PA000568. [11 pages].
1001
- 1002 **Bohaty, S.M. and J. Zachos, 2003:** Significant Southern Ocean warming even in the late middle
1003 Eocene. *Geology*, **31(11)**, 1017-1020.
1004
- 1005 **Booth, D.B., K.G. Troost, J.J. Clague, and R.B. Waitt, 2004:** The Cordilleran Ice Sheet. In: *The*
1006 *Quaternary Period in the United States* [Gillespie, A.R., S.C. Porter, and B.F. Atwater
1007 (eds.)]. Elsevier, Amsterdam, pp. 17-43.
1008

- 1009 **Bradley, R.S.**, 1999: *Paleoclimatology—Reconstructing Climate of the Quaternary*. Academic
1010 Press, San Diego, 613 pp.
1011
- 1012 **Briffa, K.R.**, Jones, P.D., Schweingruber, F.H., Osborn, T.J., 1998: Influence of volcanic
1013 eruptions on Northern Hemisphere summer temperature over the past 600 years. *Nature*,
1014 **393**, 450-455.
1015
- 1016 **Bralower, T.J.**, D.J. Thomas, J.C. Zachos, M.M. Hirschmann, U. Rohl, H. Sigurdsson, E.
1017 Thomas, and D.L. Whitney, 1995: High-resolution records of the late Paleocene thermal
1018 maximum and circum-Caribbean volcanism—Is there a causal link? *Geology*, **25**, pp.
1019 963–966.
1020
- 1021 **Callendar, G.S.**, 1938: The artificial production of carbon dioxide and its influence on
1022 temperature. *Quarterly Journal of the Royal Meteorological Society*, **64**, 223-237.
1023
- 1024 **Camp, C.D.**, and K.K. Tung, 2007: Surface warming by the solar cycle as revealed by the
1025 composite mean difference projection. *Geophysical Research Letters* **34**, L14703, doi:
1026 10.1029/2007GL030207.
1027
- 1028 **Cook, E.R.**, and L.A. Kairiukstis [eds.], 1990: *Methods of Dendrochronology: Applications in*
1029 *the Environmental Sciences*, 394 pp., Kluwer Academic, Norwell, Mass.
1030
- 1031 **Cronin, T.M.**, 1999: *Principles of Paleoclimatology*. Columbia University Press, New York, 560
1032 pp.
1033
- 1034 **Crowley, T.J.**, and G.R. North, 199: *Paleoclimatology*. Oxford University Press, New York, 339
1035 pp.
1036
- 1037 **Cuffey, K.M.** and G.D. Clow, 1997: Temperature, accumulation, and ice sheet elevation in
1038 central Greenland through the last deglacial transition. *Journal of Geophysical Research*,
1039 **102(C12)**, 26,383-26,396.

- 1040
- 1041 **D'Arrigo, R.D.**, and G.C. Jacoby, 1999: Northern North American tree-ring evidence for
 1042 regional temperature changes after major volcanic events. *Climatic Change*, **41**, 1-15.
- 1043
- 1044 **D'Hondt, S.**, 2005: Consequences of the Cretaceous/Paleogene mass extinction for marine
 1045 ecosystems. *Annual Review of Ecology, Evolution and Systematics*, **36**, 295-317.
- 1046
- 1047 **De Silva, S.L.**, and Zielinski, G.A., 1998: Global influence of the AD 1600 eruption of
 1048 Huaynaputina, Peru, *Nature*, **393**, 455-458.
- 1049
- 1050 **Donnadieu, Y.**, R. Pierrehumbert, R. Jacob, and F. Fluteau, 2006: Modeling the primary control
 1051 of paleogeography on Cretaceous climate. *Earth and Planetary Science Letters*, **248**, 426-
 1052 437.
- 1053
- 1054 **Dyke, A.S.**, and Prest, V.K., 1987: Late Wisconsinan and Holocene history of the Laurentide Ice
 1055 Sheet. *Geographie physique et Quaternaire*, **41**, 237-263.
- 1056
- 1057 **Ehhalt, D.**, M. Prather, F. Dentener, R. Derwent, E. Dlugokencky, E. Holland, I. Isaksen, J.
 1058 Katima, V. Kirchhoff, P. Matson, P. Midgley, M. Wang, 2001: Atmospheric chemistry
 1059 and Greenhouse Gases, In: *Climate Change 2001: The Scientific Basis. Contribution of*
 1060 *Working Group I to the Third Assessment Report of the Intergovernmental Panel on*
 1061 *Climate Change* [Houghton, J.T., Y. Ding, D.J. Griggs, M. Noguer, P.J. van der Linden, X.
 1062 Dai, K. Maskell, and C.A. Johnson (eds.)]. Cambridge University Press, Cambridge, United
 1063 Kingdom and New York, NY, USA, 881pp.
- 1064
- 1065 **Emiliani, C.**, 1955: Pleistocene temperatures. *Journal of Geology*, **63**: 538-578.
- 1066
- 1067 **Fairbanks, R.G.**, R.A. Mortlock, T.C. Chiu, L. Cao, A. Kaplan, T.P. Guilderson, T.W.
 1068 Fairbanks, and A.L. Bloom, 2005: Marine radiocarbon calibration curve spanning 0 to
 1069 50,000 years B.P. based on paired $^{230}\text{Th}/^{234}\text{U}/^{238}\text{U}$ and ^{14}C dates on pristine corals.
 1070 *Quaternary Science Reviews*, **24**, 1781-1796.

- 1071
- 1072 **Fischer, E.M.,** J. Luterbacher, E. Zorita, S.F.B. Tett, C. Casty, and H. Wanner, 2007: European
1073 climate response to tropical volcanic eruptions over the last half millennium. *Geophysical*
1074 *Research Letters*, **34**, L05707.
- 1075
- 1076 **Fleitmann, D.,** S.J. Burns, and M. Mudelsee, 2003: Holocene forcing of the Indian monsoon
1077 recorded in a stalagmite from southern Oman. *Science*, **300**, 1737-1739.
- 1078
- 1079 **Forster, P.,** V. Ramaswamy, P. Artaxo, T. Berntsen, R. Betts, D.W. Fahey, J. Haywood, J. Lean,
1080 D.C. Lowe, G. Myhre, J. Nganga, R. Prinn, G. Raga, M. Schulz, and R. Van Dorland,
1081 2007: Changes in atmospheric constituents and in radiative forcing. In: *Climate Change*
1082 *2007—The Physical Science Basis. Contribution of Working Group I to the Fourth*
1083 *Assessment Report of the Intergovernmental Panel on Climate Change* [Solomon, S., D.
1084 Qin, M. Manning, Z. Chen, M. Marquis, K.B. Averyt, M. Tignor, and H.L. Miller (eds.)].
1085 Cambridge University Press, Cambridge, United Kingdom, and New York, p.131-234.
- 1086
- 1087 **Foukal, P.,** C. Frohlich, H. Spruit, and T.M.L. Wigley, 2006: Variations in solar luminosity and
1088 their effect on the Earth's climate. *Nature*, **443**, 161-166.
- 1089
- 1090 **Friedrich, M.,** S. Remmelel, B. Kromer, J. Hofmann, M. Spurk, K.F. Kaiser, C. OrceI, and M.
1091 Koppers, 2004: The 12,460-year Hohenheim oak and pine tree-ring chronology from
1092 central Europe—A unique annual record for radiocarbon calibration and
1093 paleoenvironment reconstructions. *Radiocarbon*, **46**, 1111-1122.
- 1094
- 1095 **Fritts, H.,** 1976: *Tree Rings and Climate*. 567 pp., Academic Press, London.
- 1096
- 1097 **Fröhlich, C.,** Lean, J., 2004: Solar radiative output and its variability: evidence and mechanisms.
1098 *Astronomy and Astrophysics Review*, **12**, 273-320.
- 1099
- 1100 **Gallup, C.,** H. Cheng, F.W. Taylor, and R.L. Edwards, 2002: Direct determination of the time of
1101 sea level change during Termination II: *Science*, **295**, 310-313.

1102

1103 **Gao, C.,** Oman, L., Robick, A., and Stenchikov, G.L., 2007: Atmospheric volcanic loading
1104 derived from bipolar ice cores: Accounting for the spatial distribution of volcanic deposition:
1105 *J. Geophysical Research*, **112**, doi:10.1029/2006JD007461

1106

1107 **Hansen, J.,** A. Lacis, D. Rind, G. Russell, P. Stone, I. Fung, R. Ruedy, and J. Lerner, 1984:
1108 Climate sensitivity—Analysis of feedback mechanisms. In: *Climate Processes and*
1109 *Climate Sensitivity* [Hansen, J.E. and T. Takahashi (eds.)]. American Geophysical Union
1110 Geophysical Monograph 29, Maurice Ewing vol. 5, pp. 130-163.

1111

1112 **Hansen, J.,** Mki. Sato, R. Ruedy, K. Lo, D.W. Lea, and M. Medina-Elizade, 2006: Global
1113 temperature change. *Proc. Natl. Acad. Sci.*, **103**, 14288-14293,
1114 doi:10.1073/pnas.0606291103.

1115

1116

1117 **Hegerl, G.C.,** F.W. Zwiers, P. Braconnot, N.P. Gillett, Y. Luo, J.A. Marengo Orsini, N.
1118 Nicholls, J.E. Penner, and P.A. Stott, 2007: Understanding and attributing climate change.
1119 In: *Climate Change 2007—The Physical Science Basis. Contribution of Working Group I*
1120 *to the Fourth Assessment Report of the Intergovernmental Panel on Climate Change*
1121 [Solomon, S., D. Qin, M. Manning, Z. Chen, M. Marquis, K.B. Averyt, M. Tignor, and
1122 H.L. Miller (eds.)]. Cambridge University Press, Cambridge, United Kingdom, and New
1123 York, pp. 663-745.

1124

1125 **Heusser, L.E.,** M. Lyle, and A. Mix, 2000: Vegetation and climate of the northwest coast of
1126 North America during the last 500 k.y. —High-resolution pollen evidence from the northern
1127 California margin. In: Lyle, M., Richter, C., and Moore, T.C., Jr. (eds.)]. *Proceedings of the*
1128 *Ocean Drilling Program, Scientific Results*, **167**, 217-226.

1129

1130 **Hovan, S.A.,** D.K. Rea, and N.G. Pisias, 1991: Late Pleistocene continental climate and oceanic
1131 variability recorded in northwest Pacific sediments. *Paleoceanography*, **6**, 349-370.

1132

1133 **Huybers, P.**, 2007: Glacial variability over the last two million years—An extended depth
 1134 derived age model, continuous obliquity pacing, and the Pleistocene progression,
 1135 *Quaternary Science Reviews*, **26**, 37-55.

1136

1137 **Imbrie, J.**, A. Berger, E.A. Boyle, S.C. Clemens, A. Duffy, W.R. Howard, G. Kukla, J.
 1138 Kutzbach, D.G. Martinson, A. McIntyre, A.C. Mix, B. Molfino, J.J. Morley, L.C.
 1139 Peterson, N.G. Pisias, W.L. Prell, M.E. Raymo, N.J. Shackleton, and J.R. Toggweiler.
 1140 1993: On the structure and origin of major glaciation cycles. 2. The 100,000-year cycle.
 1141 *Paleoceanography*, **8**, 699-735.

1142

1143 **Imbrie, J.**, J.D. Hays, D.G. Martinson, A. McIntyre, A.C. Mix, J.J. Morley, N.G. Pisias, W.L.
 1144 Prell, and N.J. Shackleton, 1984: The orbital theory of Pleistocene climate—Support from a
 1145 revised chronology of the marine $\delta^{18}\text{O}$ record. In: *Milankovitch and climate—Understanding*
 1146 *the response to astronomical forcing* [Berger, A., J. Imbrie, J. Hays, G. Kukla, and B.
 1147 Saltzman]. D. Reidel Publishing Company, Dordrecht, pp. 269-305.

1148

1149 **Intergovernmental Panel on Climate Change (IPCC)**, 2007: Summary for policymakers. In:
 1150 *Climate Change 2007—The Physical Science Basis. Contribution of Working Group I to*
 1151 *the Fourth Assessment Report of the Intergovernmental Panel on Climate Change*
 1152 [Solomon, S., D. Qin, M. Manning, Z. Chen, M. Marquis, K.B. Averyt, M. Tignor and
 1153 H.L. Miller (eds.)]. Cambridge University Press, Cambridge, United Kingdom, and New
 1154 York, 996 pp.

1155

1156 **Jansen, E.**, J. Overpeck, K.R. Briffa, J.-C. Duplessy, F. Joos, V. Masson-Delmotte, D. Olago, B.
 1157 Otto-Bliesner, W.R. Peltier, S. Rahmstorf, R. Ramesh, D. Raynaud, D. Rind, O.
 1158 Solomina, R. Villalba, and D. Zhang, 2007: Palaeoclimate. In: *Climate Change 2007—*
 1159 *The Physical Science Basis. Contribution of Working Group I to the Fourth Assessment*
 1160 *Report of the Intergovernmental Panel on Climate Change* [Solomon, S., D. Qin, M.
 1161 Manning, Z. Chen, M. Marquis, K.B. Averyt, M. Tignor and H.L. Miller (eds.)].
 1162 Cambridge University Press, Cambridge, United Kingdom, and New York, pp. 434-497.

- 1163
1164 **Jiang, D., H. Wang, Z. Ding, X. Lang, and H. Drange, 2005:** Modeling the middle Pliocene
1165 climate with a global atmospheric general circulation model. *Journal of Geophysical*
1166 *Research*, **110**, D14107, doi:10.1029/2004JD005639.
- 1167
1168 **Johnson, W.H., A.K. Hansel, E.A. Bettis III, P.F. Karrow, G.J. Larson, T.V. Lowell, and**
1169 **Schneider, A.F., 1997:** Late Quaternary temporal and event classifications, Great Lakes
1170 region, North America. *Quaternary Research*, **47**, 1-12.
- 1171
1172 **Jouzel, J. , V. Masson-Delmotte, O. Cattani, G. Dreyfus, S. Falourd, G. Hoffmann, B. Minster, J.**
1173 **Nouet, J. M. Barnola, J. Chappellaz, H. Fischer, J. C. Gallet, S. Johnsen, M. Leuenberger, L.**
1174 **Loulergue, D. Luethi, H. Oerter, F. Parrenin, G. Raisbeck, D. Raynaud, A. Schilt, J.**
1175 **Schwander, E. Selmo, R. Souchez, R. Spahni, B. Stauffer, J. P. Steffensen, B. Stenni, T. F.**
1176 **Stocker, J. L. Tison, M. Werner, and E. W. Wolff, 2007:** Orbital and Millennial Antarctic
1177 Climate Variability over the Past 800,000 Years. *Science* **317**, 793-796, DOI:
1178 10.1126/science.1141038
- 1179
1180 **Kiehl, J. T. and Trenberth, K. E., 1997:** Earth's Annual Global Mean Energy Budget, *Bulletin of*
1181 *the American Meteorological Societz*, **78**, 197-208.
- 1182
1183 **Kump, L.R. and R.B. Alley, 1994:** Global chemical weathering on glacial timescales. In:
1184 *Material fluxes on the surface of the earth* [Hay, W.W. (ed.)]. National Academy of
1185 Sciences, New York, pp. 46-60.
- 1186
1187 **Kump, L.R., J.F. Kasting, and R.G. Crane, 2003:** *The Earth System*. Prentice Hall, New York,
1188 2nd ed., 432 pp.
- 1189
1190 **Ladurie, E.L., 1971:** *Times of feast, times of famine—A history of climate since the year 1000*.
1191 Farrar, Straus and Giroux, New York, 426 pp.
- 1192
1193 **Lamb, H.H., 1982:** *Climate History and the Modern World*. Routledge, New York, 433 pp.

1194

1195 **LaMarche**, V.C. Jr. and K.K. Hirschboeck, 1984: Frost rings in trees as records of major
1196 volcanic eruptions. *Nature*, **307**, 121-126.

1197

1198 **Lear**, C.H., Y. Rosenthal, H.K. Coxall, and P.A. Wilson, 2004: Late Eocene to Miocene ice
1199 sheet dynamics and the global carbon cycle. *Paleoceanography*, **19(4)**, PA4015,
1200 doi:10.1029/2004PA001039.

1201

1202 **Le Treut**, H., R. Somerville, U. Cubasch, Y. Ding, C. Mauritzen, A. Mokssit, T. Peterson, and
1203 M. Prather, 2007: Historical overview of climate change. In: *Climate Change 2007—The*
1204 *Physical Science Basis. Contribution of Working Group I to the Fourth Assessment*
1205 *Report of the Intergovernmental Panel on Climate Change* [Solomon, S., D. Qin, M.
1206 Manning, Z. Chen, M. Marquis, K.B. Averyt, M. Tignor and H.L. Miller (eds.)].
1207 Cambridge University Press, Cambridge, United Kingdom, and New York, pp. 93-127.

1208

1209 **Lisiecki**, L.E. and M.E. Raymo, 2005: A Pliocene-Pleistocene stack of 57 globally distributed
1210 benthic d¹⁸O records: *Paleoceanography*, **20**, PA1003, doi:10.1029/2004PA001071. (see
1211 also <http://www.lorraine-lisiecki.com/stack.html>)

1212

1213 **Lisiecki**, L.E. and M.E. Raymo, 2007: Plio-Pleistocene climate evolution—Trends and
1214 transitions in glacial cycle dynamics. *Quaternary Science Reviews*, **26**, 56-69.

1215

1216 **Livermore**, R., C.D. Hillenbrand, M. Meredith, and G. Eagles, 2007: Drake Passage and
1217 Cenozoic climate—An open and shut case? *Geochemistry, Geophysics, Geosystems*, **8**,
1218 Article Q01005.

1219

1220 **Loutre**, M.F., D. Paillard, F. Vimeux, and E. Cortijo, 2004: Does mean annual insolation have
1221 the potential to change the climate? *Earth and Planetary Science Letters*, **221**, 1-14.

1222

- 1223 **Maclennan, J., M. Jull, D. McKenzie, L. Slater, and K. Gronvold, 2002:** The link between
1224 volcanism and deglaciation in Iceland. *Geochemistry, Geophysics, Geosystems*, **3**, Article
1225 1062.
- 1226
- 1227 **Martinson, D.G., N.G. Pisias, J.D. Hays, J. Imbrie, T.C. Moore Jr., and N.J. Shackleton, 1987:**
1228 Age dating and the orbital theory of the ice ages—Development of a high-resolution 0 to
1229 300,000-year chronostratigraphy. *Quaternary Research*, **27**, 1-29.
- 1230
- 1231 **Meese, D.A., A.J. Gow, R.B. Alley, G.A. Zielinski, P.M. Grootes, M. Ram, K.C. Taylor, P.A.**
1232 **Mayewski, and J.F. Bolzan, 1997:** The Greenland Ice Sheet Project 2 depth-age scale—
1233 Methods and results. *Journal of Geophysical Research*, **102(C12)**, 26,411-26,423.
- 1234
- 1235 **Milankovitch, M., 1920:** Theorie Mathematique des Phenomenes thermiques Produits per la
1236 Radiation solaire. Gauthier-Villars, Paris. 340 pp.
- 1237
- 1238 **Milankovitch, M., 1941:** Kanon der Erdbestrahlung. Royal Serbian Academy Special
1239 Publication 132, section of Mathematical and Natural Sciences, vol. 33 (published in
1240 English by Israël Program for Scientific Translation for the U.S. Department of
1241 Commerce and the National Science Foundation, Washington D.C., 1969).
- 1242
- 1243 **Miller, K.G., M.A. Kominz, J.V. Browning, J.D. Wright, G.S. Mountain, M.E. Katz, P.J.**
1244 **Sugarman, B.S. Cramer, N. Christie-Blick, and S.F. Pekar, 2005:** The Phanerozoic
1245 record of global sea-level change. *Science*, **312**, 1293-1298.
- 1246
- 1247 **Muhs, D.R., K.R. Simmons, and B. Steinke, 2002:** Timing and warmth of the last interglacial
1248 period—New U-series evidence from Hawaii and Bermuda and a new fossil compilation
1249 for North America. *Quaternary Science Reviews*, **21**, 1355-1383.
- 1250
- 1251 **Muhs, D.R., T.W. Stafford, J.B. Swinehart, S.D. Cowherd, S.A. Mahan, C.A. Bush, R.F.**
1252 **Madole, and P.B. Maat, 1997:** Late Holocene eolian activity in the mineralogically
1253 mature Nebraska sand hills. *Quaternary Research*, **48**, 162-176.

1254

1255 **Muller, P.J., G. Kirst, G. Ruhland, I. von Storch, and A. Rosell-Mele, 1998:** Calibration of the
1256 alkenone paleotemperature index UK-37' based on core-tops from the eastern South
1257 Atlantic and the global ocean (60° N—60° S). *Geochimica et Cosmochimica Acta*, **62**,
1258 1757-1772.

1259

1260 **Muscheler, R., R. Beer, P.W. Kubik, and H.A. Synal, 2005:** Geomagnetic field intensity during
1261 the last 60,000 years based on Be-10 and Cl-36 from the Summit ice cores and C-14.
1262 *Quaternary Science Reviews*, **24**, 1849-1860.

1263

1264 **Muscheler, R., F. Joos, J. Beer, et al., 2007:** Solar activity during the last 1000 yr inferred from
1265 radionuclide records. *Quaternary Science Reviews*, **26**, 82-97.

1266

1267 **Nakamura, N. and A.H. Oort, 1988:** Atmospheric heat budgets of the polar regions. *Journal of*
1268 *Geophysical Research*, **93(D8)**, 9510-9524.

1269

1270 **National Research Council, 2006:** Surface temperature reconstructions for the last 2,000 years.
1271 National Academies Press, Washington, D.C. 160 pp.

1272

1273 **North Greenland Ice Core Project members (NGRIP), 2004:** High-resolution record of
1274 Northern Hemisphere climate extending into the last interglacial period. *Nature*, **431**,
1275 147-151.

1276

1277 **Ogg, James (compiler), 2004:** Overview of global boundary stratotype sections and points
1278 (GSSPs). International Commission on Stratigraphy, available online at
1279 <http://www.stratigraphy.org/gssp.htm>

1280

1281 **Oman, L., Robock, A., Stenchikov, G., Schmidt, G.A., and Ruedy, R., 2005:** Climatic response
1282 to high latitude volcanic eruptions. *Journal of Geophysical Research*, **110**, D13103,
1283 doi:10.1029/2004JD005487.

1284

- 1285 **Oman, L.,** Robock, A., Stenchikov, G., Thordarson, T., Koch, D., Shindell, D.T., and Gao, C.,
1286 2006: Modeling the Distribution of the Volcanic Aerosol Cloud from the 1783-1784 Laki
1287 Eruption. *Journal of Geophysical Research*, **111**, D12209, doi:10.1029/2005JD006899.
1288
- 1289 **Oppenheimer, C.,** 2003: Climatic, environmental, and human consequences of the largest
1290 known historic eruption: Tambora volcano (Indonesia) 1815. *Progress in Physical*
1291 *Geography*, **27**, 230-259.
1292
- 1293 **Pagani, M.,** M.A. Arthur, and K.H. Freeman, 1999: Miocene evolution of atmospheric carbon
1294 dioxide. *Paleoceanography*, **14**, 273-292.
1295
- 1296 **Pearson, P.N.,** P.W. Ditchfield, J. Singano, K.G. Harcourt-Brown, C.J. Nicholas, R.K. Olsson,
1297 N.J. Shackleton, and M.A. Hall, 2001: Warm tropical sea surface temperatures in the
1298 Late Cretaceous and Eocene epochs. *Nature*, **413**, 481-487.
1299
- 1300 **Peixoto, J.P.** and A.H. Oort, 1992: *Physics of Climate*. American Institute of Physics, New York,
1301 520 pp.
1302
- 1303 **Pierrehumbert, R.T.,** H. Brogniez, and R. Roca, 2007: On the relative humidity of the
1304 atmosphere. In: *The Global Circulation of the Atmosphere* [Schneider, T. and A. Sobel
1305 (eds.)]. Princeton University Press, Princeton, New Jersey, pp.143-185.
1306
- 1307 **Prentice, I.C.,** Farquhar, G.D., Fasham, M.J.R. , Goulden, M.L., Heimann, M., Jaramillo, V.J. ,
1308 Kheshgi, H.S. , Le Quéré, C., Scholes, R.J. , Wallace, D.W.R., 2001: The Scientific
1309 Basis. Contribution of Working Group I to the Third Assessment Report of the
1310 Intergovernmental Panel on Climate Change [Houghton, J.T., Y. Ding, D.J. Griggs, M.
1311 Noguer, P.J. van der Linden, X. Dai, K. Maskell, and C.A. Johnson (eds.)]. Cambridge
1312 University Press, Cambridge, United Kingdom and New York, NY, USA, 881pp.
1313
- 1314 **Rahmstorf, S.,** and H.J. Shellnhuber: 2006: *Der Klimawandel*. Beck Verlag, Munich, 144 pp.
1315

- 1316 **Ramanathan, V.**, 1975: Greenhouse effect due to chlorofluorocarbons – Climatic implications.
1317 *Science*, **190**, 50-52.
1318
- 1319 **Robock, Alan**, 2000: Volcanic eruptions and climate. *Reviews of Geophysics*, **38**, 191-219.
1320
- 1321 **Robock, Alan**, 2007: Correction to “Volcanic eruptions and climate.” *Reviews of Geophysics*,
1322 **45**, RG3005, doi:10.1029/2007RG000232.
1323
- 1324 **Robock, Alan**, Tyler Adams, Mary Moore, Luke Oman, and Georgiy Stenchikov, 2007:
1325 Southern Hemisphere atmospheric circulation effects of the 1991 Mount Pinatubo
1326 eruption. *Geophysical Research Letters*, **34**, L237, doi:10.1029/2007GL031403.
1327
- 1328 **Royer, D.L.**, R.A. Berner, and J. Park, 2007: Climate sensitivity constrained by CO₂
1329 concentrations over the past 420 million years. *Nature*, **446**, 530-532.
1330
- 1331 **Ruddiman, W.F.**, 2006, Ice-driven CO₂ feedback on ice volume. *Climate of the Past*, **2**, 43-55.
1332
- 1333 **Salzer, M.W.** and M.K. Hughs, 2006: Bristlecone pine tree rings and volcanic eruptions over the
1334 last 5000 yr. *Quaternary Research* **67** 57-68.
1335
- 1336 **Serreze, M.C.**, Barrett, A.P., Slater, A.G., Steele, M., Zhang, J.L., and Trenberth, K.E., 2007:
1337 The large-scale energy budget of the Arctic.. *Journal of Geophysical Research*, **112**,
1338 D11122.
1339
- 1340 **Shellito, C. J.**, Sloan, L.C., and M. Huber, 2003: Climate model sensitivity to atmospheric CO₂
1341 levels in the early-middle Paleogene. *Palaeogeography, Palaeoclimatology,*
1342 *Palaeoecology*, **193**, 113-123.
1343
- 1344 **Shindell, D.T.**, Schmidt, G.A., Mann, M.E., and Faluvegi, G., 2004. Dynamic winter climate
1345 response to large tropical volcanic eruptions since 1600. *Journal of Geophysical*
1346 *Research*, **109**, D05104.

1347
1348
1349
1350
1351
1352
1353
1354
1355
1356
1357
1358
1359
1360
1361
1362
1363
1364
1365
1366
1367
1368
1369
1370
1371
1372
1373

Stenchikov, Georgiy, Kevin Hamilton, Alan Robock, V. Ramaswamy, and M. Daniel Schwarzkopf, 2004: Arctic Oscillation response to the 1991 Pinatubo eruption in the SKYHI GCM with a realistic Quasi-Biennial Oscillation, *Journal of Geophysical Research*, **109**, D03112, doi: 10.1029/2003JD003699.

Stenchikov, Georgiy, Kevin Hamilton, Ronald J. Stouffer, Alan Robock, V. Ramaswamy, Ben Santer, and Hans-F. Graf, 2006: Arctic Oscillation response to volcanic eruptions in the IPCC AR4 climate models, *Journal of Geophysical Research*, **111**, D07107, doi:10.1029/2005JD006286.

Stevens, M.J., and G.R. North, 1996: Detection of the climate response to the solar cycle. *Journal of Atmospheric Science*, **53**, 2594-2608.

Stuiver, M., P.M. Grootes, and T.F. Braziunas, 1995: The GISP2 delta O-18 climate record of the past 16,500 years and the role of the sun, ocean, and volcanoes. *Quaternary Research*, **44**, 341-354.

Sun, J.M., Z.L. Ding, D. Rokosh, and N. Rutter, 1999: 580,000 year environmental reconstruction from eolian deposits at the Mu Us Desert margin, China. *Quaternary Science Reviews*, **18**, 1351-1364.

Szabo, B.J., K.R. Ludwig, D.R. Muhs, and K.R. Simmons, 1994: Thorium-230 ages of corals and duration of the last interglacial sea-level high stand on Oahu, Hawaii. *Science*, **266**, 93-96.

- 1374 **Thordarson**, T., Miller, D.J., Larsen, G., Self, S., and Sigurdsson, H., 2001: New estimates of
1375 sulfur degassing and atmospheric mass-loading by the 934 AD Eldgjá eruption, Iceland.
1376 *J. Volcanol. Geotherm. Res.*, **108**, 33-54.
1377
- 1378 **Walker**, J.C.G., P.B. Hays, and J.F. Kasting, 1981: A negative feedback mechanism for the
1379 long-term stabilization of Earth's surface-temperature. *Journal of Geophysical Research*,
1380 **86(NC-10)**, 9776-9782.
1381
- 1382 **Walter**, F.M. and D.C. Barry, 1991: Pre- and main-sequence evolution of solar activity. In: *The*
1383 *Sun in Time* [Sonnett, C.P., M.S. Giampapa, and M.S. Matthews]. University of Arizona
1384 Press, Tuscon. pp. 633-657.
1385
- 1386 **Winckler**, G. and H. Fischer, 2006: 30,000 years of cosmic dust in Antarctic ice. *Science*, **313**,
1387 491-491.
1388
- 1389 **Winograd**, I.J., T.B. Coplen, J.M. Landwehr, A.C. Riggs, K.R. Ludwig, B.J. Szabo, P.T.
1390 Kolesar, and K.M. Revesz, 1992: Continuous 500,000-year climate record from vein
1391 calcite in Devils Hole, Nevada. *Science*, **258**, 255-260.
1392
- 1393 **Winograd**, I.J., J.M. Landwehr, K.R. Ludwig, T.B. Coplen, and A.C. Riggs, 1997: Duration and
1394 structure of the past four interglaciations. *Quaternary Research*, **48**, 141-154.
1395
- 1396 **Zachos**, J., M. Pagani, L. Sloan, E. Thomas, K. Billups, 2001: Trends, rhythms, and aberrations
1397 in global climate 65 Ma to present. *Science*, **292(5517)**, 686-693.
1398
- 1399 **Zielinski**, G.A., P.A. Mayewski, L.D. Meeker, S. Whitlow, M.S. Twickler, M. Morrison, D.A.
1400 Meese, A.J. Gow, and R.B. Alley, 1994: Record of volcanism since 7000 B.C. from the
1401 GISP2 Greenland ice core and implications for the volcano-climate system. *Science*, **264**,
1402 948-950.
1403

1
2
3
4
5
6
7
8
9
10
11
12
13
14
15
16
17
18
19
20
21
22
23

CCSP Synthesis and Assessment Product 1.2

**Past Climate Variability and Change in the Arctic and at High
Latitudes**

Chapter 5 — Temperature and Precipitation History of the Arctic

Chapter Lead Authors:

Gifford Miller, University of Colorado, Boulder, CO

Julie Brigham-Grette, University of Massachusetts, Amherst , MA

Contributing Authors:

Lesleigh Anderson, U.S.Geological Survey

Henning Bauch, GEOMAR, University of Kiel

Mary Anne Douglas, University of Alberta

Mary E. Edwards, University of Southampton

Scott Elias, Royal Holloway, University of London

Bruce Finney, University of Alaska-Fairbanks

Svend Funder, University of Copenhagen

Timothy Herbert, Brown University

Larry Hinzman, University of Alaska-Fairbanks

Darrell Kaufman, University of Northern Arizona

Glen MacDonald, University of California-Los Angeles

Alan Robock, Rutgers University

Mark Serreze, University of Colorado

SAP1.2 DRAFT 3 PUBLIC COMMENT

- 24 John Smol, Queen's University
- 25 Robert Spielhagen, GEOMAR, University of Kiel
- 26 Alexander P. Wolfe, University of Alberta
- 27 Eric Wolff, British Antarctic Survey
- 28

28 **ABSTRACT**

29

30 The Arctic has undergone dramatic changes in temperature and precipitation
31 during the Cenozoic Era, the past 65 million years (m.y.) of Earth history. Arctic summer
32 temperature changes during this interval exceeded global average temperature changes
33 during both warm times and cold times, which supports the concept of Arctic
34 amplification. (Strong positive feedbacks—processes that amplify the effects of a change
35 in the controls on global temperature—produce larger changes in temperature in the
36 Arctic than elsewhere). Warm times in the past, those periods when the Arctic was either
37 mildly or substantially warmer than at present in either summer or winter season, help to
38 constrain scenarios for future warming in the Arctic. Past warm times are rarely ideal
39 analogues of future warming because the boundary conditions (such as continental
40 positions and topography) during past times of exceptional warmth were quite different.
41 Nevertheless, paleoclimate records help to define the climate sensitivity of the planet and
42 to quantify Arctic amplification.

43 At the start of the Cenozoic, 65 million years ago (Ma), the planet was ice free;
44 there was no sea ice in the Arctic Ocean and neither a Greenland nor an Antarctic ice
45 sheet. General cooling through the Cenozoic is attributed mainly to a slow decrease in
46 greenhouse gases in the atmosphere. As the Arctic cooled, high-elevation mountain
47 glaciers formed as did seasonal sea ice in the Arctic Ocean, but a detailed record of
48 changes in the Arctic is available only for the last few million years. A global warm
49 period that affected both seasons in the middle Pliocene, about 3.5 Ma, is well
50 represented in the Arctic; at that time extensive deciduous forests occupied lands that

51 now support only polar desert and tundra. Global oceanic and atmospheric circulation
52 was substantially reorganized between 3 and 2.5 Ma, and that reorganization was
53 accompanied by the development of the first continental ice sheets throughout North
54 America and Eurasia. Icebergs from these ice sheets delivered rock fragments into the
55 central North Atlantic Ocean. This change marks the onset of the Quaternary Period (2.6–
56 0 Ma), generally equated with “ice-age” time. From about 2.7 to about 0.8 Ma, the ice
57 sheets came and went about every 41 thousand years (k.y.), the same timing as changes in
58 the ongoing tilt of Earth’s axis. Ice sheets grew when Earth’s tilt was at a minimum, and
59 they melted when tilt was at a maximum. For the past 800 k.y., ice sheets have grown
60 larger and ice age times have been longer, lasting about 100 ka; those icy intervals have
61 been separated by brief warm periods of about 10 k.y. duration. The cause of this shift is
62 debated. The relatively warm interval during which human civilization developed is the
63 most recent of these 10 k.y. warm intervals, the Holocene (about 11.5–0 ka). During the
64 penultimate warm interval, about 130–120 ka, solar energy in summer in the northern
65 high latitudes was greater than at any time in the current warm interval. As a
66 consequence, the Arctic summer was about 5°C warmer than at present and almost all
67 glaciers melted completely except for the Greenland Ice Sheet, and even it was reduced
68 in size substantially from its present extent. Although sea ice is difficult to reconstruct,
69 the evidence suggests that the central Arctic Ocean retained some permanent ice cover or
70 was periodically ice free, even though the flow of warm Atlantic water into the Arctic
71 Ocean may have been greater than during the present warm interval.

72 The last glacial maximum peaked about 20 ka when parts of the Arctic were as
73 much as 20°C colder than at present. Ice recession was well underway by 16 ka, and most

74 of the Northern Hemisphere ice sheets had melted by 7 ka. Solar energy due to Earth's
75 proximity to the Sun in summer rose in the Arctic steadily from 20 ka to a maximum (10%
76 higher than at present) about 11 ka and has been decreasing since then, as the precession
77 of the equinoxes has tilted the Northern Hemisphere farther from the sun in summer. The
78 extra energy received in early Holocene summers warmed summers throughout the
79 Arctic about 1°–3°C above 20th century averages, enough to completely melt many small
80 glaciers throughout the Arctic (although the Greenland Ice Sheet was only slightly
81 smaller than present). Summer sea ice limits were substantially smaller than their 20th
82 century average, and the flow of Atlantic water into the Arctic Ocean was substantially
83 greater. As summer solar energy decreased in the second half of the Holocene, glaciers
84 re-established or advanced, sea ice extended, and the flow of warm Atlantic water into
85 the Arctic Ocean diminished. Late Holocene cooling reached its nadir during the Little
86 Ice Age (about 1250–1850 AD), when most Arctic glaciers reached their maximum
87 Holocene extent. During the warming of the past century and a half, glaciers have
88 receded throughout the Arctic, terrestrial ecosystems have advanced northward, and
89 perennial Arctic Ocean sea ice has diminished.

90 Paleoclimate reconstructions of Arctic temperatures, compared with global
91 temperature changes during four key intervals in the past 4 m.y., allow a quantitative
92 estimate of Arctic amplification. These data suggest that Arctic temperature change is
93 three to four times as large as the global average temperature change during both warm
94 and cold intervals. If global warming forecasts are correct, this relation indicates that
95 Arctic temperatures are likely to increase dramatically in the next century.

96

120 them requires understanding and characterization of its natural variability. The short time
121 interval for which instrumental data are available in the Arctic is not sufficient to characterize
122 that natural variability, so a paleoclimatic perspective is required.

123 This chapter focuses primarily on the history of temperature and precipitation in
124 the Arctic. These topics are important in their own right, and they also set the stage for
125 understanding the histories of the Greenland Ice Sheet and the Arctic sea ice, which are
126 described in Chapters 7 (Greenland Ice Sheet) and 8 (sea ice). Because of the great
127 interest in rates of change, and because of some technical details in extracting rate of
128 change from the broad history of temperature or precipitation, careful consideration of
129 rates of change is deferred to Chapter 6 (past rates of Arctic climate change).

130 Before providing the history of temperature and precipitation in the Arctic, this
131 chapter supplements the discussion in Chapter 4 (paleoclimate concepts) on forcings,
132 feedbacks, and proxies by providing additional information on those aspects particularly
133 relevant to the histories of temperature and precipitation in the Arctic. The climate history
134 of the past 65 m.y. is then summarized; it focuses on temperature and precipitation
135 changes that span the full range of the Arctic's natural climate variability and response
136 under different forcings. We place special emphasis on relevant intervals in the past with
137 a mean climate state warmer than our own. Where possible, we discuss causes of these
138 changes. From these summaries, it is possible to estimate the magnitude of polar
139 amplification and to characterize how the Arctic system responds to global warm times.

140

141 **5.2 Feedbacks Influencing Arctic Temperature and Precipitation**

142

166 although ice-age processes (like some of the other processes discussed below) clearly
167 extend well beyond the Arctic.

168

169 **5.2.1 Ice-albedo feedback**

170 Ice and snow present highly reflective surfaces. The albedo of a surface is defined
171 as the reflectivity of that surface to the wavelengths of solar radiation. Fresh ice and snow
172 have the highest albedo of any widespread surfaces on the planet (Figure 5.4), so it is
173 apparent that changes in the seasonal and areal distribution of snow and ice will exert
174 strong influences on the planetary energy balance (Peixoto and Oort, 1992). Open ocean,
175 on the other hand, has a low albedo; it absorbs almost all solar energy when the sun angle
176 is high. Changes in albedo are most important in the Arctic summer, when solar radiation
177 is at a maximum, whereas changes in the winter albedo have little influence on the energy
178 balance because little solar radiation reaches the surface then. In general, warming
179 reduces ice and snow whereas cooling allows them to extend, so the changes in ice and
180 snow act as positive feedbacks to amplify climate changes (e.g., Lemke et al., 2007).

181

182 **FIGURE 5.4 NEAR HERE**

183

184 **5.2.2 Ice-insulation feedback**

185 In addition to its effects on albedo, sea ice also causes a positive insulation
186 feedback, primarily in the wintertime. Ice effectively blocks heat transfer between
187 relatively warm ocean (at or above the freezing point of seawater) and cold atmosphere
188 (which, in the Arctic winter, averages -40°C (Chapman and Walsh, 2007). If sea ice is

212 works of Kvenvolden, 1988; 1993; MacDonald, 1990, and Haeberli et al., 1993. As
213 permafrost thaws under a warmer summer climate (Figure 5.6), it may release much more
214 greenhouse gases such as CO₂ and methane from the decomposition of organic matter
215 previously sequestered in permafrost and in widespread Arctic yedoma deposits (e.g.,
216 Vörösmarty, 2001; Thomas et al., 2002, Smith et al., 2004, Archer, 2007; Walter et al.,
217 2007). Because CO₂ and methane are greenhouse gases, atmospheric temperature is
218 likely to increase in turn, a positive feedback. Walter et al. (2007) suggest that methane
219 bubbling from the thawing of newly formed thermokarst lakes across parts of the Arctic
220 during deglaciation may account for as much as 33–87% of the increase in atmospheric
221 methane measured in ice cores. Such a release would have contributed a strong positive
222 feedback to warming during the last deglaciation, and it likely continues today (Walter et
223 al., 2006).

224

225

226

FIGURE 5.6 NEAR HERE

227

228

229 **5.2.5 Freshwater balance feedbacks and thermohaline circulation**

230 The Arctic Ocean is almost completely surrounded by continents (Figure 5.7).
231 Because precipitation is low over the ice-covered ocean (Serreze et al., 2006), the
232 freshwater input to the Arctic Ocean largely derives from the runoff from large rivers in
233 Eurasia and North America and by the inflow of relatively low-salinity Pacific water
234 through the Bering Strait. The Yenisey, Ob, and Lena are among the nine largest rivers

235 on Earth, and there are several other large rivers, such as the Mackenzie, that feed into
236 the Arctic Ocean (see Vörösmarty et al., 2008). The freshwater discharged by these rivers
237 maintains low salinities on the broad, shallow, and seasonally ice-free seas bordering the
238 Arctic Ocean. The largest of these border the Eurasian continent, where they serve as the
239 dominant area in the Arctic Ocean in which sea ice is produced (for some fundamentals
240 on Arctic sea ice, see Barry et al., 1993). Sea ice forms along the Eurasian margin and
241 then drifts toward Fram Strait; transit time is 2–3 years in the current regime. In the
242 Amerasian part of the Arctic Ocean, the clockwise-rotating Beaufort Gyre is the
243 dominant ice-drift feature (see Figure 8.1).

244 However, the transport pathway for most of the freshwater entering the Arctic
245 Ocean is the ocean's surface layer (its upper 50 m) (e.g., Schlosser et al., 2000). Low-
246 salinity surface waters are exported from the Arctic Ocean to the northern North Atlantic
247 (Nordic Seas) through western Fram Strait, after which they follow the east coast of
248 Greenland and exit the Nordic Seas through Denmark Strait. A smaller volume of
249 freshwater flows out through the inter-island channels of the Canadian Arctic
250 Archipelago, and it eventually reaches the North Atlantic through the Labrador Sea. The
251 low-saline outflow from the Arctic Ocean is compensated by a relatively warm inflow of
252 saline Atlantic water through eastern Fram Strait. Despite its warmth, Atlantic water has
253 sufficient density due to its high salinity that it is forced to sink beneath the colder, but
254 much fresher, surface water upon entering the Arctic Ocean. North of Svalbard, Atlantic
255 water spreads as a boundary current into the Arctic Basin and forms the Atlantic Water
256 Layer (Morison et al., 2000). The strong vertical gradients of salinity and temperature in
257 the Arctic Ocean produce a relatively stable stratification. However, recent observations

258 have shown that in some areas in the Eurasian part of the Arctic Ocean, the warm
259 Atlantic layer is in direct contact with the surface mixed layer (Rudels et al., 1996; Steele
260 and Boyd, 1998; Schauer et al., 2002), thereby promoting vertical heat transfer to the
261 Arctic atmosphere in winter. In recent decades circum-Arctic glaciers and ice sheets have
262 been losing mass (more snow and ice melting in summer than accumulates as snow in
263 winter) (Dowdeswell et al., 1997; Rignot and Thomas, 2002; Meier et al., 2007), and
264 since the 1930s river runoff to the Arctic Ocean has been increasing (Peterson et al.,
265 2002). Both factors increase the export of freshwater from the Arctic Ocean (Peterson et
266 al., 2006). Recent studies suggest that changes in river runoff strongly influence the
267 stability of Arctic Ocean stratification (Steele and Boyd, 1998; Martinson and Steele,
268 2001; Björk et al., 2002; Boyd et al., 2002; McLaughlin et al., 2002; Schlosser et al.,
269 2002).

270 In the North Atlantic, primarily in the Nordic Seas and the Labrador Sea,
271 wintertime cooling of the relatively warm and salty waters increases its density. The
272 denser waters then sink and flow southward to participate in the global thermohaline
273 circulation (“thermo” for temperature and “haline” for salt, the two components that
274 determine density. This circulation system also is referred to as the meridional
275 overturning circulation (MOC)). Continuing surface inflow from the south, which
276 replaces the water sinking in the Nordic and Labrador Seas, promotes persistent open
277 water rather than sea ice in these regions. In turn, this lack of sea ice promotes notably
278 warmer conditions, especially in wintertime, over and near the North Atlantic and
279 extending downwind across Europe and beyond (Seager et al., 2002). Salt rejected from
280 sea ice growing nearby also may contribute to increasingly dense sea water and to its

281 sinking.

282 If the surface waters are made sufficiently less salty by an increase in freshwater
283 from runoff of melting ice or from direct precipitation, then the rate of sinking of those
284 surface waters will diminish or stop (e.g., Broecker et al., 1985). Results of numerical
285 models indicate that if freshwater runoff into the Arctic Ocean and the North Atlantic
286 increases as surface waters warm in the northern high latitudes, then the thermohaline
287 circulation in the North Atlantic will weaken, with consequences for marine ecosystems
288 and energy transport (e.g., Rahmstorf, 1996, 2002; Marotzke, 2000; Schmittner, 2005).

289 Reducing the rate of North Atlantic thermohaline circulation may have global as
290 well as regional effects (e.g., Obata, 2007). Oceanic overturning is an important
291 mechanism for transferring atmospheric CO₂ to the deep ocean. Reducing the rate of deep
292 convection in the ocean would allow a higher proportion of anthropogenic CO₂ to remain
293 in the atmosphere. Similarly, a slowdown in thermohaline circulation would reduce the
294 turnover of nutrients from the deep ocean, with potential consequences across the Pacific
295 Ocean.

296

297 **5.2.6 Feedbacks during glacial-interglacial cycles**

298 The growth and melting of immense ice sheets, which at their peak size covered
299 approximately 30% of the modern global land area including the modern sites of New
300 York and Chicago, were paced by the orbital variations often called Milankovitch
301 forcings (e.g., Imbrie et al., 1993) described in Chapter 4 (paleoclimate concepts). There
302 is little doubt that the orbital forcings drove this glacial-interglacial cycling, but a

303 remarkably rich and varied literature debates the detailed mechanisms (see, e.g., Roe,
304 1999).

305 The generally accepted explanation of the glacial-interglacial cycling is that ice
306 sheets grew when limited summer sunshine at high northern latitudes allowed survival of
307 accumulated snow, and ice sheets shrank when abundant summer sunshine in the north
308 melted the ice. The north is more important than the south because the Antarctic has
309 remained ice covered during this cycling of the last million years and more, and there is
310 no other high-latitude land in the south on which ice sheets could grow.

311 The increased reflectivity produced by expanded ice contributed to cooling. This
312 effect is the ice-albedo feedback as described above, but with slower response controlled
313 by the flow of the great ice sheets. Atmospheric dust was more abundant in the ice ages
314 than in the intervening warm interglacials, and that additional ice-age dust contributed to
315 cooling by blocking sunlight. The changes in Earth's orbit and ice-sheet growth led to
316 complex changes in the ocean-atmosphere system that shifted carbon dioxide from the air
317 to the ocean and reduced the atmospheric greenhouse effect. The carbon-dioxide changes
318 lagged behind the orbital forcing, and thus carbon dioxide was clearly a feedback, but the
319 large global cooling of the ice ages has been successfully explained only if the reduced
320 greenhouse effect is included (Jansen et al., 2007). By analogy, overspending a credit
321 card induces debt, which is made larger by interest payments on that debt. The interest
322 payments clearly lag the debt in time and did not cause the debt, but they contribute to the
323 size of the debt, and the debt cannot be explained quantitatively unless the interest
324 payments are included.

325 Abrupt climate changes have been associated with the ice-age cycles. The most
326 prominent and best known of these are linked to jumps in the wintertime extent of sea ice
327 in the North Atlantic, which in turn were linked to changes in the large-scale circulation
328 of the ocean (e.g., Alley, 2007), as described in the previous section. The associated
329 temperature changes were very large around the North Atlantic (as much as 10°C or
330 more) but much smaller in remote regions, and they were in the opposite direction in the
331 far south (northern cooling was accompanied by slight southern warming). Hence, the
332 globally averaged temperature changes were small and were probably linked primarily to
333 ice-albedo feedback and small changes in the strength of the greenhouse effect. As
334 reviewed by Alley (2007), the large ice-age ice sheets seem to have both triggered these
335 abrupt swings and created conditions under which triggering was easier. Although such
336 events may remain possible, they are less likely without the large ice sheet on Canada.
337

338 **5.2.7 Arctic Amplification**

339 The positive feedbacks outlined above amplify the Arctic response to climate
340 forcings. The ice-albedo feedback is potentially strong in the Arctic because it hosts so
341 much snow and ice (see Serreze and Francis, 2006 for additional discussion); if
342 conditions are too warm for snow to form, no ice-albedo feedback can exist. Climate
343 models initialized from modern or similar conditions and forced in various ways are in
344 widespread agreement that global temperature trends are amplified in the Arctic and that
345 the largest changes are over the Arctic Ocean during the cold season (autumn through
346 spring) (e.g., Manabe and Stouffer, 1980; Holland and Bitz, 2003; Meehl et al., 2007).
347 Summer changes over the Arctic Ocean are relatively damped, although summer changes

348 over Arctic lands may be substantial (Serreze and Francis, 2006). The strong wintertime
349 changes over the Arctic Ocean are linked to the insulating character of sea ice.

350 Think first of an unperturbed climate in balance on annual time scales. During
351 summer, solar energy melts the sea ice cover. As the ice cover melts, areas of open water
352 are exposed. The albedo of the open water is much lower than that of sea ice, so the open
353 water gains heat. Because much of the solar energy goes into melting ice and warming
354 the ocean, the surface air temperature does not rise much and, indeed, over the melting
355 ice it stays fairly close to the freezing point. Through autumn and winter, when little or
356 no solar energy is received, this ocean heat is released back to the atmosphere. The
357 formation of sea ice itself further releases heat back to the atmosphere.

358 However, if the climate warms (e.g., through the effects of higher greenhouse gas
359 concentrations) then the summer melt season lengthens and intensifies, and more areas of
360 low-albedo open water form in summer and absorb solar radiation. As more heat is
361 gained in the upper ocean, more heat is released back to the atmosphere in autumn and
362 winter; this additional heat is expressed as a rise in air temperature. Furthermore, because
363 the ocean now contains more heat, the ice that forms in autumn and winter is thinner than
364 before. This thinner ice melts more easily in summer and produces even more low-albedo
365 open water that absorbs solar radiation, meaning even larger releases of heat to the
366 atmosphere in autumn and even thinner ice the next spring, and so on. The process can
367 also work in reverse. An initial Arctic cooling melts less ice during the summer and
368 creates less low-albedo open water. If less summer heat is gained in the ocean, then less
369 heat is released back to the atmosphere in autumn and winter, and air temperatures
370 further fall.

371 Although the albedo feedback over the ocean seems to dominate, an albedo
372 feedback over land is much more direct. Under a warming climate, snow melts earlier in
373 spring and thus low-albedo tundra, shrub, and forest cover is exposed earlier and fosters
374 further spring warming. Similarly, later autumn snow cover will foster further autumn
375 warming. More snow-free days produce a longer period of surface warming and imply
376 warmer summers. Again, the process can work in reverse: initial cooling leads to more
377 snow cover, fostering further cooling. Collectively, these processes result in stronger net
378 positive feedbacks to forced temperature change (regardless of forcing mechanism) than
379 is typical globally, thereby producing “Arctic amplification”.

380 During longer time intervals, an ice sheet such as the Laurentide Ice Sheet on
381 North America can grow, or an ice sheet such as that on Greenland can melt. This growth
382 or melting in turn influences albedo, freshwater fluxes to the ocean, broad patterns of
383 atmospheric circulation, greenhouse-gas storage or release in the ocean and on land, and
384 more.

385

386 **5.3 Proxies of Arctic Temperature and Precipitation**

387

388 Temperature and precipitation are especially important climate variables. Climate
389 change is typically driven by changes in key forcing factors, which are then amplified or
390 retarded by regional feedbacks that affect temperature and precipitation (section 5.2 and
391 4.2). Because feedbacks have strong regional variability, spatially variable responses to
392 hemispherically symmetric forcing are common throughout the Arctic (e.g., Kaufman et

393 al., 2004). Consequently, spatial patterns of temperature and precipitation must be
394 reconstructed regionally.

395 Reconstructing temperature and precipitation in pre-industrial times requires
396 reliable proxies (see section 4.3 for a general discussion of proxies) that can be used to
397 derive qualitative or, preferably, quantitative estimates of past climates. To capture the
398 expected spatial variability, proxy climate reconstructions must be spatially distributed
399 and span a wide range of geological time. In general, the use of several proxies to
400 reconstruct past climates provides the most robust evidence for past changes in
401 temperature and precipitation.

402

403 **5.3.1 Proxies for Reconstruction of Temperature**

404 **5.3.1a Vegetation/pollen records**

405 Estimates of past temperature from data that describe the distribution of
406 vegetation (primarily fossil pollen assemblages but also plant macrofossils such as fruits
407 and seeds) may be relative (warmer or colder) or quantitative (number of degrees of
408 change). Most information pertains to the growing season, because plants are dormant in
409 the winter and so are less influenced by climate than during the growing season (but see
410 below). For example, evidence of boreal forest vegetation (the presence of one or more
411 boreal tree species) would be more strongly associated with warmer growing seasons
412 than would evidence of treeless tundra—and the general position of northern treeline
413 today approximates the location of the July 10 °C isotherm.

414 Indicator species are species with well studied and relatively restricted modern
415 climatic ranges. The appearance of these species in the fossil record indicates that a

416 certain climate milestone was reached, such as exceeding a minimum summer
417 temperature threshold for successful growth or a winter minimum temperature of freezing
418 tolerance (Figure 5.8). This methodology was developed early in Scandinavia (Iversen,
419 1944); Matthews et al. (1990) used indicator species to constrain temperatures during the
420 last interglaciation in northwest Canada, and Ritchie et al. (1983) used indicator species
421 to highlight early Holocene warmth in northwest Canada. The technique has been used
422 extensively with fossil insect assemblages.

423

424

FIGURE 5.8 NEAR HERE

425

426 Methodologies for the numerical estimation of past temperatures from pollen
427 assemblages follow one of two approaches. The first is the inverse-modeling approach, in
428 which fossil data from one or more localities are used to provide temperature estimates
429 for those localities (this approach also underlies the relative estimates of temperature
430 described above). A modern “calibration set” of data (in this case, pollen assemblages) is
431 related by equations to observed modern temperature, and the functions thus obtained are
432 then applied to fossil data. This method has been developed and applied in Scandinavia
433 (e.g., Seppä et al., 2004). A variant of the inverse approach is analogue analysis, in which
434 a large modern dataset with assigned climate data forms the basis for comparison with
435 fossil spectra. Good matches are derived statistically, and the resulting set of analogues
436 provides an estimate of the past mean temperature and accompanying uncertainty
437 (Anderson et al., 1989; 1991).

438 Inverse modeling relies upon observed modern relationships. Some plant species
439 were more abundant in the past than they are today, and the fossil pollen spectra they
440 produced may have no recognizable modern counterpart—so-called “no-analogue”
441 assemblages. Outside the envelope of modern observations, fossil pollen spectra, which
442 are described in terms of pollen abundance, cannot be reliably related to past climate.
443 This problem led to the adoption of a second approach to estimating past temperature (or
444 other climate variable) called forward modeling. The pollen data are not used to develop
445 numerical values but are used to test a “hypothesis” about the status of past temperature
446 (a key ingredient of climate). The hypothesis may be a conceptual model of the status of
447 past climate, but typically it is represented by a climate-model simulation for a given time
448 in the past. The climate simulation drives a vegetation model that assigns vegetation
449 cover on the basis of bioclimatic rules (such as the winter minimums or required warmth
450 of summer growing temperatures mentioned above). The resultant map is compared with
451 a map of past vegetation developed from the fossil data. The philosophy of this approach
452 is described by Prentice and Webb (1998). Such data and models have been compared for
453 the Arctic by Kaplan et al. (2003) and Wohlfahrt et al. (2004). The great advantage of
454 this approach is that underlying the model simulation are hypothesized climatic
455 mechanisms; those mechanisms allow not only the description but also an explanation of
456 past climate changes.

457

458 **5.3.1b Dendroclimatology**

459 Seasonal differences in climate variables such as temperature and precipitation
460 throughout many parts of the world, including the high latitudes, are known to produce

461 annual rings that reflect distinct changes in the way trees grow and respond, year after
462 year, to variations in the weather (Fritts, 1976). Alternating light and dark bands
463 (couplets) of low-density early wood (spring and summer) and higher density late wood
464 (summer to late summer) have been used for decades to reproduce long time series of
465 regional climate change thought to directly influence the production of meristematic cells
466 in the trees' vascular cambium, just below the bark. Cambial activity in many parts of the
467 northern boreal forests can be short; late wood may start production in late June and
468 annual-ring width is complete by early August (e.g., Esper and Schweingruber, 2004).
469 Fundamental to the use of tree rings is the fact that the average width of a tree ring
470 couplet reflects some combination of environmental factors, largely temperature and
471 precipitation, but it can also reflect local climatic variables such as wind stress, humidity
472 and soil properties (see Bradley, 1999, for review).

473 The extraction of a climate signal from ring width and wood density
474 (dendroclimatology), relies on the identification and calibration of regional climate
475 factors and on the ability to distinguish local climate influences from regional noise
476 (Figure 5.9). How sites for tree sampling are selected is also important depending upon
477 the climatological signal of interest. Trees in marginal growth sites, perhaps on drier
478 substrates or near an ecological transition, may be ideally most sensitive to minor
479 changes in temperature stress or moisture stress. On the other hand, trees in less-marginal
480 sites may reflect conditions of more widespread change. In the high latitudes, research is
481 commonly focused on trees at both the latitude and elevation limits of tree growth or of
482 the forest-tundra ecotone.
483

484

FIGURE 5.9 NEAR HERE

485

486 Pencil-sized increment cores or sanded trunk cross sections are routinely used for
487 stereomicroscopic examination and measurement (Figure 5.10). A number of tree species
488 are examined, most commonly varieties of the genera *Larix* (larch), *Pinus* (pine), and
489 *Picea* (spruce). Raw ring-width time series are typically generated at a resolution of 0.01
490 mm along one or more radii of the tree, and these data are normalized for changes in ring
491 width that reflect the natural increase in tree girth (a young tree produces wider rings).
492 Ring widths for a number of trees are then averaged to produce a master curve for a
493 particular site. The replication of many time series throughout a wide area at a particular
494 site permits extraction of a climate-related signal and the elimination of anomalous ring
495 biases caused by changes in competition or the ecology of any particular tree. Abrupt
496 growth that caused a large change in ring width (Figure 5.9) can only be causally
497 evaluated based on forest-site characteristics; that is, if the change isn't replicated in
498 nearby trees, it's probably not related to climate.

499

500

FIGURE 5.10 NEAR HERE

501

502 Dendroclimatology is statistically laborious, and a variety of approaches are used
503 by the science community. Ring widths or ring density must first be calibrated by a
504 response-function analysis in which tree growth and monthly climatic data are compared
505 for the instrumental period. Once this is done, then cross-dated tree ring series reaching
506 back millennia can be used as predictors of past change. Principal-components analysis,

507 along with some form of multiple regression analysis, is commonly used to identify key
508 variables. A comprehensive review of statistical treatments is beyond the scope of this
509 report, but summaries can be found in Fritts (1976), Briffa and Cook (1990), Bradley
510 (1999, his Chapter 10), and Luckman (2007).

511

512 **5.3.1c Marine isotopic records**

513 The oxygen isotope composition of the calcareous shells of planktic foraminifers
514 accurately records the oxygen isotope composition of ambient seawater, modulated by
515 the temperature at which the organisms built their shells (Epstein et al., 1953; Shackleton,
516 1967; Erez and Luz, 1982; Figure 5.11). (The term $\delta^{18}\text{O}$ refers to the proportion of the
517 heavy isotope, ^{18}O , relative to the lighter, more abundant isotope, ^{16}O .) However, the low
518 horizontal and vertical temperature variability found in Arctic Ocean surface waters (less
519 than -1°C) has little effect on the oxygen isotope composition of *N. pachyderma* (sin.)
520 (maximum 0.2‰, according to Shackleton, 1974). Because meteoric waters, discharged
521 into the ocean by precipitation and (indirectly) by river runoff, have considerably lower
522 $\delta^{18}\text{O}$ values than do ocean waters, a reasonable correlation can be interpreted between
523 salinity and the oxygen isotope composition of Arctic surface waters despite the
524 complications of seasonal sea ice (Bauch et al., 1995; LeGrande and Schmidt, 2006).
525 Accordingly, the spatial variability of surface-water salinity in the Arctic Ocean is
526 recorded today by the $\delta^{18}\text{O}$ of planktic foraminifers (Spielhagen and Erlenkeuser, 1994;
527 Bauch et al., 1997).

528

529

FIGURE 5.11 NEAR HERE

530

531 The $\delta^{18}\text{O}$ values of planktic foraminifers in cores of ancient sediment from the
532 deep Arctic Ocean vary considerably in on millennial time scales (e.g., Aksu, 1985; Scott
533 et al., 1989; Stein et al., 1994; Nørgaard-Pedersen et al., 1998; 2003; 2007a,b; Polyak et
534 al., 2004; Spielhagen et al., 2004; 2005). The observed variability in foraminiferal $\delta^{18}\text{O}$
535 commonly exceeds the change in the isotopic composition of seawater that results merely
536 from storing, on glacial-interglacial time scales, isotopically light freshwater in glacial ice
537 sheets (about 1.0–1.2‰ $\delta^{18}\text{O}$) (Fairbanks, 1989; Adkins et al., 1997; Schrag et al. 2002).
538 Changes with time in freshwater balance of the near-surface waters, and in the
539 temperature of those waters, are both recorded in the $\delta^{18}\text{O}$ values of foraminifer shells.
540 Moreover, in cases where independent evidence of a regional warming of surface waters
541 is available (e.g., in the eastern Fram Strait during the last glacial maximum; Nørgaard-
542 Pedersen et al., 2003), this warming is thought to have been caused by a stronger influx
543 of saline Atlantic Water. Because salinity influences $\delta^{18}\text{O}$ of foraminifer shells from the
544 Arctic Ocean more than temperature does, it is difficult to reconstruct temperatures in the
545 past on the basis of systematic variations in calcite $\delta^{18}\text{O}$ in Arctic Ocean sediment cores.

546

547 **5.3.1d Lacustrine isotopic records**

548 Isotopic records preserved in lake sediment provide important paleoclimatic
549 information on landscape change and hydrology. Lakes are common in high-latitude
550 landscapes, and sediment deposited continuously provides uninterrupted, high-resolution
551 records of past climate (Figure 5.12).

552

553

FIGURE 5.12 NEAR HERE

554

555 Oxygen isotope ratios in precipitation reflect climate processes, especially
556 temperature (see 5.3.1e). The oxygen isotope ratios of shells and other materials in lakes
557 primarily reflect ratios of the lake water. The isotopic ratios in the lake water are
558 dominantly controlled by the isotopic ratios in precipitation—unless evaporation from the
559 lake is sufficiently rapid, compared with inflow of new water, to shift the isotopic ratios
560 towards heavier values by preferentially removing isotopically lighter water. Those lakes
561 that have streams entering and leaving (open lakes) have isotopic ratios that are generally
562 not affected much by evaporation, as do some lakes supplied only by water flow through
563 the ground (closed lakes). These lakes allow isotopic ratios of shells and other materials
564 in them to be used to reconstruct climate, especially temperature. However, some closed
565 lakes are affected notably by evaporation, in which case the isotopic ratios of the lake are
566 at least in part controlled by lake hydrology. Unless independent evidence of lake
567 hydrology is available, quantitative interpretation of $\delta^{18}\text{O}$ is difficult. Consequently, $\delta^{18}\text{O}$
568 is normally combined with additional climate proxies to constrain other variables and
569 strengthen interpretations. For example, in rare cases, ice core records that are located
570 near lakes can provide an oxygen isotope record for direct comparison (Fisher et al.,
571 2004; Anderson and Leng, 2004; Figure 5.13). Oxygen isotope ratios are relatively easy
572 to measure on carbonate shells or other carbonate materials. Greater difficulty, which
573 limits the accuracy (i.e., the time-resolution) of the records, is associated with analyses of
574 oxygen isotopes in silica from diatom shells (Leng and Marshall, 2004) and in organic
575 matter (Sauer et al., 2001; Anderson et al., 2001). Additional uncertainty arises with

576 organic matter because its site of origin is unknown: although some of it grew in the lake,
577 some was also washed in and may have been stored on the landscape for an indeterminate
578 time previously.

579

580

FIGURE 5.13 NEAR HERE

581

582

5.3.1e Ice cores

583

584

585

586

587

588

589

590

591

592

593

594

595

FIGURE 5.14 NEAR HERE

596

597

598

The underlying idea is that an air mass loses water vapor by condensation as it travels from a warm source to a cold (polar) site. This point is easily shown by the nearly

599 linear relationship between precipitation and temperature over modern ice sheets (Figure
600 5.15). Water that contains the heavy isotopes has a lower vapor pressure, so the heavy
601 isotope preferentially condenses into rain or snow, and the air mass becomes
602 progressively depleted of the heavy isotope it moves to colder sites. It can easily be
603 shown from spatial surveys (Johnsen et al., 1989) and, indeed, from modeling studies
604 using models enabled with water isotopes (e.g., Hoffmann et al., 1998; Mathieu et al.,
605 2002) that a good spatial relationship between temperature and water isotope ratio exists.
606 The relationship is

607

608

$$\delta = aT + b$$

609 where T is mean annual surface temperature, and δ is annual mean $\delta^{18}\text{O}$ or δD value in
610 precipitation in the polar regions, and the slope, a , has values typically around 0.6 for
611 Greenland $\delta^{18}\text{O}$.

612

613

FIGURE 5.15 NEAR HERE

614

615 Temperature is not the only factor that can affect isotopic ratios. Changes in the
616 season when snow falls, in the source of the water vapor, and other things are potentially
617 important (Jouzel et al., 1997; Werner et al., 2000) (Figure 5.16). For this reason, it is
618 common whenever possible to calibrate the isotopic ratios using additional
619 paleothermometers. For short intervals, instrumental records of temperature can be
620 compared with isotopic ratios (e.g., Shuman et al., 1995). The few comparisons that have
621 been done (summarized in Jouzel et al., 1997) tend to show δ/T gradients that are slightly

622 lower than the spatial gradient. Accurate reconstructions of past temperature, but with
623 low time resolution, are obtained from the use of borehole thermometry. The center of the
624 Greenland ice sheet has not finished warming from the ice age, and the remaining cold
625 temperatures reveal how cold the ice age was (Cuffey et al., 1995; Johnsen et al., 1995).
626 Additional paleothermometers are available that use a thermal diffusion effect. In this
627 effect, gas isotopes are separated slightly when an abrupt temperature change at the
628 surface creates a temperature difference between the surface and the region a few tens of
629 meters down, where bubbles are pinched off from the interconnected pore spaces in old
630 snow (called firn). The size of the gas-isotope shift reveals the size of an abrupt warming,
631 and the number of years between the indicators of an abrupt change in the ice and in the
632 bubbles trapped in ice reveals the temperature before the abrupt change—if the snowfall
633 rate before the abrupt change is known (Severinghaus et al., 1998; Severinghaus and
634 Brook, 1999; Huber et al., 2006). These methods show that the value of the δ/T slope
635 produced by many of the large changes recorded in Greenland ice cores was considerably
636 less (typically by a factor of 2) than the spatial value, probably because of a relatively
637 larger reduction in winter snowfall in colder times (Cuffey et al., 1995; Werner et al.,
638 2000; Denton et al., 2005). The actual temperature changes were therefore larger than
639 would be predicted by the standard calibration.

640

641

FIGURE 5.16 NEAR HERE

642

643 In summary, water isotopes in polar precipitation are a reliable proxy for mean
644 annual air temperature, but for quantitative use, some means of calibrating them is

645 required. They may be calibrated either against instrumental data by using an alternative
646 estimate of temperature change, or through modeling, even for ice deposited during the
647 Holocene (Schmidt et al., 2007).

648

649 **5.3.1f Fossil assemblages and sea surface temperatures**

650 Different species live preferentially at different temperatures in the modern ocean.
651 Modern observations can be used to learn the preferences of species. If we assume that
652 species maintain their preferences through time, then the mathematical expression of
653 these preferences plus the history of where the various species lived in the past can then
654 be used to interpret past temperatures (Imbrie and Kipp, 1971; CLIMAP, 1981). This line
655 of reasoning is primarily applied to near-surface (planktic) species, and especially to
656 foraminifers, diatoms, and dinoflagellates. The presence or absence and the relative
657 abundance of species can be used. Such methods are now commonly supported by sea-
658 surface temperature estimates using emerging biomarker techniques outline below.

659

660 **5.3.1g Biogeochemistry**

661 Within the past decade, two new organic proxies have emerged that can be used
662 to reconstruct past ocean surface temperature. Both measurements are based on
663 quantifying the proportions of biomarkers—molecules produced by restricted groups of
664 organisms—preserved in sediments. In the case of the “ U_{37}^k index” (Brassell et al., 1986
665 ; Prahl et al., 1988), a few closely related species of coccolithophorid algae are entirely
666 responsible for producing the 37-carbon ketones (“alkenones”) used in the
667 paleotemperature index, whereas crenarcheota (archaea) produce the tetra-ether lipids that

668 make up the TEX₈₆ index (Wuchter et al., 2004). Although the specific function that the
669 alkenones and glycerol dialkyl tetraethers serve for these organisms is unclear, the
670 relationship of the biomarker U^k₃₇ index to temperature has been confirmed
671 experimentally in the laboratory (Prah1 et al., 1988) and by extensive calibrations of
672 modern surface sediments to overlying surface ocean temperatures (Muller et al., 1998,
673 Conte et al., 2006, Wuchter et al., 2004).

674 Biomarker reconstructions have several advantages for reconstructing sea surface
675 conditions in the Arctic. First, in contrast to δ¹⁸O analyses of marine carbonates (outlined
676 above), the confounding effects of salinity and ice volume do not compromise the utility
677 of biomarkers as paleotemperature proxies (a brief discussion of caveats in the use of
678 U^k₃₇ is given below). Both the U^k₃₇ and TEX₈₆ proxies can be measured reproducibly to
679 high precision (analytical errors correspond to about 0.1°C for U^k₃₇ and 0.5°C for
680 TEX₈₆), and sediment extractions and gas or liquid chromatographic detections can be
681 automated for high sampling rates. The abundances of biomarkers also provide insights
682 into the composition of past ecosystems, so that links between the physical oceanography
683 of the high latitudes and carbon cycling can be assessed. And lastly, organic biomarkers
684 can usually be recovered from Arctic sediments that do not preserve carbonate or
685 siliceous microfossils. It should be noted, however, that the harsh conditions of the
686 northern high latitudes mean that the organisms producing the alkenone and tetraethers
687 may have been excluded at certain times and places; thus, continuous records cannot be
688 guaranteed.

689 The principal caveats in using biomarkers for paleotemperature reconstructions
690 come from ecological and evolutionary considerations. Alkenones are produced by algae

691 that are restricted to the region of abundant light (the photic zone), so paleotemperature
692 estimates based on them apply to this layer, which approximates the sea surface
693 temperature. In the vast majority of the ocean, the alkenone signal recorded by sediments
694 closely correlates with mean annual sea-surface temperature (Muller et al., 1998; Conte et
695 al., 2006; Figure 5.17). However, in the case of highly seasonal high-latitude oceans, the
696 temperatures inferred from the alkenone $U^{k'}_{37}$ index may better approximate summer
697 surface temperatures than mean annual sea-surface temperature. Furthermore, past
698 changes in the season of production could bias long-term time series of past temperatures
699 that are based on the $U^{k'}_{37}$ proxy. Depending on water column conditions, past production
700 could have been highly focused toward a short (summer?) or a more diffuse (late spring–
701 early fall?) productive season. A survey of modern surface sediments in the North
702 Atlantic (Rosell-Mele et al., 1995) shows that the seasonal bias in alkenone unsaturation
703 is not important except at high (greater than 65°N.) latitudes (Rosell-Mele et al., 1995). A
704 possible additional complication with the $U^{k'}_{37}$ proxy is that in the Nordic Seas an
705 additional alkenone (of the 37:4 type) is common, although it is rare or absent in most of
706 the world ocean including the Antarctic. The relatively fresh and cold waters of the
707 Nordic Seas may affect alkenone production by the usual species, or they may affect the
708 mixture of species that produce alkenone. Regardless, this oddity suggests caution in
709 applying the otherwise robust global calibration of alkenone unsaturation to Nordic Sea
710 surface temperature (Rosell-Mele and Comes, 1999).

711

712

FIGURE 5.17 NEAR HERE

713

714 In contrast to the near-surface restriction of the algae producing the $U^{k'}_{37}$
715 proxy, the marine crenarcheota that produce the tetraether membrane lipids used in the
716 TEX_{86} index can range widely through the water column. In situ analyses of particles
717 suspended in the water column show that the tetraether lipids are most abundant in winter
718 and spring months in many ocean provinces (Wuchter et al., 2005) and are present in
719 large amounts below 100 m depth. However, it appears that the chemical basis for the
720 TEX_{86} proxy is fixed by processes in the upper lighted (photic) zone, so that the
721 sedimentary signal originates near the sea surface (Wuchter et al., 2005), just as for the
722 $U^{k'}_{37}$ proxy. No studies have yet been conducted to assess how high-latitude seasonality
723 affects the TEX_{86} proxy.

724 As for many other proxies, use of these biomarker proxies is based on the
725 assumption that the modern relation between organic proxies and temperature was the
726 same in the past. The two modern (and genetically closely related) species producing the
727 alkenones in the $U^{k'}_{37}$ proxy can be traced back in time in a continuous lineage to the
728 Eocene (about 50 Ma), and alkenone occurrences coincide with the fossil remains of the
729 ancestral lineage in the same sediments (Marlowe et al., 1984). One might suppose that
730 past evolutionary events in the broad group of algae that includes these species might
731 have produced or eliminated other species that generated these chemicals but with a
732 different relation to temperature. However, other such species would cause jumps in
733 climate reconstructions at times of evolutionary events in the group, and no such jumps
734 are observed. The TEX_{86} proxy can be applied to marine sediments 70–100 million years
735 old. The working assumption is, therefore, that both organic proxies can be applied
736 accurately to sediments containing the appropriate chemicals.

737 Because these biomarker proxies depend on changes in relative abundance of
738 chemicals, it is important that natural processes after death of the producing organisms do
739 not preferentially break down one chemical and thus change the ratio. Fortunately, the
740 ratio appears to be stable (Prah1 et al., 1989; Grice et al., 1998, Teece et al., 1998;
741 Herbert, 2003; Schouten et al., 2004). An additional complication is that sediments can
742 be moved around by ocean currents, so that the material sampled at one place might have
743 been produced in another place under different climate conditions (Thomsen et al., 1998;
744 Ohkouchi et al., 2002). Ordinarily, lengthy transport of biomarkers into a depositional
745 site is rare and volumes are small compared with the supply from the productive ocean
746 above, so that the proxy indeed records local climate. However, at some times and places,
747 the Arctic has been comparatively unproductive, so that transport from other parts of the
748 ocean, or from land in the case of the TEX₈₆ proxy, may have been important (Weijers et
749 al., 2006).

750

751 **5.3.1h Biological proxies in lakes**

752 Lakes and ponds are common in most Arctic regions and provide useful records
753 of climate change (Smol and Cumming, 2000; Cohen, 2003; Schindler and Smol, 2006;
754 Smol 2008). Many different biological climate proxies are preserved in Arctic lake and
755 pond sediments (Pienitz et al., 2004). Diatom shells (Douglas et al., 2004) and remains of
756 non-biting midge flies (chironomid head capsules; Bennike et al., 2004) are among the
757 biological indicators most commonly used to reconstruct ancient Arctic climate (Figure
758 5.18). The approach generally used by those who study the history of lakes
759 (paleolimnologists) is first to identify useful species— those that grow only within a

760 distinct range of conditions. Then, the modern conditions preferred by these indicator
761 species are determined, as are the conditions beyond which these indicator species cannot
762 survive. (Typically used are surface sediment calibration sets or training sets to which are
763 applied statistical approaches such as canonical correspondence analysis and weighted
764 averaging regression and calibration; see Birks, 1998.) The resulting mathematical
765 relations (or transfer functions such as those used in marine records) are then used to
766 reconstruct the environmental variables of interest, on the basis of the distribution of
767 indicator assemblages preserved in dated sediment cores (Smol, 2008). Where well-
768 calibrated transfer functions are not available, such as for some parts of the Arctic, less-
769 precise climate reconstructions are commonly based on the known ecological and life-
770 history characteristics of the organisms.

771

772

FIGURE 5.18 NEAR HERE

773

774 Ideally, sedimentary characteristics would be linked directly to key climatic
775 variables such as temperature (e.g., Pienitz and Smol, 1993; Joynt and Wolfe, 2001;
776 Bigler and Hall, 2003; Bennike et al., 2004; Larocque and Hall, 2004; Woller et al. 2004,
777 Finney et al., 2004, other chapters in Pienitz et al., 2004; Barley et al., 2006; Weckström
778 et al., 2006;). However, lake sediments typically record conditions in the lake that are
779 only indirectly related to climate (Douglas and Smol, 1999). For example, lake
780 ecosystems are strongly influenced by the length of the ice-free versus the ice-covered
781 season, by the sun-blocking effect of any snow cover on ice (Figure 5.19) (e.g., Smol,
782 1988; Douglas et al., 1994; Sorvari and Korhola, 1998; Douglas and Smol, 1999; Sorvari

783 et al., 2002; Rühland et al., 2003; Smol and Douglas, 2007a) and by the existence or
784 absence of a seasonal layer of warm water near the lake surface that remains separate
785 from colder waters beneath (Figure 5.20). Shells and other features in the lake sediment
786 record the species living in the lake and conditions under which they grew. These factors
787 rather directly reflect the ice and snow cover and lake stratification and only indirectly
788 reflect the atmospheric temperature and precipitation that control the lake conditions.

789

790 FIGURE 5.19 NEAR HERE

791 FIGURE 5.20 NEAR HERE

792

793 **5.3.1i Insect proxies.**

794 Insects are common and typically are preserved well in Arctic sediment. Because
795 many insect types live only within narrow ranges of temperature or other environmental
796 conditions, the remains of particular insects in old sediments provides useful information
797 on past climate.

798 Calibrating the observed insect data to climate involves extensive modern and
799 recent studies, together with careful statistical analyses. For example, fossil beetles are
800 typically related to temperature using what is known as the Mutual Climatic Range
801 method (Elias et al., 1999; Bray et al., 2006). This method quantitatively assesses the
802 relation between the modern geographical ranges of selected beetle species and modern
803 meteorological data. A “climate envelope” is determined, within which a species can
804 thrive. When used with paleodata, the method allows for the reconstruction of several
805 parameters such as mean temperatures of the warmest and coldest months of the year.

806

807 **5.3.1j Sand dunes** When plant roots anchor the soil, sand cannot blow around to
808 make dunes. In the modern Arctic, and especially in Alaska (Figure 5.21) and Russia,
809 sand dunes are forming and migrating in many places where dry, cold conditions restrict
810 vegetation. During the last glacial interval and at some other times, dunes formed in
811 places that now lack active dunes and indicate colder or drier conditions at those earlier
812 times (Carter, 1981; Oswald et al., 1999; Beget, 2001; Mann et al., 2002). Some wind-
813 blown mineral grains are deposited in lakes. The rate at which sand and silt are deposited
814 in lakes increases as nearby vegetation is removed by cooling or drying, so analysis of the
815 sand and silt in lake sediments provides additional information on the climate (e.g.,
816 Briner et al., 2006).

817

818

FIGURE 5.21 NEAR HERE

819

820 **5.3.2 Proxies for Reconstruction of Precipitation**

821 In the case of sand dunes described above, separating the effects of changing
822 temperature from those of changing precipitation may be difficult, but additional
823 indicators such as insect fossils in lake sediments may help by constraining the
824 temperature. In general, precipitation is more difficult to estimate than is temperature, so
825 reconstructions of changes in precipitation in the past are less common, and typically less
826 quantitative, than are reconstructions of past temperature changes.

827

828 **5.3.2a Vegetation-derived precipitation estimates** Different plants live in wet
829 and dry places, so indications of past vegetation provide estimates of past wetness. Plants
830 do not respond primarily to rainfall but instead to moisture availability. Availability is
831 primarily controlled in most places by the difference between precipitation and
832 evaporation, although some soils carry water downward so efficiently that dryness occurs
833 even without much evaporation.

834 Much modern tundra vegetation grows where precipitation exceeds evaporation.
835 Plants such as *Sphagnum* (bog moss), cotton-grass (*Eriophorum*), and cloudberry (*Rubus*
836 *chamaemorus*) indicate moist growing conditions. In contrast, grasses dominate dry
837 tundra and polar semi-desert. Such differences are evident today (Oswald et al., 2003)
838 and can be reconstructed from pollen and larger plant materials (macrofossils) in
839 sediments. Some regions of Alaska and Siberia retain sand dunes that formed in the last
840 glacial maximum but are inactive today; typically, those regions are near areas that had
841 grasses then but now have plants requiring greater moisture (Colinvaux, 1964; Ager and
842 Brubaker, 1985; Lozhkin et al. 1993; Goetcheus and Birks 2001, Zazula et al., 2003).

843 In Arctic regions, snow cover may allow persistence of shrubs that would be
844 killed if exposed during the harsh winter. For example, dwarf willow can survive if snow
845 depths exceed 50 cm (Kaplan et al., 2003). Siberian stone pine requires considerable
846 winter snow to weigh down and bury its branches (Lozhkin et al, 2007). The presence of
847 these species therefore indicates certain minimum levels of winter precipitation.

848 Moisture levels can also be estimated quantitatively from pollen assemblages by
849 means of formal techniques such as inverse and forward modeling, following techniques
850 also used to estimate past temperatures. Moisture-related transfer functions have been

851 developed, in Scandinavia for example (Seppä and Hammarlund, 2000). Kaplan et al.
852 (2003) compared pollen-derived vegetation with vegetation derived from model
853 simulations for the present and key times in the past. The pollen data indicated that model
854 simulations for the Last Glacial Maximum tended to be “too moist”—the simulations
855 generated shrub-dominated biomes whereas the pollen data indicated drier tundra
856 dominated by grass.

857

858 **5.3.2b Lake-level derived precipitation estimates** In addition to their other uses
859 in paleoclimatology as described above, lakes act as natural rain gauges. If precipitation
860 increases relative to evaporation, lakes tend to rise, so records of past lake levels provide
861 information about the availability of moisture.

862 Most of the water reaching a lake first soaked into the ground and flowed through
863 spaces as groundwater, before it either seeped directly into the lake or else came back to
864 the surface in a stream that flowed into the lake. Smaller amounts of water fall directly on
865 the lake or flow over the land surface to the lake without first soaking in (e.g.,
866 MacDonald et al., 2000b). Lakes lose water to streams (“overflow”), as outflow into
867 groundwater, and by evaporation. If water supply to a lake increases, the lake level will
868 rise and the lake will spread. This spread will increase water loss from the lake by
869 increasing the area for evaporation, by increasing the area through which groundwater is
870 leaving and the “push” (hydraulic head) causing that outflow, and perhaps by forming a
871 new outgoing stream or increasing the size of an existing stream. Thus, the level of a lake
872 adjusts in response to changes in the balance between precipitation and evaporation in the
873 region feeding water to the lake (the catchment). Because either an increase in

896 Biological groups living within lakes also leave fossil assemblages that can be
897 interpreted in terms of lake level by comparing them with modern assemblages. In all
898 cases, factors other than water depth (e.g., conductivity and salinity) likely influence the
899 assemblages (MacDonald et al., 2000b), but these factors may themselves be indirectly
900 related to water depth. Aquatic plants, which are represented by pollen and macrofossils,
901 tend to dominate from nearshore to moderate depths, and shifts in the abundance of
902 pollen or seeds in one of more sediment profiles can indicate relative water-level changes
903 (Hannon and Gaillard, 1997; Edwards et al., 2000). Diatom and chironomid (midge)
904 assemblages may also be related quantitatively to lake depth by means of inverse
905 modeling and the transfer functions used to reconstruct past lake levels (Korhola et al.,
906 2000; Ilyashuk et al., 2005).

907 The great variety of lakes, and the corresponding range of sedimentary indicators,
908 requires that field scientists be broadly knowledgeable in selecting which lakes to study
909 and which techniques to use in reconstructions. For some important case studies, see
910 Hannon and Gaillard, 1997; Abbott et al., (2000), Edwards et al., (2000), Korhola et al.,
911 2000; Pienitz et al., (2000), Anderson et al., (2005), and Ilyashuk et al., 2005).

912

913 **5.3.2c Precipitation estimates from ice cores.** Ice cores provide a direct way of
914 recording the net accumulation rate at sites with permanent ice. The initial thickness of an
915 annual layer in an ice core (after mathematically accounting for the amount of air trapped
916 in the ice) is the annual accumulation. Most ice cores are drilled in cold regions that
917 produce little meltwater or runoff. Furthermore, sublimation or condensation and snow
918 drift generally account for little accumulation, so that accumulation is not too different

919 from the precipitation (e.g., Box et al., 2006). The thickness of layers deeper in the core
920 must be corrected for the thinning produced as the ice sheet spreads and thins under its
921 own weight, but for most samples this correction can be made with much accuracy by
922 using simple ice flow models (e.g., Alley et al., 1993; Cuffey and Clow, 1997).

923 The annual-layer thickness can be recorded using any component that varies
924 regularly with a defined seasonal cycle. Suitable components include visible layering
925 (e.g. Figure 5.14a), which responds to changes in snow density or impurities (Alley et al.,
926 1997), the seasonal cycle of water isotopes (Vinther et al., 2006), and seasonal cycles in
927 different chemical species (e.g. Rasmussen et al., 2006). Using more than one component
928 gives extra security to the combined output of counted years and layer thicknesses.

929 Although the correction for strain (layer thinning) increases the uncertainty in
930 estimates of absolute precipitation rate deeper in ice cores, estimates of changes in
931 relative accumulation rate along an ice core can be considered reliable (e.g., Kapsner et
932 al., 1995). Because the accumulation rate combines with the temperature to control the
933 rate at which snow is transformed to ice, and because the isotopic composition of the
934 trapped air (Sowers et al., 1989) and the number of trapped bubbles in a sample (Spencer
935 et al., 2006) record the results of that transformation, then accumulation rates can also be
936 estimated from measurements of these parameters plus independent estimation of past
937 temperature using techniques described above.

938

939 **5.4 Arctic Climate over the past 65 Ma**

940

941 During the past 65 m.y. (the Cenozoic), the Arctic has experienced a greater
942 change in temperature, vegetation, and ocean surface characteristics than has any other
943 Northern Hemisphere latitudinal band (e.g., Sewall and Sloan, 2001; Bice et al., 2006;
944 and see results presented below). Those times when the Arctic was unusually warm offer
945 insights into the feedbacks within the Arctic system that can amplify changes imposed
946 from outside the Arctic regions. Below we summarize the evidence for Cenozoic history
947 of climate in the Arctic, and we focus especially on warm times by using climate and
948 environmental proxies outlined in section 5.3.

949

950 **5.4.1 Early Cenozoic and Pliocene Warm Times**

951 Records of the $\delta^{18}\text{O}$ composition of bottom-dwelling foraminifers from the global
952 ocean document a long-term cooling of the deep sea during the past 70 m.y. (Figure 4.8;
953 Zachos et al., 2001) and the development of large Northern Hemisphere continental ice
954 sheets at 2.6–2.9 Ma (Duk-Rodkin et al., 2004). As discussed below and in Chapter 6
955 (past rates of Arctic climate change), Arctic climate history is broadly consistent with the
956 global data reported by Zachos et al. (2001): general cooling and increase in ice was
957 punctuated by short-lived and longer lived reversals, by variations in cooling rate, and by
958 additional features related to growth and shrinkage of ice once the ice was well
959 established. A detailed Arctic Ocean record that is equivalent to the global results of
960 Zachos et al. (2001) is not yet available, and because the Arctic Ocean is geographically
961 somewhat isolated from the world ocean (e.g., Jakobsson and MacNab, 2006), the
962 possibility exists that some differences would be found. Emerging paleoclimate
963 reconstructions from the Arctic Ocean derived from recently recovered sediment cores on

964 the Lomonosov Ridge (Backman et al., 2006; Moran et al., 2006) shed new light on the
965 Cenozoic evolution of the Arctic Basin, but the data have yet to be fully integrated with
966 the evidence from terrestrial records or with the sketchy records from elsewhere in the
967 Arctic Ocean (see Chapter 8, Arctic sea ice).

968 Data clearly show warm Arctic conditions during the Cretaceous and early
969 Cenozoic. For example, late Cretaceous (70 Ma) Arctic Ocean temperatures of 15°C
970 (compared to near-freezing temperatures today) are indicated by TEX₈₆-based estimates
971 (Jenkyns et al., 2004). The same indicator shows that peak Arctic Ocean temperatures
972 near the North Pole rose from about 18°C to more than 23°C during the short-lived
973 Paleocene-Eocene thermal maximum about 55 Ma (Figure 5.23) (Moran et al., 2006; also
974 see Sluijs et al., 2006; 2008). This rise was synchronous with warming on nearby land
975 from a previous temperature of about 17°C to peak temperature during the event of about
976 25°C (Weijers et al., 2007). By about 50 Ma, Arctic Ocean temperatures were about 10°C
977 and relatively fresh surface waters were dominated by aquatic ferns (Brinkhuis et al.,
978 2006). Restricted connections to the world ocean allowed the fern-dominated interval to
979 persist for about 800,000 years; return of more-vigorous interchange between the Arctic
980 and North Atlantic oceans was accompanied by a warming in the central Arctic Ocean of
981 about 3°C (Brinkhuis et al., 2006). On Arctic lands during the Eocene (55–34 Ma),
982 forests of *Metasequoia* dominated a landscape characterized by organic-rich floodplains
983 and wetlands quite different from the modern tundra (McKenna, 1980; Francis, 1988;
984 Williams et al., 2003).

985

986

FIGURE 5.23 NEAR HERE

987

988 Terrestrial evidence shows that warm conditions persisted into the early Miocene
989 (23–16 Ma), when the central Canadian Arctic Islands were covered in mixed conifer-
990 hardwood forests similar to those of southern Maritime Canada and New England today
991 (Whitlock and Dawson, 1990). *Metasequoia* was still present although less abundant than
992 in the Eocene. Still younger, deposits known as the Beaufort Formation and tentatively
993 dated to about 8–3 Ma (and thus within Miocene to Pliocene times) record an extensive
994 riverside forest of pine, birch, and spruce, which lived throughout the Canadian Arctic
995 Archipelago before geologic processes formed many of the channels that now divide the
996 islands.

997 The relatively warm climates of the earlier Cenozoic altered to the colder times of
998 the Quaternary Ice Age, which was marked by cyclic growth and shrinkage of extensive
999 land ice, during the Pliocene (5–1.8 Ma). Climate changed although continental
1000 configurations remained similar to those of the present, and most Pliocene plant and
1001 animal species were similar to those that remain today. A well-documented warm period
1002 in the middle Pliocene (about 3 Ma), just before the planet transitioned into the
1003 Quaternary ice age, supported forests that covered large regions near the Arctic Ocean
1004 that are currently polar deserts. Fossils of *Arctica islandica* (a marine bivalve that does
1005 not live near seasonal sea ice) in marine deposits as young as 3.2 Ma on Meighen Island
1006 at 80°N., likely record the peak Pliocene mean warmth of the ocean (Fyles et al., 1991).
1007 As compared with recent conditions, warmer conditions then are widely indicated
1008 (Dowsett et al., 1994). At a site on Ellesmere Island, application of a novel technique for
1009 paleoclimatic reconstruction based on ring-width and isotopic measurements of wood

1010 suggests mean-annual temperatures 14°C warmer than recently (Ballantyne et al., 2006).
1011 Additional data from records of beetles and plants indicate mid-Pliocene conditions as
1012 much as 10°C warmer than recently for mean summer conditions, and even larger
1013 wintertime warming to a maximum of 15°C or more (Elias and Matthews, 2002).

1014 Much attention has been focused on learning the causes of the slow, bumpy slide
1015 from Cretaceous hothouse temperatures to the recent ice age. As discussed below,
1016 changes in greenhouse-gas concentrations appear to have played the dominant role, and
1017 linked changes in continental positions, in sea level, and in oceanic circulation also
1018 contributed.

1019 Based on general circulation models of climate, Barron et al. (1993) found that
1020 continental position had little effect on temperature difference between Cretaceous and
1021 modern temperatures (also see Poulsen et al., 1999 and references therein). Years later,
1022 Donnadieu et al. (2006), using more sophisticated climate modeling, found that
1023 continental motions and their effects on atmospheric and oceanic circulation modified
1024 global average temperature by almost 4°C from Early to Late Cretaceous; this result does
1025 not compare directly with modern conditions, but it does suggest that continental motions
1026 can notably affect climate. However, despite much effort, modeling does not indicate that
1027 the motion of continents by itself can explain either the long-term cooling trend from the
1028 Cretaceous to the ice age or the “wiggles” within that cooling.

1029 The direct paleoclimatic data provide one interesting perspective on the role of
1030 oceanic circulation in the warmth of the later Eocene. When the Arctic Ocean was filled
1031 with water ferns living in “brackish” water (less salty than normal marine water) in an
1032 ocean that was ice-free or nearly so, the oceanic currents reaching the near-surface Arctic

1033 Ocean must have been greatly weakened relative to today for the fresh water to persist.
1034 Thus, heat transport by oceanic currents cannot explain the Arctic-Ocean warmth of that
1035 time. The resumption of stronger currents and normal salinity was accompanied by a
1036 warming of about 3°C (Brinkhuis et al., 2006), important but not dominant in the
1037 temperature difference between then and now.

1038 As discussed in section 4.2.4, the atmospheric CO₂ concentration has changed
1039 during tens of millions of years in response to many processes, and especially to those
1040 processes linked to plate tectonics and perhaps also to biological evolution. Many lines of
1041 proxy evidence (see Royer, 2006) show that atmospheric CO₂ was higher in the warm
1042 Cretaceous than it was recently, and that it subsequently fell in parallel with the cooling
1043 (Figure 5.24). Furthermore, models find that the changing CO₂ concentration is sufficient
1044 to explain much of the cooling (e.g., Bice et al., 2006; Donnadieu et al., 2006).

1045

1046 FIGURE 5.24 NEAR HERE

1047

1048 A persistent difficulty is that models driven by reconstructed CO₂ tend to
1049 underestimate Arctic warmth (e.g., Sloan and Barron, 1992). Many possible explanations
1050 have been offered for this situation: underestimation of CO₂ levels (Shellito et al., 2003;
1051 Bice et al., 2006); an enhanced greenhouse effect from polar stratospheric clouds during
1052 warm times (Sloan and Pollard, 1998; Kirk-Davidoff et al., 2002); changed planetary
1053 obliquity (Sewall and Sloan, 2004); reduced biological productivity that provided fewer
1054 cloud-condensation nuclei and thus fewer reflective clouds (Kump and Pollard, 2008);
1055 and greater heat transport by tropical cyclones (Korty et al., 2008). Several of these

1056 mechanisms use feedbacks not normally represented in climate models and that serve to
1057 amplify warming in the Arctic. Consideration of the literature cited above and of
1058 additional materials points to some combination of stronger greenhouse-gas forcing (see
1059 Alley, 2003 for a review) and to stronger long-term feedbacks than typically are included
1060 in models, rather than to large change in Earth's orbit, although that cannot be excluded.

1061 It is thought that greenhouse gases were the primary control on Arctic temperature
1062 changes because the warmth of the Paleocene-Eocene Thermal Maximum took place in
1063 the absence of any ice—and therefore the absence of any ice-albedo or snow-albedo
1064 feedbacks. As described above (see Sluijs et al., 2008 for an extensively referenced
1065 summary of the event together with new data pertaining to the Arctic), this thermal
1066 maximum was achieved by a rapid (within a few centuries or less), widespread warming
1067 coincident with a large increase in atmospheric greenhouse-gas concentrations from a
1068 biological source (whether from sea-floor methane, living biomass, soils, or other sources
1069 remains debated). Following the thermal maximum, the anomalous warmth decayed more
1070 slowly and the extra greenhouse gases dissipated for tens of thousands of years, to
1071 roughly 100,000 years ago. The event in the Arctic seems to have been positioned within
1072 a longer interval of restricted oceanic circulation into the Arctic Ocean (Sluijs et al.,
1073 2008), and it was too fast for any notable effect of plate tectonics or evolving life. The
1074 reconstructed CO₂ change thus is strongly implicated in the warming (e.g., Zachos et al.,
1075 2008).

1076 Taken very broadly, the Arctic changes parallel the global ones during the
1077 Cenozoic, except that changes in the Arctic were larger than globally averaged ones (e.g.,
1078 Sluijs et al., 2008). The global changes parallel changing atmospheric carbon-dioxide

1079 concentrations, and changing CO₂ is the likely cause of most of the temperature change
1080 (e.g., Royer, 2006; Royer et al., 2007).

1081 The well-documented warmth of the Pliocene is not fully explained. This interval
1082 is recent enough that continental positions were substantially the same as today. As
1083 reviewed by Jansen et al. (2007), many reconstructions show notable Arctic warmth but
1084 little low-latitude change; however, recent work suggests the possibility of low-latitude
1085 warmth as well (Haywood et al., 2005). Reconstructions of Pliocene atmospheric CO₂
1086 concentration (reviewed by Royer, 2006) generally agree with each other within the
1087 considerable uncertainties, but they allow values above, similar to, or even below the
1088 typical levels just before major human influence. Data remain equivocal on whether the
1089 ocean transported more heat during Pliocene warmth (reviewed by Jansen et al., 2007).
1090 The high-latitude warmth thus may have originated primarily from changes in
1091 greenhouse-gas concentrations in the atmosphere, or from changes in oceanic or
1092 atmospheric circulation, or from some combination, perhaps with a slight possibility that
1093 other processes also contributed.

1094

1095 **5.4.2 The Early Quaternary: Ice-Age Warm Times**

1096 A major reorganization of the climate system occurred between 3.0 and 2.5 Ma.
1097 As a result, the first continental ice sheets developed in the North American and Eurasian
1098 Arctic and marked the onset of the Quaternary Ice Ages (Raymo, 1994). For the first 1.5–
1099 2.0 Ma, ice age cycles appeared at a 41 k.y. interval, and the climate oscillated between
1100 glacial and interglacial states (Figure 5.25). A prominent but apparently short-lived
1101 interglacial (warm interval) about 2.4 Ma is recorded especially well in the Kap

1102 K benhavn Formation, a 100-m-thick sequence of estuarine sediments that covered an
1103 extensive lowland area near the northern tip of Greenland (Funder et al., 2001).

1104

1105 FIGURE 5.25 NEAR HERE

1106

1107 The rich and well-preserved fossil fauna and flora in the Kap K benhavn
1108 Formation (Figure 5.26) record warming from cold conditions into an interglacial and
1109 then subsequent cooling during 10,000–20,000 years. During the peak warmth, forest
1110 trees reached the Arctic Ocean coast, 1000 kilometers (km) north of the northernmost
1111 trees today. Based on this warmth, Funder et al. (2001) suggested that the Greenland Ice
1112 Sheet must have been reduced to local ice caps in mountain areas (Figure 5.26a) (see
1113 Chapter 7, Greenland Ice Sheet). Although finely resolved time records are not available
1114 throughout the Arctic Ocean at that time, by analogy with present faunas along the
1115 Russian coast, the coastal zone would have been ice-free for 2 to 3 months in summer.
1116 Today this coast of Greenland experiences year-round sea ice, and models of diminishing
1117 sea ice in a warming world generally indicate long-term persistence of summertime sea
1118 ice off these shores (e.g., Holland et al., 2006). Thus, the reduced sea ice off northern
1119 Greenland during deposition of the Kap K benhavn Formation suggests a widespread
1120 warm time in which Arctic sea ice was much diminished.

1121

1122 FIGURE 5.26 NEAR HERE

1123

1124 During Kap København times, precipitation was higher and temperatures were
1125 warmer than at the peak of the current interglacial about 7 ka, and the temperature
1126 difference were larger during winter than during summer. Higher temperatures during
1127 deposition of the Kap København were not caused by notably greater solar insolation,
1128 owing to the relative repeatability of the Milankovitch variations during millions of years
1129 (e.g., Berger et al., 1992). As discussed above, uncertainties in estimation of atmospheric
1130 carbon-dioxide concentration, ocean heat transport, and perhaps other factors at the time
1131 of the Kap København Formation are sufficiently large to preclude strong conclusions
1132 about the causes of the unusual warmth.

1133 Potentially correlative records of warm interglacial conditions are found in
1134 deposits on coastal plains along the northern and western shores of Alaska. High sea
1135 levels during interglaciations repeatedly flooded the Bering Strait, and they rapidly
1136 modified the configuration of the coastlines, altered regional continentality (isolation
1137 from the moderating influence of the sea), and reinvigorated the exchange of water
1138 masses between the North Pacific, Arctic, and North Atlantic oceans. Since the first
1139 submergence of the Bering Strait about 5.5–5 Ma (Marincovich and Gladenkov, 2001),
1140 this marine gateway has allowed relatively warm Pacific water from as far south as
1141 northern Japan to reach as far north as the Beaufort Sea (Brigham-Grette and Carter,
1142 1992). The Gubik Formation of northern Alaska records at least three warm high sea
1143 stands in the early Quaternary (Figure 5.27). During the Colvillian transgression, about
1144 2.7 Ma, the Alaskan Coastal Plain supported open boreal forest or spruce-birch woodland
1145 with scattered pine and rare fir and hemlock (Nelson and Carter, 1991). Warm marine
1146 conditions are confirmed by the general character of the ostracode fauna, which includes

1147 *Pterygocythereis vannieuwenhuisei* (Brouwers, 1987), an extinct species of a genus
1148 whose modern northern limit is the Norwegian Sea and which, in the northwestern
1149 Atlantic Ocean, is not found north of the southern cold-temperate zone (Brouwers, 1987).
1150 Despite the high sea level and relative warmth indicated by the Colvillian transgression,
1151 erratics (rocks not of local origin) in Colvillian deposits southwest of Barrow, Alaska,
1152 indicate that glaciers then terminated in the Arctic Ocean and produced icebergs large
1153 enough to reach northwest Alaska at that time.

1154

1155 FIGURE 5.27 NEAR HERE

1156

1157 Subsequently, the Bigbendian transgression (about 2.5 Ma) was also warm, as
1158 indicated by rich molluscan faunas such as the gastropod *Littorina squalida* and the
1159 bivalve *Clinocardium californiense* (Carter et al., 1986). The modern northern limit of
1160 both of these mollusk species is well to the south (Norton Sound, Alaska). The presence
1161 of sea otter bones suggests that the limit of seasonal ice on the Beaufort Sea was
1162 restricted during the Bigbendian interval to positions north of the Colville River and thus
1163 well north of typical 20th-century positions (Carter et al., 1986); modern sea otters cannot
1164 tolerate severe seasonal sea-ice conditions (Schneider and Faro, 1975).

1165 The youngest of these early Quaternary events of high sea level is the
1166 Fishcreekian transgression (about 2.1–2.4 Ma), suggested to be the same age as the Kap
1167 Kobenhavn Formation on Greenland (Brigham-Grette and Carter, 1992). However, age
1168 control is not complete, and Brigham (1985) and Goodfriend et al. (1996) suggested that
1169 the Fishcreekian could be as young as 1.4 Ma. This deposit contains several mollusk

1170 species that currently are found only to the south. Moreover, sea otter remains and the
1171 intertidal gastropod *Littorina squalida* at Fish Creek suggest that perennial sea ice was
1172 absent or severely restricted during the Fishcreekian transgression (Carter et al., 1986).
1173 Correlative deposits rich in mollusk species that currently live only well to the south are
1174 reported from the coastal plain at Nome, Alaska (Kaufman and Brigham-Grette, 1993).

1175 The available data clearly indicate episodes of relatively warm conditions that
1176 correlate with high sea levels and reduced sea ice in the early Quaternary. The high sea
1177 levels suggest melting of land ice (see Chapter 7, Greenland Ice Sheet). Thus the
1178 correlation of warmth with diminished ice on land and at sea (see Chapter 8, Arctic sea
1179 ice)—indicated by recent instrumental observations, model results, and data from other
1180 time intervals—is also found for this time interval. Improved time resolution of histories
1181 of forcing and response will be required to assess the causes of the changes, but estimates
1182 of forcings indicate that they were relatively moderate and thus that the strong Arctic
1183 amplification of climate change was active in these early Quaternary events.

1184

1185 **5.4.3 The Mid-Pleistocene Transition: 41 ka and 100 ka worlds**

1186 Since the late Pliocene, the cyclical waxing and waning of continental ice sheets
1187 have dominated global climate variability. The variations in sunshine caused by features
1188 of Earth's orbit have been very important in these ice-sheet changes, as described in
1189 Chapter 4 (paleoclimate concepts).

1190 After the onset of glaciation in North America about 2.7 Ma (Raymo, 1994), ice
1191 grew and shrank as Earth's obliquity (tilt) varied in its 41 k.y. cycle. But between 1.2 and
1192 0.7 Ma, the variations in ice volume became larger and slower, and an approximately

1193 100-k.y. period has dominated especially during the last 700 k.y. or so (Figure 5.25).
1194 Although Earth's eccentricity varies with an approximately 100-k.y. period, this variation
1195 does not cause as much change in sunshine in the key regions of ice growth as did the
1196 faster cycles, so the reasons for the dominant 100-k.y. period in ice volume remain
1197 obscure. Roe and Allen (1999) assessed six different models of this behavior and found
1198 that all fit the data rather well. The record is still too short to allow the data to
1199 demonstrate the superiority of any one model.

1200 Models for the 100-k.y. variability commonly assign a major role to the ice sheets
1201 themselves and especially to the Laurentide Ice Sheet on North America, which
1202 dominated the total global change in ice volume (e.g., Marchant and Denton, 1996). For
1203 example, Marshall and Clark (2002) modeled the growth and shrinkage of the Laurentide
1204 Ice Sheet and found that during growth the ice was frozen to the bed beneath and unable
1205 to move rapidly. After many tens of thousands of years, ice had thickened sufficiently
1206 that it trapped Earth's heat and thawed the bed, which allowed faster flow. Faster flow of
1207 the ice sheet lowered the upper surface, which allowed warming and melting (see Chapter
1208 7, Greenland Ice Sheet). Behavior such as that described could cause the main variations
1209 of ice volume to be slower than the main variations in sunshine caused by Earth's orbital
1210 features, and the slow-flowing ice might partly ignore the faster variations in sunshine
1211 until the shift to faster flow allowed a faster response. Note that this explanation remains
1212 a hypothesis, and other possibilities exist. Alternative hypotheses require interactions in
1213 the Southern Ocean between the ocean and sea ice and between the ocean and the
1214 atmosphere (Gildor et al., 2002). For example, Toggweiler (2008) suggested that because
1215 of the close connection between the southern westerly winds and meridional overturning

1216 circulation in the Southern Ocean, shifts in wind fields may control the exchange of CO₂
1217 between the ocean and the atmosphere. Carbon models support the notion that weathering
1218 and the burial of carbonate can be perturbed in ways that alter deep ocean carbon storage
1219 and that result in 100 k.y. CO₂ cycles (Toggweiler, 2008). Others have suggested that 100
1220 k.y. cycles and CO₂ might be controlled by variability in obliquity cycles (i.e., two or
1221 three 41 k.y. cycles (Huybers, 2006) or by variable precession cycles (altering the 19 k.y.
1222 and 23 k.y. cycles (Raymo, 1997)). Ruddimann (2006) recently furthered these ideas but
1223 suggested that since 900 ka, CO₂-amplified ice growth continued at the 41 k.y. intervals
1224 but that polar cooling dampened ice ablation. His CO₂-feedback hypothesis suggests a
1225 mechanism that combines the control of 100 k.y. cycles with precession cycles (19 k.y.
1226 and 23 k.y.) and with tilt cycles (41 k.y.). The cause of the switch in the length of climate
1227 cycles from about 41 k.y. to about 100 k.y, known as the mid-Pleistocene transition, also
1228 remains obscure. This transition is of particular interest because it does not seem to have
1229 been caused by any major change in Earth's orbital behavior, and so the transition may
1230 reflect some fundamental threshold within the climate system.

1231 The mid-Pleistocene transition may be related to continuation of the gradual
1232 global cooling from the Cretaceous, as described above (Raymo et al., 1997; 2006;
1233 Ruddiman, 2003). If, for example, the 100-k.y. cycle requires that the Laurentide Ice
1234 Sheet grow sufficiently large and thick to trap enough of Earth's heat to thaw the ice-
1235 sheet bed (Marshall and Clark, 2002), then long-term cooling may have reached the
1236 threshold at which the ice sheet became large enough.

1237 However, such a cooling model does not explain the key observation (Clark et al.,
1238 2006) that the ice sheets of the last 700 k.y. configured a larger volume (Clark et al.,

1239 2006) into a smaller area (Boellstorff, 1978; Balco et al., 2005a,b) than was true of earlier
1240 ice sheets. Clark and Pollard (1998) used this observation to argue that the early
1241 Laurentide Ice Sheet must have been substantially lower in elevation than in the late
1242 Pleistocene, possibly by as much as 1 km. Clark and Pollard (1998) suggested that the
1243 tens of millions of warm years back to the Cretaceous and earlier had produced thick
1244 soils and broken-up rocks below the soil. When glaciations began, the ice advanced over
1245 these water-saturated soils, which deformed easily. Just as grease on a griddle allows
1246 batter poured on top to spread easily into a wide, thin pancake, deformation of the soils
1247 beneath the growing ice (Alley, 1991) would have produced an extensive ice sheet that
1248 did not contain a large volume of ice. As successive ice ages swept the loose materials to
1249 the edges of the ice sheet, and as rivers removed most of the materials to the sea, hard
1250 bedrock was exposed in the central region. And, just as the bumps and friction of an
1251 ungreased waffle iron slow spreading of the batter to give a thicker, not-as-wide breakfast
1252 than on a greased griddle, the hard, bumpy bedrock produced an ice sheet that did not
1253 spread as far but which contained more ice.

1254 Other hypotheses also exist for these changes. A complete explanation of the
1255 onset of extensive glaciation on North America and Eurasia as well as Greenland about
1256 2.8 Ma, or of the transition from 41 k.y. to 100 k.y. ice age cycles, remains the object of
1257 ongoing investigations.

1258

1259 **5.4.4 A link between ice volume, atmospheric temperature and greenhouse**
1260 **gases**

1261 The globally-averaged temperature change during one of the large 100-k.y. ice-
1262 age cycles was about 5°–6°C (Jansen et al., 2007). The larger changes were measured in
1263 the Arctic and close to the ice sheets, such as a change of 21°–23°C atop the Greenland
1264 ice sheet (Cuffey et al., 1995). The total change in sunshine reaching the planet during
1265 these cycles was near zero, and the orbital features served primarily to move sunshine
1266 from north to south and back, or from equator to poles and back, depending on the cycle
1267 considered (see Chapter 4, paleoclimate concepts).

1268 As discussed by Jansen et al. (2007), and in section 5.2.6 above, many factors
1269 probably contributed to the large temperature change despite very small global change in
1270 total sunshine. Cooling produced growth of reflective ice that reduced the amount of
1271 sunshine absorbed by the planet. Complex changes especially in the ocean reduced
1272 atmospheric carbon dioxide, and both oceanic and terrestrial changes reduced
1273 atmospheric methane and nitrous oxide, all of which are greenhouse gases; the changes in
1274 carbon dioxide were most important. Various changes produced additional dust that
1275 blocked sunshine from reaching the planet (e.g., Mahowald et al., 2006). Cooling caused
1276 regions formerly forested to give way to grasslands or tundra that also reflected more
1277 sunshine. While Earth's orbit features drove the ice-age cycles, these feedbacks are
1278 required to provide quantitatively accurate explanations of the changes.

1279 The relation between climate and carbon dioxide has been relatively constant for
1280 at least 650,000 years (Siegenthaler et al., 2005), and the growth and shrinkage of ice,
1281 cooling and warming of the globe, and other changes have repeated along similar
1282 although not identical paths. However, some of the small differences between successive
1283 cycles are of interest, as discussed next.

1284

1285 **5.4.5 Marine Isotopic Stage 11 – a long interglaciation**

1286 Following the mid-Pleistocene transition, the growth and decay of ice sheets
1287 followed a 100 k.y. cycle: brief, warm interglaciations lasted about 10 k.y., after that ice
1288 progressively extended, and then the icy interval terminated rapidly by the transition into
1289 the next warm interglaciation (e.g., Kellogg, 1977; Ruddiman et al., 1986; Jansen et al.,
1290 1988; Bauch and Erlenkeuser, 2003; Henrich and Baumann, 1994). As discussed above,
1291 this 100 k.y. cycle may be linked to the 100 k.y. variation of the eccentricity, or out-of-
1292 roundness, of Earth's orbit about the sun, although other explanations are possible.

1293 The eccentricity exhibits an additional cycle of just greater than 400,000 years,
1294 such that the orbit goes from almost round to more eccentric to almost round in about
1295 100,000 years, but the maximum eccentricity reached in this 100,000-year cycle increases
1296 and decreases within a 400,000-year cycle (Berger and Loutre, 1991; Loutre, 2003).
1297 When the orbit is almost round, there is little effect from Earth's precession, which
1298 determines whether Earth is closer to the sun or farther from the sun during a particular
1299 season such as northern summer. About 400,000 years ago, during marine isotope stage
1300 (MIS) 11, the 400,000-year cycle caused a nearly round orbit to persist. The interglacial
1301 of MIS 11 lasted longer than previous or subsequent interglacials (see Droxler et al., 2003
1302 and references therein; Kandiano and Bauch, 2007; Jouzel et al., 2007), perhaps because
1303 the summer sunshine (insolation) at high northern latitudes did not become low enough at
1304 the end of the first 10,000 years of the interglacial to allow ice growth at high northern
1305 latitudes—because the persistently nearly round orbit (i.e., of low eccentricity) prevented
1306 adequate cooling during northern summer (Figure 5.28).

1307

1308

FIGURE 5.28 NEAR HERE

1309

1310 As discussed in Chapter 7 (Greenland Ice Sheet), indications of Arctic and
1311 subarctic temperatures at this time versus more-recent interglacials are inconsistent (also
1312 see Stanton-Frazee et al., 1999; Bauch et al., 2000; Droxler and Farrell, 2000; Helmke
1313 and Bauch, 2003). Sea level seems to have been higher at this time than at any time since,
1314 and data from Greenland are consistent with notable shrinkage or loss of the ice sheet
1315 accompanying the notable warmth, although the age of this shrinkage is not constrained
1316 well enough to be sure that the warm time recorded was indeed MIS 11 (Chapter 7).

1317

1318 **5.4.6 Marine Isotopic Stage (MIS) 5e: The Last Interglaciation**

1319 The warmest millennia of at least the past 250,000 years occurred during MIS 5,
1320 and especially during the warmest part of that interglaciation, MIS 5e (e.g., McManus et
1321 al., 1994; Fronval and Jansen, 1997; Bauch et al., 1999; Kukla, 2000). At that time global
1322 ice volumes were smaller than they are today, and Earth's orbital parameters aligned to
1323 produce a strong positive anomaly in solar radiation during summer throughout the
1324 Northern Hemisphere (Berger and Loutre, 1991). Between 130 and 127 ka, the average
1325 solar radiation during the key summer months (May, June, and July) was about 11%
1326 greater than solar radiation at present throughout the Northern Hemisphere, and a slightly
1327 greater anomaly, 13%, has been measured over the Arctic. Greater solar energy in
1328 summer, melting of the large Northern Hemisphere ice sheets, and intensification of the

1329 North Atlantic Drift (Chapman et al., 2000; Bauch and Kandiano, 2007) combined to
1330 reduce Arctic Ocean sea ice, to allow expansion of boreal forest to the Arctic Ocean
1331 shore throughout large regions, to reduce permafrost, and to melt almost all glaciers in
1332 the Northern Hemisphere (CAPE Project Members, 2006).

1333 High solar radiation in summer during MIS 5e, amplified by key boundary-
1334 condition feedbacks (especially sea ice, seasonal snow cover, and atmospheric water
1335 vapor; see above), collectively produced summer temperature anomalies 4°–5°C above
1336 present over most Arctic lands, substantially above the average Northern Hemisphere
1337 summer temperature anomaly (0°–2°C above present; CLIMAP Project Members, 1984;
1338 Bauch and Erlenkeuser, 2003). MIS 5e demonstrates the strength of positive feedbacks
1339 on Arctic warming (CAPE Project Members, 2006; Otto-Bleisner et al., 2006).

1340

1341 **5.4.6a Terrestrial MIS 5e records** At high northern latitudes, summer
1342 temperatures exert the dominant control on glacier mass balance, unless they are
1343 accompanied by strong changes in precipitation (e.g., Oerlemans, 2001; Denton et al.,
1344 2005; Koerner, 2005). Summer temperature is also the most effective predictor of most
1345 biological processes, although seasonality and the availability of moisture may influence
1346 some biological parameters such as dominance by evergreen or by deciduous vegetation
1347 (Kaplan et al., 2003). For these reasons, most studies of conditions during MIS 5e have
1348 focused on reconstructing summer temperatures. Terrestrial MIS 5e climate, especially,
1349 has been reconstructed from diagnostic assemblages of biotic proxies preserved in lake,
1350 peat, river, and shallow marine archives and from isotopic changes preserved in ice cores
1351 and carbonate deposits in lakes. Estimated winter and summer temperatures, and hence

1375 Qualitative precipitation estimates for most other sectors indicate wetter conditions than
1376 in the Holocene.

1377

1378 **5.4.6b Marine MIS 5e records** Low sedimentation rates in the central Arctic
1379 Ocean and the rare preservation of carbonate fossils limit the number of sites at which
1380 MIS 5e can be reliably identified in sediment cores. MIS 5e sediments from the central
1381 Arctic Ocean usually contain high concentrations of planktonic (surface-dwelling)
1382 foraminifers and coccoliths, which indicate a reduction in summer sea-ice coverage that
1383 permitted increased biological productivity (Gard, 1993; Spielhagen et al., 1997; 2004;
1384 Jakobsson et al., 2000; Backman et al., 2004; Polyak et al., 2004; Nørgaard-Pedersen et
1385 al., 2007a,b). However, occasional dissolution of carbonate fossils complicates the
1386 interpretation of microfossil concentrations. Also, marine sediments from MIS 5a,
1387 slightly younger and cooler than MIS 5e, sometimes have higher microfossil
1388 concentrations than do MIS 5e sediments (Gard, 1986; 1987).

1389 Arctic Ocean sediment cores recently recovered from the Lomonosov Ridge,
1390 north of Greenland, have revived the discussion of MIS 5e conditions in the Arctic
1391 Ocean. Unusually high concentrations of a subpolar foraminifer species, one which
1392 usually dwells in waters with temperatures well above freezing, were found in MIS 5e
1393 zones and interpreted to indicate warm interglacial conditions and much reduced sea-ice
1394 cover in the interior Arctic Ocean (Nørgaard-Pedersen et al., 2007a,b). Interpretation of
1395 these and other microfossils is complicated by the strong vertical stratification in the
1396 Arctic Ocean; today, warm Atlantic water (temperatures greater than 1°C) is in most
1397 areas isolated from the atmosphere by a relatively thin layer of cold (less than 1°C)

1398 fresher water; this cold water limits the transfer of heat to the atmosphere. It is not always
1399 possible to determine whether warm-water foraminifers found in marine sediment from
1400 the Arctic Ocean lived in warm waters that remained isolated from the atmosphere below
1401 the cold surface layer, or whether the warm Atlantic water had displaced the cold surface
1402 layer and was interacting with the atmosphere and affecting its energy balance.

1403 Landforms and fossils from the western Arctic and Bering Strait indicate vastly
1404 reduced sea ice during MIS 5 (Figure 5.30). The winter sea-ice limit is estimated to have
1405 been as much as 800 km farther north than its average 20th-century position, and summer
1406 sea ice may at times have been absent (Brigham-Grette and Hopkins, 1995). These
1407 reconstructions are consistent with the northward migration of treeline by hundreds of
1408 kilometers throughout much of Alaska and nearby Chukotka and with the elimination of
1409 tundra from Chukotka to the Arctic Ocean coast (Lozhkin and Anderson, 1995).

1410

1411 FIGURE 5.30 NEAR HERE

1412

1413 Sufficient data are not yet available to allow unambiguous reconstruction of MIS
1414 5e conditions in the central Arctic Ocean. Key uncertainties are related to the extent and
1415 duration of Arctic Ocean sea ice. The vertical structure of the upper 500 m of the water
1416 column is also climatically important but poorly known, in particular whether the strong
1417 vertical stratification characteristic of the modern regime persisted throughout MIS 5e, or
1418 whether reduced sea ice and changes in the hydrologic cycle and winds destabilized this
1419 stratification and allowed Atlantic water to reside at the surface in larger areas of the
1420 Arctic Ocean.

1421

1422 **5.4.7 MIS 3 Warm Intervals**

1423 The temperature and precipitation history of MIS 3 (about 70–30 ka) is difficult to
1424 reconstruct because of the paucity of continuous records and the difficulty in providing a
1425 secure time frame. The $\delta^{18}\text{O}$ record of temperature change over the Greenland ice sheet
1426 and other ice-core data show that the North Atlantic region experienced repeated episodes
1427 of rapid, high-magnitude climate change, that temperatures rapidly increased by as much
1428 as 15°C (reviewed by Alley, 2007 and references therein), and that each warm period
1429 lasted several hundred to a few thousand years. These brief climate excursions are found
1430 not only in the Greenland Ice Sheet but are also recorded in cave sediments in China
1431 (Wang et al., 2001; Dykoski, et al., 2005) and in high-resolution marine records off
1432 California (Behl and Kennett, 1996), and in the Caribbean Sea’s Cariaco Basin (Hughen
1433 et al., 1996.), the Arabian Sea (Schulz et al., 1998) and the Sea of Okhotsk (Nürnberg and
1434 Tiedmann, 2004), among many other sites. The ice-core records from Greenland contain
1435 indications of climate change in many regions on the same time scale (for example, the
1436 methane trapped in ice-core bubbles was in part produced in tropical wetlands and was
1437 essentially all produced beyond the Greenland ice sheet; Severinghaus et al., 1998).
1438 These ice-core records demonstrate clearly that the climate-change events were
1439 synchronous throughout widespread areas, and that the ages of events from many regions
1440 agree within the stated uncertainties. These events were thus hemispheric to global in
1441 nature (see review by Alley, 2007) and are considered a sign of large-scale coupling
1442 between the ocean and the atmosphere (Bard, 2002). The cause of these events is still
1443 debated. However, Broecker and Hemming (2001) and Bard (2002) among others

1444 suggested that they were likely the result of major and abrupt reorganizations of the
1445 ocean's thermohaline circulation, probably related to ice sheet instabilities that
1446 introduced large quantities of fresh water into the North Atlantic (Alley, 2007). Such
1447 large and abrupt oscillations, which were linked to changes in North Atlantic surface
1448 conditions and probably to the large-scale oceanic circulation, persisted into the Holocene
1449 (MIS 1); the youngest was only about 8.2 ka (Alley and Ágústsdóttir, 2005). However, it
1450 appears that the abrupt 8.2 ka cooling was linked to an ice-age cause, a catastrophic flood
1451 from a very large lake that had been dammed by the melting Laurentide Ice Sheet.

1452 Within MIS 3, land ice was somewhat reduced compared with the colder times of
1453 MIS 2 and MIS 4, but Arctic temperatures generally were much lower and ice more
1454 extensive than in MIS 1 (with certain exceptions). Sea level was lower at that time, the
1455 coastline was well offshore in many places, and the increased continentality may have
1456 contributed to warmer summertime temperatures that presumably were offset by colder
1457 wintertime temperatures.

1458 For example, on the New Siberian Islands in the East Siberian Sea, Andreev et al.
1459 (2001) documented the existence of graminoid-rich tundra thought to have covered wide
1460 areas of the emergent shelf while summer temperatures were perhaps as much as 2°C
1461 warmer than during the 20th century. At Elikchan 4 Lake in the upper Kolyma drainage,
1462 the sediment record contains at least three intervals (especially one about 38 ka) when
1463 summer temperatures and treeline reached late Holocene conditions (Anderson and
1464 Lozhkin, 2001). Insect faunas nearby in the lower Kolyma are thought to have thrived in
1465 summers that were 1°–4.5°C warmer than recently for similar intervals of MIS 3 Alfimov
1466 et al., 2003). In general, variable paleoenvironmental conditions were typical of the

1467 traditional Karaginskii-MIS 3 period throughout Arctic Russia; however, stratigraphic
1468 confusion within the limits of radiocarbon-dating precludes the widespread correlation of
1469 events.

1470 Relative warmth during MIS 3 appears to have been strongest in eastern Beringia;
1471 some evidence suggests that between 45 and 33 ka temperatures were only 1°–2°C lower
1472 than at present (Elias, 2007). The warmest interval in interior Alaska is known as the Fox
1473 Thermal Event, about 40–35 ka, which was marked by spruce forest tundra (Anderson
1474 and Lozhkin, 2001). Yet in the Yukon forests were most dense a little earlier, about 43–
1475 39 ka. In general (Anderson and Lozhkin, 2001), the warmest interstadial interval in all
1476 of Beringia possibly was 44–35 ka; it is well represented in proxies from interior sites
1477 and little or no vegetation response in areas closest to Bering Strait. Climatic conditions
1478 in eastern Beringia appear to have been harsher than modern conditions for all of MIS 3.
1479 In contrast, MIS 3 climates of western Beringia achieved modern or near modern
1480 conditions during several intervals. Moreover, although the transition from MIS 3 to MIS
1481 2 was clearly marked by a transition from warm-moist to cold-dry conditions in western
1482 Beringia, this transition is absent or subtle in all but a few records in Alaska (Anderson
1483 and Lozhkin, 2001).

1484

1485 **5.4.8 MIS 2, The Last Glacial Maximum (30 to 15 ka)**

1486 The last glacial maximum was particularly cold both in the Arctic and globally,
1487 and it provides useful constraints on the magnitude of Arctic amplification (see below).
1488 During peak cooling of the last glacial maximum, planetary temperatures were about 5°–
1489 6°C lower than at present (Farrera et al., 1999; Braconnot et al., 2007, Jansen et al.,

1490 2007), whereas Arctic temperatures in central Greenland were depressed more than 20°C
1491 (Cuffey et al., 1995; Dahl-Jensen et al., 1998) and similarly in Beringia (Elias et al.,
1492 1996).

1493

1494 **5.4.9 MIS 1, The Holocene: The Present Interglaciation**

1495 In the face of rising solar energy in summer that was tied to orbital features and to
1496 rising greenhouse gases, Northern Hemisphere ice sheets began to recede from near their
1497 largest extent shortly after 20 ka, and the rate of recession noticeably increased after
1498 about 16 ka (see, e.g., Alley et al., 2002 for the timing of various events during the
1499 deglaciation). Most coastlines became ice-free before 12 ka, and ice continued to melt
1500 rapidly as summer insolation reached a peak (about 9% above modern insolation) about
1501 11 ka. The transition from MIS 2 to MIS 1, which marks the start of the Holocene
1502 interglaciation, is commonly placed at the abrupt termination of the cold event called the
1503 Younger Dryas; that termination recently was estimated at about 11.7 ka (Rasmussen et
1504 al., 2006).

1505 A wide variety of evidence from terrestrial and marine archives indicates that
1506 peak Arctic summertime warmth was achieved during the early Holocene, when most
1507 regions of the Arctic experienced sustained temperatures that exceeded observed 20th
1508 century values. This period of peak warmth, which is geographically variable in its
1509 timing, is generally referred to as the Holocene Thermal Maximum. The ultimate driver
1510 of the warming was orbital forcing, which produced increased summer solar radiation
1511 across the Northern Hemisphere. At 70°N., insolation in June now is near a local
1512 minimum (the maximum was recorded about 11–12 ka). June insolation about 4 ka was

1513 about 15 W/m² larger than recently, and June insolation at the Holocene peak was about
1514 45 W/m² larger than recently, for a total change of about 10% (Figure 5.31; Berger and
1515 Loutre, 1991). Winter (January) insolation about 11 ka was only slightly lower than
1516 today, in large part because there is almost zero insolation that far north in January.

1517

1518

FIGURE 5.31 NEAR HERE

1519

1520 By 6 ka, sea level and ice volumes were close to those observed more recently,
1521 and climate forcings such as atmospheric carbon-dioxide concentration differed little
1522 from pre-industrial conditions (e.g., Jansen et al., 2007). (The exception is that far-
1523 northern summer insolation steadily decreased throughout the Holocene.) High-resolution
1524 (decades to centuries) archives containing many climate proxies are available for most of
1525 the Holocene throughout the Arctic. Consequently, the mid- to late-Holocene record
1526 allows evaluation of the range of natural climate variability and of the magnitude of
1527 climate change in response to relatively small changes in forcings.

1528

1529

5.4.9a The Holocene Thermal Maximum

1530

1531

1532

1533

1534

1535

Many of the Arctic paleoenvironmental records for the Holocene Thermal
Maximum appear to have recorded primarily summertime conditions. Many different
proxies have been exploited to derive these reconstructions by use of biological indicators
such as pollen, diatoms, chironomids, dinoflagellate cysts, and other microfossils;
elemental and isotopic geochemical indexes from lacustrine sediments, marine sediments,
and ice cores; borehole temperatures; and age distributions of radiocarbon-dated tree

1536 stumps north of (or above) current treeline, marine mollusks, and whale bones (Kaufman
1537 et al., 2004).

1538 A recent synthesis of 140 Arctic paleoclimatic and paleoenvironmental records
1539 extending from Beringia westward to Iceland (Kaufman et al., 2004) outlines the nature
1540 of the Holocene Thermal Maximum in the western Arctic (Figure 5.32). Fully 85% of the
1541 sites included in the synthesis contained evidence of a Holocene thermal maximum. Its
1542 average duration extended from 2100 years in Beringia to 3500 years in Greenland. The
1543 interval 10–4 ka contains the greatest number of sites recording Holocene Thermal
1544 Maximum conditions and the greatest spatial extent of those conditions in the western
1545 Arctic (Figure 5.32b). In the western Arctic the timing of this thermal maximum begins
1546 and ends along a strong geographic gradient (Figure 5.32c). The thermal maximum began
1547 first in Beringia, where warmer-than-present summer conditions became established at
1548 14–13 ka. Intermediate ages for its initiation (10–8 ka) are apparent in the Canadian
1549 Arctic islands and in central Greenland. The Holocene Thermal Maximum on Iceland
1550 occurred a bit later, 8–6 ka. The onset on Svalbard was earlier, by 10.8 ka (Svendsen and
1551 Mangerud, 1997). The latest general onset (7–4 ka) of Holocene Thermal Maximum
1552 conditions affected the continental portions of central and eastern Canada experienced.
1553 Similarly, the earliest termination of the Holocene Thermal Maximum occurred in
1554 Beringia, although most regions registered summer cooling by 5 ka. Much of the pattern
1555 of the onset of the Holocene Thermal Maximum can be explained at least in part by
1556 proximity to cold winds blowing off the melting Laurentide Ice Sheet in Canada, which
1557 depressed temperatures nearby until the ice melted back. Milankovitch cycling has also

1558 been suggested to explain the spatial variability of the Holocene Thermal Maximum
1559 (Maximova and Romanovsky, 1988).

1560

1561 **FIGURE 5.32 NEAR HERE**

1562

1563 Records for sea-ice conditions in the Arctic Ocean and adjacent channels have
1564 been developed by radiocarbon-dating indicators including the remains of open-water
1565 proxies such as whales and walrus, warm-water marine mollusks, and changes in the
1566 microfauna preserved in marine sediments. These reconstructions, presented in more
1567 detail in Chapter 8 (Arctic sea ice), parallel the terrestrial record for the most part. The
1568 data demonstrate that an increased mass of warm Atlantic water moved into the Arctic
1569 Ocean beginning about 11.5 ka. It peaked about 8–5 ka which, coupled with increased
1570 summer insolation, decreased the area of perennial sea-ice cover during the early
1571 Holocene. Decreased sea-ice cover in the western Arctic during the early Holocene also
1572 may be indicated by changes in concentrations of sodium from sea salt in the Penny Ice
1573 Cap (eastern Canadian Arctic; Fisher et al., 1998) and the Greenland Ice Sheet
1574 (Mayewski et al., 1997). In most regions, perennial sea ice increased in the late Holocene,
1575 although it has been suggested that sea ice declined in the Chukchi Sea (de Vernal et al.,
1576 2005), possibly in response to changing rates of Atlantic water inflow in Fram Strait.

1577 As summer temperatures increased through the early Holocene, in North America
1578 treeline expanded northward into regions formerly mantled by tundra, although the
1579 northward extent appears to have been limited to perhaps a few tens of kilometers beyond
1580 its recent position (Seppä et al., 2003; Gajewski and MacDonald, 2004). In contrast,

1581 treeline advanced much farther across the Eurasian Arctic. Tree macrofossils
1582 (Kremenetski et al., 1998; MacDonald et al., 2000a,b; 2007) collected at or beyond the
1583 current treeline indicate that tree genera such as birch (*Betula*) and larch (*Larix*) advanced
1584 beyond the modern limits of treeline across most of northern Eurasia between 11 and 10
1585 ka (Figures 5.33 and 5.34). Spruce (*Picea*) advanced slightly later than the other two
1586 genera. Interestingly, pine (*Pinus*), which now forms the conifer treeline in Fennoscandia
1587 and the Kola Peninsula, does not appear to have established appreciable forest cover at or
1588 beyond the present treeline in those regions at the far west of Europe until around 7 ka
1589 (MacDonald et al. 2000a). However, quantitative reconstructions of temperature from the
1590 Kola Peninsula and adjacent Fennoscandia suggest that summer temperatures were
1591 warmer than modern temperatures by 9 ka (Seppä and Birks, 2001; 2002; Hammarlund et
1592 al., 2002; Solovieva et al., 2005), and the development of extensive pine cover at and
1593 north of the present treeline appears to have been delayed relative to this warming. In the
1594 Taimyr Peninsula of Siberia and across nearby regions, the most northerly limit reached
1595 by trees during the Holocene was more than 200 km north of the current treeline. The
1596 treeline appears to have begun its retreat across northern Eurasia about 4 ka. The timing
1597 of the Holocene Thermal Maximum in the Eurasian Arctic overlaps the widest expression
1598 of the Holocene Thermal Maximum in the western Arctic (Figure 5.33), but it differs in
1599 two respects. The timing of onset and termination in Eurasia show much less variability
1600 than in North America, and the magnitude of the treeline expansion and retreat is far
1601 greater in the Eurasian Arctic. Fossil pollen and other indicators of vegetation or
1602 temperature from the northern Eurasian margin also support the contention of a
1603 prolonged warming and northern extension of treeline during the early through middle

1604 Holocene (see for example Hyvärinen, 1975; Seppä, 1996; Clayden et al., 1997; Velichko
1605 et al., 1997; Kaakinen and Eronen, 2000; Pisaric et al., 2001; Seppä and Birks, 2001,
1606 2002; Gervais et al., 2002; Hammarlund et al., 2002; Solovieva et al., 2005).

1607

1608 FIGURE 5.33 NEAR HERE

1609 FIGURE 5.34 NEAR HERE

1610

1611 Changes in landforms suggest that during the early to middle Holocene,
1612 permafrost in Siberia degraded. A synthesis of Russian data by Astakhov (1995) indicates
1613 that melting permafrost was apparent north of the Arctic Circle only in the European
1614 North, not in Siberia. In the Siberian North, permafrost partially thawed only very
1615 locally, and thawing was almost entirely confined to areas under thermokarst lakes that
1616 actively formed there during the early through middle Holocene. Areas south of the
1617 Arctic Circle appear to have experienced deep thawing (100–200 m depth) from the early
1618 Holocene until about 4–3 ka, when cooler summer conditions led permafrost to develop
1619 again. The deep thawing and subsequent renewal of surface permafrost in these regions
1620 produced an extensive thawed layer sandwiched between shallow (20–80 m deep) more
1621 recently frozen ground and deeper Pleistocene permafrost throughout much of
1622 northwestern Siberia.

1623 Quantitative estimates of the Holocene Thermal Maximum summer temperature
1624 anomaly along the northern margins of Eurasia and adjacent islands typically range from
1625 1° to 3°C. The geographic position of northern treeline across Eurasia is largely
1626 controlled by summer temperature and the length of the growing season (MacDonald et

1627 al., 2007), and in some areas the magnitude of treeline displacement there suggests a
1628 summer warming equivalent of 2.5°–7.0°C (see for example Birks, 1991; Wohlfarth et
1629 al., 1995; MacDonald et al., 2000a; Seppä and Birks, 2001, 2002; Hammarlund et al.,
1630 2002; Solovieva et al., 2005). Sea-surface temperature anomalies during the Holocene
1631 Thermal Maximum were as much as 4°–5°C higher than during the late Holocene for the
1632 eastern North Atlantic sector and adjacent Arctic Ocean (Salvigsen, 1992; Koç et al.,
1633 1993). Anomalies in summer temperature in the western Arctic during the Holocene
1634 Thermal Maximum ranged from 0.5° to 3°C (mean, 1.65°C). The largest anomalies were
1635 in the North Atlantic sector (Kerwin et al., 1999; Kaufman et al., 2004; Flowers et al.,
1636 2008).

1637

1638 **5.4.9b Neoglaciation**

1639 Many climate proxies are available to characterize the overall pattern of Late
1640 Holocene climate change. Following the Holocene Thermal Maximum, most proxy
1641 summer temperature records from the Arctic indicate an overall cooling trend through the
1642 late Holocene. Cooling is first recognized between 6 and 3 ka, depending on the threshold
1643 for change of each particular proxy. Records that exhibit a shift by 6–5 ka typically
1644 reflect intensified summer cooling about 3 ka (Figure 5.34).

1645 Summer cooling during the second half of the Holocene led to the expansion of
1646 mountain glaciers and ice caps around the Arctic. The term “Neoglaciation” is widely
1647 applied to this episode of glacier growth, and in some cases re-formation, following the
1648 maximum glacial retreat during the Holocene Thermal Maximum (Porter and Denton,
1649 1967). The former extent of glaciers is inferred from dated moraines and proglacial

1650 sediments deposited in lakes and marine settings. For example, ice-rafted detritus
1651 (Andrews et al., 1997) and the glacial geologic record (Funder, 1989) indicate that outlet
1652 glaciers of the Greenland Ice Sheet advanced during 6–4 ka (see Chapter 7, Greenland
1653 Ice Sheet). Multiproxy records from 10 glaciers or glaciated areas in Norway show
1654 evidence for increased activity by 5 ka (Nesje et al., 2001; Nesje et al., 2008). Major
1655 advances of outlet glaciers of northern Icelandic ice caps begin by 5 ka (Stötter et al.,
1656 1999; Geirsdottir et al., in press). In the European Arctic, glaciers expanded on Franz
1657 Josef Land (Lubinski et al., 1999) and Svalbard (Svendsen and Mangerud, 1997) by 4 ka,
1658 although sustained growth primarily began around 3 ka. An early Neoglacial advance of
1659 mountain glaciers is registered in Alaska, most prominently in the Brooks Range, the
1660 highest-latitude mountains in the state (Ellis and Calkin, 1984; Calkin, 1988). In
1661 southwest Alaska, mountain glaciers in the Ahklun Mountains did not reform until about
1662 3 ka (Levy et al., 2003). Neoglacial advances began in Arctic Canada by 5 ka (Miller et
1663 al., 2005)

1664 Additional evidence of Neoglacial seasonal cooling comes from several localities:
1665 a reduction in melt layers in the Agassiz Ice Cap (Koerner and Fisher, 1990) and in
1666 Greenland (Alley and Anandakrishnan, 1995); the decrease in $\delta^{18}\text{O}$ values in ice cores
1667 such as those from the Devon Island (Fisher, 1979) and Greenland (Johnsen et al., 1992)
1668 and indications of cooling from borehole thermometry (Cuffey et al., 1995); the retreat of
1669 large marine mammals and warm-water-dependent mollusks from the Canadian Arctic
1670 (Dyke and Savelle, 2001); the southward migration of the northern treeline across central
1671 Canada (MacDonald et al., 1993), Eurasia (MacDonald et al., 2000b), and Scandinavia
1672 (Barnekow and Sandgren, 2001); the expansion of sea-ice cover along the shores of the

1673 Arctic Ocean on Ellesmere Island (Bradley, 1990), in Baffin Bay (Levac et al., 2001),
1674 and in the Bering Sea (Cockford and Frederick, 2007); and the shift in vegetation
1675 communities inferred from plant macrofossils and pollen around the Arctic (Bigelow et
1676 al., 2003). The assemblage of microfossils and the stable isotope ratios of foraminifers
1677 indicate a shift toward colder, lower salinity conditions about 5 ka along the East
1678 Greenland Shelf (Jennings et al., 2002) and the western Nordic seas (Koç and Jansen,
1679 1994), suggesting increased influx of sea ice from the Arctic. Where quantitative
1680 estimates of temperature change are available, they generally indicate that summer
1681 temperature decreased by 1°–2°C during this initial phase of cooling.

1682 The general pattern of an early- to middle-Holocene Thermal Maximum followed
1683 by Neoglacial cooling forms a multi-millennial trend that, in most places, culminated in
1684 the 19th century. Superposed on the long-term cooling trend were many centennial-scale
1685 warmer and colder summer intervals, which are expressed to a varying extent and are
1686 interpreted with various levels of confidence in different proxy records. In northern
1687 Scandinavia, evidence for notable late Holocene cold intervals before the 16th century
1688 includes narrow tree rings (Grudd et al., 2002), lowered treeline (Eronen et al., 2002), and
1689 major glacier advances (Karlén, 1988) between 2.6 and 2.0 ka. An extended analysis of
1690 these many centennial-scale warmer and colder intervals in Russia was published by
1691 Velichko and Nechaev (2005).

1692

1693 **5.4.9c The Medieval Climate Anomaly (MCA)** Probably the most oft-cited
1694 warm interval of the late Holocene is the Medieval Climate Anomaly (MCA), earlier
1695 referred to as the Medieval Warm Period (MWP). The anomaly was recognized on the

1696 basis of several lines of evidence in Western Europe, but the term is commonly applied to
1697 other regions to refer to any of the relatively warm intervals of various magnitudes and at
1698 various times between about 950 and 1200 AD (Lamb, 1977) (Figure 5.35). In the Arctic,
1699 evidence for climate variability, such as relative warmth, during this interval is based on
1700 glacier extents, marine sediments, **speleothems**, ice cores, borehole temperatures, tree
1701 rings, and archaeology. The most consistent records of an Arctic Medieval Climate
1702 Anomaly come from the North Atlantic sector of the Arctic. The summit of Greenland
1703 (Dahl-Jensen et al., 1998), western Greenland (Crowley and Lowery, 2000), Swedish
1704 Lapland (Grudd et al., 2002), northern Siberia (Naurzbaev et al., 2002), and Arctic
1705 Canada (Anderson et al., 2008) were all relatively warm around 1000 AD. During
1706 Medieval time, Inuit populations moved out of Alaska into the eastern Canadian Arctic
1707 and hunted whale from skin boats in regions perennially ice-covered in the 20th century
1708 (McGhee, 2004).

1709

1710

FIGURE 5.35 NEAR HERE

1711

1712 The evidence for Medieval warmth throughout the rest of the Arctic is less clear.
1713 However, some indications of Medieval warmth include the general retreat of glaciers in
1714 southeastern Alaska (Reyes et al., 2006; Wiles et al., 2008) and the wider tree rings in
1715 some high-latitude tree-ring records from Asia and North America (D'Arrigo et al.,
1716 2006). However D'Arrigo et al. (2006) emphasized the uncertainties involved in
1717 estimating Medieval Climate Anomaly warmth relative to that of the 20th century, owing
1718 in part to the sparse geographic distribution of proxy data as well as to the less coherent

1719 variability of tree growth temperature estimates for this anomaly. Hughes and Diaz
1720 (1994) argued that the Arctic as a whole was not anomalously warm throughout Medieval
1721 time (also see Bradley et al., 2003b, and National Research Council, 2006). Warmth
1722 during the Medieval interval is generally ascribed to lack of explosive volcanoes that
1723 produce particles that block the sun and perhaps to greater brightness of the sun
1724 (Crowley, 2000; Goosse et al., 2005; also see Jansen et al., 2007). Warming around the
1725 North Atlantic and adjacent regions may have been linked to changes in oceanic
1726 circulation as well (Broecker, 2001).

1727

1728 **5.4.9d Climate of the past millennium and the Little Ice Age**

1729 Given the importance of understanding climate in the most recent past and the
1730 richness of the available evidence, intensive scientific effort has resulted in numerous
1731 temperature reconstructions for the past millennium (Jones, et al., 1998; Mann et al.,
1732 1998; Briffa et al., 2001; Esper et al., 2002; Crowley et al., 2003; Mann and Jones, 2003;
1733 Moberg et al., 2005; National Research Council, 2006; Jansen et al., 2007), and
1734 especially the last 500 years (Bradley and Jones, 1992; Overpeck et al., 1997). Most of
1735 these reconstructions are based on annually resolved proxy records, primarily from tree
1736 rings, and they attempt to extract a record of air-temperature change over large regions or
1737 entire hemispheres. Data from Greenland ice cores and a few annually laminated lake
1738 sediment records are typically included in these compilations, but few other records of
1739 quantitative temperature changes spanning the last millennium are available from the
1740 Arctic. In general, the temperature records are broadly similar: they show modest summer
1741 warmth during Medieval times, a variable, but cooling climate from about 1250 to 1850

1742 AD, followed by warming as shown by both paleoclimate proxies and the instrumental
1743 record. Less is known about changes in precipitation, which is spatially and temporally
1744 more variable than temperature.

1745 The trend toward colder summers after about 1250 AD coincides with the onset of
1746 the Little Ice Age (LIA), which persisted until about 1850 AD, although the timing and
1747 magnitude of specific cold intervals were different in different places. Proxy climate
1748 records, both glacial and non-glacial from around the Arctic and for the Northern
1749 Hemisphere as a whole, show that the coldest interval of the Holocene was sustained
1750 sometime between about 1500 and 1900 AD (Bradley et al., 2003a). Recent evidence
1751 from the Canadian Arctic indicates that, following their recession in Medieval times,
1752 glaciers and ice sheets began to expand again between 1250 and 1300 AD. Expansion
1753 was further amplified about 1450 AD (Anderson et al., 2008).

1754 Glacier mass balances throughout most of the Northern Hemisphere during the
1755 Holocene are closely correlated with summer temperature (Koerner, 2005), and the
1756 widespread evidence of glacier re-advances across the Arctic during the Little Ice Age is
1757 consistent with estimates of summer cooling that are based on tree rings. The climate
1758 history of the Little Ice Age has been extensively studied in natural and historical
1759 archives, and it is well documented in Europe and North America (Grove, 1988).
1760 Historical evidence from the Arctic is relatively sparse, but it generally agrees with
1761 historical records from northwest Europe (Grove, 1988). Icelandic written records
1762 indicate that the duration and extent of sea ice in the Nordic Seas were high during the
1763 Little Ice Age (Ogilvie and Jónsson, 2001).

1764 The average temperature of the Northern Hemisphere during the Little Ice Age

1765 was less than 1°C lower than in the late 20th century (Bradley and Jones, 1992; Hughes
1766 and Diaz, 1994; Crowley and Lowery, 2000), but regional temperature anomalies varied.
1767 Little Ice Age cooling appears to have been stronger in the Atlantic sector of the Arctic
1768 than in the Pacific (Kaufman et al., 2004), perhaps because ocean circulation promoted
1769 the development of sea ice in the North Atlantic, which further amplified Little Ice Age
1770 cooling there (Broecker, 2001; Miller et al., 2005).

1771 The Little Ice Age also shows evidence of multi-decadal climatic variability, such
1772 as widespread warming during the middle through late 18th century (e.g., Cronin et al.,
1773 2003). Although the initiation of the Little Ice Age and the structure of climate
1774 fluctuations during this multi-centennial interval vary around the Arctic, most records
1775 show warming beginning in the late 19th century (Overpeck et al., 1997). The end of the
1776 Little Ice Age was apparently more uniform both spatially and temporally than its
1777 initiation (Overpeck et al., 1997).

1778 The climate change that led to the Little Ice Age is manifested in proxy records
1779 other than those that reflect temperature. For example, it was associated with a positive
1780 shift in transport of dust and other chemicals to the summit of Greenland (O'Brien et al.,
1781 1995), perhaps related to deepening of the Icelandic low-pressure system (Meeker and
1782 Mayewski, 2002). According to modeling studies, the negative phase [see
1783 <http://www.ldeo.columbia.edu/res/pi/NAO/>] of the North Atlantic Oscillation could have
1784 been amplified during the Little Ice Age (Shindell et al., 2001) whereas, in the North
1785 Pacific, the Aleutian low was significantly weakened during the Little Ice Age (Fisher et
1786 al., 2004; Anderson et al., 2005).

1787 Seasonal cooling into the Little Ice Age resulted from the orbital changes as
1788 described above, together with increased explosive volcanism and probably also
1789 decreased solar luminosity as recorded by sunspot numbers as far back as 1600 AD
1790 (Renssen et al., 2005; Ammann et al., 2007; Jansen et al., 2007).

1791

1792 **5.4.10 Placing 20th century warming in the Arctic in a millennial perspective**

1793 Much scientific effort has been devoted to learning how 20th-century and 21st-
1794 century warmth compares with warmth during earlier times (e.g., National Research
1795 Council, 2006; Jansen et al., 2007). Owing to the orbital changes affecting midsummer
1796 sunshine (a drop in June insolation of about 1 W/m² at 75°N. and 2 W/m² at 90°N. during
1797 the last 1000 years; Berger and Loutre, 1991), additional forcing was needed in the 20th
1798 century to give the same summertime temperatures as achieved in the Medieval Warm
1799 Period.

1800 After it evaluated globally or even hemispherically averaged temperatures, the
1801 National Research Council (2006) found that “Presently available proxy evidence
1802 indicates that temperatures at many, but not all, individual locations were higher during
1803 the past 25 years than during any period of comparable length since A.D. 900” (p. 3).
1804 Greater uncertainties for hemispheric or global reconstructions were identified in
1805 assessing older comparisons. As reviewed next, some similar results are available for the
1806 Arctic.

1807 Thin, cold ice caps in the eastern Canadian Arctic preserve intact—but frozen—
1808 vegetation beneath them that was killed by the expanding ice. As these ice caps melt,
1809 they expose this dead vegetation, which can be dated by radiocarbon with a precision of a

1810 few decades. A recent compilation of more than 50 radiocarbon dates on dead vegetation
1811 emerging from beneath thin ice caps on northern Baffin Island shows that some ice caps
1812 formed more than 1600 years ago and persisted through Medieval times before melting
1813 early in the 21st century (Anderson et al., 2008).

1814 Records of the melting from ice caps offer another view by which 20th century
1815 warmth can be placed in a millennial perspective. The most detailed record comes from
1816 the Agassiz Ice Cap in the Canadian High Arctic, for which the percentage of summer
1817 melting of each season's snowfall is reconstructed for the past 10 k.y. (Fisher and
1818 Koerner, 2003). The percent of melt follows the general trend of decreasing summer
1819 insolation from orbital changes, but some brief departures are substantial. Of particular
1820 note is the significant increase in melt percentage during the past century; current
1821 percentages are greater than any other melt intensity since at least 1700 years ago, and
1822 melting is greater than any in sustained interval since 4–5 ka.

1823 As reviewed by Smol and Douglas (2007b), changes in lake sediments record
1824 climatic and other changes in the lakes. Extensive changes especially in the post-1850
1825 interval are most easily interpreted in terms of warming above the Medieval warmth on
1826 Ellesmere Island and probably in other regions, although other explanations cannot be
1827 excluded (also see Douglas et al., 1994). D'Arrigo et al. (2006) show tree-ring evidence
1828 from a few North American and Eurasian records that imply that summers were cooler in
1829 the Medieval Warm Period than in the late 20th century, although the statistical
1830 confidence is weak. Tree-ring and treeline studies in western Siberia (Esper and
1831 Schweingruber, 2004) and Alaska (Jacoby and D'Arrigo, 1995) suggest that warming
1832 since 1970 is has been optimal for tree growth and follows a circumpolar trend.

1833 Hantemirov and Shiyatov (2002) records from the Russian Yamal Peninsula, well north of
1834 the Arctic Circle, show that summer temperatures of recent decades are the most
1835 favorable for tree growth within the past 4 millennia.

1836 Whole-Arctic reconstructions are not yet available to allow confident comparison
1837 of late 20th century warmth with Medieval temperatures, nor has the work been done to
1838 correct for the orbital influence and thus to allow accurate comparison of the remaining
1839 forcings.

1840

1841 **5.5 Summary**

1842

1843 **5.5.1 Major features of Arctic Climate in the past 65 Ma**

1844 Section 5.4 summarized some of the extensive evidence for changes in Arctic
1845 temperatures, and to a lesser extent in Arctic precipitation, during the last 65 m.y. To
1846 some degree it also discussed “attribution”—the best scientific understanding of the
1847 causes of the climate changes. In this subsection, a brief synopsis is provided; for
1848 citations, the reader is referred to the extensive discussion just above.

1849 At the start of the Cenozoic, 65 Ma, the Arctic was much warmer year around
1850 than it was recently; forests grew on all land regions and no perennial sea ice or
1851 Greenland Ice Sheet existed. Gradual but bumpy cooling has dominated most of the last
1852 65 million years, and falling atmospheric CO₂ concentration apparently is the most
1853 important contributor to the cooling—although possible changing continental positions
1854 and their effect on atmospheric or oceanic circulation may also contribute. One especially
1855 prominent “bump,” the Paleocene-Eocene Thermal Maximum about 55 Ma, warmed the

1856 Arctic Ocean more than 5°C and the Arctic landmass about 8°C, probably in a few
1857 centuries to a millennium or so, followed by cooling for about 100 ka. Warming from
1858 release of much CO₂ (possibly initially as sea-floor methane that was then oxidized to
1859 CO₂) is the most likely explanation. In the middle Pliocene (about 3 Ma) a modest
1860 warming was sufficient to allow deciduous trees on Arctic land that at present supports
1861 only High Arctic polar-desert vegetation; whether this warming originated from changes
1862 to circulation, CO₂, or some other cause remains unclear.

1863 About 2.7 Ma, the cooling reached the threshold beyond which extensive
1864 continental ice sheets developed in the North American and Eurasian Arctic, and it
1865 marked the onset of the Quaternary Ice Age. Initially, the growth and shrinkage of the
1866 ice ages were directly controlled by changes in northern sunshine caused by features of
1867 Earth's orbit (the 41-k.y. cycle of sunshine that is tied to the obliquity (tilt) of Earth's
1868 axis is especially prominent). More recently, a 100-k.y. cycle has become more
1869 prominent, perhaps because the ice sheets became large enough that their behavior
1870 became important. Short, warm interglacials (usually lasting about 10,000 years,
1871 although the one about 440,000 years ago lasted longer) have alternated with longer
1872 glacial intervals. Recent work suggests that, in the absence of human influence, the
1873 current interglacial would continue for a few tens of thousands of years before the start
1874 of a new ice age (Berger and Loutre, 2002). Although driven by the orbital cycles, the
1875 large temperature differences between glacials and interglacials, and the globally
1876 synchronous response, reflect the effects of strong positive feedbacks, such as changes
1877 in atmospheric CO₂ and other greenhouse gases and in the areal extent of reflective
1878 snow and ice.

1879 Interactions among the various orbital cycles have caused small differences
1880 between successive interglacials. More summer sunshine was received in the Arctic
1881 during the interglacial of about 130–120 ka than has been received in the current
1882 interglacial. Thus, summer temperatures in many places were about 4°–6°C warmer than
1883 recently, and these higher temperatures reduced ice on Greenland (Chapter 7, Greenland
1884 Ice Sheet), raised sea level, and melted widespread small glaciers and ice caps.

1885 The seasonal cooling into and warming out of the most recent glacial were
1886 punctuated by numerous abrupt climate changes, and conditions persisted for millennia
1887 between jumps that were complete in years to decades. These events were very
1888 pronounced around the North Atlantic, but they had a much smaller effect on
1889 temperature elsewhere in the Arctic. Temperature changes extended to equatorial
1890 regions and caused a seesaw response in the far south (i.e., mean annual warming in the
1891 south when the north cooled). Large changes in extent of sea ice in the North Atlantic
1892 were probably responsible, linked to changes in regional to global patterns of ocean
1893 circulation; freshening of the North Atlantic favored expansion of sea-ice.

1894 These abrupt temperature changes also were a feature of the current interglacial,
1895 the Holocene, but they ended as the Laurentide Ice Sheet on Canada melted away. Arctic
1896 temperatures in the Holocene broadly responded to orbital changes, and temperatures
1897 warmed during the middle Holocene when there was more summer sunshine. Warming
1898 generally led to northward migration of vegetation and to shrinkage of ice on land and
1899 sea. Smaller oscillations in climate during the Holocene, including the so-called
1900 Medieval Warm Period and the Little Ice Age, were linked to variations in the sun-
1901 blocking effect of particles from explosive volcanoes and perhaps to small variations in

1902 solar output, or in ocean circulation, or other factors. The warming from the Little Ice
1903 Age began for largely natural reasons, but it appears to have been accelerated by human
1904 contributions and especially by increasing CO₂ concentrations in the atmosphere
1905 (Jansen, 2007).

1906

1907 **5.5.2. Arctic Amplification**

1908 The scientific understanding of climate processes shows that Arctic climate
1909 operates by use of many strong positive feedbacks (Serreze and Francis, 2006; Serreze et
1910 al., 2007a). As outlined in section 5.2, these feedbacks especially depend on the
1911 interactions of snow and ice with sunlight, the ocean, and the land surface (including its
1912 vegetation). For example, higher temperature tends to remove reflective ice and snow,
1913 more solar heat is then absorbed, and absorption of that heat promotes further warming
1914 (ice-albedo feedback). Also, higher temperature tends to remove sea ice that insulates the
1915 cold wintertime air from the warmer ocean beneath, further warming the air (ice-
1916 insolation feedback). Furthermore, higher temperature tends to allow dark shrubs to
1917 replace low-growing tundra that is easily covered by snow, intensifying the ice-albedo
1918 feedback. Similarly strong negative feedbacks are not known to stabilize Arctic climate,
1919 so physical understanding indicates that climate changes should be amplified in the
1920 Arctic as compared with lower latitude sites. This expectation is confirmed by the
1921 available data, as shown in Figure 5.36.

1922

1923

FIGURE 5.36 NEAR HERE

1924

1925 As we consider Arctic amplification, we must account for forcing. For the three
1926 younger time intervals shown in Figure 5.36, the Holocene Thermal Maximum (about 6
1927 ka), the Last Glacial Maximum (LGM, about 20 ka), and marine isotope stage 5e, also
1928 known as the last interglacial (LIG, about 130–125 ka), the climate changes were
1929 primarily forced by Milankovitch features of Earth’s orbit. The anomalies of incoming
1930 solar radiation (insolation) averaged throughout the whole planet for a year are very small
1931 for all times considered, and the orbital changes serve primarily to shift sunlight around
1932 on the planet. However, during these intervals the insolation forcing was relatively
1933 uniform throughout the Northern Hemisphere, and insolation anomalies north of 60°N.
1934 typically were only 10–20% greater than the anomalies for corresponding times averaged
1935 throughout the Northern Hemisphere. For example, at the peak of the last interglacial
1936 (130–125 ka), the Arctic (60°–90°N.) summer (May-June-July) insolation anomaly was
1937 12.7% above present, while the Northern Hemisphere anomaly was 11.4% above present
1938 (Berger and Loutre, 1991).

1939 To assess the geographic distribution of climate response, we compare Arctic and
1940 Northern Hemisphere summer temperature anomalies for the three younger time periods
1941 because of the similar forcing in the Arctic and Northern Hemisphere. During the
1942 Pliocene (and during earlier warm times discussed below but not plotted in the figure),
1943 warmth persisted much longer than the cycle time of insolation changes resulting from
1944 Earth’s orbital irregularities (about 20 ka and about 40 ka). Consequently, we compare
1945 global temperature anomalies with Arctic anomalies.

1946 A difficulty is that for some of those younger times, global and Arctic estimates
1947 of temperature anomalies are available but hemispheric estimates are not. (The global

1948 estimates clearly include hemispheric data, but those data have not been summarized in
1949 anomaly maps or hemispheric anomaly estimates that were published in the refereed
1950 scientific literature.) To obtain hemispheric estimates here, we note (as described in more
1951 detail below) that climate models driven by the known forcings show considerable
1952 fidelity in reproducing the global anomalies shown by the data for the relevant times, and
1953 that hemispheric anomalies can be assessed within these models. The hemispheric
1954 anomalies so produced are consistent with our understanding of the data, and so they are
1955 used here.

1956 The Palaeoclimate Modelling Intercomparison Project (PMIP2; Harrison et al.,
1957 2002, and see <http://pmip2.lsce.ipsl.fr/>) coordinates an international effort to compare
1958 paleoclimate simulations produced by a range of climate models, and to compare these
1959 climate model simulations with data-based paleoclimate reconstructions for a middle
1960 Holocene warm time (6 ka) and for the last glacial maximum (LGM; 21 ka). A
1961 comparison of simulations for 6 and 21 ka by the project is reported by Braconnot et al.
1962 (2007).

1963 As part of this Palaeoclimate Modelling Intercomparison Project effort, Harrison
1964 et al. (1998) compared global (mostly Northern Hemisphere) vegetation patterns
1965 simulated by using the output of 10 different climate model simulations for 6 ka. The
1966 model simulations closely agreed with the vegetation reconstructed from paleoclimate
1967 records. Similar comparisons on a regional basis for the Northern Hemisphere north of
1968 55°N. (Kaplan et al., 2003), the Arctic (CAPE Project Members, 2001), Europe (Brewer
1969 et al., 2007), and North America (Bartlein et al., 1998) also showed close matches
1970 between paleoclimate data and models for the early Holocene. Comparison of models and

1971 data for the Last Glacial Maximum (Bartlein et al., 1998; Kaplan et al., 2003), and Last
1972 Interglaciation (CAPE Last Interglacial Project Members, 2006; Otto-Bliesner et al.,
1973 2006) reached similar conclusions. (Also see Pollard and Thompson, 1997; Farrera et al.,
1974 1999; Pinot et al., 1999; Kageyama et al., 2001.) Paleoclimate data corresponded closely
1975 with model simulations of the Holocene Thermal Maximum, Last Interglaciation warmth,
1976 and Last Glacial Maximum cold. This agreement provides confidence that we can
1977 compare climate-model simulations of past times with paleoclimate-based
1978 reconstructions of summer temperatures for the Arctic in order to evaluate the magnitude
1979 of Arctic amplification. (Figure 5.34 shows such a comparison.) Clearly, however,
1980 additional data and additional analyses of existing as well as new data would improve
1981 confidence in the results and perhaps reduce the error bars.

1982 The forcing of the warmth of the middle Pliocene remains unclear. Orbital
1983 oscillations have continued throughout Earth history, but the Pliocene warmth persisted
1984 long enough to cross many orbital oscillations, which thus cannot have been responsible
1985 for the warmth.

1986 The data indicate that Arctic temperature anomalies were much larger than global
1987 ones (Figure 5.34). The regression line through the four data points has a slope of $3.6 \pm$
1988 0.6 , suggesting that the change in Arctic summer temperatures tends to be 3 to 4 times as
1989 large as the global change.

1990 This trend of larger Arctic anomalies was already well established during the
1991 greater warmth of the early Cenozoic peak warming and of the Cretaceous before that.
1992 Somewhat greater uncertainty is attached to these more ancient times in which continents
1993 were differently configured, so these data are not plotted in Figure 5.34; even so, the

1994 leading result is fully consistent with the regression. Barron et al. (1995) estimated
1995 global-average temperatures about 6°C warmer in the Cretaceous than recently. As
1996 reviewed by Alley (2003) (also see Bice et al., 2006), subsequent work suggests upward
1997 revision of tropical sea-surface temperatures by as much as a few degrees. The
1998 Cretaceous peak warmth seems to have been somewhat higher than early Cenozoic
1999 values, or perhaps similar (Zachos et al., 2001). In the Arctic, as discussed in section
2000 5.4.1, the early Cenozoic (late Paleocene) temperature records probably mostly recorded
2001 summertime conditions of about 18°C in the ocean and about 17°C on land, followed
2002 during the short-lived Paleocene-Eocene Thermal Maximum by warming to about 23°C
2003 in the summer ocean and 25°C on land (Moran et al., 2006; Sluijs et al.; 2006; 2008;
2004 Weijers et al., 2007). No evidence of wintertime ice exists, and temperatures may have
2005 remained higher than during the mid-Pliocene. Recently, the oceanic site has remained
2006 ice covered; it is near or below freezing during the summer and much colder in winter.
2007 Hence, changes in the Arctic were much larger than the globally averaged change.

2008 We have not included quantitative estimates in Figure 5.34 for the pre-Pliocene
2009 warm times, but a 3-fold Arctic amplification is consistent with the data within the broad
2010 uncertainties. The Cretaceous and early-Cenozoic warmth seems to have been forced by
2011 increased greenhouse-gas concentration, as discussed above, so the Arctic amplification
2012 seems to be independent of the forcing. This conclusion is expectable; many of the strong
2013 Arctic feedbacks serve to amplify temperature change without regard to causation—
2014 warmer summer temperatures melt reflective snow and ice, regardless of whether the
2015 warmth came from changing solar output, orbital configuration, greenhouse-gas
2016 concentrations, or other causes. Global warmth and an ice-free Arctic during the early

2017 Eocene occurred without albedo feedbacks at the same time that the tropics experienced
2018 sustained warmth (Pearson et al., 2007).

2019 Targeted studies designed to quantitatively assess Arctic amplification of climate
2020 change remain relatively rare, and they could be clarified. The available data, as assessed
2021 here, point to 3-fold to 4-fold Arctic amplification, such that, in response to the same
2022 forcing, Arctic temperature changes are 3 to 4 times as large as hemispheric-average
2023 changes, which are dominated by changes in the much larger lower latitude regions.

2024

2025 **5.5.3 Implications for the future**

2026 Paleoclimatology shows that climate has changed greatly in the Arctic with time,
2027 and that the changes typically have been much larger in the Arctic than in lower latitudes.
2028 Strong feedbacks have promoted these Arctic changes, such as the ice-albedo feedback in
2029 which summer cooling expands reflective snow and ice that in turn amplify the cooling,
2030 or warming causes melting that amplifies the warming. Changes in sea-ice coverage of
2031 the Arctic Ocean have also been critical—open water cannot fall below the freezing
2032 point, but air above ice-covered water can become very cold in the dark Arctic winter.
2033 Thus, sustained changes in sea-ice coverage may cause perhaps the largest temperature
2034 changes observed on the planet (see, e.g., Denton et al., 2005).

2035 These feedbacks have served to amplify climate changes with various causes,
2036 including those forced primarily by greenhouse-gas changes, consistent with physical
2037 understanding of the nature of the feedbacks. By simple analogy, and taken together with
2038 physical understanding, this knowledge indicates that climate changes will continue to be
2039 amplified in the Arctic. In turn, this knowledge indicates that continuing greenhouse-gas

SAP1.2 DRAFT 3 PUBLIC COMMENT

2040 forcing of global climate or other human influences will change climate more in the

2041 Arctic than in lower latitude regions.

2042

2042 **Chapter 5 Figure Captions**

2043

2044 **Figure 5.1** Median extent of sea ice in September, 2007, compared with averaged
2045 intervals during recent decades. Red curve, 1953–2000; orange curve, 1979–2000; green
2046 curve, September 2005. Inset: Sea ice extent time series plotted in square kilometers,
2047 shown from 1953–2007 in the graph below (Stroeve et al., 2008). The reduction in Arctic
2048 Ocean summer sea ice in 2007 was greater than that predicted by most recent climate
2049 models.

2050

2051 **Figure 5.2** Projected surface-temperature changes for the last decade of the 21st
2052 century (2090–2099) relative to the period 1980–1999. The map shows the IPCC multi-
2053 Atmosphere-Ocean coupled Global Climate Model [average projection for the A1B
2054 (balanced emphasis on all energy resources) scenario. The most significant substantial
2055 warming is projected for the Arctic (IPCC, 2007; that report’s Figure SPM6).

2056

2057 **Figure 5.3** Global mean observed near-surface air temperatures for January 2003,
2058 derived from Atmospheric Infrared Sounder (AIRS) data. Contrast between equatorial
2059 and Arctic temperatures is greatest during the Northern Hemisphere winter. The transfer
2060 of heat from the tropics to the polar regions is a primary feature of Earth’s climate
2061 system. Color scale is in Kelvin degrees such that $0^{\circ}\text{C}=273.15$ Kelvin. (Source:
2062 http://www-air.s.jpl.nasa.gov/graphics/features/airs_surface_temp1_full.jpg).

2063

2064 **Figure 5.4** Albedo values in the Arctic

2065 a) Advanced Very High Resolution Radiometry (AVHRR) -derived Arctic
2066 albedo values in June, 1982–2004. The multi-year average shows the strong contrast
2067 between snow- and ice-covered areas (green through red) and open water or land (blue).
2068 (Image courtesy of X. Wang, University of Wisconsin–Madison, CIMSS/NOAA)

2069 b) Albedo feedbacks. Albedo is the fraction of incident sunlight that is reflected.
2070 Snow, ice, and glaciers have high albedo. Dark objects such as the open ocean, which
2071 absorbs some 93% of the sun’s energy, have low albedo (about 0.06), absorbing some
2072 93% of the sun’s energy. Bare ice has an albedo of 0.5; however, sea ice covered with
2073 snow has an albedo of nearly 90% (*Source:*
2074 <http://nsidc.org/seaice/processes/albedo.html>).

2075

2076 **Figure 5.5** Changes in vegetation cover throughout the Arctic can influence
2077 albedo, as can altering the onset of snow melt in spring. A) Progression of the melt
2078 season in northern Alaska, May 2001 (top) and May 2002 (bottom), demonstrates how
2079 areas with exposed shrubs show earlier snow melt. B) Dark branches against reflective
2080 snow alter albedo (Sturm et al., 2005; Photograph courtesy of Matt Sturm).

2081 **Figure 5.6** Warming trend in Arctic permafrost (permanently frozen ground),
2082 1970–present. Local effects can modify this trend. A) Sites in Alaska: WD, West Dock;
2083 DH, Deadhorse; FB, Franklin Bluffs; HV, Happy Valley; LG, Livengood; GK, Gulkana;
2084 BL, Birch Lake; OM, Old Man. B) Sites in northwest Canada: WG, Wrigley; NW,
2085 Norman Wells; NA, Northern Alberta; FS, Fort Simpson. C) Sites in European Russia:
2086 VT, Vorkuta; RG, Rogovoi; KT, Karataikha; MB, Mys Bolvansky. D) Northwest Siberia:

2087 UR, Urengoi; ND, Nadym. E) Sites in Yakutia: TK, Tiksi; YK, Yakutsk. F) Sites in
2088 central Asia: KZ, Kazakhstan; MG, Mongolia (Brown and Romanovsky, 2008).

2089

2090 **Figure 5.7** Inflows and outflows of water in the Arctic Ocean. Red lines,
2091 components and paths of the surface and Atlantic Water layer in the Arctic; black arrows,
2092 pathways of Pacific water inflow from 50–200 m depth; blue arrows, surface-water
2093 circulation; green, major river inflow; red arrows, movements of density-driven Atlantic
2094 water and intermediate water masses into the Arctic (AMAP, 1998).

2095

2096 **Figure 5.8** Upper three panels: Correlation of global sea-level curve (Lambeck et
2097 al., 2002), Northern Hemisphere summer insolation (Berger and Loutre, 1991), and the
2098 Greenland Ice Sheet (GISP2) $\delta^{18}\text{O}$ record (Grootes et al., 1993), ages all given in
2099 calendar years. Bottom panel: temporal changes in the percentages of the main taxa of
2100 trees and shrubs, herbs and spores at Elikchan 4 Lake in the Magadan region of
2101 Chukotka, Russia. Lake core x-axis is depth, not time (Brigham-Grette et al., 2004).
2102 Habitat was reconstructed on the basis of modern climate range of collective species
2103 found in fossil pollen assemblages. The reconstruction can be used to estimate past
2104 temperatures or the seasonality of a particular site. The GISP2 record: Base of core
2105 roughly 60 ka (Lozhkin and Anderson, 1996). H1 above arrow, timing of Heinrich event
2106 event 1 (and so on); number 1 above curve, Dansgaard-Oschegeger event (and so on).
2107 During approximately 27 ka to nearly 55 ka, vegetation, especially treeline, recovered for
2108 short intervals to nearly Holocene conditions at the same time that the isotopic record in
2109 Greenland suggests repeated warm warm-cold cycles of change. kyr BP, thousands of

2110 years before the present.

2111

2112 **Figure 5.9** Annual tree rings composed of seasonal early and late wood are clear
2113 in this a 64-year year-old *Larix siberica* from western Siberia (Esper and Schweingruber,
2114 2004). Initial growth was restricted; narrow rings average 0.035 mm/year, punctuated by
2115 one thicker ring (one single arrow). Later (two arrows), tree-ring width abruptly at least
2116 doubled for more than three years. Ring widths increased to 0.2 mm/year (Photograph
2117 courtesy of Jan Esper, Swiss Federal Research Institute).

2118

2119 **Figure 5.10** Typical tree ring samples. a) Increment cores taken from trees with a
2120 small small-bore hollow drill. They can be easily stored and transported in plastic soda
2121 straws for analysis in the laboratory. b) Alternatively, cross sections or disks can be
2122 sanded for study. A cross section of *Larix decidua* root shows differing wood thickness
2123 within single rings, caused by exposure. (Photographs courtesy of Jan Esper and Holger
2124 Gärtner, Swiss Federal Research Institute, respectively).

2125

2126 **Figure 5.11** 14 Microscopic marine plankton known as (foraminiferaifers (see
2127 inset) grow a shell of calcium carbonate (CaCO_3) in or near isotopic equilibrium with
2128 ambient sea water. The oxygen isotope ratio measured in these shells can be used to
2129 determine the temperature of the surrounding waters. (The oxygen-isotope ratio is
2130 expressed in $\delta^{18}\text{O}$ parts per million (ppm) = $10^3[(R_{\text{sample}}/R_{\text{standard}}) - 1]$, where $R_x =$
2131 $(^{18}\text{O})/(^{16}\text{O})$ is the ratio of isotopic composition of a sample compared to that of an
2132 established standard, such as ocean water) However, factors other than temperature can

2133 influence the ratio of ^{18}O to ^{16}O . Warmer seasonal temperatures, glacial meltwater, and
2134 river runoff with depleted values all will produce a more negative (lighter) $\delta^{18}\text{O}$ [should
2135 the Greek letter be δ ?] ratio. On the other hand, cooler temperatures or higher salinity
2136 waters will drive the ratio up, making it heavier, or more positive. The growth of large
2137 continental ice sheets selectively removes the lighter isotope (^{16}O), leaving the ocean
2138 enriched in the heavier isotope (^{18}O).

2139

2140 **Figure 5.12** Lake El'gygytyn in the Arctic Far East of Russia. Open and closed
2141 lake systems in the Arctic differ hydrologically according to the balance between inflow,
2142 outflow, and the ratio of precipitation to evaporation. These parameters are the dominant
2143 influence on lake stable stable-isotopic chemistry and on the depositional character of the
2144 sediments and organic matter. Lake El'gygytyn is annually open and flows to the Bering
2145 Sea during July and August, but the outlet closes by early September as lake level drops
2146 and storms move beach gravels that choke the outlet. (Photograph by J. Brigham-Grette).

2147

2148 **Figure 5.13** Locations of Arctic and sub-Arctic lakes (blue) and ice cores (green)
2149 whose oxygen isotope records have been used to reconstruct Holocene paleoclimate.

2150 (Map adapted from the Atlas of Canada, © 2002. Her Majesty the Queen in Right of
2151 Canada, Natural Resources Canada. / Sa Majesté la Reine du chef du Canada, Ressources
2152 naturelles Canada.)

2153

2154 **Figure 5.14 a)** One-meter section of Greenland Ice Core Project-2 core from 1837
2155 m depth showing annual layers. (Photograph courtesy of Eric Cravens, Assistant Curator,

2156 U.S. National Ice Core Laboratory). b) Field site of Summit Station on top of the
2157 Greenland Ice sheet (Photograph by Michael Morrison, GISP2 SMO, University of New
2158 Hampshire; NOAA Paleoslide Set)

2159

2160 **Figure 5.15** Relation between isotopic composition of precipitation and
2161 temperature in the parts of the world where ice sheets exist. Sources of data as follows:
2162 International Atomic Energy Agency (IAEA) network (Fricke and O'Neil, 1999;
2163 calculated as the means of summer and winter data of their Table 1 for all sites with
2164 complete data. Open squares, poleward of 60° latitude (but with no inland ice-sheet
2165 sites); open circles, 45°–60° latitude; filled circles, equatorward of 45° latitude. x, data
2166 from Greenland (Johnsen et al., 1989); +, data from Antarctica (Dahe et al., 1994). About
2167 71% of Earth's surface area is equatorward of 45°, where dependence of $\delta^{18}\text{O}$ on
2168 temperature is weak to nonexistent. Only 16% of Earth's surface falls in the 45°–60°
2169 band, and only 13% is poleward of 60°. The linear array is clearly dominated by data
2170 from the ice sheets.

2171

2172 **Figure 5.16** Paleotemperature estimates of site and source waters from on
2173 Greenland: GRIP and NorthGrip, Masson-Delmotte et al., 2005). GRIP (left) and
2174 NorthGRIP (right) site (top) and source (bottom) temperatures derived from GRIP and
2175 NorthGRIP $\delta^{18}\text{O}$ and deuterium excess corrected for seawater $\delta^{18}\text{O}$ (until 6000 BP).
2176 Shaded lines in gray behind the black line provide an estimate of uncertainties due to the
2177 tuning of the isotopic model and the analytical precision. Solid line (in part above zigzag

2178 line), GRIP temperature derived from the borehole-temperature profile (Dahl-Jensen et
 2179 al., 1998).

2180

2181 **Figure 5.17** Biomarker alkenone. U_{37}^K versus measured water temperature for
 2182 ocean-water surface mixed layer (0–30 m) samples. A) Atlantic region: Empirical 3rd-
 2183 order polynomial regression for samples collected in warmer-than-4°C waters is $U_{37}^K =$
 2184 $1.004 \cdot 10^{-4} T^3 + 5.744 \cdot 10^{-3} T^2 - 6.207 \cdot 10^{-2} T + 0.407$ ($r^2 = 0.98$, $n = 413$) (Outlier data
 2185 from the southwest Atlantic margin and northeast Atlantic upwelling regime is
 2186 excluded.). B) Pacific, Indian, and Southern Ocean regions: The empirical linear
 2187 regression of Pacific samples is $U_{37}^K = 0.0391T - 0.1364$ ($r^2 = 0.97$, $n = 131$). Pacific
 2188 regression does not include the Indian and Southern Ocean data. C) Global data: The
 2189 empirical 3rd order polynomial regression, excluding anomalous southwest Atlantic
 2190 margin data, is $U_{37}^K = 5.256 \cdot 10^{-5} T^3 + 2.884 \cdot 10^{-3} T^2 - 8.4933 \cdot 10^{-2} T + 9.898$ ($r^2 =$
 2191 0.97 , $n = 588$). +, sample excluded from regressions. (Conte et al, 2006).

2192

2193 **Figure 5.18** Diatom assemblages reflect a variety of environmental conditions in
 2194 Arctic lake systems. Transitions, especially rapid change from one assemblage to another,
 2195 can reflect large changes in conditions such as light, nutrient availability, or temperature,
 2196 for example. Biogenic silica, chiefly the silica skeletal framework constructed by
 2197 diatoms, is commonly measured in lake sediments and used as an index of past changes
 2198 in aquatic primary productivity.

2199

2200 **Figure 5.19** Changing ice and snow conditions on an Arctic lake during relatively
2201 (a) cold, (b) moderate, and (c) warm conditions. During colder years, a permanent raft of
2202 ice may persist throughout the short summer, precluding the development of large
2203 populations of phytoplankton, and restricting much of the primary production to a
2204 shallow, open open-water moat. Many other physical, chemical and biological changes
2205 occur in lakes that are either directly or indirectly affected by snow and ice cover (see
2206 Table 1; Douglas and Smol, 1999). Modified from Smol (1988).

2207

2208 **Figure 5.20** A–D) Lake ice melts as it continues to warm. D) Eventually, in
2209 deeper lakes (as opposed to ponds), thermal layers may stratify or be prolonged during
2210 the summer months, further altering the limnological characteristics of the lake. Modified
2211 from Douglas (2007).

2212

2213 **Figure 5.21** The form and distribution of wind-blown silt (loess), wind-blown
2214 sand (dunes), and other deposits of wind-blown sediment in Alaska, have been used to
2215 infer both Holocene and last-glacial past wind directions. (Compiled from many sources
2216 by Muhs and Budahn, 2006.).

2217

2218 **Figure 5.22** Unnamed, hydrologically closed lake in the Yukon Flats Wildlife
2219 Refuge, Alaska. Concentric rings of vegetation developed progressively inward as water
2220 level fell, owing to a negative change in the lake's overall water balance. Historic Landsat
2221 imagery and air photographs indicate that these shorelines formed during within the last
2222 40 years or so. (Photograph by Lesleigh Anderson.)

2223

2224 **Figure 5.23** Recovered sections and palynological and geochemical results across
2225 the Paleocene-Eocene Thermal Maximum about 55 Ma; IODP Hole 302-4A (87° 52.00'
2226 N.; 136° 10.64' E.; 1288 m water depth, in the central Arctic Ocean basin). Mean annual
2227 surface-water temperatures (as indicated in the TEX₈₆' column) are estimated to have
2228 reached 23°C, similar to water in the tropics today. (Error bars for Core 31X show the
2229 uncertainty of its stratigraphic position. Orange bars, indicate intervals affected by
2230 drilling disturbance.) Stable carbon isotopes are expressed relative to the PeeDee
2231 Belemnite standard. Dinocysts tolerant of low salinity comprise *Senegalinium* spp.,
2232 *Cerodinium* spp., and *Polysphaeridium* spp., whereas *Membranosphaera* spp.,
2233 *Spiniferites ramosus* complex, and *Areoligera-Glaphyrocysta* cpx. represent typical
2234 marine species. Arrows and *A. aug* (second column) indicate the first and last
2235 occurrences of dinocyst *Apectodinium augustum*—a diagnostic indicator of Paleocene-
2236 Eocene Thermal Maximum warm conditions. (Sluijs et al., 2006).

2237

2238 **Figure 5.24** Atmospheric CO₂ and continental glaciation 400 Ma to present.
2239 Vertical blue bars, timing and palaeolatitudinal extent of ice sheets (after Crowley, 1998).
2240 Plotted CO₂ records represent five-point running averages from each of four major
2241 proxies (see Royer, 2006 for details of compilation). Also plotted are the plausible ranges
2242 of CO₂ derived from the geochemical carbon cycle model GEOCARB III (Berner and
2243 Kothavala, 2001). All data adjusted to the Gradstein et al. (2004) time scale. Continental
2244 ice sheets grow extensively when CO₂ is low. (after Jansen, 2007, that report's Figure
2245 6.1)

2246

2247 **Figure 5.25** The average isotopic composition ($\delta^{18}\text{O}$) of bottom-dwelling
2248 foraminiferaifers from in a globally distributed set of 57 sediment cores that record the
2249 last 5.3 Ma (modified from Lisiecki and Raymo, 2005). The $\delta^{18}\text{O}$ is controlled primarily
2250 by global ice volume and deep-ocean temperature, with less ice or warmer temperatures
2251 (or both) upward in the core. The influence of Milankovitch frequencies of Earth's orbital
2252 variation are present throughout, but glaciation increased about 2.7 Ma ago concurrently
2253 with establishment of a strong 41 ka variability linked to Earth's obliquity (changes in tilt
2254 of Earth's spin axis), and the additional increase in glaciation about 1.2–0.7 Ma parallels
2255 a shift to stronger 100 ka variability. Dashed lines are used because the changes seem to
2256 have been gradual. The general trend toward higher $\delta^{18}\text{O}$ that runs through this series
2257 reflects the long-term drift toward a colder Earth that began in the early Cenozoic (see
2258 Figure 4.8).

2259

2260 **Figure 5.26** a) Greenland without ice for the last time? Dark green, boreal forest;
2261 light green, deciduous forest; brown, tundra and alpine heaths; white, ice caps. The north-
2262 south temperature gradient is constructed from a comparison between North Greenland
2263 and northwest European temperatures, using standard lapse rate; distribution of
2264 precipitation assumed to retain the Holocene pattern. Topographical base, from model by
2265 Letreguilly et al. (1991) of Greenland's sub-ice topography after isostatic recovery. b)
2266 Upper part of the Kap København Formation, North Greenland. The sand was deposited
2267 in an estuary about 2.4 Ma; it contains abundant well-preserved leaves, seeds, twigs, and
2268 insect remains. (Figure and Photograph of by S.V. Funder.).

2269

2270 **Figure 5.27** The largely marine Gubik Formation, North Slope of Alaska,
2271 contains three superposed lower units that record relative sea level as high +30-+ to +40
2272 m. Pollen in these deposits suggests that borderland vegetation at each of these times was
2273 less forested; boreal forests or spruce-birch woodlands at 2.7 Ma gave way to larch and
2274 spruce forests at about 2.6 Ma and to open tundra by about 2.4 Ma (see photographs by
2275 Robert Nelson, Colby College, who analyzed the pollen; oldest at top). Isotopic reference
2276 time series of Lisecki and Raymo (2005) suggests best as assignments for these sea level
2277 events (Brigham and Carter, 1992).

2278

2279 **Figure 5.28** Glacial cycles of the past 800 ka derived from marine-sediment and
2280 ice cores (McManus, 2004). The history of deep-ocean temperatures and global ice
2281 volume inferred from $\delta^{18}\text{O}$ measured in bottom-dwelling foraminifera shells preserved in
2282 Atlantic Ocean sediments. Air temperatures over Antarctica inferred from the ratio of
2283 deuterium to hydrogen in ice from central Antarctica (EPICA, 2004). Marine isotope
2284 stage 11 (MIS 11) is an interglacial whose orbital parameters were similar to those of the
2285 Holocene, yet it lasted about twice as long as most interglacials. Note the smaller
2286 magnitude and less-pronounced interglacial warmth of the glacial cycles that preceded
2287 MIS 11. Interglaciations older than MIS 11 were less warm than subsequent
2288 interglaciations.

2289

2290 **Figure. 5.29** Polar projection showing regional maximum LIG last interglacial
2291 summer temperature anomalies relative to present summer temperatures; derived from

2292 paleotemperature proxies (see tables Tables 1 and 2, in from CAPE Last Interglacial
2293 Project Members, 2006). Circles, terrestrial; squares, marine sites.

2294

2295 **Figure 5.30** Winter sea-ice limit during MIS 5e and at present. Fossiliferous
2296 paleoshorelines and marine sediments were used by Brigham-Grette and Hopkins (1995)
2297 to evaluate the seasonality of coastal sea ice on both sides of the Bering Strait during the
2298 Last Last Interglaciatiion. Winter sea limit is estimated to have been north of the
2299 narrowest section of the strait, 800 km north of modern limits. Pollen data derived from
2300 Last Interglacial lake sediments suggest that tundra was nearly eliminated from the
2301 Russian coast at this time (Lozhkin and Anderson, 1995). In Chukotka during the warm
2302 interglaciatiion, additional open water favored some taxa tolerant of deeper winter snows.
2303 (Map of William Manley, <http://instaar.colorado.edu/QGISL/>).

2304

2305 **Figure 5.31** The Arctic Holocene Thermal Maximum. Items compared, top to
2306 bottom: seasonal insolation patterns at 70° N. (Berger & Loutre, 1991), and reconstructed
2307 Greenland air temperature from the GISP2 drilling project (Alley 2000); age distribution
2308 of radiocarbon-dated fossil remains of various tree genera from north of present treeline
2309 (MacDonald et al., 2007),); and the frequency of Western Arctic sites that experienced
2310 Holocene Thermal Maximum conditions. (Kaufman et al. 2004).

2311

2312 **Figure. 5.32** The timing of initiation and termination of the Holocene Thermal
2313 Maximum in the western Arctic (Kaufman et al., 2004). a) Regions reviewed in Kaufman
2314 et al., 2004. b) Initiation of the Holocene Thermal Maximum in the western Arctic.

2315 Longitudinal distribution (left) and frequency distribution (right). c) Spatial-temporal
2316 pattern of the Holocene Thermal Maximum in the western Arctic. Upper panel, initiation;
2317 lower panel, termination. Dot colors bracket ages of the Holocene Thermal Maximum;
2318 ages contoured using the same color scheme. Gray dots, equivocal evidence for the
2319 Holocene Thermal Maximum.

2320

2321 **Figure. 5.33** The northward extension of larch (*Larix*) treeline across the Eurasian
2322 Arctic. Treeline today compared with treeline during the Holocene Thermal Maximum
2323 and with anticipated northern forest limits (Arctic Climate Impact Assessment, 2005) due
2324 to climate warming (MacDonald et al., 2007).

2325

2326 **Fig. 5.34** Arctic temperature reconstructions. Upper panel: Holocene summer
2327 melting on the Agassiz Ice Cap, northern Ellesmere Island, Canada. “Melt” indicates the
2328 fraction of each core section that contains evidence of melting (from Koerner and Fisher,
2329 1990). Middle panel: Estimated summer temperature anomalies in central Sweden. Black
2330 bars, elevation of ^{14}C - dated sub-fossil pine wood samples (*Pinus sylvestris* L.) in the
2331 Scandes Mountains, central Sweden, relative to temperatures at the modern pine limit in
2332 the region. Dashed line, upper limit of pine growth is indicated by the dashed line.
2333 Changes in temperature estimated by assuming a lapse rate of $6\text{ }^{\circ}\text{C km}^{-1}$ (from Dahl and
2334 Nesje, 1996, ; based on samples collected by L. Kullman and by G. and J. Lundqvist).
2335 Lower panel: Paleotemperature reconstruction from oxygen isotopes in calcite sampled
2336 along the growth axis of a stalagmite from a cave at Mo i Rana, northern Norway.

2337 Growth ceased around A.D. 1750 (from Lauritzen 1996; Lauritzen and Lundberg 1998;
2338 2002). Figure from Bradley (2000).

2339

2340 **Figure 5.35** Updated composite proxy-data reconstruction of Northern
2341 Hemisphere temperatures for most of the last 2000 years, compared with other published
2342 reconstructions. Estimated confidence limits, 95%. All series have been smoothed with a
2343 40-year lowpass filter. The Medieval Climate Anomaly (MCA), about 950–1200 AD.
2344 The array of reconstructions demonstrate that the warming documented by instrumental
2345 data during the past few decades exceeds that of any warm interval of the past 2000
2346 years, including that estimated for the MCA. (Figure from Mann et al. (in press). CPS,
2347 composite plus scale methodology; CRU, East Anglia Climate Research unit, a source of
2348 instrumental data; EIV, error-in-variables); HAD, Hadley Climate Center.

2349

2350 **Figure 5.36** Paleoclimate data quantify the magnitude of Arctic amplification.
2351 Shown are paleoclimate estimates of Arctic summer temperature anomalies relative to
2352 recent, and the appropriate Northern Hemisphere or global summer temperature
2353 anomalies, together with their uncertainties, for the following: the last glacial maximum
2354 (LGM; about 20 ka), Holocene thermal maximum (HTM; about 8 ka), last interglaciation
2355 (LIG; 130–125 ka ago) and middle Pliocene (about 3.5–3.0 Ma). The trend line suggests
2356 that summer temperature changes are amplified 3 to 4 times in the Arctic. Explanation of
2357 data sources follows, for the different times for each time considered, beginning with the
2358 most recent.

2359 **Holocene Thermal Maximum (HTM):** Arctic $\Delta T = 1.7 \pm 0.8^{\circ}\text{C}$; Northern
2360 Hemisphere $\Delta T = 0.5 \pm 0.3^{\circ}\text{C}$; Global $\Delta T = 0^{\circ} \pm 0.5^{\circ}\text{C}$.

2361 A recent summary of summer temperature anomalies in the western Arctic
2362 (Kaufman et al., 2004) built on earlier summaries (Kerwin et al., 1999; CAPE Project
2363 Members, 2001) and is consistent with more-recent reconstructions (Kaplan and Wolfe,
2364 2006; Flowers et al., 2007). Although the Kaufman et al. (2004) summary considered
2365 only the western half of the Arctic, the earlier summaries by Kerwin et al., (1999) and
2366 CAPE Project Members (2001) indicated that similar anomalies characterized the eastern
2367 Arctic, and all syntheses report the largest anomalies in the North Atlantic sector. Few
2368 data are available for the central Arctic Ocean; we assume that the circumpolar dataset
2369 provides an adequate reflection of air temperatures over the Arctic Ocean as well.

2370 Climate models suggest that the average planetary anomaly was concentrated over
2371 the Northern Hemisphere. Braconnot et al. (2007) summarized the simulations from 10
2372 different climate model contributions to the PMIP2 project that compared simulated
2373 summer temperatures at 6 ka with recent temperatures. The global average summer
2374 temperature anomaly at 6 ka was $0^{\circ} \pm 0.5^{\circ}\text{C}$, whereas the Northern Hemisphere anomaly
2375 was $0.5^{\circ} \pm 0.3^{\circ}\text{C}$. These patterns are similar to patterns in model results described by
2376 Hewitt and Mitchell (1998) and Kitoh and by Murakami (2002) for 6 ka, and a global
2377 simulation for 9 ka (Renssen et al., 2006). All simulate little difference in summer
2378 temperature outside the Arctic when those temperatures are compared to with pre-
2379 industrial temperatures.

2380 **Last Glacial Maximum (LGM):** Arctic $\Delta T = 20^{\circ} \pm 5^{\circ}\text{C}$; global and Northern
2381 Hemisphere $\Delta T = -5^{\circ} \pm 1^{\circ}\text{C}$

2382 Quantitative estimates of temperature reductions during the peak of the Last
2383 Glacial Maximum are less widespread in for the Arctic than are estimates of temperatures
2384 during warm times. Ice-core borehole temperatures, which offer the most compelling
2385 evidence (Cuffey et al., 1995; Dahl-Jensen et al., 1998), are supported by evidence from
2386 biological proxies in the North Pacific sector (Elias et al., 1996a), where no ice cores are
2387 available that extend back to the Last Glacial Maximum. Because of the limited datasets
2388 for temperature reduction in the Arctic during the Last Glacial Maximum, we incorporate
2389 a large uncertainty. The global-average temperature decrease during peak glaciations,
2390 based on paleoclimate proxy data, was 5° – 6° C, and little difference existed between the
2391 Northern and Southern Hemispheres (Farrera et al., 1999; Braconnot et al., 2007;
2392 Braconnot et al., 2007). A similar temperature anomaly is derived from climate-model
2393 simulations (Otto-Bliesner et al., 2007).

2394 **Last Interglaciation (LIG):** Arctic $\Delta T = 5^{\circ} \pm 1^{\circ}$ C; global and Northern
2395 Hemisphere $\Delta T = 1^{\circ} \pm 1^{\circ}$ C)

2396 A recent summary of all available quantitative reconstructions of summer-
2397 temperature anomalies for in the Arctic during peak Last Interglaciation warmth shows a
2398 spatial pattern similar to that shown by Holocene Thermal Maximum reconstructions.
2399 The largest anomalies are in the North Atlantic sector and the smallest anomalies are in
2400 the North Pacific sector, but those small anomalies are substantially larger ($5^{\circ} \pm 1^{\circ}$ C)
2401 than they were during the Holocene Thermal Maximum (CAPE Last Interglacial Project
2402 Members, 2006). A similar pattern of Last Interglaciation summer-temperature anomalies
2403 is apparent in climate model simulations (Otto-Bliesner et al., 2006). Global and
2404 Northern Hemisphere summer-temperature anomalies are derived from summaries in

2405 CLIMAP Project Members (1984), Crowley (1990), Montoya et al. (2000), and Bauch
2406 and Erlenkeuser (2003).

2407 **Middle Pliocene:** Arctic $\Delta T = 12^{\circ} \pm 3^{\circ}\text{C}$; global $\Delta T = 4^{\circ} \pm 2^{\circ}\text{C}$)

2408 Widespread forests throughout the Arctic in the middle Pliocene offer a glimpse
2409 of a notably warm time in the Arctic, which had essentially modern continental
2410 configurations and connections between the Arctic Ocean and the global ocean.

2411 Reconstructed Arctic temperature anomalies are available from several sites that show
2412 much warmth and no summer sea ice in the Arctic Ocean basin. These sites include the
2413 Canadian Arctic Archipelago (Dowsett et al., 1994; Elias and Matthews, 2002;
2414 Ballantyne et al., 2006), Iceland (Buchardt and Símónarson, 2003), and the North Pacific
2415 (Heusser and Morley, 1996). A global summary of mid-Pliocene biomes by Salzmann et
2416 al. (2008) concluded that Arctic mean-annual-temperature anomalies were in excess of
2417 10°C ; some sites indicate temperature anomalies of as much as 15°C . Estimates of global
2418 sea-surface temperature anomalies are from Dowsett (2007).

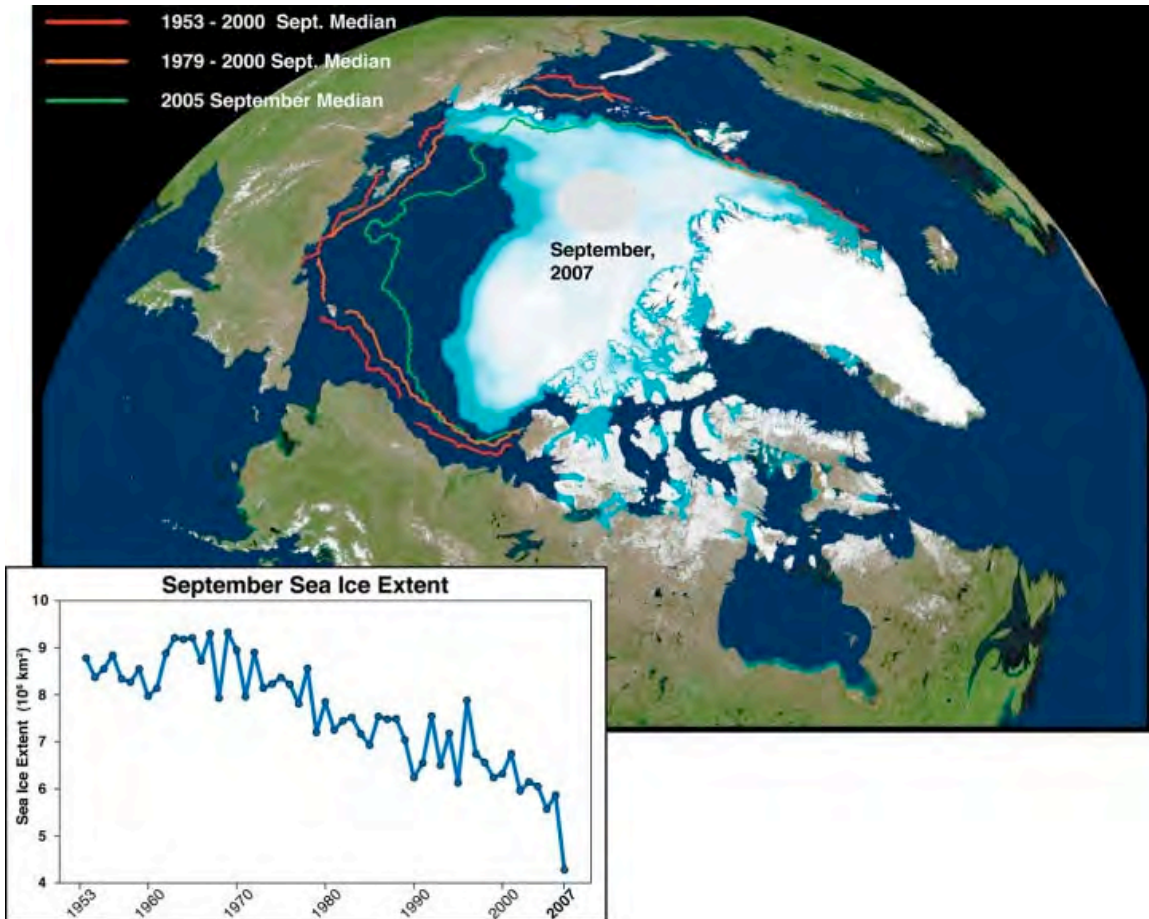
2419 Global reconstructions of mid-Pliocene temperature anomalies from proxy data
2420 and general circulation models show modest warming (average, $4^{\circ} \pm 1^{\circ}\text{C}$) across low to
2421 middle latitudes (Dowsett et al., 1999; Raymo et al., 1996; Sloan et al., 1996, Budyko et
2422 al., 1985; Haywood and Valdes, 2004; Jiang et al., 2005; Haywood and Valdes, 2006;
2423 Salzmann et al., 2008).

2424

2424

2425

2426



2427

2428

2429

2430

2431

2432

2433

2434

2435

2436

2437

2438

Figure 5.1 Median extent of sea ice in September, 2007, compared with averaged intervals during recent decades. Red curve, 1953–2000; orange curve, 1979–2000; green curve, September 2005. Inset: Sea ice extent time series plotted in square kilometers, shown from 1953–2007 in the graph below (Stroeve et al., 2008). The reduction in Arctic Ocean summer sea ice in 2007 was greater than that predicted by most recent climate models.

2436

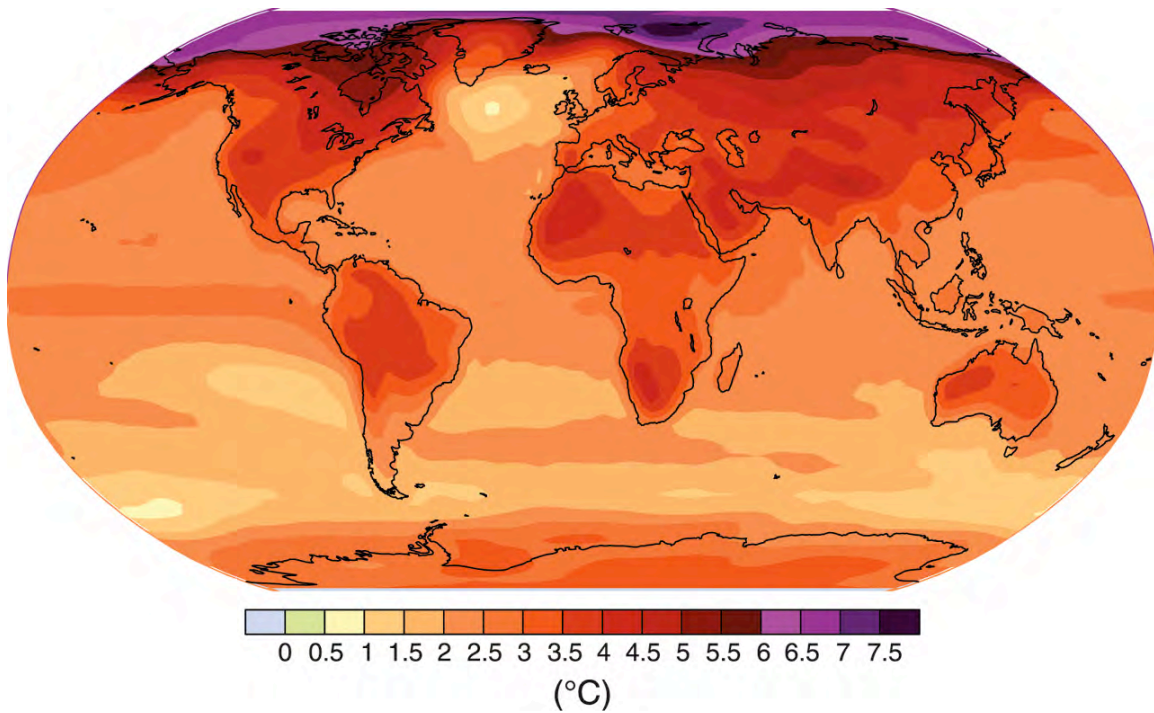
2437

2438

2438

2439

Geographical pattern of surface warming

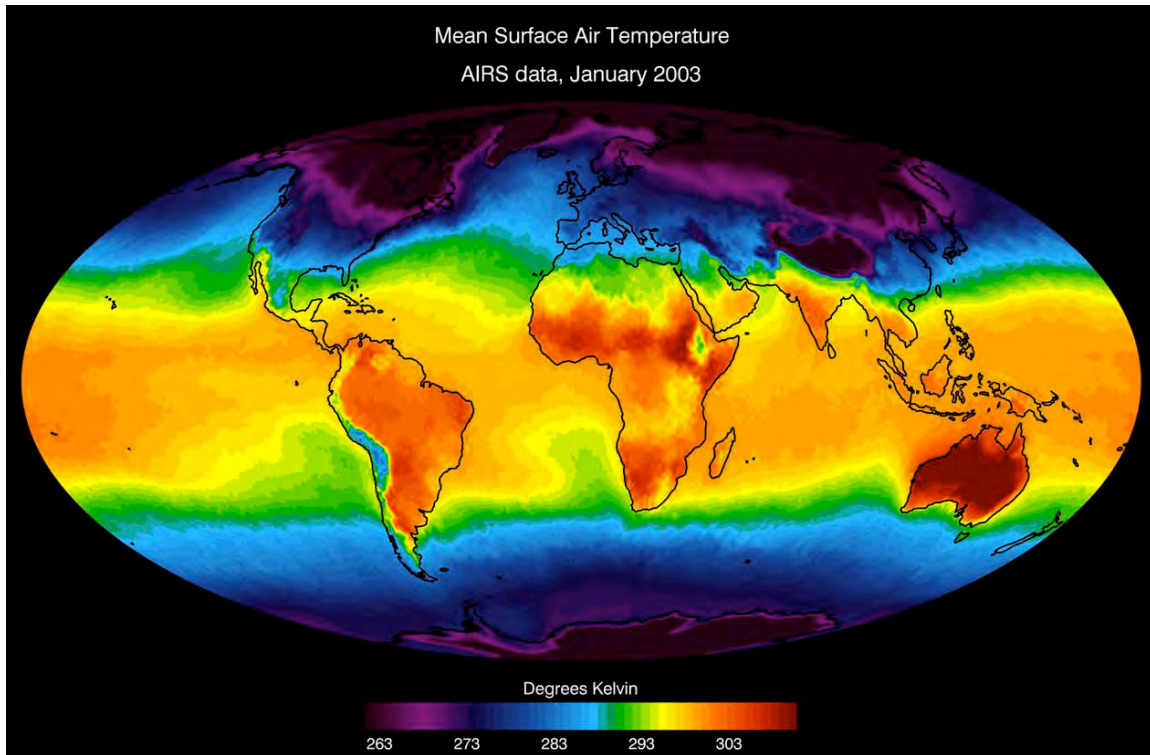


2440

2441 **Figure 5.2** Projected surface temperature changes for the last decade of the 21st century
2442 (2090-2099) relative to the period 1980-1999. The map shows the IPCC multi- multi-
2443 Atmosphere-Ocean coupled Global Climate Model average projection for the A1B
2444 (balanced emphasis on all energy resources) scenario. The most significant warming is
2445 projected to occur in the Arctic. (IPCC, 2007; Figure SPM6)

2446

2446



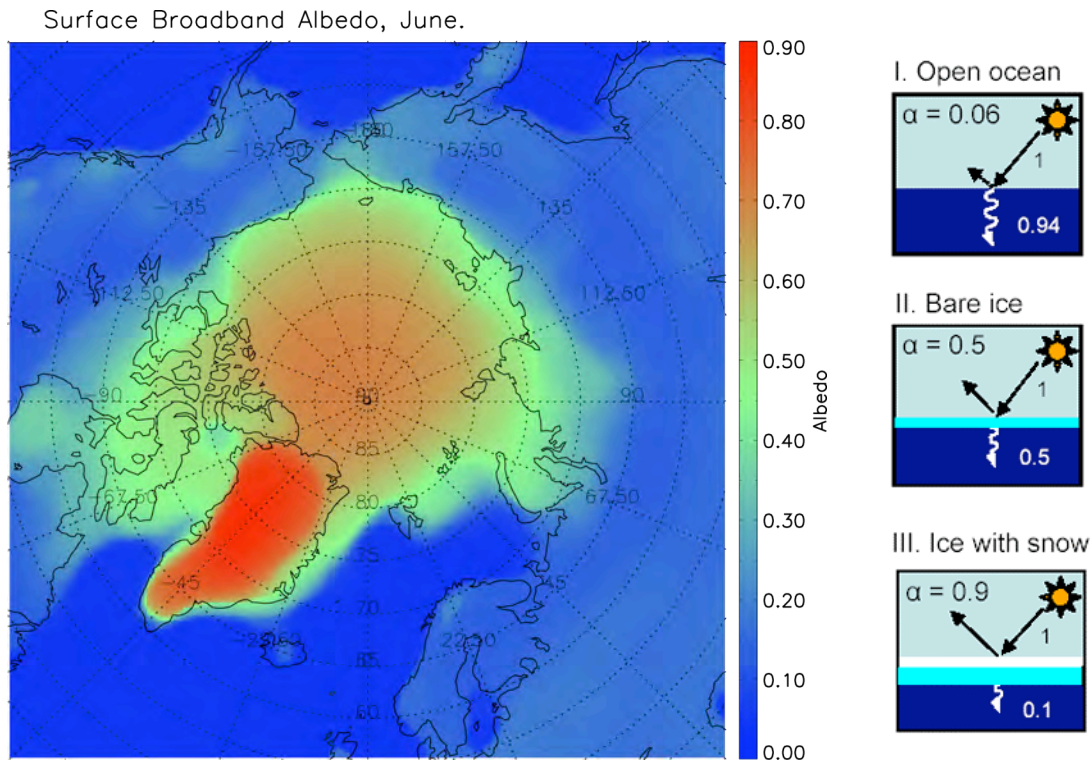
2447

2448 **Figure 5.3** Global mean observed near-surface air temperatures for the month of
2449 January, 2003 derived from the Atmospheric Infrared Sounder (AIRS) data. Contrast
2450 between equatorial and Arctic temperatures is greatest during the northern hemisphere
2451 winter. The transfer of heat from the tropics to the polar regions is a primary feature of
2452 the Earth's climate system (Color scale is in Kelvin degrees such that $0^{\circ}\text{C}=273.15$
2453 Kelvin.)

2454 (Source: http://www-airs.jpl.nasa.gov/graphics/features/airs_surface_temp1_full.jpg)

2455

2455



2456

2457 **a**

2458

2459 **Figure 5.4** Albedo values in the Arctic

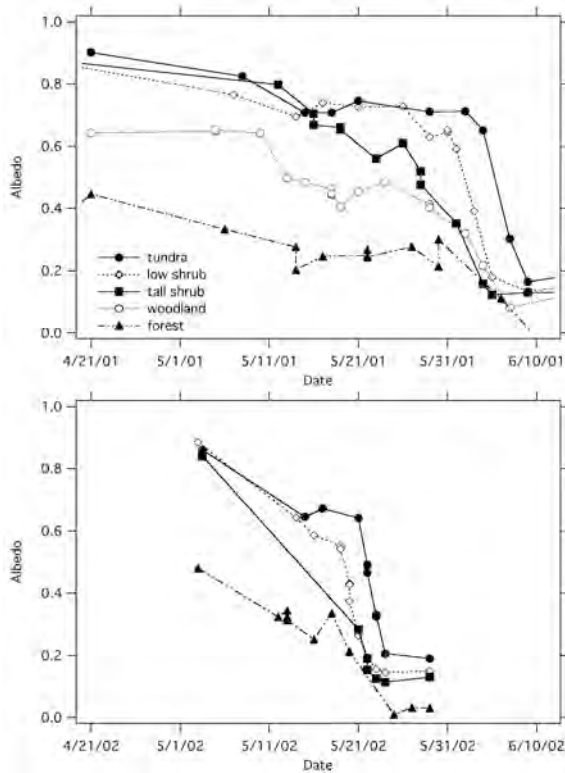
2460 **5a.** Advanced Very High Resolution Radiometry (AVHRR)-derived Arctic albedo
 2461 values in June, 1982-2004 multi-year average, showing the strong contrast between snow
 2462 and ice covered areas (green through red) and open water or land (blue). (Image courtesy
 2463 of X. Wang, University of Wisconsin-Madison, CIMSS/NOAA)

2464 **5b.** Albedo feedbacks. Albedo is the fraction of incident sunlight that is reflected. Snow,
 2465 ice, and glaciers have high albedo. Dark objects such as the open ocean, which absorbs
 2466 some 93% of the sun's energy, have low albedo (about 0.06), absorbing some 93% of the
 2467 sun's energy. Bare ice has an albedo of 0.5; however, sea ice covered with snow has an
 2468 albedo of nearly 90% (Source: <http://nsidc.org/seaice/processes/albedo.html>).

2469

b

2469



2470

a

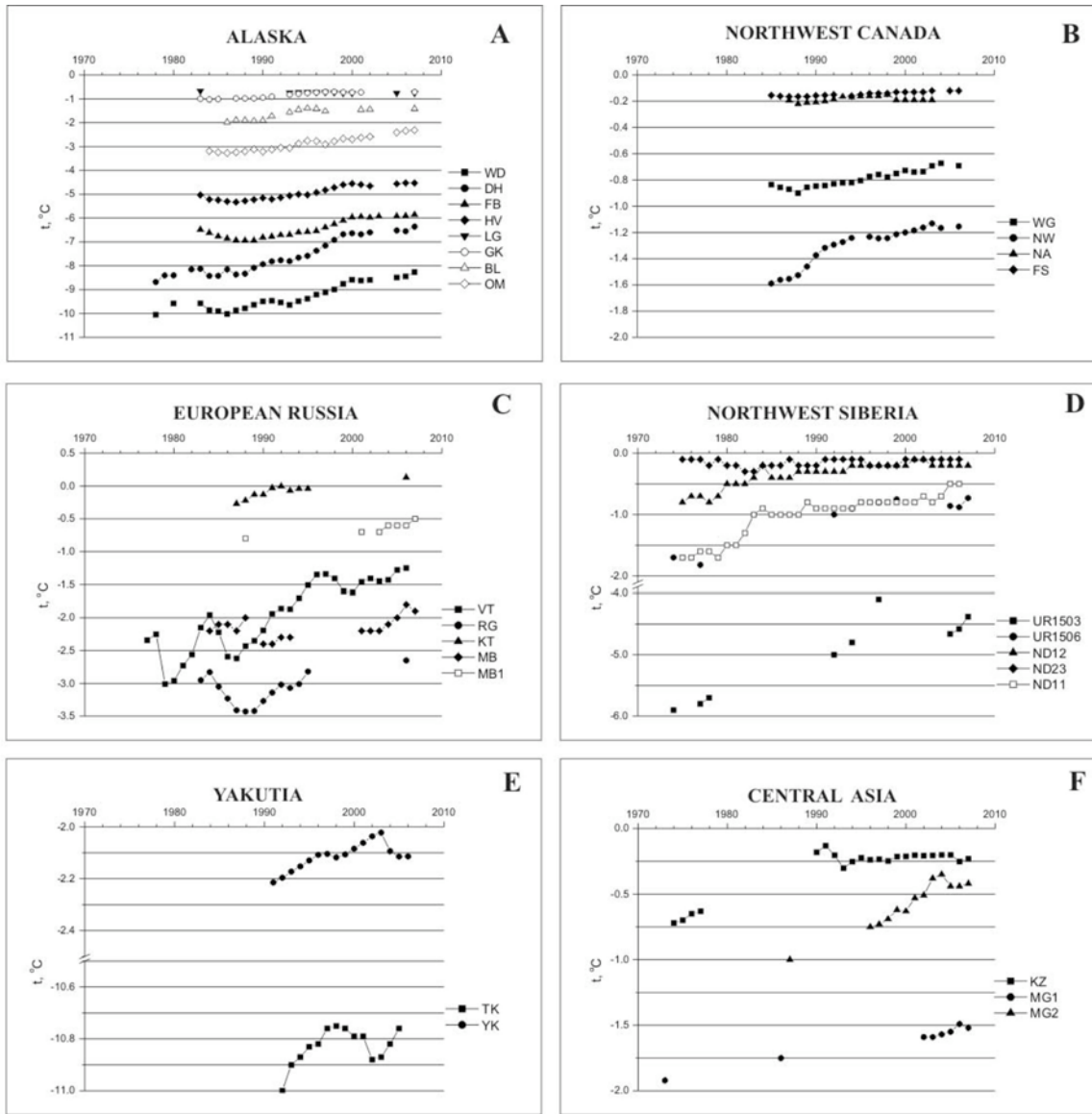
b

2471

2472

2473 **Figure 5.5** Changes in vegetation cover throughout the Arctic can influence albedo, as
 2474 can altering the onset of snow melt in spring. a) Progression of the melt season in
 2475 northern Alaska, May 2001 (top) and May 2002 (bottom), demonstrates how areas with
 2476 exposed shrubs show earlier snow melt. b) Dark branches against reflective snow alter
 2477 albedo (Sturm et al., 2005; Photograph courtesy of Matt Sturm).

2478



2479

2480 **Figure 5.6** Warming trend in Arctic permafrost (permanently frozen ground), 1970–
 2481 present. Local effects can modify this trend. A) Sites in Alaska: WD, West Dock; DH,
 2482 Deadhorse; FB, Franklin Bluffs; HV, Happy Valley; LG, Livengood; GK, Gulkana; BL,
 2483 Birch Lake; OM, Old Man. B) Sites in northwest Canada: WG, Wrigley; NW, Norman
 2484 Wells; NA, Northern Alberta; FS, Fort Simpson. C) Sites in European Russia: VT,
 2485 Vorkuta; RG, Rogovoi; KT, Karataikha; MB, Mys Bolvansky. D) Northwest Siberia: UR,

SAP1.2 DRAFT 3 PUBLIC COMMENT

2486 Urengoi; ND, Nadym. E) Sites in Yakutia: TK, Tiksi; YK, Yakutsk. F) Sites in central
2487 Asia: KZ, Kazakhstan; MG, Mongolia (Brown and Romanovsky, 2008).
2488



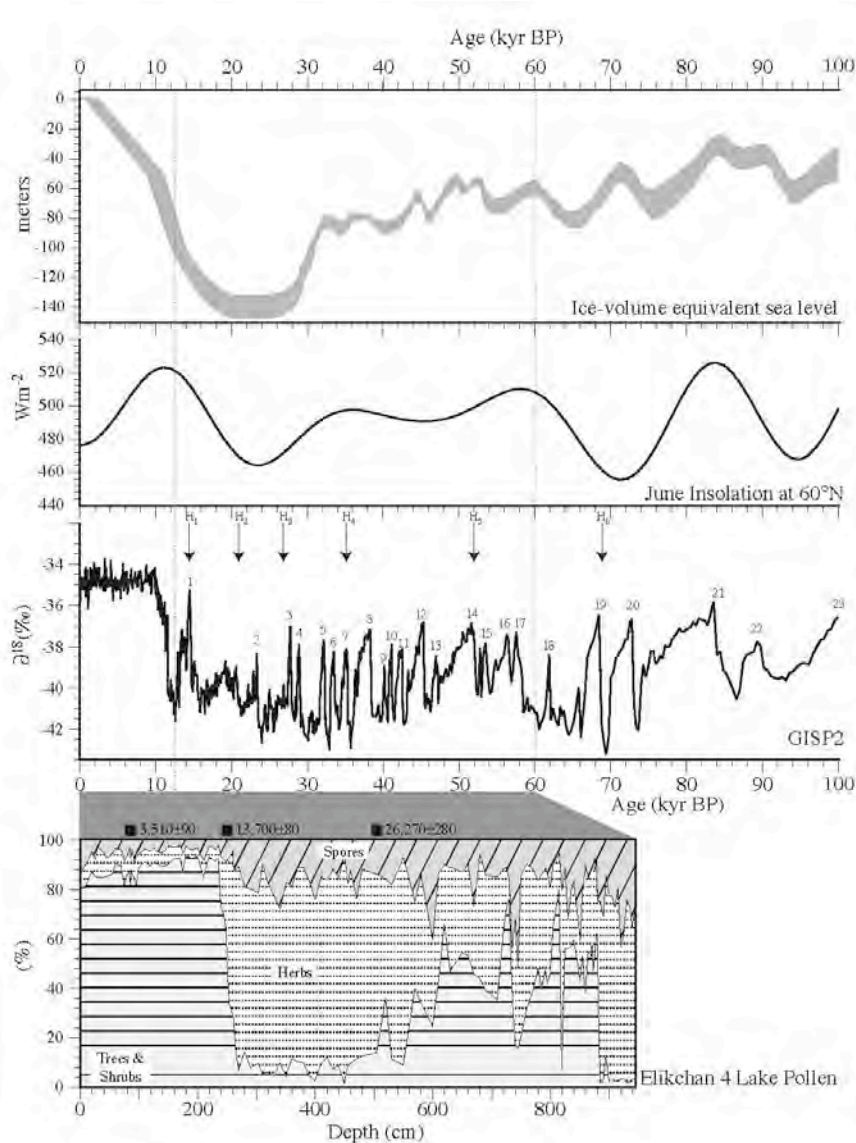
2488

2489

2490 **Figure 5.7** Inflows and outflows of water in the Arctic Ocean. Red lines, components and
 2491 paths of the surface and Atlantic Water layer in the Arctic; black arrows, pathways of
 2492 Pacific water inflow from 50–200 m depth; blue arrows, surface-water circulation; green,
 2493 major river inflow; red arrows, movements of density-driven Atlantic water and
 2494 intermediate water masses into the Arctic (AMAP, 1998).

2495

2495



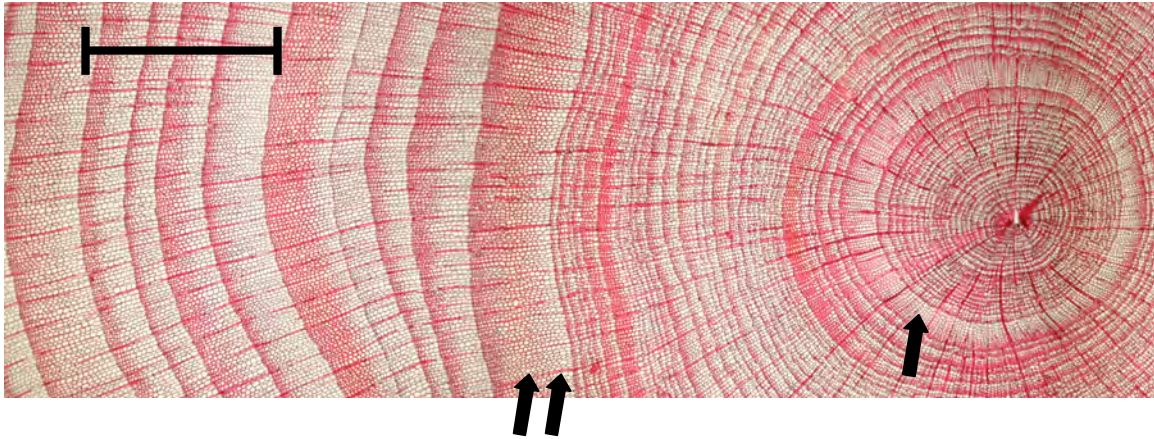
2496

2497 **Figure 5.8** Upper three panels: Correlation of global sea-level curve (Lambeck et al.,
 2498 2002), Northern Hemisphere summer insolation (Berger and Loutre, 1991), and the
 2499 Greenland Ice Sheet (GISP2) δ¹⁸O record (Grootes et al., 1993), ages all given in
 2500 calendar years. Bottom panel: temporal changes in the percentages of the main taxa of
 2501 trees and shrubs, herbs and spores at Elikchan 4 Lake in the Magadan region of
 2502 Chukotka, Russia. Lake core x-axis is depth, not time (Brigham-Grette et al., 2004).
 2503 Habitat was reconstructed on the basis of modern climate range of collective species
 2504 found in fossil pollen assemblages. The reconstruction can be used to estimate past

2505 temperatures or the seasonality of a particular site. The GISP2 record: Base of core
2506 roughly 60 ka (Lozhkin and Anderson, 1996). H1 above arrow, timing of Heinrich event
2507 event 1 (and so on); number 1 above curve, Dansgaard-Oschegeger event (and so on).
2508 During approximately 27 ka to nearly 55 ka, vegetation, especially treeline, recovered for
2509 short intervals to nearly Holocene conditions at the same time that the isotopic record in
2510 Greenland suggests repeated warm warm-cold cycles of change. kyr BP, thousands of
2511 years before the present.

2512

2513



2514

2515

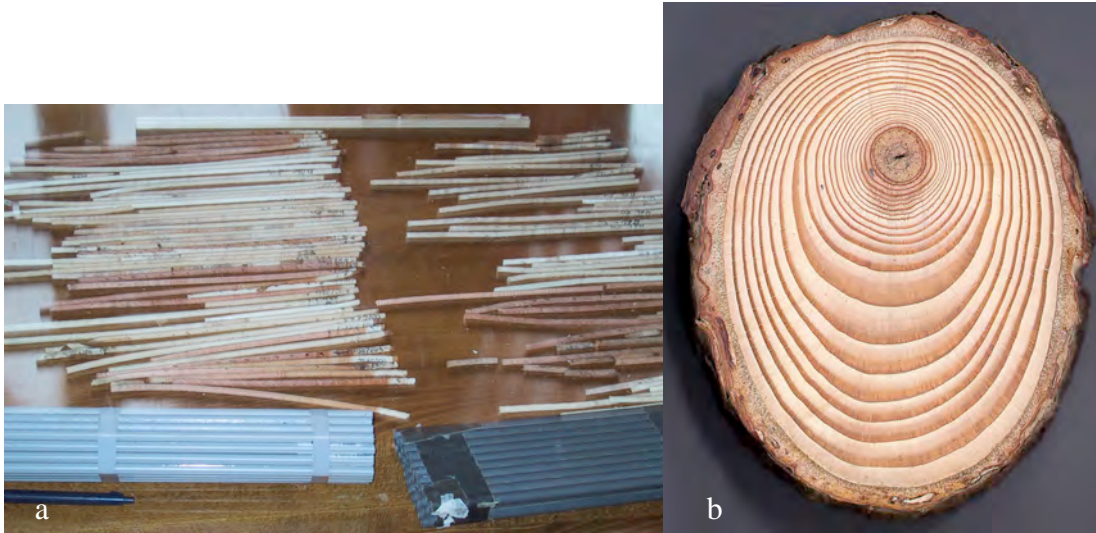
2516 **Figure 5.9** Annual tree rings composed of seasonal early and late wood are clear in this a
2517 64-year year-old *Larix siberica* from western Siberia (Esper and Schweingruber, 2004).
2518 Initial growth was restricted; narrow rings average 0.035 mm/year, punctuated by one
2519 thicker ring (one single arrow). Later (two arrows), tree-ring width abruptly at least
2520 doubled for more than three years. Ring widths increased to 0.2 mm/year (Photograph
2521 courtesy of Jan Esper, Swiss Federal Research Institute).

2522

2523

2523

2524



2525

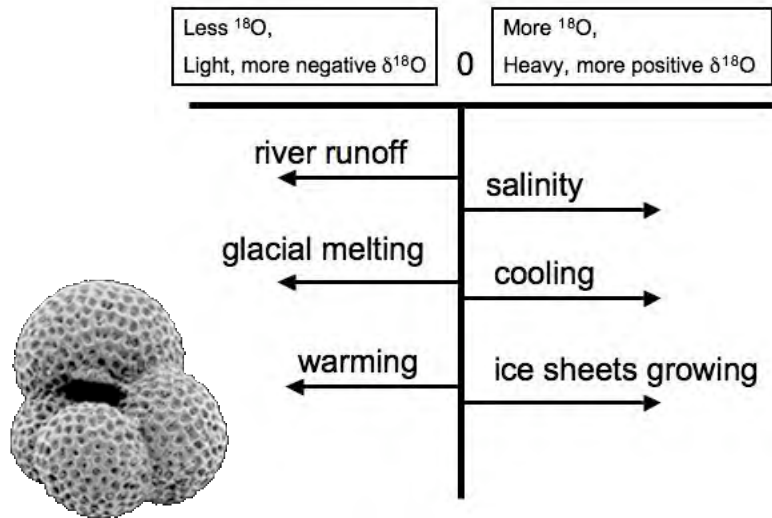
2526

2527 **Figure 5.10** Typical tree ring samples. a) Increment cores taken from trees with a small
2528 small-bore hollow drill. They can be easily stored and transported in plastic soda straws
2529 for analysis in the laboratory. b) Alternatively, cross sections or disks can be sanded for
2530 study. A cross section of *Larix decidua* root shows differing wood thickness within single
2531 rings, caused by exposure. (Photographs courtesy of Jan Esper and Holger Gärtner, Swiss
2532 Federal Research Institute, respectively).

2533

2534

2534



2535

2536 **Figure 5.11** 14 Microscopic marine plankton known as (foraminifera) (see inset)
 2537 grow a shell of calcium carbonate (CaCO_3) in or near isotopic equilibrium with ambient
 2538 sea water. The oxygen isotope ratio measured in these shells can be used to determine the
 2539 temperature of the surrounding waters. (The oxygen-isotope ratio is expressed in $\delta^{18}\text{O}$
 2540 parts per million (ppm) = $10^3[(R_{\text{sample}}/R_{\text{standard}}) - 1]$, where $R_x = (^{18}\text{O})/(^{16}\text{O})$ is the ratio of
 2541 isotopic composition of a sample compared to that of an established standard, such as
 2542 ocean water) However, factors other than temperature can influence the ratio of ^{18}O to
 2543 ^{16}O . Warmer seasonal temperatures, glacial meltwater, and river runoff with depleted
 2544 values all will produce a more negative (lighter) $\delta^{18}\text{O}$ [should the Greek letter be δ ?]
 2545 ratio. On the other hand, cooler temperatures or higher salinity waters will drive the ratio
 2546 up, making it heavier, or more positive. The growth of large continental ice sheets
 2547 selectively removes the lighter isotope (^{16}O), leaving the ocean enriched in the heavier
 2548 isotope (^{18}O).
 2549

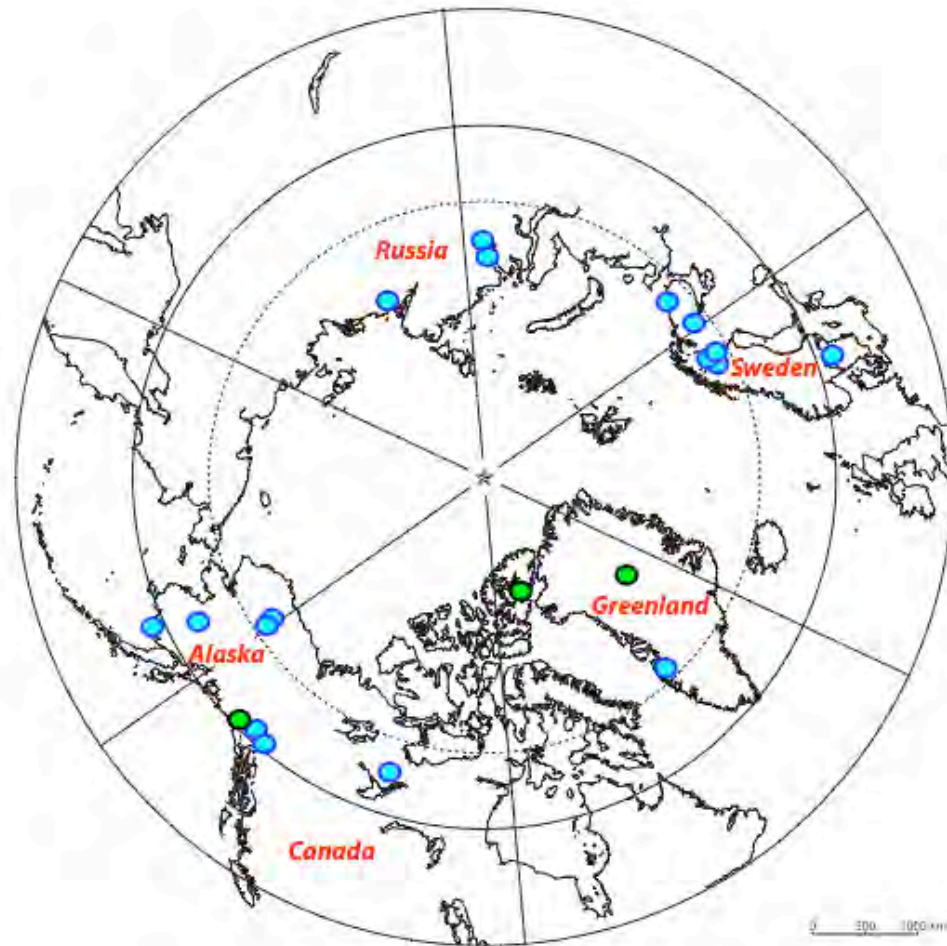
2549



2550

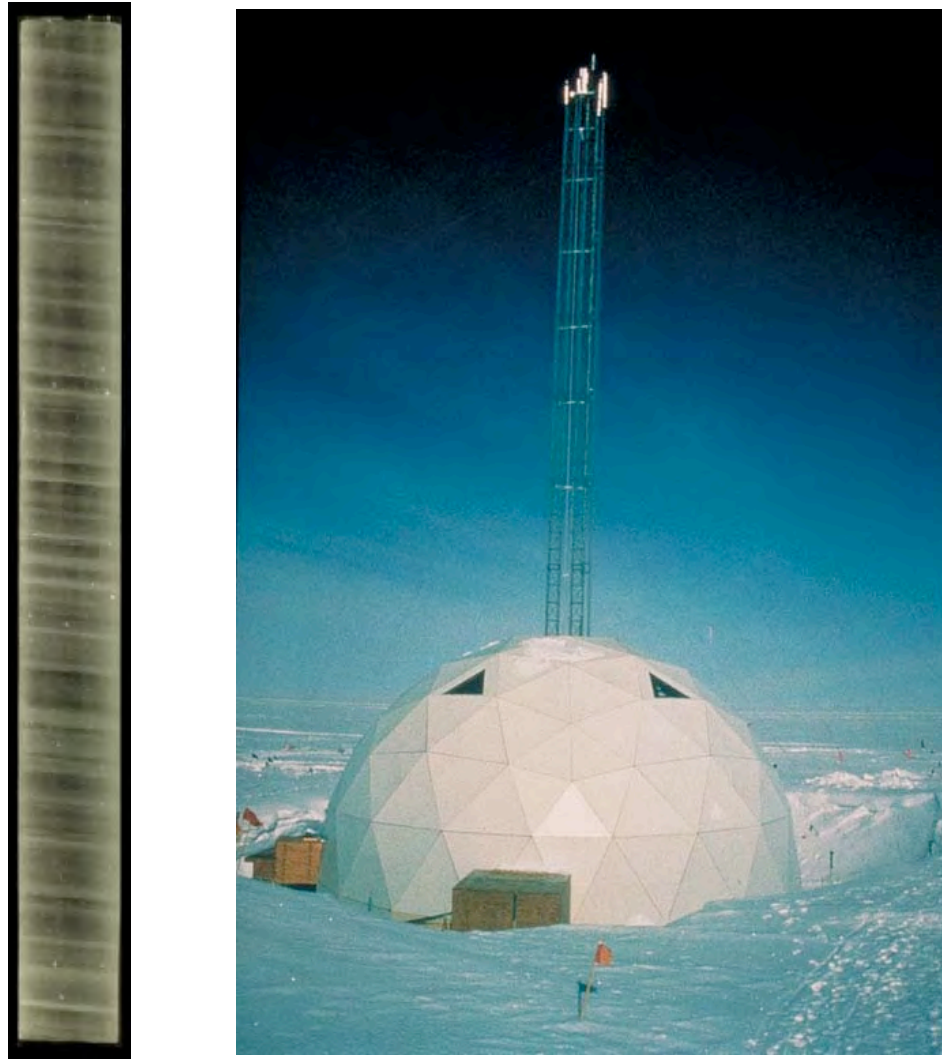
2551 **Figure 5.12** Lake El'gygytyn in the Arctic Far East of Russia. Open and closed lake
2552 systems in the Arctic differ hydrologically according to the balance between inflow,
2553 outflow, and the ratio of precipitation to evaporation. These parameters are the dominant
2554 influence on lake stable stable-isotopic chemistry and on the depositional character of the
2555 sediments and organic matter. Lake El'gygytyn is annually open and flows to the Bering
2556 Sea during July and August, but the outlet closes by early September as lake level drops
2557 and storms move beach gravels that choke the outlet. (Photograph by J. Brigham-Grette).
2558

2558



2559

2560 **Figure 5.13** Locations of Arctic and sub-Arctic lakes (blue) and ice cores (green) whose
2561 oxygen isotope records have been used to reconstruct Holocene paleoclimate. (Map
2562 adapted from the Atlas of Canada, © 2002. Her Majesty the Queen in Right of Canada,
2563 Natural Resources Canada. / Sa Majesté la Reine du chef du Canada, Ressources
2564 naturelles Canada.)



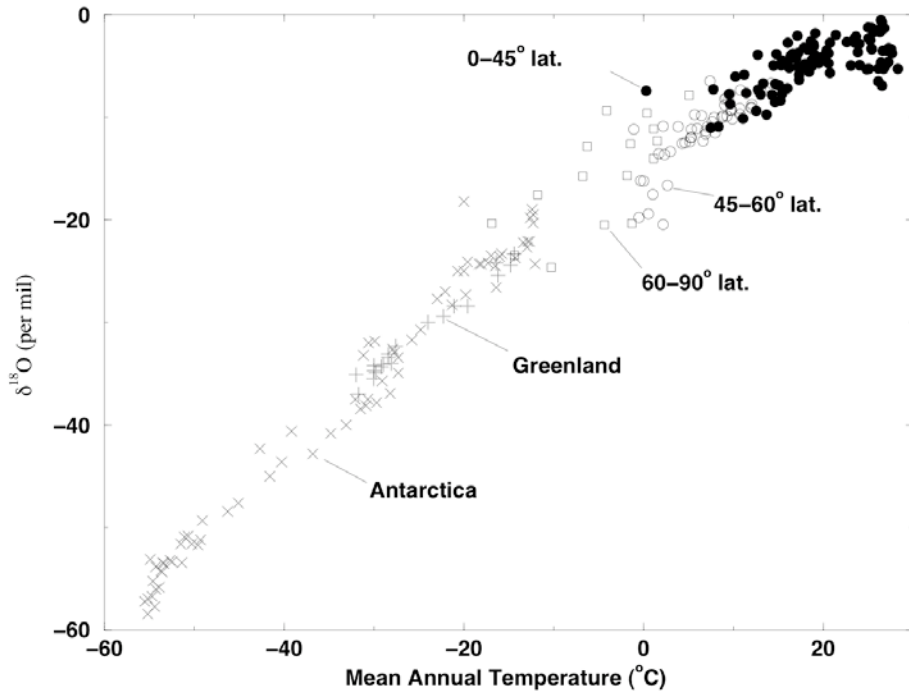
2565

a

b

2566

2567 **Figure 5.14** a) One-meter section of Greenland Ice Core Project-2 core from 1837 m
2568 depth showing annual layers. (Photograph courtesy of Eric Cravens, Assistant Curator,
2569 U.S. National Ice Core Laboratory). b) Field site of Summit Station on top of the
2570 Greenland Ice sheet (Photograph by Michael Morrison, GISP2 SMO, University of New
2571 Hampshire; NOAA Paleoslide Set)

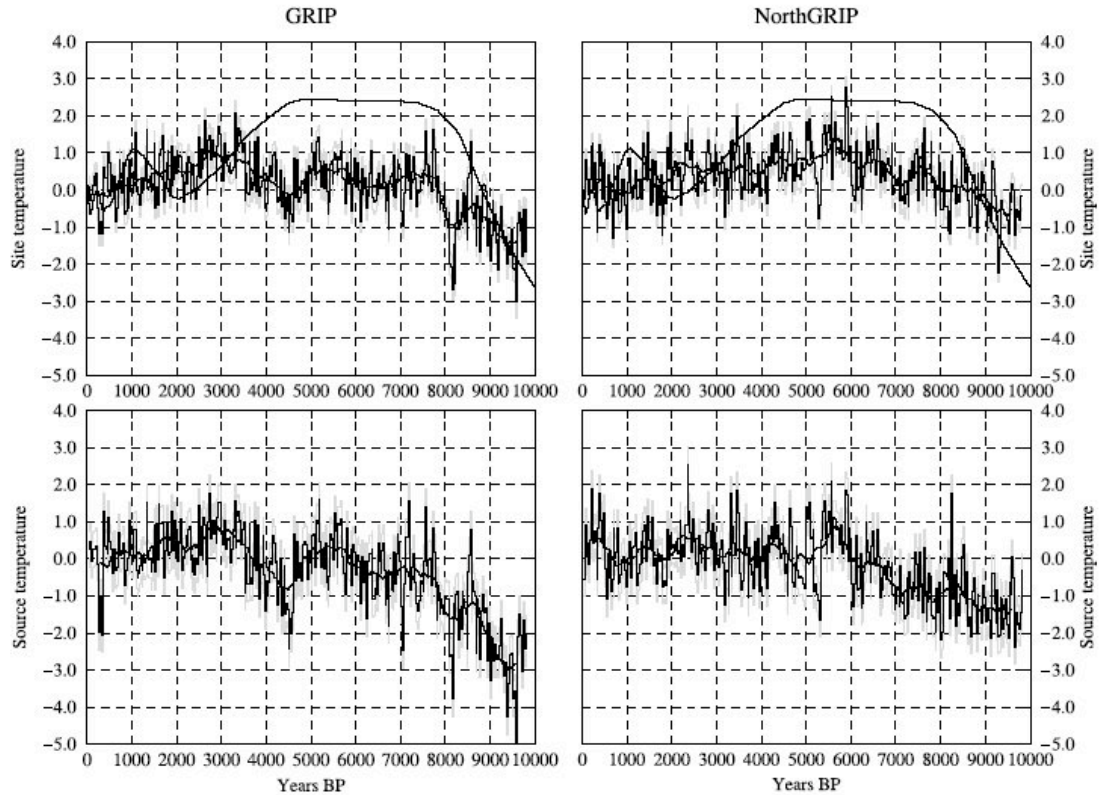


2572

2573 **Figure 5.15** Relation between isotopic composition of precipitation and temperature in
 2574 the parts of the world where ice sheets exist. Sources of data as follows: International
 2575 Atomic Energy Agency (IAEA) network (Fricke and O'Neil, 1999; calculated as the
 2576 means of summer and winter data of their Table 1 for all sites with complete data. Open
 2577 squares, poleward of 60° latitude (but with no inland ice-sheet sites); open circles, 45°–
 2578 60° latitude; filled circles, equatorward of 45° latitude. x, data from Greenland (Johnsen
 2579 et al., 1989); +, data from Antarctica (Dahe et al., 1994). About 71% of Earth's surface
 2580 area is equatorward of 45°, where dependence of $\delta^{18}\text{O}$ on temperature is weak to
 2581 nonexistent. Only 16% of Earth's surface falls in the 45°–60° band, and only 13% is
 2582 poleward of 60°. The linear array is clearly dominated by data from the ice sheets.
 2583 (Source: Alley and Cuffey, 2001)

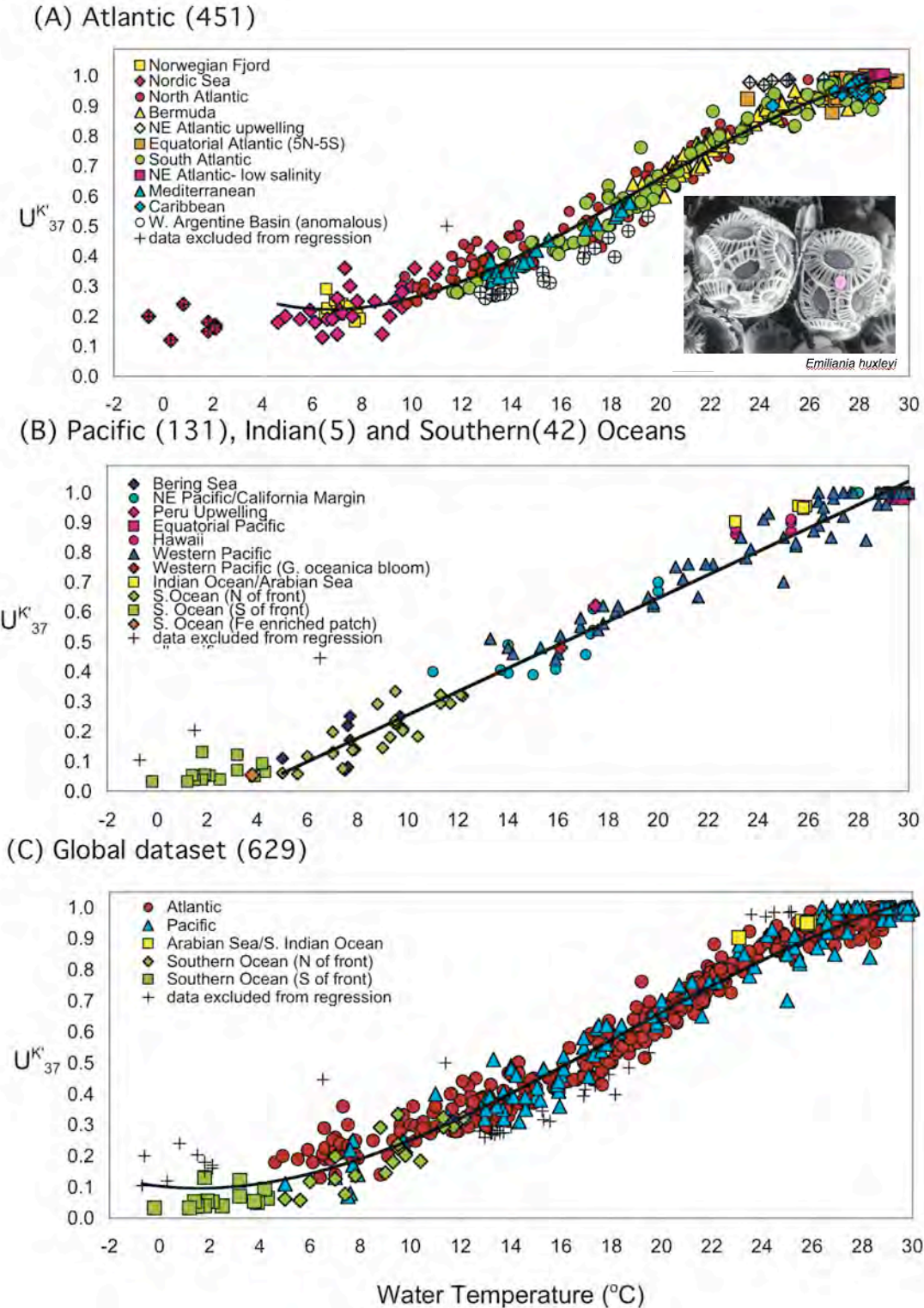
2584

2584



2585

2586 **Figure 5.16** Paleotemperature estimates of site and source waters from on Greenland:
 2587 GRIP and NorthGrip, Masson-Delmotte et al., 2005). GRIP (left) and NorthGrip (right)
 2588 site (top) and source (bottom) temperatures derived from GRIP and NorthGRIP $\delta^{18}\text{O}$ and
 2589 deuterium excess corrected for seawater $\delta^{18}\text{O}$ (until 6000 BP). Shaded lines in gray
 2590 behind the black line provide an estimate of uncertainties due to the tuning of the isotopic
 2591 model and the analytical precision. Solid line (in part above zigzag line), GRIP
 2592 temperature derived from the borehole-temperature profile (Dahl-Jensen et al., 1998).



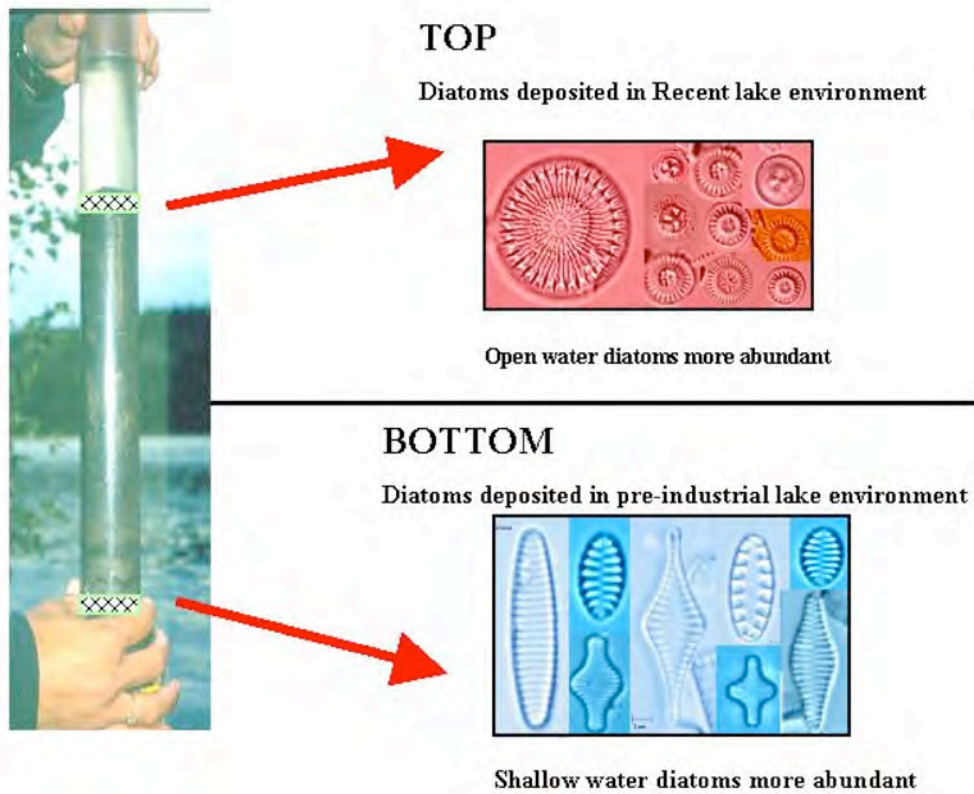
2593

2594 **Figure 5.17** Biomarker alkenone. U_{37}^K versus measured water temperature for ocean-

2595 water surface mixed layer (0–30 m) samples. A) Atlantic region: Empirical 3rd-order

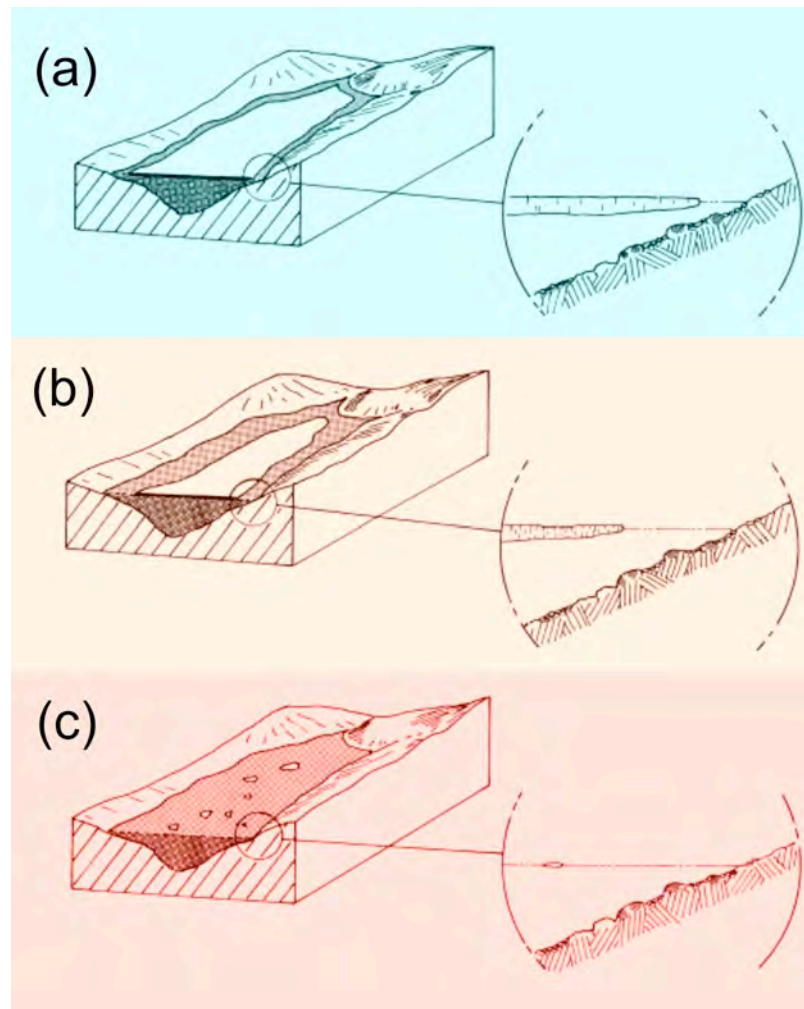
2596 polynomial regression for samples collected in warmer-than-4°C waters is $U_{37}^K = 1.004$
 2597 $10^{-4}T^3 + 5.744 \cdot 10^{-3}T^2 - 6.207 \cdot 10^{-2}T + 0.407$ ($r^2 = 0.98$, $n = 413$) (Outlier data from
 2598 the southwest Atlantic margin and northeast Atlantic upwelling regime is excluded.). B)
 2599 Pacific, Indian, and Southern Ocean regions: The empirical linear regression of Pacific
 2600 samples is $U_{37}^K = 0.0391T - 0.1364$ ($r^2 = 0.97$, $n = 131$). Pacific regression does not
 2601 include the Indian and Southern Ocean data. C) Global data: The empirical 3rd order
 2602 polynomial regression, excluding anomalous southwest Atlantic margin data, is $U_{37}^K =$
 2603 $5.256 \cdot 10^{-5}T^3 + 2.884 \cdot 10^{-3}T^2 - 8.4933 \cdot 10^{-2}T + 9.898$ ($r^2 = 0.97$, $n = 588$). +, sample
 2604 excluded from regressions. (Conte et al, 2006).

2605



2606 **Figure 5.18** Diatom assemblages reflect a variety of environmental conditions in Arctic
 2607 lake systems. Transitions, especially rapid change from one assemblage to another, can
 2608 reflect large changes in conditions such as light, nutrient availability, or temperature, for
 2609 example. Biogenic silica, chiefly the silica skeletal framework constructed by diatoms, is
 2610 commonly measured in lake sediments and used as an index of past changes in aquatic
 2611 primary productivity.

2612



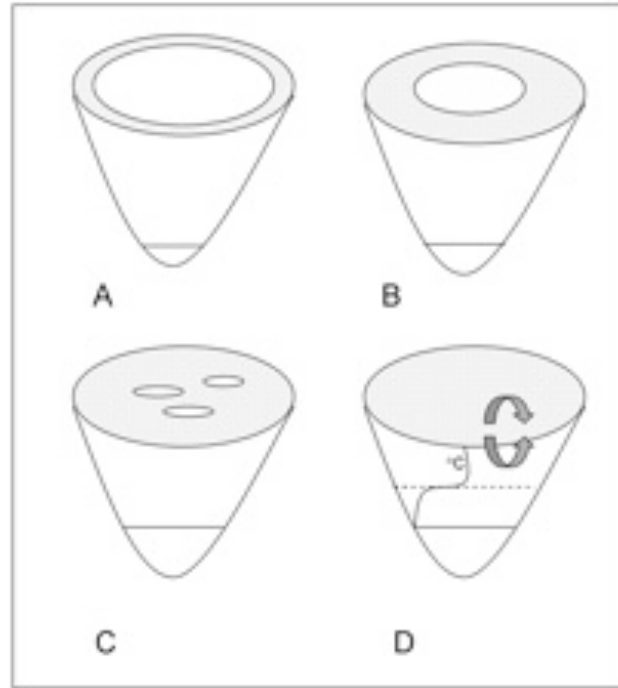
2613

2614 **Figure 5.19** Changing ice and snow conditions on an Arctic lake during relatively (a)
 2615 cold, (b) moderate, and (c) warm conditions. During colder years, a permanent raft of ice
 2616 may persist throughout the short summer, precluding the development of large
 2617 populations of phytoplankton, and restricting much of the primary production to a
 2618 shallow, open open-water moat. Many other physical, chemical and biological changes
 2619 occur in lakes that are either directly or indirectly affected by snow and ice cover (see
 2620 Table 1; Douglas and Smol, 1999). Modified from Smol (1988).

2621

2621

2622

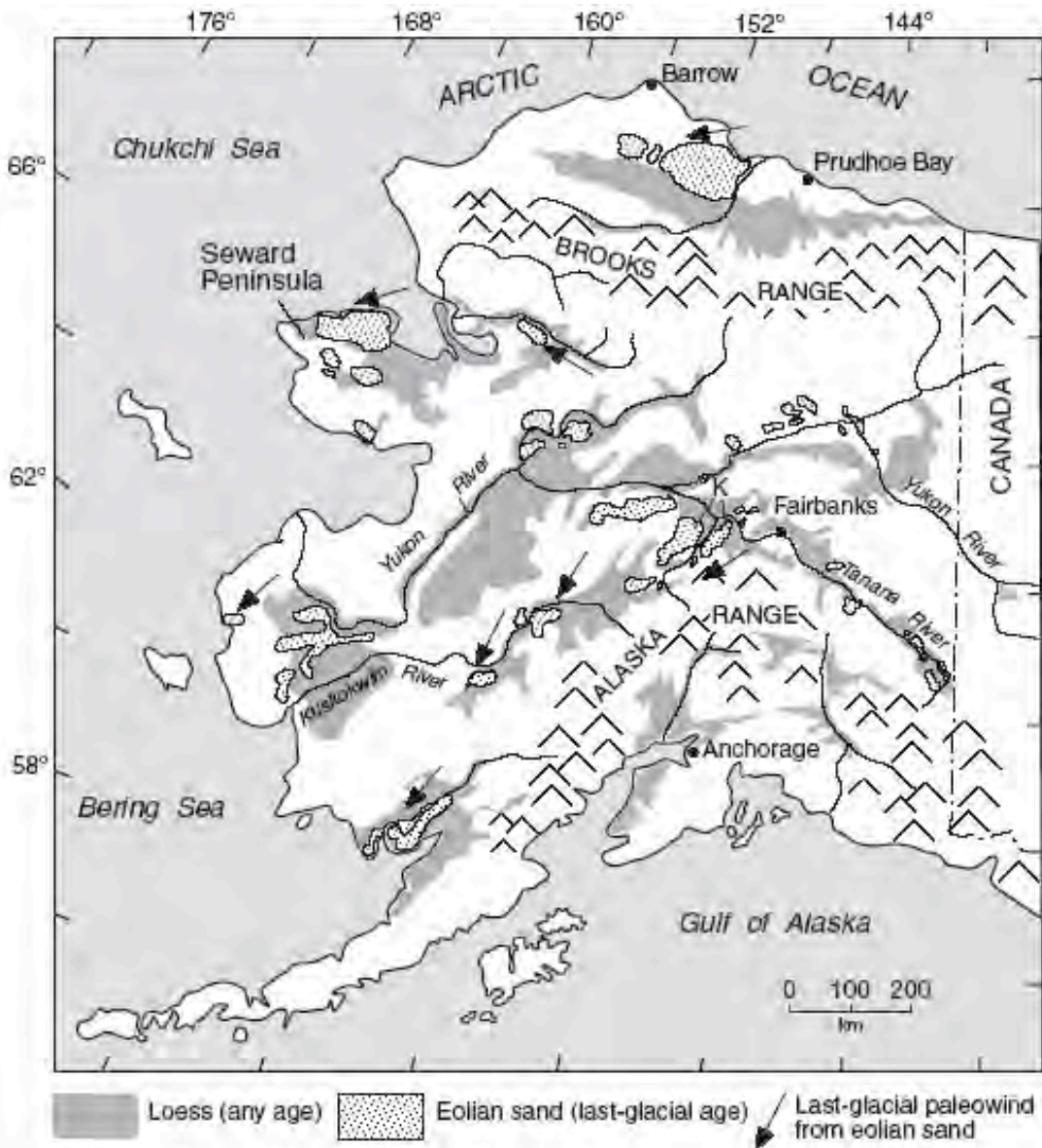


2623

2624 **Figure 5.20** Lake ice melts as it continues to warm (A – D). Eventually, in deeper lakes
2625 (vs ponds) thermal stratification may also occur (or be prolonged) during the summer
2626 months (D), further altering the limnological characteristics of the lake. Modified from
2627 Douglas (2007).

2628

2628



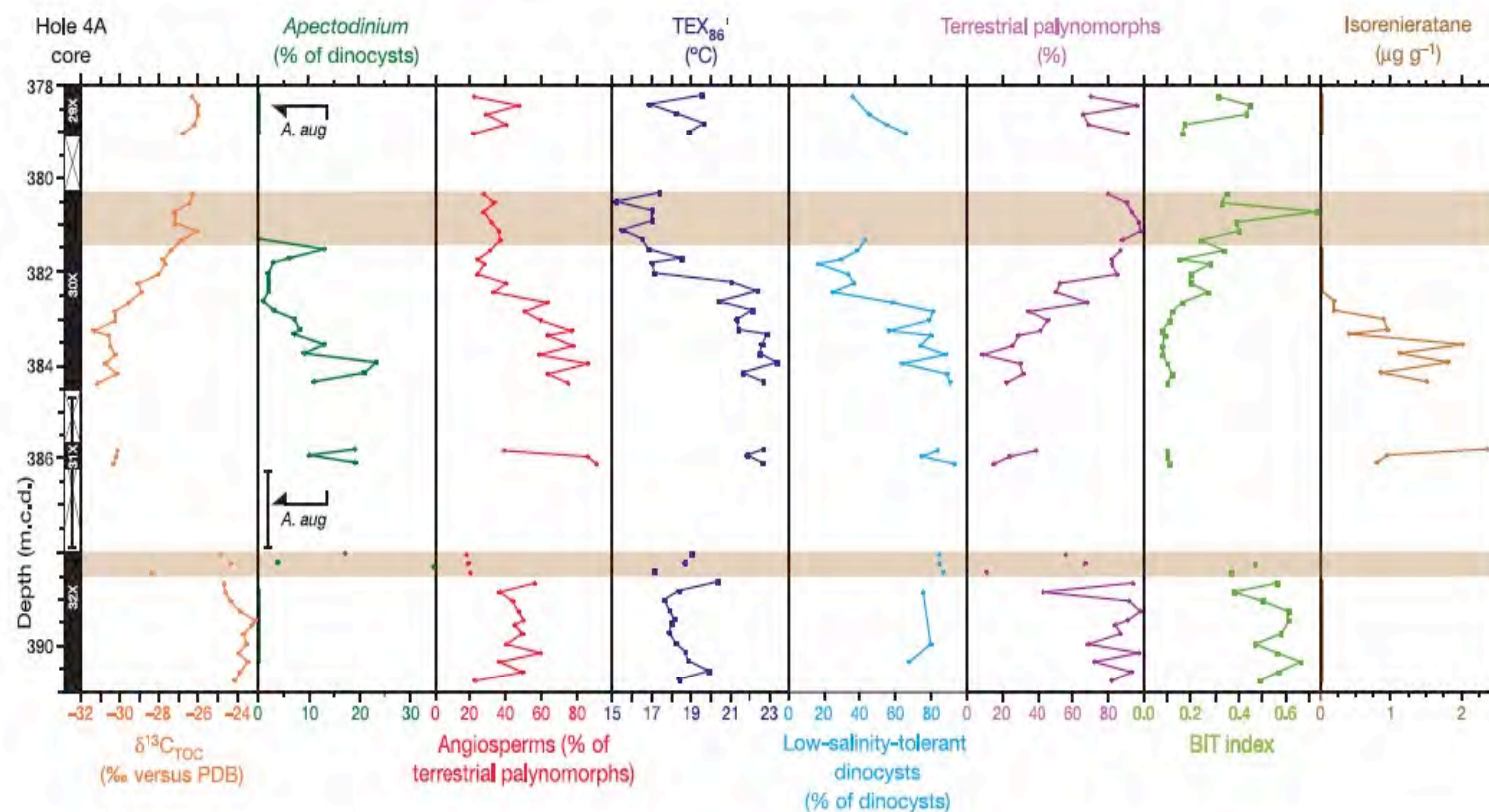
2629 **Figure 5.21** The form and distribution of wind-blown silt (loess), wind-blown sand
 2630 (dunes), and other deposits of wind-blown sediment in Alaska, have been use to infer
 2631 both Holocene and last-glacial past wind directions. (Compiled from multiple sources by
 2632 Muhs and Budahn, 2006).
 2633



2633

2634 **Figure 5.22** Unnamed, hydrologically closed lake in the Yukon Flats Wildlife Refuge,
2635 Alaska. Concentric rings of vegetation developed progressively inward as water level fell,
2636 owing to a negative change in the lake's overall water balance. Historic Landsat imagery
2637 and air photographs indicate that these shorelines formed during within the last 40 years
2638 or so. (Photograph by Lesleigh Anderson.)

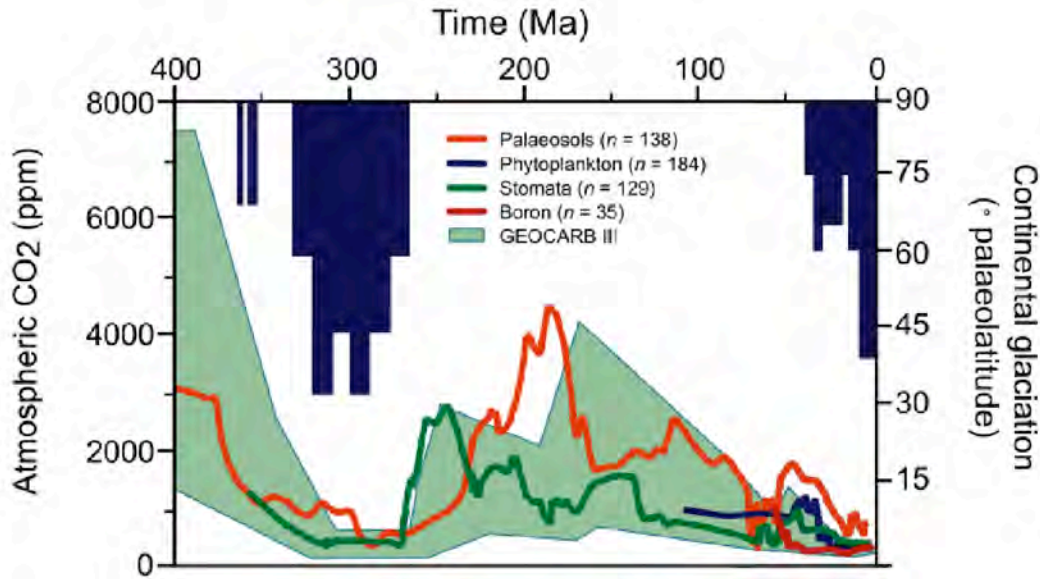
2639



2640

2641 **Figure 5.23** Recovered sections and palynological and geochemical results across the Paleocene-Eocene Thermal Maximum about 55
 2642 Ma; IODP Hole 302-4A (87° 52.00' N.; 136° 10.64' E.; 1288 m water depth, in the central Arctic Ocean basin). Mean annual surface-
 2643 water temperatures (as indicated in the TEX₈₆' column) are estimated to have reached 23°C, similar to water in the tropics today.

2644 (Error bars for Core 31X show the uncertainty of its stratigraphic position. Orange bars, indicate intervals affected by drilling
2645 disturbance.) Stable carbon isotopes are expressed relative to the PeeDee Belemnite standard. Dinocysts tolerant of low salinity
2646 comprise *Senegalinium* spp., *Cerodinium* spp., and *Polysphaeridium* spp., whereas *Membranosphaera* spp., *Spiniferites ramosus*
2647 complex, and *Areoligera-Glaphyrocysta* cpx. represent typical marine species. Arrows and *A. aug* (second column) indicate the first
2648 and last occurrences of dinocyst *Apectodinium augustum*—a diagnostic indicator of Paleocene-Eocene Thermal Maximum warm
2649 conditions. (Sluijs et al., 2006).



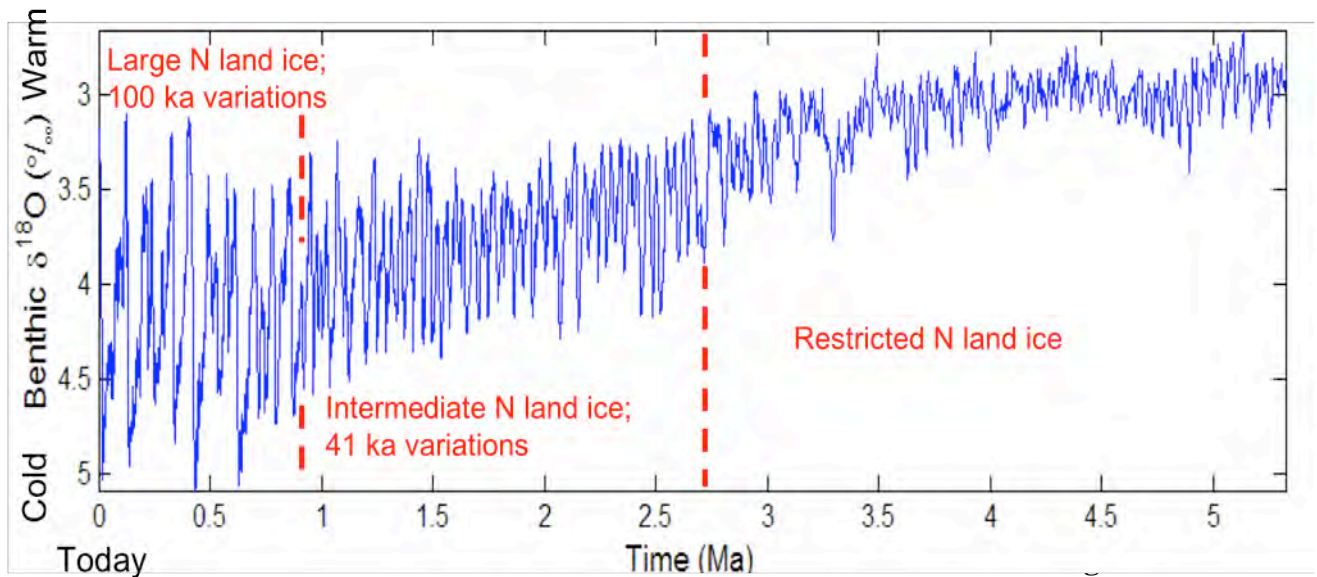
2650

2651

2652 **Figure 5.24** Atmospheric CO₂ and continental glaciation 400 Ma to present. Vertical blue
 2653 bars, timing and palaeolatitude extent of ice sheets (after Crowley, 1998). Plotted CO₂
 2654 records represent five-point running averages from each of four major proxies (see
 2655 Royer, 2006 for details of compilation). Also plotted are the plausible ranges of CO₂
 2656 derived from the geochemical carbon cycle model GEOCARB III (Bernier and Kothavala,
 2657 2001). All data adjusted to the Gradstein et al. (2004) time scale. Continental ice sheets
 2658 grow extensively when CO₂ is low. (after Jansen, 2007, that report's Figure 6.1)

2659

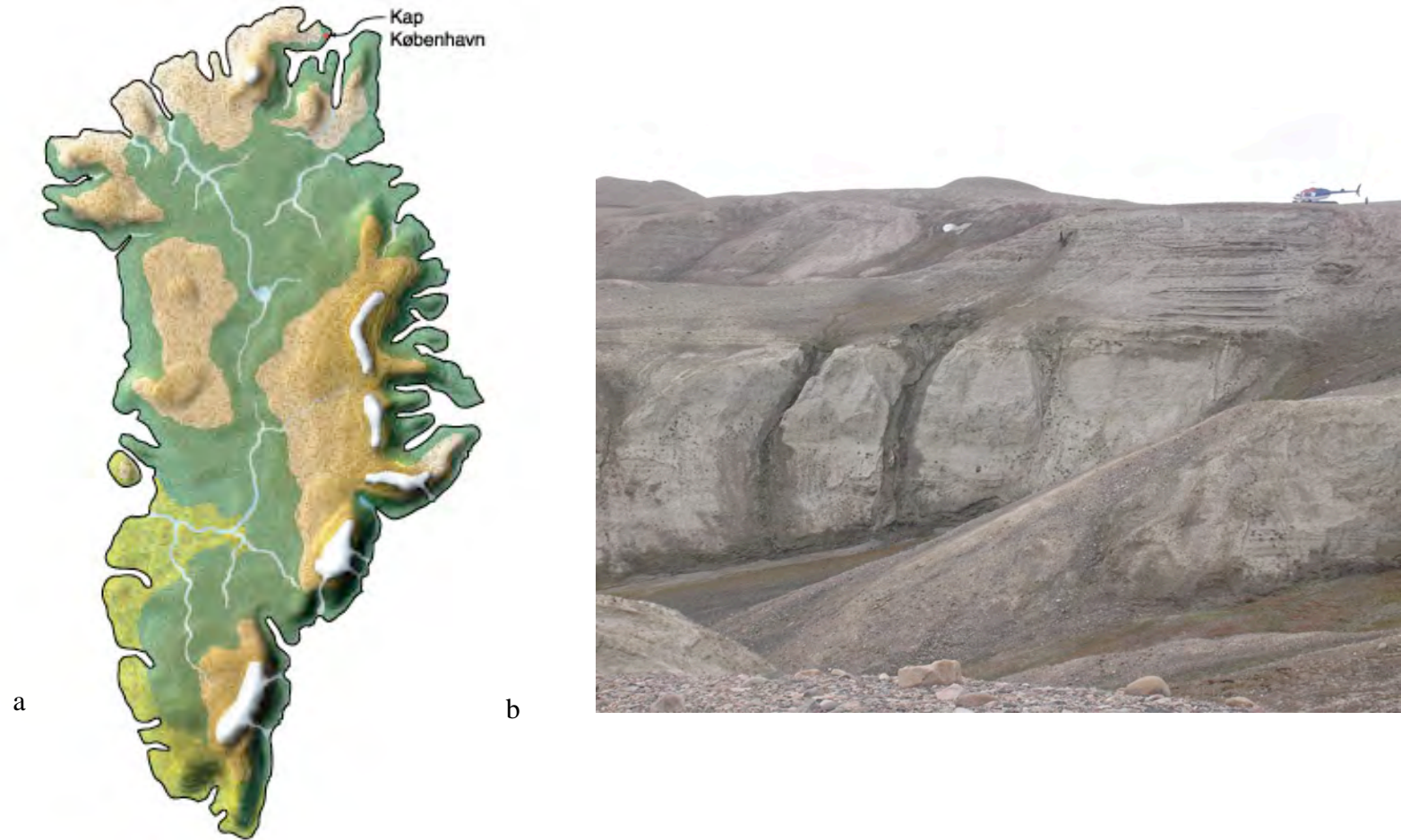
2661



2678

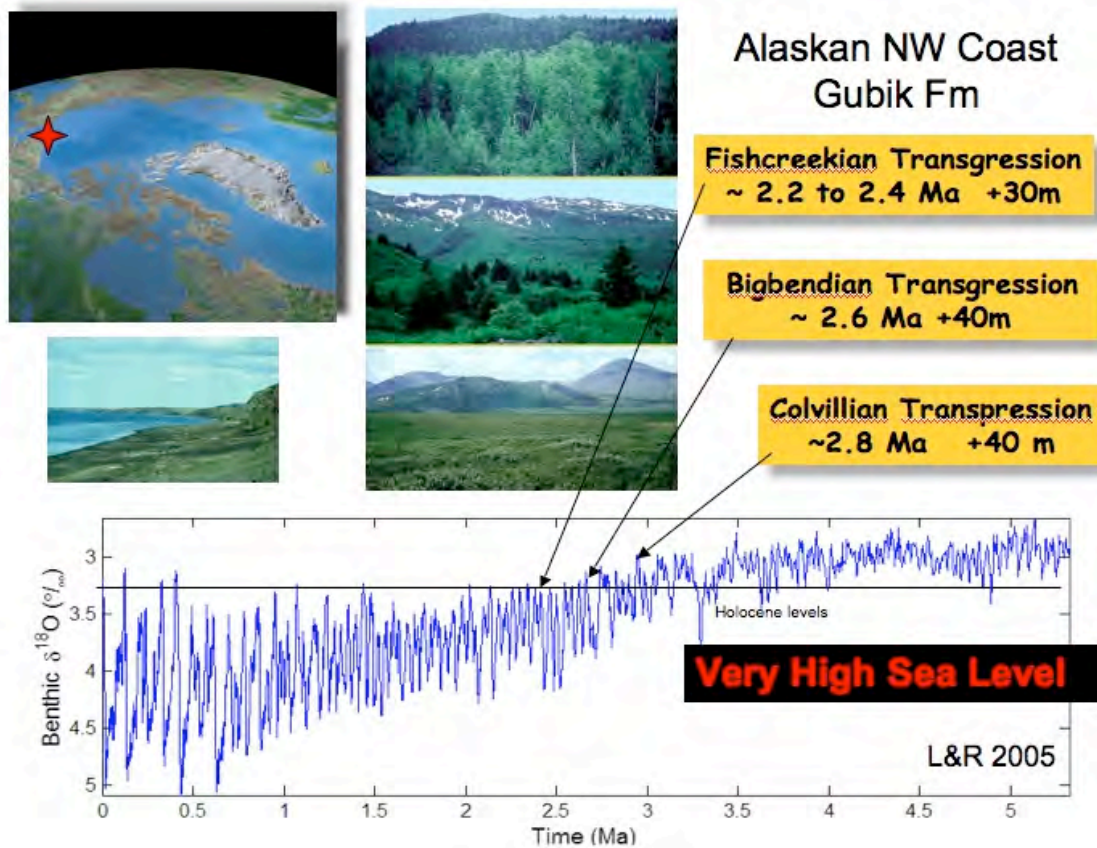
2679 **Figure 5.25** The average isotopic composition ($\delta^{18}\text{O}$) of bottom-dwelling
 2680 foraminifera from in a globally distributed set of 57 sediment cores that record the
 2681 last 5.3 Ma (modified from Lisiecki and Raymo, 2005). The $\delta^{18}\text{O}$ is controlled primarily
 2682 by global ice volume and deep-ocean temperature, with less ice or warmer temperatures
 2683 (or both) upward in the core. The influence of Milankovitch frequencies of Earth's orbital
 2684 variation are present throughout, but glaciation increased about 2.7 Ma ago concurrently
 2685 with establishment of a strong 41 ka variability linked to Earth's obliquity (changes in tilt
 2686 of Earth's spin axis), and the additional increase in glaciation about 1.2–0.7 Ma parallels
 2687 a shift to stronger 100 ka variability. Dashed lines are used because the changes seem to
 2688 have been gradual. The general trend toward higher $\delta^{18}\text{O}$ that runs through this series
 2689 reflects the long-term drift toward a colder Earth that began in the early Cenozoic (see
 2690 Figure 4.8).

2691



2692 **Figure 5.26** a) Greenland without ice for the last time? Dark green, boreal forest; light green, deciduous forest; brown, tundra and
2693 alpine heaths; white, ice caps. The north-south temperature gradient is constructed from a comparison between North Greenland and

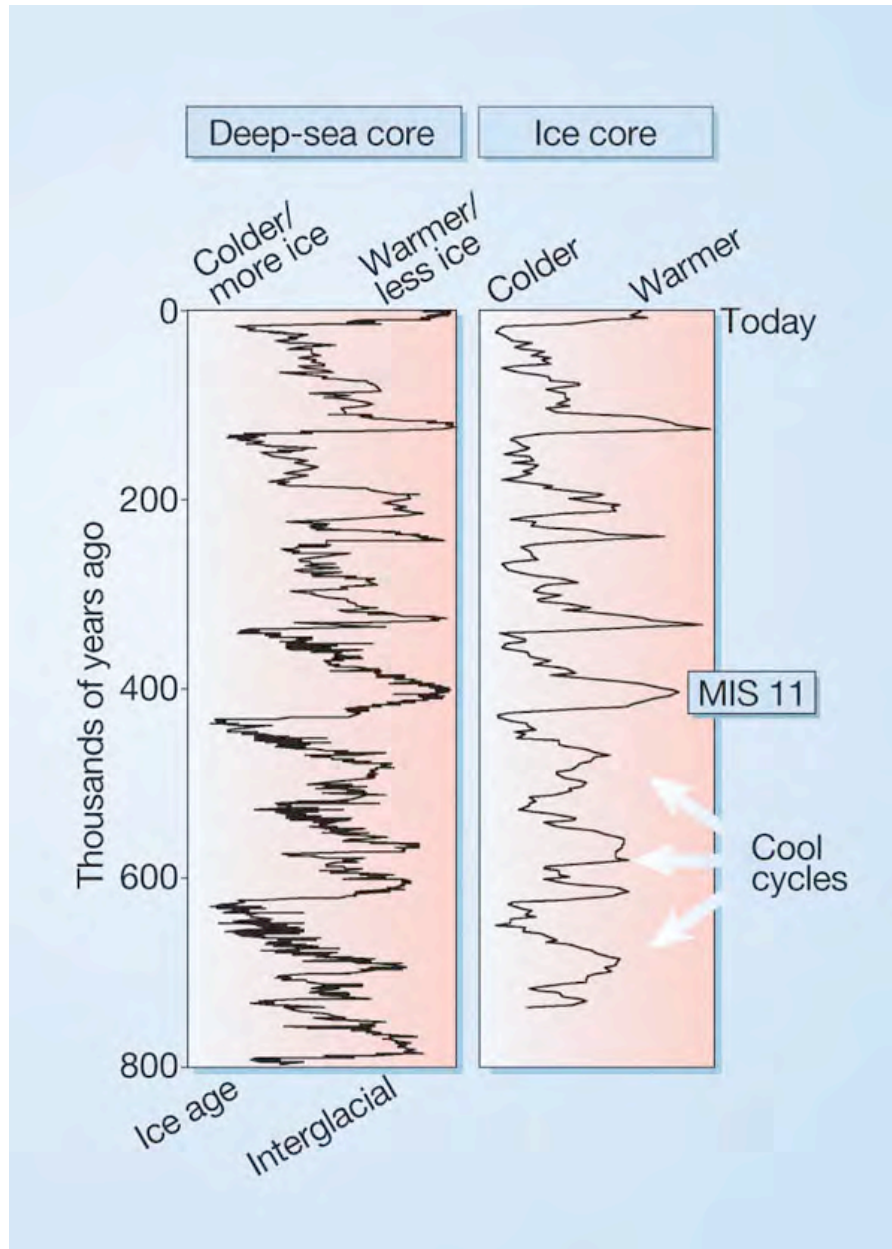
2694 northwest European temperatures, using standard lapse rate; distribution of precipitation assumed to retain the Holocene pattern.
2695 Topographical base, from model by Letreguilly et al. (1991) of Greenland's sub-ice topography after isostatic recovery. b) Upper part
2696 of the Kap København Formation, North Greenland. The sand was deposited in an estuary about 2.4 Ma; it contains abundant well-
2697 preserved leaves, seeds, twigs, and insect remains. (Figure and Photograph of by S.V. Funder.).



2698

2699

2700 **Figure 5.27** The largely marine Gubik Formation, North Slope of Alaska, contains three
 2701 superposed lower units that record relative sea level as high +30-+ to +40 m. Pollen in
 2702 these deposits suggests that borderland vegetation at each of these times was less
 2703 forested; boreal forests or spruce-birch woodlands at 2.7 Ma gave way to larch and
 2704 spruce forests at about 2.6 Ma and to open tundra by about 2.4 Ma (see photographs by
 2705 Robert Nelson, Colby College, who analyzed the pollen; oldest at top). Isotopic reference
 2706 time series of Lisecki and Raymo (2005) suggests best as assignments for these sea level
 2707 events (Brigham and Carter, 1992).



2708

2709 **Figure 5.28** Glacial cycles of the past 800 ka derived from marine-sediment and ice cores
 2710 (McManus, 2004). The history of deep-ocean temperatures and global ice volume
 2711 inferred from $\delta^{18}\text{O}$ measured in bottom-dwelling foraminifera shells preserved in Atlantic
 2712 Ocean sediments. Air temperatures over Antarctica inferred from the ratio of deuterium
 2713 to hydrogen in ice from central Antarctica (EPICA, 2004). Marine isotope stage 11 (MIS
 2714 11) is an interglacial whose orbital parameters were similar to those of the Holocene, yet
 2715 it lasted about twice as long as most interglacials. Note the smaller magnitude and less-
 2716 pronounced interglacial warmth of the glacial cycles that preceded MIS 11.

2717 Interglaciations older than MIS 11 were less warm than subsequent interglaciations.

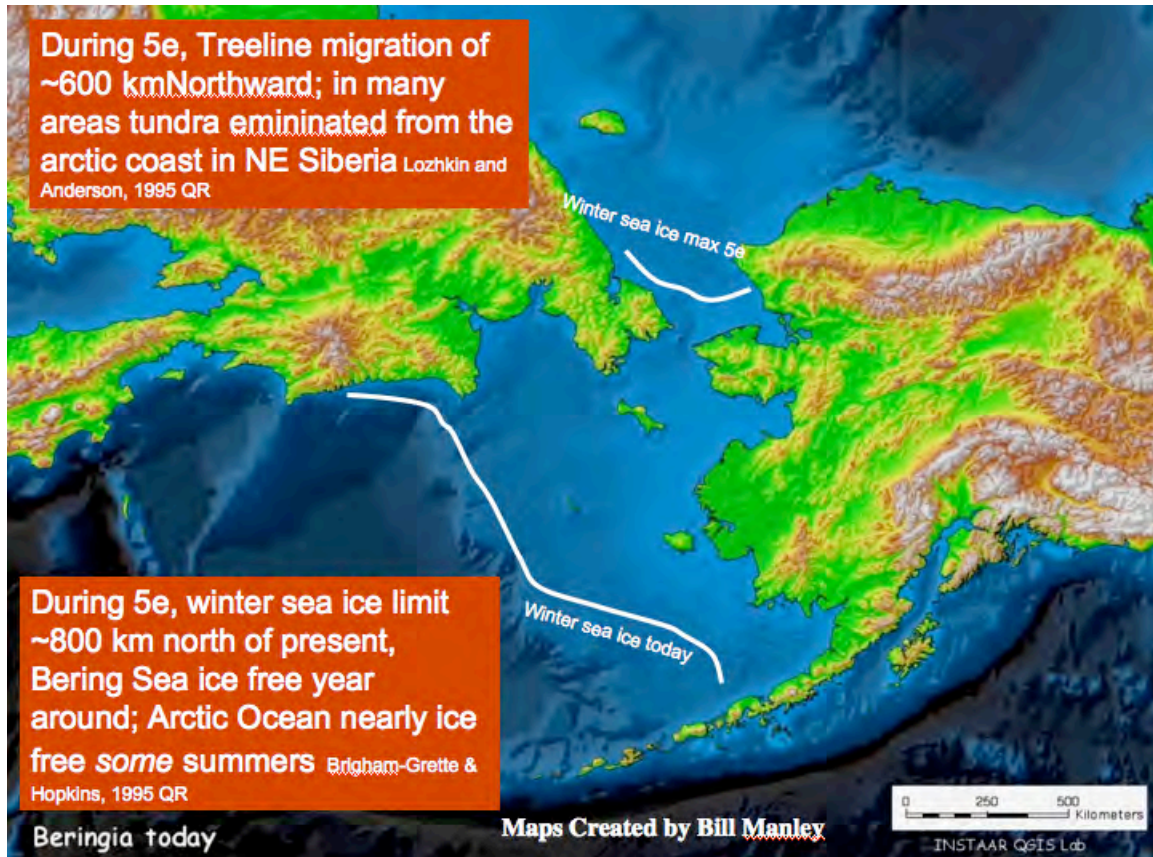
2718



2719

2720 **Figure 5.29** Polar projection showing regional maximum LIG last interglacial summer
 2721 temperature anomalies relative to present summer temperatures; derived from
 2722 paleotemperature proxies (see tables Tables 1 and 2, in from CAPE Last Interglacial
 2723 Project Members, 2006). Circles, terrestrial; squares, marine sites.

2724

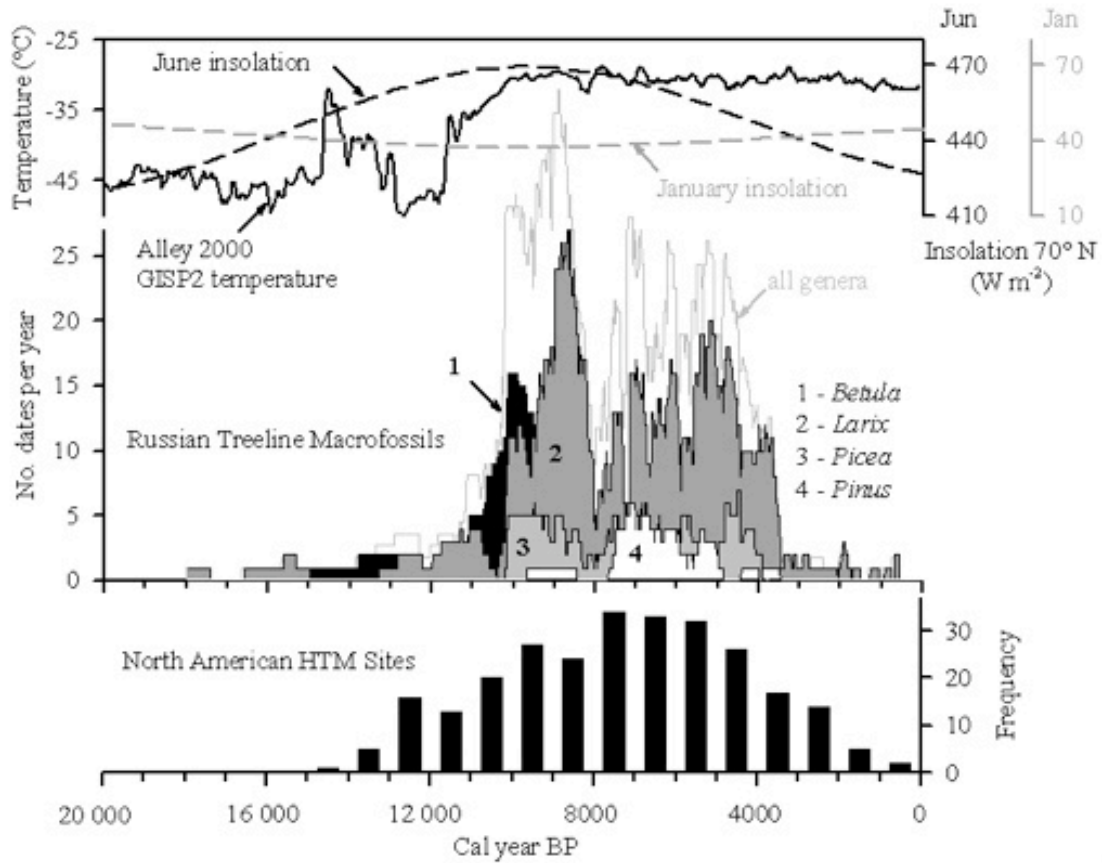


2725

2726

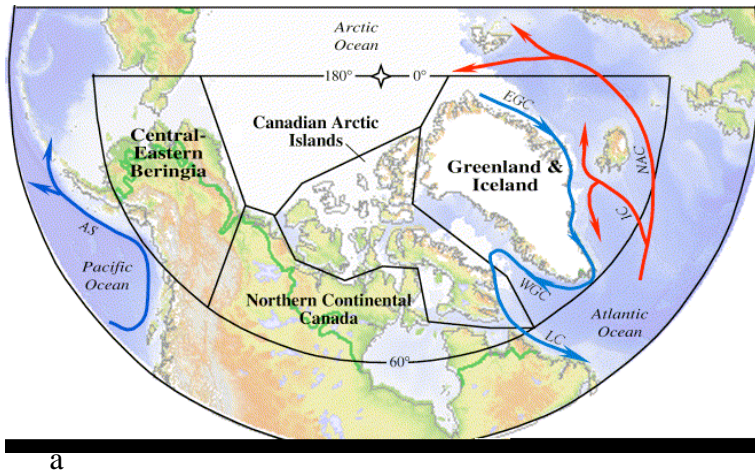
2727 **Figure 5.30** Winter sea-ice limit during MIS 5e and at present. Fossiliferous
 2728 paleoshorelines and marine sediments were used by Brigham-Grette and Hopkins (1995)
 2729 to evaluate the seasonality of coastal sea ice on both sides of the Bering Strait during the
 2730 Last Last Interglaciatiion. Winter sea limit is estimated to have been north of the
 2731 narrowest section of the strait, 800 km north of modern limits. Pollen data derived from
 2732 Last Interglacial lake sediments suggest that tundra was nearly eliminated from the
 2733 Russian coast at this time (Lozhkin and Anderson, 1995). In Chukotka during the warm
 2734 interglaciatiion, additional open water favored some taxa tolerant of deeper winter snows.
 2735 (Map of William Manley, <http://instaar.colorado.edu/QGISL/>).
 2736

2736

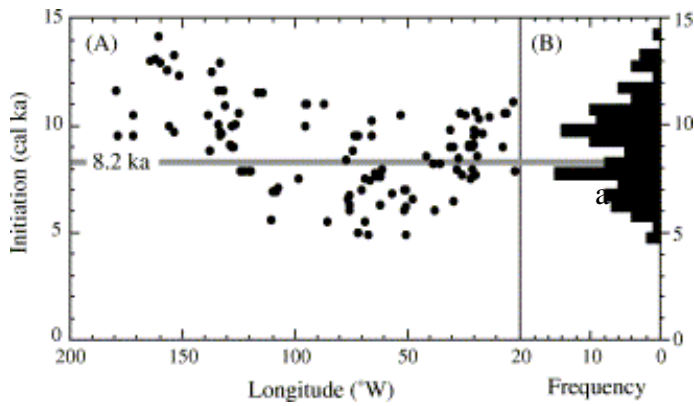


2737

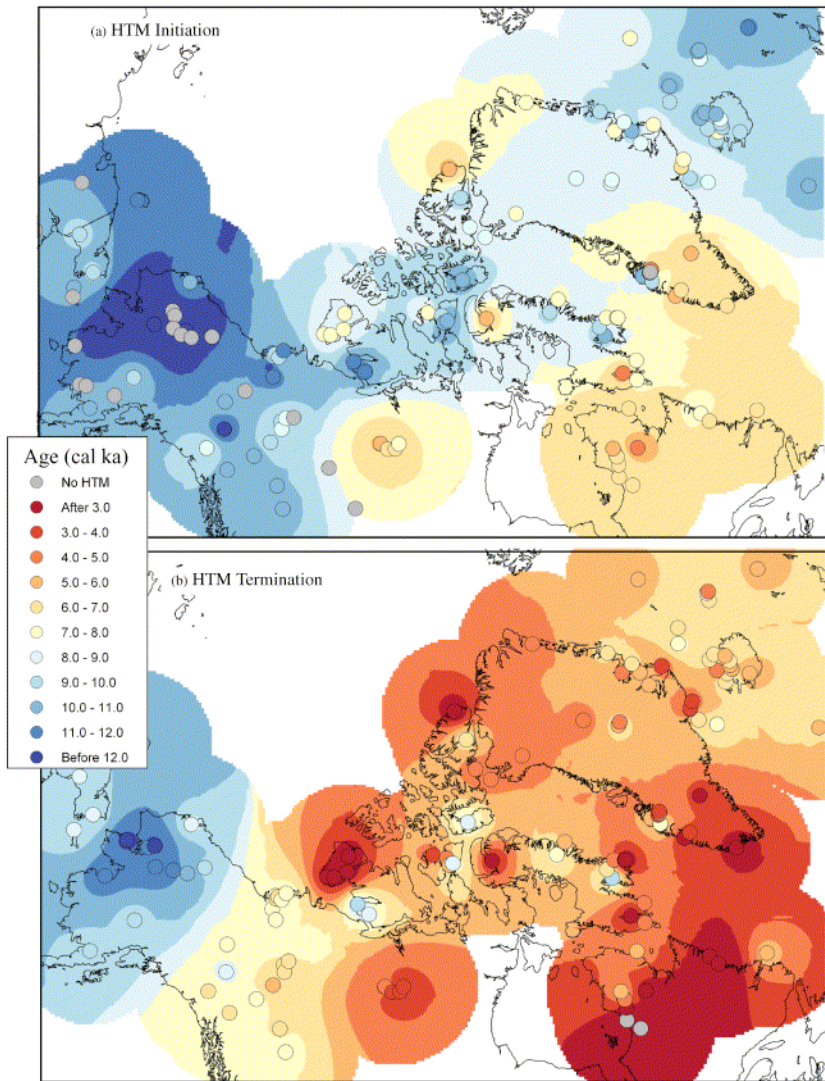
2738 **Figure 5.31** The Arctic Holocene Thermal Maximum. Items compared, top to bottom:
 2739 seasonal insolation patterns at 70° N. (Berger & Loutre, 1991), and reconstructed
 2740 Greenland air temperature from the GISP2 drilling project (Alley 2000); age distribution
 2741 of radiocarbon-dated fossil remains of various tree genera from north of present treeline
 2742 (MacDonald et al., 2007),); and the frequency of Western Arctic sites that experienced
 2743 Holocene Thermal Maximum conditions. (Kaufman et al. 2004).



a



b

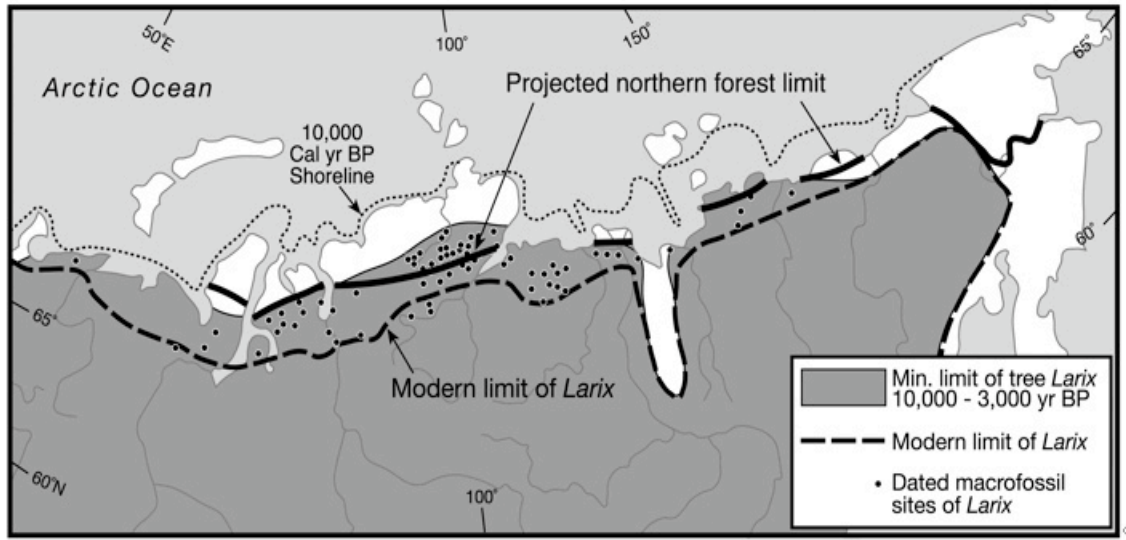


c

2744

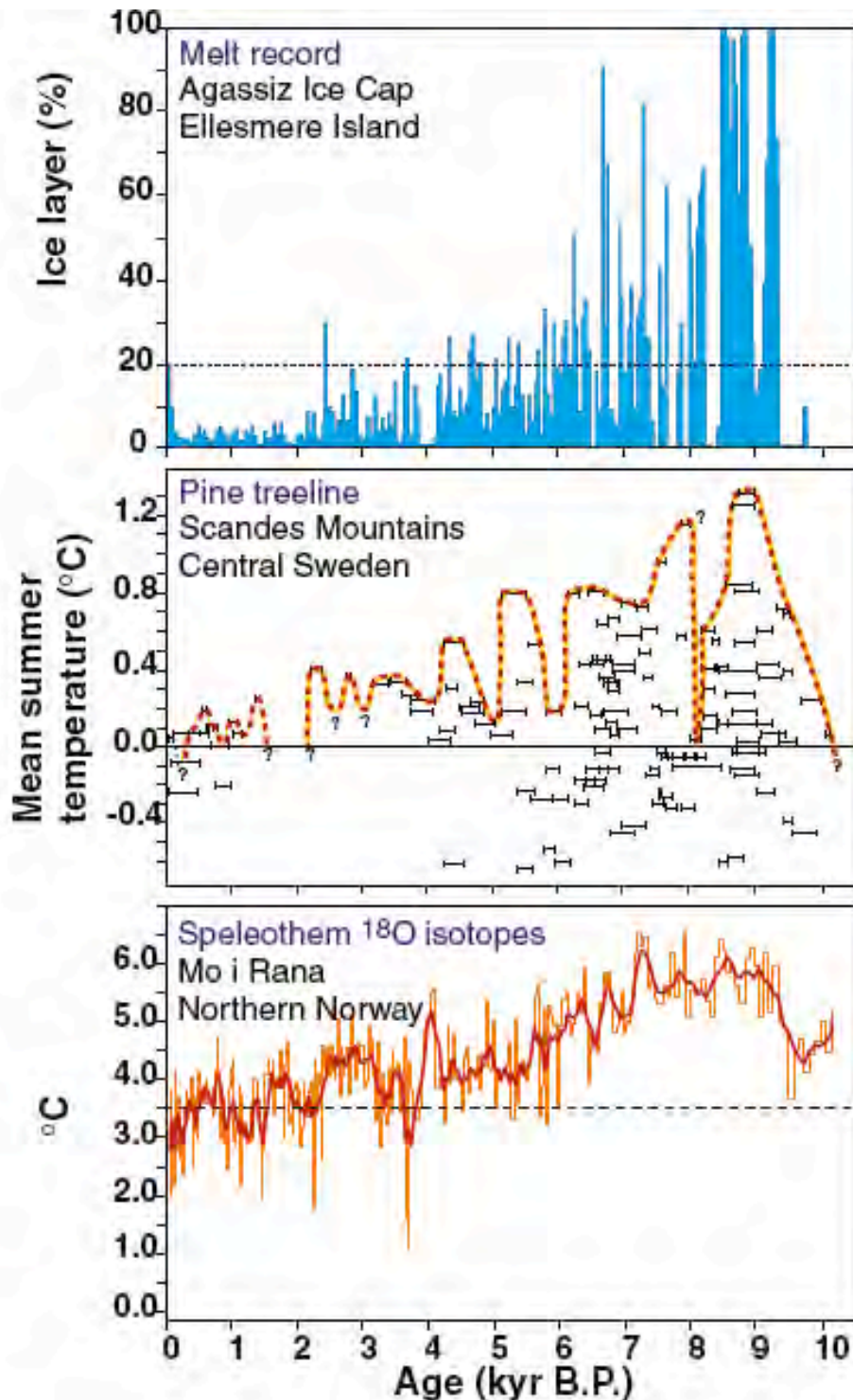
2745 **Figure. 5.32** The timing of initiation and termination of the Holocene Thermal Maximum in the western Arctic (Kaufman et al.,
2746 2004). a) Regions reviewed in Kaufman et al., 2004. b) Initiation of the Holocene Thermal Maximum in the western Arctic.
2747 Longitudinal distribution (left) and frequency distribution (right). c) Spatial-temporal pattern of the Holocene Thermal Maximum in
2748 the western Arctic. Upper panel, initiation; lower panel, termination. Dot colors bracket ages of the Holocene Thermal Maximum;
2749 ages contoured using the same color scheme. Gray dots, equivocal evidence for the Holocene Thermal Maximum.
2750

2751



2752

2753 **Figure. 5.33** The northward extension of larch (*Larix*) treeline across the Eurasian Arctic.
 2754 Treeline today compared with treeline during the Holocene Thermal Maximum and with
 2755 anticipated northern forest limits (Arctic Climate Impact Assessment, 2005) due to climate
 2756 warming (MacDonald et al., 2007).



2757

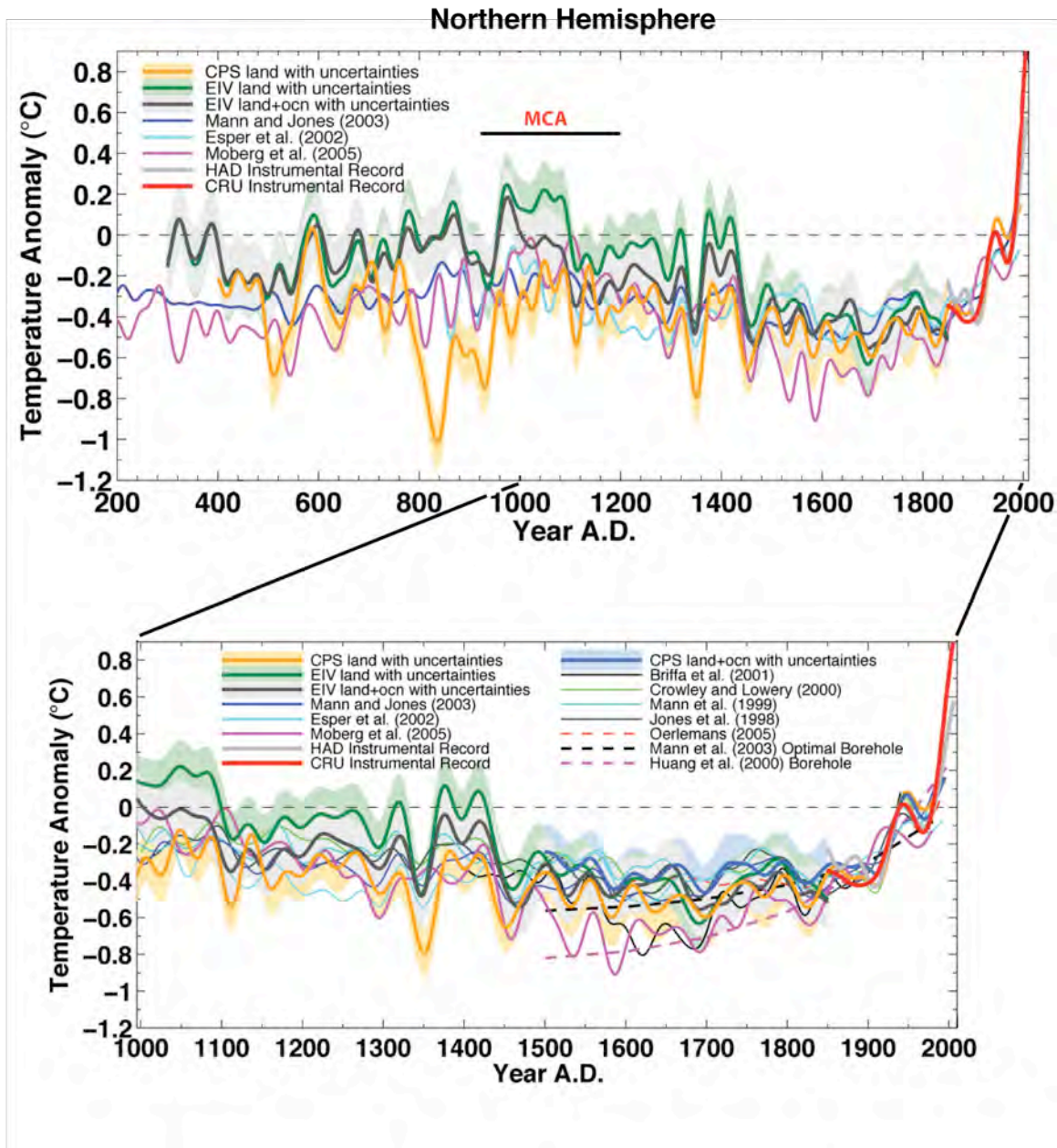
2758 **Fig. 5.34** Arctic temperature reconstructions. Upper panel: Holocene summer melting on the
 2759 Agassiz Ice Cap, northern Ellesmere Island, Canada. “Melt” indicates the fraction of each core
 2760 section that contains evidence of melting (from Koerner and Fisher, 1990). Middle panel:

SAP1.2 DRAFT 3 PUBLIC COMMENT

2761 Estimated summer temperature anomalies in central Sweden. Black bars, elevation of ^{14}C - dated
2762 sub-fossil pine wood samples (*Pinus sylvestris* L.) in the Scandes Mountains, central Sweden,
2763 relative to temperatures at the modern pine limit in the region. Dashed line, upper limit of pine
2764 growth is indicated by the dashed line. Changes in temperature estimated by assuming a lapse
2765 rate of $6\text{ }^{\circ}\text{C km}^{-1}$ (from Dahl and Nesje, 1996, ; based on samples collected by L. Kullman and
2766 by G. and J. Lundqvist). Lower panel: Paleotemperature reconstruction from oxygen isotopes in
2767 calcite sampled along the growth axis of a stalagmite from a cave at Mo i Rana, northern
2768 Norway. Growth ceased around A.D. 1750 (from Lauritzen 1996; Lauritzen and Lundberg 1998;
2769 2002). Figure from Bradley (2000).

2770

2771



2772

2773

2774

Figure 5.35. Updated composite proxy-data reconstruction of Northern Hemisphere temperatures for most of the last 2000 years, compared with other published reconstructions. Estimated confidence limits, 95%. All series have been smoothed with a 40-year lowpass filter. The Medieval Climate Anomaly (MCA), about 950–1200 AD. The array of reconstructions demonstrate that the warming documented by instrumental data during the past few decades exceeds that of any warm interval of the past 2000 years, including that estimated for the MCA.

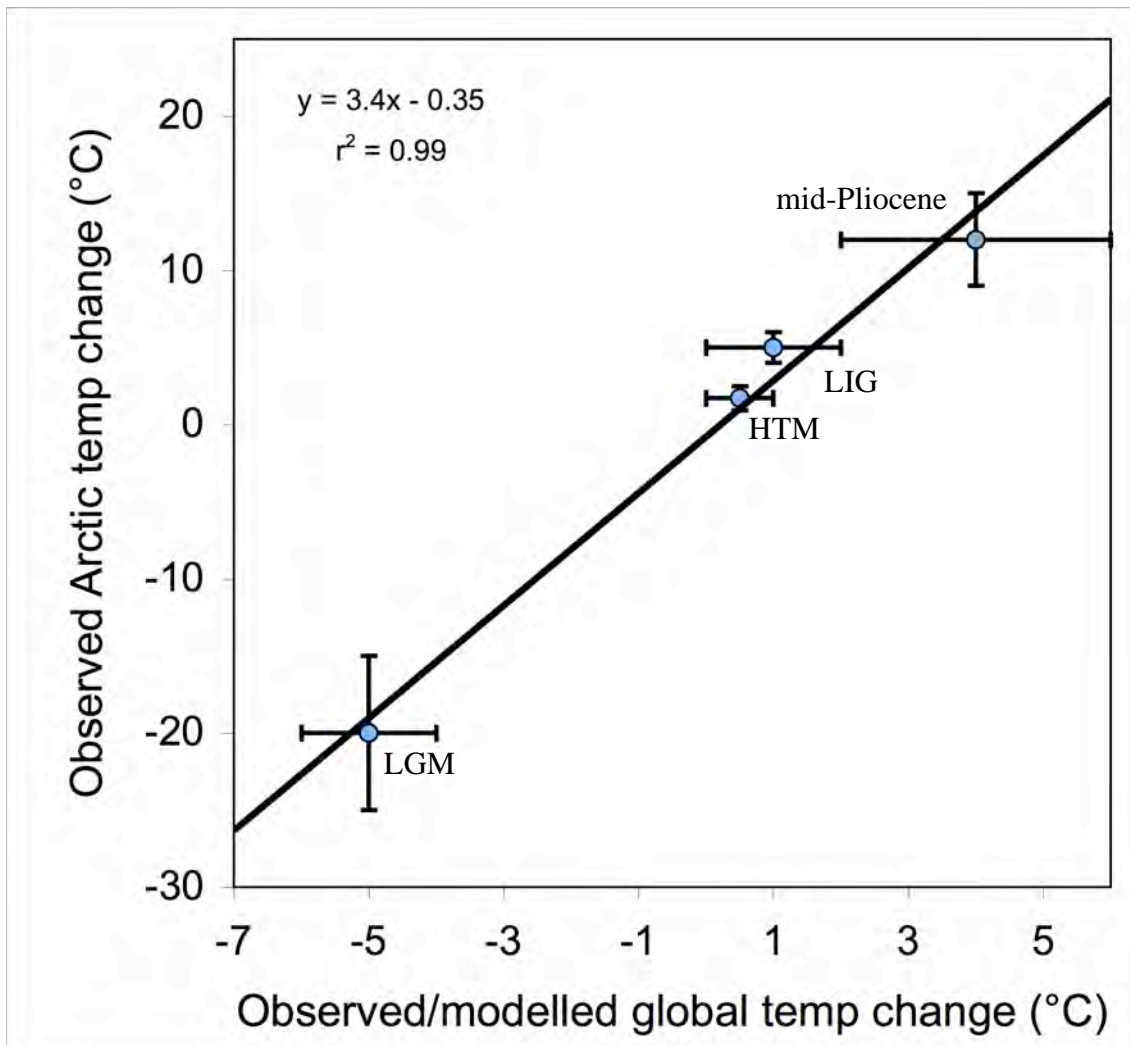
2777

2778

2779

SAP1.2 DRAFT 3 PUBLIC COMMENT

2780 (Figure from Mann et al. (in press). CPS, composite plus scale methodology; CRU, East Anglia
2781 Climate Research unit, a source of instrumental data; EIV, error-in-variables); HAD, Hadley
2782 Climate Center.



2783

2784

Figure 5.36 Paleoclimate data quantify the magnitude of Arctic amplification. Shown are

2785

paleoclimate estimates of Arctic summer temperature anomalies relative to recent, and the

2786

appropriate Northern Hemisphere or global summer temperature anomalies, together with their

2787

uncertainties, for the following: the last glacial maximum (LGM; about 20 ka), Holocene thermal

2788

maximum (HTM; about 8 ka), last interglaciation (LIG; 130–125 ka ago) and middle Pliocene

2789

(about 3.5–3.0 Ma). The trend line suggests that summer temperature changes are amplified 3 to

2790

4 times in the Arctic. Explanation of data sources follows, for the different times for each time

2791

considered, beginning with the most recent.

SAP1.2 DRAFT 3 PUBLIC COMMENT

2792 **Holocene Thermal Maximum (HTM):** Arctic $\Delta T = 1.7 \pm 0.8^{\circ}\text{C}$; Northern Hemisphere
2793 $\Delta T = 0.5 \pm 0.3^{\circ}\text{C}$; Global $\Delta T = 0^{\circ} \pm 0.5^{\circ}\text{C}$.

2794 A recent summary of summer temperature anomalies in the western Arctic (Kaufman et
2795 al., 2004) built on earlier summaries (Kerwin et al., 1999; CAPE Project Members, 2001) and is
2796 consistent with more-recent reconstructions (Kaplan and Wolfe, 2006; Flowers et al., 2007).
2797 Although the Kaufman et al. (2004) summary considered only the western half of the Arctic, the
2798 earlier summaries by Kerwin et al., (1999) and CAPE Project Members (2001) indicated that
2799 similar anomalies characterized the eastern Arctic, and all syntheses report the largest anomalies
2800 in the North Atlantic sector. Few data are available for the central Arctic Ocean; we assume that
2801 the circumpolar dataset provides an adequate reflection of air temperatures over the Arctic Ocean
2802 as well.

2803 Climate models suggest that the average planetary anomaly was concentrated over the
2804 Northern Hemisphere. Braconnot et al. (2007) summarized the simulations from 10 different
2805 climate model contributions to the PMIP2 project that compared simulated summer temperatures
2806 at 6 ka with recent temperatures. The global average summer temperature anomaly at 6 ka was
2807 $0^{\circ} \pm 0.5^{\circ}\text{C}$, whereas the Northern Hemisphere anomaly was $0.5^{\circ} \pm 0.3^{\circ}\text{C}$. These patterns are
2808 similar to patterns in model results described by Hewitt and Mitchell (1998) and Kitoh and by
2809 Murakami (2002) for 6 ka, and a global simulation for 9 ka (Renssen et al., 2006). All simulate
2810 little difference in summer temperature outside the Arctic when those temperatures are compared
2811 to with pre-industrial temperatures.

2812 **Last Glacial Maximum (LGM):** Arctic $\Delta T = 20^{\circ} \pm 5^{\circ}\text{C}$; global and Northern
2813 Hemisphere $\Delta T = -5^{\circ} \pm 1^{\circ}\text{C}$

SAP1.2 DRAFT 3 PUBLIC COMMENT

2814 Quantitative estimates of temperature reductions during the peak of the Last Glacial
2815 Maximum are less widespread in for the Arctic than are estimates of temperatures during warm
2816 times. Ice-core borehole temperatures, which offer the most compelling evidence (Cuffey et al.,
2817 1995; Dahl-Jensen et al., 1998), are supported by evidence from biological proxies in the North
2818 Pacific sector (Elias et al., 1996a), where no ice cores are available that extend back to the Last
2819 Glacial Maximum. Because of the limited datasets for temperature reduction in the Arctic during
2820 the Last Glacial Maximum, we incorporate a large uncertainty. The global-average temperature
2821 decrease during peak glaciations, based on paleoclimate proxy data, was 5° – 6°C , and little
2822 difference existed between the Northern and Southern Hemispheres (Farrera et al., 1999;
2823 Braconnot et al., 2007; Braconnot et al., 2007). A similar temperature anomaly is derived from
2824 climate-model simulations (Otto-Bliesner et al., 2007).

2825 **Last Interglaciation (LIG):** Arctic $\Delta T = 5^{\circ} \pm 1^{\circ}\text{C}$; global and Northern Hemisphere ΔT
2826 $= 1^{\circ} \pm 1^{\circ}\text{C}$)

2827 A recent summary of all available quantitative reconstructions of summer-temperature
2828 anomalies for in the Arctic during peak Last Interglaciation warmth shows a spatial pattern
2829 similar to that shown by Holocene Thermal Maximum reconstructions. The largest anomalies are
2830 in the North Atlantic sector and the smallest anomalies are in the North Pacific sector, but those
2831 small anomalies are substantially larger ($5^{\circ} \pm 1^{\circ}\text{C}$) than they were during the Holocene Thermal
2832 Maximum (CAPE Last Interglacial Project Members, 2006). A similar pattern of Last
2833 Interglaciation summer-temperature anomalies is apparent in climate model simulations (Otto-
2834 Bliesner et al., 2006). Global and Northern Hemisphere summer-temperature anomalies are
2835 derived from summaries in CLIMAP Project Members (1984), Crowley (1990), Montoya et al.
2836 (2000), and Bauch and Erlenkeuser (2003).

SAP1.2 DRAFT 3 PUBLIC COMMENT

2837 **Middle Pliocene:** Arctic $\Delta T = 12^{\circ} \pm 3^{\circ}\text{C}$; global $\Delta T = 4^{\circ} \pm 2^{\circ}\text{C}$)

2838 Widespread forests throughout the Arctic in the middle Pliocene offer a glimpse of a
2839 notably warm time in the Arctic, which had essentially modern continental configurations and
2840 connections between the Arctic Ocean and the global ocean. Reconstructed Arctic temperature
2841 anomalies are available from several sites that show much warmth and no summer sea ice in the
2842 Arctic Ocean basin. These sites include the Canadian Arctic Archipelago (Dowsett et al., 1994;
2843 Elias and Matthews, 2002; Ballantyne et al., 2006), Iceland (Buchardt and Símonarson, 2003),
2844 and the North Pacific (Heusser and Morley, 1996). A global summary of mid-Pliocene biomes
2845 by Salzmann et al. (2008) concluded that Arctic mean-annual-temperature anomalies were in
2846 excess of 10°C ; some sites indicate temperature anomalies of as much as 15°C . Estimates of
2847 global sea-surface temperature anomalies are from Dowsett (2007).

2848 Global reconstructions of mid-Pliocene temperature anomalies from proxy data and
2849 general circulation models show modest warming (average, $4^{\circ} \pm 1^{\circ}\text{C}$) across low to middle
2850 latitudes (Dowsett et al., 1999; Raymo et al., 1996; Sloan et al., 1996, Budyko et al., 1985;
2851 Haywood and Valdes, 2004; Jiang et al., 2005; Haywood and Valdes, 2006; Salzmann et al.,
2852 2008).

2853

2854

SAP1.2 DRAFT 3 PUBLIC COMMENT

2854 Chapter 5 References

2855

2856 **Abbott, M.B., B.P. Finney, M.E. Edwards, and K.R. Kelts, 2000:** Lake-level reconstructions and
2857 paleohydrology of Birch Lake, central Alaska, based on seismic reflection profiles and
2858 core transects. *Quaternary Research*, **53**, 154-166.

2859

2860 **Adkins, J.F., E.A. Boyle, L.D. Keigwin, E. Cortijio, 1997:** Variability of the North Atlantic
2861 thermohaline circulation during the last interglacial period. *Nature*, **390**, 154-156.

2862

2863 **Ager, T.A. and L.B. Brubaker, 1985:** Quaternary palynology and vegetation history of Alaska.
2864 In: *Pollen Records of Late-Quaternary North American Sediments*, [Bryant, V.M., Jr. and
2865 R.G. Holloway, (eds.)]. American Association of Stratigraphic Palynologists, Dallas, pp.
2866 353-384.

2867

2868 **Aksu, A.E., 1985:** Planktonic foraminiferal and oxygen isotope stratigraphy of CESAR cores
2869 102 and 103—Preliminary results. In: *Initial geological report on CESAR—The*
2870 *Canadian Expedition to Study the Alpha Ridge, Arctic Ocean* [Jackson, H.R., P.J. Mudie,
2871 and S.M. Blasco (eds.)]. Geological Survey of Canada Paper 84-22, pp. 115-124.

2872

2873 **Alfimov, A.V., D.I. Berman, and A.V. Sher, 2003:** Tundra-steppe insect assemblages and the
2874 reconstruction of the Late Pleistocene climate in the lower reaches of the Kolyma River.
2875 *Zoologicheskii Zhurnal*, **82**, 281-300 (In Russian).

2876

2877 **Alley, R.B., 1991:** Deforming-bed origin for southern Laurentide till sheets? *Journal of*
2878 *Glaciology*, **37(125)**, 67-76.

2879

2880 **Alley, R.B., 2003:** Paleoclimatic insights into future climate challenges. *Philosophical*
2881 *Transactions of the Royal Society of London, Series A*, **361(1810)**, 1831-1849.

2882

SAP1.2 DRAFT 3 PUBLIC COMMENT

- 2883 **Alley**, R.B., 2007: Wally was right: Predictive ability of the North Atlantic “conveyor belt”
2884 hypothesis for abrupt climate change. *Annual Review of Earth and Planetary Sciences*,
2885 **35**, 241-272.
- 2886
- 2887 **Alley**, R.B. and S. Anandakrishnan, 1995: Variations in melt-layer frequency in the GISP2 ice
2888 core: implications for Holocene summer temperatures in central Greenland. *Annals of*
2889 *Glaciology*, **21**, 64-70.
- 2890
- 2891 **Alley**, R.B. and A.M. Ágústsdóttir, 2005: The 8k event: Cause and consequences of a major
2892 Holocene abrupt climate change. *Quaternary Science Reviews*, **24**, 1123 -1149.
- 2893
- 2894 **Alley**, R.B., E.J. Brook and S. Anandakrishnan, 2002: A northern lead in the orbital band: North-
2895 south phasing of ice-age events. *Quaternary Science Reviews*, **21(1-3)**, 431-441.
- 2896
- 2897 **Alley**, R.B. and K.M. Cuffey, 2001: Oxygen- and hydrogen-isotopic ratios of water in
2898 precipitation: Beyond paleothermometry. In: *Stable Isotope Geochemistry*, [Valley, J.W.
2899 and D. Cole (eds.)]. Mineralogical Society of America Reviews in Mineralogy and
2900 Geochemistry, **43**, , p. 527-553
- 2901
- 2902 **Alley**, R.B., D.A. Meese, C.A. Shuman, A.J. Gow, K.C. Taylor, P.M. Grootes, J.W.C. White, M.
2903 Ram, E.D. Waddington, P.A. Mayewski, and G.A. Zielinski, 1993: Abrupt increase in
2904 snow accumulation at the end of the Younger Dryas event. *Nature*, **362**, 527-529.
- 2905
- 2906 **Alley**, R.B., C.A. Shuman, D.A. Meese, A.J. Gow, K.C. Taylor, K.M. Cuffey, J.J. Fitzpatrick,
2907 P.M. Grootes, G.A. Zielinski, M. Ram, G. Spinelli, and B. Elder, 1997: Visual-
2908 stratigraphic dating of the GISP2 ice core—Basis, reproducibility, and application.
2909 *Journal of Geophysical Research*, **102**, 26,367-26,381.
- 2910
- 2911 **Ammann**, C.M., F.Joos, D.S. Schimel, B.L. Otto-Bliesner, and .R.A. Tomas, 2007: Solar
2912 influence on climate during the past millennium—Results from transient simulations with
2913 the NCAR Climate System Model. *Proceedings of the National Academy of Sciences*,

SAP1.2 DRAFT 3 PUBLIC COMMENT

- 2914 U.S.A., www.pnas.org/cgi//doi/10.1073/pnas.0605064103
- 2915
- 2916 **Andersen, K.K., A. Svensson, S. Johnsen, S.O. Rasmussen, M. Bigler, R. Rothlisberger, U.**
- 2917 **Ruth, M.L. Siggaard-Andersen, J.P. Steffensen, D. Dahl-Jensen, B.M. Vinther, and H.B.**
- 2918 **Clausen, 2006: The Greenland Ice Core Chronology 2005, 15–42 kyr. Part I—**
- 2919 **Constructing the time scale. *Quaternary Science Reviews*, **25**, 3246-3257.**
- 2920
- 2921 **Anderson, N.J. and M.J. Leng, 2004: Increased aridity during the early Holocene in West**
- 2922 **Greenland inferred from stable isotopes in laminated-lake sediments. *Quaternary Science***
- 2923 ***Reviews*, **23**, 841-849.**
- 2924
- 2925 **Anderson, L., M.B. Abbott, and B.P. Finney, 2001: Holocene climate inferred from oxygen**
- 2926 **isotope ratios in lake sediments, central Brooks Range, Alaska. *Quaternary Research*, **55**,**
- 2927 **313-321.**
- 2928
- 2929 **Anderson, L., M.B. Abbott, B.P. Finney, and S.J. Burns, 2005: Regional atmospheric circulation**
- 2930 **change in the North Pacific during the Holocene inferred from lacustrine carbonate**
- 2931 **oxygen isotopes, Yukon Territory, Canada. *Quaternary Research*, **64**, 1-35.**
- 2932
- 2933 **Anderson, P.M. and A.V. Lozhkin, 2001: The stage 3 interstadial complex (Karginiskii/middle**
- 2934 **Wisconsinan interval) of Beringia: variations in paleoenvironments and implications for**
- 2935 **paleoclimatic interpretations. *Quaternary Science Reviews*, **20**, 93-125.**
- 2936
- 2937 **Anderson, P.M., P.J. Bartlein, L.B. Brubaker, K. Gajewski, and J.C. Ritchie, 1989: Modern**
- 2938 **analogues of late Quaternary pollen spectra from the western interior of North America.**
- 2939 ***Journal of Biogeography*, **16**, 573-596.**
- 2940
- 2941 **Anderson, P.M., P.J. Bartlein, L.B. Brubaker, K. Gajewski, and J.C. Ritchie, 1991: Vegetation-**
- 2942 **pollen-climate relationships for the arcto-boreal region of North America and Greenland.**
- 2943 ***Journal of Biogeography*, **18**, 565-582.**
- 2944

SAP1.2 DRAFT 3 PUBLIC COMMENT

- 2945 **Anderson, R.K., G.H. Miller, J.P. Briner, N.A. Lifton, and S.B. DeVogel, 2008:** A millennial
2946 perspective on Arctic warming from 14C in quartz and plants emerging from beneath ice
2947 caps. *Geophysical Research Letters*, **35**, L01502, doi:10.1029/2007GL032057.
2948
- 2949 **Andreev, A.A., D.M. Peteet, P.E. Tarasov, F.A. Romanenko, L.V. Filimonova, and L.D.**
2950 **Sulerzhitsky, 2001:** Late pleistocene interstadial environment on Faddeyevskiy Island,
2951 East-Siberian Sea, Russia. *Arctic, Antarctic, and Alpine Research*, **33**, 28-35.
2952
- 2953 **Andrews, J.T., L.M. Smith, R. Preston, T. Cooper, and A.E. Jennings, 1997:** Spatial and
2954 temporal patterns of iceberg rafting (IRD) along the East Greenland margin, ca. 68 N,
2955 over the last 14 cal ka. *Journal of Quaternary Science*, **12**, 1-13.
2956
- 2957 **Archer, D., 2007:** Methane hydrate stability and anthropogenic climate change. *Biogeosciences*,
2958 **4**, 521-544
2959
- 2960 **Arctic Climate Impact Assessment (ACIA), 2004:** *Impacts of a Warming Arctic—Arctic*
2961 *Climate Impact Assessment*. Cambridge University Press, Cambridge, U.K., 1042 pp.
2962
- 2963 **Arctic Monitoring and Assessment Programme (AMAP), 1998:** *AMAP Assessment Report*
2964 *Arctic Pollution Issues*. AMAP, Oslo, Norway, 871 pp.
2965
- 2966 **Astakhov, V.I., 1995:** The mode of degradation of Pleistocene permafrost in West Siberia.
2967 *Quaternary International*, **28**, 119-121.
2968
- 2969 **Backman, J., M. Jakobsson, R. Løvlie, L. Polyak, and L.A. Febo, 2004:** Is the central Arctic
2970 Ocean a sediment starved basin? *Quaternary Science Reviews*, **23**, 1435-1454.
2971
- 2972 **Backman, J., K. Moran, D.B. McInroy, L.A. Mayer, and the Expedition 302 scientists, 2006:**
2973 *Proceedings of IODP, 302*. Edinburgh (Integrated Ocean Drilling Program Management
2974 International, Inc.). doi:10.2204/iodp.proc.302.2006.
2975

SAP1.2 DRAFT 3 PUBLIC COMMENT

- 2976 **Balco**, G., C.W. Rovey, and O.H. Stone, 2005a: The First Glacial Maximum in North America.
2977 *Science*, **307**, 222.
2978
- 2979 **Balco**, G., O.H. Stone, and C..Jennings, 2005b: Dating Plio-Pleistocene glacial sediments using
2980 the cosmic-ray-produced radionuclides ^{10}Be and ^{26}Al . *American Journal of Science*, **305**,
2981 1-41.
2982
- 2983 **Ballantyne**, A.P., N.L. Rybczynski, P.A. Baker, C.R. Harington, and D. White, 2006: Pliocene
2984 Arctic temperature constraints from the growth rings and isotopic composition of fossil
2985 larch. *Palaeogeography, Palaeoclimatology, Palaeoecology*, **242**, 188-200
2986
- 2987 **Barber**, V.A. and B.P. Finney, 2000: Lake Quaternary paleoclimatic reconstructions for interior
2988 Alaska based on paleolake-level data and hydrologic models. *Journal of Paleolimnology*,
2989 **24**, 29-41.
2990
- 2991 **Bard**, E., 2002: Climate shocks—Abrupt changes over millennial time scales. *Physics Today*,
2992 **December**, 32-38.
2993
- 2994 **Barley**, E.M., I.R. Walker, and J. Kurek, L.C. Cwynar, R.W. Mathewes, K. Gajewski, and B.P.
2995 Finney, 2006: A northwest North American training set—Distribution of freshwater
2996 midges in relation to air temperature and lake depth. *Journal of Paleolimnology*, **36**, 295-
2997 314.
2998
- 2999 **Barnekow**, L. and P. Sandgren, 2001: Palaeoclimate and tree-line changes during the Holocene
3000 based on pollen and plant macrofossil records from six lakes at different altitudes in
3001 northern Sweden. *Review of Palaeobotany and Palynology*, **117**, 109-118.
3002
- 3003 **Barron**, E.J., P.J. Fawcett, D. Pollard, and S. Thompson, 1993: Model simulations of cretaceous
3004 climates - the role of geography and carbon-dioxide. *Philosophical Transactions of the*
3005 *Royal Society of London Series B-Biological Sciences*, **341(1297)**, 307-315.
3006

SAP1.2 DRAFT 3 PUBLIC COMMENT

- 3007 **Barron, E.J., P.J. Fawcett, W.H. Peterson, D. Pollard, and S.L. Thompson, 1995:** A “simulation”
3008 of mid-Cretaceous climate. *Paleoceanography*, **8**, 785-798.
- 3009
- 3010 **Barry, R.G., M.C. Serreze, J.A. Maslanik, and R.H. Preller, 1993:** The arctic sea-ice climate
3011 system — observations and modeling. *Reviews of Geophysics*, **31(4)**, 397-422.
- 3012
- 3013 **Bartlein, P.J., K.H. Anderson, P.M. Anderson, M.E. Edwards, C.J. Mock, R.S. Thompson, R.S.**
3014 **Webb, T. Webb, III, and C. Whitlock, 1998:** Paleoclimate simulations for North America
3015 over the past 21,000 years: features of the simulated climate and comparisons with
3016 paleoenvironmental data. *Quaternary Science Reviews*, **17**, 549–585.
- 3017
- 3018 **Bauch, D., J. Carstens, and G. Wefer, 1997:** Oxygen isotope composition of living
3019 *Neoglobobadrina pachyderma* (sin.) in the Arctic Ocean. *Earth and Planetary Science*
3020 *Letters*, **146**, 47-58.
- 3021
- 3022 **Bauch, D., P. Schlosser, and R.G. Fairbanks, 1995:** Freshwater balance and the sources of deep
3023 and bottom waters in the Arctic Ocean inferred from the distribution of H₂¹⁸O. *Progress*
3024 *in Oceanography*, **35**, 53-80.
- 3025
- 3026 **Bauch, H.A., H. Erlenkeuser, K. Fahl, R.F. Spielhagen, M.S. Weinelt, H. Andruleit, and R.**
3027 **Henrich, 1999:** Evidence for a steeper Eemian than Holocene sea surface temperature
3028 gradient between Arctic and sub-Arctic regions. *Palaeogeography, Palaeoclimatology,*
3029 *Palaeoecology*, **145**, 95-117.
- 3030
- 3031 **Bauch, H.A., H. Erlenkeuser, J.P. Helmke, and U. Struck, 2000:** A paleoclimatic evaluation of
3032 marine oxygen isotope stage 11 in the high-northern Atlantic (Nordic seas). *Global and*
3033 *Planetary Change*, **24**, 27-39.
- 3034
- 3035 **Bauch, H.A. and H. Erlenkeuser, 2003:** Interpreting Glacial-Interglacial Changes in Ice Volume
3036 and Climate From Subarctic Deep Water Foraminiferal d18O. In: *Earth's Climate and*
3037 *Orbital Eccentricity: The Marine Isotope Stage 11 Question*. [Droxler, A.W., R.Z. Poore,

SAP1.2 DRAFT 3 PUBLIC COMMENT

- 3038 and L.H. Burckle (eds.)]. Geophysical Monograph Series, **137**. [pages??]
3039
- 3040 **Bauch**, H.A. and E.S. Kandiano, 2007: Evidence for early warming and cooling in North
3041 Atlantic surface waters during the last interglacial. *Paleoceanography*, **22**, PA1201,
3042 doi:10.1029/2005PA001252.
3043
- 3044 **Beget**, J.E., 2001: Continuous Late Quaternary proxy climate records from loess in Beringia.
3045 *Quaternary Science Reviews* 20, 499-507.
3046
- 3047 **Behl**, R.J., and J.P. Kennett, 1996: Brief interstadial events in the Santa Barbara Basin, NE
3048 Pacific, during the past 60 kyr. *Nature*, **379**, 243-246.
3049
- 3050 **Bennike**, O., K.P. Brodersen, E. Jeppesen, and I.R. Walker, 2004: Aquatic invertebrates and
3051 high latitude paleolimnology. In: *Long-Term Environmental Change in Arctic and*
3052 *Antarctic Lakes* [Pienitz, R., M.S.V. Douglas, and J.P. Smol (eds.)]. Springer, Dordrecht,
3053 pp. 159-186.
3054
- 3055 **Berger**, A. and M.F. Loutre, 1991: Insolation values for the climate of the last million years.
3056 *Quaternary Sciences Review*, **10(4)**, 297-317.
- 3057 **Berger**, A. and M.F. Loutre, 2002: An Exceptionally long Interglacial Ahead? *Science*, **297**,
3058 1287-1288.
3059
- 3060 **Berger**, A., M.F. Loutre, and J. Laskar, 1992: Stability of the Astronomical Frequencies Over
3061 the Earth's History for Paleoclimate Studies. *Science*, **255(5044)**, 560-566.
3062
- 3063 **Berner**, R.A., and Z. Kothavala, 2001: GEOCARB III: A revised model of atmospheric CO₂
3064 over Phanerozoic time. *American Journal of Science*, **301(2)**, 182-204.
3065
- 3066 **Bice**, K.L., D. Birgel, P.A. Meyers, K.A. Dahl, K.U. Hinrichs, and R.D. Norris, 2006: A multiple
3067 proxy and model study of Cretaceous upper ocean temperatures and atmospheric CO₂

SAP1.2 DRAFT 3 PUBLIC COMMENT

- 3068 concentrations. *Paleoceanography*, **21(2)**, PA2002.
- 3069
- 3070 **Bigelow**, N., L.B. Brubaker, M.E. Edwards, S.P. Harrison, I.C. Prentice, P.M. Anderson, A.A.
3071 Andreev, P.J. Bartlein, T.R. Christensen, W. Cramer, J.O. Kaplan, A.V. Lozhkin, N.V.
3072 Matveyeva, D.F. Murraray, A.D. McGuire, V.Y. Razzhivin, J.C. Ritchie, B. Smith, D.A.
3073 Walker, K. Gajewski, V. Wolf, B.H. Holmqvist, Y. Igarashi, K. Kremenetskii, A. Paus,
3074 M.F.J. Pisaric, and V.S. Volkova, 2003: Climate change and Arctic ecosystems—1.
3075 Vegetation changes north of 55°N between the last glacial maximum, mid-Holocene, and
3076 present. *Journal of Geophysical Research*, **108**, doi:10.1029/2002JD002558.
- 3077
- 3078 **Bigler**, C. and R.I. Hall, 2003: Diatoms as quantitative indicators of July temperature—A
3079 validation attempt at century-scale with meteorological data from northern Sweden.
3080 *Palaeogeography, Palaeoclimatology, Palaeoecology*, **189**, 147-160.
- 3081
- 3082 **Birks**, H.H., 1991: Holocene vegetational history and climatic change in west Spitzbergen—
3083 Plant macrofossils from Skardtjorna, an arctic lake. *The Holocene*, **1**, 209–218.
- 3084
- 3085 **Birks**, H.J.B., 1998: Numerical tools in palaeolimnology—Progress, potentialities, and
3086 problems. *Journal of Paleolimnology*, **20**, 307-332.
- 3087
- 3088 **Björk**, G., J. Soöderkvist, P. Winsor, A. Nikolopoulos, and M. Steele, 2002: Return of the cold
3089 halocline layer to the Amundsen Basin of the Arctic Ocean—Implications for the sea ice
3090 mass balance. *Geophysical Research Letters*, **29(11)**, 1513, doi:10.1029/2001GL014157.
- 3091
- 3092 **Boellstorff**, J., 1987: North American Pleistocene stages reconsidered in light of probably
3093 Pliocene-Pleistocene continental glaciation. *Science*, **202(2004365)**, 305-307.
- 3094
- 3095 **Bonan**, G.B., D. Pollard, and S.L. Thompson, 1992: Effects of boreal forest vegetation on global
3096 climate. *Nature*, **359(6397)**, 716-718.
- 3097

SAP1.2 DRAFT 3 PUBLIC COMMENT

- 3098 **Boyd, T.J., M. Steel, R.D. Muench, and J.T. Gunn, 2002:** Partial recovery of the Arctic Ocean
3099 halocline. *Geophysical Research Letters*, **29(14)**, 1657, doi:10.1029/2001GL014047
3100
- 3101 **Box, J.E., D.H. Bromwich, B.A. Veenhuis, L.S. Bai, J.C. Stroeve, J.C. Rogers, K. Steffen, T.**
3102 **Haran, and S.H. Wang, 2006:** Greenland ice sheet surface mass balance variability (1988-
3103 2004) from calibrated polar MM5 output. *Journal of Climate*, **19(12)**, 2783-2800
3104
- 3105 **Braconnot, P., B. Otto-Bliesner, S. Harrison, F.S. Jousaume, J.-Y. Peterchmitt, A. Abe-Ouchi, M.**
3106 **Crucifix, E. Driesschaert, T. Fichefet, C.D. Hewitt, M. Kageyama, A. Kitoh, A. Laine, M.-F.**
3107 **Loutre, O. Marti, U. Merkel, G. Ramstein, P. Valdes, S.L. Weber, Y. Yu, and Y. Zhao, 2007:**
3108 **Results of PMIP2 coupled simulations of the Mid-Holocene and Last Glacial Maximum –**
3109 **Part 1: experiments and large-scale features. *Climates of the Past*, **3**, 261– 277.**
3110
- 3111 **Bradley, R.S., 1990:** Holocene paleoclimatology of the Queen Elizabeth Islands, Canadian high
3112 Arctic. *Quaternary Science Reviews*, **9**, 365-384.
3113
- 3114 **Bradley, R.S., 1999:** *Paleoclimatology: reconstructing climates of the Quaternary* (second
3115 edition), Academic Press, New York, 613 pp.
3116
- 3117 **Bradley, R. S., 2000:** Past global changes and their significance for the future. *Quaternary*
3118 *Science Reviews*, **19**, 391-402.
3119
- 3120 **Bradley, R.S., K.R. Briffa, J. Cole, and T.J. Osborn, 2003a:** The climate of the last millennium.
3121 In: *Paleoclimate, Global Change and the Future*, [Alverson, K.D., R.S. Bradley, and T.F.
3122 Pedersen (eds.)]. Springer, Berlin, pp. 105-141.
3123
- 3124 **Bradley, R.S., Hughes, M.K., and Diaz, H.F., 2003b:** Climate in Medieval Time. *Science*, **302**,
3125 404-405, doi: 10.1126/science.1090372.
3126
- 3127 **Bradley, R.S. and P.D. Jones (eds.), 1992:** *Climate Since AD 1500*. Routledge, London. 677 pp.
3128
- 3129 **Brassell, S.C., G. Eglinton, I.T. Marlowe, U. Pflaumann, and M. Sarnthein, 1986:** Molecular

SAP1.2 DRAFT 3 PUBLIC COMMENT

- 3130 stratigraphy—A new tool for climatic assessment. *Nature*, **320**, 129-133.
- 3131
- 3132 **Bray, P.J., S.P.E. Blockey, G.R. Coope, L.F. Dadswell, S.A. Elias, J.J. Lowe, and A.M. Pollard,**
- 3133 2006: Refining mutual climatic range (MCR) quantitative estimates of paleotemperature
- 3134 using ubiquity analysis. *Quaternary Science Reviews*, **25(15-16)**, 1865-1876.
- 3135
- 3136 **Brewer, S., J. Guiot, and F. Torre, 2007:** Mid-Holocene climate change in Europe: a data-model
- 3137 comparison. *Climate of the Past*, **3**, 499-512.
- 3138
- 3139 **Briffa, K. and E. Cook, 1990:** Methods of response function analysis In: *Methods of*
- 3140 *Dendrochronology* [Cook, E.R. and L.A. Kairiukstis (eds.)], sect. 5.6.
- 3141
- 3142 **Briffa, K.R., T.J. Osborn, F.H. Schweingruber, I.C. Harris, P.D. Jones, S.G. Shiyatov, and E.A.**
- 3143 **Vaganov, 2001:** Low-frequency temperature variations from a northern tree ring density
- 3144 network. *Journal of Geophysical Research*, **106**, 2929-2941.
- 3145
- 3146 **Brigham, J.K., 1985:** *Marine stratigraphy and amino acid geochronology of the Gubik*
- 3147 *Formation, western Arctic Coastal Plain, Alaska.* Doctoral dissertation, University of
- 3148 Colorado, Boulder; U.S. Geological Survey Open-File Report 85-381, 21pp.
- 3149
- 3150 **Brigham-Grette, J. and L.D. Carter, 1992:** Pliocene marine transgressions of northern Alaska—
- 3151 Circumarctic correlations and paleoclimate. *Arctic*, **43(4)**, 74-89.
- 3152
- 3153 **Brigham-Grette, J. and D.M. Hopkins, 1995:** Emergent-marine record and paleoclimate of the
- 3154 last interglaciation along the northwest Alaskan coast. *Quaternary Research*, **43**, 154-
- 3155 173.
- 3156
- 3157 **Brigham-Grette, J., A.V. Lozhkin, P.M. Anderson, and O.Y. Glushkova, 2004:**
- 3158 Paleoenvironmental conditions in western Beringia before and during the Last Glacial
- 3159 Maximum. In: *Entering America: Northeast Asia and Beringia Before the Last Glacial*
- 3160 *Maximum*, [Madsen, D.B. (ed.)]. University of Utah Press, Chapter 2, pp. 29-61.

SAP1.2 DRAFT 3 PUBLIC COMMENT

- 3161
- 3162 **Briner**, J.P., N. Michelutti, D.R. Francis, G.H. Miller, Y. Axford, M.J. Wooller, and A.P. Wolfe,
3163 2006: A multi-proxy lacustrine record of Holocene climate change on northeastern Baffin
3164 Island. *Quaternary Research*, **65**, 431-442.
- 3165
- 3166 **Brinkhuis**, H., S. Schouten, M.E. Collinson, A. Sluijs, J.S.S. Damsfte, G.R. Dickens, M. Huber,
3167 T.M. Cronin, J. Onodera, K. Takahashi, J.P. Bujak, R. Stein, J. van der Burgh, J.S.
3168 Eldrett, I.C. Harding, A.F. Lotter, F. Sangiorgi, H.V.V. Cittert, J.W. de Leeuw, J.
3169 Matthiessen, J. Backman, and K. Moran, (Expedition 302 Scientists), 2006: Episodic
3170 fresh surface waters in the Eocene Arctic Ocean. *Nature*, **441(7093)**, 606-609.
- 3171
- 3172 **Broecker**, W.S., 2001: Was the Medieval Warm Period Global? *Science*, **291** (5508) 1497-1499,
3173 doi:10.1126/science.291.5508.1497
- 3174
- 3175 **Broecker**, W.S. and S. Hemming, 2001: Climate swings come into focus. *Nature*, **294:5550**
3176 2308-2309.
- 3177
- 3178 **Broecker**, W.S., D.M. Peteet, D. Rind, 1985: Does the ocean-atmosphere system have more than
3179 one stable mode of operation. *Nature*, **315(6014)**, 21-26.
- 3180
- 3181 **Brouwers**, E.M., 1987: On *Prerygocythereis vunnieuwenhusei* Brouwers sp.nov. In: *A stereo-*
3182 *atlas of ostracode shells*, [Bate, R.H., D.J. Home, J.W. Neale, and D.J. Siveter, [eds.]].
3183 British Micropaleontological Society, London 14, Part **1**,17-20.
- 3184
- 3185 **Brown**, J. and V. Romanovsky, 2008: Report from the International Permafrost Association:
3186 State of Permafrost in the First Decade of the 21st Century. Permafrost and Periglacial
3187 Processes. *Permafrost and Periglacial Processes*, **19(2)**, 255-260.
- 3188
- 3189 **Buchardt**, B. and L.A. Símónarson, 2003: Isotope palaeotemperatures from the Tjörnes beds in
3190 Iceland: evidence of Pliocene cooling. *Palaeogeography, Palaeoclimatology,*
3191 *Palaeoecology* ,**189**, 71-95.

SAP1.2 DRAFT 3 PUBLIC COMMENT

3192

3193 **Budyko, M.I., A.B. Ronov, and A.L. Yanshin, 1985: *The History of the Earth's Atmosphere.***
3194 Leningrad, Gidrometeoirdat, 209 pp. (In Russian; English translation: Springer, Berlin,
3195 1987, 139 pp.

3196

3197 **Calkin, P.E., 1988: Holocene glaciation of Alaska (and adjoining Yukon Territory, Canada).**
3198 *Quaternary Science Reviews*, **7**, 159-184.

3199

3200 **CAPE Project Members, 2001: Holocene paleoclimate data from the Arctic: testing models of**
3201 **global climate change. *Quaternary Science Reviews*, **20**, 1275-1287.**

3202

3203 **CAPE–Last Interglacial Project Members, 2006: Last Interglacial Arctic warmth confirms**
3204 **polar amplification of climate change. *Quaternary Science Reviews*, **25**, 1383-1400.**

3205

3206 **Carter, L.D., 1981: A Pleistocene sand sea on the Alaskan Arctic Coastal Plain. *Science*,**
3207 **211(4480), 381-383.**

3208

3209 **Carter, L.D., J. Brigham-Grette, L. Marincovich, Jr., V.L. Pease, and U.S. Hillhouse, 1986: Late**
3210 **Cenozoic Arctic Ocean sea ice and terrestrial paleoclimate. *Geology*, **14**, 675-678.**

3211

3212 **Chapin, F.S. III, M. Sturm, M.C. Serreze, J.P. Mcfadden, J.R. Key, A.H. Lloyd, T.S. Rupp, A.H.**
3213 **Lynch, J.P. Schimel, J. Beringer, W.L. Chapman, H.E. Epstein, E.S. Euskirchen, L.D.**
3214 **Hinzman, G. Jia, C.L. Ping, K.D. Tape, C.D.C. Thompson, D.A. Walker, and J.M.**
3215 **Welker, 2005: Role of land-surface changes in Arctic summer warming. *Science*, **310**,**
3216 **657-660.**

3217

3218 **Chapman, M.R., N.J. Shackleton, and J.-C. Duplessy, 2000: Sea surface temperature variability**
3219 **during the last glacial-interglacial cycle—Assessing the magnitude and pattern of climate**
3220 **change in the North Atlantic. *Palaeogeography, Palaeoclimatology, Palaeoecology*, **157**,**
3221 **1-25.**

3222

SAP1.2 DRAFT 3 PUBLIC COMMENT

- 3223 **Chapman**, W.L. and J.E. Walsh, 2007: Simulations of Arctic temperature and pressure by global
3224 coupled models. *Journal of Climate*, **20(4)**, 609-632.
3225
- 3226 **Clark**, P.U. and D. Pollard, 1998: Origin of the Middle Pleistocene transition by ice sheet
3227 erosion of regolith. *Paleoceanography*, **13**, 1-9.
3228
- 3229 **Clark**, P.U., D. Archer, D. Pollard, J.D. Blum, J.A. Rial, V. Brovkin, A.C. Mix, N.G. Pisias, and
3230 M. Roy, 2006: The middle Pleistocene transition: characteristics, mechanisms, and
3231 implications for long-term changes in atmospheric pCO₂. *Quaternary Science Reviews*,
3232 **25**, 3150-3184.
3233
- 3234 **Clayden**, S.L., L.C. Cwynar, G.M. MacDonald, and A.A. Velichko, 1997: Holocene pollen and
3235 stomates from a forest-tundra site on the Taimyr Peninsula, Siberia. *Arctic and Alpine*
3236 *Research*, **29**, 327-333.
3237
- 3238 Climate Long-Range Investigation Mapping and Prediction (**CLIMAP**) Project Members, 1981:
3239 Seasonal reconstructions of the Earth's surface at the last glacial maximum. *Geological*
3240 *Society of America Map and Chart Series MC-36*, p. 1-18
3241
- 3242 Climate Long-Range Investigation Mapping and Prediction (**CLIMAP**) Project Members, 1984:
3243 The last interglacial ocean. *Quaternary Research*, **21**, 123-224.
3244
- 3245 **Cockford**, S.J. and S.G. Frederick, 2007: Sea ice expansion in the Bering Sea during the
3246 Neoglacial—Evidence from archeozoology. *The Holocene*, **17**, 699-706.
3247
- 3248 **Cohen**, A.S., 2003: *Paleolimnology—The history and evolution of lake systems*. Oxford
3249 University Press, Oxford, U.K., 528 pp.
3250
- 3251 **Colinvaux**, P.A., 1964: The environment of the Bering Land Bridge. *Ecological Monographs*,
3252 **34**, 297-329.
3253

SAP1.2 DRAFT 3 PUBLIC COMMENT

- 3254 **Conte, M.H., M. Sicre, C. Rühlemann, J.C. Weber, S. Schulte, D. Schulz-Bull, and T. Blanz,**
3255 2006: Global temperature calibration of the alkenone unsaturation index (UK'₃₇) in
3256 surface waters and comparison with surface sediments. *Geochemistry, Geophysics,*
3257 *Geosystems*, **7**, Q02005, doi:10.1029/2005GC001054.
- 3258
- 3259 **Cronin, T.M, G.S. Dwyer, T. Kamiyac, S. Schwedea, and D.A. Willarda, 2003: Medieval Warm**
3260 **Period, Little Ice Age and 20th century temperature variability from Chesapeake Bay.**
3261 *Global and Planetary Change*, **36**, 17-29
- 3262
- 3263 **Crowley, T.J., 1998: Significance of tectonic boundary conditions for paleoclimate simulations.**
3264 **In: *Tectonic Boundary Conditions for Climate Reconstructions* [Crowley, T.J., and K.C.**
3265 **Burke (eds.)]. Oxford University Press, New York, pp. 3-17.**
- 3266
- 3267 **Crowley, T.J., 1990: Are there any satisfactory geologic analogs for a future greenhouse**
3268 **warming? *Journal of Climatology*, **3**, 1282-1492.**
- 3269
- 3270 **Crowley, T.J., 2000: Causes of climate change over the past 1000 years. *Science*, **289**, 270-277.**
- 3271
- 3272 **Crowley, T.J., S.K. Baum, K.Y. Kim, G.C. Hegerl, and W.T. Hyde, 2003: Modeling ocean heat**
3273 **content changes during the last millennium. *Geophysical Research Letters*, **30**, 1932,**
3274 **doi:10.1029/2003GL017801.**
- 3275
- 3276 **Crowley, T.J. and T. Lowery, 2000: How warm was the Medieval warm period? *Ambio*, **29**, 51-**
3277 **54.**
- 3278
- 3279 **Cuffey, K.M. and G.D. Clow, 1997: Temperature, accumulation, and ice sheet elevation in**
3280 **central Greenland through the last deglacial transition. *Journal of Geophysical Research*,**
3281 ****102(C12)**, 26,383-26,396.**
- 3282
- 3283 **Cuffey, K.M., G.D. Clow, R.B. Alley, M. Stuiver, E.D. Waddington, and R.W. Saltus, 1995:**
3284 **Large Arctic temperature change at the Wisconsin-Holocene glacial transition. *Science*,**

SAP1.2 DRAFT 3 PUBLIC COMMENT

3285 **270**, 455-458.

3286

3287 **D'Arrigo**, R., Wilson, R., Jacoby, G., 2006: On the long-term context for late twentieth century
3288 warming. *Journal of Geophysical Research*, **111**, D03103, doi:10.1029/2005JD006352.

3289

3290 **Dahe**, Q., J.R. Petit, J. Jouzel, and M. Stievenard, 1994: Distribution of stable isotopes in surface
3291 snow along the route of the 1990 International Trans-Antarctic Expedition. *Journal of*
3292 *Glaciology*, **40**, 107-118.

3293

3294 **Dahl**, S.O. and A. Nesje, 1996: A new approach to calculating Holocene winter precipitation by
3295 combining glacier equilibrium-line altitudes and pine-tree limits: a case stud from
3296 Hardangerjokulen, central southern Norway. *The Holocene*, **6(4)**, 381-398,
3297 doi:10.1177/095968369600600401

3298

3299 **Dahl-Jensen**, D., K. Mosegaard, N. Gundestrup, G.D. Clow, S.J. Johnsen, A.W. Hansen, and N.
3300 Balling, 1998: Past temperature directly from the Greenland Ice Sheet. *Science*, **282**, 268-
3301 271.

3302

3303 **Dansgaard**, W., 1964: Stable isotopes in precipitation. *Tellus*, **16**, 436-468.

3304

3305 **Dansgaard**, W., J.W.C. White, and S.J. Johnsen, 1989: The abrupt termination of the Younger
3306 Dryas climate event. *Nature*, **339(6225)**, 532-534.

3307

3308 **Delworth**, T.L., and T.R. Knutson, 2000: Simulation of early 20th century global warming.
3309 *Science*, **287(5461)**, 2246-225.

3310

3311 **de Vernal**, A., C. Hillaire-Marcel, and D.A. Darby, 2005: Variability of sea ice cover in the
3312 Chukchi Sea (western Arctic Ocean) during the Holocene. *Paleoceanography*, **20**,
3313 PA4018, doi:10.1029/2005PA001157.

3314

SAP1.2 DRAFT 3 PUBLIC COMMENT

- 3315 **Denton, G.H., R.B. Alley, G.C. Comer and W.S. Broecker, 2005:** The role of seasonality in
3316 abrupt climate change. *Quaternary Science Reviews*, **24(10-11)**, 1159-1182.
3317
- 3318 **Digerfeldt, G., 1988:** Reconstruction and regional correlation of Holocene lake-level
3319 fluctuations in Lake Bysjön, South Sweden. *Boreas*, **17**, 237-263.
3320
- 3321 **Donnadieu, Y., R. Pierrehumbert, R. Jacob, and F. Fluteau, 2006:** Modeling the primary control
3322 of paleogeography on Cretaceous climate. *Earth and Planetary Science Letters*, **248**, 426-
3323 437.
3324
- 3325 **Douglas, M.S.V., 2007:** Environmental change at high latitudes. In: *Geological and*
3326 *Environmental Applications of the Diatom—Pond Scum to Carbon Sink* [Starratt, S.W.
3327 (ed.)]. The Paleontological Society Papers, **13**, 169-179.
3328
- 3329 **Douglas, M.S.V. and J.P. Smol, 1994:** Limnology of high arctic ponds (Cape Herschel,
3330 Ellesmere Island, N.W.T.). *Archiv für Hydrobiologie*, **131**, 401-434.
3331
- 3332 **Douglas, M.S.V. and J.P. Smol, 1999:** Freshwater diatoms as indicators of environmental change
3333 in the High Arctic. In: *The Diatoms—Applications for the Environment and Earth*
3334 *Sciences*, [Stoermer, E. and J.P. Smol (eds.)]. Cambridge University Press, Cambridge,
3335 U.K., 488 pp.
3336
- 3337 **Douglas, M.S.V., J.P. Smol, and W. Blake, Jr., 1994:** Marked post-18th century environmental
3338 change in high Arctic ecosystems. *Science*, **266**, 416-419.
3339
- 3340 **Douglas, M.S.V., J.P. Smol, R. Pienitz, and P. Hamilton, 2004:** Algal indicators of
3341 environmental change in arctic and antarctic lakes and ponds. In: *Long-Term*
3342 *Environmental Change in Arctic and Antarctic Lakes*, [Pienitz, R., M.S.V. Douglas, and
3343 J.P. Smol (eds.)]. Springer, Dordrecht. pp. 117-157.
3344
- 3345 **Dowdeswell, J.A., J.O. Hagen, H. Björnsson, A.F. Glazovsky, W.D. Harrison, P. Holmlund, J.**

SAP1.2 DRAFT 3 PUBLIC COMMENT

- 3346 Jania, R.M. Koerner, B. Lefauconnier, C.S.L. Ommanney, and R.H. Thomas, 1997: The
3347 mass balance of circum-Arctic glaciers and recent climate change. *Quaternary Research*,
3348 **48**, 1-14.
- 3349
- 3350 **Dowsett, H.J.**, 2007: The PRISM Palaeoclimate Reconstruction and Pliocene Sea-Surface
3351 Temperature. In: *Deep-time perspectives on climate change: marrying the signal from*
3352 *computer models and biological proxies*, [Williams, M., A.M. Haywood, F.J. Gregory,
3353 and D.N. Schmidt (eds.)] The Micropalaeontological Society, Special Publication, The
3354 Geological Society, London, pp. 459-480.
- 3355
- 3356 **Dowsett, H.J.**, J.A. Barron, R.Z. Poore, R.S. Thompson, T.M. Cronin, S.E. Ishman, S.E., D.A.
3357 Willard, 1999: Middle Pliocene paleoenvironmental reconstruction: PRISM2, U.S.
3358 Geological Survey Open File Report 99-535.
- 3359
- 3360 **Dowsett, H.J.**, and eight others, 1994: Joint investigations of the middle Pliocene climate I—
3361 PRISM paleoenvironmental reconstructions. *Global and Planetary Change*, **9**, 169-195
3362
- 3363 **Droxler, A.W.** and J.W. Farrell, 2000: Marine Isotope Stage 11 (MIS11): New insights for a
3364 warm future. *Global and Planetary Change*, **24(1)**, 1-5
3365
- 3366 **Droxler, A.W.**, R.B. Alley, W.R. Howard, R.Z. Poore and L.H. Burckle. 2003: Unique and
3367 exceptionally long interglacial marine isotope stage 11: Window into Earth future
3368 climate. In: *Earth's Climate and Orbital Eccentricity: The Marine Isotope Stage 11*
3369 *Question*, [Droxler, A.W., R.Z. Poore and L.H. Burckle (eds.)]. Geophysical Monograph,
3370 **137**, American Geophysical Union, pp. 1-14.
- 3371
- 3372 **Duk-Rodkin, A.**, R.W. Barendregt, D.G. Froese, F. Weber, R.J. Enkin, I.R. Smith, Grant D.
3373 Zazula, P. Waters, and R. Klassen, 2004: Timing and Extent of Plio-Pleistocene
3374 glaciations in North-Western Canada and East-Central Alaska. In: *Quaternary*
3375 *Glaciations-Extent and Chronology, Part II, North America*, [Ehlers, J. and P.L. Gibbard
3376 (eds.)]. Elsevier, New York, pp. 313-345.

SAP1.2 DRAFT 3 PUBLIC COMMENT

- 3377
- 3378 **Dyke**, A.S. and J.M. Savelle, 2001: Holocene history of the Bering Sea bowhead whale (*Balaena*
3379 *mysticetus*) in its Beaufort Sea summer grounds off southwestern Victoria Island, western
3380 Canadian Arctic. *Quaternary Research*, **55**, 371-379.
- 3381
- 3382 **Dykoski**, C.A., R.L. Edwards, H. Cheng, D. Yuan, Y. Cai, M. Zhang, Y. Lin, J. Qing, Z. An, and
3383 J. Revenaugh, 2005: A high-resolution, absolute-dated Holocene and deglacial Asian
3384 monsoon record from Dongge Cave, China. *Earth and Planetary Science Letters*, **233**,
3385 71-86.
- 3386
- 3387 **Edwards**, M.E., N.H. Bigelow, B.P. Finney, and W.R. Eisner, 2000: Records of aquatic pollen
3388 and sediment properties as indicators of late-Quaternary Alaskan lake levels. *Journal of*
3389 *Paleolimnology*, **24**, 55-68.
- 3390
- 3391 **Elias**, S.A., 2007: Beetle records—Late Pleistocene North America. In: *Encyclopedia of*
3392 *Quaternary Science* [Elias, S.A. (ed.)]. Elsevier, Amsterdam, pp. 222-236.
- 3393
- 3394 **Elias**, S.A., K. Anderson, and J.T. Andrews, 1996: Late Wisconsin climate in the northeastern
3395 United States and southeastern Canada, reconstructed from fossil
3396
- 3397 **Elias**, S.A., J.T. Andrews, and K.H. Anderson, 1999: New insights on the climatic constraints on
3398 the beetle fauna of coastal Alaska derived from the mutual climatic range method of
3399 paleoclimate reconstruction. *Arctic, Antarctic, and Alpine Research*, **31**, 94-98.
- 3400
- 3401 **Elias**, S.A. and J.V. Matthews, Jr., 2002: Arctic North American seasonal temperatures in the
3402 Pliocene and Early Pleistocene, based on mutual climatic range analysis of fossil beetle
3403 assemblages. *Canadian Journal of Earth Sciences*, **39**, 911-920.
- 3404 beetle assemblages. *Journal of Quaternary Science*, **11**, 417-421.
- 3405
- 3406 **Ellis**, J.M., and P.E. Calkin, 1984: Chronology of Holocene glaciation, central Brooks Range,
3407 Alaska. *Geological Society of America Bulletin*, **95**, 897-912.

SAP1.2 DRAFT 3 PUBLIC COMMENT

- 3408
- 3409 **Epstein, S.,** H. Buchsbaum, H. Lowenstam, and H.C. Urey, 1953: Revised carbonate-water
3410 isotopic temperature scale. *Geological Society of America Bulletin*, **64**, 1315-1325.
- 3411
- 3412 **Erez, J.** and B. Luz, 1982: Temperature control of oxygen-isotope fractionation of cultured
3413 planktonic foraminifera. *Nature*, **297**, 220-222.
- 3414
- 3415 **Eronen, M.,** P. Zetterberg, K.R. Briffa, M. Lindholm, J. Meriläinen, and M. Timonen, 2002: The
3416 supra-long Scots pine tree-ring record for Finnish Lapland: Part 1, chronology
3417 construction and initial inferences. *The Holocene*, **12(6)**, 673-680.
- 3418
- 3419 **Esper, J.,** E.R. Cook, and F.H. Schweingruber, 2002: Low-frequency signals in long tree-ring
3420 chronologies for reconstructing past temperature variability. *Science*, **295**, 2250-2253.
- 3421
- 3422 **Esper, J.** and F.H. Schweingruber, 2004: Large-scale treeline changes recorded in Siberia.
3423 *Geophysical Research Letters*, **31**, L06202, doi:10.1029/2003GL019178.
- 3424
- 3425 **Fairbanks, R.G.,** 1989: A 17,000-year glacio-eustatic sea level record—Influence of glacial
3426 melting rates on the Younger Dryas event and deep-ocean circulation. *Nature*, **343**, 612-
3427 616.
- 3428
- 3429 **Farrera, I.,** S.P. Harrison, I.C. Prentice, G. Ramstein, J. Guiot, P.J. Bartlein, R. Bonnelle, M.
3430 Bush, W. Cramer, U. von Grafenstein, K. Holmgren, H. Hooghiemstra, G. Hope, D.
3431 Jolly, S.-E. Lauritzen, Y. Ono, S. Pinot, M. Stute, and G. Yu, 1999: Tropical climates at
3432 the Last Glacial Maximum: a new synthesis of terrestrial palaeoclimate data. I.
3433 Vegetation, lake-levels and geochemistry. *Climate Dynamics*, **15**, 823-856.
- 3434
- 3435 **Finney, B.,** K. Rühland, J.P. Smol, and M.-A. Fallu, 2004: Paleolimnology of the North
3436 American subarctic. In: *Long-Term Environmental Change in Arctic and Antarctic Lakes*
3437 [Pienitz, R., M.S.V. Douglas, and J.P. Smol (eds.)]. Springer, Dordrecht, pp. 269-318.
- 3438

SAP1.2 DRAFT 3 PUBLIC COMMENT

- 3439 **Fisher, D.A.**, 1979: Comparison of 100,000 years of oxygen isotope and insoluble impurity
3440 profiles from the Devon Island and Camp Century ice cores. *Quaternary Research*, **11**,
3441 299-304.
- 3442
- 3443 **Fisher, D.A.** and R.M. Koerner, 2003: Holocene ice core climate history, a multi-variable
3444 approach. In: *Global Change in the Holocene*, [Mackay, A., R. Battarbee, J. Birks and F.
3445 Oldfield, (eds.)] Arnold, London, pp. 281-293.
- 3446
- 3447 **Fisher, D.A.**, R.M. Koerner, J.C. Bourgeois, G. Zielinski, C. Wake, C.U. Hammer, H.B.
3448 Clausen, N. Gundestrup, S. Johnsen, K. Goto- Azuma, T. Hondoh, E. Blake, and M.
3449 Gerasimoff, 1998: Penny Ice Cap cores, Baffin Island, Canada, and the Wisconsinan
3450 Foxe Dome connection—Two states of Hudson Bay ice cover. *Science*, **279**, 692-695.
- 3451
- 3452 **Fisher, D.A.**, C. Wake, K. Kreutz, K. Yalcin, E. Steig, P. Mayewski, L. Anderson, J. Aheng, S.
3453 Rupper, C. Zdanowicz, M. Demuth, M. Waskiewicz, D. Dahl-Jensen, K. Goto-Azuma,
3454 J.B. Bourgeois, R.M. Koerner, J. Sekerka, E. Osterberg, M.B. Abbott, B.P. Finney, and
3455 S.J. Burns, 2004: Stable isotope records from Mount Logan, Eclipse ice cores and nearby
3456 Jellybean Lake. Water cycle of the North Pacific over 2000 years and over five vertical
3457 kilometres—Sudden shift and tropical connections. *Geographie physique et Quaternaire*,
3458 **58**, 9033-9048.
- 3459
- 3460 **Flowers, G.E.**, H. Björnsson, Á. Geirsdóttir, G.H. Miller, J.L. Black, and G.K.C. Clarke, 2008:
3461 Holocene climate conditions and glacier variation in central Iceland from physical
3462 modelling and empirical evidence. *Quaternary Science Reviews*, **27**, 797-813.
- 3463
- 3464 **Francis, J.E.**, 1988: A 50-million-year-old fossil forest from Strathcona Fiord, Ellesmere Island,
3465 Arctic Canada—Evidence for a warm polar climate. *Arctic*, **41(4)**, 314-318.
- 3466
- 3467 **Fricke, H.C.** and J.R. O’Neil, 1999: The correlation between $^{18}\text{O}/^{16}\text{O}$ ratios of meteoric water
3468 and surface temperature: its use in investigating terrestrial climate change over geologic
3469 time. *Earth and Planetary Science Letters*, **170**, 181-196.

SAP1.2 DRAFT 3 PUBLIC COMMENT

3470

3471 **Fritts, H.C.**, 1976: *Tree Rings and Climate*. London Academic Press

3472

3473 **Fronval, T.** and E. Jansen, 1997: Eemian and early Weichselian (140- 60 ka) paleoceanography
3474 and paleoclimate in the Nordic seas with comparisons to Holocene conditions.

3475 *Paleoceanography*, **12**, 443-462.

3476

3477 **Funder, S.**, 1989: Quaternary geology of East Greenland. In: *Quaternary Geology of Canada*
3478 *and Greenland*, [Fulton, R.J. (ed.)]. Geological Society of America Decade of North
3479 American Geology, vol. **K1**, pp. 756-763.

3480

3481 **Funder, S.**, O. Bennike, J. Böcher, C. Israelson, K.S. Petersen, and L.A. Simonarson, 2001: Late
3482 Pliocene Greenland—The Kap Kobenhavn Formation in North Greenland. *Bulletin of the*
3483 *Geological Society of Denmark*, **48**, 117-134.

3484

3485 **Funder, S.**, I. Demidov, and Y. Yelovicheva, 2002: Hydrography and mollusc faunas of the
3486 Baltic and the White Sea-North Sea seaway in the Eemian. *Palaeogeography,*
3487 *Palaeoclimatology, Palaeoecology*, **184**, 275-304.

3488

3489 **Fyles, J.G.**, L. Marinovich, Jr., J.V. Mathews, Jr., and R. Barendregt, 1991: Unique mollusc
3490 find in the Beaufort Formation (Pliocene) Meighen Island, Arctic Canada. In: *Current*
3491 *Research, Part B, Geological Survey of Canada, Paper 91-1B*, pp. 461-468.

3492

3493 **Gajewski, K.** and G.M. MacDonald, 2004: Palynology of North American Arctic Lakes. In:
3494 *Long Term Environmental Change in Arctic and Antarctic Lakes* [R. Pienitz, M.S.V.
3495 Douglas and J.P. Smol (eds.)]. Springer, Netherlands, pp. 89-116.

3496

3497 **Gard, G.**, 1986: Calcareous nannofossil biostratigraphy north of 80° latitude in the eastern
3498 Arctic Ocean. *Boreas*, **15**, 217-229.

3499

3500 **Gard, G.**, 1987: Late Quaternary calcareous nannofossil biostratigraphy and sedimentation

SAP1.2 DRAFT 3 PUBLIC COMMENT

- 3501 patterns—Fram Strait, Arctica. *Paleoceanography*, **2**, 219-229.
- 3502
- 3503 **Gard, G.**, 1993: Late Quaternary coccoliths at the North Pole—Evidence of ice-free conditions
3504 and rapid sedimentation in the central Arctic Ocean. *Geology*, **21**, 227-230.
- 3505
- 3506 **Geirsdottir, A.**, Miller, G.H., Axford, Y. and Olafsdottir, S., in press, Holocene and latest
3507 Pleistocene climate and glacier fluctuations in Iceland. *Quaternary Science Reviews*.
- 3508
- 3509 **Gervais, B.R.**, G.M. MacDonald, J.A. Snyder, and C.V. Kremenetski, 2002: *Pinus sylvestris*
3510 treeline development and movement on the Kola Peninsula of Russia—Pollen and
3511 stomate evidence. *Journal of Ecology*, **90**, 627-638.
- 3512
- 3513 **Goetcheus, V.G.**, and H.H. Birks, 2001: Full-glacial upland tundra vegetation preserved under
3514 tephra in the Beringia National Park, Seward Peninsula, Alaska. *Quaternary Science*
3515 *Reviews*, **20(1-3)**, 135-147.
- 3516
- 3517 **Goetz, S.J.**, M.C. Mack, K.R. Gurney, J.T. Randerson, and R.A. Houghton, 2007: Ecosystem
3518 responses to recent climate change and fire disturbance at northern high latitudes—
3519 Observations and model results contrasting northern Eurasia and North America.
3520 *Environmental Research Letters*, **2**, 045031, doi:10.1088/1748-9326/2/4/045031
- 3521
- 3522 **Goodfriend, G.A.**, J. Brigham-Grette, G.H. Miller, 1996: Enhanced age resolution of the marine
3523 quaternary record in the Arctic using aspartic acid racemization dating of bivalve shells.
3524 *Quaternary Research*, **45**, 176-187
- 3525
- 3526 **Goosse, H.**, H. Renssen, A. Timmermann, and R.A. Bradley, 2005: Internal and forced climate
3527 variability during the last millennium—A model-data comparison using ensemble
3528 simulations. *Quaternary Science Reviews*, **24**, 1345-1360.
- 3529
- 3530 **Gradstein, F.M.**, J.G.Ogg, and A.G. Smith (eds.), 2004: *A Geologic Time Scale*. Cambridge
3531 University Press, Cambridge, 589 pp.

SAP1.2 DRAFT 3 PUBLIC COMMENT

3532

3533 **Grice, K., W.C.M. Klein Breteler, S. Schoten, V. Grossi, J.W. de Leeuw, and J.S. Sinnige**
3534 **Damste, 1998: Effects of zooplankton herbivory on biomarker proxy records.**
3535 ***Paleoceanography*, **13**, 686-693.**

3536

3537 **Grootes, P.M., M. Stuiver, J.W.C. White, S. Johnsen, and J. Jouzel, 1993: Comparison of**
3538 **oxygen isotope records from the GISP2 and GRIP Greenland Ice cores. *Nature*, **366**, 522-**
3539 **555.**

3540

3541 **Grove, J.M., 1988: *The Little Ice Age*. Methuen, London, 498 pp.**

3542

3543 **Grudd, H., K.R. Briffa, W. Karlén, T.S. Bartholin, P.D. Jones, and B. Kromer, 2002: A 7400-**
3544 **year tree-ring chronology in northern Swedish Lapland—Natural climatic variability**
3545 **expressed on annual to millennial timescales. *The Holocene*, **12**, 657-666.**

3546

3547 **Gudina, V.D. Kryukov, L.K. Levchuk and L.A. Sudkov, 1983: Upper-Pleistocene sediments in**
3548 **north-eastern Taimyr. *Bulletin of Commission on Quaternary Researches*, **52**, 90-97 (in**
3549 **Russian).**

3550

3551 **Haeberli, W., G.D. Cheng, A.P. Gorbunov, and S.A. Harris, 1993: Mountain permafrost and**
3552 **climatic change. *Permafrost and Periglacial Processes*, **4(2)**, 165-174.**

3553

3554 **Hammarlund, D., L. Barnekow, H.J.B. Birks, B. Buchardt, and T.W.D. Edwards, 2002:**
3555 **Holocene changes in atmospheric circulation recorded in the oxygen-isotope stratigraphy**
3556 **of lacustrine carbonates from northern Sweden. *The Holocene*, **12**, 339-351.**

3557

3558 **Hannon, G.E. and M.J. Gaillard, 1997: The plant-macrofossil record of past lake-level changes.**
3559 ***Journal of Paleolimnology*, **18**, 15-28.**

3560

3561 **Hantemirov, R.M. and S.G. Shiyatov, 2002: A continuous multi-millennial ring-width**
3562 **chronology in Yamal, northwestern Siberia. *The Holocene*, **12(6)**, 717-726.**

3563

3564 **Harrison, S., P. Braconnot, C. Hewitt, and R.J. Stouffer, 2002: Fourth International Workshop**
3565 **of the Palaeoclimate Modelling Inter- comparison Project (PMIP): Launching PMIP**
3566 **Phase II. *EOS*, **83**, 447-447.**

3567

3568 **Harrison, S.P., D. Jolly, F. Laarif, A. Abe-Ouchi, B. Dong, K. Herterich, C. Hewitt, S.**
3569 **Joussaume, J.E. Kutzbach, J. Mitchell, N. de Noblet, and P. Valdes, 1998:**
3570 **Intercomparison of simulated global vegetation distributions in response to 6 kyr BP**
3571 **orbital forcing. *Journal of Climate*, **11**, 2721-2742.**

3572

3573 **Harrison, S.P., J.E. Kutzbach, I.C. Prentice, P.J. Behling, and M.T. Sykes, 1995: The response**
3574 **of northern hemisphere extratropical climate and vegetation to orbitally induced changes**
3575 **in insolation during the last interglaciation. *Quaternary Research*, **43**(2), 174-184.**

3576

3577 **Haywood, A.M., P. Dekens, A.C. Ravelo, and M. Williams, 2005: Warmer tropics during the**
3578 **mid-Pliocene? Evidence from alkenone paleothermometry and a fully coupled ocean-**
3579 **atmosphere GCM. *Geochemistry, Geophysics, Geosystems*, **6**, Q03010,**
3580 **doi:10.1029/2004GC000799.**

3581

3582 **Haywood, A.M. and P.J. Valdes, 2004: Modeling Pliocene warmth: contribution of atmosphere,**
3583 **oceans and cryosphere. *Earth and Planetary Science Letters*, **218**, 363-377.**

3584

3585 **Haywood, A.M. and P.J. Valdes, 2006: Vegetation cover in a warmer world simulated using a**
3586 **dynamic global vegetation model for the Mid-Pliocene. *Palaeogeography,***
3587 ***Palaeoclimatology, Palaeoecology*, **237**, 412-427.**

3588

3589 **Helmke, J.P. and H.A. Bauch, 2003: Comparison of glacial and interglacial conditions between**
3590 **the polar and subpolar North Atlantic region over the last five climatic cycles.**

3591 ***Paleoceanograph*, **18**(2), 1036, doi:10.1029/2002PA000794**

3592

3593 **Henrich R. and K.-H. Baumann, 1994: Evolution of the Norwegian current and the**

SAP1.2 DRAFT 3 PUBLIC COMMENT

3594 Scandinavian ice sheets during the past 2.6 m.y.: evidence from ODP Leg 104 biogenic
3595 carbonate and terrigenous records. *Palaeogeography, Palaeoclimatology, Palaeoecology*,
3596 **108**, 75-94.

3597

3598 **Herbert**, T.D., 2003: *Alkenone paleotemperature determinations*. In: *Treatise in Marine*
3599 *Geochemistry*, [Elderfield, H. and K.K. Turekian (eds.)]. Elsevier, Amsterdam, pp. 391-
3600 432.

3601

3602 **Heusser**, L. and J. Morley, 1996: Pliocene climate of Japan and environs between 4.8 and 2.8
3603 Ma: a joint pollen and marine faunal study. *Marine Micropaleontology*, **27**, 85-106.

3604

3605 **Hewitt**, C.D. and J.F.B. Mitchell, 1998: A Fully Coupled GCM Simulation of the Climate of the
3606 Mid-Holocene. *Geophysical Research Letters*, **25**, 361-364.

3607

3608 **Hoffmann**, G., M. Werner, and M. Heimann, 1998: Water isotope module of the ECHAM
3609 atmospheric general circulation model—A study on timescales from days to several
3610 years. *Journal of Geophysical Research*, **103**, 16,871-16,896.

3611

3612 **Holland**, M.M. and C.M. Bitz, 2003: Polar amplification of climate change in coupled models.
3613 *Climate Dynamics*, **21**, 221-232.

3614

3615 **Holland**, M.H., C.M., Bitz, and B. Tremblay, 2006: Future abrupt reductions in the summer
3616 Arctic sea ice. *Geophysical Research Letters*, **33**, L23503, doi:10.1029/2006GL028024.

3617

3618 **Huber**, C., M. Leuenberger, R. Spahni, J. Flückiger, J. Schwander, T. F. Stocker, S. Johnsen, A.
3619 Landals, and J. Jouzel, 2006: Isotope calibrated Greenland temperature record over
3620 Marine Isotope Stage 3 and its relation to CH₄. *Earth and Planetary Science Letters*, **243**,
3621 504-519.

3622

3623 **Hughen**, K., J. Overpeck, R.F. Anderson, K.M. and Williams, 1996: The potential for
3624 palaeoclimate records from varved Arctic lake sediments: Baffin Island, Eastern

SAP1.2 DRAFT 3 PUBLIC COMMENT

- 3625 Canadian Arctic. In: *Lacustrine Environments. Palaeoclimatology and*
3626 *Palaeoceanography from Laminated Sediments* [Kemp, A.E.S. (ed.)]. Geological
3627 Society, London, Special Publications 116, pp. 57-71.
3628
- 3629 **Hughes**, M.K. and H.F. Diaz, 1994: Was there a ‘Medieval Warm Period’ and if so, where and
3630 when? *Journal of Climatic Change*, **265**, 109-142.
3631
- 3632 **Huybers**, P., 2006: Early Pleistocene glacial cycles and the integrated summer insolation
3633 forcing. *Science*, *313*, 508-511.
3634
- 3635 **Hyvärinen**, H., 1976: Flandrian pollen deposition rates and tree-line history in northern
3636 Fennoscandia. *Boreas*, **5(3)**, 163-175.
3637
- 3638 **Ilyashuk**, E.A, B.P. Ilyashuk, D. Hammarlund, and I. Larocque, 2005: Holocene climatic and
3639 environmental changes inferred from midge records (Diptera: Chironomidae,
3640 Chaoboridae, Ceratopogonidae) at Lake Berkut, southern Kola Peninsula, Russia.
3641 *Holocene*, **15**, 897-914.
3642
- 3643 **Imbrie**, J. and N.G. Kipp, 1971: A new micropaleontological method for Quantitative
3644 Paleoclimatology: Application to a late Pleistocene Caribbean Core. In: *The Late*
3645 *Cenozoic Glacial Age*,. [Turekian, K.K. (ed.)]. Yale Univeristy Press, New Haven, CT,
3646 pp. 71-181.
3647
- 3648 **Imbrie**, J., A. Berger, E.A. Boyle, S.C. Clemens, A. Duffy, W.R. Howard, G. Kukla, J.
3649 Kutzbach, D.G. Martinson, A. McIntyre, A.C. Mix, B. Molfino, J.J. Morley, L.C.
3650 Peterson, N.G. Pisias, W.L. Prell, M.E. Raymo, N.J. Shackleton, and J.R. Toggweiler,
3651 1993: On the structure and origin of major glaciation cycles. 2. The 100,000-year cycle.
3652 *Paleoceanography*, **8**, 699-735.
3653
- 3654 **IPCC**, 1990: *Climate Change: The IPCC scientific assessment*, [Houghton,J.T., G.J. Jenkins,
3655 and J.J. Ephraums, (eds.)]. Cambridge University Press, Cambridge.

SAP1.2 DRAFT 3 PUBLIC COMMENT

- 3656
- 3657 **IPCC**, 2007: Summary for Policymakers. In: *Climate Change 2007: The Physical Science Basis*
3658 — *Contribution of Working Group I to the Fourth Assessment Report of the*
3659 *Intergovernmental Panel on Climate Change*, [Solomon, S., D. Qin, M. Manning, Z.
3660 Chen, M. Marquis, K.B. Averyt, M.Tignor and H.L. Miller (eds.)]. Cambridge University
3661 Press, Cambridge, United Kingdom and New York, 996 pp.
- 3662
- 3663 **Iversen, J.**, 1944: *Viscum, Hedera* and *Ilex* as climatic indicators. A contribution to the study of
3664 past-glacial temperature climate. *Geologiska Foreningens Forhandlingar*, **66**, 463-483.
- 3665
- 3666 **Jacoby, G.C.** and R.D. D'Arrigo, 1995: Tree ring width and density evidence of climatic and
3667 potential forest change in Alaska. *Global Biogeochemical Cycles*, **9(2)**, 227-234.
- 3668
- 3669 **Jakobsson, M.**, and R. Macnab, 2006: A comparison between GEBCO sheet 5.17 and the
3670 International Bathymetric Chart of the Arctic Ocean (IBCAO) version 1.0. *Marine*
3671 *Geophysical Researches*, **27(1)**, 35-48.
- 3672
- 3673 **Jakobsson, M.**, R. Løvlie, H. Al-Hanbali, E. Arnold, J. Backman, and M. Mörth, 2000:
3674 Manganese color cycles in Arctic Ocean sediments constrain Pleistocene chronology.
3675 *Geology*, **28**, 23-26.
- 3676
- 3677 **Jansen, E.**, E. Bleil, R. Henrich, L. Kringstad, and B. Slettemark, B., 1988: Paleoenvironmental
3678 changes in the Norwegian Sea and the northeast atlantic during the last 2.8 m.y.: deep sea
3679 drilling project/ocean drilling program sites 610, 642, 643 and 644. *Paleoceanography*, **3**,
3680 563-581.
- 3681
- 3682 **Jansen, E.**, J. Overpeck, K.R. Briffa, J.-C. Duplessy, F. Joos, V. Masson-Delmotte, D. Olago, B.
3683 Otto-Bliesner, W.R. Peltier, S. Rahmstorf, R. Ramesh, D. Raynaud, D. Rind, O.
3684 Solomina, R. Villalba, and D. Zhang, 2007: Palaeoclimate. In: *Climate Change 2007—*
3685 *The Physical Science Basis. Contribution of Working Group I to the Fourth Assessment*
3686 *Report of the Intergovernmental Panel on Climate Change*, [Solomon, S., D. Qin, M.

SAP1.2 DRAFT 3 PUBLIC COMMENT

- 3687 Manning, Z. Chen, M. Marquis, K.B. Averyt, M. Tignor, and H.L. Miller (eds.)].
3688 Cambridge University Press, Cambridge, U.K., and New York.
3689
- 3690 **Jenkyns, H.C., A. Forster, S. Schouten, and J.S. Sinninghe Damsté, 2004: High temperatures in**
3691 **the Late Cretaceous Arctic Ocean. *Nature*, **432(7019)**, 888-892.**
3692
- 3693 **Jennings, A., K. Knudsen, M. Hald, C. Hansen, and J. Andrews, 2002: A mid-Holocene shift in**
3694 **Arctic sea-ice variability on the East Greenland Shelf. *The Holocene*, **12**, 49-58.**
3695
- 3696 **Jiang D., H. Wang, Z. Ding, X. Lang, H. Drange, 2005: Modeling the middle Pliocene climate**
3697 **with a global atmospheric general circulation model. *Journal of Geophysical Research*,**
3698 ***110*, D14107, doi:10.1029/2004JD005639.**
3699
- 3700 **Johnsen, S., H. Clausen, W. Dansgaard, K. Fuhrer, N. Gundestrup, C. Hammer, P. Iversen, J.**
3701 **Jouzel, B. Stauffer, and J. Steffensen, 1992: Irregular glacial interstadials recorded in a**
3702 **new Greenland ice core. *Nature*, **359**, 311-313.**
3703
- 3704 **Johnsen, S.J., D. Dahl-Jensen, W. Dansgaard, and N. Gundestrup, 1995: Greenland**
3705 **palaeotemperatures derived from GRIP bore hole temperature and ice core isotope**
3706 **profiles. *Tellus*, **47B**, 624-629.**
3707
- 3708 **Johnsen, S.J., W. Dansgaard, and J.W.C. White, 1989: The origin of Arctic precipitation under**
3709 **present and glacial conditions. *Tellus*, **41B**, 452-468.**
3710
- 3711 **Jones, P.D., K.R. Briffa, T.P. Barnett, and S.F.B. Tett, 1998: High-resolution palaeoclimatic**
3712 **records for the last millennium: interpretation, integration and comparison with General**
3713 **Circulation Model control-run temperatures. *Holocene*, **8**, 455-471.**
3714
- 3715 **Jouzel, J., V. Masson-Delmotte, O. Cattani, G. Dreyfus, S. Falourd, G. Hoffmann, B. Minster, J.**
3716 **Nouet, J. M. Barnola, J. Chappellaz, H. Fischer, J.C. Gallet, S. Johnsen, M. Leuenberger,**
3717 **L. Loulergue, D. Luethi, H. Oerter, F. Parrenin, G. Raisbeck, D. Raynaud, A. Schilt, J.**

SAP1.2 DRAFT 3 PUBLIC COMMENT

- 3718 Schwander, E. Selmo, R. Souchez, R. Spahni, B. Stauffer, J.P. Steffensen, B. Stenni, T.F.
3719 Stocker, J.L. Tison, M. Werner, and E.W. Wolff, 2007: Orbital and Millennial Antarctic
3720 Climate Variability over the Past 800,000 Years. *Science*, **317**, 793-796,
3721 doi:10.1126/science.1141038.
3722
- 3723 **Jouzel, J.**, R.B. Alley, K.M. Cuffey, W. Dansgaard, P. Grootes, G. Hoffmann, S.J. Johnsen, R.D.
3724 Koster, D. Peel, C.A. Shuman, M. Stievenard, M. Stuiver, and J. White, 1997: Validity of
3725 the temperature reconstruction from water isotopes in ice cores. *Journal of Geophysical*
3726 *Research*, **102**, 26471-26487.
3727
- 3728 **Joynt, E.H., III** and A.P. Wolfe, 2001: Paleoenvironmental inference models from sediment
3729 diatom assemblages in Baffin Island lakes (Nunavut, Canada) and reconstruction of
3730 summer water temperature. *Canadian Journal of Fisheries and Aquatic Sciences*, **58**,
3731 1222-1243.
3732
- 3733 **Kaakinen, A.** and M. Eronen, 2000: Holocene pollen stratigraphy indicating climatic and tree-
3734 line changes derived from a peat section at Ortino, in the Pechora lowland, northern
3735 Russia. *The Holocene*, **10**, 611-620.
3736
- 3737 **Kageyama, M.**, O. Peyron, S. Pinot, P. Tarasov, J. Guiot, S. Joussaume, and G. Ramstein, 2001:
3738 The Last Glacial Maximum climate over Europe and western Siberia: a PMIP
3739 comparison between models and data. *Climate Dynamics*, **17**, 23-43.
3740
- 3741 **Kandiano, E.S.** and H.A. Bauch, 2007: Phase relationship and surface water mass change in the
3742 Northeast Atlantic during Marine Isotope Stage 11 (MIS11). *Quaternary Research*,
3743 **68(3)**, 445-455
3744
- 3745 **Kaplan, J.O.**, N.H. Bigelow, P.J. Bartlein, T.R. Christiansen, W. Cramer, S.P. Harrison, N.V.
3746 Matveyeva, A.D. McGuire, D.F. Murray, I.C. Prentice, V.Y. Razzhivin, B. Smith, D.A.
3747 Walker, P.M. Anderson, A.A. Andreev, L.B. Brubaker, M.E. Edwards, A.V. Lozhkin,
3748 and J.C. Ritchie, 2003: Climate change and arctic ecosystems II—Modeling paleodata-

SAP1.2 DRAFT 3 PUBLIC COMMENT

- 3749 model comparisons, and future projections. *Journal of Geophysical Research*, **108(D19)**,
3750 8171, doi:10.1029/2002JD002559.
- 3751
- 3752 **Kaplan**, M.R. and A.P. Wolfe, 2006: Spatial and temporal variability of Holocene temperature
3753 trends in the North Atlantic sector. *Quaternary Research*, **65**, 223-231.
- 3754
- 3755 **Kapsner**, W.R., R.B. Alley, C.A. Shuman, S. Anandakrishnan, and P.M. Grootes, 1995:
3756 Dominant influence of atmospheric circulation on snow accumulation in Greenland over
3757 the past 18,000 years. *Nature*, **373**, 52-54.
- 3758
- 3759 **Karlén**, W., 1988: Scandinavian glacial and climate fluctuations during the Holocene.
3760 *Quaternary Science Reviews*, **7**, 199-209.
- 3761
- 3762 **Kaspar**, F., N. Kühl, U. Cubasch, and T. Litt, 2005: A model-data-comparison of European
3763 temperatures in the Eemian interglacial, *Geophysical Research Letters*, **32**, L11703,
3764 doi:10.1029/2005GL022456.
- 3765
- 3766 **Kaufman**, D.S., T.A. Ager, N.J. Anderson, P.M. Anderson, J.T. Andrew, P.J. Bartlein, L.B.
3767 Brubaker, L.L. Coats, L.C. Cwynar, M.L. Duvall, A.S. Dyke, M.E. Edwards, W.R.
3768 Eisner, K. Gajewski, A. Geirsdóttir, F.S. Hu, A.E. Jennings, M.R. Kaplan, M.W. Kerwin,
3769 A.V. Lozhkin, G.M. MacDonald, G.H. Miller, C.J. Mock, W.W. Oswald, B.L. Otto-
3770 Bliesver, D.F. Porinchu, K. Ruüland, J.P. Smol, E.J. Steig, and B.B. Wolfe, 2004:
3771 Holocene thermal maximum in the western Arctic (0–180°W). *Quaternary Science*
3772 *Reviews*, **23**, 529-560.
- 3773
- 3774 **Kaufman**, D.S. and J. Brigham-Grette, 1993: Aminostratigraphic correlations and
3775 paleotemperature implications, Pliocene-Pleistocene high sea level deposits, northwestern
3776 Alaska. *Quaternary Science Reviews*, **12**, 21-33.
- 3777
- 3778 **Kellogg**, T.B., 1977: Paleoclimatology and paleo-oceanography of the Norwegian and Greenland
3779 seas: the last 450,000 years. *Marine Micropaleontology*, **2**, 235-249.

SAP1.2 DRAFT 3 PUBLIC COMMENT

3780

3781 **Kerwin**, M., J.T. Overpeck, R.S. Webb, A. DeVernal, D.H. Rind and R.J. Healy, 1999: The role
3782 of oceanic forcing in mid-Holocene northern hemisphere climatic change.

3783 *Paleoceanography* **14**, 200-210.

3784

3785 **Kirk-Davidov**, D.B., D.P. Schrag, and J.G. Anderson, 2002: On the feedback of stratospheric
3786 clouds on polar climate. *Geophysical Research Letters*, **29(11)**, 1556.

3787

3788 **Kitoh**, A. and S. Murakami, 2002: Tropical Pacific Climate at the mid-Holocene and the Last
3789 Glacial Maximum simulated by a coupled ocean-atmosphere general circulation model,

3790 *Paleoceanography*, **17**, 1-13

3791

3792 **Knutson**, T.R., T.L. Delworth, K.W. Dixon, I.M. Held, J. Lu, V. Ramaswamy, M.D.

3793 Schwarzkopf, G. Stenchikov, and R.J. Stouffer, 2006: Assessment of twentieth-century
3794 regional surface temperature trends using the GFDL CM2 coupled models. *Journal of*

3795 *Climate*, **19(9)**, 1624-1651.

3796

3797 **Koç**, N. and E. Jansen, 1994: Response of the high-latitude Northern Hemisphere to climate
3798 forcing—Evidence from the Nordic Seas. *Geology*, **22**, 523-526.

3799

3800 **Koç**, N., E. Jansen, and H. Haflidason, 1993: Paleoceanographic reconstruction of surface
3801 ocean conditions in the Greenland, Iceland and Norwegian Seas through the last 14 ka

3802 based on diatoms. *Quaternary Science Reviews*, **12**, 115-140.

3803

3804 **Koerner**, R.M., 2005: Mass Balance of glaciers in the Queen Elizabeth Islands, Nunavut,
3805 Canada. *Annals of Glaciology*, **42(1)**, 417-423.

3806

3807 **Koerner**, R.M. and D.A. Fisher, 1990: A record of Holocene summer climate from a Canadian
3808 high-Arctic ice core. *Nature*, **343**, 630-631.

3809

3810 **Korhola**, A., H. Olander, and T. Blom, 2000: Cladoceran and chironomid assemblages as

SAP1.2 DRAFT 3 PUBLIC COMMENT

- 3811 quantitative indicators of water depth in sub-Arctic Fennoscandian lakes. *Journal of*
3812 *Paleolimnology*, **24**, 43-54.
- 3813
- 3814 **Korty**, R.L., K.A. Emanuel, and J.R. Scott, 2008: Tropical cyclone-induced upper-ocean mixing
3815 and climate: Application to equable climates. *Journal of Climate*, **21(4)**, 638-654.
- 3816
- 3817 **Kremenetski**, C.V., L.D. Sulerzhitsky, and R. Hantemirov, 1998: Holocene history of the
3818 northern range limits of some trees and shrubs in Russia. *Arctic and Alpine Research*, **30**,
3819 317-333.
- 3820
- 3821 **Kukla**, G.J., 2000: The last interglacial. *Science*, **287**, 987–988.
- 3822
- 3823 **Kump**, L.R. and D. Pollard, 2008: Amplification of Cretaceous Warmth by Biological Cloud
3824 Feedbacks. *Science*, **11,(5873)**, 195, doi:10.1126/science.1153883.
- 3825
- 3826 **Kvenvolden**, K.A., 1988: Methane hydrate—a major reservoir of carbon in the shallow
3827 geosphere? *Chemical Geology*, **71**, 41–51.
- 3828
- 3829 **Kvenvolden**, K.A., 1993: A primer on gas hydrates. In: *The Future of Energy Gases*, [Howel,
3830 D.G. (Ed)]. U.S. Geological Survey Professional Paper 1570, pp. 279-291.
- 3831
- 3832 **Lamb**, H.H., 1977: *Climate History and the Future. Climate—Past, Present and Future*.
3833 Methuen, London, vol. 2, 835 pp.
- 3834
- 3835 **Lambeck**, K., Y. Yokoyama, and T. Purcell, 2002: Into and out of the Last Glacial Maximum:
3836 sea-level change during oxygen isotope stages 3 and 2. *Quaternary Science Reviews*, **21**,
3837 343-360.
- 3838
- 3839 **Larocque**, I. and R.I. Hall, 2004: Holocene temperature estimates and chironomid community
3840 composition in the Abisko Valley, northern Sweden. *Quaternary Science Reviews*, **23**,
3841 2453-2465.

3842

3843 **Lauritzen**, S.-E., 1996: Calibration of speleothem stable isotopes against historical records: a
3844 Holocene temperature curve for north Norway?. In: *Climatic Change: the Karst Record*
3845 [Lauritzen, S.-E. (Ed.)] Vol. 2 Karst Waters Institute Special Publication, Charles Town,
3846 West Virginia, pp. 78-80.

3847

3848 **Lauritzen**, S.E. and J. Lundberg, 1998: Rapid temperature variations and volcanic events during
3849 the Holocene from a Norwegian speleothem record. Past Global Changes and their
3850 Significance for the Future. Volume of Abstracts, IGBP-PAGES, Bern 00, p. 88.

3851

3852 **LeGrande**, A.N., and G.A. Schmidt, 2006: Global gridded data set of the oxygen isotopic
3853 composition in seawater. *Geophysical. Research Letters*, **33**, L12604,
3854 doi:10.1029/2006GL026011.

3855

3856 **Lemke**, P., J. Ren, R.B. Alley, I. Allison, J. Carrasco, G. Flato, Y. Fujii, G. Kaser, P. Mote, R.H.
3857 Thomas, and T. Zhang, 2007: Observations: Changes in Snow, Ice and Frozen Ground.
3858 In: *Climate Change 2007: The Physical Science Basis— Contribution of Working Group*
3859 *I to the Fourth Assessment Report of the Intergovernmental Panel on Climate Change*,
3860 [Solomon, S., D. Qin, M. Manning, Z. Chen, M. Marquis, K.B. Averyt, M. Tignor and
3861 H.L. Miller (eds.)]. Cambridge University Press, Cambridge and New York, 996 pp.

3862

3863 **Leng**, M.J. and J.D. Marshall, 2004: Palaeoclimate interpretation of stable isotope data from lake
3864 sediment archives. *Quaternary Science Reviews*, **23**, 811-831.

3865

3866 **Levac**, E., A. de Vernal, and W.J. Blake, 2001: Sea-surface conditions in northernmost Baffin
3867 Bay during the Holocene—Palynological evidence. *Journal of Quaternary Science*, **16**,
3868 353-363.

3869

3870 **Levy**, L.B., D.S. Kaufman, and A. Werner, 2003: Holocene glacier fluctuations, Waskey Lake,
3871 northeastern Ahklun Mountains, southwestern Alaska. *Holocene*, **14**, 185-193.

3872

SAP1.2 DRAFT 3 PUBLIC COMMENT

- 3873 **Ling**, F. and T.J. Zhang, 2007: Modeled impacts of changes in tundra snow thickness on ground
3874 thermal regime and heat flow to the atmosphere in Northernmost Alaska. *Global and*
3875 *Planetary Change* **57(3-4)**, 235-246.
- 3876
- 3877 **Lisiecki**, L.E. and M.E. Raymo, 2005: A Pliocene-Pleistocene stack of 57 globally distributed
3878 benthic d¹⁸O records. *Paleoceanography*, **20**, PA1003, doi:10.1029/2004PA001071.
- 3879
- 3880 **Lisiecki**, L.E. and M.E. Raymo, 2007: Plio-Pleistocene climate evolution—Trends and
3881 transitions in glacial cycle dynamics. *Quaternary Science Reviews*, **26**, 56-69.
- 3882
- 3883 **Loutre**, M.F., 2003: Clues from MIS 11 to predict the future climate – a modeling point of view.
3884 *Earth and Planetary Science Letters*, **212(1-2)**, 213-224
- 3885
- 3886 **Lozhkin**, A.V. and P.M. Anderson, 1995: The last interglaciation of northeast Siberia.
3887 *Quaternary Research*, **43**, 147-158.
- 3888
- 3889 **Lozhkin**, A.V. and P.M. Anderson, 1996: A late Quaternary pollen record from Elikchan 4 Lake,
3890 northeast Siberia. *Geology of the Pacific Ocean*, **12**, 6-9-616.
- 3891
- 3892 **Lozhkin**, A.V., P.M. Anderson, W.R. Eisner, L.G. Ravako, D.M. Hopkins, L.B. Brubaker, P.A.
3893 Colinvaux, and M.C. Miller, 1993: Late Quaternary lacustrine pollen records from
3894 southwestern Beringia. *Quaternary Research*, **9**, 314-324.
- 3895
- 3896 **Lozhkin**, A.V., P.M. Anderson, T.V. Matrosova, and P.S. Minyuk, 2007: The pollen record from
3897 El'gygytgyn Lake: implications for vegetation and climate histories of northern Chukotka
3898 since the late middle Pleistocene. *Journal of Paleolimnology*, **37(1)**, 135-153.
- 3899
- 3900 **Lubinski**, D.J., S.L. Forman, and G.H. Miller, 1999: Holocene glacier and climate fluctuations
3901 on Franz Josef Land, Arctic Russia, 80°N. *Quaternary Science Reviews*, **18**, 85-108.
- 3902
- 3903 **Luckman**, B.H., 2007: Dendroclimatology. In: *Encyclopedia of Quaternary Science* [Elias, S.

SAP1.2 DRAFT 3 PUBLIC COMMENT

3904 (ed.)] **1**, 465-475.

3905

3906 **MacDonald, G.J.**, 1990: Role of methane clathrates in past and future climates. *Climatic*
3907 *Change*, **16(3)** 247-281.

3908

3909 **MacDonald, G.M.**, T. Edwards, K. Moser, and R. Pienitz, 1993: Rapid response of treeline
3910 vegetation and lakes to past climate warming. *Nature*, **361**, 243-246.

3911

3912 **MacDonald, G.M.**, B.R. Gervais, J.A. Snyder, G.A. Tarasov, and O.K. Borisova, 2000a:
3913 Radiocarbon dated *Pinus sylvestris* L. wood from beyond treeline on the Kola Peninsula,
3914 Russia. *The Holocene*, **10**, 143-147.

3915

3916 **MacDonald, G.M.**, K.V. Kremenetski, and D.W. Beilman, D.W., 2007: Climate change and the
3917 northern Russian treeline zone. *Philosophical Transactions of the Royal Society B*,
3918 doi:10.1098/rstb.2007.2200.

3919

3920 **MacDonald, G.M.**, A.A. Velichko, C.V. Kremenetski, O.K. Borisova, A.A. Goleva, A.A.
3921 Andreev, L.C. Cwynar, R.T. Riding, S.L. Forman, T.W.D. Edwards, R. Aravena, D.
3922 Hammarlund, J.M. Szeicz, and V.N. Gattaulin, 2000b: Holocene treeline history and
3923 climate change across northern Eurasia. *Quaternary Research*, **53**, 302-311.

3924

3925 **Macdonald, R.W.** and J.M. Bowers, 1996: Contaminants in the arctic marine environment:
3926 priorities for protection. *ICES Journal of Marine Science*, **53**, 537-563.

3927

3928 **Mahowald, N. M.**, D. R. Muhs, S. Levis, P. J Rasch, M. Yoshioka, C. S. Zender, and C. Luo,
3929 2006: Change in atmospheric mineral aerosols in response to climate: Last glacial period,
3930 preindustrial, modern, and doubled carbon dioxide climates, *ournal of Geophysical*
3931 *Research*, **111**, D10202, doi:10.1029/2005JD006653

3932

3933 **Manabe, S.** and R.J. Stouffer, 1980: Sensitivity of a global climate model to an increase of CO₂
3934 in the atmosphere. *Journal of Geophysical Research*, **85(C10)**, 5529-5554.

SAP1.2 DRAFT 3 PUBLIC COMMENT

3935

3936 **Mann**, M.E., R.S. Bradley, and M.K. Hughes, 1998: Global-scale temperature patterns and
3937 climate forcing over the past six centuries. *Nature*, **392**, 779-787.

3938

3939 **Mann**, D.H., D.M. Peteet, R.E. Reanier, and M.L. Kunz, 2002: Responses of an arctic landscape
3940 to Late glacial and early Holocene climatic changes: The importance of moisture:
3941 *Quaternary Science Reviews*, **21**, 997-1021, doi: 10.1016/S0277-3791(01)00116-0.

3942

3943 **Mann**, M.E., and P.D. Jones, 2003: Global surface temperatures over the past two millennia.
3944 *Geophysical Research Letters*, **30(15)**, 1820, doi:10.1029/2003GL017814

3945

3946 **Mann**, M.E., A. Zhang, M.K. Hughes, R.S. Bradley, S.K. Miller, S. Rutherford, and S. Ni, F., **in**
3947 **press**: Proxy-based Reconstructions of Hemispheric and Global Surface Temperature
3948 Variations over the past Two Millennia. *Proceedings of the National Academy of*
3949 *Sciences*.

3950

3951 **Marchant**, D.R., and G.H. Denton, 1996: Miocene and Pliocene paleoclimate of the Dry Valleys
3952 region, southern Victoria Land: A geomorphological approach. *Marine*
3953 *Micropaleontology*, **27**, 253-271.

3954

3955 **Marincovitch**, L., Jr. and A.Y. Gladenkov, 2000: New evidence for the age of Bering Strait.
3956 *Quaternary Science Reviews*, **20(1-3)**, 329-335.

3957

3958 **Marlowe** I.T., J.C. Green, A.C. Neal, S.C. Brassell, G. Eglinton, P.A. Course, 1984: Long-chain
3959 (N-C37-C39) alkenones in the prymnesiophyceae - distribution of alkenones and other
3960 lipids and their taxonomic significance. *British Phycological Journal*, **19(3)**, 203-216.

3961

3962 **Marotzke**, J., 2000: Abrupt climate change and thermohaline circulation—Mechanisms and
3963 predictability. *Proceedings of the National Academy of Sciences, U.S.A.*, **97(4)**, 1347-
3964 1350.

3965

SAP1.2 DRAFT 3 PUBLIC COMMENT

- 3966 **Marshall**, S.J. and P.U. Clark, 2002: Basal temperature evolution of North American ice sheets
3967 and implications for the 100-kyr cycle. *Geophysical Research Letters*, **29(24)**, 2214.
3968
- 3969 **Martinson**, D.G. and M. Steele, 2001: Future of the Arctic sea ice cover—Implications of an
3970 Antarctic analog. *Geophysical Research Letters*, **28**, 307-310.
3971
- 3972 **Masson-Delmotte**, V., J. Jouzel, A. Landais, M. Stievenard, S.J. Johnsen, J.W.C. White, M.A.
3973 Werner, A. Sveinbjornsdottir, and K. Fuhrer, 2005: GRIP deuterium excess reveals rapid
3974 and orbital-scale changes in Greenland moisture origin. *Science*, **309**, 118-121.
3975
- 3976 **Mathieu**, R., D. Pollard, J.E. Cole, J.W.C. White, R.S. Webb, and S.L. Thompson, 2002:
3977 Simulation of stable water isotope variations by the GENESIS GCM for modern
3978 conditions. *Journal of Geophysical Research*, **107**, doi:10.1029/2001JD900255.
3979
- 3980 **Matthews**, J.V., Jr., C.E. Schweger, and J. Janssens, 1990: The last (Koy-Yukon) interglaciation
3981 in the northern Yukon—Evidence from unit 4 at Chijee's Bluff, Bluefish Basin.
3982 *Geographie physique et Quaternaire*, **44**, 341-362.
3983
- 3984 **Mayewski**, P.A., L.D. Meeker, M.S. Twickler, S.I. Whitlow, Q. Yang, W.B. Lyons, and M.
3985 Prentice, 1997: Major features and forcing of high-latitude Northern Hemisphere
3986 atmospheric circulation using a 110,000-year-long glaciochemical series. *Journal of*
3987 *Geophysical Research*, **102**, 26,345-26,366.
3988
- 3989 **Maximova**, L.N. and V.E. Romanovsky, 1988: A hypothesis of the Holocene permafrost
3990 evolution. *Proceedings of the Fifth International Conference on Permafrost*, Norwegian
3991 Institute of Technology, Trondheim, Norway, 102-106.
3992
- 3993 **McGhee**, R., 2004: *The last imaginary place; a human history of the Arctic world*. Key Porter,
3994 Ontario, 296 pp.
3995

SAP1.2 DRAFT 3 PUBLIC COMMENT

- 3996 **McKenna**, M.C., 1980. Eocene paleolatitude, climate and mammals of Ellesmere Island.
3997 *Paleogeography, Paleoclimatology and Paleoecology*, **30**, 349-362.
3998
- 3999 **McLaughlin**, F., E. Carmack, R. Macdonald, A.J. Weaver, and J. Smith, 2002: The Canada
4000 Basin, 1989–1995—Upstream events and far-field effects of the Barents Sea. *Journal of*
4001 *Geophysical Research*, **107(C7)**, 3082, doi:10.1029/2001JC000904.
4002
- 4003 **McManus**, J.F., 2004: A great grand-daddy of ice cores. *Nature*, **429**, 611-612.
4004
- 4005 **Meehl**, G.A., T.F. Stocker, W.D. Collins, P. Friedlingstein, A.T. Gaye, J.M. Gregory, A. Kitoh,
4006 R. Knutti, J.M. Murphy, A. Noda, S.C.B. Raper, I.G. Watterson, A.J. Weaver and Z.-C.
4007 Zhao, 2007: Global Climate Projections. In: *Climate Change 2007: The Physical Science*
4008 *Basis — Contribution of Working Group I to the Fourth Assessment Report of the*
4009 *Intergovernmental Panel on Climate Change*, [Solomon, S., D. Qin, M. Manning, Z.
4010 Chen, M. Marquis, K.B. Averyt, M. Tignor and H.L. Miller (eds.)]. Cambridge
4011 University Press, Cambridge, United Kingdom and New York, pp. 747-845.
4012
- 4013 **Meeker**, L.D. and P.A. Mayewski, 2002: A 1400-year high-resolution record of atmospheric
4014 circulation over the North Atlantic and Asia. *Holocene*, **12**, 257-266.
4015
- 4016 **Meier**, M.F., M.B. Dyurgerov, U.K. Rick, S. O'Neel, W.T. Pfeffer, R.S. Anderson, S.P.
4017 Anderson, and A.F. Glazovsky, 2007: Glaciers Dominate Eustatic Sea-Level Rise in the
4018 21st Century. *Science*, **317(5841)**, 1064-1067 doi: 10.1126/science.1143906
4019
- 4020 **Miller**, G.H., A.P. Wolfe, J.P. Briner, P.E. Sauer, and A. Nesje, 2005: Holocene glaciation and
4021 climate evolution of Baffin Island, Arctic Canada. *Quaternary Science Reviews*, **24**,
4022 1703-1721.
4023
- 4024 **Moberg**, A., D.M. Sonechkin, K. Holmgren, N.M. Datsenko, and W. Karlen, 2005: Highly
4025 variable northern hemisphere temperatures reconstructed from low- and high-resolution
4026 proxy data. *Nature*, **433**, 613-617.

SAP1.2 DRAFT 3 PUBLIC COMMENT

- 4027
- 4028 **Montoya, M., H. von Storch, and T.J. Crowley, 2000:** Climate Simulation for 125 kyr BP with a
4029 Coupled Ocean–Atmosphere General Circulation Model. *Journal of Climate*, **13**, 1057-
4030 1072.
- 4031
- 4032 **Moran, K., J. Backman, H. Brinkhuis, S.C. Clemens, T. Cronin, G.R. Dickens, F. Eynaud, J.**
4033 **Gattacceca, M. Jakobsson, R.W. Jordan, M. Kaminski, J. King, N. Koc, A. Krylov, N.**
4034 **Martinez, J. Matthiessen, D. McInroy, T.C. Moore, J. Onodera, M. O’Regan, H. Palike,**
4035 **B. Rea, D. Rio, T. Sakamoto, D.C. Smith, R. Stein, K. St. John, I. Suto, N. Suzuki, K.**
4036 **Takahashi, M. Watanabe, M. Yamamoto, J. Farrell, M. Frank, P. Kubik, W. Jokat, and Y.**
4037 **Kristoffersen, 2006:** The Cenozoic palaeoenvironment of the Arctic Ocean. *Nature*, **441**,
4038 601-605.
- 4039
- 4040 **Morison, J., K. Aagaard, and M. Steele, 2000:** Recent environmental changes in the arctic.
4041 *Arctic*, **53(4)**, 359-371.
- 4042
- 4043 **Muhs, D.R. and J.R. Budahn, 2006:** Geochemical evidence for the origin of late Quaternary
4044 loess in central Alaska. *Canadian Journal of Earth Science*, **43**, 323-337
- 4045
- 4046 **Muller, P.J., G. Kirst, G. Ruhland, I. von Storch, and A. Rossell-Mele, 1998:** Calibration of the
4047 alkenone paleotemperature index Uk³⁷ based on core-tops from the eastern South
4048 Atlantic and the global ocean (60°N–60°S). *Geochimica et Cosmochimica Acta*, **62**,
4049 1757-1772.
- 4050
- 4051 **National Research Council, 2006:** *Surface temperature reconstructions for the last 2,000 years.*
4052 National Academies Press, Washington, DC. 160pp.
- 4053
- 4054 **Naurzbaev, M.M., E.A. Vaganov, O.V. Sidorova, and F.H. Schweingruber, 2002:** Summer
4055 temperatures in eastern Taimyr inferred from a 2427-year late-Holocene tree-ring
4056 chronology and earlier floating series. *The Holocene*, **12**, 727-736.
- 4057

SAP1.2 DRAFT 3 PUBLIC COMMENT

- 4058 **Nelson, R.E.**, and Carter, L.D. 1991. Preliminary interpretation of vegetation and paleoclimate in
4059 northern Alaska during the late Pliocene Colvillian marine transgression. In: *Geologic*
4060 *studies in Alaska*, [Bradley, D.C. and A.B. Ford (eds.)]. U.S.Geological Survey Bulletin
4061 1999, pp. 219-222.
- 4062
- 4063 **Nesje, A.**, J. Bakke, S.O. Dahl, O. Lie, and J.A. Matthews, 2008: Norwegian mountain glaciers
4064 in the past, present and future. *Global and Planetary Change*, **60**, 10-27.
- 4065
- 4066 **Nesje, A.** , J.A. Matthews, S.O. Dahl, M.S. Berrisford, and C. Andersson, 2001: Holocene
4067 glacier fluctuations of Flatebreen and winter precipitation changes in the Jostedalbreen
4068 region, western Norway, based on glaciolacustrine records. *The Holocene*, **11**, 267-280.
- 4069
- 4070 **Nørgaard-Pedersen, N.**, N. Mikkelsen, and Y. Kristoffersen, 2007a: Arctic Ocean record of last
4071 two glacial-interglacial cycles off North Greenland/Ellesmere Island—Implications for
4072 glacial history. *Marine Geology*, **244(2007)**, 93-108.
- 4073
- 4074 **Nørgaard-Pedersen, N.**, N. Mikkelsen, S.J. Lassen, Y. Kristoffersen, and E. Sheldon, 2007b:
4075 Reduced sea ice concentrations in the Arctic Ocean during the last interglacial period
4076 revealed by sediment cores off northern Greenland. *Paleoceanography*, **22**, PA1218,
4077 doi:10.1029/2006PA001283.
- 4078
- 4079 **Nørgaard-Pedersen, N.**, R.F. Spielhagen, H. Erlenkeuser, P.M. Grootes, J. Heinemeier, and J.
4080 Knies, 2003: The Arctic Ocean during the Last Glacial Maximum—Atlantic and polar
4081 domains of surface water mass distribution and ice cover. *Paleoceanography*, **18**, 8-1 to
4082 8-19.
- 4083
- 4084 **Nørgaard-Pedersen, N.**, R.F. Spielhagen, J. Thiede, and H. Kassens, 1998: Central Arctic
4085 surface ocean environment during the past 80,000 years. *Paleoceanography*, **13**, 193-204.
- 4086
- 4087 **Nürnberg, D.** and R. Tiedemann, 2004: Environmental changes in the Sea of Okhotsk during the
4088 last 1.1 million years. *Paleoceanography*, **19**, PA4011.

SAP1.2 DRAFT 3 PUBLIC COMMENT

- 4089
- 4090 **O'Brien**, S.R., P.A. Mayewski, L.D. Meeker, D.A. Meese, M.S. Twickler, and S.I. Whitlow,
4091 1995: Complexity of Holocene climate as reconstructed from a Greenland ice core.
4092 *Science*, **270**, 1962-1964.
- 4093
- 4094 **Obata**, A., 2007: Climate-carbon cycle model response to freshwater discharge into the
4095 North Atlantic. *Journal of Climate*, **20(24)** 5962-5976.
- 4096
- 4097 **Ogilvie**, A.E.J. and T. Jónsson, 2001: "Little Ice Age" Research: A Perspective from Iceland.
4098 *Climate Change*, **48**, 9-52.
- 4099
- 4100 **Ogilvie**, A.E.J. and I. Jónsdóttir, 2000. Sea ice, climate and Icelandic fisheries in historical times.
4101 *Arctic*, **53(4)**, 383-394.
- 4102
- 4103 **Ohkouchi**, N., T.I. Eglinton, L.D. Keigwin, and J.M. Hayes, 2002: Spatial and temporal offsets
4104 between proxy records in a sediment drift. *Science*, **298**, 1224-1227.
- 4105
- 4106 **Oswald**, W.W., L.B. Brubaker, and P.M. Anderson, 1999, Late Quaternary vegetational history
4107 of the Howard Pass area, northwestern Alaska. *Canadian Journal of Botany*, **77(4)**, 570-
4108 581
- 4109
- 4110 **Oswald**, W.W., L.B. Brubaker, F.S. Hu, and G.W. Kling, 2003: Holocene pollen records from
4111 the central Arctic Foothills, northern Alaska—Testing the role of substrate in the
4112 response of tundra to climate change. *Journal of Ecology*, **91**, 1034-1048
- 4113
- 4114 **Otto-Bliesner**, B.L., C.D. Hewitt, T.M. Marchitto, E. Brady, A. Abe-Ouchi, M. Crucifix, S.
4115 Murakami, and S.L. Weber, 2007: Last Glacial Maximum ocean thermohaline
4116 circulation: PMIP2model inter-comparisons and data constraints. *Geophysical Research*
4117 *Letters*, **34**, L12706, doi:10.1029/2007GL029475.
- 4118

SAP1.2 DRAFT 3 PUBLIC COMMENT

- 4119 **Otto-Bliesner**, B.L., S.J. Marshall, J.T. Overpeck, G.H. Miller, A. Hu, and CAPE Last
4120 Interglacial Project members, 2006, Simulating Arctic climate warmth and icefield retreat
4121 in the Last Interglaciatiion. *Science*, **311**, 1751-1753, doi:10.1126/science.1120808
4122
- 4123 **Overpeck**, J., K. Hughen, D. Hardy, R. Bradley, R. Case, M. Douglas, B. Finney, K. Gajewski,
4124 C. Jacoby, A. Jennings, S. Lamoureux, A. Lasca, G. MacDonald, J. Moore, M. Retelle, S.
4125 Smith, A. Wolfe, and G. Zielinski, 1997: Arctic environmental change of the last four
4126 centuries. *Science*, **278**, 1251-1256.
4127
- 4128 **Pagani**, M., K. Caldeira, D. Archer, and J.C. Zachos, 2006: An Ancient Carbon Mystery.
4129 *Science*, **314**, 1556 - 1557 doi: 10.1126/science.1136110
- 4130 **Pearson**, P.N., B.E. van Dongen, C.J. Nicholas, R.D. Pancost, S. Schouten, J.M. Singano, and
4131 B.S. Wade, 2007: Stable warm tropical climate through the Eocene Epoch. *Geology*, **35**,
4132 211-214.
4133
- 4134 **Peterson**, B.J., R.M. Holmes, J.W. McClelland, C.J. Vorosmarty, R.B. Lammers, A.I.
4135 Shiklomanov, I.A. Shiklomanov, and S. Rahmstorf, 2002: Increasing river discharge to
4136 the Arctic Ocean. *Science*, **298**, 2171-2173.
4137
- 4138 **Peterson**, B.J., J. McClelland, R. Murry, R.M. Holmes, J.E. Walsh, and K. Aagaard, 2006:
4139 Trajectory shifts in the Arctic and subarctic freshwater cycle. *Science*, **313**, 1061-1066.
4140
- 4141 **Pienitz**, R., M.S.V. Douglas, and J.P. Smol (eds.), 2004: *Long-Term Environmental Change in*
4142 *Arctic and Antarctic Lakes*. Dordrecht, Germany: Springer, 579 pp.
4143
- 4144 **Pienitz**, R. and J.P. Smol, 1993: Diatom assemblages and their relationship to environmental
4145 variables in lakes from the boreal forest-tundra ecotone near Yellowknife, Northwest-
4146 Territories, Canada. *Hydrobiologia*, **269**, 391-404.
4147
- 4148 **Pienitz**, R., J.P. Smol, W.M. Last, P.R. Leavitt, and B.F. Cumming, 2000: Multi-proxy Holocene

SAP1.2 DRAFT 3 PUBLIC COMMENT

- 4149 palaeoclimatic record from a saline lake in the Canadian Subarctic. *The Holocene*, **10(6)**,
4150 673-686 doi:10.1191/09596830094935
4151
- 4152 **Pierrehumbert**, R.T., H. Brogniez, and R. Roca, 2007: On the relative humidity of the
4153 atmosphere. In: *The Global Circulation of the Atmosphere* [Schneider, T. and A. Sobel
4154 (eds.)]. Princeton University Press, Princeton, New Jersey, pp.143-185.
4155
- 4156 **Peixoto**, J.P. and A.H. Oort, 1992: *Physics of Climate*. American Institute of Physics, New York,
4157 520 pp.
4158
- 4159 **Pinot**, S., G. Ramstein, S.P. Harrison, I.C. Prentice, J. Guiot, M. Stute. and S. Joussaume, 1999:
4160 Tropical paleoclimates of the Last Glacial Maximum: comparison of Paleoclimate
4161 Modelling Intercomparison Project (PMIP) simulations and paleodata. *Climate*
4162 *Dynamics*, **15**, 857-874.
4163
- 4164 **Pisaric**, M.F J., G.M. MacDonald, A.A Velichko, and L.C. Cwynar, 2001: The late-glacial and
4165 post-glacial vegetation history of the northwestern limits of Beringia, from pollen,
4166 stomates and tree stump evidence. *Quaternary Science Reviews*, **20**, 235-245.
4167
- 4168 **Pollard**, D. and S.L. Thompson, 1997: Climate and ice-sheet mass balance at the Last Glacial
4169 Maximum from the GENESIS Version 2 global climate model. *Quaternary Science*
4170 *Reviews*, **16**, 841-864
4171
- 4172 **Polyak**, L., W.B. Curry, D.A. Darby, J. Bischof, and T.M. Cronin, 2004: Contrasting
4173 glacial/interglacial regimes in the western Arctic Ocean as exemplified by a sedimentary
4174 record from the Mendeleev Ridge. *Palaeogeography, Palaeoclimatology, Palaeoecology*,
4175 **203**, 73-93.
4176
- 4177 **Porter**, S.C. and G.H. Denton, 1967: Chronology of neoglaciation. *American Journal of Science*,
4178 **165**, 177-210.
4179

SAP1.2 DRAFT 3 PUBLIC COMMENT

- 4180 **Poulsen, C.J., E.J. Barron, W.H. Peterson, and P.A. Wilson, 1999:** A reinterpretation of mid-
4181 Cretaceous shallow marine temperatures through model-data comparison.
4182 *Paleoceanography*, **14(6)** 679-697.
- 4183
- 4184 **Prahl, F.G., G.J. de Lange, M. Lyle, and M.A. Sparrow, 1989:** Post-depositional stability of
4185 long-chain alkenones under contrasting redox conditions. *Nature*, **341**, 434-437.
- 4186
- 4187 **Prahl, F.G., L.A. Muelhausen, and D.L. Zahnle, 1988:** Further evaluation of long-chain
4188 alkenones as indicators of paleoceanographic conditions. *Geochimica et Cosmochimica*
4189 *Acta*, **52**, 2303-2310.
- 4190
- 4191 **Prentice, I.C. and T. Webb III, 1998:** BIOME 6000—Reconstructing global mid-Holocene
4192 vegetation patterns from palaeoecological records. *Journal of Biogeography*, **25**, 997-
4193 1005.
- 4194
- 4195 **Rahmstorf, S., 1996:** On the freshwater forcing and transport of the Atlantic thermohaline
4196 circulation. *Climate Dynamics*, **12**, 799-811.
- 4197
- 4198 **Rahmstorf, S., 2002:** Ocean circulation and climate during the past 120,000 years. *Nature*, **419**,
4199 207-214.
- 4200
- 4201 **Rasmussen, S.O., K.K. Andersen, A.M. Svensson, J.P. Steffensen, B.M. Vinther, H.B. Clausen,**
4202 **M.L. Siggaard-Andersen, S.J. Johnsen, L.B. Larsen, D. Dahl-Jensen, M. Bigler, R.**
4203 **Rothlisberger, H. Fischer, K. Goto-Azuma, M.E. Hansson, and U. Ruth, 2006:** A new
4204 Greenland ice core chronology for the last glacial termination. *Journal of Geophysical*
4205 *Research*, **111**, D061202, doi:10.1029/2005JD006079.
- 4206
- 4207 **Raymo, M.E., 1994:** The initiation of northern hemisphere glaciation. *Annual Review of Earth*
4208 *and Planetary Sciences*, **22**, 353-383, doi:10.1146/annurev.ea.22.050194.002033
- 4209
- 4210 **Raymo, M. E., 1997:** The timing of major climate terminations, *Paleoceanography*, **12**, 577-585.

SAP1.2 DRAFT 3 PUBLIC COMMENT

- 4211
4212 **Raymo, M.E., B. Grant, M. Horowitz, and G.H. Rau, 1996:** Mid-Pliocene warmth—Stronger
4213 greenhouse and stronger conveyor. *Marine Micropaleontology*, **27**, 313-326.
4214
- 4215 **Raymo, M.E., L.E. Lisiecki, and K.H. Nisancioglu, 2006:** Plio-Pleistocene ice volume, Antarctic
4216 climate, and the global $\delta^{18}\text{O}$ record. *Science*, **313**, 492-495.
4217
- 4218 **Raymo, M.E., D.W. Oppo, and W. Curry, 1997:** The mid-Pleistocene climate transition: A deep
4219 sea carbon isotopic perspective: *Paleoceanography*, **12**, 546-559.
4220
- 4221 **Renssen, H., E. Driesschaert, M.F. Loutre, and T. Fichefet, 2006:** On the importance of initial
4222 conditions for simulations of the Mid-Holocene climate. *Climate of the Past*, **2**, 91-97.
4223
- 4224 **Renssen, H., H. Goosse, T. Fichefet, V. Brovkin, E. Dresschaert, and F. Wolk, 2005:** Simulating
4225 the Holocene climate evolution at northern high latitudes using a coupled atmosphere–sea
4226 ice–ocean–vegetation model. *Climate Dynamics*, **24**, 23-43.
4227
- 4228 **Reyes, A.V., G.C. Wiles, D.J. Smith, D.J. Barclay, S. Allen, S. Jackson, S. Larocque, S. Laxton,**
4229 **D. Lewis, P.E. Calkin, and J.J. Clague, 2006:** Expansion of alpine glaciers in Pacific
4230 North America in the first millennium A.D. *Geology*, **34**, 57-60.
4231
- 4232 **Rignot, E. and R.H. Thomas, 2002:** Mass balance of polar ice sheets. *Science* **297**, 1502-1506.
4233
- 4234 **Rigor, I.G. and J.M. Wallace, 2004:** Variations in the age of Arctic sea-ice and summer sea-ice
4235 extent. *Geophysical Research Letters*, **31**, L09401, doi:10.1029/2004GL019492.
4236
- 4237 **Rimbu, N., G. Lohmann, and K. Grosfeld, 2007:** Northern Hemisphere atmospheric blocking in
4238 ice core accumulation records from northern Greenland. *Geophysical Research Letters*,
4239 **34**, L09704, doi:10.1029/2006GL029175.
4240
- 4241 **Ritchie, J.C., 1984:** *Past and Present Vegetation of the Far Northwest of Canada*. University of

SAP1.2 DRAFT 3 PUBLIC COMMENT

4242 Toronto Press, Toronto, 251 pp.

4243

4244 **Ritchie, J.C., L.C. Cwynar, and R.W. Spear, 1983: Evidence from northwest Canada for an early**
4245 **Holocene Milankovitch thermal maximum. *Nature*, **305**, 126-128.**

4246

4247 **Rivers, A.R., and A.H. Lynch, 2004: On the influence of land cover on early Holocene climate**
4248 **in northern latitudes. *Journal of Geophysical Research-Atmospheres*, **109(D21)**, D21114.**

4249

4250 **Roe, G.H. and M.R. Allen, 1999: A comparison of competing explanations for the 100,000-yr**
4251 **ice age cycle. *Geophysical Research Letters*, **26(15)**, 2259-2262.**

4252

4253 **Rosell-Mele, A. and P. Comes, 1999: Evidence for a warm Last Glacial Maximum in the Nordic**
4254 **sea or an example of shortcomings in Uk37 δ and Uk37 to estimate low sea surface**
4255 **temperature? *Paleoceanography*, **14**, 770-776.**

4256

4257 **Rosell-Mele, A., G. Eglinton, U. Pflaumann, and M. Sarnthein, 1995: Atlantic core top**
4258 **calibration of the Uk37 index as a sea-surface temperature indicator. *Geochimica et***
4259 ***Cosmochimica Acta*, **59**, 3099-3107.**

4260

4261 **Royer, D.L., 2006: CO₂-forced climate thresholds during the Phanerozoic. *Geochimica et***
4262 ***Cosmochimica Acta*, **70(23)**, 5665-5675.**

4263

4264 **Royer, D.L., R.A. Berner, and J. Park, 2007: Climate sensitivity constrained by CO₂**
4265 **concentrations over the past 420 million years. *Nature*, **446**, 530-532.**

4266

4267 **Ruddiman, W.F., 2003: Insolation, Ice Sheets and Greenhouse Gases. *Quaternary Science***
4268 ***Reviews*, **22**, 1597.**

4269

4270 **Ruddiman, W.F., 2006: Ice-driven CO₂ feedback on ice volume. *Climate of the Past*, **2**, 43-55.**

4271

4272 **Ruddiman, W.F., N.J. Shackleton, and A. McIntyre, 1986: North Atlantic sea-surface**

SAP1.2 DRAFT 3 PUBLIC COMMENT

4273 temperatures for the last 1.1 million years. In: *North Atlantic Paleoceanography*,
4274 [Summerhayes, C.P. and N.J. Shackleton, (eds.)]. Geological Society of London, Special
4275 Publication, **21**, 155-173.

4276

4277 **Rudels, B., L.G. Anderson, E.P. Jones, and G. Kattner, 1996:** Formation and evolution of the
4278 surface mixed layer and halocline of the Arctic Ocean. *Journal of Geophysical Research*,
4279 **101**, 8807-8821.

4280

4281 **Rühland, K., A. Priesnitz, and J.P. Smol, 2003:** Evidence for recent environmental changes in
4282 50 lakes the across Canadian Arctic treeline. *Arctic, Antarctic, and Alpine Research*, **35**,
4283 110-23.

4284

4285 **Salvigsen, O., S.L. Forman, and G.H. Miller, 1992:** Thermophilous mollusks on Svalbard during
4286 the Holocene and their paleoclimatic implications. *Polar Research*, **11**, 1-10.

4287

4288 **Salzmann, U., A.M. Haywood, D.J. Lunt, P.J. Valdes, and D.J. Hill, 2008:** A new global biome
4289 reconstruction and data-model comparison for the Middle Pliocene. *Global Ecology and*
4290 *Biogeography*, **17**, 432-447.

4291

4292 **Sauer, P.E., G.H. Miller, and J.T. Overpeck, 2001:** Oxygen isotope ratios of organic matter in
4293 Arctic lakes as a paleoclimate proxy—Field and laboratory investigations. *Journal of*
4294 *Paleolimnology*, **25**, 43-64.

4295

4296 **Schauer, U., B. Rudels, E.P. Jones, L.G. Anderson, R.D. Muench, G. Björk, J.H. Swift, V.**
4297 **Ivanov, and A.-M. Larsson, 2002:** Confluence and redistribution of Atlantic water in the
4298 Nansen, Amundsen and Makarov basins. *Annals of Geophysics*, **20**, 257- 273.

4299

4300 **Schindler, D.W. and J.P. Smol, 2006:** Cumulative effects of climate warming and other human
4301 activities on freshwaters of Arctic and subarctic North America. *Ambio*, **35**, 160-68.

4302

4303 **Schlosser, P., B. Ekwurzel, S. Khatiwala, B. Newton, W. Maslowski, and S. Pfirman, 2000:**

SAP1.2 DRAFT 3 PUBLIC COMMENT

- 4304 Tracer studies of the Arctic freshwater budget. In: *The Freshwater Budget of the Arctic*
4305 *Ocean* [Lewis, E.L. (ed.)]. Kluwer Academic Publishers, Norwell, Mass. pp. 453- 478.
4306
- 4307 **Schlosser, P., R. Newton, B. Ekwurzel, S. Khatiwala, R. Mortlock, and R. Fairbanks, 2002:**
4308 Decrease of river runoff in the upper waters of the Eurasian Basin, Arctic Ocean, between
4309 1991 and 1996—Evidence from d¹⁸O data. *Geophysical Research Letters*, **29(9)**, 1289,
4310 doi:10.1029/ 2001GL013135.
4311
- 4312 **Schmidt, G.A., A.N. LeGrande, and G. Hoffman, 2007: Water isotope expressions of intrinsic**
4313 **and forced variability in a coupled ocean-atmosphere model. *Journal Geophysical***
4314 ***Research*, **112**, D10103, doi:10.1029/2006JD007781.**
4315
- 4316 **Schmittner, A., 2005: Decline of the marine ecosystem caused by a reduction in the Atlantic**
4317 **overturning circulation. *Nature*, **434**, 628-33.**
4318
- 4319 **Schneider, K.B. and B. Faro, 1975: Effects of sea ice on sea otters (*Enhydra lutris*). *Journal of***
4320 ***Mammalogy*, **56**, 91-101.**
4321
- 4322 **Schouten, S., E.C. Hopmans, and J.S.S. Damsté, 2004: The effect of maturity and depositional**
4323 **redox conditions on archaeal tetraether lipid palaeothermometry. *Organic Geochemistry*,**
4324 ****35(5)**, 567-571**
4325
- 4326 **Schrag, D.P., J.F. Adkins, K. McIntyre, J.L. Alexander, D.A. Hodell, C.D. Charles, and J.F.**
4327 **McManus, 2002: The oxygen isotopic composition of seawater during the Last Glacial**
4328 **Maximum. *Quaternary Science Reviews*, **21(1-3)**, 331-342**
4329
- 4329 **Schulz, H., U. von Rad, and H. Erlenkeuser, 1998: Correlation between Arabian Sea and**
4330 **Greenland climate oscillations of the past 110,000 years: *Nature*, **393**, 54-57.**
4331
- 4332 **Scott, D.B., P.J. Mudie, V. Baki, K.D. MacKinnon, and F.E. Cole, 1989: Biostratigraphy and**
4333 **late Cenozoic paleoceanography of the Arctic Ocean—Foraminiferal, lithostratigraphic,**
4334 **and isotopic evidence. *Geological Society of America Bulletin*, **101**, 260-277.**

- 4335
- 4336 **Seager, R., D.S. Battisti, J. Yin, N. Gordon, N. Naik, A.C. Clement, and M.A. Cane, 2002:** Is the
4337 Gulf Stream responsible for Europe's mild winters? *Quarterly Journal of the Royal*
4338 *Meteorological Society*, **128(586)**, 2563-2586.
- 4339
- 4340 **Seppä, H., 1996:** Post-glacial dynamics of vegetation and tree-lines in the far north of
4341 Fennoscandia. *Fennia*, **174**, 1-96.
- 4342
- 4343 **Seppä, H. and H.J.B. Birks, 2001:** July mean temperature and annual precipitation trends during
4344 the Holocene in the Fennoscandian tree-line area—Pollen-based climate reconstructions.
4345 *The Holocene*, **11**, 527-539.
- 4346
- 4347 **Seppä, H. and H.J.B. Birks, 2002:** Holocene climate reconstructions from the Fennoscandian
4348 tree-line area based on pollen data from Toskaljavri. *Quaternary Research*, **57**, 191-199.
- 4349
- 4350 **Seppä, H. and D. Hammarlund, 2000:** Pollen-stratigraphical evidence of Holocene hydrological
4351 change in northern Fennoscandia supported by independent isotopic data. *Journal of*
4352 *Paleolimnology*, **24(1)**, 69-79.
- 4353
- 4354 **Seppä, H., H.J.B. Birks, A. Odland, A. Poska, and S. Veski, 2004:** A modern pollen-climate
4355 calibration set from northern Europe—Developing and testing a tool for
4356 palaeoclimatological reconstructions. *Journal of Biogeography*, **31**, 251-267.
- 4357
- 4358 **Seppä, H., L.C. Cwynar, and G.M. MacDonald, 2003:** Post-glacial vegetation reconstruction and
4359 a possible 8200 cal. Yr BP event from the low arctic of continental Nunavut, Canada.
4360 *Journal of Quaternary Science*, **18**, 621-629.
- 4361
- 4362 **Serreze, M.C. and J.A. Francis, 2006:** The Arctic amplification debate. *Climatic Change*, **76**,
4363 241-264.
- 4364
- 4365 **Serreze, M.C., A.P. Barrett, A.G. Slater, M. Steele, J. Zhang, and K.E. Trenberth, 2007a:** The

SAP1.2 DRAFT 3 PUBLIC COMMENT

- 4366 large-scale energy budget of the Arctic. *Journal of Geophysical Research*, **112**, D11122,
4367 doi:10.1029/2006JD008230.
- 4368
- 4369 **Serreze**, M.C., A.P. Barrett, A.G. Slater, R.A. Woodgate, K. Aagaard, R.B. Lammers, M. Steele,
4370 R. Moritz, M. Meredith, and C.M. Lee, 2006: The large-scale freshwater cycle of the
4371 Arctic, *Journal of Geophysical Research-Oceans*, **111(C11)**, C11010.
- 4372
- 4373 **Serreze**, M.C., M.M. Holland, and J. Stroeve, 2007b: Perspectives on the Arctic's shrinking sea
4374 ice cover. *Science*, **315**, 1533-1536.
- 4375
- 4376 **Severinghaus**, J.P. and E.J. Brook, 1999: Abrupt climate change at the end of the last glacial
4377 period inferred from trapped air in polar ice. *Science*, **286**, 930-934.
- 4378
- 4379 **Severinghaus**, J.P., T. Sowers, E.J. Brook, R.B. Alley and M.L. Bender. 1998: Timing of abrupt
4380 climate change at the end of the Younger Dryas interval from thermally fractionated
4381 gases in polar ice. *Nature*, **391(6663)**, 141-146.
- 4382
- 4383 **Sewall**, J.O. and L.C. Sloan, 2004: Disappearing Arctic sea ice reduces available water in the
4384 American west. *Geophysical Research Letters*, **31**, doi:10.1029/2003GL019133.
- 4385
- 4386 **Sewall**, J.O. and L.C. Sloan, 2001: Equable Paleogene climates: The result of a stable, positive
4387 Arctic Oscillation? *Geophysical Research Letters*, **28(19)**, 3693-3695.
- 4388
- 4389 **Shackleton**, N.J., 1967: Oxygen isotope analyses and paleotemperatures reassessed. *Nature*,
4390 **215**, 15-17.
- 4391
- 4392 **Shackleton**, N.J., 1974: Attainment of isotopic equilibrium between ocean water and the
4393 benthonic foraminifera genus *Uvigerina*—Isotopic changes in the ocean during the last
4394 glacial. *Coll. Int. du CNRS*, **219**, 203-209.
- 4395

SAP1.2 DRAFT 3 PUBLIC COMMENT

- 4396 **Shellito**, C. J., L.C. Sloan, and M. Huber, 2003: Climate model sensitivity to atmospheric CO₂
4397 levels in the early-middle Paleogene. *Palaeogeography, Palaeoclimatology,*
4398 *Palaeoecology*, **193**, 113-123.
- 4399
- 4400 **Shindell**, D.T., G.A. Schmidt, M.E. Mann, D. Rind, and A. Waple, 2001: Solar forcing of
4401 regional climate change during the Maunder Minimum. *Science*, **294**, 2149-2152.
- 4402
- 4403 **Shuman**, C.A., R.B. Alley, S. Anandakrishnan, J.W.C. White, P.M. Grootes and C.R. Stearns,
4404 1995: Temperature and accumulation at the Greenland Summit: comparison of high-
4405 resolution isotope profiles and satellite passive microwave brightness temperature trends.
4406 *Journal of Geophysical Research*, **100(D5)**, 9165-9177.
- 4407
- 4408 **Siegenthaler**, U., T.F. Stocker, E. Monnin, E. Lüthi, J. Schwander, B. Stauffer, D. Raynaud,
4409 J.M. Barnola, H. Fischer, V. Masson-Delmotte, and J. Jouzel, 2005: Stable carbon cycle-
4410 climate relationship during the late Pleistocene. *Science*, **310**, 1313-1317,
4411 doi:10.1126/science.1120130
- 4412
- 4413 **Sloan**, L.C. and E.J. Barron, 1992: A comparison of eocene climate model results to quantified
4414 paleoclimatic interpretations. *Palaeogeography, Palaeoclimatology, Palaeoecology*,
4415 **93(3-4)**, 183-202
- 4416
- 4417 **Sloan**, L., T.J. Crowley, and D. Pollard, 1996: Modeling of middle Pliocene climate with the
4418 NCAR GENESIS general circulation model. *Marine Micropaleontology*, **27**, 51-61.
- 4419
- 4420 **Sloan**, L.C., and D. Pollard, 1998: Polar stratospheric clouds: A high latitude warming
4421 mechanism in an ancient greenhouse world. *Geophysical Research Letters*, **25(18)**, 3517-
4422 3520.
- 4423
- 4424 **Sluijs**, A., U. Rohl, S. Schouten, H.J. Brumsack, F. Sangiorgi, J.S.S. Damste, and H. Brinkhuis,
4425 2008: Arctic late Paleocene-early Eocene paleoenvironments with special emphasis on

SAP1.2 DRAFT 3 PUBLIC COMMENT

- 4426 the Paleocene-Eocene thermal maximum (Lomonosov Ridge, Integrated Ocean Drilling
4427 Program Expedition 302). *Paleoceanography*, **23**(1), PA1S11.
- 4428
- 4429 **Sluijs, A.**, S. Schouten, M. Pagani, M. Woltering, H. Brinkhuis, J.S.S. Damste, G.R. Dickens, M.
4430 Huber, G.J. Reichart, R. Stein, J. Matthiessen, L.J. Lourens, N. Pedentchouk, J. Backman
4431 and K. Moran, 2006: Subtropical arctic ocean temperatures during the Palaeocene/Eocene
4432 thermal maximum. *Nature*, **441**, 610-613.
- 4433
- 4434 **Smith, L.C.**, G.M. MacDonald, A.A. Velichko, D.W. Beilman, O.K. Borisova, K.E. Frey, K.V.
4435 Kremenetski, and Y. Sheng, 2004: Siberian peatlands a net carbon sink and global
4436 methane source since the early Holocene. *Science*, **303**(5656), 353-356.
- 4437
- 4438 **Smol, J.P.**, 1988: Paleoclimate proxy data from freshwater Arctic diatoms. *Internationale*
4439 *Vereinigung für Limnologie*, **23**, 837-44.
- 4440
- 4441 **Smol, J.P.**, 2008: *Pollution of lakes and rivers—A paleoenvironmental perspective*. Blackwell
4442 Publishing, Oxford, U.K., 2nd ed., 280 pp.
- 4443
- 4444 **Smol, J.P.** and B.F. Cumming, 2000: Tracking long-term changes in climate using algal
4445 indicators in lake sediments. *Journal of Phycology*, **36**, 986-1011.
- 4446
- 4447 **Smol, J.P.** and M.S.V. Douglas, 2007a: From controversy to consensus—Making the case for
4448 recent climatic change in the Arctic using lake sediments. *Frontiers in Ecology and the*
4449 *Environment*, **5**, 466-474
- 4450
- 4451 **Smol, J.P.** and M.S.V. Douglas, 2007b: Crossing the final ecological threshold in high Arctic
4452 ponds. *Proceedings of the National Academy of Sciences, U.S.A.*, **104**, 12,395-12,397.
- 4453
- 4454 **Solovieva, N.**, P.E. Tarasov, and G.M. MacDonald, 2005: Quantitative reconstruction of
4455 Holocene climate from the Chuna Lake pollen record, Kola Peninsula, northwest Russia.
4456 *The Holocene*, **15**, 141-148.

SAP1.2 DRAFT 3 PUBLIC COMMENT

- 4457
- 4458 **Sorvari, S.** and A. Korhola, 1998: Recent diatom assemblage changes in subarctic Lake
4459 Saanajarvi, NW Finnish Lapland, and their paleoenvironmental implications. *Journal of*
4460 *Paleolimnology*, **20(3)**, 205-215.
- 4461
- 4462 **Sorvari, S.**, A. Korhola, and R. Thompson, 2002: Lake diatom response to recent Arctic warming
4463 in Finnish Lapland. *Global Change Biology*, **8**, 171-181.
- 4464
- 4465 **Sowers, T.**, Bender, M., Raynaud, D., 1989: Elemental and isotopic composition of occluded O₂
4466 and N₂ in polar ice. *Journal of Geophysical Research-Atmospheres*, **94(D4)**, 5137-5150.
- 4467
- 4468 **Spencer, M.K.**, R.B. Alley and J.J. Fitzpatrick, 2006: Developing a bubble number-density
4469 paleoclimatic indicator for glacier ice. *Journal of Glaciology*, **52(178)**, 358-364.
- 4470
- 4471 **Spielhagen, R.F.**, K-H Baumann, H. Erlenkeuser, N.R. Nowaczyk, N. Nørgaard-Pedersen, C.
4472 Vogt, and D. Weiel, 2004: Arctic Ocean deep-sea record of northern Eurasian ice sheet
4473 history. *Quaternary Science Reviews*, **23(11-13)**, 1455-1483.
- 4474
- 4475 **Spielhagen, R.F.**, G. Bonani, A. Eisenhauer, M. Frank, T. Frederichs, H. Kassens, P.W. Kubik,
4476 N. Nørgaard-Pedersen, N. R. Nowaczyk, A. Mangini, S. Schäper, R. Stein, J. Thiede, R.
4477 Tiedemann, and M. Wahsner, 1997: Arctic Ocean evidence for late Quaternary initiation
4478 of northern Eurasian ice sheets. *Geology*, **25(9)**, 783-786.
- 4479
- 4480 **Spielhagen, R.F.** and H. Erlenkeuser, 1994: Stable oxygen and carbon isotopes in planktic
4481 foraminifers from Arctic Ocean surface sediments—Reflection of the low salinity surface
4482 water layer. *Marine Geology*, **119(3/4)**, 227-250.
- 4483
- 4484 **Spielhagen, R.F.**, H. Erlenkeuser, and C. Siebert, 2005: History of freshwater runoff across the
4485 Laptev Sea (Arctic) during the last deglaciation. *Global and Planetary Change*, **48(1-3)**,
4486 187-207.
- 4487

SAP1.2 DRAFT 3 PUBLIC COMMENT

- 4488 **Stanton-Fraze**, C., D.A. Warnke, K. Venz, D.A. Hodell, 1999: The stage 11 problem as seen
4489 from ODP site 982, In: *Marine Oxygen Isotope Stage 11 and Associated Terrestrial*
4490 *Records*, [R.Z. Poore, L. Burckle, A. Droxler, W.E. McNulty (eds.)]. U.S. Geological
4491 Survey Open-file Report 99-312, 1999, pp.75.
4492
- 4493 **Steele**, M. and T. Boyd, 1998: Retreat of the cold halocline layer in the Arctic Ocean. *Journal of*
4494 *Geophysical Research*, **103**, 10,419-10,435.
4495
- 4496 **Stein**, R., S.I. Nam, C. Schubert, C. Vogt, D. Fütterer, and J. Heinemeier, 1994: The last
4497 deglaciation event in the eastern central Arctic Ocean. *Science*, **264**, 692-696.
4498
- 4499 **Stötter**, J., M. Wastl, C. Caseldine, and T. Häberle, 1999: Holocene palaeoclimatic
4500 reconstruction in Northern Iceland—Approaches and results. *Quaternary Science*
4501 *Reviews*, **18**, 457-474.
4502
- 4503 **Stroeve**, J., M. Serreze, S. Drobot, S. Gearheard, M. Holland, J. Maslanik, W. Meier, and T.
4504 Scambos, 2008: Arctic Sea Ice Extent Plummets in 2007. *EOS, Transactions, American*
4505 *Geophysical Union*, **89(2)**, 13-14.
4506
- 4507 **Sturm**, M., T. Douglas, C. Racine, and G.E. Liston, 2005: Changing Snow and shrub conditions
4508 affect albedo with global implications. *Journal of Geophysical Research*, **110**, G01004,
4509 doi:10.1029/2005JG000013.
4510
- 4511 **Svendsen**, J.I. and J. Mangerud, 1997: Holocene glacial and climatic variations on Spitsbergen,
4512 Svalbard. *The Holocene*, **7**, 45-57.
4513
- 4514 **Teece**, M.A., J.M. Getliff, J.W. Leftley, R.J. Parkes, and J.R. Maxwell, 1998: Microbial
4515 degradation of the marine prymnesiophyte *Emiliana huxleyi* under oxic and anoxic
4516 conditions as a model for early diagenesis—Long chain alkadienes, alkenones and alkyl
4517 alkenoates. *Organic Geochemistry*, **29**, 863-880.
4518

SAP1.2 DRAFT 3 PUBLIC COMMENT

- 4519 **Thomas, D.J., J.C. Zachos, T.J. Bralower, E. Thomas, and S. Bohaty, 2002:** Warming the fuel
4520 for the fire: Evidence for the thermal dissociation of methane hydrate during the
4521 Paleocene-Eocene thermal maximum. *Geology*, **30(12)**, 1067-1070.
4522
- 4523 **Thomsen, C., D.E. Schulz-Bull, G. Petrick, and J.C. Duinker, 1998:** Seasonal variability of the
4524 long-chain alkenone flux and the effect on the Uk37 index in the Norwegian Sea.
4525 *Organic Geochemistry*, **28**, 311-323.
4526
- 4527 **Toggweiler, J. R., 2008:** Origin of the 100,000-year timescale in Antarctic temperatures and
4528 atmospheric CO₂. *Paleoceanography*, **23**, PA2211, doi:10.1029/2006PA001405.
4529
- 4530 **Troitsky, S.L., 1964:** Osnoviye zakonomernosti izmeneniya sostava fauny po razrezam
4531 morskikh meshmorenykh sloev ust-eniseyskoy vpadiny i nishne-pechorskoy
4532 depressii. *Akademia NAUK SSSR, Trudy instituta geologii i geofiziki*, **9**, 48-65 (in
4533 Russian).
4534
- 4535 **Vassiljev, J., 1998:** The simulated response of lakes to changes in annual and seasonal
4536 precipitation—Implication for Holocene lake-level changes in northern Europe. *Climate*
4537 *Dynamics*, **14**, 791-801.
4538
- 4539 **Vassiljev, J., S.P. Harrison, and J. Guiot, 1998:** Simulating the Holocene lake-level record of
4540 Lake Bysjon, southern Sweden. *Quaternary Research*, **49**, 62-71.
4541
- 4542 **Velichko, A.A., A.A. Andreev, and V.A. Klimanov, 1997:** Climate and vegetation dynamics in
4543 the tundra and forest zone during the Late Glacial and Holocene. *Quaternary*
4544 *International*, **41/42**, 71-96.
4545
- 4546 **Velichko, A.A., and V.P. Nechaev (eds), 2005:** *Cenozoic climatic and environmental changes in*
4547 *Russia*. [H.E. Wright, Jr., T.A. Blyakharchuk, A.A. Velichko and Olga Borisova (eds. of
4548 English version)]. The Geological Society of America Special Paper, **382**, 226 pp.
4549

SAP1.2 DRAFT 3 PUBLIC COMMENT

- 4550 **Vinther**, B.M., H.B. Clausen, S.J. Johnsen, S.O. Rasmussen, K.K. Andersen, S.L. Buchardt, D.
4551 Dahl-Jensen, I.K. Seierstad, M.L. Siggaard-Andersen, J.P. Steffensen, A. Svensson, J.
4552 Olsen, and J. Heinemeier, 2006: A synchronized dating of three Greenland ice cores
4553 throughout the Holocene. *Journal of Geophysical Research*, **111**, D13102,
4554 doi:13110.11029/12005JD006921.
4555
- 4556 **Vörösmarty**, C.J., L.D. Hinzman, B.J. Peterson, D.H. Bromwich, L.C. Hamilton, J. Morison,
4557 V.E. Romanovsky, M. Sturm, and R.S. Webb. 2001: The Hydrologic Cycle and its Role
4558 in Arctic and Global Environmental Change: A Rationale and Strategy for Synthesis
4559 Study. Fairbanks, Alaska: Arctic Research Consortium of the U.S., 84 pp.
4560
- 4561 **Vörösmarty**, C., L. Hinzman, and J. Pundsack, 2008: Introduction to special section on Changes
4562 in the Arctic Freshwater System: Identification, Attribution, and Impacts at Local and
4563 Global Scales. *Journal of Geophysical Research-Biogeosciences*, **113(G1)**, G01S91.
4564
- 4565 **Walter**, K.M., S.A. Zimov, J.P. Chanton, D. Verbyla, and F. S. Chapin, III, 2006: Methane
4566 Bubbling from Siberian Thaw Lakes as a Positive Feedback to Climate Warming. *Nature*,
4567 **443**, 71-75.
4568
- 4569 **Walter** K.M., M. Edwards S.A. Zimov G. Grosse F.S. Chapin, III, 2007: Thermokarst lakes as a
4570 source of atmospheric CH₄ during the last deglaciation. *Science*, **318,(5850)**, 633-636.
4571
- 4572 **Wang**, Y.J., H. Cheng, R. L. Edwards, Z. S. An, J. Y. Wu, C.-C. Shen, J. A. Dorale' 2001: A
4573 high-resolution absolute-dated late Pleistocene monsoon record from Hulu Cave, China.
4574 *Science*, **294**, 2345-2348.
4575
- 4576 **Weaver**, A.J., C.M. Bitz, A.F. Fanning, and M.M. Holland, 1999: Thermohaline circulation—
4577 High latitude phenomena and the difference between the Pacific and Atlantic. *Annual*
4578 *Review of Earth and Planetary Sciences*, **27**, 231-285.
4579
- 4580 **Weckström**, J., A. Korhola, P. Erästö, and L. Holmström, 2006: Temperature patterns over the

- 4581 past eight centuries in northern Fennoscandia inferred from sedimentary diatoms.
 4582 *Quaternary Research*, **66**, 78-86.
 4583
- 4584 **Weijers, J.W.H., S. Schouten, O.C. Spaargaren, and J.S.S. Damsté, 2006:** Occurrence and
 4585 distribution of tetraether membrane lipids in solid—Implications for the use of the TEX₈₆
 4586 proxy and the BIT index. *Organic Geochemistry*, **37(12)**, 1680-1693.
 4587
- 4588 **Weijers, J.W.H., S. Schouten, A. Sluijs, H. Brinkhuis, and J.S.S. Damste, 2007:** Warm arctic
 4589 continents during the Palaeocene-Eocene thermal maximum. *Earth and Planetary
 4590 Science Letters*, **261(1-2)**, 230-238.
 4591
- 4592 **Werner, M., U. Mikolajewicz, M. Heimann, and G. Hoffmann, 2000:** Borehole versus isotope
 4593 temperatures on Greenland—Seasonality does matter. *Geophysical Research Letters*, **27**,
 4594 723-726.
 4595
- 4596 **Whitlock, C. and M.R. Dawson, 1990:** Pollen and vertebrates of the early Neogene Haughton
 4597 Formation, Devon Island, Arctic Canada. *Arctic*, **43(4)**, 324-330.
 4598
- 4599 **Wiles, G.C., D.J. Barclay, P.E. Calkin, and T.V. Lowell, 2008:** Century to millennial-scale
 4600 temperature variations for the last two thousand years indicated from glacial geologic
 4601 records of Southern Alaska. *Global and Planetary Change*, **60**, 15-125.
 4602
- 4603 **Williams, C..J., A.H. Johnson, B.A. LePage, D.R. Vann and T. Sweda, 2003:** Reconstruction of
 4604 Tertiary Metasequoia Forests II. Structure, Biomass and Productivity of Eocene Floodplain
 4605 Forests in the Canadian Arctic, *Paleobiology*, **29**, 271-292.
 4606
- 4607 **Wohlfahrt, J., S.P. Harrison, and P. Braconnot, 2004:** Synergistic feedbacks between ocean and
 4608 vegetation on mid- and high-latitude climates during the Holocene. *Climate Dynamics*,
 4609 **22**, 223-238.
 4610
- 4611 **Wohlfarth, B., G. Lemdahl, S. Olsson, T. Persson, I. Snowball, J. Ising, and V. Jones, 1995:**
 4612 Early Holocene environment on Bjornoya (Svalbard) inferred from multidisciplinary lake

SAP1.2 DRAFT 3 PUBLIC COMMENT

- 4613 ^A sediment studies. *Polar*^B *Research*, **14**, 253-275.
- 4614
- 4615 **Wooller**, M.J., D. Francis, M.L. Fogel, G.H. Miller, I.R. Walker, and A.P. Wolfe, 2004:
- 4616 Quantitative paleotemperature estimates from delta O-18 of chironomid head capsules
- 4617 preserved in arctic lake sediments. *Journal of Paleolimnology*, **31(3)**, 267-274.
- 4618
- 4619 **Wuchter**, C., S. Schouten, M.J.L. Coolen, and J.S.S. Damsté, 2004: Temperature-dependent
- 4620 variation in the distribution of tetraether membrane lipids of marine Crenarchaeota—
- 4621 Implications for TEX86 paleothermometry. *Paleoceanography*, **19(4)**, PA4028
- 4622
- 4623 **Zachos**, J.C., Dickens, G.R., Zeebe, R.E., 2008: An early Cenozoic perspective on greenhouse
- 4624 warming and carbon-cycle dynamics. *Nature*, **451** (7176), 279-283.
- 4625
- 4626 **Zachos**, Z., P. Pagani, L. Sloan, E. Thomas, and K. Billups, 2001: Trends, rhythms, and
- 4627 aberrations in global climate 65 Ma to present. *Science*, **292**, 686-693.
- 4628
- 4629 **Zazula** G.D., D.G. Froese, C.E. Schweger, R.W. Mathewes, A.B. Beaudoin, A.M. Telka, C.R.
- 4630 Harington, and J.A. Westgate, 2003: Ice-age steppe vegetation in east Beringia - tiny
- 4631 plant fossils indicate how this frozen region once sustained huge herds of mammals.
- 4632 *Nature*, **423**, 603-603.
- 4633

1
2
3
4
5
6
7
8
9
10
11
12
13
14
15

CCSP Synthesis and Assessment Product 1.2

**Past Climate Variability and Change in the Arctic and at High
Latitudes**

Chapter 6 — Past Rates of Climate Change in the Arctic

Chapter Lead Authors

James White, University of Colorado, Boulder, CO

Richard Alley, Pennsylvania State University, University Park, PA

Contributing Authors

Anne Jennings, University of Colorado

Sigfus Johnsen, University of Copenhagen

Gifford Miller, University of Colorado

Steven Nerem, University of Colorado

15 **ABSTRACT**

16
17 Climate has changed on numerous time scales for various reasons and has always
18 done so. In general, longer lived changes are somewhat larger but much slower than
19 shorter lived changes. Processes linked with continental drift have affected atmospheric
20 and oceanic currents and the composition of the atmosphere over tens of millions of
21 years; in the Arctic, a global cooling trend has altered conditions near sea level from ice-
22 free year-round to icy. Within the icy times, variations in Arctic sunshine over tens of
23 thousands of years in response to features of Earth’s orbit caused regular cycles of
24 warming and cooling that were roughly half the size of the continental-drift-linked
25 changes. This “glacial-interglacial” cycling has been amplified by colder times bringing
26 reduced greenhouse gases and greater reflection of sunlight especially from more-
27 extended ice. This glacial-interglacial cycling has been punctuated by sharp-onset, sharp-
28 end (in some instances less than 10 years) millennial oscillations, which near the North
29 Atlantic were roughly half as large as the glacial-interglacial cycles but which were much
30 smaller Arctic-wide and beyond. The current warm period of the glacial-interglacial cycle
31 has been influenced by cooling events from single volcanic eruptions, slower but longer
32 lasting changes from random fluctuations in frequency of volcanic eruptions and from
33 weak solar variability, and perhaps by other classes of events. Very recently, human
34 effects have become evident, but they do not yet show either a size or duration that
35 exceeds peak values of natural fluctuations further in the past. However, some projections
36 indicate that human influences could become anomalously large in size and duration, and
37 in speed.

38

39 **6.1. Introduction**

40

41 Climate change, as opposed to change in the weather (the distinction is defined
42 below), occurs on all time scales, ranging from several years to billions of years. The rate
43 of change, typically measured in degrees Celsius (°C) per unit of time (years, decades,
44 centuries, or millennia, for example, if climate is being considered) is a key determinant
45 of the effect of the change on living things such as plants and animals; collections and
46 webs of living things, such as ecosystems; and humans and human societies. Consider,
47 for example, a 10°C change in annual average temperature, roughly the equivalent to
48 going from Birmingham, Alabama, to Bangor, Maine. If such a change took place during
49 thousands of years, as happens when the earth's orbit varies and portions of the planet
50 receive more or less energy from the Sun, ecosystems and aspects of the environment,
51 such as sea level, would change, but the slow change would allow time for human
52 societies to adapt. A 10°C change that appears in 50 years or less, however, is
53 fundamentally different (National Research Council, 2002). Ecosystems would be able to
54 complete only very limited adaptation because trees, for example, typically are unable to
55 migrate that fast by seed dispersal. Human adaptation would be limited as well, and
56 widespread challenges would face agriculture, industry, and public utilities in response to
57 changing patterns of precipitation, severe weather, and other events. Such abrupt climate
58 changes on regional scales are well documented in the paleoclimate record (National
59 Research Council, 2002; Alley et al., 2003). This rate of change is about 100 times as fast
60 as the warming of the last century.

61 Not all parts of the climate system can change this rapidly. Global temperature
62 change is slowed by the heat capacity of the oceans, for example (e.g., Hegerl et al.,
63 2007). Local changes, particularly in continental interiors or where sea-ice changes
64 modify the interaction between ocean and atmosphere, can be faster and larger. Changes
65 in atmospheric circulation are potentially faster than changes in ocean circulation, owing
66 to the difference in mass and thus inertia of these two circulating systems. This
67 difference, in turn, influences important climate properties that depend on oceanic or
68 atmospheric circulation. The concentration of carbon dioxide in the atmosphere, for
69 example, depends in part on ocean circulation, and thus it does not naturally vary rapidly
70 (e.g., Monnin et al., 2001). Methane concentration in the atmosphere, on the other hand,
71 has increased by more than 50% within decades (Severinghaus et al., 1998), as this gas is
72 more dependent on the distribution of wetlands, which in turn depend on atmospheric
73 circulation to bring rains.

74 In the following pages we examine past rates of environmental change observed
75 in Arctic paleoclimatic records. We begin with some basic definitions and clarification of
76 concepts. Climate change can be evaluated absolutely, using numerical values such as
77 those for temperature or rainfall, or they can be evaluated relative to the effects they
78 produce (National Research Council, 2002). Different groups often have differing views
79 on what constitutes “important.” Hence, we begin with a common vocabulary.

80

81 **6.2. Variability Versus Change; Definitions and Clarification of Usage**

82

83 Climate scientists and weather forecasters are familiar with opposite sides of very

84 common questions. Does this hot day (or month, or year) prove that global warming is
85 occurring? or does this cold day (or month, or year) prove that global warming is not
86 occurring? Does global warming mean that tomorrow (or next month, or next year) will
87 be hot? or does the latest argument against global warming mean that tomorrow (or next
88 month, or next year) will be cold? Has the climate changed? When will we know that the
89 climate has changed? To people accustomed to seven-day weather forecasts, in which the
90 forecast beyond the first few days is not very accurate, the answers are often not very
91 satisfying. The next sections briefly discuss some of the issues involved.

92

93 **6.2.1 Weather Versus Climate**

94 The globally averaged temperature difference between an ice age and an
95 interglacial is about 5°–6°C (Cuffey and Brook, 2000; Jansen et al., 2007). The 12-hour
96 temperature change between peak daytime and minimum nighttime temperatures at a
97 given place, or the 24-hour change, or the seasonal change, may be much larger than that
98 glacial-interglacial change (e.g., Trenberth et al., 2007). In assessing the “importance” of
99 a climate change, it is generally accepted that a single change has greater effect on
100 ecosystems and economies, and thus is more “important,” if that change is less expected,
101 arrives more rapidly, and stays longer (National Research Council, 2002). In addition, a
102 step change that then persists for millennia might become less important than similar-
103 sized changes that occurred repeatedly in opposite directions at random times.

104 Historically, climate has been taken as a running average of weather conditions at
105 a place or throughout a region. The average is taken for a long enough time interval to
106 largely remove fluctuations caused by “weather.” Thirty years is often used for

107 averaging.

108 Weather, to most observers, implies day-to-day occurrences, which are
109 predictable for only about two weeks. Looking further ahead than that is limited by the
110 chaotic nature of the atmospheric system; that is, by the sensitivity of the system to initial
111 conditions (e.g., Lorenz, 1963; Le Treut et al., 2007), as described next. All thermometers
112 have uncertainties, even if only a fraction of a degree, and all measurements by
113 thermometers are taken at particular places and not in between. All temperature estimates
114 at and between thermometers are thus subject to some uncertainty. A weather-forecasting
115 model can correctly be started from a range of possible starting conditions that differ by
116 an amount equal to or less than the measurement uncertainties. For short times of hours
117 or even days, the different starting conditions provided by the modern observational
118 system typically have little effect on the weather; vary the starting data within the known
119 uncertainties, and the output of the model will not be affected much. However, if the
120 model is run for times beyond a few days to perhaps a couple of weeks, the different
121 starting conditions produce very different forecasts. The forecasts are “bounded”—they
122 do not produce blizzards in the tropics or tropical temperatures in the Arctic wintertime,
123 for example; and they do produce “forecasts” recognizably possible for all regions
124 covered—but the forecasts differ greatly in the details of where and when convective
125 thunderstorms or frontal systems occur and how much precipitation will be produced
126 during what time period. To many observers, “weather” refers to those features of Earth’s
127 coupled atmosphere-ocean system that are predictable to two weeks or so but not beyond.

128 For many climatologists, however, somewhat longer term events are often lumped
129 under the general heading of “weather.” The year-to-year temperature variability in

130 global average temperature associated with the El Nino–La Nina phenomenon may be a
131 few tenths of a degree Celsius (e.g., Trenberth et al., 2002), and similar or slightly larger
132 variability can be caused by volcanic eruptions (e.g., Yang and Schlesinger, 2002). The
133 influences of such phenomena are short lived compared with a 30-year average, but they
134 are long lived compared with the two-week interval described just above. Volcanic
135 eruptions may someday prove to be predictable beyond two weeks (U.S. Geological
136 Survey scientists successfully predicted one of the Mt. St. Helens eruptions more than
137 two weeks in advance (Tilling et al., 1990)), and the effects following an eruption
138 certainly are predictable for longer times. El Ninos are predictable beyond two weeks.
139 However, if one is interested in the climatic conditions at a particular place, a proper
140 estimate would include the average behavior of volcanoes and El Ninos, but it would not
141 be influenced by the accident that the starting and ending points of the 30-year averaging
142 period happened to sample a higher or lower number of these events than would be found
143 in an average 30-year period.

144 The issues of the length of time considered and the starting time chosen are
145 illustrated in Figure 6.1. Annual temperatures for the continental United States since 1960
146 are shown. The variability shown is linked to El Nino, volcanic eruptions, and other
147 factors. If we use a 4-year window to illustrate the issue, it is apparent that for any given
148 4-year period, the temperature trend can appear to warm, to cool, or to stay flat. Also
149 shown are the 3-, 7-, 11-, 15-, and 19-year linear trends centered on 1990. Depending on
150 the number of years chosen, the trend can be strongly warming to strongly cooling. The
151 warm El Nino years of 1987 and 1988, and the cooling trend in 1992 and 1993 caused by
152 the eruption of Mt. Pinatubo, affect our perception of the time trend, or climate. Notice

153 that of the 45 four-year regression lines possible between 1960 and 2007 (17 are shown
154 in Figure 6.1) only one meets the usual statistical criterion of having a slope different
155 from zero with at least 95% confidence. Climate is often considered as a 30-year average,
156 and all 30-year regression lines that can be placed on Figure 6.1 (years 1960–1989, 1961–
157 1990, ..., 1978–2007) have a positive slope (warming) with greater than 95% confidence.
158 Thus, all of the short-time-interval lines shown on Figure 6.1 are part of a warming
159 climate but clearly reflect weather as well.

160

161

FIGURE 6.1 NEAR HERE

162

163 **6.2.2 Style of Change**

164 In some situations a 30-year climatology appears inappropriate. As recorded in
165 Greenland ice cores, local temperatures fell many degrees Celsius within a few decades
166 about 13 ka during the Younger Dryas time, a larger change than the interannual
167 variability. The temperature remained low for more than a millennium, and then it
168 jumped up about 10°C in about a decade, and it has remained substantially elevated since
169 (Clow, 1997; Severinghaus et al., 1998; Cuffey and Alley, 2000). It is difficult to imagine
170 any observer choosing the temperature average of a 30-year period that included that
171 10°C jump and then arguing that this average was a useful representation of the climate.
172 The jump is perhaps the best-known and most-representative example of abrupt climate
173 change (National Research Council, 2002; Alley et al., 2003), and the change is ascribed
174 to what is now known colloquially as a “tipping point.” Tipping points occur when a slow
175 process reaches a threshold that “tips” the climate system into a new mode of operation

176 (e.g., Alley, 2007). Analogy to a canoe tipping over suddenly in response to the slowly
177 increasing lean of a paddler is appropriate.

178 Tipping behavior is readily described sufficiently long after the event, although it
179 is much less evident that a climate scientist could have predicted the event just before it
180 occurred, or that a scientist experiencing the event could have stated with confidence that
181 conditions had tipped. Research on this topic is advancing, and quantitative statements
182 can be made about detection of events, but timely detection may remain difficult (Keller
183 and McInerney, 2007).

184

185 **6.2.3 How to Talk About Rates of Change**

186 The term “abrupt climate change” has been defined with some authority in the
187 report of the National Research Council (2002). However, many additional terms such as
188 “tipping point” remain colloquial, although arguably they can be related to well-accepted
189 definitions. For the purposes of this report, preference will be given to common English
190 words whenever possible, with explanations of what is meant, without relying on new
191 definitions of words or on poorly defined words.

192

193 **6.2.4 Spatial Characteristics of Change**

194 The Younger Dryas cold event, introduced above in section 6.2.2, led to
195 prominent cooling around the North Atlantic, weaker cooling around much of the
196 Northern Hemisphere, and weak warming in the far south; uncertainty remains about
197 changes in many places, and the globally averaged effect probably was minor (reviewed
198 by Alley, 2007). The most commonly cited records of the Younger Dryas are those that

199 show large signals. Informal discussions by many investigators with people outside our
200 field indicate that the strong local signals are at least occasionally misinterpreted as
201 global signals. It is essential to recognize the geographic as well as time limitations of
202 climate events and their paleoclimatic records.

203 Further complicating this discussion is the possibility that an event may start in
204 one region and then require some climatically notable time interval to propagate to other
205 regions. Limited data supported by our basic understanding of how climate processes
206 work suggest that the Younger Dryas cold event began and ended in the north, that the
207 response was delayed by decades or longer in the far south, and that it was transmitted
208 there through the ocean (Steig and Alley, 2003; Stocker and Johnsen, 2003). Cross-dating
209 climate records around the world to the precision and accuracy needed to confirm that
210 relative timing is a daunting task. The mere act of relating records from different areas
211 then becomes difficult; an understanding of the processes involved is almost certainly
212 required to support the interpretation.

213

214 **6.3 Issues Concerning Reconstruction of Rates of Change from Paleoclimatic**

215 **Indicators**

216

217 In an ideal world, a chapter on rates of change would not be needed. If climate
218 records were available from all places and all times, with accurate and precise dates, then
219 rate of change would be immediately evident from inspection of those records. However,
220 as suggested in the previous section, such a simple interpretation is seldom possible.

221 Consider a hypothetical example. A group of tree trunks, bulldozed by a glacier

222 and incorporated into glacial sediments, is now exposed at a coastal site. Many trees were
223 killed at approximately the same time. The patterns of thick and thin rings, dense and
224 less-dense wood, and isotopic variation of the wood layers contain climatic information
225 (e.g., White et al., 1994). The climatic fluctuations that controlled the tree-ring
226 characteristics can be dated precisely relative to each other—for example, this isotopic
227 event occurred 7 years after that one. However, the precise age of the start and end of that
228 climate record may not be available.

229 If much additional wood of various ages is available nearby, and if a large effort
230 is expended, it may be possible to use the patterns of thick and thin rings and other
231 features to match overlapping trees of different ages and thus to tie the record to still-
232 living trees and provide a continuous record absolutely dated to the nearest year. If this is
233 not possible, but the trees grew within the time span for which radiocarbon can be used, it
234 may be possible to learn the age of the record to within a few decades or centuries, but no
235 better. If the record is older than can be dated using radiocarbon, and other dating
236 techniques are not available, even larger errors may be attached to estimates of the time
237 interval occupied by the record.

238 Uncertainties are always associated with reconstructed climate changes (were the
239 thick and thin rings controlled primarily by temperature changes or by moisture changes?
240 for example), but once temperatures or rainfall amounts are estimated for each year,
241 calculation of the rate of change from year to year will involve no additional error
242 because each year is accurately identified. However, learning the spatial pattern of
243 climate change may not be possible, because it will not be possible to relate the events
244 recorded by the tree rings to events in records from other places with their own dating

245 difficulties.

246 Sometimes, however, it is possible to learn the spatial pattern of the climate
247 change and to learn how the rate of change at one place compared with the rate of change
248 elsewhere. Volcanic eruptions are discrete events, and major eruptions typically are short
249 lived (hours to days), so that the layer produced by a single eruption in various lake and
250 marine sediments and glaciers is almost exactly the same age in all. If the same pattern of
251 volcanic fallout is found in many cores of lake or ocean sediment or ice, then it is
252 possible to compare the rate of change at those different sites. The uncertainties in
253 knowing the time interval between two volcanic layers may be small or large, but
254 whatever the time interval is, it will be the same in all cores containing those two layers.

255 These and additional considerations motivate the additional discussion of rates of
256 climate change provided here.

257

258 **6.3.1 Measurement of Rates of Change in Marine Records**

259 In Arctic and subarctic marine sediments, radiocarbon dating remains the standard
260 technique for obtaining well-dated records during the last 40,000 to 50,000 years.

261 Radiocarbon dating is relatively inexpensive, procedures are well developed, and

262 materials that can be dated usually are more common than is true for other techniques.

263 Radiocarbon dating is now conventionally calibrated against other techniques such as

264 tree-ring or uranium-series-disequilibrium techniques, which are more accurate but less

265 widely applicable. The calibration continues to improve (e.g., Stuiver et al., 1998;

266 Hugen et al., 2000; 2004). Instruments also improve. In particular, the accelerator mass

267 spectrometer (AMS) radiocarbon analysis allows dating of milligram quantities of

268 foraminifers, mollusks and other biogenic materials. A single seed or tiny shell can be
269 dated, and this analysis of smaller samples than was possible with previous techniques in
270 turn allows finer time resolution in a single core. Taken together, these advances have
271 greatly improved our ability to generate well-constrained age models for high-latitude
272 marine sediment cores. In addition, coring systems such as the Calypso corer have been
273 deployed in the Arctic to recover much longer (10–60 m) sediment cores. This corer
274 allows sampling of relatively long time intervals even in sites where sediment has
275 accumulated rapidly. Sites with faster sediment accumulation allow easier “reading” of
276 the history of short-lived events, so higher resolution paleoenvironmental records can
277 now be generated from high-latitude continental-margin and deep-sea sites. Where dates
278 can be obtained from many levels in a core, it is feasible to evaluate centennial and even
279 multidecadal variability from these archives (e.g., Ellison et al., 2006; Stoner et al.,
280 2007).

281 However, in the Arctic, particularly along eastern margins of oceans where cold
282 polar and Arctic water masses influence the environment, little carbonate that can be
283 dated by radiocarbon techniques is produced, and much of the carbonate produced
284 commonly dissolves after the producing organism dies. In addition, the carbon used in
285 growing the shells is commonly “old” (that is, the carbon entered the ocean some decades
286 or centuries before being used by the creature in growing its shell; the date obtained is
287 approximately the time when the carbon entered the ocean, and it must be corrected for
288 the time interval between the carbon entering the ocean and being incorporated into the
289 shell). This marine reservoir correction is often more uncertain in the Arctic than
290 elsewhere (e.g., Björck et al., 2003) in part because of the strong but time-varying effect

291 of sea ice, which blocks exchange between atmosphere and ocean. This uncertainty
292 continues to hamper development of highly constrained chronologies. Some important
293 regions, such as near the eastern side of Baffin Island, have received little study since
294 radiocarbon dating by accelerator mass spectrometry was introduced, so the chronology
295 and Holocene climate evolution of this important margin are still poorly known.

296 As researchers attempt to develop centennial to multidecadal climate records from
297 marine cores and to correlate between records at sub-millennial resolution, the limits of
298 the dating method are often reached, hampering our ability to determine whether high-
299 frequency variability is synchronous or asynchronous between sites. Resource limitations
300 generally restrict radiocarbon dating to samples no closer together than about 500-year
301 intervals. In marine areas with rapid biological production where sufficient biogenic
302 carbonate is available to obtain highly accurate dates, the instrumental error on individual
303 radiocarbon dates may be as small as ± 20 years. But, in many Arctic archives, it is not
304 possible to obtain enough carbonate material to achieve that accuracy, and many dates are
305 obtained with standard deviations (one sigma) errors of ± 80 years to a couple of
306 centuries.

307 A new approach that uses a combination of paleomagnetic secular variation
308 (PSV) records and radiocarbon dating has improved relative correlation and chronology
309 well above the accuracy that each of these methods can achieve on its own (Stoner et al.,
310 2007). Earth's magnetic field varies in strength and direction with time, and the field
311 affects the magnetization of sediments deposited. Gross features in the field (reversals of
312 direction) have been used for decades in the interpretation of geologic history, but much

336 Where radiocarbon dates can be obtained at the same depth in a core as tephra layers,
337 deviations of calibrated ages from the known age of a tephra can be used to determine the
338 marine-reservoir age at that location and time (Eiriksson et al., 2004; Kristjansdottir,
339 2005, Jennings et al., 2006). An example is the Vedde Ash, a widely dispersed explosive
340 Icelandic tephra that provides a 12,000-year-old constant-time horizon (an isochron)
341 during the Younger Dryas cold period, when marine reservoir ages are poorly constrained
342 and very different from today's. On the North Iceland shelf, changes in the marine
343 reservoir age are associated with shifts in the Arctic and polar fronts, which have
344 important climatic implications (Eiriksson et al., 2004; Kristjansdottir, 2005). As many as
345 22 tephra layers have been identified in Holocene marine cores off north Iceland
346 (Kristjansdottir et al., 2007). Eiriksson et al. (2004) recovered 10 known-age tephra
347 layers of Holocene age. Some of the Icelandic tephtras have wide geographic distributions
348 either because they were ejected by very large explosive eruptions or because tephra
349 particles were transported on sea ice whereas, nearer to their source, the tephra layers are
350 more numerous and locally distributed. Transport on sea ice may spread the deposition
351 time of a layer to months or years, but the layer will still remain a very short-interval time
352 marker.

353

354 **6.3.2 Measurement of Rates of Change in Terrestrial Records**

355 Terrestrial archives across the Arctic have been tapped to evaluate changes in the
356 climate system in prehistoric times, with particular emphasis on changes in summer
357 temperature, although moisture balance has been addressed in some studies. With
358 sufficient age control, environmental proxies extracted from these archives can be used to

359 evaluate rates of change. Archives that accumulate sediment in a regular and continuous
360 pattern have the highest potential for reconstructing rates of change. The most promising
361 archives are lake sediments and tree rings, both of which add material incrementally over
362 time. Long-lived trees reach only to the fringes of the Arctic, so most reconstructions rely
363 on climate proxies preserved in the sediments that accumulate in lake basins. Trees do
364 extend to relatively high latitudes in Alaska and portions of the Eurasian Arctic, where
365 they contribute high-resolution, usually annually resolved, paleoclimate records of the
366 past several centuries, but they rarely exceed 400 years duration (Overpeck et al., 1997).
367 The steady accumulation of calcium carbonate precipitates in caves may also provide a
368 continuous paleoenvironmental record (Lauritzen and Lundberg, 2004), although these
369 archives are relatively rare in the Arctic. This overview focuses on how well we can
370 reconstruct times of rapid change in terrestrial sediment archives from the Arctic,
371 focusing on changes that occurred on time scales of decades to centuries during the past
372 150,000 years or so, the late Quaternary.

373 Much of the terrestrial Arctic was covered by continental ice sheets during the last
374 glacial maximum (until about 15 ka), and large areas outside the ice sheet margins were
375 too cold for lake sediment to accumulate. Consequently, most lake records span the time
376 since deglaciation, typically the past 10,000 to 15,000 years. In a few Arctic regions,
377 longer, continuous lacustrine records more than 100,000 years long have been recovered,
378 and these rare records provide essential information about past environments and about
379 rates of change in the more distant past (e.g., (Lozhkin and Anderson, 1995; Brubaker et
380 al., 2005; Hu et al., 2006; Brigham-Grette et al., 2007). In addition to these continuous
381 records, discontinuous lake-sediment archives are found in formerly glaciated regions.

382 These sites provide continuous records spanning several millennia through past warm
383 times. In special settings, usually where the over-riding ice was very cold, slow-moving,
384 and relatively thin, lake basins have preserved past sediment accumulations intact,
385 despite subsequent over-riding by ice sheets during glacial periods (Miller et al., 1999;
386 Briner et al., 2007).

387 The rarity of terrestrial archives that span the last glaciation hampers our ability to
388 evaluate how rapid, high-magnitude changes seen in ice-core records (Dansgaard-
389 Oeschger, or D-O events) and marine sediment cores (Heinrich, or H events) are
390 manifested in the terrestrial arctic environment.

391

392 **6.3.2a Climate indicators and ages**

393 Deciphering rates of change from lake sediment, or any other geological archive,
394 requires a reliable environmental proxy and a secure geochronology.

395 Climate and environmental proxies: Most high-latitude biological proxies record
396 peak or average summer air temperatures. The most commonly employed
397 paleoenvironmental proxies are biological remains, particularly pollen grains and the
398 siliceous cell walls (frustules) of microscopic, unicellular algae called diatoms, which
399 preserve well and are very abundant in lake sediment. In a summary of the timing and
400 magnitude of peak summer warmth during the Holocene across the North American
401 Arctic, Kaufman et al. (2004) noted that most records rely on pollen and plant
402 microfossils to infer growing-season temperature of terrestrial vegetation. Diatom
403 assemblages primarily reflect changes in water chemistry, which also carries a strong
404 environmental signal. More recently, biological proxies have expanded to include larval

405 head capsules of non-biting midges (chironomids) that are well preserved in lake
406 sediment. The distribution of the larval stages of chironomid taxa exhibit a strong
407 summer-temperature dependence in the modern environment (Walker et al., 1997), which
408 allows fossil assemblages to be interpreted in terms of past summer temperatures.

409 In addition to biological proxies that provide information about past
410 environmental conditions, a wide range of physical and geochemical tracers also provide
411 information about past environments. Biogenic silica (mostly produced by diatoms),
412 organic carbon (mostly derived from the decay of aquatic organisms), and the isotopes of
413 carbon and nitrogen in the organic carbon residues can be readily measured on small
414 volumes of sediment, allowing the generation of closely spaced data—a key requirement
415 for detecting rapid environmental change. Some lakes have sufficiently high levels of
416 calcium and carbonate ions that calcium carbonate precipitates in the sediment. The
417 isotopes of carbon and oxygen extracted from calcium carbonate deposits in lake
418 sediment offer proxies of past temperatures and precipitation, and they have been used to
419 reconstruct times of rapid climate change at high latitudes (e.g., Hu et al., 1999b).

420 Promising new developments in molecular biomarkers (Hu et al., 1999a; Sauer et
421 al., 2001; Huang et al., 2004; D’Andrea and Huang, 2005) offer the potential of a wide
422 suite of new climate proxies that might be measured at relatively high resolution as
423 instrumentation becomes increasingly automated.

424 Dating lake sediment: In addition to the extraction of paleoenvironmental proxies
425 at sufficient resolution to identify rapid environmental changes in the past, a secure
426 geochronology also must be developed for the sedimentary archive. Methods for
427 developing a secure depth-age relationship generally falls into one of three categories:

428 direct dating, identification of key stratigraphic markers dated independently at other
429 sites, and dating by correlation with an established record elsewhere. Much similarity
430 exists between the techniques applied in lakes and in marine environments, although
431 some differences do exist.

432 Direct dating: The strengths and weaknesses of various dating methods applied to
433 Arctic terrestrial archives have been reviewed recently (Abbott and Stafford, 1996;
434 Oswald et al., 2005; Wolfe et al., 2005). Radiocarbon is the primary dating method for
435 archives dating from the past 15,000 years and sometimes beyond, although conditions
436 endemic to the Arctic (and described next) commonly prevent application of the
437 technique back as far as 40,000 to 50,000 years, the limit achieved elsewhere. The
438 primary challenge to accuracy of radiocarbon dates in Arctic lakes is the low primary
439 productivity of both terrestrial and aquatic vegetation throughout most of the Arctic,
440 coupled with the low rate at which organic matter decomposes on land. These two factors
441 work together so that dissolved organic carbon incorporated into lake sediment contains a
442 considerable proportion of material that grew on land, was stored on land for long times,
443 and was then washed into the lake. The carbon in this terrestrial in-wash is much older
444 than the sediment in which it is deposited, and it produces dissolved-organic-carbon ages
445 that are anomalously old by centuries to millennia (Wolfe et al., 2005). Dissolved organic
446 carbon contains many compounds, including humic acids; these acids tend to have the
447 lowest reservoir ages among the compounds and so are most often targeted when no other
448 options are available.

449 The large and variable reservoir age of dissolved organic carbon has led most
450 researchers to avoid it for dating, and instead they concentrate on sufficiently large,

451 identifiable organic remains such as seeds, shells, leaves, or other materials, typically
452 called macrofossils. Macrofossils of things living on land, such as land plants, almost
453 always yield accurate radiocarbon ages because the carbon in the plant was fully and
454 recently exchanged (equilibrated) with the atmosphere. Similarly, aquatic plants are
455 equilibrated with the carbon in the lake water, which for most lakes is equilibrated with
456 the atmosphere. However, some lakes contain sufficient calcium carbonate, which
457 typically contains old carbon not equilibrated with the atmosphere, such that the ^{14}C
458 activity of the lake water is not in equilibrium with the atmosphere, a fundamental
459 assumption for accurate radiocarbon dating. In these settings, known as hard-water lakes,
460 macrofossils of terrestrial origin are targeted for dating. In lakes without this hard-water
461 effect, either terrestrial or aquatic macrofossils may be targeted. Although macrofossil
462 dates have been shown to be more reliable than bulk-carbon dates in Arctic lakes, in
463 many instances terrestrial macrofossils washed into lake basins are derived from stored
464 reservoirs (older rocks or sediments) in the landscape and have radiocarbon ages
465 hundreds of years older than the deposition of the enclosing lake sediments.

466 For young sediment (20th century), the best dating methods are ^{210}Pb (age range
467 of about 100–150 years) and identification of the atmospheric nuclear testing spike of the
468 early 1960s, usually either with peak abundances of ^{137}Cs , $^{239,240}\text{Pu}$ or ^{241}Am . These
469 methods usually provide high-precision age control for sediments deposited within the
470 past century.

471 Some lakes preserve annual laminations, owing to strong seasonality in either
472 biological or physical parameters. If laminations can be shown to be annual, chronologies
473 can be derived by counting the number of annual laminations, or varves (Francus et al.,

474 2002; Hughen et al., 1996; Snowball et al., 2002).

475 For late Quaternary sediments beyond the range of radiocarbon dating, dating
476 methods include optically stimulated luminescence (OSL) dating, amino acid
477 racemization (AAR) dating, cosmogenic radionuclide (CRN) dating, uranium-series
478 disequilibrium (U-series) dating and, for volcanic sediment, potassium-argon or argon-
479 argon (K-Ar or $^{40/39}\text{Ar}$) dating (e.g., Bradley, 1999; Cronin, 1999). With the exception of
480 U-series dating, none of these methods has the precision to accurately date the timing of
481 rapid changes directly. But these methods are capable of defining the time range of a
482 sediment package and, if reasonable assumptions can be made about sedimentation rates,
483 then the rate at which measured proxies changed can be derived within reasonable
484 uncertainties. U-series dating has stringent depositional-system requirements that must be
485 met to be applicable. For the terrestrial realm, calcium carbonate accumulations
486 precipitated in a regular fashion in caves (flowstones, stalagmites, stalactites) offer the
487 optimal materials. In these instances, high-precision ages can be derived for the entire
488 Late Quaternary time period.

489 Stratigraphic markers: As noted in the previous subsection, the Arctic includes
490 major centers of volcanism in the North Atlantic (Iceland) and the North Pacific (Alaska
491 and Kamchatka) sectors. Explosive volcanism from both regions can produce large
492 volumes of source- and time-diagnostic tephra distributed extensively across the Arctic.
493 These tephra layers provide time-synchronous marker horizons that can be used to
494 constrain the geochronology of lacustrine sediment records. The tephra layers can also
495 serve to precisely synchronize records derived from lacustrine, marine, and ice-sheet
496 archives, thereby allowing a better assessment of leads and lags in the climate system and

497 the phasing of abrupt changes identified in different archives. Most tephras have
498 diagnostic geochemical signatures that allow them to be securely identified with a source
499 and, with modest age constraints, to a given eruptive event. If that event is well dated in
500 regions near the source, such tephras then become dating tools in a technique known as
501 tephrochronology.

502 As indicated in section 6.3.1, systematic centennial to millennial changes in
503 Earth's magnetic field (paleomagnetic secular variation) (Fig. 6.2) have been used to
504 correlate between several high-latitude lacustrine sedimentary archives and between
505 marine and lacustrine records in the same region (Snowball et al., 2007; Stoner et al.,
506 2007). Lacustrine records of paleomagnetic secular variation calibrated with varved
507 sediments have been used for dating in Scandinavia (Saarinen, 1999; Ojala and Tiljander,
508 2003; Snowball and Sandgren, 2004)]. Recent work on marine sediments suggests that
509 paleomagnetic secular variation can provide a useful means of correlating marine and
510 terrestrial records.

511 “Wiggle matching”: In some instances, very high resolution down-core analytical
512 profiles from sedimentary archives with only moderate age constraints can be
513 conclusively correlated with a well-dated high-resolution record at a distant locality, such
514 as Greenland ice core records, with little uncertainty. Although the best examples of such
515 correlations are not from the Arctic (e.g., Hughen et al., 2004a), this method remains a
516 potential tool for providing age control for Arctic lake sediment records.

517

518 **6.3.2b Potential for reconstructing rates of environmental change in the**
519 **terrestrial Arctic**

520 A goal of paleoclimate research is to understand rapid changes on human time
521 scales of decades to centuries. The major challenges in meeting this goal for the Arctic
522 include uncertainties in the time scales of terrestrial archives and in the interpretation of
523 various environmental proxies. Although uncertainties are widespread in both aspects,
524 neither presents a fundamental impediment to the primary goal, quantifying rates of
525 change.

526 Precision versus accuracy: Many Arctic lake archives are dated with high
527 precision, but with greater uncertainty in their accuracy. One can say, for example, that a
528 particular climate change recorded in a section of core occurred within a 500-year
529 interval with little uncertainty, but the exact age of the start and end of that 500-year
530 interval are much less certain. This uncertainty is due to systematic errors in the
531 proportion of old carbon incorporated into the humic acid fraction of the dissolved
532 organic carbon used to date the lake sediment. Although this fraction, or “reservoir age,”
533 varies through the Holocene, changes in the reservoir age occur relatively slowly.

534 Figure 6.3 shows a segment of a sediment core from the eastern Canadian Arctic,
535 for which six humic acid dates define an age-depth relation with an uncertainty of only
536 ± 65 years, but the humic acid ages are systematically 500–600 years too old. In this
537 situation, rates of change for decades to centuries can be calculated with confidence,
538 although determining whether a rapid change at this site correlated with a rapid change
539 elsewhere is much less certain owing to the large uncertainty in the accuracy of the humic
540 acid dates.

541

542

FIGURE 6.3 NEAR HERE

543

544 Figure 6.4 similarly provides an example of rapid change in an environmental
545 proxy in an Arctic lake sediment core, for which the rate of change can be estimated with
546 certainty, but the timing of the change is less certain.

547

548

FIGURE 6.4 NEAR HERE

549

550 **6.3.3 Measurement of Rates of Change in Ice-Core Records**

551 Ice-core records have figured especially prominently in the discussion of rates of
552 change during the time interval for which such records are available. One special
553 advantage of ice cores is that they collect climate indicators from many different regions.
554 In central Greenland, for example, the dust trapped in ice cores has been isotopically and
555 chemically fingerprinted: it comes from central Asia (Biscaye et al., 1997), the methane
556 has widespread sources in Arctic and in low latitudes (e.g., Harder et al., 2007), and the
557 snowfall rate and temperature are primarily local indicators (see review by Alley, 2000).
558 This aspect of ice-core records allows one to learn whether climate in widespread regions
559 changed at the same time or different times and to obtain much better time resolution
560 than is available by comparing individual records and accounting for the associated
561 uncertainties in their dating.

562 Ice cores also exhibit very high time resolution. In many Greenland cores,
563 individual years are recognized so that sub-annual dating is possible. Some care is needed
564 in the interpretation. For example, the template for the history of temperature change in
565 an ice core is typically the stable-isotope composition of the ice. (The calibration of this

566 template to actual temperature is achieved in various ways, as discussed in chapter 7, but
567 the major changes in the isotopic ratios correlate with major changes in temperature with
568 very high confidence, as discussed there.) However, owing to post-depositional processes
569 such as diffusion in **firn** and ice (Johnsen, 1977; Whillans and Grootes, 1985; Cuffey and
570 Steig, 1998; Johnsen et al., 2000), the resolution of the isotope records does decrease with
571 increasing age and depth. Initially the decrease is due to processes in the porous firn, and
572 later it is due to more rapid diffusion in the warmer ice close to the bottom of the ice
573 sheet. The isotopic resolution may reveal individual storms shortly after deposition but be
574 smeared into several years in ice tens of thousands of years old. Normally in Greenland,
575 accumulation rates of less than about 0.2 m/yr of ice are insufficient to preserve annual
576 cycles for more than a few decades; higher accumulation rates allow the annual layers to
577 survive the transformation of low-density snow to high-density ice, and the cycles then
578 survive for millennia before being gradually smoothed.

579 Records of dust concentration appear to be almost unaffected by smoothing
580 processes, but some chemical constituents seem to be somewhat mobile and thus to have
581 their records smoothed over a few years in older samples (Steffensen et al., 1997;
582 Steffensen and Dahl-Jensen, 1997). Unfortunately, despite important recent progress
583 (Rempel and Wettlaufer, 2003), the processes of chemical diffusion are not as well
584 understood as are isotopic ratios, so confident modeling of the chemical diffusion is not
585 possible and the degree of smoothing is not as well quantified as one would like.
586 Persistence of relatively sharp steps in old ice that is still in normal stratigraphic order
587 demonstrates that the diffusion is not extensive. The high-resolution features of the dust
588 and chemistry records have been used to date the glacial part of the GISP2 core by using

589 mainly annual cycles of dust (Meese et al., 1997) and the NGRIP core by using annual
590 layers in different ionic constituents together with the visible dust layers (cloudy bands;
591 Fig. 6.5) back to 42 ka (Andersen et al., 2006, Svensson et al., 2006). Figure 6.5 shows
592 the visible cloudy bands in a 72 ka section of the NGRIP core. The cloudy bands are
593 generally assumed to be due to tiny gas bubbles that form on dust particles as the core is
594 brought to surface. During storage of core in the laboratory, these bands fade somewhat.
595 However, the very sharp nature of the bands when the core is recovered suggests that
596 diffusive smoothing has not been important, and that high-time-resolution data are
597 preserved.

598

599 **FIGURE 6.5 NEAR HERE**

600

601 **6.4 Classes of Changes and Their Rates**

602

603 The day-to-night and summer-to-winter changes are typically larger—but have
604 less persistent effect on the climate—than long-lived features such as ice ages. This
605 observation suggests that it is wise to separate rates of change on the basis of persistence.
606 As discussed in section 4.2 on forcings, effects from the aging of the Sun can be
607 discounted on “short” time scales of 100 m.y. or less, but many other forcings must be
608 considered. Several are discussed below. For the last ice-age cycle, special reliance is
609 placed on Greenland ice-core records because of their high time resolution and confident
610 paleothermometry. But Greenland is only a small part of the whole Arctic, and this
611 limitation should be borne in mind.

612

613 **6.4.1 Tectonic Time Scales**

614 As discussed in section 4.2 on forcings, drifting continents and related slow shifts
615 in global biogeochemical cycling, together with evolving life forms, can have profound
616 local and global effects on climate during tens of millions of years. If a continent moves
617 from equator to pole, the climate of that continent will change greatly. In addition, by
618 affecting ocean currents, ability to grow ice sheets, cloud patterns, and more, the moving
619 continent may have an effect on global and regional climates as well, although this effect
620 will in general be much more subtle than the effect on the continent's own climate (e.g.,
621 Donnadieu et al., 2006).

622 Within the last tens of millions of years, the primary direct effect of drifting
623 continents on the Arctic probably has been to modify the degree to which the Arctic
624 Ocean connects with the lower latitudes, by altering the “gateways” between land masses.
625 The Arctic Ocean, primarily surrounded by land masses, has persisted throughout that
626 time (Moran et al., 2006). Much attention has been directed to the possibility that the
627 warmth of the Arctic during certain times, such as the Eocene (which began about 50
628 Ma), was linked to increased transport of ocean heat as compared with other, colder
629 times. However, both models and data indicate that this possibility appears unlikely (e.g.,
630 Bice et al., 2000). The late Eocene Arctic Ocean appears to have supported a dense
631 growth of pond weed (*Azolla*), which is understood to grow in brackish waters (those
632 notably fresher than full marine salinity) (Moran et al., 2006). A more-vigorous ocean
633 circulation then would have introduced fully marine waters and would have transported
634 the pond weed away. A great range of studies indicates that larger atmospheric carbon-

635 dioxide concentrations during that earlier time were important in causing the warmth
636 (Royer et al., 2007).

637 The Arctic of about 50 Ma appears to have been ice free, at least near sea level,
638 and thus minimum wintertime temperatures must have been above freezing. Section 7.3.1
639 includes some indications of temperatures in that time, with perhaps 20°C a useful
640 benchmark for Arctic-wide average annual temperature. Recent values are closer to –
641 15°C, which would indicate a cooling of roughly 35°C within about 50 m.y. The implied
642 rate is then in the neighborhood of 0.7°C/million years or 0.0000007°C/yr. One could
643 pick time intervals during which little or no change occurred, and intervals within the last
644 50 m.y. during which the rate of change was somewhat larger; a “tectonic” value of about
645 1°C/million years or less may be useful.

646

647 **6.4.2 Orbital Time Scales**

648 As described in section 4.3 on forcings, features of Earth’s orbit cause very small
649 changes in globally averaged incoming solar radiation (insolation) but large changes
650 (more than 10%) in local sunshine. These orbital changes serve primarily to move
651 sunshine from north to south and back or from poles to equator and back, depending on
652 which of the orbital features is considered. The leading interpretation (e.g., Imbrie et al.,
653 1993) is that ice sheets grow and the world enters an ice age when reduced summer
654 sunshine at high northern latitudes allows survival of snow without melting; ice sheets
655 melt, and the world exits an ice age, when greater summer sunshine at high northern
656 latitudes melts snow there. Because the globally averaged forcing is nearly zero but the
657 globally averaged response is large (e.g., Jansen et al., 2007), the Earth system must have

658 strong amplifying processes (feedbacks). Changes in greenhouse-gas concentrations
659 (especially carbon dioxide), how much of the Sun's energy is reflected (ice-albedo
660 feedback, plus some changes in vegetation), and blocking of the Sun by dust are
661 prominent in interpretations, and all appear to be required to explain the size and pattern
662 of the reconstructed changes (Jansen et al., 2007).

663 The globally averaged change from ice-age to interglacial is typically estimated as
664 $5^{\circ}\text{--}6^{\circ}\text{C}$ (e.g., Jansen et al., 2007). Changes in the Arctic clearly were larger. In central
665 Greenland, typical glacial and interglacial temperatures differed by about 15°C , and the
666 maximum warming from the most-recent ice age was about 23°C (Cuffey et al., 1995).
667 Very large changes occurred where ice sheets grew during the ice age and melted during
668 the subsequent warming, related to the cooling effect of the higher elevation of the ice
669 sheets, but the elevation change is not the same as a climatic effect.

670 In central Greenland, the coldest time of the ice age was about 24 ka, although as
671 discussed in chapter 7, some records place the extreme value of the most recent ice age
672 slightly more recently. Kaufman et al. (2004) analyzed the timing of the peak warmth of
673 the Holocene throughout broad regions of the Arctic; near the melting ice sheet on North
674 America, peak warmth was delayed until most of the ice was gone, whereas far from the
675 ice sheet peak warmth was reached before 8 ka, in some regions by a few millennia.

676 A useful order-of-magnitude estimate may be that the temperature change
677 associated with the end of the ice age was about 15°C in about 15 thousand years (k.y.) or
678 about $1^{\circ}\text{C}/\text{k.y.}$ or $0.001^{\circ}\text{C}/\text{yr}$, and peak rates were perhaps twice that. The ice-age cycle
679 of the last few hundred thousand years is often described as consisting of about 90 k.y. of
680 cooling followed by about 10 k.y. of warming, or something similar, implying faster

681 warming than cooling (see Fig. 7.9). Thus, rates notably slower than $1^{\circ}\text{--}2^{\circ}\text{C/ka}$ are
682 clearly observed at times.

683 Kaufman et al. (2004) indicated that the warmest times of the current or Holocene
684 interglacial (MIS 1) in the western-hemisphere part of the Arctic were, for average land,
685 $1.6 \pm 0.8^{\circ}\text{C}$ above mean 20th-century values. Warmth peaked before 12 ka in western
686 Alaska but after 3 ka in some places near Hudson Bay; a typical value is near 7–8 ka.
687 Thus, the orbital signal during the Holocene has been less than or equal to approximately
688 0.2°C/ka , or $0.0002^{\circ}\text{C/yr}$.

689

690 **6.4.3 Millennial or Abrupt Climate Changes**

691 Exceptional attention has been focused on the abrupt climate changes recorded in
692 Greenland ice-cores and in many other records from the most recent ice age and earlier
693 (see National Research Council, 2002; Alley et al., 2003; Alley, 2007).

694 The more recent of these changes has been well known for decades from many
695 studies primarily in Europe that worked with lake and bog sediments and the moraines
696 left by retreating ice sheets. However, most research focused on the slower ice-age
697 cycles, which were easier to study in paleoclimatic archives.

698 The first deep ice core through the Greenland ice sheet, at Camp Century in 1966,
699 produced a $\delta^{18}\text{O}$ isotope profile that showed unexpectedly rapid and strong climatic shifts
700 through the entire last glacial period (Dansgaard et al., 1969; 1971; Johnsen et al., 1972).
701 The fastest observed sharp transitions from cold to warm seemed to have been on the
702 time scale of centuries, clearly much faster than **Milankovitch time scales**.

703 These results did not stimulate much additional research immediately; the record
704 lay close to the glacier bed, and it may be that many investigators suspected that the
705 records had been altered by ice-flow processes. There were, however, data from quite
706 different archives pointing to the same possibility of large and rapid climate change. For
707 example, the Grand Pile pollen profile (Woillard, 1978; Woillard, 1979) showed that the
708 last interglacial (MIS 5) ended rapidly during an interval estimated at 150 ± 75 yrs,
709 comparable to the Camp Century findings. The Grand Pile pollen data also pointed to
710 many sharp warming events during the last ice age.

711 The next deep core in Greenland at the Dye-3 radar station was drilled by the
712 United States, Danish, and Swiss members of the Greenland Ice Sheet Program
713 (Dansgaard et al., 1982). The violent climatic changes, as Willi Dansgaard termed them,
714 matched the often-ignored Camp Century results. The cause for these strong climatic
715 oscillations had already been hinted at by Ruddiman and Glover (1975) and Ruddiman
716 and McIntyre (1981), who studied oceanic evidence for the large climatic oscillations
717 involving strong warming into the Bolling interval, cooling into the Younger Dryas, and
718 warming into the Preboreal. They assigned the cause for these strong climatic anomalies
719 to thermohaline circulation changes combined with strong zonal winds partly driving the
720 surface currents in the north Atlantic; these forces drove sharp north-south shifts of the
721 polar front. In light of the ice core data, the oscillations around the Younger Dryas were
722 part of a long row of similar events, which Dansgaard et al. (1984) and Oeschger et al.
723 (1984) likewise assigned to circulation changes in the north Atlantic. Broecker et al.
724 (1985) argued for bi-stable North Atlantic circulation as the cause for the Greenland
725 climatic jumps.

726 The results of the Dye-3 core went a long way toward settling the issue of the
727 existence of abrupt climate change. Further results from year-by-year ice sampling during
728 the Younger Dryas warming from this same core pushed the definition of “abrupt” from
729 the century time scale to the decadal and nearly annual scale (Dansgaard et al., 1989).
730 Alley et al. (1993) suggested the possibility that much of an abrupt change was
731 completed in a single year for at least one climatic variable (snow accumulation at the
732 GISP2 site).

733 In addition to the GISP2, GRIP, and DYE-3 cores, ice core evidence has been
734 strengthened by new deep ice cores at Siple Dome in West Antarctica and North-GRIP in
735 northern Greenland. New high-resolution measurement techniques have provided
736 subannual resolution for several parameters, and these data have been used for the North-
737 GRIP core to provide absolute dating, the GICC05 chronology, back to 60 ka (Svensson
738 et al., 2005; Rasmussen et al., 2006; Vinther et al., 2006). The GISP2 and GRIP ice cores
739 have also been synchronized with the North-GRIP core through MIS 2 (Rasmussen et al.,
740 2006; in press).

741 The temperature shifts into the warm intervals in the millennial climate changes,
742 which are called interstadials (Johnsen et al., 1992; Dansgaard et al., 1993), have been
743 found to vary from 10° to 16°C on the basis of borehole thermometry (Cuffey et al.,
744 1995; Johnsen et al., 1995; Jouzel et al., 1997) and of studies of the isotopic effect of
745 thermal **firn** diffusion on gas isotopes (Severinghaus et al., 1998; Lang et al., 1999;
746 Leuenberger et al., 1999; Landais et al., 2004; Huber et al., 2006).

747 The North-GRIP core, the most recent of the Greenland deep cores and the one on
748 which the most effort was expended in counting annual layers, shows that typically the

749 rapid warmings into interstadials are recorded as increases in only 20 years in the 20-year
750 averages of isotopic values during MIS 2 and MIS 3; this information indicates
751 temperature changes of 0.5°C/yr or faster.

752 In the Holocene period, the approximately 160-year-long cold event about 8.2 ka,
753 which produced 4°–5°C cooling in Greenland (Leuenberger et al., 1999), began in less
754 than 20 years, and perhaps much less. The cooling is believed to have been caused by the
755 emptying of Lake Agassiz (reviewed by Alley and Agustsdottir, 2005), and the rapid
756 transitions found bear witness to the dynamic nature of the North Atlantic circulation in
757 jumping to a new mode.

758 The Younger Dryas and the 8.2 ka cold event (section 7.3.5a) are well known in
759 Europe and in Arctic regions, but they appear to have been much weaker or absent in
760 other Arctic regions (see reviews by Alley and Agustsdottir (2005) and Alley (2007);
761 note that strong signals of these events are found in some but not all lower-latitude
762 regions). The signal of the Younger Dryas did extend across the Arctic to Alaska (see
763 Peteet, 1995a,b; Hajdas et al., 1998). Lake sediment records from the eastern Canadian
764 Arctic contain evidence for both excursions (Miller et al., 2005).

765 The 8.2 ka event is recorded at two sites as a notable readvance of cirque glaciers
766 and outlet glaciers of local ice caps at $8,200 \pm 100$ years (Miller et al., 2005). In some
767 lakes not dominated by runoff of meltwater from glaciers, a reduction in primary
768 productivity is apparent at the same time. These records suggest that colder summers
769 during the event without a dramatic reduction in precipitation produced positive mass
770 balances and glacier re-advances. For most local glaciers, this readvance was the last
771 important one before they receded behind their Little Ice Age margins. Organic carbon

772 accumulation in a West Greenland lake sediment record suggests a decrease in biotic
773 productivity synchronous with the negative $\delta^{18}\text{O}$ excursion in the GRIP ice core
774 (Willemse and Törnqvist, 1999).

775 Few Arctic lakes contain records that extend through Younger Dryas time. And
776 despite the strong signal indicative of rapid, dramatic Younger Dryas cooling in
777 Greenland ice cores, no definitive records document or refute accompanying glacier
778 expansion or cold around the edge of the Greenland ice sheet (Funder and Hansen, 1996;
779 Björck et al., 2002) (discussed in chapter 7), near Svalbard (Svendson and Mangerud,
780 1992), or in Arctic Canada (Miller et al., 2005). These observations are consistent with
781 the joint observations that the events primarily occurred in wintertime, whereas most
782 paleoclimatic indicators are more sensitive to summertime conditions. Moreover, the
783 events manifested primarily in the North Atlantic and surroundings, and their amplitude
784 was reduced away from the North Atlantic (Denton et al., 2005; Alley, 2007; also see
785 Björck et al., 2002). This means in turn that the rate of climate change associated with
786 these events, although truly spectacular in the north Atlantic, was much smaller
787 elsewhere (poorly constrained, but perhaps only one-tenth as large in many parts of the
788 Arctic, and a region of zero temperature change somewhere on the planet separated the
789 northern regions of cooling from the southern regions of weak warming). The globally
790 averaged signal in temperature change was weak, although in some regions rainfall seems
791 to have changed very markedly (e.g., Cai et al., 2008).

792

793 **6.4.4 Higher-Frequency Events Especially in the Holocene**

794 The Holocene record, although showing greatly muted fluctuations in temperature

795 as compared with earlier times, is not entirely without variations. As noted above, a slow
796 variation during the Holocene is linked with orbital forcing and decay of the great ice
797 sheets. Riding on the back of this variation are oscillations of roughly 1°C or less, at
798 various temporal spacings. Great effort has been expended in determining what is signal
799 versus noise in these records, because the signals are so small, and issues of whether
800 events are broadly synchronous or not become important.

801 A few rather straightforward conclusions can be stated with some confidence. Ice-
802 core records from Greenland show the forcing and response of individual volcanic
803 eruptions. A large explosive eruption caused a cooling of roughly 1°C in Greenland, and
804 the cooling and then warming each lasted roughly 1 year (Grootes and Stuiver, 1997;
805 Stuiver et al., 1997), although a cool “tail” lasted longer. Thus, the temperature changes
806 associated with volcanic eruptions are strong, 1°C/year, but not sustained. Because
807 volcanic eruptions are essentially random in time, accidental clustering in time can
808 influence longer term trends stochastically.

809 The possible role of solar variability in Holocene changes (and in older changes;
810 e.g., Braun et al., 2005) is of considerable interest. Ice-core records are prominent in
811 reconstruction of solar forcing (e.g., Bard et al., 2007; Muscheler et al., 2007).
812 Identification of climate variability correlated with solar variability then allows
813 assessment of the solar influence and the rates of change caused by the solar variability.

814 Much study has focused on the role of the Sun in the oscillations within the
815 interval from the so-called Medieval Warm Period through the Little Ice Age and the
816 subsequent warming to recent conditions. The reader is especially referred to Hegerl et al.
817 (2007). In Greenland, the Little Ice Age–Medieval Warm Period oscillation had an

818 amplitude of roughly 1°C. Attribution exercises show that much of this amplitude can be
819 explained by volcanic forcing in response to the changing frequency of large eruptions
820 (Hegerl et al., 2007). In addition, some of this temperature change might reflect oceanic
821 changes (Broecker, 2000; Renssen et al., 2006), but some fraction is probably attributable
822 to solar forcing (Hegerl et al., 2007). Although the time from Medieval Warm Period to
823 Little Ice Age to recent warmth is about 1 millennium, there are warmings and coolings
824 in that interval that suggest that the changes involved are probably closer to 1°C/century;
825 some fraction of that change is attributable to solar forcing and some to volcanic and
826 perhaps to oceanic processes. Because recent studies tend to indicate greater importance
827 for volcanic forcing than for solar forcing (Hegerl et al., 2007), changes of 0.3°C/century
828 may be a reasonable estimate of an upper limit for the solar forcing observed (but with
829 notable uncertainty). Weak variations of the ice-core isotopic ratios that correlate with the
830 sunspot cycles and other inferred solar periodicities similarly indicate a weak solar
831 influence (Stuiver et al., 1997; Grootes and Stuiver, 1997). Whether a weak solar
832 influence acting on millennial time scales is evident in poorly quantified paleoclimatic
833 indicators (Bond et al., 2001) remains a hotly debated topic. The ability to explain the
834 Medieval Warm Period–Little Ice Age oscillation without appeal to such a periodicity
835 and the evidently very small role of any solar forcing in those events largely exclude a
836 major role for such millennial oscillations in the Holocene.

837 The warming from the Little Ice Age extends into the instrumental record,
838 generally consistent with the considerations above. In the reconstruction of Delworth and
839 Knutson (2000), the Arctic sections show warming of roughly 1°C in the first half of the
840 20th century (and with peak warming rates of twice that average). The warming likely

841 arose from some combination of volcanic, solar, and human (McConnell et al., 2007)
842 forcing, and perhaps some oceanic forcing. The warming was followed by weak cooling
843 and then a similar warming in the latter 20th century (roughly 1°C per 30 years) primarily
844 attributable to human forcing with little and perhaps opposing natural forcing (Hegerl et
845 al., 2007).

846 As noted in section 4.2 on forcings (see above; also see Bard and Delaguye,
847 2008), the lack of correlation between indicators of climate and indicators of past
848 magnetic-field strength, or between indicators of climate and indicators of in-fall rate of
849 extraterrestrial materials, means that any role of these possible forcings must be minor
850 and perhaps truly zero.

851

852 **6.5 Summary**

853

854 The discussion in the previous section produced estimates of peak rates of climate
855 change associated with different causes. These estimates are plotted in a summary
856 fashion in Figure 6.6. As one goes to longer times, the total size of changes increases, but
857 the rate of change decreases. Such behavior is unsurprising; a sprinter changes position
858 very rapidly but does not sustain the rate, so that in a few hours the marathon runner
859 covers more ground. To illustrate this concept, regression lines were added through the
860 tectonic, ice-age, volcano, volcanoes, and solar points; abrupt climate changes and
861 human-caused changes were omitted from this regression because of difficulty in
862 estimating an Arctic-wide value.

863

864 FIGURE 6.6 NEAR HERE

865

866 The local effects of the abrupt climate changes in the North Atlantic are clearly
867 anomalous compared with the general trend of the regression lines, and changes were
868 both large and rapid. These events have commanded much scientific attention for
869 precisely this reason. However, globally averaged, these events are unimpressive: they
870 fall well below the regression lines, thus demonstrating clearly the difference between
871 global and regional behavior. An Arctic-wide assessment would plot closer to the
872 regression lines than do either the local Greenland or global values.

873 Thus far, human influence does not stand out relative to other, natural causes of
874 climate change. However, the projected changes can easily rise above those trends,
875 especially if human influence continues for more than a hundred years and rises above
876 the IPCC “mid-range” A1B scenario. No generally accepted way exists to formally assess
877 the effects or importance of size versus rate of climate change, so no strong conclusions
878 should be drawn from the observations here.

879 The data clearly show that strong natural variability has been characteristic of the
880 Arctic at all time scales considered. The data suggest the twin hypotheses that the human
881 influence on rate and size of climate change thus far does not stand out strongly from
882 other causes of climate change, but that projected human changes in the future may do so.

883 The report here relied much more heavily on ice-core data from Greenland than is
884 ideal in assessing Arctic-wide changes. Great opportunities exist for generation and
885 synthesis of other data sets to improve and extend the results here, using the techniques
886 described in this chapter. If widely applied, such research could remove the over-reliance

887 on Greenland data.

888

888 **Chapter 6 Figure Captions**

889

890 **Figure 6.1** “Weather” versus “climate,” in annual temperatures for the
891 continental United States, 1960–2007. Red lines, trends for 4-year segments that
892 show how the time period affects whether the trend appears to depict warming,
893 cooling, or no change. Various lines show averages of different number of years,
894 all centered on 1990: Dark blue dash, 3 years; dark blue, 7 years; light blue dash,
895 11 years; light blue, 15 years; and green, 19 years. The perceived trend can be
896 warming, cooling, or no change depending on the length of time considered.
897 Climate is normally taken as a 30-year average; all 30-year-long intervals (1960–
898 1989 through 1978–2007) warmed significantly (greater than 95% confidence),
899 whereas only 1 of the 45 possible trend-lines (17 are shown) has a slope that is
900 markedly different from zero with more than 95% confidence. Thus, a climate-
901 scale interpretation of these data indicates warming, whereas shorter-term
902 (“weather”) interpretations lead to variable but insignificant trends. Data from
903 United States Historical Climatology Network,
904 <http://www.ncdc.noaa.gov/oa/climate/research/cag3/cag3.html> (Easterling et al.,
905 1996).

906

907 **Figure 6.2** Paleomagnetic secular variations records (left), tephrochronology
908 records (right), and calibrated radiocarbon ages for cores MD99-2269 and -2322 (center)
909 provide a template for Holocene stratigraphy of the Denmark Straits region (after Stoner
910 et al., 2007, and Kirstjansdottir et al., 2007). Solid lines, tephra horizons in core 2269.

911

912 **Figure 6.3** Precision versus accuracy in radiocarbon dates. Blue circle,
913 accelerated mass spectrometry (AMS) ^{14}C date on the humic acid (HA) fraction of the
914 total dissolved organic carbon (DOC) extracted from a sediment core from the eastern
915 Canadian Arctic. Red circle, AMS ^{14}C date on macrofossil of aquatic moss from 75.6 cm,
916 the same stratigraphic depth as a HA-DOC date. Dashed line is the best estimate of the
917 age-depth model for the core. Samples taken 1–2 cm apart for HA-DOC dates show a
918 systematic down-core trend suggesting that the precision is within the uncertainty of the
919 measurements (± 40 to ± 80 years), whereas the discrepancy between macrofossil and HA-
920 DOC dates from the same stratigraphic depth demonstrates an uncertainty in the accuracy
921 of the HA-DOC ages of nearly 600 years. Data from Miller et al. (1999).

922

923 **Figure 6.4** Down-core changes in organic carbon (measured as loss-on-ignition
924 (LOI)) in a lake sediment core from the eastern Canadian Arctic. At the base of the
925 record, organic carbon increased sharply from about 2% to greater than 20% in less than
926 100 years, but the age of the rapid change has an uncertainty of 500 years. Data are from
927 Briner et al. (2006).

928

929 **Figure 6.5** A linescan image of NGRIP ice core interval 2528.35–2530.0 m
930 depth. Gray layers, annual cloudy bands; annual layers are about 1.5 cm thick. Age of
931 this interval is about 72 ka, which corresponds with Greenland Interstadial 19. (Svensson
932 et al., 2005)

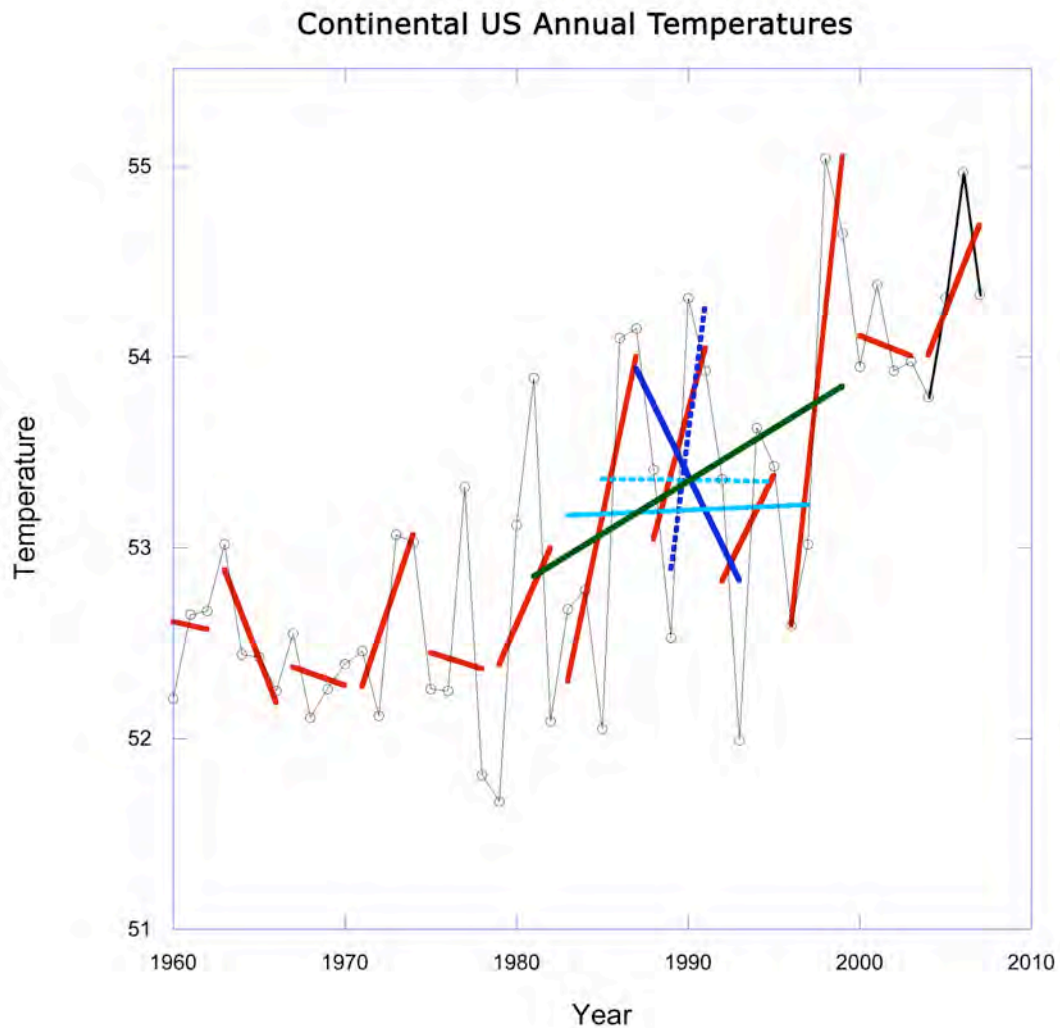
933

934 **Figure 6.6** Summary of estimated peak rates of change and sizes of changes
935 associated with various classes of cause. Error bars are not provided because of difficulty
936 of quantifying them, but high precision is not implied. Both panels have logarithmic
937 scales on both axes (log-log plots) to allow the huge range of behavior to be shown in a
938 single figure. The natural changes during the Little Ice Age–Medieval Warm Period have
939 been somewhat arbitrarily partitioned as 0.6°C for changes in volcanic-eruption
940 frequency (labeled “volcanoes” to differentiate from the effects of a single eruption,
941 labeled “volcano”), and 0.3°C for solar forcing to provide an upper limit on solar causes;
942 a larger volcanic role and smaller solar role would be easy to defend (Hegerl et al., 2007),
943 but a larger solar role is precluded by available data and interpretations. The abrupt
944 climate changes are shown for local Greenland values and for a poorly constrained global
945 estimate of 0.1°C . These numbers are intended to represent the Arctic as a whole, but
946 much Greenland ice-core data have been used in determinations. The instrumental record
947 has been used to assess human effects (see Delworth and Knutson, 2000 and Hegerl et al.,
948 2007). The “human” contribution may have been overestimated and natural fluctuations
949 may have contributed to the late-20th-century change, but one also cannot exclude the
950 possibility that the “human” contribution was larger than shown here and that natural
951 variability offset some of the change. The ability of climate models to explain widespread
952 changes in climate primarily on the basis of human forcing, and the evidence that there is
953 little natural forcing during the latter 20th century (Hegerl et al., 2007), motivate the plot
954 as shown. Also included for scaling is the projection for the next century (from 1980–
955 1999 to 2080–2099 means) for the IPCC SRES A1B emissions scenario (one often
956 termed “middle of the road”) scaled from Figure 10.7 of Meehl et al. (2007); see also

957 Chapman and Walsh (2007). This scenario is shown as the black square labeled A1B; a
958 different symbol shows the fundamental difference of this scenario-based projection from
959 data-based interpretations for the other results on the figure. Human changes could be
960 smaller or larger than shown as A1B, and they may continue to possibly much larger
961 values further into the future. There is no guarantee that human disturbance will end
962 before the end of the 21st century, as plotted here. The regression lines pass through
963 tectonic, ice-age, solar, volcano, and volcanoes; they are included solely to guide the eye
964 and not to imply mechanisms.
965

965

966



967

968

969

970

971

972

973

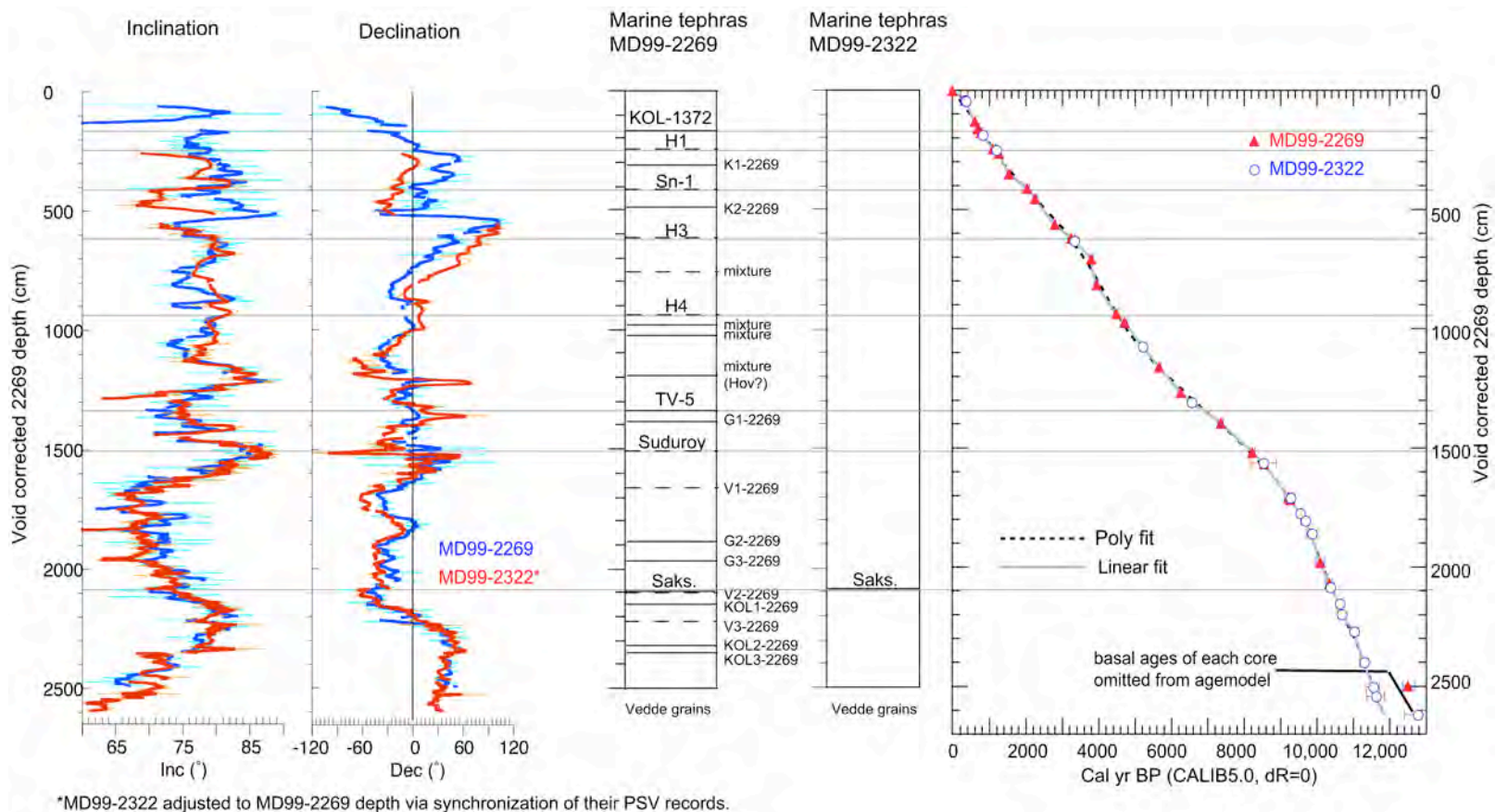
974

975

976

Figure 6.1. A “Weather” versus “climate,” in annual temperatures for the continental United States, 1960–2007. Red lines, trends for 4-year segments that show how the time period affects whether the trend appears to depict warming, cooling, or no change. Various lines show averages of different number of years, all centered on 1990: Dark blue dash, 3 years; dark blue, 7 years; light blue dash, 11 years; light blue, 15 years; and green, 19 years. The perceived trend can be warming, cooling, or no change depending on the length of time considered. Climate is normally taken as a 30-year average; all 30-year-long intervals (1960–1989 through

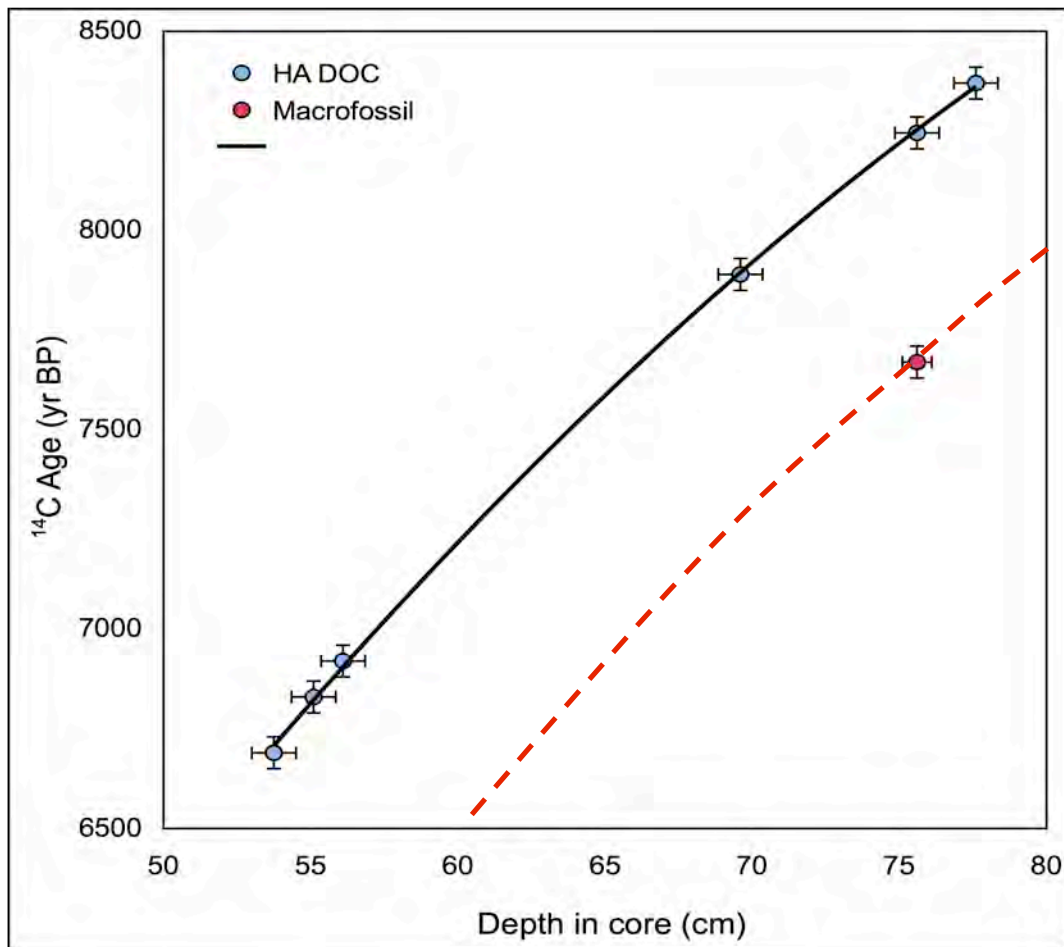
977 1978–2007) warmed significantly (greater than 95% confidence), whereas
978 only 1 of the 45 possible trend-lines (17 are shown) has a slope that is
979 markedly different from zero with more than 95% confidence. Thus, a
980 climate-scale interpretation of these data indicates warming, whereas
981 shorter-term (“weather”) interpretations lead to variable but insignificant
982 trends. Data from United States Historical Climatology Network,
983 <http://www.ncdc.noaa.gov/oa/climate/research/cag3/cag3.html> (Easterling
984 et al., 1996).
985



986

987 **Figure 6.2** Paleomagnetic secular variations records (left), tephrochronology records (right), and calibrated radiocarbon ages for cores
 988 MD99-2269 and -2322 (center) provide a template for Holocene stratigraphy of the Denmark Straits region (after Stoner et al., 2007,
 989 and Kirstjansdottir et al., 2007). Solid lines, tephra horizons in core 2269.

990



991

992

993 **Figure 6.3** Precision versus accuracy in radiocarbon dates. Blue circle, accelerated mass994 spectrometry (AMS) ¹⁴C date on the humic acid (HA) fraction of the total dissolved

995 organic carbon (DOC) extracted from a sediment core from the eastern Canadian Arctic.

996 Red circle, AMS ¹⁴C date on macrofossil of aquatic moss from 75.6 cm, the same

997 stratigraphic depth as a HA-DOC date. Dashed line is the best estimate of the age-depth

998 model for the core. Samples taken 1–2 cm apart for HA-DOC dates show a systematic

999 down-core trend suggesting that the precision is within the uncertainty of the

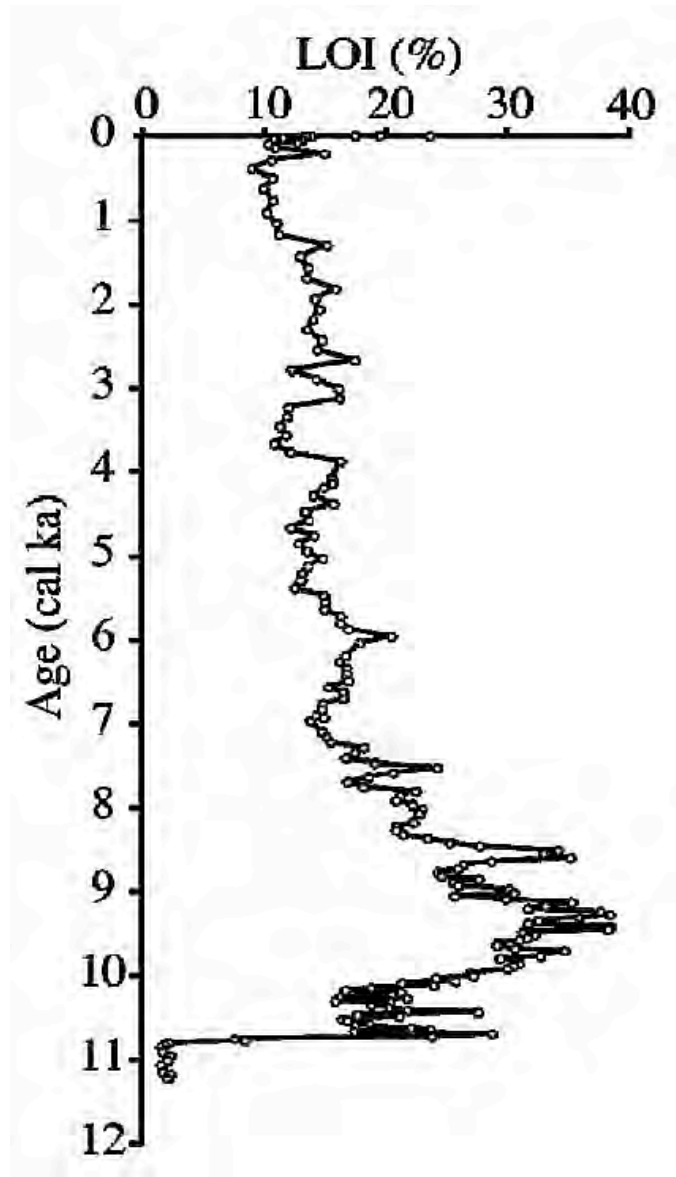
1000 measurements (± 40 to ± 80 years), whereas the discrepancy between macrofossil and HA-

1001 DOC dates from the same stratigraphic depth demonstrates an uncertainty in the accuracy

1002 of the HA-DOC ages of nearly 600 years. Data from Miller et al. (1999).

1003

1003



1004

1005

1006 **Figure 6.4** Down-core changes in organic carbon (measured as loss-on-ignition (LOI)) in
 1007 a lake sediment core from the eastern Canadian Arctic. At the base of the record, organic
 1008 carbon increased sharply from about 2% to greater than 20% in less than 100 years, but
 1009 the age of the rapid change has an uncertainty of 500 years. Data are from Briner et al.
 1010 (2006).

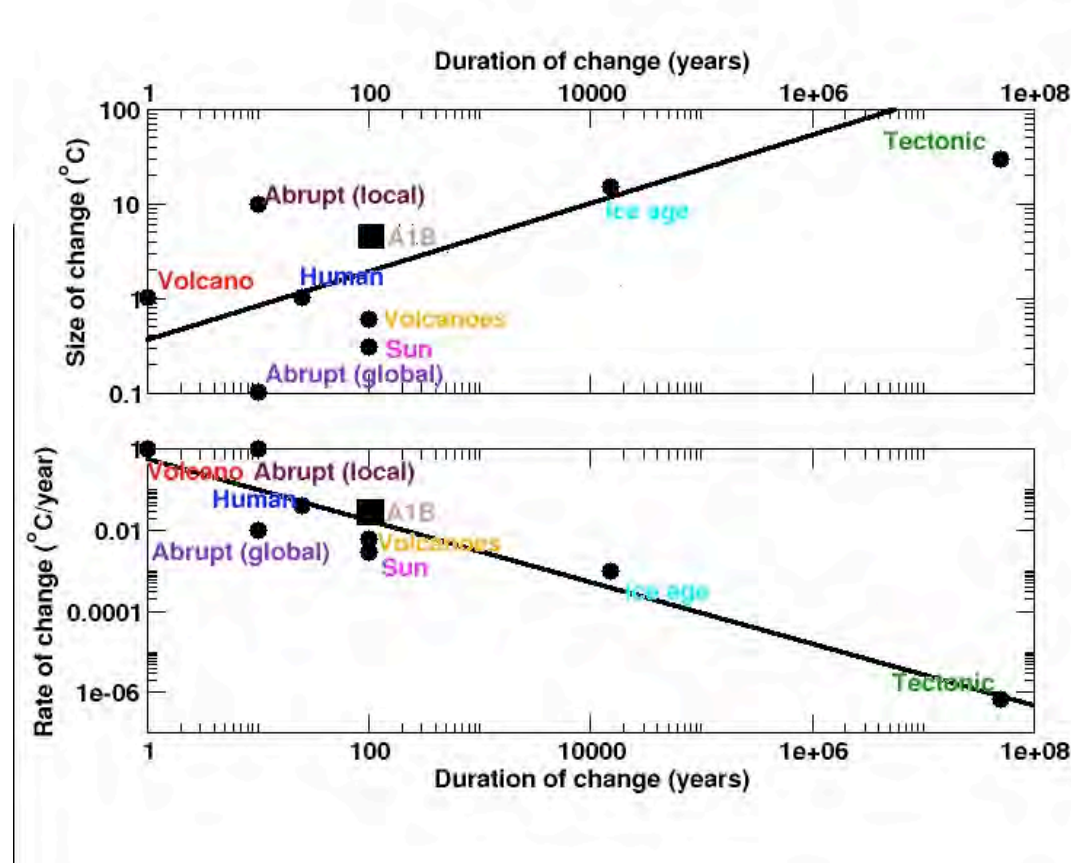
1011
1012
1013
1014
1015
1016
1017



1018

1019 **Figure 6.5.** A linescan image of NGRIP ice core interval 2528.35–2530.0 m depth. Gray layers, annual cloudy bands; annual layers
1020 are about 1.5 cm thick. Age of this interval is about 72 ka, which corresponds with Greenland Interstadial 19. (Svensson et al., 2005)

1021



1022

1023 **Figure 6.6.** Summary of estimated peak rates of change and sizes of changes associated with
 1024 various classes of cause. Error bars are not provided because of difficulty of quantifying them,
 1025 but high precision is not implied. Both panels have logarithmic scales on both axes (log-log
 1026 plots) to allow the huge range of behavior to be shown in a single figure. The natural changes
 1027 during the Little Ice Age–Medieval Warm Period have been somewhat arbitrarily partitioned as
 1028 0.6°C for changes in volcanic-eruption frequency (labeled “volcanoes” to differentiate from the
 1029 effects of a single eruption, labeled “volcano”), and 0.3°C for solar forcing to provide an upper
 1030 limit on solar causes; a larger volcanic role and smaller solar role would be easy to defend
 1031 (Hegerl et al., 2007), but a larger solar role is precluded by available data and interpretations.
 1032 The abrupt climate changes are shown for local Greenland values and for a poorly constrained
 1033 global estimate of 0.1°C. These numbers are intended to represent the Arctic as a whole, but
 1034 much Greenland ice-core data have been used in determinations. The instrumental record has
 1035 been used to assess human effects (see Delworth and Knutson, 2000 and Hegerl et al., 2007).
 1036 The “human” contribution may have been overestimated and natural fluctuations may have

1037 contributed to the late-20th-century change, but one also cannot exclude the possibility that the
1038 “human” contribution was larger than shown here and that natural variability offset some of the
1039 change. The ability of climate models to explain widespread changes in climate primarily on the
1040 basis of human forcing, and the evidence that there is little natural forcing during the latter 20th
1041 century (Hegerl et al., 2007), motivate the plot as shown. Also included for scaling is the
1042 projection for the next century (from 1980–1999 to 2080–2099 means) for the IPCC SRES A1B
1043 emissions scenario (one often termed “middle of the road”) scaled from Figure 10.7 of Meehl et
1044 al. (2007); see also Chapman and Walsh (2007). This scenario is shown as the black square
1045 labeled A1B; a different symbol shows the fundamental difference of this scenario-based
1046 projection from data-based interpretations for the other results on the figure. Human changes
1047 could be smaller or larger than shown as A1B, and they may continue to possibly much larger
1048 values further into the future. There is no guarantee that human disturbance will end before the
1049 end of the 21st century, as plotted here. The regression lines pass through tectonic, ice-age, solar,
1050 volcano, and volcanoes; they are included solely to guide the eye and not to imply mechanisms.
1051

1052 **Chapter 6 References Cited**

1053

1054 **Abbott, M.B.** and T.W.J. Stafford, 1996: Radiocarbon geochemistry of modern and ancient
1055 arctic lake systems, Baffin Island, Canada. *Quaternary Research*, **45**, 300-311.

1056

1057 **Alley, R.B.**, 2000: The Younger Dryas cold interval as viewed from central Greenland.
1058 *Quaternary Science Reviews*, **19**, 213-226.

1059

1060 **Alley, R.B.**, 2007: Wally was right: Predictive ability of the North Atlantic “conveyor belt”
1061 hypothesis for abrupt climate change. *Annual Review of Earth and Planetary Sciences*,
1062 **35**, 241-272.

1063

1064 **Alley, R.B.** and A.M. Agustsdottir, 2005: The 8k event: Cause and consequences of a major
1065 Holocene abrupt climate change, *Quaternary Science Reviews*, **24**, 1123 -1149.

1066

1067 **Alley, R.B.**, J. Marotzke, W.D. Nordhaus, J.T. Overpeck, D.M. Peteet, R.A. Pielke, Jr., R.T.
1068 Pierrehumbert, P.B. Rhines, T.F. Stocker, L.D. Talley, and J.M. Wallace, 2003: Abrupt
1069 climate change. *Science*, **299**, 2005-2010.

1070

1071 **Alley, R.B.**, D.A. Meese, C.A. Shuman, A.J. Gow, K.C. Taylor, P.M. Grootes, J.W.C. White, M.
1072 Ram, E.D. Waddington, P.A. Mayewski, and G.A. Zielinski, 1993: Abrupt increase in
1073 snow accumulation at the end of the Younger Dryas event. *Nature*, **362**, 527-529.

1074

1075 **Andersen, K.K.**, A. Svensson, S.O. Rasmussen, J.P. Steffensen, S.J. Johnsen, M. Bigler, R.
1076 Röthlisberger, U. Ruth, M.-L. Siggaard-Andersen, D. Dahl-Jensen, B.M. Vinther, and
1077 H.B. Clausen, 2006: The Greenland ice core chronology 2005, 15-42 ka. Part 1:
1078 Constructing the time scale. *Quaternary Science Reviews*, **25(23-24)**, 3246-3257.

1079

1080 **Bard, E.** and G. Delaygue, 2008: Comment on - "Are there connections between the Earth's
1081 magnetic field and climate?" *Earth and Planetary Science Letters*, **265**, 302-307.

1082

1083 **Bard, E., G.M. Raisbeck, F. Yiou, and J. Jouzel, 2007: Comment – Solar activity during the last**
1084 1000 yr inferred from radionuclide records. *Quaternary Science Reviews*, **26**, 2301-2304.

1085

1086 **Bice, K.L., C.R. Scotese, D. Seidov, and E.J. Barron, 2000: Quantifying the role of geographic**
1087 change in Cenozoic ocean heat transport using uncoupled atmosphere and ocean models.
1088 *Palaeogeography Palaeoclimatology Palaeoecology*, **161**, 295-310.

1089

1090 **Biscaye, P.E., F.E. Grousset, M. Revel, S. VanderGaast, G.A. Zielinski, A. Vaars, and G. Kukla,**
1091 1997: Asian provenance of glacial dust (stage 2) in the Greenland Ice Sheet Project 2 Ice
1092 Core, Summit, Greenland. *Journal of Geophysical Research – Oceans*, **102(C12)**, 26765-
1093 26781.

1094

1095 **Björck, S., O. Bennike, P. Rose, C.S. Andreson, S., Bohncke, E. Kaas, and D. Conley, 2002:**
1096 Anomalously mild Younger Dryas summer conditions in southern Greenland. *Geology*,
1097 **30**, 427-430.

1098

1099 **Björck, S., N. Koç, and G. Skot, 2003: Consistently large marine reservoir ages in the**
1100 Norwegian Sea during the last deglaciation. *Quaternary Science Reviews*, **22**, 429-435.

1101

1102 **Bond, G., B. Kromer, J. Beer, R. Muscheler, M.N. Evans, W. Showers, S. Hoffman, R. Lotti-**
1103 **Bond, I. Hajdas, and G. Bonani, 2001: Persistent solar influence on North Atlantic**
1104 climate during the Holocene. *Science*, **294**, 2130-2136.

1105

1106 **Bradley, R.S., 1999: *Paleoclimatology: Reconstructing Climate of the Quaternary*. Academic**
1107 Press, San Diego, 613 pp.

1108

1109 **Braun, H., L.M. Christ, S. Rahmstorf, A. Ganopolski, A.Mangini, C. Kubatzki, K. Roth, and B.**
1110 **Kromer, 2005: Possible solar origin of the 1,470-year glacial climate cycle demonstrated**
1111 in a coupled model. *Nature*, **438**, 208-211.

1112

- 1113 **Brigham-Grette, J., M. Melles, P. Minyuk, and Scientific Party, 2007: Overview and**
1114 **significance of a 250 ka paleoclimate record from El'gygytgyn Crater Lake, NE Russia.**
1115 ***Journal of Paleolimnology*, **37(1)**, 1-16.**
1116
- 1117 **Briner, J.P., Y. Axford, S.L. Forman, G.H. Miller, and A.P. Wolfe, 2007: Multiple generations**
1118 **of interglacial lake sediment preserved beneath the Laurentide Ice Sheet. *Geology*, **35**,**
1119 **887-890.**
1120
- 1121 **Briner, J.P., N. Michelutti, D.R. Francis, G.H. Miller, Y. Axford, M.J. Wooller, and A.P. Wolfe,**
1122 **2006: A multi-proxy lacustrine record of Holocene climate change on northeastern Baffin**
1123 **Island, Arctic Canada. *Quaternary Research*, **65**, 431-442.**
1124
- 1125 **Broecker, W.S., 2000: Was a change in thermohaline circulation responsible for the Little Ice**
1126 **Age? *Proceedings of the National Academy of Sciences of the United States of America*,**
1127 ****97**, 1339-1342**
1128
- 1129 **Broecker, W.S., D.M. Peteet, and D. Rind, 1985: Does the ocean-atmosphere system have more**
1130 **than one stable mode of operation? *Nature*, **315**, 21-26.**
1131
- 1132 **Brubaker, L.B., P.M. Anderson, M.E. Edwards, and A.V. Lozhkin, 2005: Beringia as a glacial**
1133 **refugium for boreal trees and shrubs—New perspectives from mapped pollen data.**
1134 ***Journal of Biogeography*, **32**, 833-848.**
1135
- 1136 **Cai, B.G., R.L. Edwards, H. Cheng, M. Tan, X. Wang, and T.S. Liu, 2008: A dry episode during**
1137 **the Younger Dryas and centennial-scale weak monsoon events during the early**
1138 **Holocene—A high-resolution stalagmite record from southeast of the Loess Plateau,**
1139 **China. *Geophysical Research Letters*, **35(2)**, Article L02705**
1140
- 1141 **Chapman, W.L., and J.E. Walsh, 2007: Simulations of Arctic Temperature and Pressure by**
1142 **Global Coupled Models. *J. Climate*, **20**, 609–632.**
1143

- 1144
1145 **Cronin, T.M.**, 1999: *Principles of Paleoclimatology*. Columbia University Press, New York, 560
1146 pp.
1147
- 1148 **Cuffey, K.M.** and E.J. Brook, 2000: Ice sheets and the ice-core record of climate change. In:
1149 *Earth system science—From biogeochemical cycles to global change* [Jacobson, M.C.,
1150 R.J. Charlson, H. Rodhe and G.H. Orians (eds.)], Academic Press, Burlington, MA, pp.
1151 459 -497.
1152
- 1153 **Cuffey, K.M.**, G.D. Clow, R.B. Alley, M. Stuiver, E.D. Waddington, and R.W. Saltus, 1995:
1154 Large arctic temperature change at the Wisconsin-Holocene glacial transition. *Science*,
1155 **270(5235)**, 455-458.
1156
- 1157 **Cuffey, K.M.** and G.D. Clow, 1997: Temperature, accumulation, and ice sheet elevation in
1158 central Greenland through the last deglacial transition. *Journal of Geophysical Research*,
1159 **102(C12)**, 26,383-26,396.
1160
- 1161 **Cuffey, K.M.** and E.J. Steig, 1998: Isotopic diffusion in polar firn—Implications for
1162 interpretation of seasonal climate parameters in ice-core records, with emphasis on
1163 central Greenland. *Journal of Glaciology*, **44(147)**, 273-284.
1164
- 1165 **D’Andrea, W.J.** and Y. Huang, 2005: Long-chain alkenones in Greenland lake sediments—Low
1166 $\delta^{13}\text{C}$ values and exceptional abundance. *Organic Geochemistry*, **36**, 1234-1241.
1167
- 1168 **Dansgaard, W.**, H.B. Clausen, N. Gundestrup, C.U. Hammer, S.J. Johnsen, P.M. Kristinsdottir,
1169 and N. Reeh, 1982: A new Greenland deep ice core. *Science*, **218(4579)**, 1273-1277.
1170
- 1171 **Dansgaard, W.**, S.J. Johnsen, H.B. Clausen, D. Dahl-Jensen, N.S. Gundestrup, C.U. Hammer,
1172 C.S. Hvidberg, J.P. Steffensen, A.E. Sveinbjörnsdottir, J. Jouzel, and G. Bond, 1993:
1173 Evidence for general instability of past climate from a 250-kyr ice-core record. *Nature*,
1174 **364(6434)**, 218-220.

- 1175
- 1176 **Dansgaard, W., S.J. Johnsen, H.B. Clausen, D. Dahl-Jensen, N. Gundestrup, C.U. Hammer, and**
1177 **H. Oeschger, 1984: North Atlantic climatic oscillations revealed by deep Greenland ice**
1178 **cores. In: *Climatic Processes and Climate Sensitivity* [Hansen, J.E. and T. Takahashi**
1179 **(eds.)]. Geophysical Monograph Series 29, American Geophysical Union, Washington,**
1180 **DC, pp. 288-298.**
- 1181
- 1182 **Dansgaard, W., S.J. Johnsen, H.B. Clausen, and C.C. Langway, Jr., 1971: Climatic record**
1183 **revealed by the Camp Century ice core. In: *The Late Cenozoic Glacial Ages*, [Turekian,**
1184 **K.K. (ed.)]. Yale University Press, USA, pp. 37-56.**
- 1185
- 1186 **Dansgaard, W., S.J. Johnsen, J. Møller, and C.C. Langway, Jr., 1969: One thousand centuries of**
1187 **climatic record from Camp Century on the Greenland ice sheet. *Science*, **166(3903)**, 377-**
1188 **381.**
- 1189
- 1190 **Dansgaard, W., J.W.C. White, and S.J. Johnsen, 1989: The abrupt termination of the Younger**
1191 **Dryas climate event. *Nature*, **339**, 532-534.**
- 1192
- 1193 **Denton, G. H., R.B. Alley, G.C. Comer, and W.S. Broecker, 2005: The role of seasonality in**
1194 **abrupt climate change. *Quaternary Science Reviews*, **24**, 1159-1182.**
- 1195
- 1196 **Delworth, T.L. and T.R. Knutson, 2000: Simulation of early 20th century global warming.**
1197 ***Science*, **287**, 2246.**
- 1198
- 1199 **Donnadieu, Y., R. Pierrehumbert, R. Jacob, and F. Fluteau, 2006: Modelling the primary control**
1200 **of paleogeography on Cretaceous climate. *Earth and Planetary Science Letters*, **248**, 426-**
1201 **437.**
- 1202
- 1203 **Easterling, D.R., T.R. Karl, E.H. Mason, P.Y. Hughes, and D.P. Bowman, 1996: *United States***
1204 ***Historical Climatology Network (U.S. HCN) Monthly Temperature and Precipitation***

- 1205 *Data*. ORNL/CDIAC-87, NDP-019/R3. Carbon Dioxide Information Analysis Center,
1206 Oak Ridge National Laboratory, U.S. Department of Energy, Oak Ridge, TN.
1207
- 1208 **Eiriksson, J., G. Larsen, K.L. Knudsen, J. Heinemeier, and L.A. Simonarson, 2004:** Marine
1209 reservoir age variability and water mass distribution in the Iceland Sea. *Quaternary*
1210 *Science Reviews*, **23**, 2247-2268.
1211
- 1212 **Ellison, C.R.W., M.R. Chapman, and I.R. Hall, 2006:** Surface and deep ocean interactions
1213 during the cold climate event 8200 years ago. *Science*, **312**, 1929-1932.
1214
- 1215 **Francus, P., R. Bradley, M. Abbott, F. Keimig, and W. Patridge, 2002:** Paleoclimate studies of
1216 minerogenic sediments using annually resolved textural parameters. *Geophysical*
1217 *Research Letters*, **29**, 59-1 to 59-4.
1218
- 1219 **Funder, S. and L. Hansen, 1996:** The Greenland ice sheet—A model for its culmination and
1220 decay during and after the last glacial maximum. *Bulletin of the Geological Society of*
1221 *Denmark*, **42**, 137-152.
1222
- 1223 **Grootes, P.M. and M. Stuiver, 1997:** Oxygen 18/16 variability in Greenland snow and ice with
1224 10(-3)- to 10(5)-year time resolution. *Journal of Geophysical Research—Oceans*,
1225 **102(C12)**, 26,455-26,470.
1226
- 1227 **Hajdas, I., G. Bonani, P. Boden, D.M. Peteet, and D.H. Mann, 1998:** Cold reversal on Kodiak
1228 Island, Alaska, correlated with the European Younger Dryas by using variations of
1229 atmospheric C-14 content. *Geology*, **26(11)**, 1047-1050.
1230
- 1231 **Harder, S.L., D.T. Shindell, G.A. Schmidt, and E.J. Brook, 2007:** A global climate model study
1232 of CH₄ emissions during the Holocene and glacial-interglacial transitions constrained by
1233 ice core data. *Global Biogeochemical Cycles*, **21**, GB1011.
1234
- 1235 **Hegerl, G.C., F.W. Zwiers, P. Braconnot, N.P. Gillett, Y. Luo, J.A. Marengo Orsini, N.**

- 1236 Nicholls, J.E. Penner, and P.A. Stott, 2007: Understanding and Attributing Climate
1237 Change. In: *Climate Change 2007—The Physical Science Basis. Contribution of Working*
1238 *Group I to the Fourth Assessment Report of the Intergovernmental Panel on Climate*
1239 *Change*, [Solomon, S., D. Qin, M. Manning, Z. Chen, M. Marquis, K.B. Averyt, M.
1240 Tignor and H.L. Miller (eds.)]. Cambridge University Press, Cambridge, United
1241 Kingdom and New York, pp. 663-745.
- 1242
- 1243 **Hu**, F.S., J.I. Hedges, E.S. Gorden, and L.B. Brubaker, 1999a: Lignin biomarkers and pollen in
1244 postglacial sediments of an Alaskan lake. *Geochimica Cosmochimica Acta*, **63**, 1421-
1245 1430.
- 1246
- 1247 **Hu**, F.S., D.M. Nelson, G.H. Clarke, K.M. Ruhland, Y. Huang, D.S. Kaufman, and J.P. Smol,
1248 2006: Abrupt climatic events during the last glacial-interglacial transition in Alaska.
1249 *Geophysical Research Letters*, **33**, L18708, doi:10.1029/2006GL027261.
- 1250
- 1251 **Hu**, F.S., D. Slawinski, H.E.J. Wright, E. Ito, R.G. Johnson, K.R. Kelts, R.F. McEwan, and A.
1252 Boedigheimer, 1999b: Abrupt changes in North American climate during early Holocene
1253 times. *Nature*, **400**, 437-440.
- 1254
- 1255 **Huang**, Y., B. Shuman, Y. Wang, and T. Webb, III, 2004: Hydrogen isotope ratios of individual
1256 lipids in lake sediments as novel tracers of climatic and environmental change—A
1257 surface sediment test. *Journal Paleolimnology*, **31**, 363-375.
- 1258
- 1259 **Huber**, C., M. Leuenberger, R. Spahni, J. Flückiger, J. Schwander, T.F. Stocker, S. Johnsen, A.
1260 Landais, and J. Jouzel, 2006: Isotope calibrated Greenland temperature record over
1261 Marine Isotope Stage 3 and its relation to CH₄. *Earth and Planetary Science Letters*,
1262 **243(3-4)**, 504-519.
- 1263
- 1264 **Hughen**, H.A., J.R. Southon, S.J. Lehman, and J.T. Overpeck, 2000: Synchronous radiocarbon
1265 and climate shifts during the last deglaciation. *Science*, **290**, 1951-1954.
- 1266

- 1267 **Hughen**, K.A., M.G.L. Baillie, E. Bard, A. Bayliss, J.W. Beck, C. Bertrand, P.G. Blackwell,
 1268 C.E. Buck, G. Burr, K.B. Cutler, P.E. Damon, R.L. Edwards, R.G. Fairbanks, M.
 1269 Friedrich, T.P. Guilderson, B. Kromer, F.G. McCormac, S. Manning, C. Bronk Ramsey,
 1270 P.J. Reimer, R.W. Reimer, S. Remmele, J.R. Southon, M. Stuiver, S. Talamo, F.W.
 1271 Taylor, J. van der Plicht, and C.E. Weyhenmeyer, 2004a: Marine04 marine radiocarbon
 1272 age calibration, 0-26 Cal Kyr BP. *Radiocarbon*, **46**, 1059-1086.
 1273
- 1274 **Hughen**, K., S. Lehman, J. Southon, J. Overpeck, O. Marchal, C. Herring, and J. Turnbull,
 1275 2004b: ^{14}C Activity and global carbon cycle changes over the past 50,000 years. *Science*,
 1276 **303**, 202-207.
 1277
- 1278 **Hughen**, K., J. Overpeck, R.F. Anderson, and K.M. Williams, 1996: The potential for
 1279 palaeoclimate records from varved Arctic lake sediments: Baffin Island, Eastern
 1280 Canadian Arctic. In: *Lacustrine Environments. Palaeoclimatology and*
 1281 *Palaeoceanography from Laminated Sediments*, [Kemp, A.E.S. (ed.)], Geological
 1282 Society, London, Special Publications 116, pp. 57-71.
 1283
- 1284 **Imbrie**, J., A. Berger, E.A. Boyle, S.C. Clemens, A. Duffy, W.R. Howard, G. Kukla, J.
 1285 Kutzbach, D.G. Martinson, A. McIntyre, A.C. Mix, B. Molino, J.J. Morley, L.C.
 1286 Peterson, N.G. Pisias, W.L. Prell, M.E. Raymo, N.J. Shackleton, and J.R. Toggweiler,
 1287 1993: On the structure and origin of major glaciation cycles .2. the 100,000-year cycle.
 1288 *Paleoceanography*, **8(6)** 699-735.
 1289
- 1290 **Jansen**, E., J. Overpeck, K.R. Briffa, J.-C. Duplessy, F. Joos, V. Masson-Delmotte, D. Olago, B.
 1291 Otto-Bliesner, W.R. Peltier, S. Rahmstorf, R. Ramesh, D. Raynaud, D. Rind, O.
 1292 Solomina, R. Villalba and D. Zhang. 2007. Palaeoclimate. In: *Climate Change 2007—*
 1293 *The Physical Science Basis. Contribution of Working Group I to the Fourth Assessment*
 1294 *Report of the Intergovernmental Panel on Climate Change*, [Solomon, S., D. Qin, M.
 1295 Manning, Z. Chen, M. Marquis, K.B. Averyt, M. Tignor and H.L. Miller (eds.)].
 1296 Cambridge University Press, Cambridge, United Kingdom and New York, pp. 434-497.
 1297

- 1298 **Jennings, A.E., Hald, M., Smith, M., Andrews, J.T., 2006:** Freshwater forcing from the
1299 Greenland Ice Sheet during the Younger Dryas: Evidence from southeastern Greenland
1300 shelf cores. *Quaternary Science Reviews* 25: 282-298.
1301
- 1302 **Johnsen, S.J., 1977:** Stable isotope homogenization of polar firn and ice. In: *Isotopes and*
1303 *Impurities in Snow and Ice*. Proceedings of International Union of Geodesy and
1304 Geophysics symposium XVI, General Assembly, Grenoble, France, August and
1305 September 1975, pp. 210-219. IAHS-AISH Publication 118, Washington, DC
1306
- 1307 **Johnsen, S.J., H.B. Clausen, K.M. Cuffey, G. Hoffmann, J. Schwander, and T. Creyts, 2000:**
1308 Diffusion of stable isotopes in polar firn and ice—The isotope effect in firn diffusion. In:
1309 *Physics of Ice Core Records* [Hondoh, T. (ed.)]. Hokkaido University Press, Sapporo, pp.
1310 121-140.
1311
- 1312 **Johnsen, S.J., H.B. Clausen, W. Dansgaard, K. Fuhrer, N. Gundestrup, C.U. Hammer, P.**
1313 **Iversen, J.P. Steffensen, J. Jouzel, and B. Stauffer, 1992:** Irregular glacial interstadials
1314 recorded in a new Greenland ice core. *Nature*, **359(6393)**, 311-313.
1315
- 1316 **Johnsen, S., D. Dahl-Jensen, W. Dansgaard, and N. Gundestrup, 1995:** Greenland
1317 palaeotemperatures derived from GRIP bore hole temperature and ice core isotope
1318 profiles. *Tellus B*, **47(5)**, 624-629.
1319
- 1320 **Johnsen, S.J., W. Dansgaard, H.B. Clausen, and C.C. Langway, Jr., 1972:** Oxygen isotope
1321 profiles through the Antarctic and Greenland ice sheets. *Nature*, **235(5339)**, 429-434.
1322
- 1323 **Jouzel, J., R.B. Alley, K.M. Cuffey, W. Dansgaard, P. Grootes, G. Hoffmann, S.J. Johnsen, R.D.**
1324 **Koster, D. Peel, C.A. Shuman, M. Stievenard, M. Stuiver, and J. White, 1997:** Validity of
1325 the temperature reconstruction from water isotopes in ice cores. *Journal of Geophysical*
1326 *Research*, **102(C12)**, 26,471-26,487.
1327

- 1328 **Kaufman, D.S.**, T.A. Ager, N.J. Anderson, P.M. Anderson, J.T. Andrews, P.J. Bartlein, L.B.
 1329 Brubaker, L.L. Coats, L.C. Cwynar, M.L. Duvall, A.S. Dyke, M.E. Edwards, W.R.
 1330 Eisner, K. Gajewski, A. Geirsdóttir, F.S. Hu, A.E. Jennings, M.R. Kaplan, M.W. Kerwin,
 1331 A.V. Lozhkin, G.M. MacDonald, G.H. Miller, C.J. Mock, W.W. Oswald, B.L. Otto-
 1332 Bliesner, D.F. Porinchu, K. Rühland, J.P. Smol, E.J. Steig, and B.B. Wolfe, 2004:
 1333 Holocene thermal maximum in the western Arctic (0–180°W). *Quaternary Science*
 1334 *Reviews*, **23**, 529-560.
- 1335
- 1336 **Keller, K.** and D. McInerney, 2007. The dynamics of learning about a climate threshold. *Climate*
 1337 *Dynamics*, **30**, 321-332, doi:10.1007/s00382-007-0290-5.
- 1338
- 1339 **Kristjansdottir, G.B.**, 2005: Holocene climatic and environmental changes on the Iceland
 1340 shelf— $\delta^{18}\text{O}$, Mg/Ca, and tephrochronology of core MD99-2269. PhD dissertation,
 1341 Department of Geological Sciences, University of Colorado, Boulder, 423 pp.
- 1342
- 1343 **Kristjansdottir, G.B.**, J.S. Stoner, A.E. Jennings, J.T. Andrews, and K. Gronvold, 2007:
 1344 Geochemistry of Holocene cryptotephra from the North Iceland Shelf (MD99-2269)—
 1345 Intercalibration with radiocarbon and paleomagnetic chronostratigraphies. *The Holocene*,
 1346 **17(2)**: 155-176.
- 1347
- 1348 **Landais, A.**, J.M. Barnola, V. Masson-Delmotte, J. Jouzel, J. Chappellaz, N. Caillon, C. Huber,
 1349 M. Leuenberger, and S.J. Johnsen, 2004: A continuous record of temperature evolution
 1350 over a sequence of Dansgaard-Oeschger events during Marine Isotopic Stage 4 (76 to 62
 1351 kyr BP). *Geophysical Research Letters*, **31**, L22211, doi:22210.21029/22004GL021193.
- 1352
- 1353 **Lang, C.**, M. Leuenberger, J. Schwander, and S. Johnsen, 1999: 16°C rapid temperature
 1354 variation in central Greenland 70,000 years ago. *Science*, **286(5441)**, 934-937.
- 1355
- 1356 **Lauritzen, S.-E.** and J. Lundberg, 2004: Isotope Stage 11, the "Super-Interglacial," from a north
 1357 Norwegian speleothem. In: *Studies of Cave Sediments: Physical and Chemical Records*
 1358 *of Paleoclimate*, [Sasowsky, I.D. and J. Mylroie (eds.)]. Kluwer Academic, New York,

1359 pp. 257-272.

1360

1361 **Le Treut**, H., R. Somerville, U. Cubasch, Y. Ding, C. Mauritzen, A. Mokssit, T. Peterson, and
 1362 M. Prather, 2007: Historical Overview of Climate Change. In: *Climate Change 2007—*
 1363 *The Physical Science Basis. Contribution of Working Group I to the Fourth Assessment*
 1364 *Report of the Intergovernmental Panel on Climate Change*, [Solomon, S., D. Qin, M.
 1365 Manning, Z. Chen, M. Marquis, K.B. Averyt, M. Tignor and H.L. Miller (eds.)].
 1366 Cambridge University Press, Cambridge, United Kingdom and New York, pp. 93-127.

1367

1368 **Leuenberger**, M., C. Lang, and J. Schwander, 1999: Delta ¹⁵N measurements as a calibration
 1369 tool for the paleothermometer and gas-ice age differences—A case study for the 8200
 1370 B.P. event on GRIP ice. *Journal of Geophysical Research*, **104(D18)**, 22,163-22,170.

1371

1372 **Lorenz**, E.N., 1963: Deterministic Nonperiodic Flow. *Journal of the Atmospheric Sciences*,
 1373 **20(2)**,130-141.

1374

1375 **Lozhkin**, A.V. and P.M. Anderson, 1995: The last interglaciation of northeast Siberia.
 1376 *Quaternary Research*, **43**, 147-158.

1377

1378 **McConnell**, J.R., R. Edwards, G.L. Kok, M.G. Flanner, C.S. Zender, E.S. Saltzman, J.R. Banta,
 1379 D.R. Pasteris, M.M. Carter, and J.D.W. Kahl, 2007: 20th-century industrial black carbon
 1380 emissions altered arctic climate forcing. *Science*, **317**, 1381-1384.

1381

1382 **Meese**, D.A., A.J. Gow, R.B. Alley, G.A. Zielinski, P.M. Grootes, M. Ram, K.C. Taylor, P.A.
 1383 Mayewski, and J.F. Bolzan, 1997: The Greenland Ice Sheet Project 2 depth-age scale—
 1384 Methods and results. *Journal of Geophysical Research*, **102(C12)**, 26,411-26,423.

1385

1386 **Meehl**, G.A., T.F. Stocker, W.D. Collins, P. Friedlingstein, A.T. Gaye, J.M. Gregory, A. Kitoh,
 1387 R. Knutti, J.M. Murphy, A. Noda, S.C.B. Raper, I.G. Watterson, A.J. Weaver and Z.-C.
 1388 Zhao, 2007: Global Climate Projections. In: *Climate Change 2007: The Physical Science*
 1389 *Basis. Contribution of Working Group I to the Fourth Assessment Report of the*

- 1390 *Intergovernmental Panel on Climate Change*, [Solomon, S.,D. Qin, M. Manning, Z.
1391 Chen, M. Marquis, K.B. Averyt, M. Tignor and H.L. Miller (eds.)]. Cambridge
1392 University Press, Cambridge, United Kingdom and New York, pp. 747-845.
1393
- 1394 **Miller**, G.H., W.N. Mode, A.P. Wolfe, P.E. Sauer, O. Bennike, S.L. Forman, S.K. Short, and
1395 T.W.J. Stafford, 1999: Stratified interglacial lacustrine sediments from Baffin Island,
1396 Arctic Canada—Chronology and paleoenvironmental implications. *Quaternary Science*
1397 *Reviews*, **18**, 789-810.
1398
- 1399 **Miller**, G.H., A.P. Wolfe, J.P. Briner, P.E. Sauer, and A. Nesje, 2005: Holocene glaciation and
1400 climate evolution of Baffin Island, Arctic Canada. *Quaternary Science Reviews*, **24**,
1401 1703-1721.
1402
- 1403 **Monnin**, E., A. Indermuhle, A. Dallenbach, J. Fluckiger, B. Stauffer, T.F. Stocker, D. Raynaud,
1404 and J.M. Barnola, 2001: Atmospheric CO2 concentrations over the last glacial
1405 termination. *Science*, **291(5501)** 112-114.
1406
- 1407 **Moran**, K., J. Backman, H. Brinkhuis, S.C. Clemens, T. Cronin, G.R. Dickens, F. Eynaud, J.
1408 Gattacceca, M. Jakobsson, R.W. Jordan, M. Kaminski, J. King, N. Koc, A. Krylov, N.
1409 Martinez, J. Matthiessen, D. McInroy, T.C. Moore, J. Onodera, M. O'Regan, H. Palike,
1410 B. Rea, D. Rio, T. Sakamoto, D.C. Smith, R. Stein, K. St. John, I. Suto, N. Suzuki, K.
1411 Takahashi, M. Watanabe, M. Yamamoto, J. Farrell, M. Frank, P. Kubik, W. Jokat and Y.
1412 Kristoffersen, 2006: The Cenozoic palaeoenvironment of the Arctic Ocean. *Nature*, **441**,
1413 601-605.
1414
- 1415 **Muscheler**, R., F. Joos, J. Beer, S.A. Miller, M. Vonmoos, and I. Snowball, 2007: Solar activity
1416 during the last 1000 yr inferred from radionuclide records. *Quaternary Science Reviews*,
1417 **26**, 82-97.
1418
- 1419 **National Research Council**, 2002: *Abrupt Climate Change, Inevitable Surprises*. National
1420 Academy Press, Washington, DC, 230 pp.

- 1421
- 1422 **Oeschger, H., J. Beer, U. Siegenthaler, B. Stauffer, W. Dansgaard, and C.C. Langway, Jr., 1984:**
1423 Late glacial climate history from ice cores. In: *Climate Processes and Climate Sensitivity*,
1424 [Hansen, J.E. and T. Takahashi, (eds.)]. Geophysical Monograph Series 29, American
1425 Geophysical Union, Washington, DC, pp. 299-306.
- 1426
- 1427 **Ojala, A.E.K. and M. Tiljander, 2003: Testing the fidelity of sediment chronology—Comparison**
1428 of varve and paleomagnetic results from Holocene lake sediments from central Finland.
1429 *Quaternary Science Reviews*, **22**, 1787-1803.
- 1430
- 1431 **Oswald, W.W., P.M. Anderson, T.A. Brown, L.B. Brubaker, F.S. Hu, A.V. Lozhkin, W. Tinner,**
1432 and P. Kaltenrieder, 2005: Effects of sample mass and macrofossil type on radiocarbon
1433 dating of arctic and boreal lake sediments. *The Holocene*, **15**, 758-767.
- 1434
- 1435 **Overpeck, J., K. Hughen, D. Hardy, R. Bradley, R. Case, M. Douglas, B. Finney, K. Gajewski,**
1436 G. Jacoby, A. Jennings, S. Lamoureux, A. Lasca, G. MacDonald, J. Moore, M. Retelle, S.
1437 Smith, A. Wolfe, and G. Zielinski, 1997: Arctic environmental change of the last four
1438 centuries. *Science*, **278**, 1251-1256.
- 1439
- 1440 **Peteet, D. 1995a: Global Younger Dryas. *Quaternary International*, **28**, 93-104.**
- 1441
- 1442 **Peteet, D.M., 1995b: Global Younger Dryas. Vol. 2. Preface. *Quaternary Science Reviews*, **14**,**
1443 811.
- 1444
- 1445 **Rasmussen, S.O., K.K. Andersen, A.M. Svensson, J.P. Steffensen, B.M. Vinther, H.B. Clausen,**
1446 M.-L. Siggaard-Andersen, S.J. Johnsen, L.B. Larsen, D. Dahl-Jensen, M. Bigler, R.
1447 Röthlisberger, H. Fischer, K. Goto-Azuma, M.E. Hansson, and U. Ruth, 2006: A new
1448 Greenland ice core chronology for the last glacial termination. *Journal of Geophysical*
1449 *Research*, **111**, D06102, doi:06110.01029/02005JD006079.
- 1450

- 1451 **Rasmussen, S.O., I.K. Seierstad, K.K. Andersen, M. Bigler, D. Dahl-Jensen, and S.J. Johnsen,**
 1452 2007: Synchronization of the NGRIP, GRIP, and GISP2 ice cores across MIS 2 and
 1453 palaeoclimatic implications. *Quaternary Science Review*, **27**, 18-28.
 1454
- 1455 **Reeh, N.,** 1985: Greenland ice-sheet mass balance and sea-level change. In: *Glaciers, Ice Sheets*
 1456 *and Sea Level: Effect of a CO₂-Induced Climatic Change*. DOE/ER/60235-1, Department
 1457 of Energy, Washington, DC, pp. 155-171.
 1458
- 1459 **Rempel, A.W. and J.S. Wettlaufer,** 2003: Segregation, transport, and interaction of climate
 1460 proxies in polycrystalline ice. *Canadian Journal of Physics*, **81(1–2)**, 89-97.
 1461
- 1462 **Renssen, H., H. Goosse, and R. Muscheler,** 2006: Coupled climate model simulation of
 1463 Holocene cooling events—Oceanic feedback amplifies solar forcing. *Climate of the Past*,
 1464 **2**, 79-90.
 1465
- 1466 **Royer, D.L., R.A. Berner, and J. Park,** 2007: Climate sensitivity constrained by CO₂
 1467 concentrations over the past 420 million years. *Nature*, **446**, 530-532.
 1468
- 1469 **Ruddiman, W.F. and L.K. Glover,** 1975: Subpolar North Atlantic circulation at 9300 yr BP—
 1470 Faunal evidence. *Quaternary Research*, **5**, 361-389.
 1471
- 1472 **Ruddiman, W.F. and A. McIntyre,** 1981: The North Atlantic Ocean during the last deglaciation.
 1473 *Palaeogeography, Palaeoclimatology, Palaeoecology*, **35**, 145-214.
 1474
- 1475 **Saarinen, T.,** 1999: Paleomagnetic dating of late Holocene sediments in Fennoscandia.
 1476 *Quaternary Science Reviews*, **18**, 889-897.
 1477
- 1478 **Sauer, P.E., T.I. Eglinton, J.M. Hayes, A. Schimmelmann, and A.L. Sessions,** 2001: Compound-
 1479 specific D/H ratios of lipid biomarkers from sediments as a proxy for environmental and
 1480 climatic conditions. *Geochimica Cosmochimica Acta*, **65**, 213-222.
 1481

- 1482 **Serreze, M.C., M.M. Holland, and J. Stroeve, 2007:** Perspectives on the Arctic's shrinking sea-
1483 ice cover. *Science*, **315(5818)**, 1533, doi:10.1126/science.1139426.
1484
- 1485 **Severinghaus, J.P., T. Sowers, E.J. Brook, R.B. Alley, and M.L. Bender, 1998:** Timing of abrupt
1486 climate change at the end of the Young Dryas interval from thermally fractionated gases
1487 in polar ice. *Nature*, **391**, 141-146.
1488
- 1489 **Snowball, I. F., L. Zillén, and M.-J. Gaillard, 2002.** Rapid early Holocene environmental
1490 changes in northern Sweden based on studies of two varved lake sediment sequences. *The*
1491 *Holocene* **12**, 7-16.
1492
- 1493 **Snowball, I. and P. Sandgren, 2004:** Geomagnetic field intensity changes in Sweden between
1494 9000 and 450 cal B.P.—Extending the record of archaeomagnetic jerks by means of lake
1495 sediments and the pseudo-Thellier technique. *Earth and Planetary Science Letters*, **277**,
1496 361-376.
1497
- 1498 **Snowball, I., L. Zillén, A. Ojala, T. Saarinen, and P. Sandgren, 2007:** FENNOSTACK and
1499 FENNORPIS—Varve-dated Holocene palaeomagnetic secular variation and relative
1500 palaeointensity stacks for Fennoscandia. *Earth and Planetary Science Letters*, **255**, 106-
1501 115.
1502
- 1503 **Steffensen, J.P., H.B. Clausen, C.U. Hammer, M. Legrand, and M. De Angelis, 1997:** The
1504 chemical composition of cold events within the Eemian section of the Greenland Ice Core
1505 Project ice core from Summit, Greenland. *Journal of Geophysical Research*, **102(C12)**,
1506 26,747-26,754.
1507
- 1508 **Steffensen, J.P. and D. Dahl-Jensen, 1997:** Modelling of alterations of the stratigraphy of ionic
1509 impurities in very old ice core strata. *Eos, Transactions, American Geophysical Meeting*
1510 *Fall Meeting, San Francisco, USA*, **78**, F7 Poster U21A-22.
1511
- 1512 **Steig, E.J. and R.B. Alley, 2003:** Phase relationships between Antarctic and Greenland climate

- 1513 records. *Annals of Glaciology*, **35**, 451-456.
- 1514
- 1515 **Stocker**, T.F. and S.J. Johnsen, 2003: A minimum thermodynamic model for the bipolar seesaw.
- 1516 *Paleoceanography*, **18**, 1087.
- 1517
- 1518 **Stoner**, J.S., A. Jennings, G.B. Kristjansdottir, G. Dunhill, J.T. Andrews, and J. Hardardottir,
- 1519 2007: A paleomagnetic approach toward refining Holocene radiocarbon-based
- 1520 chronologies—Paleoceanographic records from the North Iceland (MD99-2269) and East
- 1521 Greenland (MD99-2322) margins. *Paleoceanography*, **22**, PA1209,
- 1522 doi:10.1029/2006PA001285.
- 1523
- 1524 **Stuiver**, M., T.F. Braziunas, P.M. Grootes, and G.A. Zielinski, 1997: Is there evidence for solar
- 1525 forcing of climate in the GISP2 oxygen isotope record? *Quaternary Research*, **48**, 259-
- 1526 266.
- 1527
- 1528 **Stuiver**, M., P.J. Reimer, E. Bard, J.W. Beck, K.A. Hughen, B. Kromer, F.G. McCormack, J.
- 1529 van der Plicht, and M. Spurk, 1998: INTCAL98 Radiocarbon age calibration 24,000 cal
- 1530 BP. *Radiocarbon*, **40**, 1041-1083.
- 1531
- 1532 **Svendson**, J.I. and J. Mangerud, 1992: Paleoclimatic inferences from glacial fluctuations on
- 1533 Svalbard during the last 20 000 years. *Climate Dynamics*, **6**, 213-220.
- 1534
- 1535 **Svensson**, A., K.K. Andersen, M. Bigler, H.B. Clausen, D. Dahl-Jensen, S.M. Davies, S.J.
- 1536 Johnsen, R. Muscheler, S.O. Rasmussen, R. Röthlisberger, J.P. Steffensen, and B.M.
- 1537 Vinther, 2006: The Greenland Ice Core chronology 2005, 15–42 ka. Part 2—Comparison
- 1538 to other records. *Quaternary Science Reviews*, **25(23-24)**, 3258-3267.
- 1539
- 1540 **Svensson**, A., S.W. Nielsen, S. Kipfstuhl, S.J. Johnsen, J.P. Steffensen, M. Bigler, U. Ruth, and
- 1541 R. Röthlisberger, 2005: Visual stratigraphy of the North Greenland Ice Core Project
- 1542 (NorthGRIP) ice core during the last glacial period. *Journal of Geophysical Research*,
- 1543 **110**, D02108, doi:02110.01029/02004JD005134.

1544

1545 **Tilling**, R.I., L. Topinka, and D.A. Swanson, 1990: *Eruptions of Mount St. Helens: Past,*
1546 *Present, and Future.* U.S. Geological Survey Special Interest Publication, 56 pp.

1547

1548 **Trenberth**, K.E., P.D. Jones, P. Ambenje, R. Bojariu, D. Easterling, A. Klein Tank, D. Parker,
1549 F. Rahimzadeh, J.A. Renwick, M. Rusticucci, B. Soden, and P. Zhai, 2007: Observations:
1550 Surface and Atmospheric Climate Change. In: *Climate Change 2007: The Physical*
1551 *Science Basis. Contribution of Working Group I to the Fourth Assessment Report of the*
1552 *Intergovernmental Panel on Climate Change*, [Solomon, S., D. Qin, M. Manning, Z.
1553 Chen, M. Marquis, K.B. Averyt, M. Tignor, and H.L. Miller (eds.)]. Cambridge
1554 University Press, Cambridge, United Kingdom and New York, pp. 236-336.

1555

1556 **Trenberth**, K.E., J.M. Caron, D.P. Stepaniak, and S. Worley, 2002: Evolution of El Niño-
1557 Southern Oscillation and global atmospheric surface temperatures. *Journal of*
1558 *Geophysical Research–Atmospheres*, **107(D7-8)**, 4065.

1559

1560 **Vinther**, B.M., H.B. Clausen, S.J. Johnsen, S.O. Rasmussen, K.K. Andersen, S.L. Buchardt, D.
1561 Dahl-Jensen, I.K. Seierstad, M.-L. Siggaard-Andersen, J.P. Steffensen, A.M. Svensson, J.
1562 Olsen, and J. Heinemeier, 2006: A synchronized dating of three Greenland ice cores
1563 throughout the Holocene. *Journal of Geophysical Research*, **111**, D13102,
1564 doi:13110.11029/12005JD006921.

1565

1566 **Walker**, I.R., A.J. Levesque, L.C. Cwynar, and A.F. Lotter, 1997: An expanded surface-water
1567 palaeotemperature inference model for use with fossil midges from eastern Canada.
1568 *Journal of Paleolimnology*, **18**, 165-178.

1569

1570 **Whillans**, I.M. and P.M. Grootes, 1985: Isotopic diffusion in cold snow and firn. *Journal of*
1571 *Geophysical Research*, **90(D2)**, 3910-3918.

1572

- 1573 **White, J.W.C., J.R. Lawrence, and W.S. Broecker, 1994: Modeling and Interpreting D/H Ratios**
1574 **in Tree-Rings - A test-case of white-pine in the northeastern United States. *Geochimica et***
1575 ***Cosmochimica Acta*, **58(2)**, 851-862.**
1576
- 1577 **Willemse, N.W. and T.E. Törnqvist, 1999: Holocene century-scale temperature variability from**
1578 **West Greenland lake records. *Geology*, **27**, 580-584.**
1579
- 1580 **Woillard, G.M., 1979: Abrupt end of the last interglacial ss in north-east France. *Nature*,**
1581 ****281(5732)**, 558-562.**
1582
- 1583 **Woillard, G.M., 1978: Grande Pile peat bog—A continuous pollen record for the last 140.000**
1584 **years. *Quaternary Research*, **9**, 1-21.**
1585
- 1586 **Wolfe, A.P., G.H. Miller, C. Olsen, S.L. Forman, P.T. Doran, and S.U. Holmgren, 2005:**
1587 **Geochronology of high-latitude lake sediments. In: *Long-term Environmental Change in***
1588 ***Arctic and Antarctic Lakes—Developments in Paleoenvironmental Research*, [Pienitz,**
1589 **R., M.S.V. Douglas, and J.P. Smol (eds.)]. Springer, New York, pp. 19-52.**
1590
- 1591 **Yang, F.L., M.E. Schlesinger, 2002: On the surface and atmospheric temperature changes**
1592 **following the 1991 Pinatubo volcanic eruption: A GCM study. *Journal of Geophysical***
1593 ***Research-Atmospheres*, **107(D8)**, 4073, doi:10.1029/2001JD000373.**

1
2
3
4
5
6
7
8
9
10
11
12
13
14
15
16
17
18
19
20
21

CCSP Synthesis and Assessment Product 1.2

**Past Climate Variability and Change in the Arctic and at High
Latitudes**

Chapter 7 — Past Extent and Status of the Greenland Ice Sheet

Chapter Lead Author:

Richard B. Alley, Pennsylvania State University, University
Park, PA

Contributing Authors:

John T. Andrews, University of Colorado

Garry K.C. Clarke, University of British Columbia

Kurt M. Cuffey, University of California

Svend Funder, University of Copenhagen

Shawn J. Marshall, University of Calgary

Jerry X. Mitrovica, University of Toronto

Daniel R. Muhs, U.S. Geological Survey

Bette Otto-Bliesner, National Center for Atmospheric

Research

21 **ABSTRACT**

22 The Greenland Ice Sheet is expected to shrink or disappear with warming, a
23 conclusion based on a survey of paleoclimatic and related information. Recent
24 observations show that the Greenland Ice Sheet has melted more in years with warmer
25 summers. Mass loss by melting is therefore expected to increase with warming. But
26 whether the ice sheet shrinks or grows, and at what pace, depend also on snowfall and
27 iceberg production. The Arctic is a complicated system. Reconstructions of past climate
28 and ice sheet configuration (the “paleo-record”) are valuable sources of information that
29 complement process-based models. The paleo-record shows that the Greenland Ice Sheet
30 consistently lost mass when the climate warmed, and grew when the climate cooled.
31 Such changes have occurred even at times of slow or zero sea-level change, so changing
32 sea level cannot be the cause of at least some of the ice sheet changes. In contrast, there
33 are no documented major ice-sheet changes that occurred independent of temperature
34 changes. Moreover, snowfall has increased when the climate warmed, but the ice sheet
35 lost mass nonetheless; increased accumulation in the ice sheet’s center has not been
36 sufficient to counteract increased melting and flow near the edges. Most documented
37 forcings of change, and the changes to the ice sheet themselves, spanned periods of
38 several thousand years, but limited data also show rapid response to rapid forcings. In
39 particular, regions near the ice margin have responded within decades. However, major
40 changes of central regions of the ice sheet are thought to require centuries to millennia.
41 The paleo-record does not yet strongly constrain how rapidly a major shrinkage or nearly
42 complete loss of the ice sheet could occur. The evidence suggests nearly total loss may
43 result from warming of more than a few degrees above mean 20th century values, but this

44 threshold is poorly defined (perhaps as little as 2°C or more than 7°C). Paleoclimatic
45 records are sufficiently sketchy that the ice sheet may have grown temporarily in
46 response to warming, or changes may have been induced by factors other than
47 temperature, without having been recorded.

48

49 **7.1 The Greenland Ice Sheet**

50 **7.1.1. Overview**

51 The Greenland Ice Sheet (Figure 7.1) contains by far the largest volume of ice of
52 any present-day Northern Hemisphere mass. The ice sheet is approximately 1.7 million
53 square kilometers (km²) in area, extending as much as 2200 km north to south. The
54 maximum ice thickness is 3367 m, its average thickness is 1600 m (Thomas et al., 2001),
55 and its volume is 2.9 million km³ (Bamber et al., 2001). Some of the bedrock beneath this
56 ice has been depressed below sea level by the weight of the ice, and a little of this
57 bedrock would remain below sea level following removal of the ice and rebound of the
58 bedrock (Bamber et al., 2001). However, most of the ice that rests on bedrock is above
59 sea level and so would contribute to sea-level rise if it were melted: if the entire ice sheet
60 melted, it is estimated that sea-level would rise about 7.3 m (Lemke et al., 2007).

61

62

FIGURE 7.1 NEAR HERE

63

64 The ice sheet consists primarily of old snow that has been squeezed to ice under
65 the weight of new snow that accumulates every year. Snow accumulation on the upper
66 surface tends to increase ice-sheet size. Ice sheets lose mass primarily by melting in low-

67 elevation regions and by forming icebergs that break off the ice margins (calving) and
68 drift away to melt elsewhere. Sublimation, snowdrift (Box et al., 2006), and melting or
69 freezing at the bed beneath the ice are minor terms in the budget, although melting
70 beneath floating extensions called ice shelves before icebergs break off may be important
71 (see 7.1.2, below).

72 Estimates of net snow accumulation on the Greenland Ice Sheet have been
73 presented by Hanna et al. (2005) and Box et al. (2006), among others. Hanna et al. (2005)
74 found for 1961–1990 (an interval of moderately stable conditions before more-recent
75 warming) that surface snow accumulation (precipitation minus evaporation) was about
76 573 gigatons per year (Gt/yr) and that 280 Gt/yr of meltwater left the ice sheet. The
77 difference of 293 Gt/yr is similar to the estimated iceberg calving flux within broad
78 uncertainties (Reeh, 1985; Bigg, 1999; Reeh et al., 1999). (For reference, return of 360 Gt
79 of ice to the ocean would raise global sea level by 1 millimeter (mm); Lemke et al.,
80 2007.) More-recent trends are toward warming temperatures, increasing snowfall, and
81 more rapidly increasing meltwater runoff (Hanna et al., 2005; Box et al., 2006). Large
82 interannual variability causes the statistical significance of many of these trends to be
83 relatively low, but the independent trends exhibit internal consistency (e.g., warming is
84 expected to increase both melting and snowfall, on the basis of modeling experiments and
85 simple physical arguments, and both trends are observed in independent studies (Hanna
86 et al., 2005; Box et al., 2006)).

87 Increased iceberg calving has also been observed in response to faster flow of
88 many outlet glaciers and shrinkage or loss of ice shelves (see 7.1.2, below, for discussion
89 of the parts of an ice sheet) (e.g., Rignot and Kanagaratnam, 2006; Alley et al. 2005).

90 Increased iceberg calving has also been observed in response to faster flow of many
91 outlet glaciers and shrinkage or loss of ice shelves (see 7.1.2, below, for discussion of the
92 parts of an ice sheet) (e.g., Rignot and Kanagaratnam, 2006; Alley et al. 2005). The
93 Intergovernmental Panel on Climate Change (IPCC; Lemke et al., 2007) found that
94 “Assessment of the data and techniques suggests a mass balance of the Greenland Ice
95 Sheet of between +25 and -60 Gt (-0.07 to 0.17 mm) SLE [sea level equivalent] per year
96 from 1961-2003 and -50 to -100 Gt (0.14 to 0.28 mm SLE) per year from 1993-2003,
97 with even larger losses in 2005”. Updates are provided by Alley et al. (2007) (Figure
98 7.2) and by Cazenave (2006). Rapid changes have been occurring in the ice sheet, and in
99 the ability to observe the ice sheet, so additional updates are virtually certain to be
100 produced.

101

102 **FIGURE 7.2 NEAR HERE**

103

104 The long-term importance of these trends is uncertain—short-lived oscillation or
105 harbinger of further shrinkage? This uncertainty motivates some of the interest in the
106 history of the ice sheet.

107

108 **7.1.2 Ice-sheet behavior**

109 Where delivery of snow or ice (typically as snowfall) exceeds removal (typically by
110 meltwater runoff), a pile of ice develops. Such a pile that notably deforms and flows is
111 called a glacier, ice cap, or ice sheet. (For a more comprehensive overview, see Paterson,
112 1994; Hughes, 1998; Van der Veen, 1999; or Hooke, 2005, among well-known texts.)

113 Use of these terms is often ambiguous. “Glacier” most typically refers to a relatively
114 small mass in which flow is directed down one side of a mountain, whereas “ice cap”
115 refers to a small mass with flow diverging from a central dome or ridge, and “ice sheet”
116 to a very large ice cap of continental or subcontinental scale. A faster moving “jet” of ice
117 flanked by slower flowing parts of an ice sheet or ice cap may be referred to as an ice
118 stream, but also as an outlet glacier or simply glacier (especially if the configuration of
119 the underlying bedrock is important in delineating the faster moving parts), complicating
120 terminology. Thus, the prominent Jakobshavn Glacier (Jakobshavn Isbrae, or Jakobshavn
121 ice stream) is part of the ice sheet on Greenland, flowing in a deep bedrock trough but
122 with slower-moving ice flanking the faster-moving ice near the surface.

123 A glacier or ice sheet spreads under its own weight, deforming internally. The
124 deformation rate increases with the cube of the driving stress, which is proportional to the
125 ice thickness and to the surface slope of the ice. Ice may also move by sliding across the
126 interface between the bottom of the ice and what lies beneath it, i.e., its substrate. Ice
127 motion is typically slow or zero where the ice is frozen to the substrate, but is faster
128 where the ice-substrate interface is close to the melting point. Ice motion can also take
129 place through the deformation of subglacial sediments. This mechanism is important
130 only where subglacial sediments are present and thawed. The contribution of these basal
131 processes ranges from essentially zero to almost all of the total ice motion. Except for
132 floating ice shelves (see below in this section), Greenland’s ice generally does not exhibit
133 the gross dominance by basal processes seen in some West Antarctic ice streams.

134 Most glaciers and ice sheets tend toward a steady configuration. Snow
135 accumulation in higher, colder regions supplies mass, which flows to lower, warmer

136 regions where mass is lost by melting and runoff or by calving of icebergs that drift away
137 to melt elsewhere.

138 Some ice masses tend to an oscillating condition, marked by ice buildup during a
139 period of slow flow, and then a short-lived surge of rapid ice flow; however, under steady
140 climatic conditions, these oscillations repeat with some regularity and without huge
141 changes in the average size across cycles

142 Accelerations in ice flow, whether as part of a surging cycle, or in response to
143 long-term ice-sheet evolution or climatically forced change, may occur through several
144 mechanisms. These mechanisms include thawing of a formerly frozen bed, increase in
145 meltwater reaching the bed causing increased lubrication (Zwally et al., 2002; Joughin et
146 al., 1996; Parizek and Alley, 2004), and changes in meltwater drainage causing retention
147 of water at the base of the glacier, which increases lubrication (Kamb et al., 1985). Ice-
148 flow slowdown can similarly be induced by reversing these causes.

149 Recently, attention has been focused on changes in ice shelves. Where ice flows
150 into a bordering water body, icebergs may calve from grounded (non-floating) ice.
151 Alternatively, the flowing ice may remain attached to the glacier or ice sheet as it flows
152 into the ice-marginal body of water. The attached ice floats on the water and calves from
153 the end of the floating extension, which is called an ice shelf. Ice shelves frequently run
154 aground on local high spots in the bed of the water body on which they float. Ice shelves
155 that occupy embayments or fjords may rub against the rocky or icy sides, and friction
156 from this restrains, or “buttresses,” ice flow. Loss of this buttressing through shrinkage or
157 loss of an ice shelf then allows faster flow of the ice feeding the ice shelf (Payne et al.,
158 2004; Dupont and Alley, 2005; 2006).

159 Although numerous scientific papers have addressed the affects of changing
160 lubrication or loss of ice-shelf buttressing affecting ice flow, comprehensive ice-flow
161 models generally have not incorporated these processes. These comprehensive models
162 also failed to accurately project recent ice-flow accelerations in Greenland and in some
163 parts of the Antarctic ice sheet (Alley et al., 2005; Lemke et al., 2007; Bamber et al.,
164 2007). This issue is cited by IPCC (2007), which provided sea-level projections
165 “excluding future rapid dynamical changes in ice flow” (Table SPM3, WG1) and noted
166 that this exclusion prevented “a best estimate or an upper bound for sea level rise” (p.
167 SPM 15). A paleoclimatic perspective can help inform our understanding of these issues.

168 As noted above in this section, when subjected to a **step forcing** (e.g., a rapid
169 warming that moves temperatures from one sustained level to another), an ice sheet
170 typically responds by evolving to a new steady state (Paterson, 1994). For example, an
171 increase in accumulation rate thickens the ice sheet. The thicker ice sheet discharges mass
172 faster and, if the ice margin does not move as the ice sheet thickens, the ice sheet
173 becomes on average steeper, which also speeds ice discharge. These changes eventually
174 cause the ice sheet to approach a new configuration—a new steady state—that is in
175 balance with the new forcing. For central regions of cold ice sheets, the time required to
176 complete most of the response to a step change in rate of accumulation (i.e., the response
177 time) is proportional to the ice thickness divided by the accumulation rate. These
178 characteristic times are a few thousands of years (millennia) for the modern Greenland
179 Ice Sheet and a few times longer for the ice-age ice sheet (e.g., Alley and Whillans, 1984;
180 Cuffey and Clow, 1997).

181 A change in the position of the ice-margin will steepen or flatten the mean slope

182 of the ice sheet, speeding or slowing flow. The edge of the ice-sheet will respond first..
183 This response, in turn, will cause a wave of adjustment that propagates toward the ice-
184 sheet center. Fast-flowing marginal regions can be affected within years, whereas the full
185 response of the slow-flowing central regions to a step-change at the coast requires a few
186 millennia.

187 Warmer ice deforms more rapidly than colder ice. In inland regions, ice sheet
188 response to temperature change is somewhat similar to response to accumulation-rate
189 change with cooling causing slower deformation, which favors thickening hence higher
190 ice flux through the increased thickness (and perhaps with increasing surface slope also
191 speeding flow), re-establishing equilibrium. However, because most of the deformation
192 occurs in deep ice, and a surface-temperature change requires many millennia to
193 penetrate to that deep ice to affect deformation, most of the response is delayed for a few
194 millennia or longer while the temperature change penetrates to the deep layers, and then
195 the response requires a few more millennia. The calculation is not simple, because the
196 motion of the ice carries its temperature along with it. If melting of the upper surface of
197 an ice sheet develops over a region in which the bottom of the ice is frozen to the
198 substrate, thawing of that basal interface may be caused by penetration of surface
199 meltwater to the bed if water-filled crevasses develop at the surface. The actual
200 penetration of the water-filled crevasse is likely to occur in much less than a single year,
201 perhaps in only a few minutes, rather than over centuries to millennia (Alley et al., 2005).

202 Numerous ice-sheet models (e.g., Huybrechts, 2002) demonstrate the relative
203 insensitivity of inland ice thickness to many environmental parameters. This insensitivity
204 has allowed reasonably accurate ice-sheet reconstructions using computational models

205 that assume perfectly plastic ice behavior and a fixed yield strength (Reeh 1984; the only
206 piece of information needed in these reconstructions of inland-ice configuration is the
207 footprint of the ice sheet; one need not specify accumulation rate hence mass flux, for
208 example). This insensitivity can be understood from basic physics.

209 As noted above in this section, the stress that drives ice deformation increases
210 linearly with ice thickness and with the surface slope, and the rate of ice deformation
211 increases with the cube of this stress. Velocity from deformation is obtained by
212 integrating the deformation rate through thickness, and ice flux is the depth-averaged
213 velocity multiplied by thickness. Therefore, for ice frozen to the bed, the ice flux
214 increases with the cube of the surface slope and the fifth power of the thickness. (Ice flux
215 in an ice sheet with a thawed bed would retain strong dependence on surface slope and
216 thickness, but with different numerical values.) If the ice-marginal position is fixed (say,
217 because the ice has advanced to the edge of the continental shelf and cannot advance
218 farther across the very deep water), then the typical surface slope of the ice sheet is also
219 proportional to the ice thickness (divided by the fixed half-width), giving an eighth-
220 power dependence of ice flux on inland thickness. Although an eighth-power dependence
221 is not truly perfectly plastic, it does serve to greatly limit inland-thickness changes—
222 doubling the inland thickness would increase ice flux 256-fold. Because of this
223 insensitivity of the inland thickness to many controlling parameters, changes in ice-sheet
224 volume are controlled more by changes in the areal extent of the ice sheet than by
225 changes in the thickness in central regions (Reeh, 1984; Paterson, 1994).

226 Such simple mechanistic scalings of ice sheet behaviors can be useful in a
227 pragmatic sense, and they have been used to interpret ice-sheet behavior in the past.

228 However, in modern usage, our physical understanding of ice sheet behaviors is fully
229 coupled three-dimensional (or reduced-dimensional) ice-dynamical models (e.g.,
230 Huybrechts, 2002; Parizek and Alley, 2004; Clarke et al., 2005), which help researchers
231 assimilate and understand relevant data.

232

233 **7.2 Paleoclimatic Indicators Bearing on Ice-Sheet History**

234 The basis for paleoclimatic reconstruction is discussed in Cronin (1999) and
235 Bradley (1999), among other sources. Here, additional attention is focused on those
236 indicators that help in reconstruction of the history of the ice sheet. Marine indicators are
237 discussed first, followed by terrestrial archives.

238

239 **7.2.1 Marine Indicators**

240 As discussed in section 7.3 below, the Greenland Ice Sheet has at many times in
241 the past been more extensive than it is now, and much of that extension occupied regions
242 that now are below sea level. Furthermore, iceberg-rafted debris and meltwater from the
243 ice sheet can leave records in marine settings related to the extent of the ice sheet and its
244 flux of ice. Marine sediments also preserve important indicators of temperature and of
245 other conditions that may have affected the ice sheet.

246 Research cruises to the marine shelf and slope margins of west and east
247 Greenland dedicated to understanding changes over the times most relevant to its history
248 have been undertaken only in the last ten to twenty years. Initially, attention was focused
249 along the east Greenland shelf (Marienfeld, 1992b; Mienert et al., 1992; Dowdeswell et
250 al., 1994a), but in the last few years several cruises have extended to the west Greenland

251 margin as well (Lloyd, 2006; Moros et al., 2006). Research on adjacent deep-sea basins,
252 such as Baffin Bay or Fram Basin off North Greenland, is more complicated because the
253 late Quaternary (less than 450 thousand years old (ka)) sediments contain inputs from
254 several adjacent ice sheets (Dyke et al., 2002; Aksu, 1985; Andrews et al., 1998a; Hiscott
255 et al., 1989). (We use calendar years rather than radiocarbon years unless indicated;
256 conversions include those of Stuiver et al., 1998 and Fairbanks et al., 2005; all ages
257 specified as “ka” or “Ma” are in years before present, where “present” is conventionally
258 taken as the year 1950.) Regardless, only a few geographic areas on the Greenland shelf
259 have been investigated. In terms of time, the majority of marine cores from the Greenland
260 shelf span the retreat from the last ice age (less than 15 ka). The use of datable volcanic
261 ashes (tephras—a recognizable tephra or ash layer from a single eruption is commonly
262 found throughout broad regions and has the same age in all cores) from Icelandic sources
263 offers the possibility of linking records from around Greenland from the time of the layer
264 known as Ash Zone II (about 54 ka) to the present (with appropriate cautions; Jennings et
265 al., 2002a).

266 The sea-floor around Greenland is relatively shallow above “sills” formed during
267 the rifting that opened the modern oceans. Such sills connect Greenland to Iceland
268 through Denmark Strait and to Baffin Island through Davis Strait. These 500–600-m-
269 deep sills separate sedimentary records of ice sheet histories into “northern” and
270 “southern” components. Even farther north, sediments shed from north Greenland are
271 transported especially into the Fram Basin of the Arctic Ocean (Darby et al., 2002).

272 The circulation of the ocean around Greenland today transports debris-bearing
273 icebergs from the ice sheet. It is largely controlled by a clockwise pattern: cold, fresh

274 waters exit the Arctic Ocean through Fram Strait and flow southward along the East
275 Greenland margin as the East Greenland Current (Hopkins, 1991). These waters turn
276 north after rounding the southern tip of Greenland. In the vicinity of Denmark Strait,
277 warmer water from the Atlantic (modified Atlantic Water from the Irminger Current)
278 turns and flows parallel to the East Greenland Current. This surface current is called the
279 West Greenland Current once it has rounded the southern tip of Greenland. On the East
280 Greenland shelf, this modified Atlantic Water becomes an “intermediate-depth” water
281 mass (reaching to the deeper parts of the continental shelf, but not to the depths of the
282 ocean beyond the continental shelf), which moves along the deeper topographic troughs
283 on the continental shelf and penetrates into the margins of the calving Kangerdlugssuaq
284 ice stream (Jennings and Weiner, 1994; Syvitski et al., 1996). Baffin Bay contains three
285 water masses: Arctic Water in the upper 100–300 meters (m) in all areas, West Greenland
286 Intermediate Water (modified Atlantic Water) between 300–800 m, and Deep Baffin Bay
287 Water throughout the Bay at depths greater than 1200 m (Tang et al., 2004).

288 Some of the interest in the Greenland Ice Sheet is linked to the possibility that
289 meltwater could greatly influence the formation of deep water in the North Atlantic.
290 Furthermore, changes in deep-water formation in the past are linked to climate changes
291 that affected the ice sheet (e.g., Alley, 2007). The major deep-water flow is directed
292 southward through and south of Denmark Strait (McCave and Tucholke, 1986). The
293 sediment deposit known as the Erik Drift off southwest Greenland is a product of this
294 flow (Stoner et al., 1995). Convection in the Labrador Sea forms an upper component of
295 this North Atlantic Deep Water.

296 Evidence from marine cores and seismic data has been used to reconstruct

297 variations in the Greenland Ice Sheet during the last glacial cycle (and, occasionally, into
298 older times). Four types of evidence apply: (1) ice-rafted debris and indications of
299 changes in sediment sources; (2) glacial deposition onto trough-mouth fans; (3) stable-
300 isotope and biotic data that indicate intervals when meltwater was released from the ice
301 sheet; and (4) geophysical data that indicate sea-floor erosion and deposition. Each is
302 discussed briefly in section 7.2.1, below.)

303

304 **7.2.1a Ice-rafted debris and its provenance**

305 Coarse-grained rock material (such as sand and pebbles) cannot be carried far
306 from a continent by wind or current, so the presence of such materials in marine cores is
307 of great interest. Small amounts might be delivered in tree roots or attached to uprooted
308 kelp holdfasts (Gilbert, 1990; Smith and Bayliss-Smith, 1998), and rarely a meteorite
309 might be identified, but large quantities of coarse rock material found far from land
310 indicate transport in ice, and so this material is called ice-rafted debris (IRD). Both sea
311 ice and icebergs can carry coarse material, complicating interpretations. However,
312 iceberg-rafted debris usually includes some number of grains larger than 2 mm in size
313 and consistent with the grain-size distribution of glacially transported materials, whereas
314 the sediment entrained in sea ice is typically finer (Lisitzin, 2002). In order to link the
315 Greenland Ice Sheet with ice-rafted debris described in marine cores, we must be able to
316 link that debris to specific bedrock sites (i.e., identify its provenance or site of origin).
317 However, such studies are only in their infancy. Proxies for sediment source include
318 radiogenic isotopes (such as ϵNd ; Grousset et al., 2001; Farmer et al., 2003), biomarkers
319 that can be linked to different outcrops of dolomite (Parnell et al., 2007), magnetic

320 properties of sediment (Stoner et al., 1995), and quantitative mineralogical assessment of
321 sediment composition (Andrews, 2008).

322

323 **7.2.1b Trough mouth fans**

324 The sediments in trough-mouth fans contain histories of sediment sources that
325 may include ice sheets. Sediment is commonly transferred across the continental shelf
326 along large troughs that form major depositional features called trough-mouth fans
327 (TMF) where the troughs widen and flatten at the continental rise (Vorren and Laberg,
328 1997; O'Cofaigh et al., 2003). Along the East Greenland margin, trough-mouth fans exist
329 off Scoresby Sund (Dowdeswell et al., 1997), the Kangerdlugssuaq Trough (Stein, 1996),
330 and the Angamassalik Trough (St. John and Krissek, 2002). Along the west Greenland
331 margin, the most conspicuous such fan is a massive body off Disko Bay associated with
332 erosion by Jakobshavn Glacier and other outlet glaciers in that region. During periods
333 when the ice sheet reached the shelf break, glacial sediments were shed downslope as
334 debris flows (producing coarse, poorly sorted deposits containing large grains in a fine-
335 grained matrix), whereas periods when the ice sheet was well back from the shelf break
336 are marked by sediments containing materials typical of open-marine environments, such
337 as shells of foraminifers) and typical terrestrial materials (including ice-rafted debris).

338

339 **7.2.1c Foraminifers and stable-isotopic ratios of shells**

340 Foraminifers—mostly marine, single-celled planktonic animals with chalky
341 shells—are widely distributed in sediments, and shells of surface-dwelling (planktic) and
342 bottom-dwelling (benthic) species are commonly found. The particular species present

343 and the chemical and isotopic characteristics of their shells reflect environmental
344 conditions. Variations in the ratios of the stable isotopes of oxygen, ^{18}O to ^{16}O ($\delta^{18}\text{O}$) are
345 especially widely used. These ratios respond to changes in the global ice volume. Water
346 containing the lighter isotope (^{16}O) evaporates from the ocean more readily, and ice
347 sheets are ultimately composed of that evaporated water, so during times when the ice
348 sheets are larger, the ocean is isotopically heavier. This effect is well known, and it can
349 be corrected for with considerable confidence if the age of a sample is known.
350 Temperature also affects $\delta^{18}\text{O}$; warmer air temperatures favor incorporation of the lighter
351 isotope into the shell. Near ice sheets, the abrupt appearance of light isotopes is most
352 commonly associated with meltwater that delivered isotopically light and fresh water
353 (Jones and Keigwin, 1988; Andrews et al., 1994). Around the Greenland Ice Sheet, most
354 such records are from near-surface planktic foraminifers of the species *N. pachyderma*
355 sinistral (Fillon and Duplessy, 1980; van Kreveld et al., 2000; Hagen and Hald, 2002),
356 although there are some data from benthic foraminifers (Andrews et al., 1998a; Jennings
357 et al., 2006).

358

359 **7.2.1d Seismic and geophysical data**

360 Several major shelf troughs and trough-mouth fans have been studied by seismic
361 investigations. Most are high-resolution studies of the sediments nearest the sea floor
362 (seismostratigraphy; O'Cofaigh et al., 2003), although some data on deeper strata are
363 available (airgun profiles; Stein, 1996; Wilken and Mienert, 2006). Sonar reveals the
364 shape of the upper surface of the sediment, and features such as the tracks left by drifting
365 icebergs that plowed through the sediment (Dowdeswell et al., 1994b; Dowdeswell et al.,

366 1996; Syvitski et al., 2001) and the streamlining of the sediment surface caused by
367 glaciation.

368

369 **7.2.2 Terrestrial Indicators**

370 Land-based records, like their marine equivalents, can reveal the history of
371 changes in areal extent of ice and of the climate conditions that existed around the ice
372 sheet. Terrestrial records are typically more discontinuous in space and time than are
373 marine records, because net erosion (which removes sediments containing climatic
374 records) is dominant on land whereas net deposition is dominant in most marine settings.
375 Nonetheless, useful records of many time intervals have been assembled from terrestrial
376 indicators. Here, common indicators are briefly described. This treatment is
377 representative rather than comprehensive. Furthermore, the great wealth of indicators,
378 and the interwoven nature of their interpretation, precludes any simple subdivision.

379

380 ***7.2.2a Geomorphic indicators***

381 The land surface itself records the action of ice and thus provides information on
382 ice-sheet history. Glacial deposits known as moraines are especially instructive, but
383 others are also important.

384 Moraines are composed of sediment deposited around glaciers from material
385 carried on, in, or under the moving ice (e.g., Sugden and John, 1976). A preserved
386 moraine may mark either the maximum extent reached by ice during some advance or a
387 still-stand during retreat. Normally, older moraines are destroyed by ice readvance,
388 although remnants of moraines overrun by a subsequent advance are occasionally

389 preserved and identifiable, especially if the ice that readvanced was frozen to its bed and
390 thus nearly or completely stationary where the ice met the moraine. Because most older
391 moraines are reworked by subsequent advances, most existing moraines record only the
392 time of the most recent glacial maximum and pauses or subsidiary readvances during
393 retreat.

394 The limiting ages of moraines can be estimated from radiocarbon (carbon-14)
395 dating of carbon-bearing materials incorporated into a moraine (the moraine must be
396 younger than those materials) or deposited in lakes that formed on or behind moraines
397 following ice retreat (the moraine must be older than those materials). Increasingly,
398 moraines are dated by measurement of beryllium-10 or other isotopes produced in
399 boulders by cosmic rays (e.g., Gosse and Phillips, 2001). Cosmic rays penetrate only
400 about 1 m in rock. Thus, boulders that are quarried from beneath the ice following
401 erosion of about 1 m or more of overlying material, or large boulders that fell onto the ice
402 and rolled over during transport, typically start with no cosmogenic nuclides in their
403 upper surfaces but accumulate those nuclides proportional to exposure time. Corrections
404 for loss of nuclides by boulder erosion, for inheritance of nuclides from before
405 deposition, and other factors may be nontrivial but potentially reveal further information.
406 Additional techniques of dating can sometimes be used, including historical records and
407 the increase with time of the size of lichen colonies (e.g., Locke et al., 1979; Geirsdottir
408 et al., 2000), soil development, and breakdown of rocks (clast weathering).

409 Related information on glacial behavior and ages is also available from the land
410 surface. For ages of events, a boulder need not be in a moraine to be dated using
411 cosmogenic isotopes, and surfaces striated and polished by glacial action can be dated

412 similarly. Glacial retreat often reveals wood or other organic material that died when it
413 was overrun during an advance and that can also be dated using radiocarbon techniques.

414 In moraines produced by small glaciers, the highest elevation to which a moraine
415 extends is commonly close to the equilibrium-line altitude at the time when the moraine
416 formed. (The equilibrium-line altitude is the altitude above which net snow accumulation
417 occurred and below which mass loss occurred—mass moved into the glacier above that
418 elevation and out below that elevation, controlling the deposition of rock material.)

419 Glaciation produces identifiable landforms, especially if the ice was thawed at the base
420 and thus slid freely across its substrate, so contrasts in the appearance of landforms can
421 be used to map the limits of glaciation (or of wet-based glaciation) where moraines are
422 not available.

423 Glaciers respond to many environmental factors, but for most glaciers the balance
424 between snow accumulation and melting is the major control on glacier size.

425 Furthermore, with notable exceptions, melting is usually affected more by temperature
426 than is accumulation. The equilibrium vapor pressure (the ability of warmer air to hold
427 more moisture) increases roughly 7% per °C. For a variety of glaciers that balance snow
428 accumulation by melting, the increase in melting is approximately 35% ($\pm 10\%$) per °C
429 (e.g., Oerlemans, 1994; 2001; Denton et al., 2005). Thus, glacier extent can usually be
430 used as a proxy for temperature (duration and warmth of the melt-season) , primarily
431 summertime temperature.

432

433 *7.2.2b Biological indicators and related features*

434 Living things are sensitive to climate. The species found in a tropical rain forest

435 differ from those found on the tundra. By comparing modern species from different
436 places that have different climates, or by looking at changes in species at one place for
437 the short interval of the instrumental record, the relation with climate can be estimated.
438 Assuming that this relation has not changed with time, longer records of climate then can
439 be estimated from occurrence of different species in older sediments (e.g., Schofield et
440 al., 2007). These climate records then can be tied, to some degree, to the state of the ice
441 sheet.

442 Lake sediments are especially valuable as sources of biotic indicators, because
443 sedimentation (and thus the record) is continuous and the ecosystems in and around lakes
444 tend to be rich (e.g., Bjorck et al., 2002; Ljung and Bjorck, 2004; Andresen et al., 2004).
445 Pollen (e.g., Ljung and Bjorck, 2004; Schofield et al., 2007), microfossils, and
446 macrofossils (such as chironomids, or midge flies (Brodersen and Bennike, 2003)) are all
447 used to great advantage in reconstructing past climates. The isotopic composition of
448 shells or of inorganic precipitates in lakes records some combination of temperature and
449 of the isotopic composition of the water . Physical aspects of lake sediments, including
450 those linked to biological processes (e.g., loss on ignition, which primarily measures the
451 relative abundance of organic matter in the sediment) are also related to climate. In places
452 where the weight of the ice previously depressed the land below sea level and subsequent
453 rebound raised the land back above sea level and formed lakes (see 7.2.2c, below), the
454 time of onset of lacustrine conditions and the modern height of the lake together provide
455 key information on ice-sheet history (e.g., Bennike et al., 2002).

456 Raised marine deposits in Greenland and surroundings provide an additional and
457 important source of biological indicators of climate change. Many marine deposits now

458 reside above sea level, because of the interplay of changing sea level, geological
459 processes of uplift and subsidence, and isostatic response (ice-sheet growth depressing
460 the land and subsequent ice-sheet shrinkage allowing rebound, with a lagged response;
461 again, see 7.2.2c, below) . Biological materials within those deposits, and especially
462 shells, can be dated by radiocarbon or uranium-thorium techniques (see 7.2.2d, below).
463 Those dates then help fill in the history of relative sea level that can be used to infer ice-
464 sheet loading histories and to reconstruct climates on the basis of the species present
465 (e.g., Dyke et al., 1996).

466

467 *7.2.2c Glacial isostatic adjustment and relative sea-level indicators near the ice*
468 *sheet*

469 Within the geological literature, sea level is generally defined as the distance
470 between the sea surface and sea bottom. (This convention contrasts with the concept of
471 an absolute sea level whose position (the sea surface) is measured relative to some
472 absolute datum, such as the center of Earth.) This definition of sea level is consistent with
473 geological markers of past sea-level change (such as ancient shorelines, shells, and
474 driftwood), which reflect changes in the height of either of the two bounding surfaces
475 (i.e., an ancient shoreline can be exposed because the surface of the ocean dropped, or
476 land uplifted, or a net combination of land and ocean height changes). During the time
477 periods considered in this report, the dominant process responsible for such changes, at
478 least on a global scale, has been the mass transfer between ice reservoirs and oceans
479 associated with the ice-age cycles and the deformational response of Earth to this transfer
480 of mass. This deformational response is formally termed **glacial isostatic adjustment**.

481 The growth and shrinkage of ice have generally been sufficiently slow that glacial
482 isostatic adjustment of the solid Earth is characterized by both immediate **elastic** and
483 slow viscous (i.e., flow) effects. As an example, if a large ice sheet were to form instantly
484 and then persist for more than a few thousand years, the land would respond by nearly
485 instantaneous elastic sinking, followed by slow subsidence toward isostatic equilibrium
486 as deep, hot rock moved outward from beneath the ice sheet. Roughly speaking, the final
487 depression would be about 30% of the thickness of the ice. Thus the ancient Laurentide
488 Ice Sheet, which covered most of Canada and the northeastern United States and whose
489 peak thickness was 3–4 km, produced a crustal depression of about 1 km. (For
490 comparison, that ice sheet contained enough water to make a layer about 70 m thick
491 across the world oceans, much less than the local deformation beneath the ice.) Outside
492 the depressed region covered by ice, land is gradually pushed upward to form a
493 peripheral bulge. As the ice subsequently melts, the central region of depression
494 rebounds, and relative sea level will fall for thousands of years beyond the end of the
495 melting phase. For example, at sites in Hudson Bay, sea-level continues to fall on the
496 order of 1 centimeter per year (cm/yr) despite the disappearance of most of the
497 Laurentide Ice Sheet some 8000 years ago. Moreover, the loss of ice cover allows the
498 peripheral bulge to subside, leading to a sea-level rise in such areas (e.g., along the east
499 coast of the United States) that also continues to the present. As one considers sites
500 farther away from the high-latitude ice cover, in the so-called “far field,” the sea-level
501 change is dominated during deglaciation by the addition of meltwater into the global
502 oceans. However, in periods of stable ice cover, for example during the present
503 interglacial, changes in sea level continue as a consequence of the ongoing gravitational

504 and deformational effects of glacial isostatic adjustment. As an example, glacial isostatic
505 adjustment in parts of the equatorial Pacific is responsible for a fall in sea level of about 3
506 m during the last 5,000 years and for the associated exposure of corals and ancient
507 shoreline features of this age (Mitrovica and Peltier, 1991; Mitrovica and Milne, 2002;
508 Dickinson, 2001). We will return to this point in section 7.2.2d, below.

509 Nearby (near-field) relative sea-level changes, where the term “relative” denotes
510 the height of an ancient marker relative to the present-day level of the sea, have
511 commonly been used to constrain models of the geometry of ice complexes, particularly
512 since the Last Glacial Maximum (about 24 ka) (e.g., Lambeck et al., 1998; Peltier, 2004).
513 Fleming and Lambeck (2004) compared a set of about 600 relative sea-level data points
514 from sites in Greenland; all but the southeast coast and the west coast near Melville Bugt
515 were represented. Numerical models of glacial isotatic adjustment constrained the history
516 of the Greenland Ice Sheet after the Last Glacial Maximum. The Fleming and Lambeck
517 (2004) data set comprised primarily fossil mollusk shells that lived at or below the sea
518 surface but that now are exposed above sea level; because of the unknown depth at which
519 the mollusks lived, they provide a limiting value on sea level. However, Fleming and
520 Lambeck (2004) also included observations on the transition of modern lakes from
521 formerly marine conditions, and constraints associated with the present (sub-sea) location
522 of initially terrestrial archaeological sites (see also Weidick, 1996; Kuijpers et al., 1999).
523 Tarasov and Peltier (2002, 2003) analyzed their own compilation of local sea-level
524 records by coupling glacial isostatic adjustment and climatological models; from this
525 information they inferred ice history into the last interglacial.

526 Like all glacial isostatic adjustment models, these studies are hampered by

527 uncertainties in the viscoelastic structure of Earth (Mitrovica, 1996), which is generally
528 prescribed by the thickness of the elastic plate and the radial profile of viscosity within
529 the underlying mantle, and this uncertainty has implications for the robustness of the
530 inferred ice history. In addition, the analysis of sea-level records in Greenland is
531 complicated by signals from at least two other distant sources: (1) the adjustment of the
532 peripheral bulge associated with the (de)glaciation of the larger North American
533 Laurentide Ice Sheet, because this bulge extends into Greenland (e.g., Fleming and
534 Lambeck, 2004); and (2) the net addition of meltwater from contemporaneous melting
535 (or, in times of glaciation, growth) of all other global ice reservoirs. Therefore, some
536 constraints on the volume and extent of the Laurentide ice sheet, and the volume of more-
537 distant ice sheets and glaciers, are required for the analysis of sea-level data from
538 Greenland.

539

540 *7.2.2d Far-field indicators of relative sea-level high-stands*

541 Past changes in the volume of the Greenland Ice Sheet are recorded in far-field
542 sea level. All other sources of sea-level change, as well as the change due to glacial
543 isostatic adjustment, are also recorded in far-field sea-level records, so a single history of
544 sea level provides information related to ice-volume change (and to other factors such as
545 thermal expansion and contraction of ocean water) but no information on the relative
546 contribution of individual sources.

547 The record of past sea level can be reconstructed in many ways. An especially
548 powerful method of reconstruction uses the record of marine deposits or emergent coral
549 reefs that are now found above sea level on geologically relatively stable coasts and

550 islands (that is, in regions not markedly affected by processes linked to plate tectonics).
551 Such records are literally high-water marks (or “bathtub rings”) of past high sea levels.
552 Coastal landforms and deposits provide powerful and independent records of sea-level
553 history compared with the often-cited deep-sea oxygen-isotope record of glacial and
554 interglacial periods. For recording sea-level history, coastal landforms have two
555 advantages as compared with the deep-sea oxygen-isotope record: (1) if corals are
556 present, they can be dated directly; and (2) estimates of ancient sea level may—
557 depending on the geological setting—be possible.

558 Coastal landforms record high stands of the sea when coral-reefs grew as fast as
559 sea level rose (upper panel in Figure 7.3) or when a stable sea-level high stand eroded
560 marine terraces into bedrock (lower panel in Figure 7.3). Thus, emergent marine deposits,
561 either reefs or terraces, on geologically active, rising coastlines record interglacial periods
562 (Figure 7.4). On a geologically stable or slowly sinking coast, reefs will emerge only
563 from sea-level stands that were higher than at present (Figure 7.4). Past sea levels can
564 thus be determined from stable coastlines or even rising coastlines, if one can make
565 reasoned models of uplift rates. Geologic records of high sea-level stands on geologically
566 relatively stable coasts are especially useful. Although valuable geologic records are
567 found on rising coasts, estimates of past sea level derived from such coasts depend on
568 assumptions about the rate of tectonic uplift, and therefore they embody more
569 uncertainty.

570

571 FIGURE 7.3 NEAR HERE

572 FIGURE 7.4 NEAR HERE

573

574 The direct dating of emergent marine deposits is possible because uranium (U) is
575 dissolved in ocean water but thorium (Th) and protactinium (Pa) are not. Certain marine
576 organisms, particularly corals, co-precipitate U directly from seawater during growth. All
577 three of the naturally occurring isotopes of uranium— ^{238}U and ^{235}U (both primordial
578 parents) and ^{234}U (a decay product of ^{238}U)—are therefore incorporated into living corals.
579 ^{238}U decays to ^{234}U , which in turn decays to ^{230}Th . The parent isotope ^{235}U decays to
580 ^{231}Pa . Thus, activity ratios of $^{230}\text{Th}/^{234}\text{U}$, $^{238}\text{U}/^{234}\text{U}$, and $^{231}\text{Pa}/^{235}\text{U}$ can provide three
581 independent clocks for dating the same fossil coral (e.g., Edwards et al., 1997). Since the
582 1980s, most workers have employed thermal ionization mass spectrometry (TIMS) to
583 measure U-series nuclides; this method has increased precision, requires much smaller
584 samples, and can extend the useful time period for dating back to at least about 500,000
585 years.

586 The coastlines where the most reliable records of past high sea levels can be
587 found are in the tropics and subtropics, where ocean temperatures are warm enough that
588 coral-reefs grow. Within this broad equatorial region, the ideal coastlines for studies of
589 past high sea levels are those that are distant from boundaries of tectonic plates. Such
590 coastlines lie near geologically relatively quiescent continental margins or as islands well
591 within the interiors of large tectonic plates. Even in such locations, however, interpreting
592 past sea levels can include much uncertainty. We highlight two major reasons for this
593 uncertainty.

594 First, many islands well within the crustal tectonic plate that underlies the Pacific
595 Ocean, for example, are part of hot-spot volcanic chains. (A major source of internal heat,

596 called a hot spot, leads to a volcano on the overriding tectonic plate; as the plate drifts
597 laterally, the slower-moving hot spot becomes positioned below a different part of the
598 plate, and a new volcano is formed as the previously active volcano becomes extinct.
599 Eventually, a chain of volcanoes is produced, such as the Hawaiian-Emperor seamount
600 chain). As a volcano grows in elevation, its weight isostatically depresses the land it sits
601 on in the same way that the weight of an ice sheet does, and the cold upper elastic layer
602 of the Earth flexes to form a broad ring-shaped ridge around the low caused by the
603 volcano. Oahu, in the Hawaiian Island chain, is a good example of an island that is
604 apparently experiencing slow uplift, and an associated local sea-level fall, due to volcanic
605 loading on the “Big Island” of Hawaii (Muhs and Szabo, 1994).

606 Second, the existence of a sea-level highstand of a given age in a stable geologic
607 setting does not necessarily imply that ice volumes were lower at that time relative to the
608 present day, even if the highstand is dated to a previous interglacial. As discussed above,
609 glacial isostatic adjustment, because it involves slow viscous flow of rock, produces
610 global-scale changes in sea-level even during periods when ice volumes are stable. As an
611 example, for the last 5,000 years (long after the end of the last glacial interval), ocean
612 water has moved away from the equatorial regions and toward the former Pleistocene ice
613 complexes to fill the voids left by the subsidence of the peripheral bulge regions
614 produced by the ice sheets. As a result, sea level has fallen (and continues to fall) about
615 0.5 mm/yr in those far-field equatorial regions (Mitrovica and Peltier, 1991; Mitrovica
616 and Milne, 2002). This process, known as equatorial ocean siphoning, has developed so-
617 called 3-meter beaches and exposed coral reefs that have been dated to the end of the last
618 deglaciation and that are endemic to the equatorial Pacific (e.g., Dickinson, 2001). Thus,

619 the interpretation of such apparent highstands requires correction for glacial isostatic
620 adjustments such that the residual record reflects true changes in ice volume.

621

622 *7.2.2e Geodetic indicators*

623 Geodetic data are yielding both local and regional constraints on recent changes
624 in the mass of ice-sheets. As an example, land-based measurements of changes in gravity
625 and crustal motions, estimated by using the global positioning system (GPS), are being
626 used to monitor deformation (associated with changes in the distribution of mass) at the
627 periphery of the Greenland Ice Sheet (e.g., Kahn et al., 2007). A drawback of these
628 techniques is that few sites have been monitored because of the difficulty of establishing
629 high-quality GPS sites. In contrast, data from the Gravity Recovery and Climate
630 Experiment (GRACE) satellite mission are revealing trends in gravity across the polar ice
631 sheets (at a spatial resolution of about 400 km) from which estimates of both regional and
632 integrated mass flux are being obtained (e.g., Velicogna and Wahr, 2006). A general
633 problem in all attempts to infer recent ice sheet balance, whether from land-based or
634 satellite gravity, GPS, or even altimeter measurements of ice height (e.g., Johannessen et
635 al., 2005; Thomas et al., 2006), is that a measurements must be corrected for the
636 continuing influence of glacial isostatic adjustments. As discussed above (section 7.2.2c),
637 this correction involves uncertainty associated with both the ice sheet history and the
638 viscoelastic structure of Earth.

639 Accurate glacial isostatic adjustment corrections are also central to regional
640 estimates of ice-sheet mass balance. For the last century global sea-level change has been
641 inferred principally by analyzing records from widely distributed tide gauges (simple sea-

642 level monitoring devices). Most residual rates (those corrected for glacial isostatic
643 adjustment) of tide gauges yield an average 20th century sea-level rise in the range 1.5–
644 2.0 mm/yr (Douglas, 1997).

645 Furthermore, geographic trends in the residual rates may constrain the sources of
646 the meltwater. In particular, Mitrovica et al. (2001) and Plag and Juttner (2001) have
647 demonstrated that the rapid melting of different ice sheets will have substantially
648 different signatures, or fingerprints, in the spatial pattern of sea-level change. These
649 patterns are linked to the gravitational effects of the lost ice (sea level is raised near an ice
650 sheet because of the gravitational attraction of the ice mass for the adjacent ocean water)
651 and to the elastic (as opposed to viscoelastic) deformation of Earth driven by the rapid
652 unloading. Some ambiguity in determining the source of meltwater arises because of
653 uncertainty in both the original correction for glacial isostatic adjustment and in the
654 correction for the poorly known signature of ocean thermal expansion, as well as from
655 the non-uniform distribution of tide gauge sites.

656 Other geodetic indicators related to Earth’s rotational state also constrain
657 estimates of recent changes in the mass of ice-sheets (Munk, 2002; Mitrovica et al.,
658 2006). Earth’s rotation is affected by any redistribution of mass on or inside the planet.
659 Transfer of mass from the poles to the equator slows the planet’s rotation (like a spinning
660 ice skater extending her arms to slow her rotation). Moreover, any transfer of mass that is
661 not symmetric about the poles causes “wobble,” or true polar wander (TPW) (that is, the
662 position of the north rotation pole moves relative to the surface of the planet). True polar
663 wander for the last century has been estimated using both astronomical and satellite
664 geodetic data. In contrast, changes in the rotation rate (or, as geodesists say, length of

665 day), have been determined for the last few decades by using satellite measurements and
666 for the last few millennia by using observations of eclipses recorded by ancient cultures.
667 Specifically, the timing of ancient eclipses recorded by these cultures differs from the
668 timing one would expect by simply projecting the Earth-Moon-Sun system back in time
669 using the modern rotation rate of Earth. The discrepancy indicates a gradual slowing of
670 Earth's rate of rotation (Munk, 2002). The difference in the rotation-rate history during
671 the last few millennia (after correcting for slowing of Earth's rotation associated with the
672 "drag" of the tides) as compared with the rotation rate of last few decades provides a
673 measure of any anomalous recent melting of polar ice reservoirs. (This difference does
674 not uniquely constrain the individual sources of the meltwater because all sources will be
675 about equally efficient, for a given mass loss rate, at driving these changes in rotation.)
676 True polar wander, after correction for glacial isostatic adjustment, serves as an important
677 complement to this rotation-rate analysis because it does give some information about the
678 source of the meltwater. As an example, melting from the Antarctic, because it is located
679 at the pole, generates very little true polar wander, whereas melting from the Greenland
680 Ice Sheet, whose center of mass lies about 15 degrees off Earth's rotation axis, is capable
681 of driving substantial true polar wander (Munk, 2002; Mitrovica et al., 2006).

682

683 *7.2.2f Ice cores*

684 Ice cores preserve information about many climatic variables that affected the ice
685 sheet, and about how the ice sheet responded to changes in those variables.

686 Temperature histories derived from ice cores are especially accurate. Several
687 indicators are used, as described next, such as the isotopic ratios of accumulated snow,

688 ice-sheet temperature profiles (using borehole thermometry), and various techniques
689 based on use of gas-isotopic indicators . Agreement among these different indicators
690 increases confidence in the results.

691 Let us first consider isotopic ratios of the oxygen and hydrogen in accumulated
692 snow (e.g., Jouzel et al., 1997). The ocean contains both normal and “heavy” water:
693 roughly one molecule in 500 incorporates at least one extra neutron in the nucleus of an
694 oxygen or hydrogen atom. Evaporation is less likely, and condensation hence
695 precipitation more likely, for the heavier species. As water evaporated from the ocean is
696 carried by an air mass inland over an ice sheet, the heavy species preferentially rain or
697 snow out. The colder the air mass, the more vapor is removed, the more depleted of the
698 heavy species is the remaining vapor, and the lighter the isotopic ratios in the next rain or
699 snow. Hence, the isotopic composition of precipitation is linked to temperature of the air
700 mass and, over polar ice sheets, the temperature of the air mass is typically linked to the
701 surface temperature. { {Oxygen- and hydrogen-isotope ratios are both studied, and they
702 help locate the source of precipitation, track the changing isotopic composition of the
703 moving air mass (“path effects”), and indicate the ice-sheet temperature as well. Because
704 site temperature is most important for this review, one species is sufficient. Results will
705 be discussed here as $\delta^{18}\text{O}$, the difference between the $^{18}\text{O}:^{16}\text{O}$ ratio of a sample and of
706 standard mean ocean water, normalized by the ratio of the standard and expressed not as
707 percent but as per mil (‰) (percent is parts per hundred, and per mil is parts per
708 thousand).

709 Although linked to site temperature, $\delta^{18}\text{O}$ can be affected by many factors (Jouzel
710 et al., 1997; Alley and Cuffey, 2001), such as change in the ratio of summertime to

711 wintertime precipitation. Hence, additional means of determining past temperatures are
712 required. One of the most reliable is based on the physical temperature of the ice. Just as
713 a frozen turkey takes a long time in a hot oven to warm in the middle, intermediate depths
714 of the central Greenland Ice Sheet are colder than ice above or below. Surface ice
715 temperatures equilibrate with air temperature, and basal ice receives some warmth from
716 Earth's heat flow, but the center of the ice sheet has not finished warming from the ice-
717 age cold. If ice flow is understood well at a site, the modern profile of the physical
718 temperature of the ice with increasing depth provides a low-time-resolution history of the
719 surface temperature with increasing time. Joint interpretation of the isotopic ratios and
720 temperatures measured in boreholes (Cuffey et al., 1995; Cuffey and Clow, 1997), or
721 independent interpretation of the borehole temperatures and then comparison with the
722 isotopic ratios (Dahl-Jensen et al., 1998), helps to outline the history of temperature.
723 Furthermore, the relation between isotopic ratio and temperature (α ‰ per °C) becomes a
724 useful paleoclimatic indicator, and changes in this ratio α with time can be used to test
725 hypotheses about the overall changes in seasonality of snowfall and other factors.

726 The isotopic composition of gases trapped in bubbles in the ice sheet provides an
727 additional indicator of temperature.. New-fallen snow contains many interconnected air
728 spaces. Snow turns to ice without melting in central regions of cold ice sheets through
729 solid-state mechanisms that operate more rapidly under higher temperature or higher
730 pressure. Snow in an ice sheet usually transforms to ice within the top few tens of
731 meters. The intermediate material is called firn, and the transformation is complete when
732 bubbles are isolated so that the air spaces are no longer interconnected to the surface.
733 Wind moving over the ice sheet typically mixes gases in the pore spaces of the firn only

734 in the uppermost few meters or less. Diffusion mixes the gases deeper than this. Gases
735 are slightly separated by gravity (Sowers et al., 1992), with the air trapped in bubbles
736 slightly isotopically heavier, than in the free atmosphere, proportional to the thickness of
737 the air column in which diffusion dominates.

738 If a sudden temperature change occurs at the surface, the temperature change
739 requires typically about 100 years to penetrate to the depth of bubble trapping. However,
740 when a temperature gradient is applied across gases in diffusive equilibrium, the gases
741 are separated by thermal fractionation as well as by gravity, with the heavier gases moved
742 thermally to the colder end (Severinghaus et al., 1998). Equilibrium of gases is obtained
743 in a few years, far faster than the time for heat flow to remove the temperature gradient
744 across the firn. Within a few years after an abrupt temperature change at the surface,
745 newly forming bubbles will begin to trap air with very slight (but easily measured)
746 anomalies in gas-isotope compositions, and this trapping of slightly anomalous air will
747 continue for a century or so. Because different gases have different sensitivities to
748 temperature gradients and to gravity, measuring isotopic ratios of several gases (such as
749 argon and nitrogen) allows researchers to determine the temperature difference that
750 existed vertically in the firn at the time of bubble trapping and to determine the thickness
751 of firn in which wind was not mixing the gas (Severinghaus et al., 1998). If the surface
752 temperature changed very quickly, the magnitude of the temperature difference across the
753 firn will peak at the magnitude of the surface-temperature change; if it changed slowly,
754 the temperature difference across the firn will always be less than the total temperature
755 change at the surface. If the climate was relatively steady before an abrupt temperature
756 change, such that the depth-density profile of the firn came into balance with the

757 temperature and the accumulation rate, and if the accumulation rate is known
758 independently (see below), then the number of years or amount of ice between the gas-
759 phase and ice-phase indications of abrupt change provides information on the mean
760 temperature before the abrupt change (Severinghaus et al., 1998). With so many
761 independent thermometers, highly confident paleothermometry is possible.

762 Ice cores can provide information on climatic indicators other than temperature.
763 Past ice-accumulation rates are most readily obtained by measuring the thickness of
764 annual layer in ice cores corrected for ice-flow thinning (e.g., Alley et al., 1993). In other
765 methods, the thickness of firn can be approximated by measurements of gas-isotope
766 fractionation or of the number and density of bubbles (Spencer et al., 2006); these
767 measurements combined with temperature estimates constrain accumulation rates as well.
768 Aerosols (very small liquid and solid particles) of all types fall with snow and are
769 incorporated into the ice sheet; with knowledge of the accumulation rate (hence dilution
770 of the aerosols), time histories of atmospheric loading of those aerosols can be estimated
771 (e.g., Alley et al., 1995a). Dust and volcanic fallout (e.g., Zielinski et al., 1994) help
772 constrain the cooling effects of aerosols (particles) blocking the Sun. Cosmogenic
773 isotopes (beryllium-10 is most commonly measured) reflect cosmic-ray bombardment of
774 the atmosphere, which is modulated by the strength of Earth's magnetic field and by solar
775 activity (e.g., Finkel and Nishiizumi, 1997). The observed correlation in paleoclimatic
776 records between indicators of climate and indicators of solar activity (Stuiver et al., 1997;
777 Muscheler et al., 2005; Bard and Frank, 2006)—and the lack of correlation with
778 indicators of magnetic-field strength (Finkel and Nishiizumi, 1997; Muscheler et al.,
779 2005)—help researchers understand climate changes.

780 Ages in ice cores are estimated by counting annual layers (e.g., Alley et al., 1993;
781 Andersen et al., 2006) and by correlation with other records (Blunier and Brook, 2001).
782 Several indicators of atmospheric composition from Greenland ice cores that were
783 matched with similar (but longer) records from Antarctica (Suwa et al., 2006) showed
784 that old ice exists in central Greenland (Suwa et al., 2006; Chappellaz et al., 1997) at
785 depths where flow processes have mixed the layers (Alley et al., 1997). In regions of
786 continuous and unmixed layers, other features in ice cores, such as chemically distinctive
787 ash from particular volcanic eruptions, can be correlated with independently dated
788 records (e.g., Finkel and Nishiizumi, 1997; Zielinski et al. 1994). Flow models also can
789 be used to aid in dating.

790 The past elevation of ice-sheets is indicated by the total gas content of the ice
791 (Raynaud et al., 1997) at a given depth and age. As noted above in this section, bubbles
792 are pinched off (pore close-off) from interconnected air spaces in the firn a few tens of
793 meters down. The density of the ice at this pore close-off is nearly constant after a fairly
794 well known and small correction for climatic conditions. Because air pressure varies with
795 elevation and elevation varies with ice thickness, the total number of trapped molecules
796 of gas per unit volume of ice is correlated with ice-sheet thickness. Small elevation
797 changes cannot be detected (because of additional fluctuations in total gas content that
798 are likely linked to changing layering in the firn that affects trapped bubbles), but
799 elevation changes of greater than 500 m are detectable with confidence (Raynaud et al.,
800 1997).

801 Additional information on ice-sheet changes comes from the current distribution
802 of isochronous surfaces (surfaces that have the same age throughout) in the ice sheet. An

803 explosive volcanic eruption will deposit an acidic ash layer of a single age on the surface
804 of the ice sheet, and that layer can be identified after burial by using radar (Whillans,
805 1976). Ages of reflectors can be determined at ice-core sites (e.g., Eisen et al., 2004), and
806 the layers can then be mapped throughout broad areas (Jacobel and Welch, 2005). A
807 model can be used to predict the current distribution of isochronous surfaces (as well as
808 some other properties, such as temperature) for any hypothesis that combines the history
809 of climatic forcing (primarily accumulation rate affecting burial and temperature) and
810 ice-sheet flow (primarily changes in surface elevation and extent) (e.g., Clarke et al.,
811 2005). Optimal histories can be estimated in this way.

812

813 **7.3 History of the Greenland Ice Sheet**

814 **7.3.1 Ice-Sheet Onset and Early Fluctuations**

815 Prior to 65 million years ago (Ma), dinosaurs lived on a high-CO₂, warm world
816 that usually lacked permanent ice at sea level. The high latitudes were warm (crocodilians
817 lived along coastlines near the pole, suggesting coldest-month temperatures above 5°C
818 and mean annual temperatures above 14°C (Markwick, 1998). Sluijs et al. (2006) showed
819 that the ocean surface warmed near the North Pole from about 18°C to peak temperatures
820 of 23°C during the short-lived Paleocene-Eocene Thermal Maximum about 55 Ma. Such
821 warm temperatures preclude permanent ice near sea level and, indeed, no evidence of
822 such ice has been found (Moran et al., 2006).

823 Cooling following the Paleocene-Eocene Thermal Maximum may have allowed
824 ice to reach sea level fairly quickly; sand and coarser materials found in a core from the
825 Arctic Ocean sea floor and dated at about 46 Ma (Moran et al. 2006; St. John, 2008) is

826 most easily (but not with absolute certainty) interpreted as indicating ice rafting linked to
827 glaciers. Ice-rafted debris likely traceable at least in part to glaciers rather than to sea ice
828 is found in a core recovered from about 75°N latitude in the Norwegian-Greenland Sea
829 off East Greenland; the core is dated between about 38 and 30 Ma (late Eocene into
830 Oligocene time). Certain characteristics of this debris point to an East Greenland source
831 and exclude Svalbard, the next-nearest land mass (Eldrett et al., 2007). It is not known
832 whether this ice-rafted debris represents isolated mountain glaciers or more-extensive ice-
833 sheet cover.

834 The central Arctic Ocean sediment core of Moran et al. (2006) shows a highly
835 condensed record that suggests erosion or little deposition across this interval of ice
836 rafting off Greenland studied by Eldrett et al. (2007; see previous paragraph) and until
837 about 16 Ma. Ice-rafted debris, interpreted as representing iceberg as well as sea-ice
838 transport, was actively delivered to the open-ocean site studied by Moran et al. (2006) at
839 16 Ma, and volumes increased about 14 Ma and again about 3.2 Ma (also see Shackleton
840 et al., 1984; Thiede et al., 1998; Kleiven et al., 2002). St. John and Krissek (2002)
841 suggested onset of sea-level glaciation in southeastern Greenland at about 7.3 Ma, on the
842 basis of ice-rafted debris near Greenland in the Irminger Basin. Because of its
843 geographical pattern, the increase in ice-rafted debris about 3.2 Ma is thought to have had
844 sources in Greenland, Scandinavia, and the North American landmass (Laurentide Ice
845 Sheet). However, tying the debris to particular source rocks (e.g., Hemming et al., 2002)
846 has not been possible. Additionally, no direct evidence shows whether this debris was
847 supplied to the ocean by an extensive ice sheet or by vigorous glaciers that drained
848 coastal mountains in the absence of ice from Greenland's central lowlands. Despite the

849 lack of conclusive evidence, Greenland seems to have supported at least some glaciation
850 since at least 38 Ma; glaciation left more records after about 14 Ma (middle Miocene).
851 Thus, as Earth cooled from the “hothouse” conditions extant during the time of dinosaurs,
852 ice sheets began to form on Greenland.

853 Following the establishment of ice in Greenland, a notable warm interval of about
854 2.4 million years (m.y.) is recorded by the Kap København Formation of North
855 Greenland. This formation is a 100-m-thick unit of sand, silt, and clay deposited
856 primarily in shallow marine conditions. Fossil biota in the deposit switch from Arctic to
857 subarctic to boreal assemblages during the depositional interval. The unit was deposited
858 rapidly, perhaps in 20,000 years or less. Funder et al. (2001) postulated complete
859 deglaciation of Greenland at this time, primarily on the basis of the great summertime
860 warmth indicated at this far-northern site, although clearly there is no comprehensive
861 record of the whole ice sheet.

862

863 **7.3.2 The Most Recent Million Years**

864 Fragmented records on land combined with lack of unequivocal indicators in the
865 ocean complicate ice-sheet reconstructions. Nonetheless, many additional indications of
866 ice-sheet change are available between the time of the Kap København Formation and the
867 most recent 100,000 years. Locally, ice expanded during colder times and ice retreated
868 during warmer times, but data provide no comprehensive overviews of the ice sheet. This
869 section (7.3.2) summarizes data especially from marine isotope stage (MIS) 11 (about
870 440 ka) to MIS 5 (about 130 ka), although dating uncertainties allow the possibility that
871 some of the samples are older than MIS 11, and detailed consideration of MIS 5 is

895 and other contemporaneous ice masses.

896 Far from the Greenland Ice Sheet, some fragmentary and poorly dated deposits
897 suggest a higher-than-present sea-level stand during MIS 11, about 400 ka. Sea-level
898 history of MIS 11 [about 362–420 ka] is of particular interest to paleoclimatologists
899 because the Earth-Sun orbital geometry during that interglacial epoch is similar to the
900 configuration during the current interglacial (Berger and Loutre, 1991).

901 Hearty et al. (1999) proposed that marine deposits found in a cave on the
902 tectonically stable island of Bermuda date to the MIS 11 interglacial epoch. These marine
903 deposits are about 21 m above modern sea level, and they contain coral pebbles that have
904 been dated by U-series techniques. Hearty et al. (1999) interpreted the deposits to date to
905 about 400 ka, although the coral pebbles were dated older than 500 ka. The authors’
906 interpretation is based primarily on an overlying deposit that dates to about 400 ka.
907 Although the deposit appears to record an old sea stand markedly higher than present, the
908 chronology is still uncertain.

909 An Alaskan marine deposit is also found at altitudes of up to 22 m (Kaufman et
910 al., 1991), similar to altitudes of the cave deposit on Bermuda. The deposit, representing
911 what has been called the “Anvilian marine transgression,” extends along the Seward
912 Peninsula and Arctic Ocean coast of Alaska. This part of Alaska is tectonically stable. It
913 is landward of Pelukian (MIS 5 (about 74–130 ka)) marine deposits. Amino-acid ratios in
914 mollusks (Kaufman and Brigham-Grette, 1993) show that the Anvilian deposit is easily
915 distinguishable from last-interglacial (locally called Pelukian) deposits, but it is younger
916 than deposits thought to be of Pliocene age (about 1.8–5.3 Ma). Kaufman et al. (1991)
917 reported that basaltic lava overlies deposits of the Nome River glaciation, which in turn

918 overlie Anvilian marine deposits. An average of several analyses on the lava yields an
919 age of 470 ± 190 ka. Within the broad limits permitted by this age, and using reasonable
920 rates of changes in the amino-acid ratios of marine mollusks, Kaufman et al. (1991)
921 proposed that the Anvilian marine transgression dates to about 400 ka and correlates with
922 MIS 11.

923 Other far-field evidence supports the concept that during MIS 11 sea level was
924 higher than at present. Oxygen-isotope and faunal data from the Cariaco Basin off
925 Venezuela provide independent evidence of a higher-than-present sea level during MIS
926 11 (Poore and Dowsett, 2001). If the Bermudan cave deposits and the Anvilian marine
927 deposits of Alaska prove to be genuine manifestations of a ~400 ka-old high sea stand,
928 the implication for climate history is that all of the Greenland Ice Sheet (Willerslev et al.,
929 2007; see section 7.3.2b, below), all of the West Antarctic ice sheet, and part of the East
930 Antarctic ice sheet would have disappeared at this time (these being generally accepted as
931 the most vulnerable ice masses); preservation of the Greenland Ice Sheet would require
932 much more loss from the East Antarctic ice sheet, which is widely considered to be
933 relatively stable (e.g., Huybrechts and de Wolde, 1999).

934 Until recently, no reliably dated emergent marine deposits from MIS 9 [about
935 303–331 ka] had been found on tectonically stable coasts, although coral reefs of this age
936 have been recognized for some time on the tectonically rising island of Barbados (Bender
937 et al., 1979). Stirling et al. (2001) reported that well-preserved fringing reefs are found on
938 Henderson Island in the southeastern Pacific Ocean. Reef elevations on this tectonically
939 stable island are as high as about 29 m above sea level, and U-series dates between about
940 334 ± 4 and 293 ± 5 ka correlate with MIS 9. Despite the good preservation of the corals

941 and the reefs they are found in, and the reliable U-series ages, it is uncertain how high sea
942 level was at this time. Although Henderson Island is geologically stable, it is
943 experiencing slow uplift (less than 0.1 m/1,000 yr) due to volcanic loading by the
944 emplacement of nearby Pitcairn Island. A correction for maximum uplift rate, therefore,
945 could put the MIS 9 ancient level estimate below present sea level. Multer et al. (2002)
946 reported U-series ages of about 370 ka for a coral (*Montastrea annularis*) from a fossil
947 reef drilled at a locality called Pleasant Point in Florida Bay. This coral showed clear
948 evidence of open-system conditions (i.e., it was not completely chemically isolated from
949 its surroundings since formation, a requirement for the measured age to be accurate), and
950 the age is probably closer to 300–340 ka, if we use the correction scheme of Gallup et al.
951 (1994). If so, the age suggests that during MIS 9, sea level was close to but not much
952 above the present level.

953 As with MIS 9, several MIS 7 (about 190–241 ka) reef or terrace records have
954 been found on tectonically rising coasts (Bender et al., 1979; Gallup et al., 1994; Edwards
955 et al., 1997), but far fewer have been found on tectonically relatively stable coasts.
956 However, two recent reports show evidence of MIS 7 sea-level high stands on
957 tectonically stable islands. One is a pair of U-series ages of about 200 ka from coral-
958 bearing marine deposits about 2 m above sea level on Bermuda (Muhs et al., 2002). The
959 other is a single coral age from the Florida Keys (Muhs et al., 2004). They collected
960 samples of near-surface *Montastrea annularis* corals in quarry spoil piles on Long Key.
961 Analysis of a single sample shows an apparent age of 235 ± 4 ka. The higher-than-
962 modern initial $^{234}\text{U}/^{238}\text{U}$ value indicates a probable bias to an older age by about 7 ka;
963 thus, the true age may be closer to about 220–230 ka, if we again use the Gallup et al.

964 (1994) correction scheme. If valid, these data suggest that sea level may have stood close
965 to its present level during the interglacial period MIS 7. Much more study is needed to
966 confirm these preliminary ages, however.

967 Taken together, these data point to MIS 11 as a time in which sea level likely was
968 notably higher than at present, although the data are sufficiently sparse that stronger
969 conclusions are not warranted. If so, melting of Greenland ice seems likely, mostly on the
970 basis of elimination: Greenland meltwater is thought to be able to supply much of the
971 sea-level rise needed to explain the observations, and the alternative—extracting an
972 additional 7 m of sea-level rise through melting in East Antarctica—is not considered as
973 likely). Marine isotope stages 9 and 7 seem to have had sea levels similar to modern ones.

974

975 ***7.3.2b Ice-sheet indications***

976 The cold MIS 6 ice age (about 130–188 ka) may have produced the most
977 extensive ice in Greenland (Wilken and Meinert, 2006). Recently described glacial
978 deposits in east Greenland support this view (Adrielsson and Alexanderson, 2005),
979 although more-extensive, older deposits are known locally (Funder et al., 2004). Funder
980 et al. (1998) reconstructed thick ice (greater than 1000 m) during MIS 6 in areas of
981 Jameson Land (east Greenland) that now are ice free. However, no confident ice-sheet-
982 wide reconstructions based on paleoclimatic data are available for MIS 6 ice.

983 Both northwest and east Greenland preserve widespread marine deposits from
984 early in the MIS 5 interglacial (the interglacial previous to the present one) (about 74–130
985 ka), and particularly from the warmest subdivision of MIS 5, called MIS 5e (about 123
986 ka). Depression of the land from the weight of MIS 6 ice allowed incursion of seawater

987 as ice melted during the transition to MIS 5e. The resulting deposits were not reworked
988 by the subsequent incursion of seawater during the transition from the most recent
989 glaciation (MIS 2, which peaked about 12–24 ka) to the modern interglacial (MIS 1, less
990 than 11 ka). Thus, seawater moved farther inland during the transition from MIS 6
991 (glacial) to MIS 5 (interglacial) than during the transition from MIS 2 (most recent
992 glacial) to MIS 1 (current interglacial).

993 Several hypotheses can explain this difference. Perhaps most simply, there may
994 have been more ice on Greenland causing greater isostatic depression during MIS 6 than
995 during MIS 2. However, if some or all of the older deposits survived being overridden by
996 cold-based ice of MIS 2, additional possibilities exist. Because isostatic uplift occurs
997 while ice is thinning but before the ice margin melts enough to allow incursion of
998 seawater, perhaps the MIS 6 ice melted faster and allowed incursion of seawater over
999 more-depressed land than was true for MIS 2 ice. Additionally, at the time during MIS 6
1000 that ice in Greenland receded and thus allowed incursion of seawater, global sea level
1001 might have been higher than it was during MIS 2 (perhaps because of relatively earlier
1002 melting of MIS 6 ice on North America or elsewhere beyond Greenland). More-detailed
1003 modeling of glacial isostatic adjustment will be required to test these hypotheses.
1004 Nonetheless, the leading hypothesis seems to be that ice was more extensive in MIS 6
1005 than in MIS 2.

1006 A particularly interesting new result comes from analysis of materials found in ice
1007 cores from the deepest part of the ice sheet. Willerslev et al. (2007) attempted to amplify
1008 DNA in three samples: (1) silty ice at the base of the Greenland Ice Sheet from the Dye-3
1009 drill site (on the southern dome of the ice sheet) and the GRIP drill site (at the crest of the

1010 main dome of the ice sheet), (2) “clean” ice just above the silty ice of these sites, and (3)
1011 the Kap København formation. The Kap København, clean-ice, and GRIP silty samples
1012 did not yield identifiable quantities of DNA (probably indicating post-depositional
1013 changes for Kap København perhaps during room-temperature storage following
1014 collection, and showing that long-distance transport is not important for supplying large
1015 quantities of DNA to the ice of the central part of the sheet).. However, it was possible to
1016 prepare extensive materials from the Dye 3 silty ice. These materials indicate a northern
1017 boreal forest, compared to the tundra environment that exists in coastal sites at the same
1018 latitude and lower elevation today. . The taxa indicate mean July temperatures then above
1019 10°C and minimum winter temperatures above –17°C at an elevation of about 1 km
1020 above sea level (allowing for isostatic rebound following ice melting). Dating of this
1021 warm, reduced-ice time is uncertain, but an age of 450–800 ka is probably consistent
1022 with the indications of high sea level in MIS 11.

1023 Nishiizumi et al. (1996) reported on radioactive cosmogenic isotopes in rock core
1024 collected from beneath the ice at the GISP2 site (central Greenland, 28 km west of the
1025 GRIP site at the Greenland summit). Joint analysis of beryllium-10 and aluminum-26
1026 indicated a few-millennia-long interval of exposure to cosmic rays (hence ice cover of
1027 thickness less than 1 m or so) about 500 ± 200 ka. This information is consistent with,
1028 and thus provides further support for, the DNA results of Willerslev et al. (2007). This
1029 work was presented at a scientific meeting and in an abstract but not in a refereed
1030 scientific journal, and thus it is subject to lower confidence than is other evidence
1031 discussed in this report.

1032 No long, continuous climate records from Greenland itself are available for the

1033 time interval occupied by the boreal forest at Dye-3 reported by Willerslev et al. (2007).
1034 Marine-sediment records from around the North Atlantic point toward MIS 11, at about
1035 440 ka, as the most likely time of anomalous warmth. Owing to orbital forcing factors
1036 (reviewed in Droxler et al., 2003), this interglacial seems to have been anomalously long
1037 compared with those before and after. As discussed above, indications of sea level above
1038 modern level exist for this interval (Kindler and Hearty, 2000), but much uncertainty
1039 remains (see Rohling et al., 1998; Droxler et al., 2003). Records of sea-surface-
1040 temperature in the North Atlantic indicate that MIS 11 temperatures were similar to those
1041 from the current interglacial (Holocene) within 1°–2°C; slightly cooler, similar, or
1042 slightly warmer conditions have all been reported (e.g., Bauch et al., 2000; de Abreu et
1043 al. 2005; Helmke et al., 2003; McManus et al., 1999, Kandiano and Bauch, 2003). The
1044 longer of these records show no other anomalously warm times within the age interval
1045 most consistent with the Willerslev et al. (2007) dates. (Notice, however, that during MIS
1046 5e locally higher temperatures are indicated in Greenland than are indicated in the far-
1047 field sea-surface temperatures. Thus, the absence of warm temperatures far from the ice
1048 sheet does not guarantee the absence of warm temperatures close to the ice sheet; see
1049 7.3.3, below.) The independent indications of high global sea level during MIS 11, as
1050 discussed above in section 7.3.2a, and of major Greenland Ice Sheet shrinkage or loss at
1051 that time, are mutually consistent.

1052 The Greenland Ice Sheet is thought to complete most of its response to a step
1053 forcing in climate within a few millennia (e.g., Alley and Whillans, 1984; Cuffey and
1054 Clow, 1997). Thus, any of the interglacials during the last 420,000 years was long enough
1055 for the ice sheet to have completed most of its response to the end-of-ice-age forcings

1056 (although smaller forcings during the interglacials may have precluded a completely
1057 steady state). Thus, it is not obvious how a longer-yet-not-warmer interglacial, as
1058 suggested by MIS 11 indicators in the North Atlantic away from Greenland, would have
1059 caused notable or even complete loss of the Greenland Ice Sheet, although this result
1060 cannot be ruled out completely. Many possible interpretations remain: greater Greenland
1061 warming in MIS 11 than indicated by marine records from well beyond the ice sheet,
1062 large age error in the Willerslev et al.(2007) estimates, great warmth at Dye-3 yet a
1063 reduced but persistent Greenland Ice Sheet nearby, and others. One possible
1064 interpretation is that the threshold for notable shrinkage or loss of Greenland ice is just
1065 1°–2°C above the temperature reached during MIS 5e, thus falling within the error
1066 bounds of the data.

1067 The data strongly indicate that Greenland’s ice was notably reduced, or lost, sometime
1068 after ice coverage became extensive and large ice ages began, while temperatures
1069 surrounding Greenland were not grossly higher than they have been recently. The rate of
1070 mass loss within the warm period is unconstrained; the long interglacial at MIS 11 allows
1071 the possibility of very slow loss or much faster loss. If the cosmogenic isotopes in the
1072 GISP2 rock core are interpreted at face value, then the time over which ice was absent
1073 was only a few millennia.

1074

1075 **7.3.3 Marine Isotope Stage 5e**

1076 ***7.3.3a Far-field sea-level indications***

1077 Investigators studying sea-level history have paid most attention to sea level
1078 during the last interglacial, MIS 5 (about 71–122 ka), and specifically to MIS 5e (about

1079 123 ka). The evidence of past sea level during MIS 5e along tectonically stable coasts is
1080 summarized here (Muhs, 2002). Sea-level high stand during MIS 5e is best estimated
1081 from coral reef and marine deposits now above sea level at sites in Australia, the
1082 Bahamas, Bermuda, and the Florida Keys.

1083 On the coast and islands of tectonically stable Western Australia, emergent coral
1084 reefs and marine deposits now 2–4 m above sea level are widespread and well-preserved.
1085 U-series ages of the fossil corals at mainland localities and Rottneest Island range from
1086 128 ± 1 to 116 ± 1 ka (Stirling et al., 1995, 1998). The main period of last-interglacial
1087 coral growth was a restricted interval from about 128–121 ka (Stirling et al., 1995, 1998).
1088 Because the highest corals are about 4 m above sea level at present but grew at some
1089 unknown depth below sea level, 4 m is a minimum for the amount of last-interglacial sea-
1090 level rise.

1091 The islands of the Bahamas are tectonically stable, although they may be slowly
1092 subsiding owing to carbonate loading on the Bahamian platform. Fossil reefs in the
1093 Bahamas are well preserved (Chen et al., 1991), reefs have elevations up to 5 m above
1094 sea level, and many corals are in growth position. On San Salvador Island, reef ages
1095 range from 130.3 ± 1.3 to 119.9 ± 1.4 ka. The sea level record of the Bahamas is
1096 particularly valuable because many reefs contain the coral *Acropora palmata*, a species
1097 that almost always lives within the upper 5 m of the water column (Goreau, 1959). Thus,
1098 fossil reefs containing this species place a fairly precise constraint on the former water
1099 depth.

1100 As discussed above (section 7.3.2a), Bermuda is tectonically stable. Bermuda
1101 does not host MIS 5e fossil reefs, but numerous coral-bearing marine deposits fringe the

1102 island. A number of U-series ages of corals from Bermuda range from about 119 ka to
1103 about 113 ka (Muhs et al., 2002). The deposits are found 2–3 m above present sea level,
1104 although overlying wind-blown sand prevents precise estimates of where the former
1105 shoreline lay.

1106 The Florida Keys, not far from the Bahamas, are also tectonically stable. Fruijtier
1107 et al. (2000) reported ages for corals from Windley Key, Upper Matecumbe Key, and
1108 Key Largo that, when corrected for high initial $^{234}\text{U}/^{238}\text{U}$ values (Gallup et al., 1994), are
1109 in the range of 130–121 ka. The last-interglacial MIS 5 reef on Windley Key is 3–5 m
1110 above present sea level, on Grassy Key it is 1–2 m above sea level, and on Key Largo it
1111 is 3–4 m above modern sea level.

1112 The collective evidence from Australia, Bermuda, the Bahamas, and the Florida
1113 Keys shows that sea level was above its present stand during MIS 5e. On the basis of
1114 measurements of the reefs themselves, sea level then was at least 4–5 m higher than sea
1115 level now. An additional correction should be applied for the water depth at which the
1116 various coral species grew. Most coral species found in Bermuda, the Bahamas, and the
1117 Florida Keys require water depths of at least a few meters for optimal growth, and many
1118 live tens of meters below the ocean surface. For example, *Montastrea annularis*, the most
1119 common coral found in MIS 5e reefs of the Florida Keys, has an optimum growth depth
1120 of 3–45 m and can live as deep as 80 m (Goreau, 1959). A minimum rise in sea level is
1121 calculated thusly: fossil reefs are 3 m above present sea level, and the most conservative
1122 estimate of the depth at which they grew is 3 m. Thus, the MIS 5e sea level was at least 6
1123 m higher than modern-day sea level (Figures 7.5, 7.6). A summary of additional sites led
1124 Overpeck et al. (2006) to indicate a sea-level rise of 4 m to more than 6 m during MIS 5e.

1125

1126

FIGURE 7.5 NEAR HERE

1127

FIGURE 7.6 NEAR HERE

1128

1129

1130

1131

1132

1133

1134

1135

1136

1137

1138

1139

7.3.3b Conditions in Greenland

1140

1141

1142

1143

1144

1145

1146

1147

Existing estimates generally presume that glacial isostatic adjustment have not notably affected the sites at the key times. The data set, and the accuracy of the dates (also see Thompson and Goldstein, 2005) are becoming sufficient to support, in future work, improved corrections for glacial isostatic adjustment. The implications of a 4 m to more than 6 m sea-level highstand during the last interglacial are as follows: (1) all or most of the Greenland Ice Sheet would have melted; or (2) all or most of the West Antarctic ice sheet would have melted; or (3) parts of both would have melted. Both ice sheets may indeed have melted in part, but greater melting is likely from Greenland (Overpeck et al., 2006), as described in section 7.3.3c, below.

1148 albedo and other feedbacks. Simulated warming around Greenland exhibited local
1149 maxima of 4-5°C in those northwestern and eastern coastal regions for which terrestrial
1150 and shallow-marine data are available and show matching warmings; elsewhere over
1151 Greenland and surroundings, typical warmings of ~3°C were simulated.

1152 The sea-level record in East Greenland (Scoresby Sund) indicates a two-step
1153 inundation at the start of MIS 5e. Of the possible interpretations, Funder et al. (1998)
1154 favored one in which early deglaciation of the coastal region of Greenland preceded
1155 much of the melting of non-Greenland land ice, so that early coastal flooding after
1156 deglaciation of isostatically depressed land was followed by uplift and then by flooding
1157 attributable to sea-level rise as that far-field land ice melted. Additional testing of this
1158 idea would be very interesting, as it suggests that the Greenland Ice Sheet has responded
1159 rapidly to climate forcing in the past.

1160 Much of the evidence of climate change in Greenland comes from ice-core
1161 records. As discussed next, these changes cannot be estimated independent of a
1162 discussion of the ice sheet, because of the possibility of thickness change. Hence, the
1163 changes in the ice sheet are discussed before additional evidence bearing on forcing and
1164 response.

1165

1166 ***7.3.3c Ice-sheet changes***

1167 The Greenland Ice Sheet during MIS 5e covered a smaller area than it does now.
1168 How much smaller is not known with certainty. The most compelling evidence is the
1169 absence of pre-MIS 5e ice in the ice cores from south, northwest, and east Greenland (the
1170 locations Dye-3, Camp Century, and Renland drilling sites, respectively). In all of these

1171 cores, the climate record extends through the entire last glacial epoch and then terminates
1172 at the bed in a layer of ice deposited in a much warmer climate (Koerner, 1989; Koerner
1173 and Fisher, 2002). This basal ice is most likely MIS 5e ice. Moreover, the composition of
1174 this ice is not an average of glacial and interglacial values, as would be expected if it
1175 were a mixture of ices from earlier cold and warm climates. Instead, the ice composition
1176 exclusively indicates a climate considerably warmer than that of the Holocene. (One
1177 cannot entirely eliminate the possibility that each core independently bottomed on a rock
1178 that had been transported up from the bed, and that older ice lies beneath each rock, but
1179 this seems highly improbable.)

1180 At Dye-3, the oxygen isotope composition of this basal ice layer is reported as
1181 $\delta^{18}\text{O} = -23\text{‰}$, which means that it is 23‰ (or 2.3%) lighter than standard mean ocean
1182 water. Moreover, a value of $\delta^{18}\text{O} = -30\text{‰}$ is reported for modern snowfall in the source
1183 region (up-flow from the site of Dye-3). At Camp Century, a value of $\delta^{18}\text{O} = -25\text{‰}$ is
1184 reported for basal ice; a value of $\delta^{18}\text{O} = -31.5\text{‰}$ is reported in the source region (see
1185 Table 2 of Koerner, 1989). These changes of about 7‰ are much larger than the MIS 5e-
1186 to-MIS 1 climatic signal (about 3.3‰, according to the central Greenland cores; see
1187 below in this section). Thus, the MIS 5e ice at Dye-3 and Camp Century not only
1188 indicates a warmer climate but also a much lower source elevation: the ice sheet was re-
1189 growing when these MIS 5e ices were deposited.

1190 In combination, these two observations (absence of pre-MIS 5e ice, and
1191 anomalously low-elevation sources of the basal ice) indicate that the Greenland margin
1192 had retreated considerably during MIS 5e. Of greatest importance is that retreat of the
1193 margin northward past Dye-3 implies that the southern dome of the ice sheet was nearly

1194 or completely gone.

1195 In this context it is useful to understand the genesis of the basal ice layer, and the
1196 layer at Dye-3 in particular. Unfortunately the picture is cloudy—not unlike the basal ice
1197 itself, which has a small amount of silt and sand dispersed through it, making it opaque.
1198 This silty basal layer is about 25 m thick (Souchez et al., 1998). Overlying it is “clean”
1199 (not notably silty) ice that appears to be typical of polar ice sheets. Its total gas content
1200 and gas composition indicate that the ice formed by normal densification of firn in a cold,
1201 dry environment. The oxygen isotope composition of this clean ice is -30.5% . The
1202 bottom 4 m of the silty ice is radically different; its oxygen isotope value is -23% , and its
1203 gas composition indicates substantial alteration by water. The total gas content of this
1204 basal silty ice is about half that of normal cold ice formed from solid-state transformation
1205 of firn, the carbon dioxide content is 100 times normal, and the oxygen/nitrogen ratio is
1206 less than 20% that of normal cold ice. This basal silty layer may be superimposed ice (ice
1207 formed by refreezing of meltwater in snow on a glacier or ice sheet, as Koerner (1989)
1208 suggested for the entire silty layer), or it may be non-glacial snowpack, or it may be a
1209 remnant of segregation ice in permafrost (permafrost commonly contains relatively
1210 “clean” although still impure lenses of ice, called segregation ice).

1211 In any case, the upper 21 m of the silty ice may be explained as a mixture of these
1212 two end members (Souchez et al. 1998). As they deform, ice sheets do mix ice layers by
1213 small-scale structural folding (e.g., Alley et al., 1995b), by interactions between rock
1214 particles, by grain-boundary diffusion, and possibly by other processes. Unfortunately,
1215 there is no way to distinguish rigorously how much this ice really is a mixture of these
1216 end-member components and how much of it is warm-climate (presumably MIS 5e)

1217 normal ice-sheet ice. The difficulty is that the bottom layer is not itself well mixed (its
1218 gas composition is highly variable), so a mixing model for the middle layer uses an
1219 essentially arbitrary composition for one end member. Souchez et al. (1998) used the
1220 composition at the top of the bottom layer for their mixing calculations, but it could just
1221 as well be argued that the composition here is determined by exchange with the overlying
1222 layer and is not a fixed quantity.

1223 As discussed in section 7.3.2b, above, in a recent study, Willerslev et al. (2007)
1224 examined biological molecules in the silty ice from Dye-3, including DNA and amino
1225 acids. They concluded that organic material contained in that Dye-3 ice originated in a
1226 boreal forest (remnants of diagnostic plants and insects were identified). This
1227 environment implies a very much warmer climate than at the present margin in
1228 Greenland (e.g., July temperatures at 1 km elevation above 10°C), and hence it also
1229 suggests a great antiquity for this material; no evidence suggests that MIS 5e in
1230 Greenland was nearly this warm. Indeed, Willerslev et al. (2007) also inferred the age of
1231 the organic material and the age of exposure of the rock particles, using several methods.
1232 They concluded that a 450–800 ka age is most likely, although uncertainties in all four of
1233 their dating techniques prevented a definitive statement. This conclusion suggests that the
1234 bottom ice layer (the source of rock material in the overlying mixed layer) is much older
1235 than MIS 5e.

1236 This evidence admits of two principal interpretations. One is that this material
1237 survived the MIS 5e deglaciation by being contained in permafrost. The second is that the
1238 MIS 5e deglaciation did not extend as far north as the Dye-3 site, and that local
1239 topography allowed ice to persist, isolated from the large-scale flow. This latter

1240 hypothesis (apparently favored by Willerslev et al., 2007) does not explain the several-
1241 hundred-thousand-year hiatus within the ice, however, or the purely interglacial
1242 composition of the entire basal ice, both of which favor the permafrost interpretation.
1243 (Both hypotheses can be modified slightly to allow short-distance ice-flow transport to
1244 the Dye-3 site; e.g., Clarke et al., 2005.)

1245 Ice-sheets can also slide at their margins. Sliding near the modern margin of the
1246 Greenland ice sheet (e.g., Joughin et al., 2008a) provides a way to rapidly re-establish the
1247 ice sheet in deglaciated regions and to preserve soil or permafrost materials as the ice re-
1248 grows, as described next. Marginal regions of the Greenland ice sheet are thawed at the
1249 bottom and slide over the materials beneath (e.g., Joughin et al., 2008a)—on a thin film
1250 of water or possibly thicker water or soft sediments. During a time of cooling, sliding
1251 advances the ice margin more rapidly than would be possible if the ice were frozen to the
1252 bed. Furthermore, the sliding will bring to a given point ice that was deposited elsewhere
1253 and at higher elevation; subsequently, that ice may freeze to the bed. As discussed below
1254 (section 7.3.5b), widespread evidence shows a notable advance of the ice-sheet margin
1255 during the last few millennia. Regions near the ice-sheet margin, and icebergs calving
1256 from that margin, now contain ice that was deposited somewhere in the accumulation
1257 zone at higher elevation and that slid into position (e.g., Petrenko et al., 2006). Were
1258 sliding not present, one might expect that re-glaciation of a site such as Dye-3 would
1259 have required cooling until the site became an accumulation zone, followed by slow
1260 buildup of the ice sheet.

1261 In contrast to all the preceding information from south-, northwest-, and east-
1262 Greenland ice cores, the ice cores from central Greenland (the GISP2 and GRIP cores;

1263 Suwa et al., 2006) and north-central Greenland (the NGRIP core) do contain MIS 5e ice
1264 that is normal, cold-environment, ice-sheet ice. Unfortunately, none of these cores
1265 contains a complete or continuous MIS 5e chronology. Layering of the GISP2 and GRIP
1266 cores is disrupted by ice flow (Alley et al., 1995b) and, in the NGRIP core, basal melting
1267 has removed the early part of MIS 5e and any older ice (Dahl-Jensen et al., 2003). The
1268 central Greenland cores do reveal two important facts: MIS 5e was warmer than MIS 1
1269 (oxygen isotope ratios were 3.3‰ higher than modern ones), and the elevation in the
1270 center of the ice sheet was similar to that of the modern ice sheet, although the ice sheet
1271 was probably slightly thinner in MIS 5e (within a few hundred meters of elevation, based
1272 on the total gas content). Thus, if we consider also evidence from the other cores, the ice
1273 sheet shrank substantially under a warm climate, but it persisted in a narrower, steeper
1274 form.

1275 What climate conditions were responsible for driving the ice sheet into this
1276 configuration? The answer is not clear. None of the paleoclimate proxy information is
1277 continuous over time, both precipitation and temperature changes are important, and
1278 some factors related to ice flow are poorly constrained. Cuffey and Marshall (2000; also
1279 see Marshall and Cuffey, 2000) were the first to address this question using the
1280 information from the central Greenland cores as constraints. In particular, Cuffey and
1281 Marshall (2000) noted that oxygen isotope ratios were at least 3.3‰ higher during MIS
1282 5e, and they used this value to constrain the climate forcing on an ice sheet model.
1283 Because the isotopic composition depends on the elevation of the ice-sheet surface as
1284 well as on temperature change at a constant elevation, these analyses generated both
1285 climate histories and ice-sheet histories. Results depended critically on the isotopic

1286 sensitivity parameter relating isotopic composition to temperature and on the way past
1287 accumulation rates are estimated, which have large uncertainties. Furthermore, there was
1288 no attempt to model increased flow in response to changes of calving margins, or
1289 increased flow in response to production of surface meltwater (see Lemke et al., 2007).
1290 Thus, the ice sheet model was conservative; a given climatic temperature change
1291 produced a smaller response in the modeled ice sheet than is expected in nature.

1292 In the reconstruction favored by Cuffey and Marshall (isotopic sensitivity $\alpha =$
1293 0.4‰ per $^{\circ}\text{C}$), the southern dome of Greenland completely melted after a sustained (for at
1294 least 2,000 years) climate warming of approximately 7°C higher than present. In a
1295 different scenario (sensitivity $\alpha = 0.67\text{‰}$ per $^{\circ}\text{C}$), the southern ice sheet margin did not
1296 retreat past Dye-3 after a sustained warming of 3.5°C . Thus an intermediate scenario
1297 (sustained warming of $5^{\circ}\text{--}6^{\circ}\text{C}$) is required, in this view, to cause the margin to retreat just
1298 to Dye-3. Given the conservative representation of ice dynamics in the model, a smaller
1299 sustained warming would in fact be sufficient to accomplish such a retreat. How much
1300 smaller is not known, but it could be quite small. Outflow of ice can increase by a factor
1301 of two in response to modest changes in air and ocean temperatures at the calving
1302 margins (see Lemke et al., 2007).

1303 Mass balance depends on numerous variables that are not modeled, introducing
1304 much uncertainty. Examples of these variables are storm-scale weather controls on the
1305 warmest periods within summers, similar controls on annual snowfall, and increased
1306 warming due to exposure of dark ground as the ice sheet retreats. In contrast to the under-
1307 representation of ice dynamics, however, no major observations show that the models are
1308 fundamentally in error with respect to mass-balance forcings. A hint of a serious error is,

1309 however, provided by the record of accumulation rate from central Greenland. During the
1310 past about 11,000 years (MIS 1) variations in snow accumulation and in temperature
1311 show no consistent correlation, whereas most models assume that snowfall (and hence
1312 accumulation) will increase with temperature. This lack of correlation suggests that
1313 models are over-predicting the extent to which increased snowfall will partly balance
1314 increased melt in a warmer climate. If this MIS 1 situation in central Greenland applied to
1315 much of the ice sheet in MIS 5e, then models would require less warming to match the
1316 reconstructed ice-sheet footprint. Again, the real ice sheet appears to be more vulnerable
1317 than the model ones. We refer to this observation as only a “hint” of a problem, however,
1318 because snowfall on the center of Greenland may not represent snowfall over the whole
1319 ice sheet, for which other climatological influences come into play.

1320 The climate forcing for the Cuffey and Marshall (2000) ice dynamics model, like
1321 that of most recent models that explore Greenland’s glacial history, is driven by a single
1322 paleoclimate record, the isotope-based surface temperature at the Summit ice core sites.
1323 From this information, temperature and precipitation fields are derived and then
1324 combined to obtain a mass balance forcing over space and time, which is then applied to
1325 the entire ice sheet. This approach can be criticized for eliminating all local-scale climate
1326 variability, but few observations would allow such variability to be adequately specified.

1327 Recent efforts to estimate the minimum MIS 5e ice volume for Greenland have
1328 much in common with the Cuffey and Marshall (2000) approach, but they focus on
1329 adding observational constraints that optimize the model parameters. For example, the
1330 new ability to model the movement of materials passively entrained in ice sheets (Clarke
1331 and Marshall, 2002) now allows the predicted and observed isotope profiles at ice core

1332 sites to be compared. By using these capabilities, Tarasov and Peltier (2003) produced
1333 new estimates of MIS 5e ice volume that were constrained by the measured ice-
1334 temperature profiles at GRIP and GISP2 and by the $\delta^{18}\text{O}$ profiles at GRIP, GISP2, and
1335 NorthGRIP. Their conservative estimate is that the Greenland Ice Sheet contributed
1336 enough meltwater to cause a 2.0–5.2 m rise in MIS 5e sea level; the more likely range is
1337 2.7–4.5 m—lower than the 4.0–5.5 m estimate of Cuffey and Marshall (2000). Ice-core
1338 sites closer to the ice sheet margins, such as Camp Century and Dye-3, better constrain
1339 ice extent than do the central Greenland sites (Lhomme et al., 2005). These authors added
1340 a tracer transport capability to the model used by Marshall and Cuffey (2000) and
1341 attempted to optimize the model fit to the isotope profiles at GRIP, GISP2, Dye-3 and
1342 Camp Century. For now, their estimate of a 3.5–4.5 m maximum MIS 5e sea-level rise
1343 attributable to meltwater from the Greenland Ice Sheet is the most comprehensive
1344 estimate based on this technique (Lhomme et al., 2005).

1345 The discussion just previous rested on interpretation of paleoclimatic data from
1346 the central Greenland ice cores to drive a model to match the inferred ice-sheet
1347 “footprint” (and sometimes other indicators) and thus learn volume changes in relation to
1348 temperature changes. An alternative approach is to use what we know about climate
1349 forcings to drive a coupled ocean-atmosphere climate model and then test the output of
1350 that model against paleoclimatic data from around the ice sheet. If the model is
1351 successful, then the modeled conditions can be used over the ice sheet to drive an ice-
1352 sheet model to match the reconstructed ice-sheet footprint. From response to forcing
1353 changes we then learn volume changes. This latter approach avoids the difficulty of
1354 inferring the “ α ” parameter relating isotopic composition of ice to temperature, and of

1355 assuming a relation between temperature and snow accumulation, although this latter
1356 approach obviously raises other issues. The latter approach was used by Otto-Bliesner et
1357 al. (2006; also see Overpeck et al., 2006).

1358 The primary forcings of Arctic warmth during MIS 5e are the seasonal and
1359 latitudinal changes in solar insolation at the top of the atmosphere associated with
1360 periodic, cyclical changes in Earth's orbit. (Berger, 1978). Earth's orbit varies in its
1361 obliquity (the inclination of Earth's spin axis to the orbital plane, which peaked at about
1362 130 ka), eccentricity (the out-of-roundness of Earth's elliptical orbit around the Sun), and
1363 precession (the timing of closest approach to the Sun on the elliptical orbit relative to
1364 hemispheric seasons). The net effect of these factors was anomalously high summer
1365 insolation in the Northern Hemisphere during the first half of this interglacial (about 130–
1366 123 ka) (Otto-Bliesner et al., 2006; Overpeck et al., 2006). Atmosphere-Ocean General
1367 Circulation Models of the climate (AOGCMs) have used the MIS 5e seasonal and
1368 latitudinal insolation changes to calculate both the seasonal temperatures and
1369 precipitation of the atmosphere, as well as changes to sea ice and ocean temperatures.
1370 These models simulate approximately correct sensitivity to the MIS 5e orbital forcing.
1371 They reproduce the proxy-derived summer warmth for the Arctic of up to 5°C, and they
1372 place the largest warming over northern Greenland, northeast Canada, and Siberia
1373 (CAPE, 2006; Jansen et al., 2007).

1374 In one of the models that has been extensively analyzed, the NCAR CCSM
1375 (National Center for Atmospheric Research Community Climate System Model), the
1376 orbitally induced warmth of MIS 5e causes loss of snow and sea ice, which in turn causes
1377 positive albedo feedbacks that reduce reflection of sunlight (Otto-Bliesner et al., 2006).

1378 The insolation anomalies increased sea-ice melting early in the northern spring and
1379 summer seasons, and reduced the extent of Arctic sea ice from April into November. The
1380 simulated reduced summer sea ice allows the North Atlantic to warm, particularly along
1381 coastal regions of the Arctic and the surrounding waters of Greenland. Feedbacks
1382 associated with the reduced sea ice around Greenland and decreased snow depths on
1383 Greenland further warm Greenland during the summer months. In combination with
1384 simulated precipitation rates, which overall were not substantially different from present
1385 rates, the simulated mass balance of the Greenland Ice Sheet resulting from the model
1386 was negative. Then, as now, the surface of the ice sheet melted primarily in the summer.

1387 The NCAR CCSM model has a mid-range climate sensitivity among
1388 comprehensive atmosphere-ocean models; that is, this model generates mid-range
1389 warming in response to doubling of CO₂ or other specified forcing (Kiehl and Gent,
1390 2004). Temperatures and precipitation produced by the NCAR CCSM model for 130 ka
1391 were then used to drive an ice-flow model. (The model used an updated version of that
1392 used by Cuffey and Marshall (2000), and thus it also lacked representations of some
1393 physical processes that would accelerate ice-sheet response and increase sensitivity to
1394 climate change.) The ice-flow model simulated the likely configuration of the MIS 5e
1395 Greenland Ice Sheet, for comparison with paleoclimatic data on ice-sheet configuration.
1396 In this model, the Greenland Ice Sheet proved sensitive to the warmer summer
1397 temperatures when melting was taking place. Increased melting outweighed the increase
1398 in snowfall. For all but the summit of Greenland and isolated coastal sites, increased rates
1399 of melting and the extended ablation season led to a negative mass balance in response to
1400 the orbitally induced changes in temperature and snowfall. As the simulated ice sheet

1401 retreated for several millennia, the loss of ice mass lowered the surface of the Greenland
1402 Ice Sheet, which amplified the negative mass-balance and accelerated retreat. The
1403 Greenland Ice Sheet responded to the seasonal orbital forcings because it is particularly
1404 sensitive to warming in summer and autumn, rather than in winter when temperatures are
1405 too cold for melting. The modeled Greenland Ice Sheet melted in response to both direct
1406 effects (warmer atmospheric temperatures) and indirect effects (reduction of its altitude
1407 and size).

1408 The simulated MIS 5e Greenland Ice Sheet was a steep-sided ice sheet in central
1409 and northern Greenland (Otto-Bliesner et al., 2006) (Figure 7.7). The model did not
1410 incorporate feedbacks associated with the exposure of bedrock as the ice sheet retreated,
1411 potential meltwater-driven or ice-shelf-driven ice-dynamical processes, or time-evolving
1412 orbital forcing, so the model was probably less sensitive and more slowly responsive to
1413 warming than the real ice sheet, as noted just above. The lateral extent of the modeled
1414 minimal Greenland Ice Sheet was constrained by ice core data (see above). If the
1415 Greenland Ice Sheet's southern dome did not survive the peak interglacial warmth, as
1416 suggested by those data (Koerner and Fisher, 2002; Lhomme et al., 2005), then the model
1417 suggests that the Greenland Ice Sheet contributed enough meltwater to account for 1.9–
1418 3.0 m of sea-level rise (another 0.3–0.4 m rise was produced by meltwater from ice on
1419 Arctic Canada and Iceland) for several millennia during the last interglacial. The
1420 evolution through time of the Greenland Ice Sheet's retreat and the linked rate at which
1421 sea level rose cannot be constrained by paleoclimatic observational data or current ice-
1422 sheet models. Furthermore, because the ice-sheet model was forced by conditions
1423 appropriate for 130 ka rather than being forced by more realistic, slowly time-varying

1424 conditions, the details of the modeled time-evolution of the Greenland Ice Sheet are not
1425 expected to exactly match reality. Sensitivity studies that set melting of the Greenland Ice
1426 Sheet at a more rapid rate than suggested by the ice-sheet model indicate that the
1427 meltwater added to the North Atlantic was not sufficient to induce oceanic and other
1428 climate changes that would have inhibited melting of the Greenland Ice Sheet (Otto-
1429 Bliesner et al., 2006).

1430

1431

FIGURE 7.7 NEAR HERE

1432

1433 The atmosphere-ocean modeling driven by known forcings produces
1434 reconstructions that match many data from around Greenland and the Arctic. The earlier
1435 work of Cuffey and Marshall (2000) had found that a very warm and snowy MIS 5e, or a
1436 more modest warming with less increase in snowfall, could be consistent with the data,
1437 and the atmosphere-ocean model favors the more modest temperature change. (The
1438 results of the different approaches, although broadly compatible, do not agree in detail,
1439 however.) The Otto-Bliesner et al. (2006) modeling leads to a somewhat smaller sea-level
1440 rise from melting of the Greenland Ice Sheet than does the earlier work of Cuffey and
1441 Marshall (2000). A temperature rise of 3°–4°C and a sea-level rise of 3–4 m may be
1442 consistent with the data, with notable uncertainties.

1443 Considering all of the efforts summarized above, as little as 1–2 m or as much as
1444 4–5 m of ice may have been removed from the Greenland Ice Sheet during MIS 5e, in
1445 response to climatic temperature changes of perhaps 2°–7°C. At least the higher numbers
1446 for the warming are based on estimates that include the feedbacks from melting of the ice

1447 sheet. Central values in the 3–4 m and 3°–4°C range may be appropriate.

1448

1449 **7.3.4 Post-MIS 5e Cooling to the Last Glacial Maximum (LGM, or MIS 2)**

1450 ***7.3.4a Climate forcing***

1451 Both climate and ice-sheet reconstructions become more confident for times
1452 younger than MIS 5e. The climatic records derived from ice cores are especially good.
1453 The Greenland ice cores, primarily from the GRIP, NGRIP, and GISP2 cores but also
1454 from Camp Century, Dye-3, and Renland cores, provide what are probably the most
1455 reliable paleoclimatic records of any sites on Earth (e.g., Cuffey et al., 1995; Dahl-Jensen
1456 et al., 1998; Johnsen et al., 2001; Jouzel et al., 1997; Severinghaus et al., 1998).

1457 The paleoclimate information derived from near-field marine records is less
1458 robust. Because sediment accumulated rapidly in depositional centers adjacent to
1459 glaciated margins, relatively few cores span all of the last 130,000 years. In core HU90-
1460 013 (Figure 7.8) from the Erik Drift (Stoner et al., 1995), rapid sedimentation buried the
1461 sediments from MIS 5e to about 13 m depth. At that site, the $\delta^{18}\text{O}$ of planktonic
1462 foraminiferal shells changes markedly from MIS 5e to 5d. The change, of close to 1.5‰,
1463 is consistent with cooling as well as ice growth on land, and it is associated with a rapid
1464 increase in magnetic susceptibility that indicates delivery of glacially derived sediments.

1465

1466 **FIGURE 7.8 NEAR HERE**

1467

1468 The broad picture, which is based on ice-core, far-field and near-field marine
1469 records, and more, indicates the following:

- 1470 • a general cooling from MIS 5e (about 123 ka) to MIS 2 (coldest temperatures were at
1471 about 24 ka; Alley et al., 2002),
1472 • warming to the mid-Holocene/MIS 1 a few millennia ago,
1473 • cooling into the Little Ice Age of one to a few centuries ago,
1474 • and then a bumpy warming (see section 7.3.5b, below).

1475 The cooling trend from MIS 5e involved temperature minima in MIS 5d, 5b, and 4 before
1476 reaching the coldest of these minima in MIS 2, with maxima in MIS 5c, 5a, and 3.

1477 Throughout the cooling from MIS 5e to MIS 2, and the subsequent warming into
1478 MIS 1 (the Holocene), shorter-lived “millennial” events occurred. During these events,
1479 central Greenland warmed abruptly—roughly 10°C in a few years to decades—cooled
1480 gradually, then cooled more abruptly, gradually warmed slightly, and then repeated the
1481 sequence (Figure 7.9) (also see Alley, 1998). The abrupt coolings were usually spaced
1482 about 1500 years apart, although longer intervals are often observed (e.g., Alley et al.,
1483 2001; Braun et al., 2005).

1484

1485 **FIGURE 7.9 NEAR HERE**

1486

1487 Marine sediment cores from around the North Atlantic and beyond show
1488 temperature histories closely tied to those recorded in Greenland (Bond et al., 1993).
1489 Indeed, the Greenland ice cores appear to have recorded quite clearly the template for
1490 millennial climate oscillations around much of the planet (although that template requires
1491 a modified seesaw in far-southern regions (Figure 7.9) (Stocker and Johnsen, 2003)).

1492 Closer to the ice sheet, marine cores display strong oscillations that correlate in

1493 time with that template, but with more complexity in the response (Andrews, 2008).
1494 Figure 7.10, panel A shows data from a transect of cores (Andrews, 2008) and compares
1495 the marine near-surface isotopic variations with $\delta^{18}\text{O}$ data from the Renland ice core, just
1496 inland from Scoresby Sund (Johnsen et al., 1992a; 2001) (Figure 7.8). The complexity
1497 observed in this comparison likely arises because of the rich nature of the marine
1498 indicators. As noted in section 7.2.1c, above, the oxygen isotope composition of surface-
1499 dwelling foraminiferal shells becomes lighter when the temperature increases and also
1500 when meltwater supply is increased to the system (or meltwater removal is reduced). If
1501 cooling is caused by freshwater-induced reduction in the formation of deep water, then
1502 one may observe either heavier or lighter isotopic ratios, depending on whether the core
1503 primarily reflects the temperature change or the freshwater change. Some of the signals in
1504 Figure 7.10, panel A likely involve delivery of additional meltwater (which could have
1505 had various sources, such as melting of icebergs) to the vicinity of the core during colder
1506 times.

1507

1508 **FIGURE 7.10 NEAR HERE**

1509

1510 The slower tens-of-millennia cycling of the climate records is well explained by
1511 features of Earth's orbit and by associated influences of Earth-system response to the
1512 orbital features (especially changes in atmospheric CO_2 and other greenhouse gases, ice-
1513 albedo feedbacks, and effects of changing dust loading), and strongly modulated by the
1514 response of the large ice sheets (e.g., Broecker, 1995). The faster changes are rather
1515 clearly linked to switches in the behavior of the North Atlantic (e.g., Alley, 2007): colder

1516 intervals mark times of more-extensive wintertime sea ice, and warmer intervals mark
1517 times of lesser sea ice (Denton et al., 2005). These links are in turn coupled to changes in
1518 deep-water formation in the North Atlantic and thus to “conveyor-belt” circulation (e.g.,
1519 Broecker, 1995; Alley, 2007). (Note that a fully quantitative mechanistic understanding
1520 of forcing and response of these faster changes is still being developed; e.g., Stastna and
1521 Peltier, 2007.)

1522 Of particular interest relative to the ice sheets is the observation that iceberg-
1523 rafted debris is much more abundant throughout the North Atlantic during some cold
1524 intervals, called Heinrich events (Figure 7.9). The material in this debris is largely tied to
1525 sources in Hudson Bay and Hudson Strait at the mouth of Hudson Bay, and thus to the
1526 North American Laurentide Ice Sheet, but it also contains other materials from almost
1527 everywhere around the North Atlantic (Hemming, 2004).

1528

1529 ***7.3.4b Ice-sheet changes***

1530 With certain qualifications, the behavior of the Greenland Ice Sheet during this
1531 interval was closely tied to the climate: the ice sheet expanded with cooling and retreated
1532 with warming. Records are generally inadequate to assess response to millennial changes,
1533 and dating is typically sufficiently uncertain that lead-or-lag relations cannot be
1534 determined with high confidence, but colder temperatures were accompanied by more-
1535 extensive ice.

1536 Furthermore, with some uncertainty, the larger footprint of the Greenland Ice
1537 Sheet during colder times corresponded with a larger ice volume. This conclusion
1538 emerges both from limited data on total gas content of ice cores (Raynaud et al., 1997)

1539 indicating small changes in thickness, and from physical understanding of the ice-flow
1540 response to changing temperature, accumulation rate, ice-sheet extent, and other changes
1541 in the ice. As described in section 7.1.2, above, the retreat of ice-sheet margins tends to
1542 thin central regions, whereas the advance of margins tends to thicken central regions.
1543 Moreover, because ice thickness in central regions is relatively insensitive to changes in
1544 accumulation rate (or other factors), marginal changes largely dominate the ice-volume
1545 changes.

1546 The best records of ice-sheet response during the cooling into MIS 2 are probably
1547 those from the Scoresby Sund region of east Greenland (Funder et al., 1998). These
1548 records indicate

- 1549 • ice advances during the coolings of MIS 5d and 5b that did not fully fill the Scoresby
1550 Sund fjord,
- 1551 • retreats during the relatively warmer MIS 5c and 5a (although 5c and 5a were colder
1552 than MIS 5e or MIS 1; e.g., Bennike and Bocher, 1994),
- 1553 • advance to the mouth of Scoresby Sund, probably during MIS 4,
- 1554 • and remaining there into MIS 2, building the extensive moraine at the mouth of the
1555 Sund.

1556 Whether ice advanced beyond the mouth of the Sund during this interval remains
1557 unclear. Most reconstructions place the ice edge very close to the mouth (e.g.,
1558 Dowdeswell et al., 1994a; Mangerud and Funder, 1994). However, the recent work of
1559 Hakansson et al. (2007) indicates wet-based ice on the south side of the mouth of the
1560 Sund that is 250 m above modern sea level at the Last Glacial Maximum (MIS 2). Such a
1561 position almost certainly requires ice advance past the mouth. Seismic studies and cores

1562 on the Scoresby Sund trough-mouth fan offshore indicate that on the southern portion of
1563 the fan debris flows have been deposited fairly recently, whereas on the northern portion
1564 this activity pre-dates MIS 5 (O'Cofaigh et al., 2003). It is not clear how such debris flow
1565 activity occurred unless the ice had advanced well onto the shelf (O'Cofaigh et al., 2003).

1566 To the south of Scoresby Sund, at Kangerdlugssuaq, ice extended to the edge of
1567 the continental shelf during about 31–19 ka (Andrews et al., 1997, 1998a; Jennings et al.,
1568 2002a). These data, combined with widespread geomorphic evidence that ice reached the
1569 shelf break around south Greenland, are then the primary evidence for extensive ice cover
1570 of this age in southern Greenland (Funder et al., 2004; Weidick et al., 2004).

1571 In the Thule region of northwestern Greenland, the data are consistent both with
1572 the broad climate picture (the MIS 5e to MIS 2 sequence) and with ice-sheet response as
1573 in Scoresby Sund (advances in colder MIS 5d, 5b, 4 (about 59–73 ka) and especially MIS
1574 2, retreats in warmer 5c and 5a, possibly in MIS 3 (about 24–59 ka) , and surely in MIS
1575 1; see Figure 7.6 for general chronology) (Kelly et al., 1999). However, the dating is not
1576 secure enough to insist on much beyond the warmth of MIS 5e (marked by retreated ice),
1577 the cold of MIS 2 (marked by notably expanded ice), and the ice's subsequent retreat.

1578 The extent of ice at the glacial maximum also remains in doubt in the
1579 northwestern part of the Greenland ice sheet. The submarine moraines at the edge of the
1580 continental shelf are poorly dated. Ice from Greenland did merge with that from
1581 Ellesmere Island, thus joining the great Greenland Ice Sheet with the Inuitian sector of
1582 the North American Laurentide Ice Sheet (England, 1999; Dyke et al., 2002). However,
1583 whether ice advanced to the edge of the continental shelf in widespread regions to the
1584 north and south of the merger zone is poorly understood (Blake et al., 1996; Kelly et al.,

1585 1999). A recent reconstruction (Funder et al., 2004) favors advance of grounded ice to the
1586 shelf edge in the northwest, merging with North American ice, and with the merged ice
1587 spreading to the northeast and southwest along what is now Nares Strait to feed ice
1588 shelves extending toward the Arctic Ocean and Baffin Bay.. The lack of a high marine
1589 limit just south of Smith Sund in the northwest is prominent in that interpretation—more-
1590 extensive ice would have pushed the land down more and allowed the ocean to advance
1591 farther inland following deglaciation, and then subsequent isostatic uplift would have
1592 raised the marine deposits higher. But, a trade-off does exist between slow retreat and
1593 small retreat in controlling the marine limit. This trade-off has been explored by some
1594 workers (e.g., Huybrechts, 2002; Tarasov and Peltier, 2002), but the relative sea-level
1595 data are not as sensitive to the earlier part (about 24 ka) as to the later, and so strong
1596 conclusions are not available.

1597 Thus, the broad picture of ice advance in cooling conditions and ice retreat in
1598 warming conditions is quite clear. Remaining issues include the extent of advance onto
1599 the continental shelf (and if it was limited, why), and the rates and times of response.

1600 Let's look first at ice extent. The generally accepted picture has been one of
1601 expansion to the edge of the continental shelf in the south, much more limited expansion
1602 in the north, and a transition somewhere between Kangerdlugssuaq and Scoresby Sund
1603 on the east coast (Dowdeswell et al., 1996). On the west coast, the moraines that typically
1604 lie 30–50 km beyond the modern coastline (and even farther along troughs) are usually
1605 identified with MIS 2. The shelf-edge moraines (usually called Hellefisk moraines and
1606 usually roughly twice as far from the modern coastline as the presumably MIS 2
1607 moraines) are usually identified with MIS 6, although few solid dates are available

1608 (Funder and Larsen, 1989). On the east coast, the evidence from the mouth of Scoresby
1609 Sund and the trough-mouth fan, noted above in this section, opens the possibility of
1610 more-extensive ice there than is indicated by the generally accepted picture; ice may have
1611 extended to the mid-shelf or the shelf edge. Similarly, the work of Blake et al. (1996) in
1612 Greenland's far northwest may indicate that ice reached the shelf edge. The indications of
1613 Blake et al. (1996) are geomorphically consistent with wet-based ice. The increasing
1614 realization that cold-based ice is sometimes extensive yet geomorphically inactive (e.g.,
1615 England, 1999) further complicates interpretations. No evidence overturns the
1616 conventional view of expansion to the shelf-edge in the south, expansion to merge with
1617 North American ice in the northwest, and expansion onto the continental shelf but not to
1618 the shelf-edge elsewhere. Thus, this interpretation is probably favored, but additional data
1619 would clearly be of interest.

1620 Glaciological understanding indicates that ice sheets almost always respond to
1621 climatic or other environmental forcings (such as sufficiently large sea-level change). The
1622 most prominent exception may be advance to the edge of the continental shelf under
1623 conditions that would allow further advance if a huge topographic step in the sea floor
1624 were not present. (Similarly, ice may not respond to relatively small climate changes,
1625 such as during the advance stage of the tidewater-glacier cycle (Meier and Post, 1987)). If
1626 this assessment is accurate, and if the Greenland Ice Sheet at the time of the Last Glacial
1627 Maximum terminated somewhere on the continental shelf rather than at the shelf edge
1628 around part of the coastline, then glaciological understanding indicates that the ice sheet
1629 should have responded to short-lived climate changes.

1630 The near-field marine record is consistent with such fluctuations, as discussed

1631 next. However, owing to the complexity of the controls on the paleoclimatic indicators,
1632 unambiguous interpretations are not possible.

1633 Several marine sediment cores extend back through MIS 3 and even into MIS 4
1634 (the cores were obtained from Baffin Bay, the Erik Drift off southwestern Greenland, the
1635 Irminger and Blosseville Basins (e.g., cores SU90-24 & PS2264, Figure 7.8), and from
1636 the Denmark Strait) (Figure 7.8). In many of those cores, the $\delta^{18}\text{O}$ of near-surface
1637 planktic foraminifers varies widely during MIS 3. These variations were initially
1638 documented by Fillon and Duplessy (1980) in cores HU75-041 and -042 from south of
1639 Davis Strait (Figures 7.8 and 7.10, panel B), and this documentation preceded the
1640 recognition of large millennial oscillations (Dansgaard-Oeschger or D-O events; Johnsen
1641 at al., 1992b, Dansgaard et al., 1993) in the Greenland ice core records. In addition, Fillon
1642 and Duplessy (1980) also contributed information on the down-core numbers of volcanic-
1643 ash (tephra) shards in these two cores. These authors identified “Ash Zone B” in core
1644 HU75-042, which is correlated with the North Atlantic Ash Zone II, for which the current
1645 best-estimate age is about 54 ka (Figure 7.10B; it is associated with the end of interstadial
1646 15 as identified by Dansgaard et al., 1993). Subsequent work, especially north and south
1647 of Denmark Strait, has also shown large oscillations in planktonic foraminiferal $\delta^{18}\text{O}$
1648 (Elliott et al., 1998; Hagen, 1999; van Kreveland et al., 2000; Hagen and Hald, 2002). As
1649 noted in section 7.3.4a, above, and shown in Figure 7.10A, the transect of cores appears
1650 to show both climate forcing and ice-sheet response in the millennial oscillations,
1651 although strong conclusions are not possible.

1652 Cores from the Scoresby Sund and Kangerdlugssuaq trough mouth fans, two of
1653 the major outlets of the eastern Greenland Ice Sheet, also have distinct layers that are rich

1654 in ice-rafted debris (Stein et al., 1996; Andrews et al., 1998a; Nam and Stein, 1999).
1655 Cores HU93030-007 and MD99-2260 from the Kangerdlugssuaq trough-mouth fan
1656 (Dunhill, 2005) (Figure 7.8) consist of alternating layers with more and less ice-rafted
1657 debris that overlie a massive debris flow. Material above the debris flow is dated about 35
1658 ka. The debris-rich layers have radiocarbon dates that are approximately coeval with
1659 Heinrich events 3 and 2. (Figure 7.9) On the Scoresby Sund trough-mouth fan, Stein et al
1660 (1996) also recorded intervals rich in ice-rafted debris that they quantified by counting
1661 the number of clasts greater than 2 mm as observed on X-rays. Although these cores are
1662 not as well dated as many from sites south of the Scotland-Greenland Ridge, they do
1663 indicate that such debris was delivered to the fan in pulses that may be approximately
1664 coeval with the North Atlantic Heinrich events.

1665 Although several reports have invoked the Iceland Ice Sheet as a major
1666 contributor to North Atlantic sediment (Bond and Lotti, 1995; Elliot et al., 1998;
1667 Grousset et al., 2001), Farmer et al. (2003) and Andrews (2008) have questioned this
1668 assertion. They argue that the eastern Greenland Ice Sheet has been an ignored source of
1669 ice-rafted debris in the eastern North Atlantic south of the Scotland-Greenland Ridge. In
1670 particular, Andrews (2008) argued that the data from Iceland and Denmark Strait
1671 precluded any Icelandic contribution for Heinrich event 3. As noted by Huddard et al
1672 (2006), the area of the Iceland Ice Sheet during the Last Glacial Maximum was only
1673 200,000 km² with an annual loss of ~600 km³, and only ~150 km³ of this loss was
1674 associated with calving. This is less than one-half the estimated calving rate of the
1675 present day Greenland Ice Sheet (Reeh, 1985).

1676 The marine evidence from the western margin of the Greenland Ice Sheet for

1677 fluctuations of the ice sheet during MIS 3 is confounded by two facts: there are no
1678 published chronologies from the trough-mouth fan off Disko Island, and the stratigraphic
1679 record from Baffin Bay consists of glacially derived sediments from the Greenland Ice
1680 Sheet and from the Laurentide Ice Sheet including its Innuitian section (Dyke et al.,
1681 2002). Evidence for major ice-sheet events during MIS 3 is abundant, as is seen
1682 throughout Baffin Bay in layers rich in carbonate clasts transported from adjacent
1683 continental rocks (Aksu, 1985; Andrews et al., 1998b; Parnell et al., 2007) (Figure 7.11).

1684

1685

FIGURE 7.11 NEAR HERE

1686

1687 Core PS1230 from Fram Strait, which records the export of sediments from ice
1688 sheets around the Arctic Ocean (Darby et al., 2002), shows ice-rafted debris intervals
1689 associated with major contributions from north Greenland about 32, 23, and 17 ka. These
1690 debris intervals correspond closely in timing with ice-rafted debris events from the Arctic
1691 margins of the Laurentide Ice Sheet.

1692 The fact that ice-rafted debris does not directly indicate ice-sheet behavior
1693 presents a continuing difficulty. Iceberg rafting of debris at an offshore site may increase
1694 owing to several possible factors: faster flow of ice from an adjacent ice sheet; flow of ice
1695 containing more clasts; loss of an ice shelf (most ice shelves experience basal melting,
1696 tending to remove debris in the ice, so ice-shelf loss would allow calving of bergs bearing
1697 more debris); cooling of ocean waters that allows icebergs—and their debris—to reach a
1698 site, loss of extensive coastal sea ice that allows icebergs to reach sites more rapidly
1699 (Reeh, 2004), alterations in currents or winds that control iceberg drift tracks, or other

1700 changes. The very large changes in volume of incoming sediment from the North
1701 American Laurentide Ice Sheet during Heinrich events (Hemming, 2004) are generally
1702 interpreted to be true indicators of ice-dynamical changes (e.g., Alley and MacAyeal,
1703 1994), but even that is debated (e.g., Hulbe et al., 2004). Thus, the marine-sediment
1704 record is consistent with Greenland fluctuations in concert with millennial variability
1705 during the cooling into MIS 2. Moreover, trained observers have interpreted the records
1706 as indicating millennial oscillations of the Greenland Ice Sheet in concert with climate,
1707 but those fluctuations cannot be demonstrated uniquely.

1708

1709 **7.3.5 Ice-Sheet Retreat from the Last Glacial Maximum (MIS 2)**

1710 ***7.3.5a Climatic history and forcing***

1711 As shown in **Figure 7.9** (also see Alley et al., 2002), the coldest conditions recorded in
1712 Greenland ice cores since MIS 6 were reached about 24 ka, which corresponds closely in
1713 time with the minimum in local midsummer sunshine and with Heinrich Event H2. The
1714 suite of sediment cores from Denmark Strait (**Figures 7.8 and 7.10A**) plus data from
1715 other sediment cores (VM28-14 and HU93030-007) indicate that the most extreme values
1716 indicating Last Glacial Maximum in $\delta^{18}\text{O}$ of marine foraminifera occurred ~18–20 ka
1717 (slightly younger than the Last Glacial Maximum values in the ice cores) with values of
1718 4.6‰ indicating cold, salty waters.

1719 The “orbital” warming signal in ice-core records and other climate records is
1720 fairly weak until perhaps 19 ka or so (Alley et al., 2002). The very rapid onset of warmth
1721 about 14.7 ka (the Bølling interstadial) is quite prominent. However, more than a third of
1722 the total deglacial warming was achieved before that abrupt step, and that pre-14.7 ka

1723 orbital warming was interrupted by Heinrich event H1. Bølling warmth was followed by
1724 general cooling (by two prominent but short-lived cold events, usually called the Older
1725 Dryas and the Inter-Allerød cold period), before faster cooling led into the Younger
1726 Dryas about 12.8 ka. Gradual warming then occurred through the Younger Dryas,
1727 followed by a step warming at the end of the Younger Dryas about 11.5 ka. This abrupt
1728 warming was followed by ramp warming to above recent values by 9 ka or so, punctuated
1729 by the short-lived cold event of the Preboreal Oscillation about 11.2–11.4 ka (Bjorck et
1730 al., 1997; Geirsdottir et al., 1997; Hald and Hagen, 1998; Fisher et al., 2002; Andrews
1731 and Dunhill, 2004; van der Plicht et al., 2004; Kobashi et al., in press), and followed by
1732 the short-lived cold event about 8.3–8.2 ka (the “8k event”; e.g., Alley and Agustsdottir,
1733 2005).

1734 The cold times of Heinrich events H2, H1, the Younger Dryas, the 8k event, and
1735 probably other short-lived cold events including the Preboreal Oscillation are linked to
1736 greatly expanded wintertime sea ice in response to decreases in near-surface salinity and
1737 to the strength of the overturning circulation in the North Atlantic (see review by Alley,
1738 2007). The cooling associated with these oceanic changes probably affected summers in
1739 and around Greenland (but see Bjorck et al., 2002 and Jennings et al., 2002a), but they
1740 were most influential in wintertime (Denton et al., 2005).

1741 Peak MIS 1/Holocene warmth before and after the 8.2-ka event was, for roughly
1742 millennial averages, $\sim 1.3^{\circ}\text{C}$ above late Holocene values in central Greenland, based on
1743 frequency of occurrence of melt layers in the GISP2 ice core (Alley and Anandakrishnan,
1744 1995), with mean-annual changes slightly larger although still smaller than $\sim 2^{\circ}\text{C}$ (and
1745 with correspondingly larger wintertime changes); other indicators are consistent with this

1746 interpretation (Alley et al., 1999). Indicators from around Greenland similarly show mid-
1747 Holocene warmth, although with different sites often showing peak warmth at slightly
1748 different times (Funder and Fredskild, 1989). Peak Holocene warmth was followed by
1749 cooling (with oscillations) into the Little Ice Age. The ice-core data indicate that the
1750 century- to few-century-long anomalous cold of the Little Ice Age was $\sim 1^{\circ}\text{C}$ or slightly
1751 more (Johnsen, 1977; Alley and Koci, 1990; Cuffey et al., 1994).

1752

1753 ***7.3.5b Ice-sheet changes***

1754 The Greenland Ice Sheet lost about 40% of its area (Funder et al., 2004) and a
1755 notable fraction of its volume (see below; also Elverhoi et al., 1998) after the peak of the
1756 last glaciation about 24–19 ka. These losses are much less than those of the warmer
1757 Laurentide and Fennoscandian Ice Sheets (essentially complete loss) and much more than
1758 those in the colder Antarctic.

1759 The time of onset of retreat from the Last Glacial Maximum is poorly defined
1760 because most of the evidence is now below sea level. Funder et al. (1998) suggested that
1761 the ice was most extended in the Scoresby Sund area from about 24,000 to about 19,000
1762 ka, on the basis of a comparison of marine and terrestrial data. This interval started at the
1763 coldest time in Greenland ice cores (which corresponds with the millennial Heinrich
1764 event H2) and extends to roughly the time when sea-level rise became notable because
1765 many ice masses around the world retreated (e.g., Peltier and Fairbanks, 2006).

1766 Extensive deglaciation that left clear records is typically more recent. For
1767 example, a core from Hall Basin (core 79, Figure 7.8), the northernmost of a series of
1768 basins that lie between northwest Greenland and Ellesmere Island, has a date on hand-

1769 picked foraminifers of about 16.2 ka. This date implies that the outlet to the Arctic Ocean
1770 had retreated by this time (Mudie et al., 2006). At Sermilik Fjord in southwest Greenland,
1771 retreat from the shelf preceded about 16 ka (Funder, 1989c). The ice was at the modern
1772 coastline or back into the fjords along much of the coast by approximately Younger
1773 Dryas time (13–11.5 ka, but with no implication that this position is directly linked to the
1774 climatic anomaly of the Younger Dryas) (Funder, 1989c; Marienfeld, 1992b; Andrews et
1775 al., 1996; Jennings et al., 2002b; Lloyd et al., 2005; Jennings et al., 2006). In the
1776 Holocene, the marine evidence of ice-rafted debris from the east-central Greenland
1777 margin (Marienfeld, 1992a; Andrews et al., 1997; Jennings et al., 2002a; Jennings et al.,
1778 2006) shows a tripartite record with early debris inputs, a middle-Holocene interval with
1779 very little such debris, and a late Holocene (neoglacial) period that spans the last 5–6 ka
1780 of steady delivery of such debris (Figure 7.12).

1781

1782

FIGURE 7.12 NEAR HERE

1783

1784 Along most of the Greenland coast, radiocarbon dates much older than the end of
1785 Younger Dryas time are rare, likely because of persistent cover by the Greenland Ice
1786 Sheet. Radiocarbon dates become common near the end of the Younger Dryas and
1787 especially during the Preboreal interval, and they remain common for all younger ages,
1788 indicating deglaciation (Funder, 1989a,b,c). The term “Preboreal” typically refers to the
1789 millennium-long interval following the Younger Dryas; the Preboreal Oscillation is a
1790 shorter lived cold event within this interval, but the terminology has sometimes been used
1791 loosely in the literature. Owing to uncertainty about the radiocarbon “reservoir” age of

1792 the waters in which mollusks lived and other issues, it typically is not possible to assess
1793 whether a given date traces to the Preboreal Oscillation or the longer Preboreal. These
1794 uncertainties typically preclude linking a particular date with Preboreal or with Younger
1795 Dryas.

1796 Given the prominence of the end of the Younger Dryas cold event in ice-core
1797 records (it was marked by a temperature increase of about 10°C in about 10 years;
1798 Severinghaus et al., 1998), it may seem surprising at first that widespread moraines
1799 abandoned in response to that warming have not been identified with confidence. Part of
1800 the difficulty is solved by the hypothesis of Denton et al. (2005), who argued that most of
1801 the warming occurred in winter. Bjorck et al. (2002) and Jennings et al. (2002a) argued
1802 for notable summertime warmth in Greenland during the Younger Dryas, but from
1803 Denton et al. (2005) and Lie and Paasche (2006), at least some warming or lengthening
1804 of the melt season probably occurred at the end of the Younger Dryas. The terminal
1805 Younger Dryas warming then would be expected to have affected glacier and ice-sheet
1806 behavior.

1807 All ice-core records from Greenland show clearly that the temperature drop into
1808 the Younger Dryas was followed by a millennium of slow warming before the rapid
1809 warming at the end (Johnsen et al., 2001; North Greenland Ice Core Project Members,
1810 2004). The slow warming perhaps reflected rising mid-summer insolation (a function of
1811 Earth's orbit) during that time. The Younger Dryas was certainly long enough for coastal
1812 mountain glaciers to reflect both the cooling into the event and the warming during the
1813 event before the terminal step. The ice-sheet margin probably would have been
1814 influenced by these changes as well (as discussed in section 7.3.4b, above, and in this

1815 section below). If the ice margin did advance with the cooling into the Younger Dryas,
1816 and did retreat during the Younger Dryas and its termination, then moraine sets would be
1817 expected from near the start of the Younger Dryas and from the cooling of the Preboreal
1818 Oscillation after the Younger Dryas (perhaps with minor moraines marking small events
1819 during the latter-Younger Dryas retreat). Because so much of the ice-sheet margin was
1820 marine at the start of the Younger Dryas, events of that age would not be recorded well.

1821 Much study has focused on the spectacular late-glacial moraines of the Scoresby
1822 Sund region of east Greenland (Funder et al., 1998; Denton et al., 2005). Funder et al.
1823 (1998) suggested that the last resurgence of glaciers in the region, known as the Milne
1824 Land Stade, was correlated with the Preboreal Oscillation, although a Younger Dryas age
1825 for at least some of the moraines, perhaps with both Preboreal Oscillation and Younger
1826 and Dryas present, cannot be excluded (Funder et al., 1998; Denton et al., 2005). Data
1827 and modeling remain sufficiently sketchy that strong conclusions do not seem warranted,
1828 but the available results are consistent with rapid response of the ice to forcing, with
1829 warming causing retreat.

1830 Retreat of the ice sheet from the coastline passed the position of the modern ice
1831 margin about 8 ka and continued well inland, perhaps more than 10 km in west
1832 Greenland (Funder, 1989c), up to 20 km in north Greenland (Funder, 1989b), and
1833 perhaps as much as 60 km in parts of south Greenland (Tarasov and Peltier, 2002).
1834 Reworked marine shells and other organic matter of ages 7–3 ka found on the ice surface
1835 and in younger moraines document this retreat (Weidick et al., 1990; Weidick, 1993). In
1836 west Greenland, the general retreat from the coast was interrupted by intervals during
1837 which moraines formed, especially about 9.5–9 ka and 8.3 ka (Funder, 1989c). These

1838 moraines are not all of the same age and are not, in general, directly traceable to the
1839 short-lived 8k cold event about 8.3–8.2 ka (Long et al., 2006). Timing of the onset of late
1840 Holocene readvance is not tightly constrained. Funder (1989c) suggested about 3 ka for
1841 west Greenland, the approximate time when relative a sea-level fall (from isostatic
1842 rebound of the land) switched to begin a relative sea-level rise of about 5 m (perhaps in
1843 part a response to depression of the land by the advancing ice load). Similar
1844 considerations place the onset of readvance somewhat earlier in the south, where relative
1845 sea-level fall switched to relative rise of about 10 m beginning about 8–6 ka (Sparrenbom
1846 et al., 2006a; 2006b).

1847 The late Holocene advance culminated in different areas at different times,
1848 especially in the mid-1700s, 1850–1890, and near 1920 (Weidick et al., 2004). Since
1849 then, ice has retreated from this maximum.

1850 Evidence of relative sea-level changes is consistent with this history (Funder,
1851 1989d; Tarasov and Peltier, 2002; 2003; Fleming and Lambeck, 2004). Flights of raised
1852 beaches or other marine indicators are observed on many coasts of Greenland, and they
1853 lie as much as 160 m above modern sea level in west Greenland.

1854 Fleming and Lambeck (2004) used an iterative technique to reconstruct the ice-
1855 sheet volume over time to match relative sea-level curves. They obtained an ice-sheet
1856 volume at the time of the Last Glacial Maximum about 42% larger than modern (3.1 m of
1857 additional sea-level equivalent in the ice sheet, compared with the modern value of 7.3 m
1858 of sea-level equivalent; interestingly, Huybrechts (2002) obtained a model-based estimate
1859 of 3.1 m of excess ice at the Last Glacial Maximum). Fleming and Lambeck (2004)
1860 estimated that 1.9 m of the 3.1 m of excess ice during the Last Glacial Maximum

1861 persisted at the end of the Younger Dryas. In their reconstruction, ice of the Last Glacial
1862 Maximum terminated on the continental shelf in most places, but it extended to or near
1863 the shelf edge in parts of southern Greenland, northeast Greenland, and in the far
1864 northwest where the Greenland Ice Sheet coalesced with the Innuitian ice from North
1865 America. Ice along much of the modern coastline was more than 500 m thick, and it was
1866 more than 1500 m thick in some places. Mid-Holocene retreat of about 40 km behind the
1867 present margin before late Holocene advance was also indicated. Rigorous error limits
1868 are not available, and modeling of the Last Glacial Maximum did not include the effects
1869 of the Holocene retreat behind the modern margin, so additional uncertainty is
1870 introduced.

1871 In the ICE5G model, Peltier (2004) (with a Greenland Ice Sheet history based on
1872 Tarasov and Peltier, 2002) found that the relative sea-level data were inadequate to
1873 constrain Greenland ice-sheet volume accurately. In particular, these constraints provide
1874 only a partial history of the ice-sheet footprint and no information on the small—but
1875 nonzero—changes inland. Thus, Tarasov and Peltier (2002; 2003) and Peltier (2004)
1876 chose to combine ice-sheet and glacial isostatic adjustment modeling with relative-sea-
1877 level observations to derive a model of the ice-sheet geometry extending back to the
1878 Eemian (MIS 5e, about 125–130 ka). The previous ICE4G reconstruction had been
1879 characterized by an excess ice volume during the Last Glacial Maximum, relative to the
1880 present, of 6 m; this volume is reduced to 2.8 m in ICE5G. Later shrinkage of the
1881 Greenland Ice Sheet largely occurred in the last 10 ka in the ICE5G reconstruction, and
1882 proceeded to a mid-Holocene (7-6 ka) volume about 0.5 m less than at present, before
1883 regrowth to the modern volume.

1884 The 20th century warmed from the Little Ice Age to about 1930, sustained
1885 warmth into the 1960s, cooled, and then warmed again since about 1990 (e.g., Box et al.,
1886 2006). The earlier warming caused marked ice retreat in many places (e.g., Funder,
1887 1989a; 1989b; 1989c), and retreat and mass loss are now widespread (e.g., Alley et al.,
1888 2005). Study of declassified satellite images shows that at least for Helheim Glacier in
1889 the southeast of Greenland, the ice was in a retreated position in 1965, advanced after that
1890 during a short-lived cooling, and has again switched to retreat (Joughin et al., 2008b).
1891 This latest phase of retreat is consistent with global positioning system–based inferences
1892 of rapid melting in the southeastern sector of the Greenland Ice Sheet (Khan et al., 2007).
1893 It is also consistent with GRACE satellite gravity observations, which indicate a mean
1894 mass loss in the period April 2002–April 2006 equivalent to 0.5 mm/yr of globally
1895 uniform sea-level rise (Velicogna and Wahr, 2006).

1896 As discussed in section 7.2.2e, above, geodetic measurements of perturbations in
1897 Earth’s rotational state can also help constrain the recent ice-mass balance. Munk (2002)
1898 suggested that length-of-day and true polar wander data were well fit by a model of
1899 ongoing glacial isostatic adjustment, and that this fit precluded a contribution from the
1900 Greenland Ice Sheet to recent sea-level rise. Mitrovica et al. (2006) reanalyzed the
1901 rotation data and applied a new theory of true polar wander induced by glacial isostatic
1902 adjustment. They found that an anomalous 20th-century contribution of as much as about
1903 1 mm/yr of sea-level rise is consistent with the data; the partitioning of this value into
1904 signals from melting of mountain glaciers, Antarctic ice, and the Greenland Ice Sheet is
1905 non-unique. Interestingly, Mitrovica et al. (2001) analyzed a set of robust tide-gauge
1906 records and found that the geographic trends in the glacial isostatic adjustment–corrected

1907 rates suggested a mean 20th century melting of the Greenland Ice Sheet equivalent to
1908 about 0.4 mm/yr of sea-level rise.

1909

1910 **7.4 Discussion**

1911 Glaciers and ice sheets are highly complex, and they are controlled by numerous
1912 climatic factors and by internal dynamics. Textbooks have been written on the controls,
1913 and no complete list is possible. The attribution of a given ice-sheet change to a particular
1914 cause is generally difficult, and it requires appropriate modeling and related studies.

1915 It remains, however, that in the suite of observations as a whole, the behavior of
1916 the Greenland Ice Sheet has been more closely tied to temperature than to anything else.
1917 The Greenland Ice Sheet shrank with warming and grew with cooling. Because of the
1918 generally positive relation between temperature and precipitation (e.g., Alley et al.,
1919 1993), the ice sheet has tended to grow with reduced precipitation (snowfall) and to
1920 shrink when the atmospheric mass supply increased, so precipitation changes cannot have
1921 controlled ice-sheet behavior. However, local or regional events may at times have been
1922 controlled by precipitation.

1923 The hothouse world of the dinosaurs and into the Eocene occurred with no
1924 evidence of ice reaching sea level in Greenland. The long-term cooling that followed is
1925 correlated in time with appearance of ice in Greenland.

1926 Once ice appeared, paleoclimatic archives record fluctuations that closely match
1927 not only local but also widespread records of temperature, because local temperatures
1928 correlate closely with more-widespread temperatures. Because any ice-albedo feedback
1929 or other feedbacks from the Greenland Ice Sheet itself are too weak to have controlled

1930 temperatures far beyond Greenland, the arrow of causation cannot have run primarily
1931 from the ice sheet to the widespread climate.

1932 One must consider whether something controlled both the temperature and the ice
1933 sheet, but this possibility appears unlikely. The only physically reasonable control would
1934 be sea level, in which warming caused melting of ice beyond Greenland, and the resultant
1935 sea-level rise forced retreat of the Greenland Ice Sheet by floating marginal regions and
1936 speeding iceberg calving and ice-flow spreading. However, data point to times when this
1937 explanation is not sufficient. There at least is a suggestion at MIS 6 that Greenland
1938 deglaciation led strong global sea-level rise, as described in section 7.3.2b, above. Ice
1939 expanded from MIS 5e to MIS 5d from a reduced ice sheet, which would have had little
1940 contact with the sea. Much of the retreat from the MIS 2 maximum took place on land,
1941 although fjord glaciers did contact the sea. Ice re-expanded after the mid-Holocene
1942 warmth against a baseline of very little change in sea level but in general with slight sea-
1943 level rise—opposite to expectations if sea-level controls the ice sheet. Similarly, the
1944 advance of Helheim Glacier after the 1960s occurred with a slightly rising global sea
1945 level and probably a slightly rising local sea level.

1946 At many other times the ice-sheet size changed in the direction expected from
1947 sea-level control as well as from temperature control, because trends in temperature and
1948 sea level were broadly correlated. Strictly on the basis of the paleoclimatic record, it is
1949 not possible to disentangle the relative effects of sea-level rise and temperature on the ice
1950 sheet. However, it is notable that terminal positions of the ice are marked by sedimentary
1951 deposits; although erosion in Greenland is not nearly as fast as in some mountain belts
1952 such as coastal Alaska, notable sediment supply to grounding lines continues. And, as

1953 shown by Alley et al. (2007), such sedimentation tends to stabilize an ice sheet against
1954 the effects of relative rise in sea level. Although a sea-level rise of tens of meters could
1955 overcome this stabilizing effect, the ice would need to be unaffected for many millennia
1956 by other environmental forcings, such as changing temperature, to allow that much sea-
1957 level rise (Alley et al., 2007). Strong temperature control on the ice sheet is observed for
1958 recent events (e.g., Zwally et al., 2002; Thomas et al., 2003; Hanna et al., 2005; Box et
1959 al., 2006) and has been modeled (e.g., Huybrechts and de Wolde, 1999; Huybrechts,
1960 2002; Toniazzo et al., 2004; Ridley et al., 2005; Gregory and Huybrechts, 2006).

1961 Thus, it is clear that many of the changes in the ice sheet were forced by
1962 temperature. In general, the ice sheet responded oppositely to that expected from changes
1963 in precipitation: it retreated with increasing precipitation. Events explainable by sea-level
1964 forcing but not by temperature change have not been identified. Sea-level forcing might
1965 yet prove to have been important during cold times of extensively advanced ice; however,
1966 the warm-time evidence of Holocene and MIS 5e changes that cannot be explained by
1967 sea-level forcing indicates that temperature control was dominant.

1968 Temperature change may affect ice sheets in many ways, as discussed in section
1969 7.1.2. Warming of summertime conditions increases meltwater production and runoff
1970 from the ice-sheet surface, and may increase basal lubrication to speed mass loss by
1971 iceberg calving into adjacent seas. Warmer ocean waters (or more-vigorous circulation of
1972 those waters) can melt the undersides of ice shelves, which reduces friction at the ice-
1973 water interface and so increases flow speed and mass loss by iceberg calving. In general,
1974 the paleoclimatic record is not yet able to separate these influences, which leads to the
1975 broad use of “temperature” in discussing ice-sheet forcing. In detail, ocean temperature

1976 will not exactly correlate with atmospheric temperature, so the possibility may exist that
1977 additional studies could quantify the relative importance of changes in ocean and in air
1978 temperatures.

1979 Most of the forcings of past ice-sheet behavior considered here have been applied
1980 slowly. Orbital changes in sunshine, greenhouse-gas forcing, and sea level have all varied
1981 on 10,000-year timescales. Purely on the basis of paleoclimatic evidence, it is generally
1982 not possible to separate the ice-volume response to incremental forcing from the
1983 continuing response to earlier forcing. In a few cases, sufficiently high time resolution
1984 and sufficiently accurate dating are available to attempt this separation for ice-sheet area.
1985 At least for the most recent events during the last decades of the 20th century and into the
1986 21st century, ice-marginal changes have tracked forcing, with very little lag. The data on
1987 ice-sheet response to earlier rapid forcing, including the Younger Dryas and Preboreal
1988 Oscillation, remain sketchy and preclude strong conclusions, but results are consistent
1989 with rapid temperature-driven response.

1990 A summary of many of the observations is given in Figure 7.13, which shows
1991 changes in ice-sheet volume in response to temperature forcing from an assumed
1992 “modern” equilibrium (before the warming of the last decade or two). Error bars cannot
1993 be placed with confidence. A discussion of the plotted values and error bars is given in
1994 the caption to Figure 7.13. Some of the ice-sheet change may have been caused directly
1995 by temperature and some by sea-level effects correlated with temperature; the techniques
1996 used cannot separate them (nor do modern models allow complete separation; Alley et
1997 al., 2007). However, as discussed above in this section, temperature likely dominated,
1998 especially during warmer times when contact with the sea was reduced because of ice-

1999 sheet retreat. Again, no rates of change are implied. The large error bars on Figure 7.13
2000 remain disturbing, but general covariation of temperature forcing and sea-level change
2001 from Greenland is indicated. The decrease in sensitivity to temperature with decreasing
2002 temperature also is physically reasonable; if the ice sheet were everywhere cooled to well
2003 below the freezing point, then a small warming would not cause melting and the ice sheet
2004 would not shrink.

2005

2006

FIGURE 7.13 NEAR HERE

2007

2008 **7.5 Synopsis**

2009 Paleoclimatic data show that the Greenland Ice Sheet has changed greatly with
2010 time. Physical understanding indicates that many environmental factors can force
2011 changes in the size of an ice-sheet. Comparison of the histories of important forcings and
2012 of ice-sheet size implicates cooling as causing ice-sheet growth, warming as causing
2013 shrinkage, and sufficiently large warming as causing loss. The evidence for temperature
2014 control is clearest for temperatures similar to or warmer than recent temperatures (the last
2015 few millennia). Snow accumulation rate is inversely related to ice-sheet volume (less ice
2016 when snowfall is higher), and thus the snow-accumulation rate in general is not the
2017 leading control on ice-sheet change. Rising sea level tends to float marginal regions of ice
2018 sheets and force retreat, so the generally positive relation between sea level and
2019 temperature means that typically both reduce the volume of the ice sheet. However, for
2020 some small changes during the most recent millennia, marginal fluctuations in the ice
2021 sheet have been opposed to those expected from local relative sea-level forcing but in the

2022 direction expected from temperature forcing. These fluctuations, plus the tendency of ice-
2023 sheet margins to retreat from the ocean during intervals of shrinkage, indicate that sea-
2024 level change is not the dominant forcing at least for temperatures similar to or above
2025 those of the last few millennia. High-time-resolution histories of ice-sheet volume are not
2026 available, but the limited paleoclimatic data consistently show that short-term and long-
2027 term responses to temperature change are in the same direction. The best estimate from
2028 paleoclimatic data is thus that warming will shrink the Greenland Ice Sheet, and that
2029 warming of a few degrees is sufficient to cause ice-sheet loss. Tightly constrained
2030 numerical estimates of the threshold warming required for ice-sheet loss are not
2031 available, nor are rigorous error bounds, and rate of loss is very poorly constrained.
2032 Numerous opportunities exist for additional data collection and analyses that would
2033 reduce these uncertainties.
2034

2034 **FIGURE CAPTIONS**

2035

2036

2037

2038

2039

2040

2041

2042

2043

2044

2045

2046

2047

2048

2049

2050

2051

2052

2053

2054

2055

2056

2057

Figure 7.1. Satellite image (SeaWiFS) of the Greenland Ice Sheet and surroundings, from July 15, 2000 (<http://www.gsfc.nasa.gov/gsfc/earth/pictures/earthpic.htm>).

Figure 7.2. Recently published estimates of the mass balance of the Greenland Ice Sheet through time (modified from Alley et al., 2007). A Total Mass Balance of 0 indicates neither growth nor shrinkage, and -180 Gt yr^{-1} indicates ice-sheet shrinkage contributing to sea-level rise of 0.5 mm/yr, as indicated. Each box extends from the beginning to the end of the time interval covered by the estimate, with the upper and lower lines indicating the uncertainties in the estimates. A given color is associated with a particular technique, and the different letters identify different studies. Two estimates have arrows attached, because those authors indicated that the change is probably larger than shown. The dotted box in the upper right is a frequently-cited study that applies only to the central part of the ice sheet, which is thickening, and misses the faster thinning in the margins.

FIGURE 7.3. Cross-sections showing idealized geomorphic and stratigraphic expression of coastal landforms and deposits found on low-wave-energy carbonate coasts of Florida and the Bahamas (upper) and high-wave-energy rocky coasts of Oregon and California (lower). Redrawn from Muhs et al. (2004) and references therein. (Vertical elevations are greatly exaggerated.)

2058 **FIGURE 7.4.** Relations of oxygen isotope records in foraminifers of deep-sea
2059 sediments to emergent reef or wave-cut terraces on an uplifting coastline (upper) and a
2060 tectonically stable or slowly subsiding coastline (lower). Emergent marine deposits
2061 record interglacial periods. Oxygen isotope data shown are from the SPECMAP record
2062 (Imbrie et al., 1984). Redrawn from Muhs et al. (2004).

2063

2064 **FIGURE 7.5.** Photographs of last-interglacial (MIS 5e) reef and corals on Key
2065 Largo, Florida, their elevations, probable water depths, and estimated paleo-sea level.
2066 Photographs by D.R. Muhs.

2067

2068 **FIGURE 7.6.** . Oxygen isotope data from the SPECMAP record (Imbrie et al.,
2069 1984), with indications of sea-level stands for different interglacials, assuming minimal
2070 glacial isostatic adjustments to the observed reef elevations.

2071

2072 **Figure 7.7.** Modeled configuration of the Greenland Ice Sheet today (left) and in
2073 MIS 5e (right), from Otto-Bliesner et al. (2006).

2074

2075 **Figure 7.8.** Location map with core locations discussed in the text. Full core
2076 identities are as follows: 79=LSSLL2001-079; 75-41 and -42=HU75-4,-42; 77-
2077 017=HU77-017; 76-033=HU76-033; 90-013=HU90-013; 1230=PS1230; 2264=PS2264;
2078 1225 and 1228=JM96-1225,-1228; 007=HU93-007; 2322=MD99-2322; 90-24=SU90-24.
2079 HS=Hudson Strait, source for major Heinrich events; R = location of the Renland Ice
2080 Cap.

2081

2082 **Figure 7.1** Ice-isotopic records ($\delta^{18}\text{O}$, a proxy for temperature, with less-negative
2083 values indicating warmer conditions) from GISP2, Greenland (Grootes and Stuiver,
2084 1997) (scale on right) and Byrd Station, Antarctica (scale on left), as synchronized by
2085 Blunier and Brook (2001), with various climate-event terminology indicated. Ice age
2086 terms are shown in blue (top); the classical Eemian/Sangamonian is slightly older than
2087 shown here, as is the peak of marine isotope stage (MIS, shown in purple) 5, known as
2088 5e. Referring specifically to the GISP2 curve, the warm Dansgaard-Oeschger events or
2089 stadial events, as numbered by Dansgaard et al. (1993), are indicated in red; Dansgaard-
2090 Oeschger event 24 is older than shown here. Occasional terms (L = Little Ice Age, 8 = 8k
2091 event, P=Preboreal Oscillation (PBO), Y = Younger Dryas, B = Bolling-Allerod, and
2092 LGM = Last Glacial Maximum) are shown in pink. Heinrich events are numbered in
2093 green just below the GISP2 isotopic curve, as placed by Bond et al. (1993). The Antarctic
2094 warm events A1–A7, as identified by Blunier and Brook (2001), are indicated for the
2095 Byrd record. Modified from Alley (2007).

2096

2097 **Figure 7.10.** A) Variations in $\delta^{18}\text{O}$ from a series of cores north to south of
2098 Denmark Strait (see Fig. 7.8), namely: PS2264, JM96-1225 and 1228 plotted against the
2099 $\delta^{18}\text{O}$ from the Renland Ice Cap. B) $\delta^{18}\text{O}$ variations in cores HU75-42 (NW Labrador
2100 Sea). C) Stable oxygen variations in cores HU77-017 from north of Davis Strait.

2101

2102 **Figure 7.11.** Variations in detrital carbonate (pieces of old rock) in core HU76-
2103 033 from Baffin Bay (Fig. 7.8) showing down-core variations in magnetic susceptibility

2104 and $\delta^{18}\text{O}$.

2105

2106 **Figure 7.12.** Holocene ice-rafted debris concentrations from MD99-2322 off
2107 Kangerdlugssuaq Fjord, east Greenland (Fig. 7.8) showing log values of the percent of
2108 sediment > 1 mm and the weight % of quartz in the < 2 mm sediment fraction.

2109

2110 **Figure 7.13.** A best-guess representation of the dependence of the volume of the
2111 Greenland Ice Sheet on temperature. Large uncertainties should be understood, and any
2112 ice-volume changes in response to sea-level changes correlated with temperature changes
2113 are included (although, as discussed in the text, temperature changes probably dominated
2114 forcing, especially at warmer temperatures when the reduced ice sheet had less contact
2115 with the sea). Recent values of temperature and ice volume (perhaps appropriate for 1960
2116 or so) are assigned 0,0. The Last Glacial Maximum was probably about 6°C colder than
2117 modern for global average (e.g., Cuffey and Brook, 2000; data and results summarized in
2118 Jansen et al., 2007). Cooling in central Greenland was about 15°C (with peak cooling
2119 somewhat more; Cuffey et al., 1995). Some of the central-Greenland cooling was
2120 probably linked to strengthening of the temperature inversion that lowers near-surface
2121 temperatures relative to the free troposphere (Cuffey et al., 1995). A cooling of about
2122 10°C is thus plotted. The ice-volume-change estimates of Peltier (2004; ICE5G) and
2123 Fleming and Lambeck (2004) are used, with the upper end of the uncertainty taken to be
2124 the ICE4G estimate (see Peltier, 2004), and somewhat arbitrarily set as 1 m on the lower
2125 side. The arrow indicates that the ice sheet in MIS 6 was more likely than not slightly
2126 larger than in MIS 2, and that some (although inconsistent) evidence of slightly colder

2127 temperatures is available (e.g., Bauch et al., 2000). The mid-Holocene result from ICE5G
2128 (Peltier, 2004) of an ice sheet smaller than modern by about 0.5 m of sea-level equivalent
2129 is plotted; the error bars reflect the high confidence that the mid-Holocene ice sheet was
2130 smaller than modern, with similar uncertainty assumed for the other side. Mid-Holocene
2131 temperature is taken from the Alley and Anandakrishnan (1995) summertime melt-layer
2132 history of central Greenland, with their 0.5°C uncertainty on the lower side, and a wider
2133 uncertainty on the upper side to include larger changes from other indicators (which are
2134 probably weighted by wintertime changes that have less effect on ice-sheet mass balance,
2135 and so are not used for the best estimate; Alley et al., 1999). As discussed in 7.3.3b and c,
2136 MIS 5e (the Eemian) is plotted with a warming of 3.5°C and a sea-level rise of 3.5 m.
2137 The uncertainties on sea-level change come from the range of data-constrained models
2138 discussed in 7.3.3c. The temperature uncertainties reflect the results of Cuffey and
2139 Marshall (2000) on the high side, and the lower values simulated over Greenland by
2140 Otto-Bliesner et al. (2006). Loss of the full ice sheet is also plotted, to reflect the warmer
2141 conditions that may date to MIS 11 if not earlier, and perhaps also to the Pliocene times
2142 of the Kap København Formation. Very large warming is indicated by the paleoclimatic
2143 data from Greenland, but much of that warming probably was a feedback from loss of the
2144 ice sheet itself (Otto-Bliesner et al., 2006). Data from around the North Atlantic for MIS
2145 11 and other interglacials do not show substantially higher temperatures than during MIS
2146 5e, allowing the possibility that sustaining MIS 5e levels for a longer time led to loss of
2147 the ice sheet. Slight additional warming is indicated here, within the error bounds of the
2148 other records, based on assessment that MIS 5e was sufficiently long for much of the ice-
2149 sheet response to have been completed, so that additional warmth was required to cause

2150 additional retreat. The volume of ice possibly persisting in highlands even after loss of
2151 central regions of the ice sheet is poorly quantified; 1 m is indicated.

2152

2153

2153

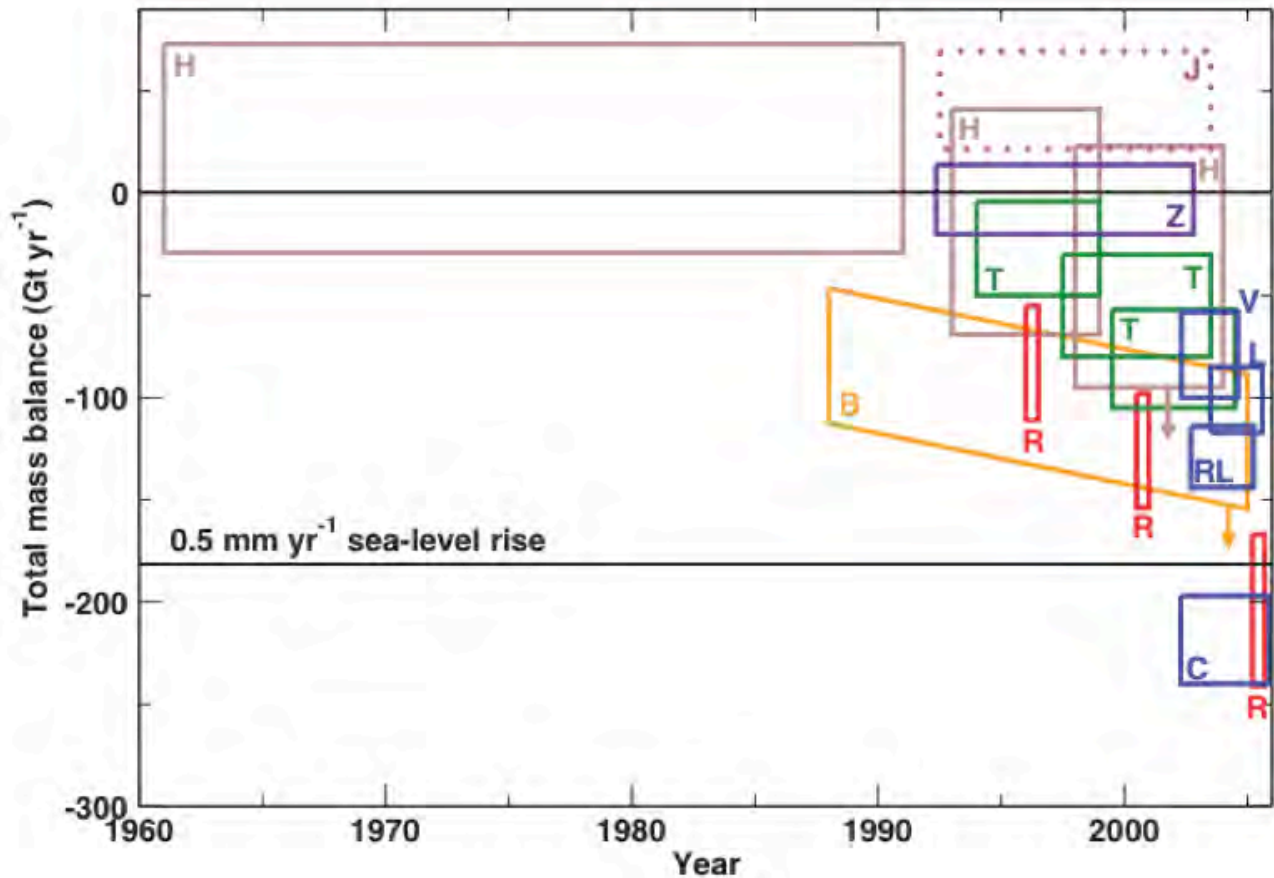
2154



2155

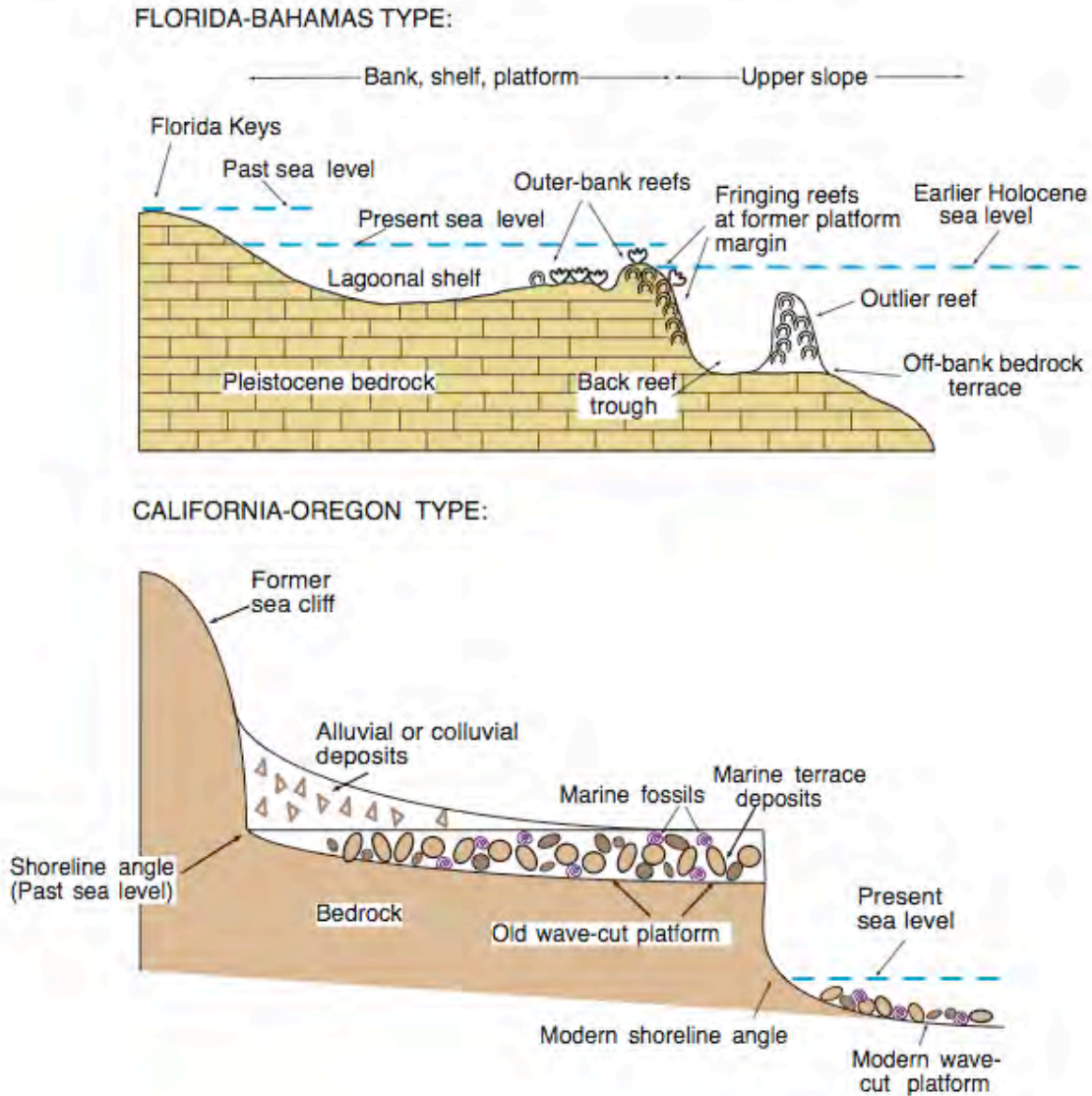
2156 **Figure 7.1** Satellite image (SeaWiFS) of the Greenland Ice Sheet and surroundings,
2157 from July 15, 2000 (<http://www.gsfc.nasa.gov/gsfcc/earth/pictures/earthpic.htm>).

2158

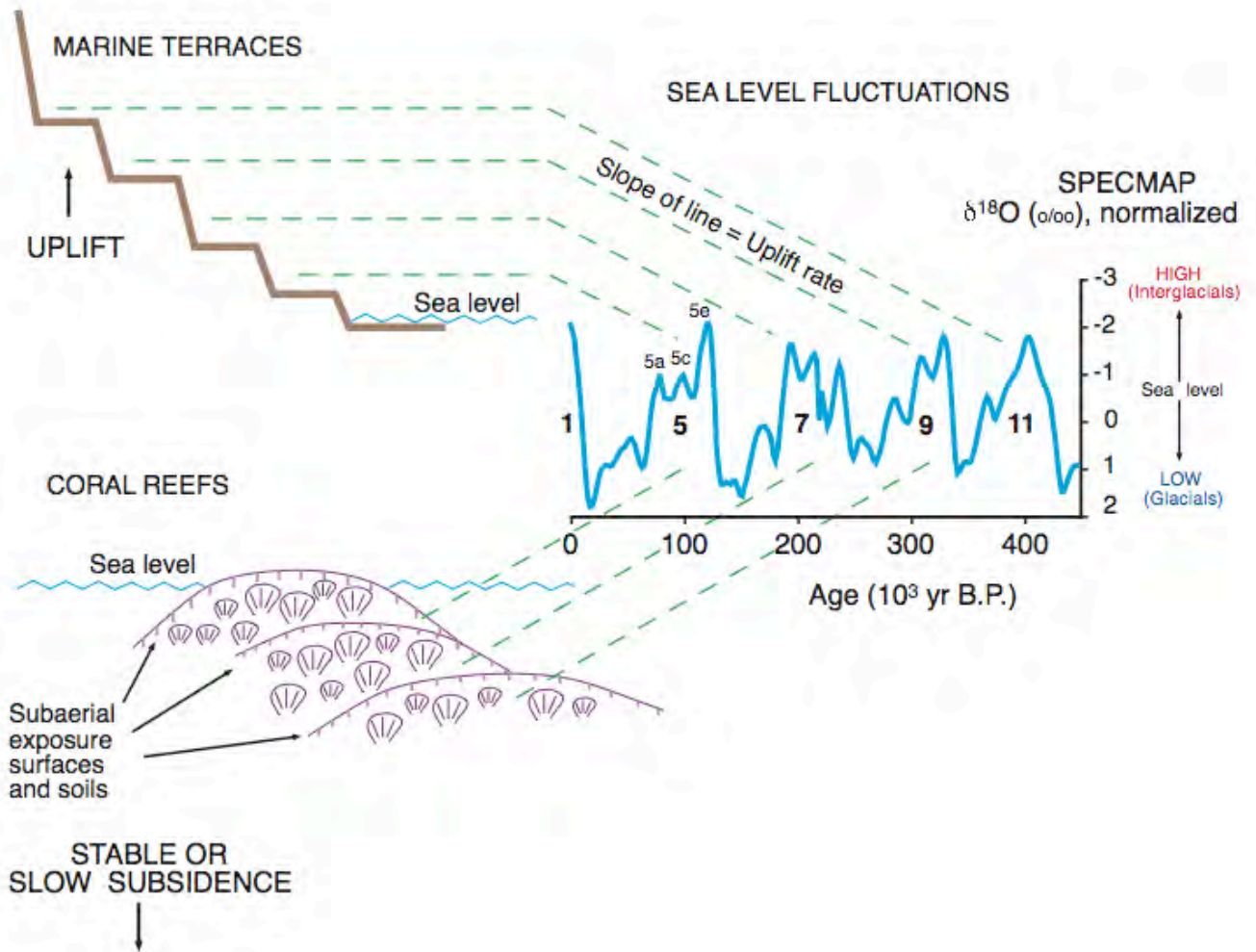


2158

2159 **Figure 7.2** Recently published estimates of the mass balance of the Greenland Ice Sheet
 2160 through time (modified from Alley et al., 2007). A Total Mass Balance of 0 indicates
 2161 neither growth nor shrinkage, and -180 Gt yr⁻¹ indicates ice-sheet shrinkage contributing
 2162 to sea-level rise of 0.5 mm/yr, as indicated. Each box extends from the beginning to the
 2163 end of the time interval covered by the estimate, with the upper and lower lines indicating
 2164 the uncertainties in the estimates. A given color is associated with a particular technique,
 2165 and the different letters identify different studies. Two estimates have arrows attached,
 2166 because those authors indicated that the change is probably larger than shown. The dotted
 2167 box in the upper right is a frequently-cited study that applies only to the central part of
 2168 the ice sheet, which is thickening, and misses the faster thinning in the margins.



2169 **Figure 7.3** Cross-sections showing idealized geomorphic and stratigraphic expression of
 2170 coastal landforms and deposits found on low-wave-energy carbonate coasts of Florida
 2171 and the Bahamas (upper) and high-wave-energy rocky coasts of Oregon and California
 2172 (lower). (Vertical elevations are greatly exaggerated.)
 2173



2173

2174 **Figure 7.4** Relations of oxygen isotope records in foraminifers of deep-sea sediments to
 2175 emergent reef or wave-cut terraces on an uplifting coastline (upper) and a tectonically
 2176 stable or slowly subsiding coastline (lower). Emergent marine deposits record
 2177 interglacial periods. Oxygen isotope data shown are from the SPECMAP record (Imbrie
 2178 et al., 1984). Redrawn from Muhs et al. (2004).

2179

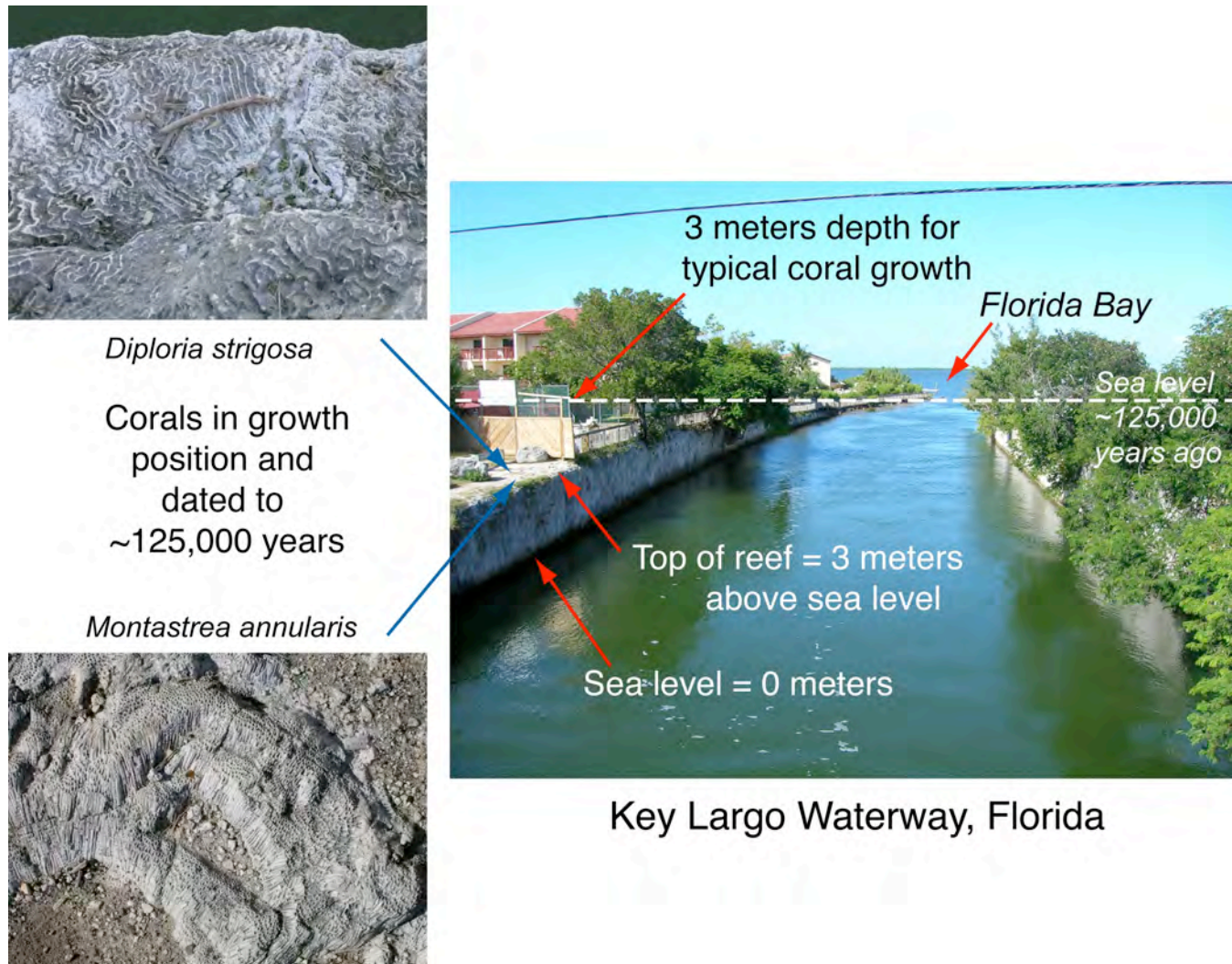


Figure 7.5 Photographs of last-interglacial (MIS 5e) reef and corals on Key Largo, Florida, their elevations, probable water depths, and estimated paleo-sea level. Photographs by D.R. Muhs.

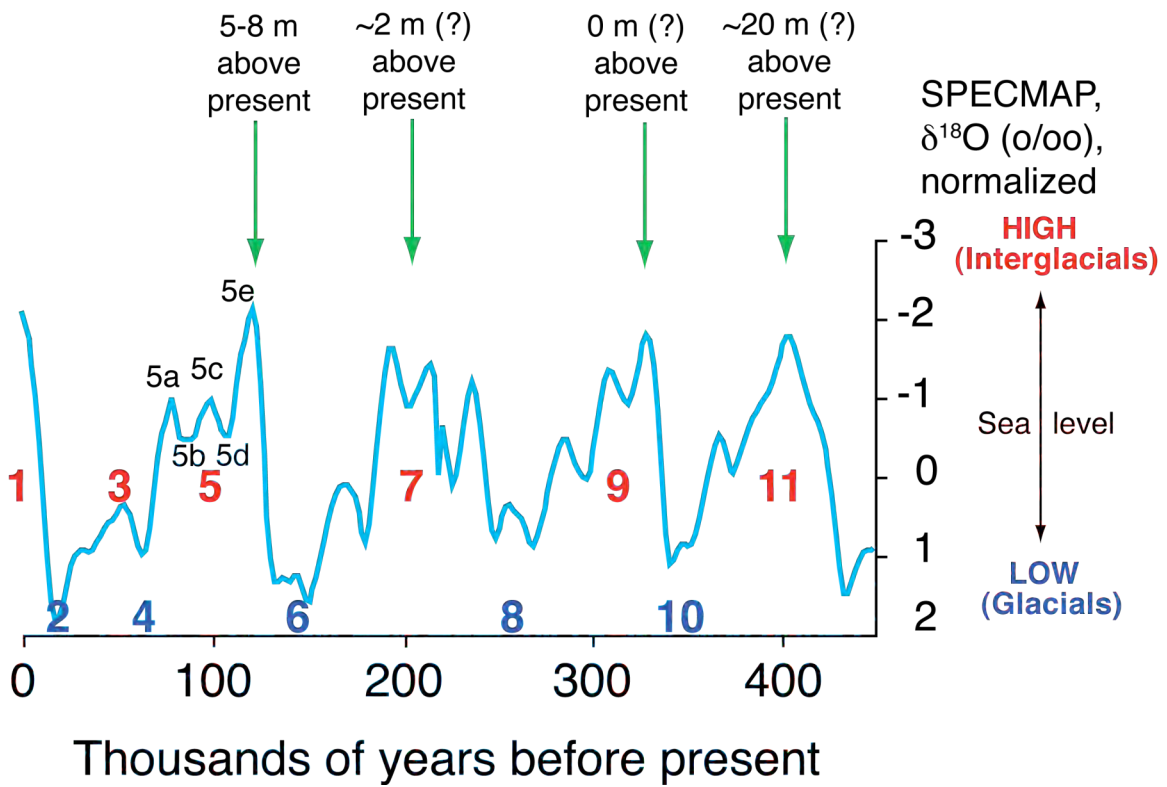


Figure 7.6 Oxygen isotope data from the SPECMAP record (Imbrie et al., 1984), with indications of sea-level stands for different interglacials, assuming minimal glacial isostatic adjustments to the observed reef elevations. Numbers identify Marine Isotope Stages (MIS) 1 through 11.

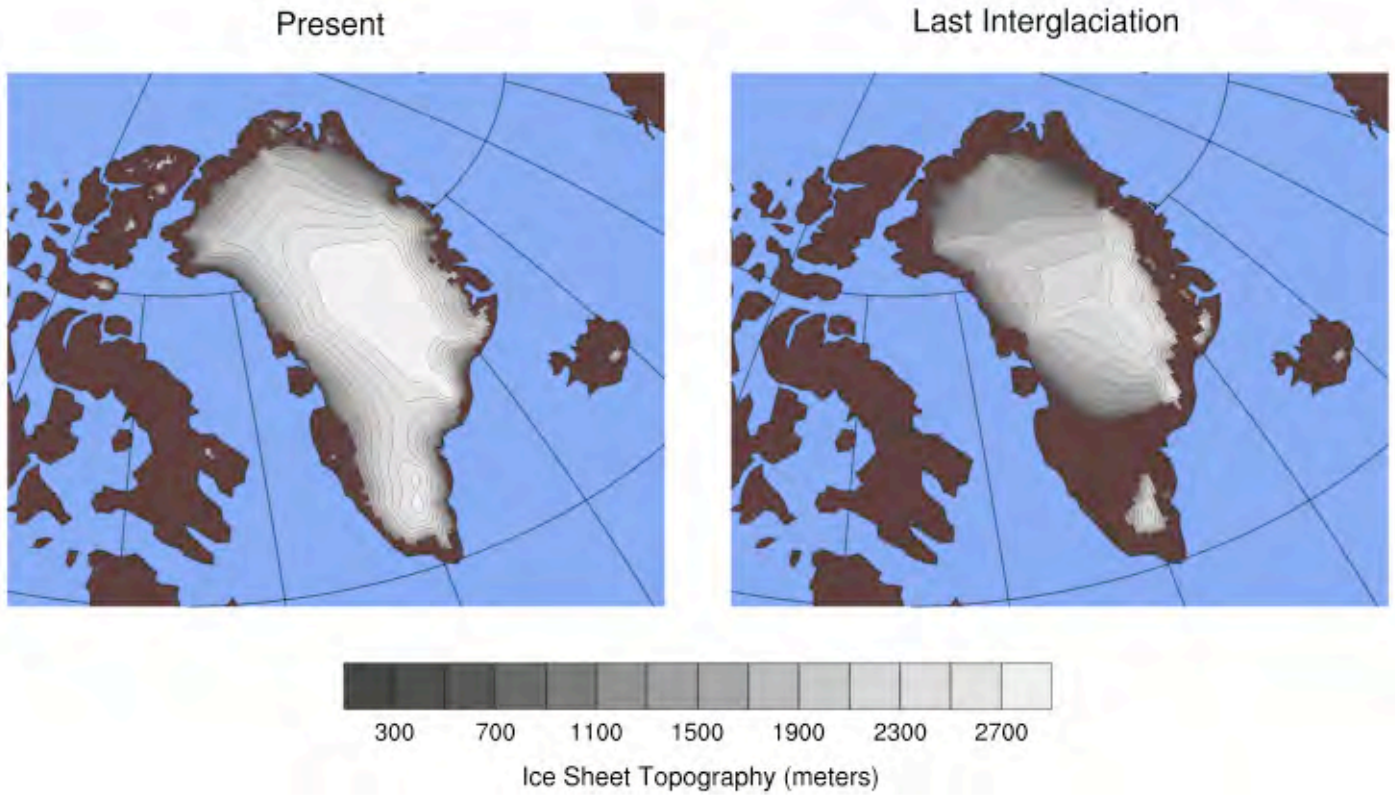


Figure 7.7 Modeled configuration of the Greenland Ice Sheet today (left) and in MIS 5e (right), from Otto-Bliesner et al. (2006).

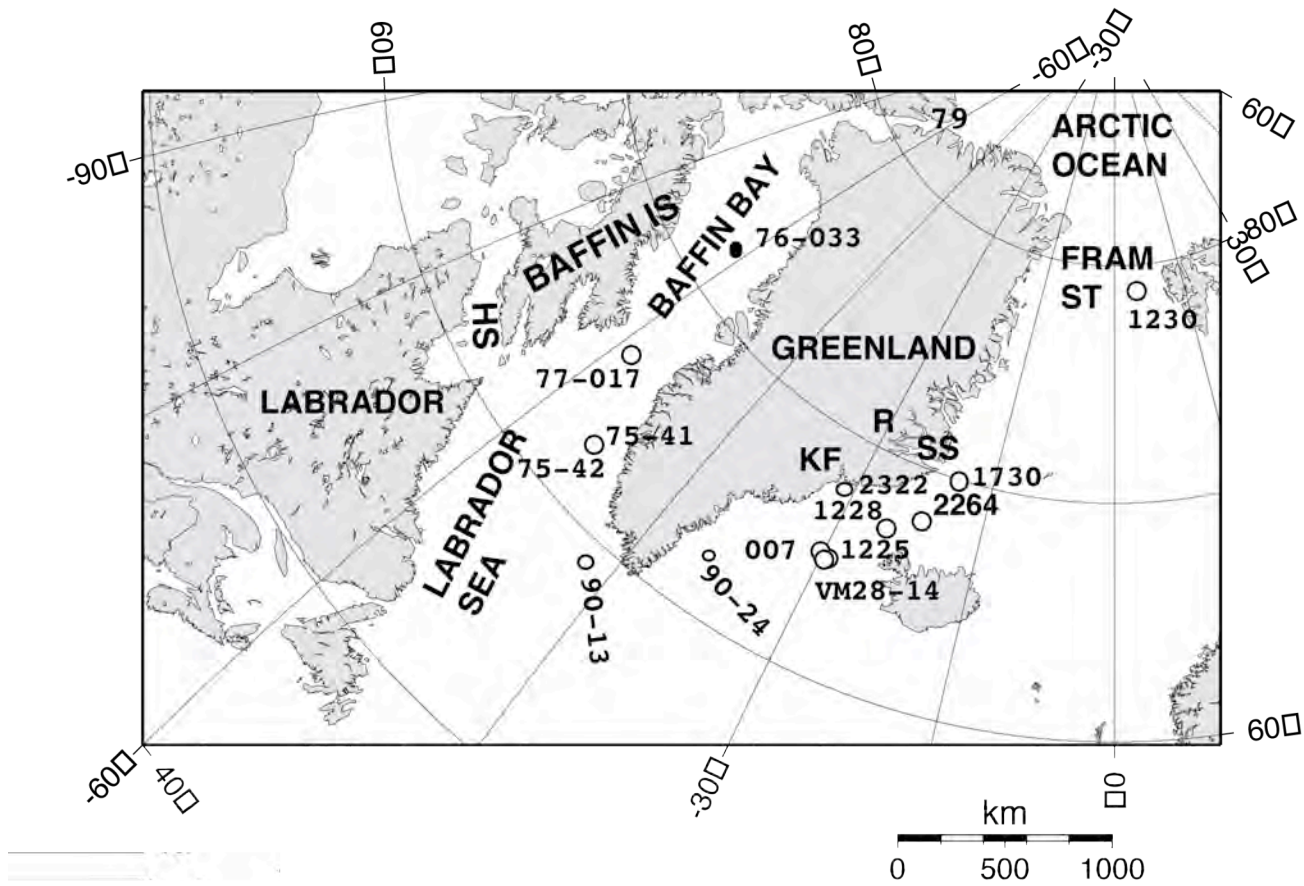


Figure 7.8 Location map with core locations discussed in the text. Full core identities are as follows: 79=LSSLL2001-079; 75-41 and -42=HU75-4,-42; 77-017=HU77-017; 76-033=HU76-033; 90-013=HU90-013; 1230=PS1230; 2264=PS2264; 1225 and 1228=JM96-1225,-1228; 007=HU93-007; 2322=MD99-2322; 90-24=SU90-24. HS=Hudson Strait, source for major Heinrich events; R = location of the Renland Ice Cap.

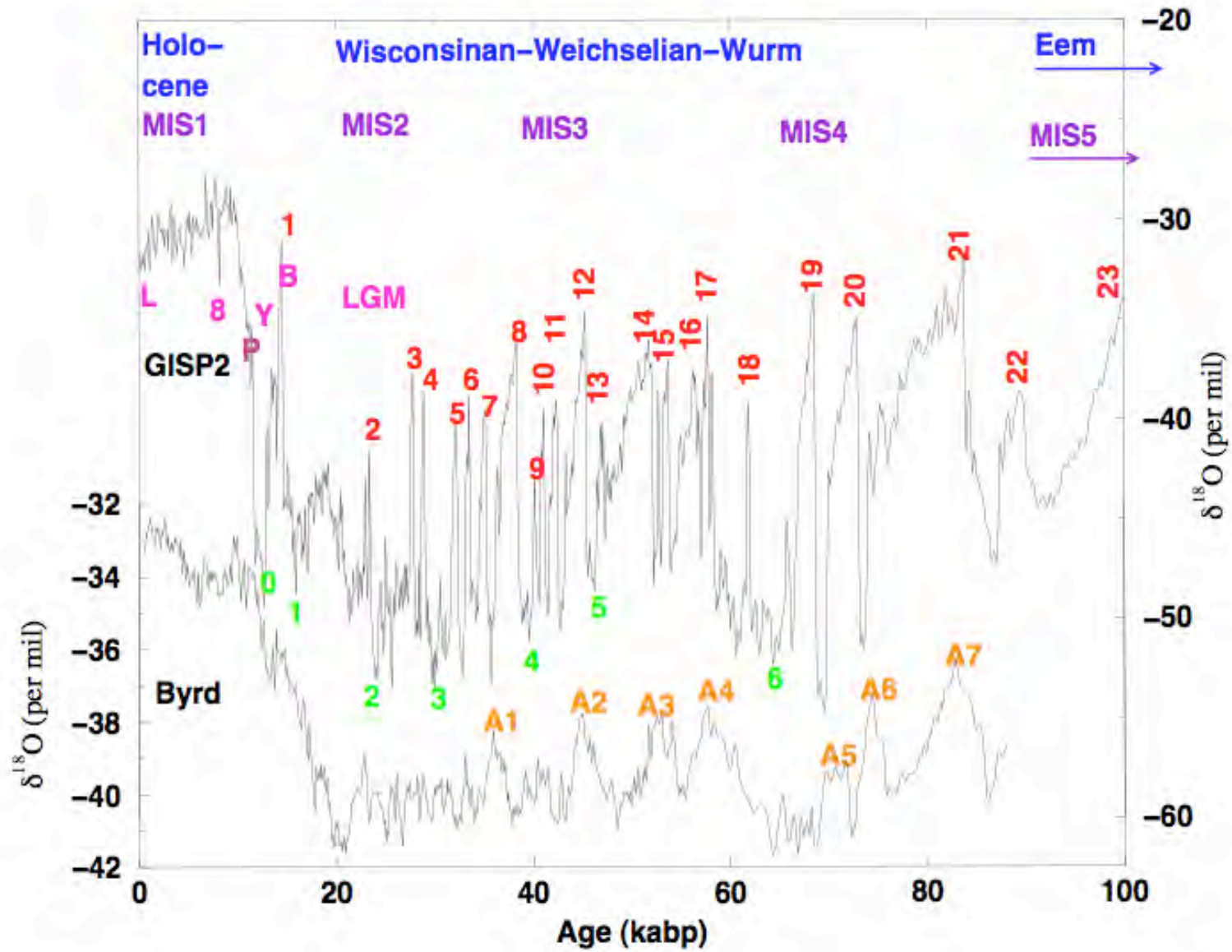


Figure 7.9 Ice-isotopic records ($\delta^{18}\text{O}$, a proxy for temperature, with less-negative values indicating warmer conditions) from GISP2, Greenland (Grootes and Stuiver, 1997) (scale on right) and Byrd Station, Antarctica (scale on left), as synchronized by Blunier and Brook (2001), with various climate-event terminology indicated. Ice age terms are shown in blue (top); the classical Eemian/Sangamonian is slightly older than shown here, as is the peak of marine isotope stage (MIS, shown in purple) 5, known as 5e. Referring specifically to the GISP2 curve, the warm Dansgaard-Oeschger events or stadial events, as numbered by Dansgaard et al. (1993), are indicated in red; Dansgaard-Oeschger event 24 is older than shown here. Occasional terms (L = Little Ice Age, 8 = 8k event, P=Preboreal Oscillation (PBO), Y = Younger Dryas, B = Bølling-Allerød, and LGM = Last Glacial Maximum) are shown in pink. Heinrich events are numbered in green just below the GISP2 isotopic curve, as placed by Bond et al. (1993). The Antarctic warm events A1–A7, as identified by Blunier and Brook (2001), are indicated for the Byrd record. Modified from Alley (2007).

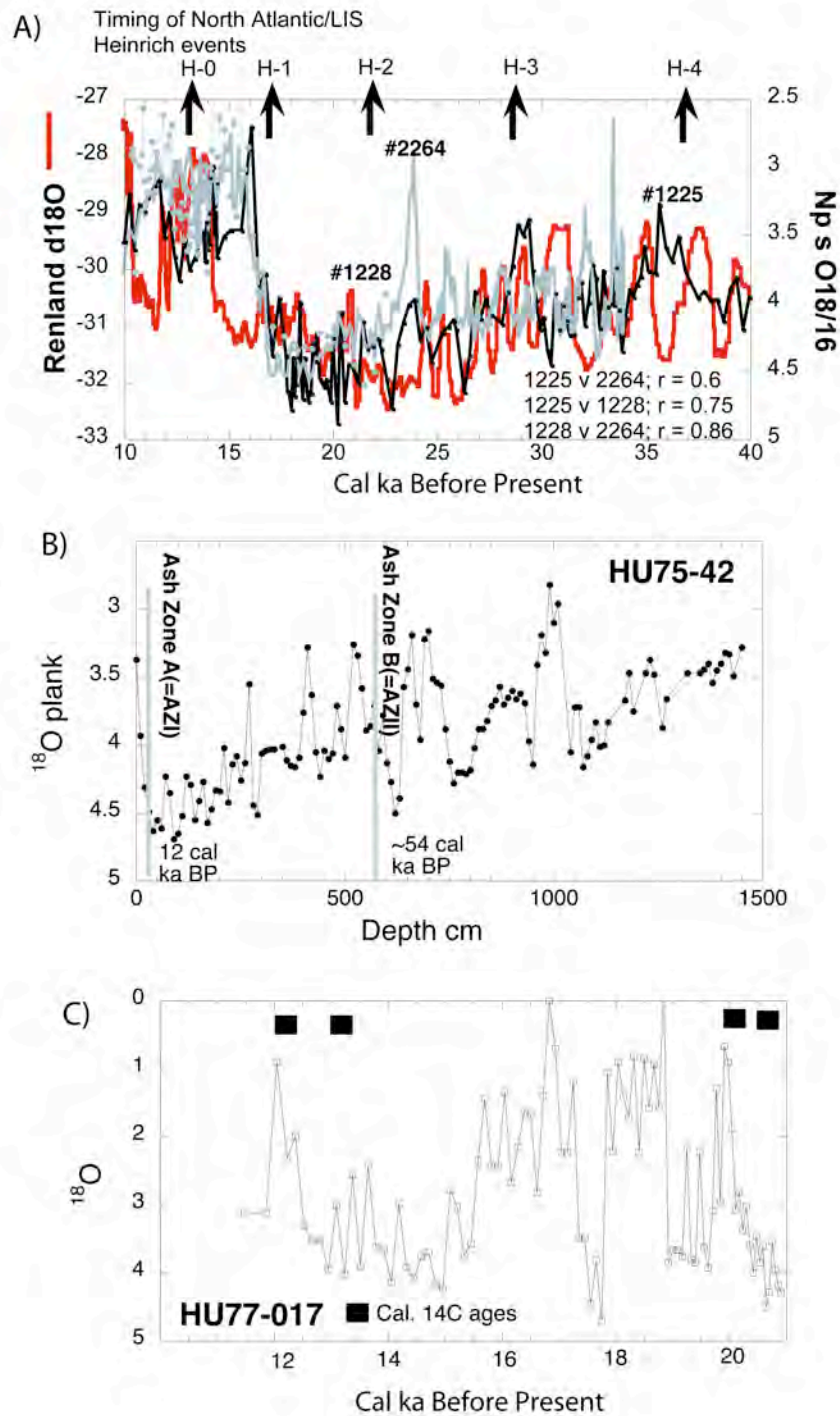


Figure 7.10 A) Variations in $\delta^{18}O$ from a series of cores north to south of Denmark Strait (see Fig. 7.8), namely: PS2264, JM96-1225 and 1228 plotted against the $\delta^{18}O$ from the Renland Ice Cap. B) $\delta^{18}O$ variations in cores HU75-42 (NW Labrador Sea). C) Stable oxygen variations in cores HU77-017 from north of the Davis Strait.

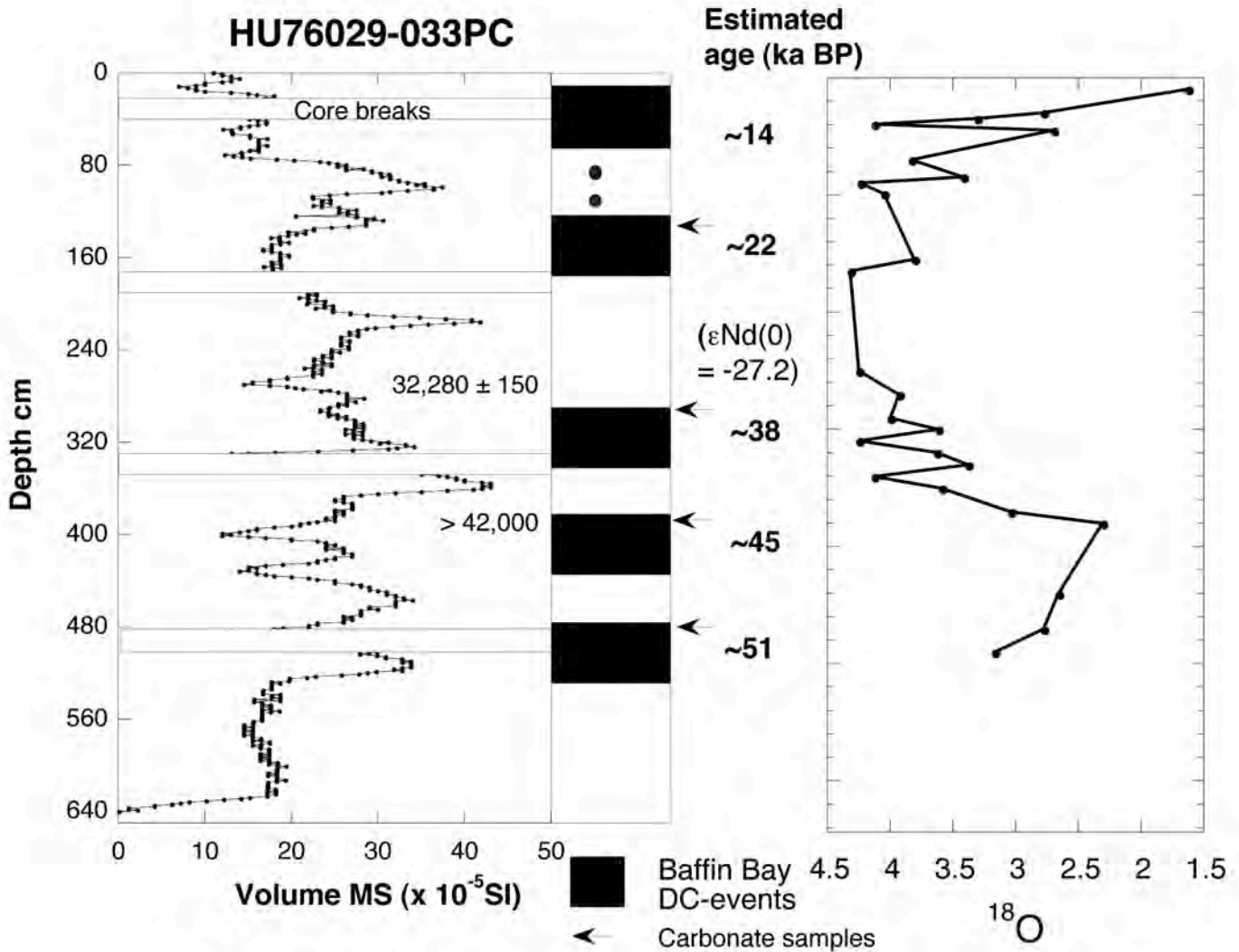


Figure 7.11 Variations in detrital carbonate (pieces of old rock) in core HU76-033 from Baffin Bay (Figure 7.8) showing down-core variations in magnetic susceptibility and $\delta^{18}O$.

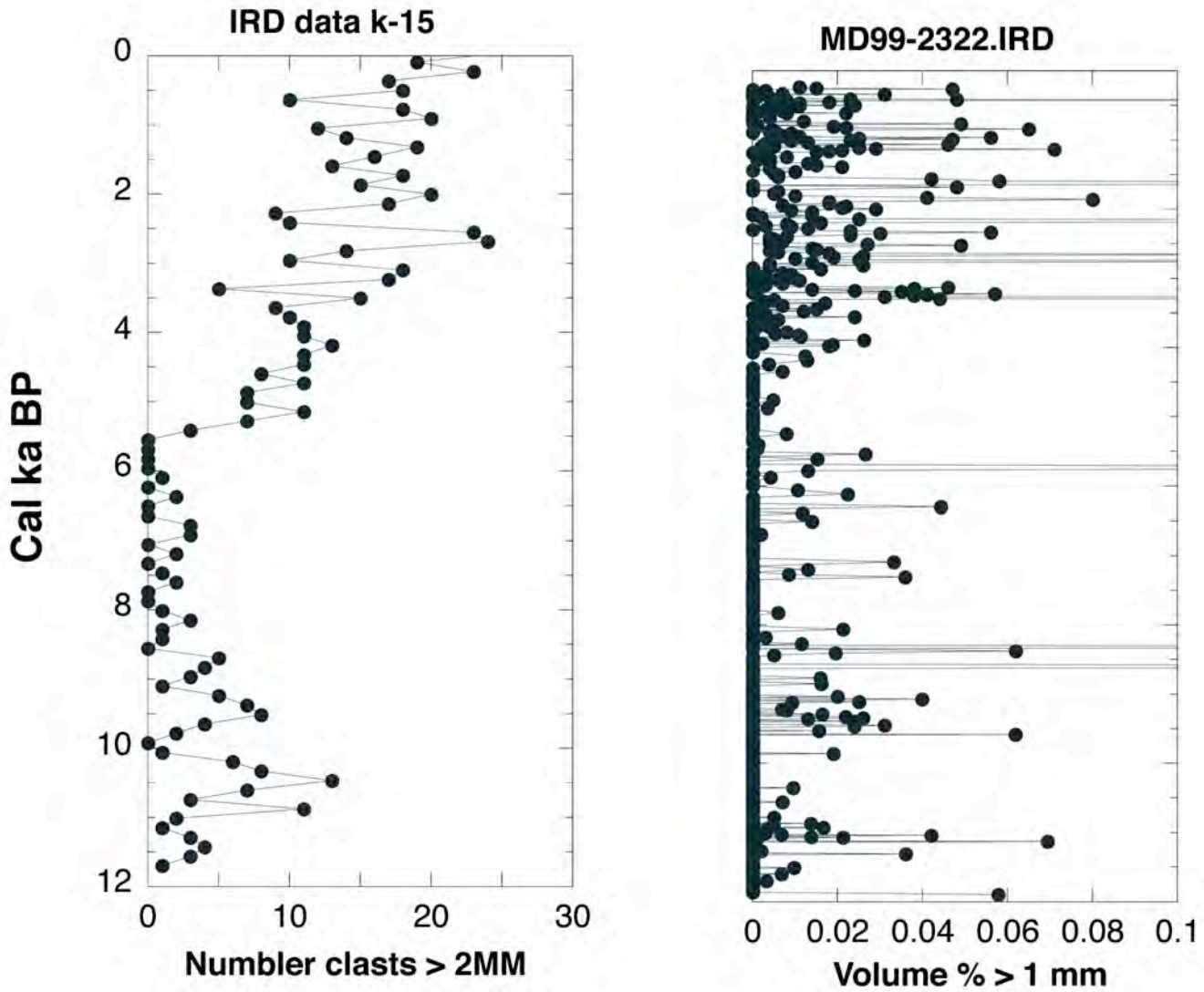
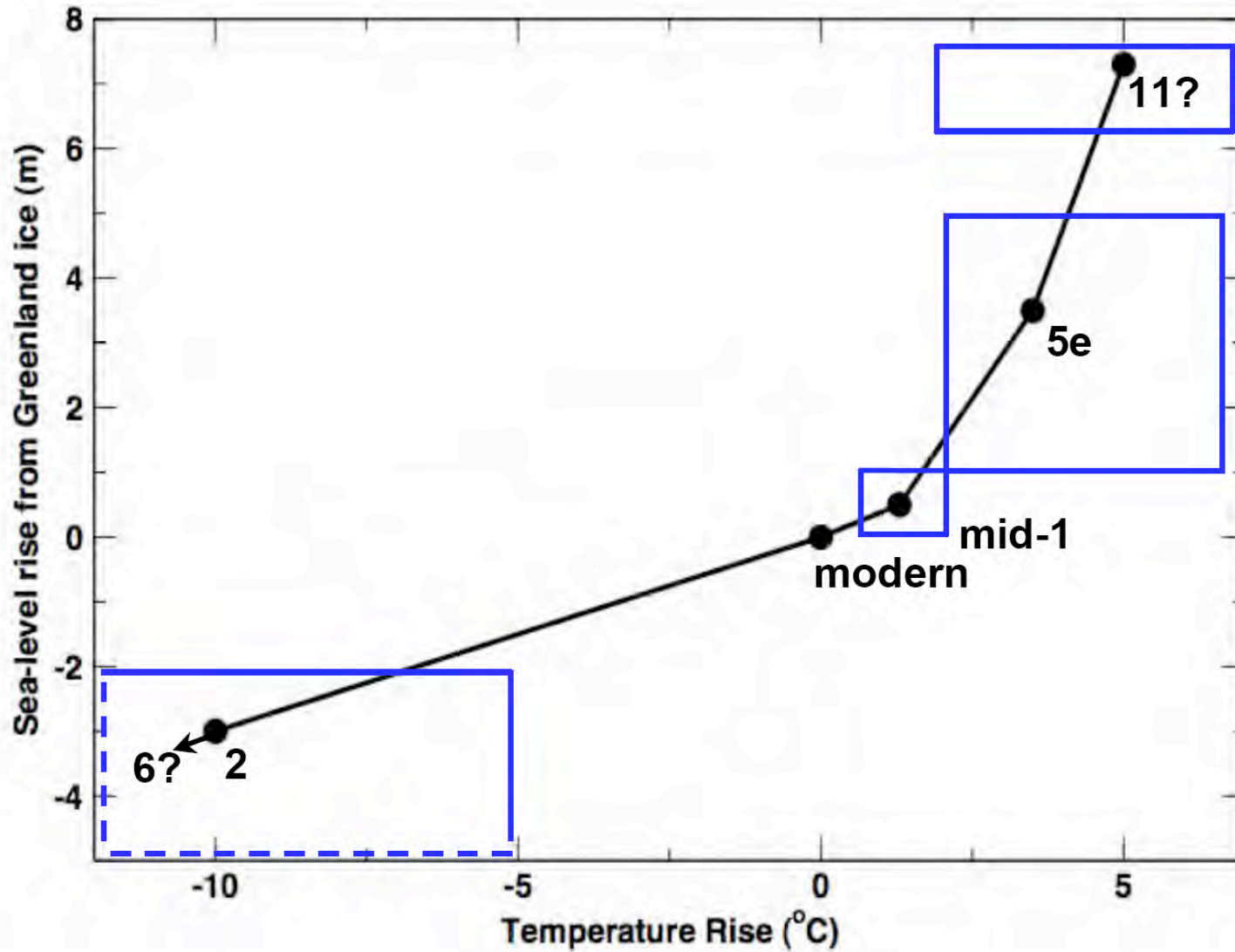


Figure 7.12 Holocene ice-rafted debris concentrations from MD99-2322 off Kangerdlugssuaq Fjord, east Greenland (Figure 7.8) showing log values of the percent of sediment > 1 mm and the weight % of quartz in the < 2mm sediment fraction.

1



2 **Figure 7.13** A best-guess representation of the dependence of the volume of the Greenland Ice Sheet on temperature. Large
3 uncertainties should be understood, and any ice-volume changes in response to sea-level changes correlated with temperature changes
4 are included (although, as discussed in the text, temperature changes probably dominated forcing, especially at warmer temperatures
5 when the reduced ice sheet had less contact with the sea). Recent values of temperature and ice volume (perhaps appropriate for 1960
6 or so) are assigned 0,0. The Last Glacial Maximum was probably $\sim 6^{\circ}\text{C}$ colder than modern for global average (e.g., Cuffey and Brook,
7 2000; data and results summarized in Jansen et al., 2007). Cooling in central Greenland was $\sim 15^{\circ}\text{C}$ (with peak cooling somewhat
8 more; Cuffey et al., 1995). Some of the central-Greenland cooling was probably linked to strengthening of the temperature inversion
9 that lowers near-surface temperatures relative to the free troposphere (Cuffey et al., 1995). A cooling of $\sim 10^{\circ}\text{C}$ is thus plotted. The
10 ice-volume-change estimates of Peltier (2004; ICE5G) and Fleming and Lambeck (2004) are used, with the upper end of the
11 uncertainty taken to be the ICE4G estimate (see Peltier, 2004), and somewhat arbitrarily set as 1 m on the lower side. The arrow
12 indicates that the ice sheet in MIS 6 was more likely than not slightly larger than in MIS 2, and that some (although inconsistent)
13 evidence of slightly colder temperatures is available (e.g., Bauch et al., 2000). The mid-Holocene result from ICE5G (Peltier, 2004)
14 of an ice sheet smaller than modern by ~ 0.5 m of sea-level equivalent is plotted; the error bars reflect the high confidence that the mid-
15 Holocene ice sheet was smaller than modern, with similar uncertainty assumed for the other side. Mid-Holocene temperature is taken
16 from the Alley and Anandakrishnan (1995) summertime melt-layer history of central Greenland, with their 0.5°C uncertainty on the
17 lower side, and a wider uncertainty on the upper side to include larger changes from other indicators (which are probably weighted by
18 wintertime changes that have less effect on ice-sheet mass balance, and so are not used for the best estimate; Alley et al., 1999). As
19 discussed in 7.3.3b and c, MIS 5e (the Eemian) is plotted with a warming of 3.5°C and a sea-level rise of 3.5 m. The uncertainties on
20 sea-level change come from the range of data-constrained models discussed in 7.3.3c. The temperature uncertainties reflect the results
21 of Cuffey and Marshall (2000) on the high side, and the lower values simulated over Greenland by Otto-Bliesner et al. (2006). Loss of
22 the full ice sheet is also plotted, to reflect the warmer conditions that may date to MIS 11 if not earlier, and perhaps also to the

23 Pliocene times of the Kap København Formation. Very large warming is indicated by the paleoclimatic data from Greenland, but
24 much of that warming probably was a feedback from loss of the ice sheet itself (Otto-Bliesner et al., 2006). Data from around the
25 North Atlantic for MIS 11 and other interglacials do not show significantly higher temperatures than during MIS 5e, allowing the
26 possibility that sustaining MIS 5e levels for a longer time led to loss of the ice sheet. Slight additional warming is indicated here,
27 within the error bounds of the other records, based on assessment that MIS 5e was sufficiently long for much of the ice-sheet response
28 to have been completed, so that additional warmth was required to cause additional retreat. The volume of ice possibly persisting in
29 highlands even after loss of central regions of the ice sheet is poorly quantified; 1 m is indicated.

30 **Chapter 7 References Cited**

31

32

Adrielson, L. and H. Alexanderson, 2005: Interactions between the Greenland Ice Sheet and the Liverpool Land coastal ice cap during the last two glaciation cycles. *Journal of Quaternary Science*, **20**, 269-283.

35

36

Aksu, A. E., 1985: Climatic and oceanographic changes over the past 400,000 years—Evidence from deep-sea cores on Baffin Bay and David Strait. In: *Quaternary Environments—Eastern Canadian Arctic, Baffin Bay and Western Greenland* [Andrews, J.T. (ed.)]. Allen and Unwin, Boston, pp. 181-209.

40

41

Alley, R.B., 2007. Wally was right—Predictive ability of the North Atlantic “conveyor belt” hypothesis for abrupt climate change. *Annual Review of Earth and Planetary Sciences*, **35**, 241-272.

44

45

Alley, R.B. and S. Anandakrishnan, 1995: Variations in melt-layer frequency in the GISP2 ice core—Implications for Holocene summer temperatures in central Greenland. *Annals of Glaciology*, **21**, 64-70.

48

49

Alley, R.B. and K.M. Cuffey. 2001. Oxygen- and hydrogen-isotopic ratios of water in precipitation—Beyond paleothermometry. In: *Stable Isotope Geochemistry*, [Valle, J.W. and D. Cole (eds.)]. Reviews in Mineralogy and Geochemistry, **43**, 527-553.

53

54

Alley, R.B. and B.R. Koci, 1990: Recent warming in central Greenland? *Annals of Glaciology*, **14**, 6-8.

56

57

Alley, R.B. and I.M. Whillans, 1984: Response of the East Antarctic ice sheet to sea-level rise. *Journal of Geophysical Research*, **89C**, 6487-6493.

59

60

Alley, R.B., A.M. Agustsdottir, and P.J. Fawcett, 1999: Ice-core evidence of

61 late-Holocene reduction in north Atlantic ocean heat transport. In: *Mechanisms of*
62 *Global Climate Change at Millennial Time Scales* [Clark, P.U., R.S. Webb and L.D.
63 Keigwin (eds.)]. Geophysical Monograph 112, American Geophysical Union,
64 Washington, DC, p. 301-312.

65

66 **Alley, R.B., S. Anandakrishnan, and P. Jung, 2001:** Stochastic resonance in
67 the North Atlantic. *Paleoceanography*, **16**, 190-198.

68

69 **Alley, R.B., E.J. Brook and S. Anandakrishnan, 2002:** A northern lead in the
70 orbital band—North-south phasing of ice-age events. *Quaternary Science Reviews*,
71 21, 431-441 (2002).

72

73 **Alley, R.B., P.U. Clark, P. Huybrechts, and I. Joughin, 2005a:** Ice-sheet and
74 sea-level changes. *Science*, **310**, 456-460.

75

76 **Alley, R.B., T.K. Dupont, B.R. Parizek, and S. Anandakrishnan, 2005b:**
77 Access of surface meltwater to beds of sub-freezing glaciers—Preliminary insights.
78 *Annals of Glaciology*, **40**, 8-14.

79

80 **Alley, R.B., R.C. Finkel, K. Nishiizumi, S. Anandakrishnan, C.A. Shuman,**
81 **G.R. Mershon, G.A. Zielinski, and P.A. Mayewski, 1995a:** Changes in continental
82 and sea-salt atmospheric loadings in central Greenland during the most recent
83 deglaciation. *Journal of Glaciology*, **41(139)**, 503-514.

84

85 **Alley, R.B., A.J. Gow, S.J. Johnsen, J. Kipfstuhl, D.A. Meese, and Th.**
86 **Thorsteinsson, 1995b:** Comparison of deep ice cores. *Nature*, **373**, 393-394.

87

88 **Alley, R.B., A.J. Gow, D.A. Meese, J.J. Fitzpatrick, E.D. Waddington, and**
89 **J.F. Bolzan, 1997:** Grain-scale processes, folding, and stratigraphic disturbance in the
90 GISP2 ice core. *Journal of Geophysical Research*, **102(C12)**, 26,819-26,830.

91

92 **Alley, R.B.,** D.A. Meese, C.A. Shuman, A.J. Gow, K.C. Taylor, P.M. Grootes,
93 J.W.C. White, M. Ram, E.D. Waddington, P.A. Mayewski, and G.A. Zielinski, 1993:
94 Abrupt increase in snow accumulation at the end of the Younger Dryas event. *Nature*,
95 **362**, 527-529.

96
97 **Alley, R.B.,** M.K. Spencer, and S. Anandakrishnan, 2007: Ice-sheet mass
98 balance: assessment, attribution and prognosis. *Annals of Glaciology*, **46**, 1-7.

99
100 **Andersen, K.K.,** A. Svensson, S.J. Johnsen, S.O. Rasmussen, M. Bigler, R.
101 Rothlisberger, U. Ruth, M.L. Siggaard-Andersen, J.P. Steffensen, D. Dahl-Jensen,
102 B.M. Vinther, and H.B. Clausen, 2006: The Greenland ice core chronology 2005, 15-
103 42 ka. Part 1—Constructing the time scale. *Quaternary Science Reviews*, **25**, 3246-
104 3257.

105
106 **Andresen, C.S.,** S. Bjorck, O. Bennike, and G. Bond, 2004: Holocene climate
107 changes in southern Greenland—Evidence from lake sediments. *Journal of*
108 *Quaternary Science*, **19**, 783-795.

109
110 **Andrews, J.T.,** 2008: The role of the Iceland Ice Sheet in sediment delivery to
111 the North Atlantic during the late Quaternary—How important was it? Evidence from
112 the area of Denmark Strait. *Journal of Quaternary Science*, **23**, 3-20.

113
114 **Andrews, J.T.** and G. Dunhill, 2004: Early to mid-Holocene Atlantic water
115 influx and deglacial meltwater events, Beaufort Sea slope, Arctic Ocean. *Quaternary*
116 *Research*, **61**, 14-21.

117
118 **Andrews, J.T.,** T.A. Cooper, A.E. Jennings, A.B. Stein, and H. Erlenkeuser,
119 1998a: Late Quaternary iceberg-rafted detritus events on the Denmark
120 Strait/Southeast Greenland continental slope (about 65° N)—Related to North
121 Atlantic Heinrich Events? *Marine Geology*, **149**, 211-228.

122

123 **Andrews, J.T., Erlenkeuser, H., Tedesco, K., Aksu, A., and Jull, A.J.T., 1994:**
124 Late Quaternary (Stage 2 and 3) meltwater and Heinrich events, NW Labrador Sea.
125 *Quaternary Research*, **41**, 26-34.

126
127 **Andrews, J.T., Jennings, A.E., Cooper, T., Williams, K.M., and Mienert, J.,**
128 1996: Late Quaternary sedimentation along a fjord to shelf (trough) transect, East
129 Greenland (ca. 68°N). In: *Late Quaternary Paleoceanography of North Atlantic*
130 *Margins* [Andrews, J.T., W. Austin, H. Bergsten, and A.E. Jennings (eds.)].
131 Geological Society, London, pp. 153-166.

132
133 **Andrews, J.T., M.E. Kirby, A. Aksu, D.C. Barber, and D. Meese, 1998b:** Late
134 Quaternary detrital carbonate (DC-) events in Baffin Bay (67°–74° N)—Do they
135 correlate with and contribute to Heinrich Events in the North Atlantic? *Quaternary*
136 *Science Reviews*, **17**, 1125-1137.

137
138 **Andrews, J.T., L.M. Smith, R.Preston, T. Cooper, and A.E. Jennings, 1997:**
139 Spatial and temporal patterns of iceberg rafting (IRD) along the East Greenland
140 margin, ca. 68 N, over the last 14 cal.ka. *Journal of Quaternary Science*, **12**, 1-13.

141
142 **Bamber, J.L., R.L. Layberry, and S.P. Gogineni, 2001:** A new ice thickness
143 and bed data set for the Greenland Ice Sheet 1—Measurement, data reduction, and
144 errors. *Journal of Geophysical Research*, **106**, 33,773-33,780.

145
146 **Bamber, J.L., R.B. Alley, and I. Joughin, 2007:** Rapid Response of modern
147 day ice sheets to external forcing. *Earth and Planetary Science Letters*, **257**, 1-13.

148
149 **Bard, E. and M. Frank, 2006:** Climate change and solar variability—What's
150 new under the sun? *Earth and Planetary Science Letters*, **248**, 1-14.

151
152 **Bauch, H.A., H. Erlenkeuser, J.P. Helmke, and U. Struck, 2000:** A
153 paleoclimatic evaluation of marine oxygen isotope stage 11 in the high-northern

154 Atlantic (Nordic seas). *Global and Planetary Change*, **24**, 27-39.

155

156 **Bender, M.L., R.G. Fairbanks., F.W. Taylor, R.K. Matthews, J.G. Goddard,**
157 and W.S. Broecker, 1979: Uranium-series dating of the Pleistocene reef tracts of
158 Barbados, West Indies. *Geological Society of America Bulletin, Part I*, **90**, 577-594.

159

160 **Bennike, O. and J. Bocher,** 1994: Land biotas of the last interglacial-glacial
161 cycle on Jameson Land, East Greenland. *Boreas*, **23**, 479-487.

162

163 **Bennike, O., S. Bjorck, and K. Lambeck,** 2002: Estimates of South Greenland
164 late-glacial ice limits from a new relative sea level curve. *Earth and Planetary*
165 *Science Letters*, **197**, 171-186.

166

167 **Berger, A.L.,** 1978: Long-term variations of caloric insolation resulting from
168 the earth's orbital elements. *Quaternary Research*, **9**, 139-167.

169

170 **Berger, A. and Loutre, M.F.,** 1991: Insolation values for the climate of the
171 last 10 million years. *Quaternary Science Reviews*, **10**, 297-317.

172

173 **Bigg, G.R.,** 1999: An estimate of the flux of iceberg calving from Greenland.
174 *Arctic, Antarctic, and Alpine Research*, **31**, 174-178.

175

176 **Bjorck, S., M. Rundgren, O. Ingolfsson, and S. Funder,** 1997: The Preboreal
177 oscillation around the Nordic Seas—Terrestrial and lacustrine responses. *Journal of*
178 *Quaternary Science*, **12**, 455-465.

179

180 **Bjorck, S., O. Bennike, P. Rosen, C.S. Andresen, S. Bohncke, E. Kaas, and**
181 **D. Conley,** 2002: Anomalously mild Younger Dryas summer conditions in southern
182 Greenland. *Geology*, **30**, 427-430.

183

184 **Blake, W., Jr., H.R. Jackson, and C.G. Currie,** 1996: Seafloor evidence for

185 glaciation, northernmost Baffn Bay. *Bulletin of the Geological Survey of Denmark*,
186 **43**, 157-168.

187

188 **Blunier**, T. and E.J. Brook, 2001: Timing of millennial-scale climate change
189 in Antarctica and Greenland during the last glacial period. *Science*, **291**, 109-112.

190

191 **Bond**, G., W. Broecker, S. Johnson, J. McManus, L. Labeyrie, J. Jouzel, and
192 G. Bonani, 1993: Correlation between climate records from North Atlantic sediments
193 and Greenland ice. *Nature*, **365**, 507-508.

194

195 **Bond**, G.C. and R. Lotti, 1995: Iceberg discharges into the North Atlantic on
196 millennial time scales during the last glaciation. *Science*, **267**, 1005-1009.

197

198 **Box**, J.E., D.H. Bromwich, B.A. Veenhuis, L.-S. Bai, J.C. Stroeve, J.C.
199 Rogers, K. Steffen, T. Haran, and S.-H. Wang, 2006: Greenland ice-sheet surface
200 mass balance variability (1988-2004) from calibrated Polar MM5 output. *Journal of*
201 *Climate*, **19(12)**, 2783–2800.

202

203 **Bradley**, R.S., 1999: *Paleoclimatology—Reconstructing Climate of the*
204 *Quaternary*. Academic Press, San Diego, 613 pp.

205

206 **Braun**, H., M. Christl, S. Rahmstorf, A. Ganopolski, A. Mangini, C.
207 Kubatzki, K. Roth, and B. Kromer, 2005: Possible solar origin of the 1,470-year
208 glacial climate cycle demonstrated in a coupled model. *Nature*, **438**, 208-211.

209

210 **Brodersen**, K.P. and O. Bennike, 2003: Interglacial Chironomidae (Diptera)
211 from Thule, Northwest Greenland—Matching modern analogues to fossil
212 assemblages. *Boreas*, **32**, 560-565.

213

214 **Broecker**, W.S., 1995: *The Glacial World According to Wally*. Eldigio Press,
215 Palisades, NY, 89 pp.

216

217

CircumArctic PaleoEnvironments (CAPE)—Last Interglacial Project

218

Members (P. Anderson, O. Bermike, N. Bigelow, J. Brigham-Grette, M. Duvall, M.

219

Edwards, B. Frechette, S. Funder, S. Johnsen, J. Knies, R. Koerner, A. Lozhkin, S.

220

Marshall, J. Matthiessen, G. Macdonald, G. Miller, M. Montoya, D. Muhs, B. Otto-

221

Bliesner, J. Overpeck, N. Reeh, H.P. Sejrup, R. Spielhagen, C. Turner and A.

222

Velichko), 2006: Last Interglacial Arctic warmth confirms polar amplification of

223

climate change. *Quaternary Science Reviews*, **25**, 1383-1400.

224

225

Cazenave, A., 2006: How fast are the ice sheets melting? *Science*, **314**, 1250-

226

1252.

227

228

Chappellaz, J., E. Brook, T. Blunier, and B. Malaize, 1997: CH₄ and delta O-

229

18 of O-2 records from Antarctic and Greenland ice—A clue for stratigraphic

230

disturbance in the bottom part of the Greenland Ice Core Project and the Greenland

231

Ice Sheet Project 2 ice cores. *Journal of Geophysical Research*, **102(C12)**, 26,547-

232

26,557.

233

234

Chen, J.H., H.A. Curran, B. White, and G.J. Wasserburg, 1991: Precise

235

chronology of the last interglacial period—²³⁴U-²³⁰Th data from fossil coral reefs in

236

the Bahamas: *Geological Society of America Bulletin*, **103**, 82-97.

237

238

Clarke, G.K.C. and S.J. Marshall, 2002: Isotopic balance of the Greenland Ice

239

Sheet—Modeled concentrations of water isotopes from 30,000 BP to present.

240

Quaternary Science Reviews, **21**, 419-430.

241

242

Clarke, G.K.C., N. Lhomme, and S.J. Marshall, 2005: Tracer transport in the

243

Greenland Ice Sheet—Three-dimensional isotopic stratigraphy. *Quaternary Science*

244

Reviews, **24**, 155-171.

245

246

Cronin, T.M., 1999: *Principles of Paleoclimatology*. Columbia University

247 Press, New York, 560 pp.

248

249 **Cuffey, K.M.** and E.J. Brook, 2000: Ice sheets and the ice-core record of
250 climate change. In: *Earth System Science—From Biogeochemical Cycles to Global*
251 *Change* [Jacobson, M.C., R.J. Charlson, H. Rodhe, and G.H. Orians (eds.)].
252 Academic Press, New York, pp. 459-497.

253

254 **Cuffey, K.M.** and G.D. Clow, 1997: Temperature, accumulation, and ice sheet
255 elevation in central Greenland through the last deglacial transition. *Journal of*
256 *Geophysical Research*, **102(C12)**, 26,383-26,396.

257

258 **Cuffey, K.M.** and S.J. Marshall, 2000: Substantial contribution to sea-level
259 rise during the last interglacial from the Greenland Ice Sheet. *Nature*, **404**, 591-594.

260

261 **Cuffey, K.M.,** R.B. Alley, P.M. Grootes, J.F. Bolzan, and S. Anandakrishnan,
262 1994: Calibration of the $d^{18}O$ isotopic paleothermometer for central Greenland, using
263 borehole temperatures. *Journal of Glaciology*, **40(135)**, 341-349.

264

265 **Cuffey, K.M.,** G.D. Clow, R.B. Alley, M. Stuiver, E.D. Waddington, and
266 R.W. Saltus, 1995: Large Arctic temperature change at the glacial-Holocene
267 transition. *Science*, **270**, 455-458.

268

269 **Dahl-Jensen, D.,** K. Mosegaard, N. Gundestrup, G.D. Clow, S.J. Johnsen,
270 A.W. Hansen, and N. Balling, 1998: Past temperatures directly from the Greenland
271 Ice Sheet. *Science*, **282**, 268-271.

272

273 **Dahl-Jensen, D.,** N. Gundestrup, S.P. Gogineni, and H. Miller, 2003: Basal
274 melt at NorthGRIP modeled from borehole, ice-core and radio-echo sounded
275 observations. *Annals of Glaciology*, **37**, 207-212.

276

277 **Dansgaard, W.,** S.J. Johnsen, H.B. Clausen, D. Dahl-Jensen, N.S.

278 Gundestrup, C.U. Hammer, C.S. Hvidberg, J.P. Steffensen, A.E. Sveinbjorndottir, J.
279 Jouzel, and G. Bond, 1993: Evidence for general insatbility of past climate from a
280 250-kyr ice-core record. *Nature*, **364**, 218-220.

281

282 **Darby, D.A., J. Bischof, R.F. Spielhagen, S.A. Marshall, and S.W. Herman,**
283 2002: Arctic ice export events and their potential impact on global climate during the
284 late Pleistocene. *Palaeoceanography*, **17**, doi. 10.1029/2001PA000639, 000615-
285 000631 to 000615-000617.

286

287 **De Abreu, C., F.F. Abrantes, N.J. Shackleton, P.C. Tzedakis, J.F. McManus,**
288 D.W. Oppo, and M.A. Hall, 2005: Ocean climate variability in the eastern North
289 Atlantic during interglacial marine isotope stage 11—A partial analogue to the
290 Holocene? *Paleoceanography*, **20**, Art. No. PA3009.

291

292 **Denton, G.H., R.B. Alley, G.C. Comer, and W.S. Broecker,** 2005: The role of
293 seasonality in abrupt climate change. *Quaternary Science Reviews*, **24**, 1159-1182.

294

295 **Dickinson, W.R.,** 2001: Paleoshoreline record of relative Holocene sea levels
296 on Pacific Islands. *Earth-Science Reviews*, **55**, 191-234.

297

298 **Dowdeswell, J.A., G. Uenzelmann-Neben, R.J. Whittington, P. and**
299 Marienfeld, 1994a: The Late Quaternary sedimentary record in Scoresby Sund, East
300 Greenland. *Boreas*, **23**, 294-310.

301

302 **Dowdeswell, J.A., R.J. Whittington, and P. Marienfeld,** 1994b: The origin of
303 massive diamicton facies by iceberg rafting and scouring, Scoresby Sund, East
304 Greenland. *Sedimentology*, **41**, 21-35.

305

306 **Dowdeswell, J.A., N.H. Kenyon, A. Elverhoi, J.S. Laberg, F.-J. Hollender, J.**
307 Mienert, and M.J. Siegert, 1996: Large-scale sedimentation on the glacier-influenced
308 Polar North Atlantic margins—Long-range side-scan sonar evidence. *Geophysical*

309 *Research Letters*, **23**, 3535-3538.

310

311 **Dowdeswell**, J.A., N.H. Kenyon, and J.S. Laberg, 1997: The glacier-
312 influenced Scoresby Sund Fan, east Greenland continental margin—Evidence from
313 GLORIA and 3.5 kHz records. *Marine Geology*, **143**, 207-221.

314

315 **Droxler**, A.W., R.B. Alley, W.R. Howard, R.Z. Poore, and L.H. Burckle,
316 2003: Unique and exceptionally long interglacial marine isotope stage 11—Window
317 into Earth future climate. In: *Earth's Climate and Orbital Eccentricity—The Marine*
318 *Isotope Stage 11 Question* [Droxler, A.W., R.Z. Poore and L.H. Burckle (eds.)].
319 Geophysical Monograph 137, American Geophysical Union, p. 1-14.

320

321 **Dunhill**, G., 2005: Iceland and Greenland margins—A comparison of
322 depositional processes under different glaciological and oceanographic settings. PhD
323 dissertation, Geological Sciences, University of Colorado, Boulder.

324

325 **Dupont**, T.K. and R.B. Alley, 2005: Assessment of the importance of ice-
326 shelf buttressing to ice-sheet flow. *Geophysical Research Letters*, **32**, L04503, doi
327 10.1029/2004GL022024.

328

329 **Dupont**, T.K. and R.B. Alley, 2006: Role of small ice shelves in sea-level
330 rise. *Geophysical Research Letters*, **33**, L09503.

331

332 **Dyke**, A.S., J.E. Dale, and R.N. McNeely, 1996: Marine molluscs as
333 indicators of environmental change in glaciated North America and Greenland during
334 the last 18,000 years. *Geographie Physique et Quaternaire*, **50**, 125-184.

335

336 **Dyke**, A.S., J.T. Andrews, P.U. Clark, J.H. England, G.H. Miller, J. Shaw,
337 and J.J. Veillette, 2002: The Laurentide and Innuitian ice sheets during the Last
338 Glacial Maximum. *Quaternary Science Reviews*, **21**, 9-31.

339

340 **Edwards, R.L., H. Cheng, M.T. Murrell, and S.J. Goldstein, 1997:**
341 Protactinium-231 dating of carbonates by thermal ionization mass spectrometry—
342 Implications for Quaternary climate change: *Science*, **276**, 782-786.

343
344 **Eisen, O., U. Nixdorf, F. Wilhelms, and H. Miller, 2004:** Age estimates of
345 isochronous reflection horizons by combining ice core, survey, and synthetic radar
346 data. *Journal of Geophysical Research*, **109(B4)**, Art. No. B04106.

347
348 **Eldrett, J.S., I.C. Harding, P.A. Wilson, E. Butler, and A.P. Roberts, 2007:**
349 Continental ice in Greenland during the Eocene and Oligocene. *Nature*, **446**, 176-179.

350
351 **Elliot, M., L. Labeyrie, G. Bond, E. Cortijo, J.-L. Turon, N. Tiseray, and J.-C.**
352 **Duplessy, 1998:** Millennial-scale iceberg discharges in the Irminger Basin during the
353 last glacial period—Relationship with the Heinrich events and environmental settings.
354 *Paleoceanography*, **13**, 433-446.

355
356 **Elverhoi, A., J.A. Dowdeswell, S. Funder, J. Mangerud, and R. Stein, 1998:**
357 Glacial and oceanic history of the polar North Atlantic margins—An overview.
358 *Quaternary Science Reviews*, **17**, 1-10.

359
360 **England, J., 1999:** Coalescent Greenland and Inuitian ice during the Last
361 Glacial Maximum—Revising the Quaternary of the Canadian High Arctic.
362 *Quaternary Science Reviews*, **18**, 421-456.

363
364 **Fairbanks, R.G., R.A. Mortlock, C. Tzu-Chien, L. Cao, A. Kaplan, T.P.**
365 **Guilderson, T.W. Fairbanks, A.L. Bloom, P.M. Grootes, and M.-J. Nadeau, 2005:**
366 Radiocarbon calibration curve spanning 0 to 50,000 years BP based on paired
367 ²³⁰Th/²³⁴U/²³⁸U and ¹⁴C dates on pristine corals. *Quaternary Science Reviews*, **24**,
368 1781-1796.

369
370 **Farmer, G.L. D.C., Barber, and J.T. Andrews, 2003:** Provenance of Late

371 Quaternary ice-proximal sediments in the North Atlantic—Nd, Sr and Pd isotopic
372 evidence. *Earth and Planetary Science Letters*, **209**, 227-243.

373

374 **Fillon**, R.H. and J.C. Duplessy, 1980: Labrador Sea bio-, tephro-, oxygen
375 isotopic stratigraphy and Late Quaternary paleoceanographic trends. *Canadian*
376 *Journal Earth Sciences*, **17**, 831-854.

377

378 **Finkel**, R.C. and K. Nishiizumi, 1997: Beryllium 10 concentrations in the
379 Greenland Ice Sheet Project 2 ice core from 3-40 ka. *Journal of Geophysical*
380 *Research*, **102(C12)**, 26,699-26,706.

381

382 **Fisher**, T.G., D.G. Smith, and J.T. Andrews, 2002: Preboreal oscillation
383 caused by a glacial Lake Agassiz flood. *Quaternary Science Reviews*, **21**, 873-878.

384

385 **Fleming**, K. and K. Lambeck, 2004: Constraints on the Greenland Ice Sheet
386 since the Last Glacial Maximum from sea-level observations and glacial-rebound
387 models. *Quaternary Science Reviews*, **23**, 1053-1077.

388

389 **Fruijtjer**, C., T. Elliot, and W. Schlager, 2000: Mass-spectrometric ^{234}U - ^{230}Th
390 ages from the Key Largo Formation, Florida Keys, United States—Constraints on
391 diagenetic age disturbance. *Geological Society of America Bulletin*, **112**, 267-277.

392

393 **Funder**, S., 1989a: Quaternary geology of east Greenland. In: Chapter 13 of
394 *Quaternary Geology of Canada and Greenland* [Fulton, R.J. (ed.)]. Geological
395 Survey of Canada, Geology of Canada, no. 1, 839 pp.; also Geological Society of
396 America, the Geology of North America, v. K-1, p. 756-763.

397

398 **Funder**, S., 1989b: Quaternary geology of north Greenland. In: Chapter 13 of
399 *Quaternary Geology of Canada and Greenland* [Fulton, R.J. (ed.)]. Geological
400 Survey of Canada, Geology of Canada, no. 1, 839 pp.; also Geological Society of
401 America, the Geology of North America, v. K-1, p. 763-769.

402

403 **Funder, S.**, 1989c: Quaternary geology of west Greenland. In: Chapter 13 of
404 *Quaternary Geology of Canada and Greenland* [R.J. Fulton (ed.)]. Geological Survey
405 of Canada, Geology of Canada, no. 1, 839 pp.; also Geological Society of America,
406 the Geology of North America, v. K-1, p. 749-756.

407

408 **Funder, S.**, 1989d: Sea level history. In: Chapter 13 of *Quaternary Geology*
409 *of Canada and Greenland* [R.J. Fulton (ed.)]. Geological Survey of Canada, Geology
410 of Canada, no. 1, 839 pp.; also Geological Society of America, the Geology of North
411 America, v. K-1, p. 772-774.

412

413 **Funder, S.** and B. Fredskild, 1989: Paleofaunas and floras. In: Chapter 13 of
414 *Quaternary Geology of Canada and Greenland* [Fulton, R.J. (ed.)]. Geological
415 Survey of Canada, Geology of Canada, no. 1; also Geological Society of America, the
416 Geology of North America, v. K-1, p. 775-783.

417

418 **Funder, S.** and H.C. Larsen, 1989: Quaternary geology of the shelves
419 adjacent to Greenland. In: Chapter 13 of *Quaternary Geology of Canada and*
420 *Greenland* [Fulton, R.J. (ed.)]. Geological Survey of Canada, Geology of Canada, no.
421 1; also Geological Society of America, The Geology of North America, v. K-1, p.
422 769-772.

423

424 **Funder, S.**, C. Hjort, J.Y. Landvik, S.I. Nam, N. Reeh, and R. Stein, 1998:
425 History of a stable ice margin East Greenland during the Middle and Upper
426 Pleistocene. *Quaternary Science Reviews*, **17**, 77-123.

427

428 **Funder, S.**, O. Bennike, J. Böcher, C. Israelson, K.S. Petersen, and L.A.
429 Símonarson, 2001: Late Pliocene Greenland—The Kap København Formation in
430 North Greenland. *Bulletin of the Geological Society of Denmark*, **48**, 117–134.

431

432 **Funder, S.**, A.E. Jennings, and M.J. Kelly, 2004: Middle and late Quaternary

433 glacial limits in Greenland. In: *Quaternary Glaciations—Extent and Chronology,*
434 *Part II* [Ehlers, J. and P.L. Gibbard (eds.)]. Elsevier, New York, pp. 425-430.

435

436 **Gallup, C.D., R.L. Edwards, and R.G. Johnson, 1994:** The timing of high sea
437 levels over the past 200,000 years: *Science*, **263**, 796-800.

438

439 **Geirsdottir, A., H. Hardardottir, and J. Eirsson, 1997:** The depositional
440 history of the Younger Dryas–Preboreal Budi moraines in south-central Iceland.
441 *Arctic and Alpine Research*, **29**, 13-23.

442

443 **Geirsdottir, A., J. Hardardottir, and J.T. Andrews, 2000:** Late Holocene
444 terrestrial geology of Miki and I.C. Jacobsen Fjords, East Greenland. *The Holocene*,
445 **10**, 125-134.

446

447 **Gilbert, R., 1990:** Rafting in glacial marine environments. In: *Glacial marine*
448 *Environments—Processes and Sediments* [Dowdeswell, J.A. and J.D. Scourse (eds.)].
449 Geological Society, London, 105-120.

450

451 **Goreau, T.F., 1959:** The ecology of Jamaican coral reefs I—Species
452 composition and zonation. *Ecology*, **40(1)**, 67-90.

453

454 **Gosse, J.C. and F.M. Phillips, 2001:** Terrestrial in situ cosmogenic nuclides—
455 Theory and application. *Quaternary Science Reviews*, **20**, 1475-1560.

456

457 **Gregory, J.M. and P. Huybrechts, 2006:** Ice-sheet contributions to future sea-
458 level change. *Philosophical Transactions of the Royal Society A: Mathematical,*
459 *Physical and Engineering Sciences*, **364(1844)**, 1709-1731.

460

461 **Grootes, P.M. and M. Stuiver, 1997:** Oxygen 18/16 variability in Greenland
462 snow and ice with 10(-3)- to 10(5)-year time resolution. *Journal of Geophysical*
463 *Research*, **102C**, 26,455-26,470.

464

465

466

467

468

469

470

471

472

473

474

475

476

477

478

479

480

481

482

483

484

485

486

487

488

489

490

491

492

493

494

Grousset, F.E., E. Cortijo, S. Huon, L. Herve, T. Richter, D. Burdloff, J. Duprat, and O. Weber, 2001: Zooming in on Heinrich layers. *Paleoceanography*, **16, 240-259.**

Hagen, S., 1999: North Atlantic paleoceanography and climate history during the last ~70 cal. ka years. PhD dissertation, Department of Geology, University of Tromso, Norway, 110 pp.

Hagen, S. and Hald, M., 2002: Variation in surface and deep water circulation in the Denmark Strait, North Atlantic, during marine isotope stages 3 and 2. *Paleoceanography*, **17, 13-11 to 13-16 (10.1029/2001PA000632).**

Hakansson, L., J. Briner, H. Alexanderson, A. Aldahan, and G. Possnert, 2007: ¹⁰Be ages from central east Greenland constrain the extent of the Greenland Ice Sheet during the Last Glacial Maximum. *Quaternary Science Reviews*, **26(19-21) 2316-2321, doi:10.1016/j.quascirev.2007.08.001**

Hald, M. and S. Hagen, 1998: Early Preboreal cooling in the Nordic seas region triggered by meltwater. *Geology*, **26, 615-618.**

Hanna, E., P. Huybrechts, I. Janssens, J. Cappelen, K. Steffens, and A. Stephens, 2005: Runoff and mass balance of the Greenland Ice Sheet—1958-2003. *Journal of Geophysical Research*, **110, D13108, doi:10.1029/2004JD005641**

Hearty, P.J., P. Kindler, H. Cheng, and R.L. Edwards, 1999: A +20 m middle Pleistocene sea-level highstand (Bermuda and the Bahamas) due to partial collapse of Antarctic ice: *Geology*, **27, 375-378.**

Helmke, J.P., H.A. Bauch, and H. Erlenkeuser, 2003: Development of glacial and interglacial conditions in the Nordic seas between 1.5 and 0.35 Ma. *Quaternary*

495 *Science Reviews*, **22**, 1717-1728.

496

497 **Hemming**, S.R., 2004: Heinrich events—Massive late Pleistocene detritus
498 layers of the North Atlantic and their global climate imprint. *Reviews of Geophysics*,
499 **42**, Art. No. RG1005.

500

501 **Hemming**, S.R., T.O. Vorren, and J. Kleman, 2002: Provinciality of ice
502 rafting in the North Atlantic—Application of Ar-40/Ar-39 dating of individual ice
503 rafted hornblende grains. *Quaternary International*, **95**, 75-85.

504

505 **Hooke**, R. LeB., 2005: *Principles of Glacier Mechanics*. Cambridge
506 University Press, Cambridge, 429 pp.

507

508 **Hopkins**, T.S., 1991: The GIN Sea—A synthesis of its physical oceanography
509 and literature review 1972-1985. *Earth Science Reviews*, **30**, 175-318.

510

511 **Huddard**, A., D. Sugden, A. Dugmore, H. Norddahl, and H.G. Petersson,
512 2006: A modelling insight into the Icelandic Last Glacial Maximum ice sheet.
513 *Quaternary Science Reviews*, **25**, 2283-2296.

514

515 **Hughes**, T.J., 1998: *Ice Sheets*. Oxford University Press, New York, 343 pp.

516

517 **Hulbe**, C.L., D.R. MacAyeal, G.H. Denton, J. Kleman, and T.V. Lowell,
518 2004: Catastrophic ice shelf breakup as the source of Heinrich event icebergs.
519 *Paleoceanography*, **19**, Art. No. PA1004.

520

521 **Huybrechts**, P., 2002: Sea-level changes at the LGM from ice-dynamic
522 reconstructions of the Greenland and Antarctic ice sheets during the glacial cycles.
523 *Quaternary Science Reviews*, **21**, 203-231.

524

525 **Huybrechts**, P. and J. de Wolde, 1999: The dynamic response of the

526 Greenland and Antarctic ice sheets to multiple-century climatic warming. *Journal of*
527 *Climate*, **12**, 2169-2188.

528

529 **Intergovernmental Panel on Climate Change (IPCC)**, 2007: Summary for
530 policymakers. In: *Climate Change 2007—The Physical Science Basis. Contribution*
531 *of Working Group I to the Fourth Assessment Report of the Intergovernmental Panel*
532 *on Climate Change* [Solomon, S., D. Qin, M. Manning, Z. Chen, M. Marquis, K.B.
533 Averyt, M.Tignor and H.L. Miller (eds.)]. Cambridge University Press, Cambridge
534 and New York, 18 pp.

535

536 **Jacobel**, R.W. and B.C. Welch, 2005: A time marker at 17.5 kyr BP detected
537 throughout West Antarctica. *Annals of Glaciology*, **41**, 47-51.

538

539 **Jansen**, E., J. Overpeck, K.R. Briffa, J.-C. Duplessy, F. Joos, V. Masson-
540 Delmotte, D. Olago, B. Otto-Bliesner, W.R. Peltier, S. Rahmstorf, R. Ramesh, D.
541 Raynaud, D. Rind, O. Solomina, R. Villalba, and D. Zhang, 2007: Palaeoclimate. In:
542 *Climate Change 2007: The Physical Science Basis. Contribution of Working Group I*
543 *to the Fourth Assessment Report of the Intergovernmental Panel on Climate Change*
544 [Solomon, S., D. Qin, M. Manning, Z. Chen, M. Marquis, K.B. Averyt, M. Tignor
545 and H.L. Miller (eds.)]. Cambridge University Press, Cambridge, United Kingdom
546 and New York, NY, USA.

547

548 **Jennings**, A.E. and N.J. Weiner, 1994: East Greenland climate change over
549 the last 1300 years from foraminiferal evidence. *PaleoBios*, **16(Supplement to No.**
550 **2)**, 38

551

552 **Jennings**, A.E., K. Gronvold, R. Hilberman, M. Smith, and M. Hald, 2002a:
553 High resolution study of Icelandic tephra in the Kangerlussuaq Trough, SE East
554 Greenland, during the last deglaciation. *Journal of Quaternary Science*, **17**, 747-757.

555

556 **Jennings**, A.E., K.L. Knudsen, M. Hald, C.V. Hansen, and J.T. Andrews,

557 2002b: A mid-Holocene shift in Arctic sea ice variability on the East Greenland shelf.
558 *The Holocene*, **12**, 49-58.

559

560 **Jennings**, A.E., M. Hald, L.M. Smith, and J.T. Andrews, 2006: Freshwater
561 forcing from the Greenland Ice Sheet during the Younger Dryas—Evidence from
562 Southeastern Greenland shelf cores. *Quaternary Science Reviews*, **25**, 282-298.

563

564 **Johannessen**, O.M., K. Khvorostovsky, M.W. Miles, and L.P. Bobylev, 2005:
565 Recent ice-sheet growth in the interior of Greenland. *Science*, **310**, 1013-1016.

566

567 **Johnsen**, S.J., 1977: Stable isotope homogenization of polar firn and ice. In:
568 *Proceedings of a Symposium on Isotopes and Impurities in Snow and Ice, I.U.G.G.*
569 *XVI, General Assembly, Grenoble Aug. Sept. 1975*, IAHS-AISH Publ. 118,
570 Washington D.C., pp. 210-219.

571

572 **Johnsen**, S., H.B. Clausen, W. Dansgaard, N.S. Gundestrup, M. Hansson, P.
573 Johnsson, P. Steffensen, and A.E. Sveinbjornsdottir, 1992a: A “deep” ice core from
574 East Greenland. *Meddelelser om Gronland, Geoscience*, **29**, 3-22

575

576 **Johnsen**, S.J., H.B. Clausen, W. Dansgaard, K. Fuhrer, N. Gundestrup, C.U.
577 Hammer, P. Iversen, J. Jouzel, B. Stauffer, and J.P. Steffensen, 1992b: Irregular
578 glacial interstadials recorded in a new Greenland ice core. *Nature*, **359**, 311-313.

579

580 **Johnsen**, S.J., D. Dahl-Jensen, N. Gundestrup, J.P. Steffensen, H.B. Clausen,
581 H. Miller, V. Masson-Delmotte, A.E. Sveinbjornsdottir, and J. White, 2001: Oxygen
582 isotope and palaeotemperature records from six Greenland ice-core stations: Camp
583 Century, Dye-3, GRIP, GISP2, Renland and NorthGRIP. *Journal of Quaternary*
584 *Science*, **16**, 299-307.

585

586 **Jones**, G.A. and L.D. Keigwin, 1988: Evidence from the Fram Strait (78 N)
587 for early deglaciation. *Nature*, **336**, 56-59.

588

589 **Joughin, I.**, S. Tulaczyk, M. Fahnestock, and R. Kwok, 1996: A mini-surge
590 on the Ryder Glacier, Greenland, observed by satellite radar interferometry. *Science*,
591 **274**, 228-230.

592

593 **Joughin, I.**, Das, S.B., King, M.A., Smith, B. E., Howat, I.M., and Moon, T.,
594 2008a: Seasonal Speedup Along the Western Flank of the Greenland Ice Sheet.
595 *Science*, published online, 10.1126/science.1153288 (Science Express Reports).

596

597 **Joughin, I.**, I. Howat, R.B. Alley, G. Ekstrom, M. Fahnestock, T. Moon, M.
598 Nettles, M. Truffer, and V.C. Tsai, 2008b: Ice front variation and tidewater behavior
599 on Helheim and Kangerdlugssuaq Glaciers, Greenland. *Journal of Geophysical*
600 *Research*, **113**, F01004, doi:10.1029/2007JF000837.

601

602 **Jouzel, J.**, R.B. Alley, K.M. Cuffey, W. Dansgaard, P. Grootes, G. Hoffmann,
603 S.J. Johnsen, R.D. Koster, D. Peel, C.A. Shuman, M. Stievenard, M. Stuiver, and J.
604 White, 1997: Validity of the temperature reconstruction from water isotopes in ice
605 cores. *Journal of Geophysical Research*, **102(C12)**, 26,471-26,487.

606

607 **Kahn, S.A.**, J. Wahr, L.A. Stearns, G.S. Hamilton, T. van Dam, K.M. Larson,
608 and O. Francis, 2007: Elastic uplift in southeast Greenland due to rapid ice mass loss.
609 *Geophysical Resesarch Letters*, **34**, L21701. doi:10.1029/2007GL031468.

610

611 **Kamb, B.**, C.F. Raymond, W.D. Harrison, H. Engelhardt, K.A. Echelmeyer,
612 N. Humphrey, M.M. Brugman, and T. Pfeffer, 1985: Glacier Surge Mechanism:
613 1982-1983 surge of Variegated Glacier, Alaska. *Science*, **227**, 469-479.

614

615 **Kandiano, E.S.** and H.A. Bauch, 2003: Surface ocean temperatures in the
616 north-east Atlantic during the last 500,000 years—Evidence from foraminiferal
617 census data. *Terra Nova*, **15**, 265-271.

618

619 **Kaufman, D.S.** and J. Brigham-Grette, 1993: Aminostratigraphic correlations
620 and paleotemperature implications, Pliocene–Pleistocene high sea level deposits,
621 northwestern Alaska. *Quaternary Science Reviews*, **12**, 21-33.

622

623 **Kaufman, D.S.**, R.C. Walter, J. Brigham-Grette, and D.M. Hopkins, 1991:
624 Middle Pleistocene age of the Nome River glaciation, northwestern Alaska.
625 *Quaternary Research*, **36**, 277-293.

626

627 **Kelly, M.**, S. Funder, M. Houmark-Nielsen, K.L. Knudsen, C. Kronborg, J.
628 Landvik, and L. Sorby, 1999: Quaternary glacial and marine environmental history of
629 northwest Greenland—A review and reappraisal. *Quaternary Science Reviews*, **18**,
630 373-392.

631

632 **Kiehl, J.T.** and P.R. Gent, 2004: The Community Climate System model,
633 version two. *Journal of Climate*, **17**, 3666-3682.

634

635 **Kindler, P.** and P.J. Hearty, 2000: Elevated marine terraces from Eleuthera
636 (Bahamas) and Bermuda: sedimentological, petrographic and geochronological
637 evidence for important deglaciation events during the middle Pleistocene. *Global and*
638 *Planetary Change*, **24**, 41-58.

639

640 **Kleiven, H.F.**, E. Jansen, T. Fronval, and T.M. Smith, 2002: Intensification of
641 Northern Hemisphere glaciations in the circum Atlantic region (3.5-2.4 Ma) —Ice-
642 rafted detritus evidence. *Palaeogeography, Palaeoclimatology, Palaeoecology*, **184**,
643 213-223.

644

645 **Kobashi, T.**, J.P. Severinghaus, and J.-M. Barnola. In press. $4\pm 1.5^{\circ}\text{C}$ abrupt
646 warming 11,270 years ago identified from trapped air in Greenland ice. *Earth and*
647 *Planetary Science Letters*.

648

649 **Koerner, R.M.**, 1989: Ice core evidence for extensive melting of the

650 Greenland Ice Sheet in the last interglacial. *Science*, **244**, 964-968.

651

652 **Koerner**, R.M. and D.A. Fisher, 2002: Ice-core evidence for widespread
653 Arctic glacier retreat in the last interglacial and the early Holocene. *Annals of*
654 *Glaciology*, **35**, 19-24.

655

656 **Kuijpers**, A., N. Abrahamsen, G. Hoffmann, V. Huhnerbach, P. Konradi, H.
657 Kunzendorf, N. Mikkelsen, J. Thiede, and W. Weinrebe, scientific party of RV
658 Poseidon, surveyors of the Royal Danish Administration for Navigation, and
659 Hydrology, 1999: Climate change and the Viking-age fjord environment of the
660 Eastern Settlement, South Greenland. *Geology of Greenland Survey Bulletin*, **183**, 61-
661 67.

662

663 **Lambeck**, K., C. Smither, and P. Johnston, 1998: Sea-level change, glacial
664 rebound and mantle viscosity for northern Europe. *Geophysical Journal*
665 *International*, **134**, 102-144.

666

667 **Lemke**, P., J. Ren, R.B. Alley, I. Allison, J. Carrasco, G. Flato, Y. Fujii, G.
668 Kaser, P. Mote, R.H. Thomas, and T. Zhang, 2007: Observations: Changes in Snow,
669 Ice and Frozen Ground. In: *Climate Change 2007: The Physical Science Basis.*
670 *Contribution of Working Group I to the Fourth Assessment Report of the*
671 *Intergovernmental Panel on Climate Change* [Solomon, S., D. Qin, M. Manning, Z.
672 Chen, M. Marquis, K.B. Averyt, M. Tignor and H.L. Miller (eds.)]. Cambridge
673 University Press, Cambridge and New York, 996 pp.

674

675 **Lhomme**, N., G.K.C. Clarke, and S.J. Marshall, 2005: Tracer transport in the
676 Greenland Ice Sheet—Constraints on ice cores and glacial history. *Quaternary*
677 *Science Reviews*, **24**, 173-194.

678

679 **Lisitzin**, A.P., 2002: *Sea-Ice and Iceberg Sedimentation in the Ocean—*
680 *Recent and Past*. Springer-Verlag, Berlin, 563 pp.

681

682 **Lloyd, J. M.,** L.A. Park, A. Kuijpers, and M. Moros, 2005: Early Holocene
683 palaeoceanography and deglacial chronology of Disko Bugt, West Greenland.
684 *Quaternary Science Reviews*, **24**, 1741-1755.

685

686 **Lloyd, J.M.,** 2006: Late Holocene environmental change in Disko Bugt, west
687 Greenland— Interaction between climate, ocean circulation and Jakobshavn Isbrae.
688 *Boreas*, **35**, 35-49.

689

690 **Ljung, K.** and S. Bjorck, 2004: A lacustrine record of the Pleistocene-
691 Holocene boundary in southernmost Greenland. *GFF (Geological Society of Sweden)*,
692 **126**, 273-278, Part 3.

693

694 **Locke, W.W.I.,** J.T. Andrews, and P.J. Webber, 1979: *A Manual for*
695 *Lichenometry*. British Geomorphological Research Group, Technical Bulletin 26, 47
696 pp.

697

698 **Long, A.J.,** D.H. Roberts, and S. Dawson, 2006: Early Holocene history of
699 the west Greenland Ice Sheet and the GH-8.2 event. *Quaternary Science Reviews*, **25**,
700 904-922.

701

702 **Mangerud, J.** and Funder, S., 1994: The interglacial-glacial record at the
703 mouth of Scoresby Sund, East Greenland. *Boreas*, **23**, 349-358.

704

705 **Marienfeld, P.,** 1992a: Recent sedimentary processes in Scoresby Sund, East
706 Greenland. *Boreas*, **21**: 169-186.

707

708 **Marienfeld, P.,** 1992b: Postglacial sedimentary history of Scoresby Sund,
709 East Greenland. *Polarforschung*, **60**, 181-195.

710

711 **Marshall, S.J.** and K.M. Cuffey, 2000: Peregrinations of the Greenland Ice

712 Sheet divide in the last glacial cycle—Implications for central Greenland ice cores.
713 *Earth and Planetary Science Letters*, **179**, 73-90.

714

715 **Marwick**, P.J., 1998: Fossil crocodylians as indicators of Late Cretaceous and
716 Cenozoic climates—Implications for using palaeontological data in reconstructing
717 palaeoclimate. *Palaeogeography, Palaeoclimatology, Palaeoecology*, **137**, 205-271.

718

719 **McCave**, I.N. and B.E. Tucholke, 1986: Deep current-controlled
720 sedimentation in the western North Atlantic. In: *The Geology of North America: The*
721 *Western North Atlantic Region* [Vogt, P.R. and B.E. Tucholke (eds.)]. Geological
722 Society of America, pp. 451-468.

723

724 **McManus**, J.F., D.W. Oppo, and J.L. Cullen, 1999: A 0.5-million-year record
725 of millennial-scale climate variability in the North Atlantic. *Science*, **283**, 971-975.

726

727 **Meier**, M.F. and A. Post, 1987: Fast tidewater glaciers. *Journal of*
728 *Geophysical Research*, **92(B9)**, 9051-9058.

729

730 **Mienert**, J., J.T. Andrews, and J.D. Milliman, 1992: The East Greenland
731 continental margin (65 N) since the last deglaciation—Changes in sea floor properties
732 and ocean circulation. *Marine Geology*, **106**: 217-238.

733

734 **Milne**, G.A., J.X. Mitrovica, H.G. Scherneck, J.L. Davis, J.M. Johansson, H.
735 Koivula, and M. Vermeer, 2004: Continuous GPS measurements of postglacial
736 adjustment in Fennoscandia— 2. Modeling results. *Journal of Geophysical Research*,
737 **109(B2)**, Art. No. B02412.

738

739 **Mitrovica**, J.X., 1996: Haskell [1935] Revisited. *Journal Geophysical*
740 *Research*, **101**, 555-569.

741

742 **Mitrovica**, J.X. and G.A. Milne, 2002: On the origin of Late Holocene

743 highstands within equatorial ocean basins, *Quaternary Science Reviews*, **21**, 2179-
744 2190.

745

746 **Mitrovica**, J.X. and W.R. Peltier, 1991: On post-glacial geoid relaxation over
747 the equatorial oceans. *Journal Geophysical Research*, **96**, 20,053-20,071.

748

749 **Mitrovica**, J.X., M.E. Tamisiea, J.L. Davis, and G.A. Milne, 2001: Recent
750 mass balance of polar ice sheets inferred from patterns of global sea-level change.
751 *Nature*, **409**, 1026-1029.

752

753 **Mitrovica**, J.X., J. Wahr, I. Matsuyama, A. Paulson, and M.E. Tamisiea,
754 2006: Reanalysis of ancient eclipse, astronomic and geodetic data—A possible route
755 to resolving the enigma of global sea-level rise. *Earth and Planetary Science Letters*,
756 **243**, 390-399.

757

758 **Moran**, K., J. Backman, H. Brinkhuis, S.C. Clemens, T. Cronin, G.R.
759 Dickens, F. Eynaud, J. Gattacceca, M. Jakobsson, R.W. Jordan, M. Kaminski, J.
760 King, N. Koc, A. Krylov, N. Martinez, J. Matthiessen, D. McInroy, T.C. Moore, J.
761 Onodera, M. O'Regan, H. Palike, B. Rea, D. Rio, T. Sakamoto, D.C. Smith, R. Stein,
762 K. St. John, I. Suto, N. Suzuki, K. Takahashi, M. Watanabe, M. Yamamoto, J. Farrell,
763 M. Frank, P. Kubik, W. Jokat and Y. Kristoffersen, 2006: The Cenozoic
764 palaeoenvironment of the Arctic Ocean. *Nature*, **441**, 601-605.

765

766 **Moros**, M., K.G. Jensen, and A. Kuijpers, 2006: Mid- to late-Holocene
767 hydrological variability and climatic variability in Disko Bugt, central West
768 Greenland. *The Holocene*, **16**, 357-367.

769

770 **Mudie**, P.J., A. Rochon, M.A. Prins, D. Soenarjo, S.R. Troelstra, E. Levac,
771 D.B. Scott, L. Roncaglia, and A. Kuijpers, 2006: Late Pleistocene-Holocene marine
772 geology of Nares Strait region—Palaeoceanography from foraminifera and
773 dinoflagellate cysts, sedimentology and stable isotopes. *Polarforschung*, **74(1/3)**, 169-

774 183. hdl:10013/epic.29931.d001

775

776 **Muhs, D.R.**, 2002: Evidence for the timing and duration of the last
777 interglacial period from high-precision uranium-series ages of corals on tectonically
778 stable coastlines. *Quaternary Research*, **58**, 36-40.

779

780 **Muhs, D.R.** and B.J. Szabo, 1994: New uranium-series ages of the
781 Waimanalo Limestone, Oahu, Hawaii—Implications for sea level during the last
782 interglacial period: *Marine Geology*, **118**, 315-326.

783

784 **Muhs, D.R.**, K.R. Simmons, and B. Steinke, 2002: Timing and warmth of the
785 last interglacial period—New U-series evidence from Hawaii and Bermuda and a new
786 fossil compilation for North America. *Quaternary Science Reviews*, **21**, 1355-1383.

787

788 **Muhs, D.R.**, J.F. Wehmiller, K.R. Simmons, and L.L. York, 2004: Quaternary
789 sea level history of the United States. In: *The Quaternary Period in the United States*
790 [Gillespie, A.R., S.C. Porter, and B.F. Atwater, (eds.)]. Elsevier, Amsterdam, pp. 147-
791 183.

792

793 **Multer, H.G.**, E. Gischler, J. Lundberg, K.R. Simmons, and E.A. Shinn,
794 2002: Key Largo Limestone revisited—Pleistocene shelf-edge facies, Florida Keys,
795 USA: *Facies*, **46**, 229-272.

796

797 **Munk, W.**, 2002: Twentieth century sea level—An enigma. *Proceedings of*
798 *the National Academy of Sciences of the United States of America*, **99**, 6550-6555.

799

800 **Muscheler, R.**, R. Beer, P.W. Kubik, and H.A. Synal, 2005: Geomagnetic
801 field intensity during the last 60,000 years based on Be-10 and Cl-36 from the
802 Summit ice cores and C-14. *Quaternary Science Reviews*, **24**, 1849-1860.

803

804 **Nam, S. I.** and R. Stein, 1999: Late Quaternary variations in sediment

805 accumulation rates and their paleoenvironment implications: a case study from the
806 East Greenland continental margin. *GeoResearch Forum*, **5**, 223-240.

807 **Nishiizumi, K.**, R.C. Finkel, K.V. Ponganis, T. Graf, C.P. Kohl, and K. Marti,
808 1996: In situ produced cosmogenic nuclides in GISP2 rock core from Greenland
809 Summit (Abstract, Fall Meeting 1996). *Eos, Transactions of the American*
810 *Geophysical Union*, **77(46) Supplement**, F428, Abstract OS41B-10.

811

812 **North Greenland Ice Core Project Members.** 2004. High-resolution record
813 of Northern Hemisphere climate extending into the last interglacial period. *Nature*,
814 **431**, 147-151.

815

816 **O'Cofaigh, C.**, J. Taylor, J.A. Dowdeswell, and C.J. Pudsey, 2003: Palaeo-ice
817 streams, trough mouth fans and high-latitude continental slope sedimentation. *Boreas*,
818 **32**, 37-55.

819

820 **Oerlemans, J.**, 1994: Quantifying global warming from the retreat of glaciers.
821 *Science*, **264**, 243–245.

822

823 **Oerlemans, J.**, 2001: *Glaciers and Climatic Change*. A.A. Balkema
824 Publishers, Lisse, 148 pp.

825

826 **Otto-Bliesner, B.L.**, J.T. Overpeck, S.J. Marshall, and G. Miller, 2006:
827 Simulating Arctic climate warmth and icefield retreat in the Last Interglaciation.
828 *Science*, **311**, 1751-1753.

829

830 **Overpeck, J.T.**, B.L. Otto-Bliesner, G.H., Miller, D.R. Muhs, R.B. Alley, and
831 J.T. Kiehl, 2006: Paleoclimatic evidence for future ice-sheet instability and rapid sea-
832 level rise, *Science*, **311**, 1747-1750.

833

834 **Parizek, B.R.** and R.B. Alley, 2004: Implications of increased Greenland
835 surface melt under global-warming scenarios: ice-sheet simulations. *Quaternary*

836 *Science Reviews*, **23**, 1013-1027.

837

838 **Parnell, J., S. Bowden, C. Taylor, and J.T. Andrews, 2007:** Biomarker
839 determination as a provenance tool for detrital carbonate events (Heinrich events?) —
840 Fingerprinting Quaternary glacial sources in Baffin Bay. *Earth and Planetary Science*
841 *Letters*, **257**, 71-82.

842

843 **Paterson, W.S.B., 1994:** *The Physics of Glaciers*. Pergamon, Oxford, 3rd ed.
844 480 pp.

845

846 **Payne, A.J., A. Vieli, A.P. Shepherd, D.J. Wingham, and E. Rignot, 2004:**
847 Recent dramatic thinning of largest West Antarctic ice stream triggered by oceans.
848 *Geophysical Research Letters*, **31**, L23401. doi: 10.1029/2004GL021284.

849

850 **Peltier, W.R., 2004:** Global glacial isostasy and the surface of the ice-age
851 Earth—The ICE-5G (VM2) Model and GRACE. *Annual Review of Earth and*
852 *Planetary Sciences*, **32**, 111-149. (doi:10.1146/annurev.earth.32.082503.144359)

853

854 **Peltier, W.R. and R.G. Fairbanks, 2006:** Global glacial ice volume and Last
855 Glacial Maximum duration from an extended Barbados sea level record. *Quaternary*
856 *Science Reviews*, **25**, 3322-3337.

857

858 **Petrenko, V.V., Severinghaus, J.P., Brook, E.J., Reeh, N., Schaefer, H., 2006:**
859 Gas records from the West Greenland ice margin covering the Last Glacial
860 Termination: a horizontal ice core. *Quaternary Science Reviews*, **25**, 865-875.

861

862 **Plag, H.-P. and H.-U. Juttner, 2001:** Inversion of global tide gauge data for
863 present-day ice load changes. In: *Proceedings of the International Symposium on*
864 *Environmental Research in the Arctic and Fifth Ny-Alesund Science Seminar*
865 [Yamanouchi, T. (ed.)]. *Memoirs of the National Institute of Polar Research (Japan)*,
866 **54**, 301-317.

867

868 **Poore, R.Z.** and H.J. Dowsett, 2001: Pleistocene reduction of polar ice caps—
869 Evidence from Cariaco Basin marine sediments. *Geology*, **29**, 1-74.

870

871 **Raynaud, D.,** J. Chappellaz, C. Ritz, and P. Martinerie, 1997: Air content
872 along the Greenland Ice Core Project core—A record of surface climatic parameters
873 and elevation in central Greenland. *Journal of Geophysical Research*, **102(C12)**,
874 26,607-26,613.

875

876 **Reeh, N.,** 1984: Reconstruction of the glacial ice covers of Greenland and the
877 Canadian Arctic islands by 3-dimensional, perfectly plastic ice-sheet modeling.
878 *Annals of Glaciology*, **5**, 115-121.

879

880 **Reeh, N.,** 1985: Greenland Ice-Sheet Mass Balance and Sea-Level change. In:
881 *Glaciers, Ice Sheets, and Sea Level—Effect of a CO₂ induced climatic change*.
882 National Academy Press, Washington D.C., pp. 155-171.

883

884 **Reeh, N.,** 2004: Holocene climate and fjord glaciations in Northeast
885 Greenland—Implications for IRD deposition in the North Atlantic. *Sedimentary*
886 *Geology*, **165**, 333-342.

887

888 **Reeh, N.,** C. Mayer, H. Miller, H.H. Thomsen, and A. Weidick, 1999: Present
889 and past climate control on fjord glaciations in Greenland—Implications for IRD-
890 deposition in the sea. *Geophysical Research Letters*, **26**, 1039-1042.

891

892 **Ridley, J.K.,** P. Huybrechts, J.M. Gregory, and J.A. Lowe, 2005: Elimination
893 of the Greenland Ice Sheet in a high CO₂ climate. *Journal of Climate*, **18**, 3409-
894 3427.

895

896 **Rignot, E.** and P. Kanagaratnam, 2006: changes in the velocity structure of
897 the Greenland Ice Sheet. *Science*, **311**, 986-990.

898

899 **Rohling**, E.J., M. Fenton, F.J. Jorissen, P. Bertrand, G. Ganssen, and J.P.
900 Caulet. 1998. Magnitudes of sea-level lowstands of the past 500,000 years. *Nature*,
901 **394**, 162-165.

902

903 **Schofield**, J.E., K.J. Edwards, and J.A. McMullen, 2007: Modern pollen-
904 vegetation relationships in subarctic southern Greenland and the interpretation of
905 fossil pollen data from the Norse landnam. *Journal of Biogeography*, **34**, 473-488.

906

907 **Severinghaus**, J.P., T. Sowers, E.J. Brook, R.B. Alley, and M.L. Bender,
908 1998: Timing of abrupt climate change at the end of the Younger Dryas interval from
909 thermally fractionated gases in polar ice. *Nature*, **391**,141-146.

910

911 **Shackleton**, N.J., J. Backman, H. Zimmerman, D.V. Kent, M.A. Hall, D.G.
912 Roberts, D. Schnitker, J.G. Baldauf, A. Desprairies, R. Homrighausen, P. Huddlestun,
913 J.B. Keene, A.J. Kaltenback, K.A.O. Krumsiek, A.C. Morton, J.W. Murray, and J.
914 Westbergsmith, 1984: Oxygen isotope calibration of the onset of ice-rafting and
915 history of glaciation in the North-Atlantic region. *Nature*, **307**, 620-623.

916

917 **Sluijs**, A., S. Schouten, M. Pagani, M. Woltering, H. Brinkhuis, J.S.S.
918 Damste, G.R. Dickens, M. Huber, G.J. Reichart, R. Stein, J. Matthiessen, L.J.
919 Lourens, N. Pedentchouk, J. Backman and K. Moran, 2006: Subtropical arctic ocean
920 temperatures during the Palaeocene/Eocene thermal maximum. *Nature*, **441**, 610-613.

921

922 **Smith**, J.M.B. and T.P. Bayliss-Smith, 1998: Kelp-plucking—Coastal erosion
923 facilitated by bull-kelp *Durvillaea antarctica* at subantarctic Macquarie Island.
924 *Antarctic Science*, **10**, 431-438.

925

926 **Souchez**, R., A. Bouzette, H.B. Clausen, S.J. Johnsen, and J. Jouzel, 1998: A
927 stacked mixing sequence at the base of the Dye 3 core, Greenland. *Geophysical*
928 *Research Letters*, **25**, 1943-1946.

929

930 **Sowers, T., M. Bender, D. Raynaud, and Y.S. Korotkevich, 1992:** Delta-N-15
931 of N₂ in air trapped in polar ice—A tracer of gas-transport in the firn and a possible
932 constraint on ice age/gas age-differences. *Journal of Geophysical Research*, **97(D14)**,
933 15,683-15,697.

934

935 **Sparrenbom, C.J., O. Bennike, S. Bjorck, and K. Lambeck, 2006a:** Holocene
936 relative sea-level changes in the Qaqortoq area, southern Greenland. *Boreas*, **35**, 171-
937 187.

938

939 **Sparrenbom, C.J., O. Bennike, S. Bjorck, and K. Lambeck, 2006b:** Relative
940 sea-level changes since 15 000 cal. yr BP in the Nanortalik area, southern Greenland.
941 *Journal of Quaternary Science*, **21**, 29-48.

942

943 **Spencer, M.K., R.B. Alley, and J.J. Fitzpatrick, 2006:** Developing a bubble
944 number-density paleoclimatic indicator for glacier ice. *Journal of Glaciology*,
945 **52(178)**, 358-364.

946

947 **Stastna, M. and Peltier, W.R., 2007:** On box models of the North Atlantic
948 thermohaline circulation: intrinsic and extrinsic millennial timescale variability in
949 response to deterministic and stochastic forcing. *Journal of Geophysical Research*,
950 **112**, C10023.

951

952 **St. John, K.E. and Krissek, L.A., 2002:** The late Miocene to Pleistocene ice-
953 rafting history of southeast Greenland. *Boreas*, **31**, 28-35.

954

955 **St. John, K., 2008:** Cenozoic ice-rafting history of the central Arctic Ocean—
956 Terrigenous sands on the Lomonosov Ridge. *Paleoceanography*, **23**, PA1S05.
957 doi:10.1029/2007PA001483.

958

959 **Stein, A.B., 1996:** Seismic stratigraphy and seafloor morphology of the

960 Kangerlugssuaq region, East Greenland—Evidence for glaciations to the Continental
961 shelf break during the late Weischelian and earlier. MSc thesis, University of
962 Colorado, Boulder, 293 pp.

963

964 **Stein, R.,** Nam, S.-I., Grobe, H., and Hubberten, H., 1996: Late Quaternary
965 glacial history and short-term ice-rafted debris fluctuations along the East Greenland
966 continental margin. In: *Late Quaternary Paleoceanography of North Atlantic*
967 *Margins* [Andrews, J.T., W.A. Austen, H. Bergsetn, and A.E. Jennings (eds.)].
968 Geological Society, London, pp. 135-151.

969

970 **Stirling, C.H.,** T.M. Esat, M.T. McCulloch, and K. Lambeck, 1995: High-
971 precision U-series dating of corals from Western Australia and implications for the
972 timing and duration of the last interglacial. *Earth and Planetary Science Letters*, **135**,
973 115-130.

974

975 **Stirling, C.H.,** T.M. Esat, K. Lambeck, and M.T. McCulloch, 1998: Timing
976 and duration of the last interglacial—Evidence for a restricted interval of widespread
977 coral reef growth. *Earth and Planetary Science Letters*, **160**, 745-762.

978

979 **Stirling, C.H.** T.M., Esat, K. Lambeck, M.T. McCulloch, S.G. Blake, D.-C.
980 Lee, and A.N. Halliday, 2001: Orbital forcing of the marine isotope stage 9
981 interglacial: *Science*, **291**, 290-293.

982

983 **Stocker, T.F.** and S.J. Johnsen, 2003: A minimum thermodynamic model for
984 the bipolar seesaw. *Paleoceanography*, **18**, Art. No. 1087.

985

986 **Stoner, J.S.,** J.E.T. Channell, and C. Hillaire-Marcel, 1995: Magnetic
987 properties of deep-sea sediments off southwest Greenland—Evidence for major
988 differences between the last two deglaciations. *Geology*, **23**: 241-244.

989

990 **Stuiver, M.,** T.F. Braziunas, P.M. Grootes, and G.A. Zielinski, 1997: Is there

991 evidence for solar forcing of climate in the GISP2 oxygen isotope record? *Quaternary*
 992 *Research*, **48**, 259-266.

993

994 **Stuiver**, M., P.J. Reimer, E. Bard, J.W. Beck, K.A. Hughen, B. Kromer, F.G.
 995 McCormack, J. van der Plicht, and M. Spurk, 1998: INTCAL98 Radiocarbon age
 996 calibration 24,000-0 cal BP. *Radiocarbon*, **40**, 1041-1083.

997

998 **Sugden**, D. and B. John, 1976: *Glaciers and Landscape*. Arnold, London, and
 999 Halsted, New York, 376 pp.

1000

1001 **Suwa**, M., J.C. von Fischer, M.L. Bender, A. Landais, and E.J. Brook, 2006:
 1002 Chronology reconstruction for the disturbed bottom section of the GISP2 and the
 1003 GRIP ice cores— Implications for Termination II in Greenland. *Journal of*
 1004 *Geophysical Research*, **111(D2)**, Art. No. D02101.

1005

1006 **Syvitski**, J.P.M., J.T. Andrews, and J.A. Dowdeswell, 1996: Sediment
 1007 deposition in an iceberg-dominated glacial marine environment, East Greenland—Basin
 1008 fill implications. *Global and Planetary Change*, **12**, 251-270.

1009

1010 **Syvitski**, J.P.M., A. Stein, J.T. Andrews, and J.D. Milliman, 2001: Icebergs
 1011 and seafloor of the East Greenland (Kangerlussuaq) continental margin. *Arctic,*
 1012 *Antarctic and Alpine Research*, **33**, 52-61.

1013

1014 **Tang**, C.C.L., C.K. Ross, and T. Yao, 2004: The circulation, water masses
 1015 and sea-ice of Baffin Bay. *Progress in Oceanography*, **63**, 183-228.

1016

1017 **Tarasov**, L. and W. Richard Peltier, 2002: Greenland glacial history and local
 1018 geodynamic consequences. *Geophysical Journal International*, **150(1)**, 198-229.

1019 doi:10.1046/j.1365-246X.2002.01702.x

1020

1021 **Tarasov**, L. and W.R. Peltier, 2003: Greenland glacial history, borehole

1022 constraints, and Eemian extent. *Journal of Geophysical Research*, **108(B3)**, Art. No.
1023 2143.

1024

1025 **Thiede, J., A. Winkler, T. Wolf-Welling, O. Eldholm, A.M. Myhre, K.H.**
1026 **Baumann, R. Henrick, and R. Stein, 1998: Late Cenozoic history of the Polar North**
1027 **Atlantic—Results from ocean drilling. *Quaternary Science Reviews*, **17**, 185-208.**

1028

1029 **Thomas, R.H. and PARCA Investigators, 2001: Program for Arctic Regional**
1030 **Climate Assessment (PARCA) —Goals, key findings, and future directions. *Journal***
1031 ***of Geophysical Research*, **106(D24)**, 33,691-33705.**

1032

1033 **Thomas, R., W. Abdalati, E. Frederick, W. Krabill, S. Manizade, and K.**
1034 **Steffen, 2003: Investigation of surface melting and dynamic thinning on Jakobshavn**
1035 **Isbrae, Greenland. *Journal of Glaciology*, **49**, 231-239.**

1036

1037 **Thomas, R., E. Frederick, W. Krabill, S. Manizade, and C. Martin, 2006:**
1038 **Progressive increase in ice loss from Greenland. *Geophysical Research Letters*, **33**,**
1039 **L10503, doi:10.1029/2006GL026075.**

1040

1041 **Thompson, W.G. and S.L. Goldstein, 2005: Open-system coral ages reveal**
1042 **persistent suborbital sea-level cycles. *Science*, **308**, 401-404.**

1043

1044 **Toniazzo, T., J.M. Gregory, and P. Huybrechts, 2004: Climatic impact of a**
1045 **Greenland deglaciation and its possible irreversibility. *Journal of Climate*, **17**, 21-33.**

1046

1047 **van der Plicht, J., B. Van Geel, S.J.P. Bohncke, J.A.A. Bos, M. Blaauw,**
1048 **A.O.M. Speranza, R. Muscheler, and S. Bjorck, 2004: The Preboreal climate reversal**
1049 **and a subsequent solar-forced climate shift. *Journal of Quaternary Science*, **19**, 263-**
1050 **269.**

1051

1052 **van der Veen, C.J.,1999: *Fundamentals of Glacier Dynamics*. Balkema,**

1053 Rotterdam. 462 pp.

1054

1055 **van Kreveld, S.**, M. Sarthein, H. Erlenkeuser, P. Grootes, S. Jung, M.J.

1056 Nadeau, U. Pflaumann, and A. Voelker, 2000: Potential links between surging ice

1057 sheets, circulation changes, and the Dansgaard-Oeschger cycles in the Irminger Sea,

1058 60-18 ka. *Paleoceanography*, **15**, 425-442.

1059

1060 **Velicogna, I.** and J. Wahr, 2006: Acceleration of Greenland ice mass loss in

1061 spring 2004. *Nature*, **443**, 329-331.

1062

1063 **Vorren, T.O.** and J.S. Laberg, 1997: Trough mouth fans—Palaeoclimate and

1064 ice-sheet monitors. *Quaternary Science Reviews*, **16**, 865-886.

1065

1066 **Weidick, A.** 1993: Neoglacial change of ice cover and the related

1067 response of the Earth's crust in West Greenland. *Grønl. Geol. Unders. Rapp.* **159**,

1068 121–126.

1069 **Weidick, A.**, 1996: Neoglacial changes of ice cover and sea level in

1070 Greenland—A classical enigma. In: *The Paleo-Eskimo Cultures of Greenland*

1071 [Gronnow, B. and J. Pind (eds.)]. Danish Polar Center, Copenhagen, pp. 257-270.

1072

1073 **Weidick, A.**, H. Oerter, N. Reeh, H.H. Thomsen, and L. Thorning, 1990: The

1074 recession of the Inland Ice margin during the Holocene Climatic Optimum in the

1075 Jakobshavn-Isfjord area of west Greenland. *Global and Planetary Change*, **82**, 389-

1076 399.

1077

1078 **Weidick, A.**, M. Kelly, and O. Bennike, 2004: Later Quaternary development

1079 of the southern sector of the Greenland Ice Sheet, with particular reference to the

1080 Qassimiut lobe. *Boreas*, **33**, 284-299.

1081

1082 **Whillans, I.M.**, 1976: Radio-echo layers and recent stability of West

1083 Antarctic ice sheet. *Nature*, **264**, 152-155.

1084

1085 **Wilken**, M. and J. Mienert, 2006: Submarine glacial debris flows, deep-
1086 sea channels and past ice-stream behaviour of the East Greenland continental margin.
1087 *Quaternary Science Reviews*, **25**, 784-810.

1088

1089 **Willerslev**, E., E. Cappellini, W. Boomsma, R. Nielsen, M.B. Hebsgaard,
1090 T.B. Brand, M. Hofreiter, M. Bunce, H.N. Poinar, D. Dahl-Jensen, S. Johnsen, J.P.
1091 Steffensen, O. Bennike, J.L. Schwenninger, R. Nathan, S. Armitage, C.J. de Hoog, V.
1092 Alfimov, M. Christi, J. Beer, R. Muscheler, J. Barker, M. Sharkp, K.E.H. Penkman, J.
1093 Haile, P. Taberlet, M.T.P. Bilbert, A. Casoli, E. Campani, and M.J. Collins, 2007:
1094 Ancient biomolecules from deep ice cores reveal a forested Southern Greenland.
1095 *Science*, **317**, 111-114.

1096

1097 **Zielinski**, G.A., P.A. Mayewski, L.D. Meeker, S. Whitlow, M.S. Twickler, M.
1098 Morrison, D.A. Meese, A.J. Gow, and R.B. Alley, 1994: Record of volcanism since
1099 7000 B.C. from the GISP2 Greenland ice core and implications for the volcano-
1100 climate system. *Science*, **264**, 948-950.

1101

1102 **Zwally**, H.J., W. Abdalati, T. Herring, K. Larson, J. Saba, and K. Steffen,
1103 2002: Surface melt-induced acceleration of Greenland ice-sheet flow. *Science*, **297**,
1104 218-222.

1 **CCSP Synthesis and Assessment Product 1.2**
2 **Past Climate Variability and Change in the Arctic and at High Latitudes**

3
4 **Chapter 8 — History of Sea Ice in the Arctic**

5
6 **Chapter Lead Author**

7 Leonid Polyak, Byrd Polar Research Center, Ohio State University

8 **Contributing Authors**

9 John Andrews, University of Colorado

10 Julie Brigham-Grette, University of Massachusetts

11
12 Dennis Darby, Old Dominion University

13 Arthur Dyke, Geological Survey of Canada

14 Svend Funder, University of Copenhagen

15 Marika Holland, National Center for Atmospheric Research

16
17 Anne Jennings, University of Colorado

18 James Savelle, Geological Survey of Canada

19 Mark Serreze, University of Colorado

20
21 Eric Wolff, British Antarctic Survey

22

22 **ABSTRACT**

23
24 The volume of Arctic sea ice is rapidly declining, and to put that decline into perspective
25 we need to know the history of Arctic sea ice in the geologic past. Sedimentary proxy records
26 from the Arctic Ocean floor and from the surrounding coasts can provide clues. Although
27 incomplete, existing data outline the development of Arctic sea ice during the last several million
28 years. Some data indicate that sea ice consistently covered at least part of the Arctic Ocean for no
29 less than 13–14 million years, and that ice was most widespread during the last approximately 2
30 million years in relationship with Earth’s overall cooler climate. Nevertheless, episodes of
31 considerably reduced ice cover or even a seasonally ice-free Arctic Ocean probably punctuated
32 even this latter period. Ice diminished episodically during warmer climate events associated with
33 changes in Earth’s orbit on the time scale of tens of thousands of years. Ice cover in the Arctic
34 began to diminish in the late 19th century and has accelerated during the last several decades.
35 The current reduction in Arctic ice is the largest in at least the last few thousand years and is
36 progressing at a very fast rate that appears to have no analogs in past records. Because ice cover
37 is diminishing so rapidly, a comprehensive investigation of past warming events in the Arctic is
38 essential. Data obtained from this investigation will provide critical information for assessing the
39 magnitude and rate of the approaching ice loss and for understanding conditions in the reduced-
40 ice or seasonally ice-free Arctic.

41 8.1 Introduction

42

43

44

45

46

47

48

49

50

51

52

53

54

55

56

57

58

59

60

61

62

63

64

The most defining feature of the surface of the Arctic Ocean and adjacent seas is its sea ice cover, which waxes and wanes with the seasons, and which also changes in extent and thickness on interannual and longer time scales. These changes are controlled by climate, notably by temperature (e.g., Smith et al., 2003), but they also affect atmospheric and hydrographic conditions in high latitudes (Kinnard et al., 2008; Steele et al., 2008). Observations during the past several decades document substantial retreat and thinning of the Arctic sea ice cover: retreat is accelerating, and it is expected to continue. The Arctic Ocean may become seasonally ice free as early as 2040 (Holland et al., 2006a; Comiso et al., 2008; Stroeve et al., 2008). A reduction in sea ice will promote Arctic warming through a feedback mechanism between ice and its reflectivity (the ice-albedo feedback mechanism), and this reduction will thus influence weather systems in the northern high and perhaps middle latitudes. Changes in ice cover and freshwater flux out of the Arctic Ocean will also affect oceanic circulation of the North Atlantic, which has profound influence on climate in Europe and North America (Seager et al., 2002; Holland et al., 2006b). Furthermore, continued retreat of sea ice will accelerate coastal erosion owing to increased wave action. Ice loss will modify the Arctic Ocean food web and its large predators, such as polar bears and seals, that depend on the ice cover. These changes, in turn, will affect indigenous human populations that harvest such species. All of these possibilities make it important to know how fast Arctic ice will diminish and the consequences of that reduction, a task that requires thorough understanding of the natural variability of ice cover in the recent and longer term past.

65 **8.2 Background on Arctic Sea-Ice Cover**

66

67 **8.2.1 Ice Extent, Thickness, Drift and Duration**

68 Arctic sea ice cover grows to its maximum extent by the end of winter and shrinks to a
69 minimum in September. For the period of reliable satellite observations (1979–2007), extremes
70 in Northern Hemisphere ice extent are 16.44×10^6 square kilometers (km^2) for March 1979 and
71 4.28×10^6 km^2 for September 2007 (http://nsidc.org/data/seaice_index/; Stroeve et al., 2008). Ice
72 extent is defined as the region of the ocean of which at least 15% is covered by ice. The ice cover
73 can be broadly divided into a perennial ice zone where ice is present throughout the year and a
74 seasonal ice zone where ice is present only seasonally. A considerable fraction of Arctic sea ice
75 is perennial, which differs strongly from Antarctic sea ice which is nearly all seasonal. Ice
76 concentrations in the perennial ice zone typically exceed 97% in winter but fall to 85–95% in
77 summer. Sea ice concentrations in the seasonal ice zone are highly variable, and in general (but
78 not always) they decrease toward the southern sea ice margin.

79 The thickness of sea ice, which varies markedly in both space and time, can be described
80 by a probability distribution. For the Arctic Ocean as a whole, the peak of this distribution (as
81 thick as the ice ever gets) is typically cited at about 3 meters (m) (Serreze et al., 2007b), but
82 growing evidence (discussed below) suggests that during recent decades not only is the area of
83 sea ice shrinking, but that it is also thinning substantially. Although many different types of sea
84 ice can be defined, the two basic categories are first-year ice, which represents a single year's
85 growth, and multiyear ice, which has survived one or more melt seasons. Undeformed first-year
86 ice typically is as much as 2 m thick. Although in general multiyear ice is thicker (greater than 2
87 m), first-year ice that is locally pushed into ridges can be as thick as 20–30 m.

88 Under the influence of winds and ocean currents, the Arctic sea ice cover is in nearly
89 constant motion. The large-scale circulation principally consists of the Beaufort Gyre, a mean
90 annual clockwise motion in the western Arctic Ocean with a drift speed of 1–3 centimeters per
91 second, and the Transpolar Drift, the movement of ice from the coast of Siberia east across the
92 pole and into the North Atlantic by way of Fram Strait, which lies between northern Greenland
93 and Svalbard. Ice velocities in the Transpolar Drift increase toward Fram Strait, where the mean
94 drift speed is 5–20 centimeters per second (Figure 8.1) (Thorndike, 1986; Gow and Tucker,
95 1987). About 20% of the total ice area of the Arctic Ocean is discharged each year through Fram
96 Strait, the majority of which is multiyear ice. This ice subsequently melts in the northern North
97 Atlantic, and since the ice is relatively fresh compared with sea water, this melting adds
98 freshwater to the ocean in those regions.

99

100 FIGURE 8.1 NEAR HERE

101

102 **8.2.2 Influences on the Climate System**

103 Seasonal changes in the amount of heat at the surface (net surface heat flux) associated
104 with sea ice modulate the exchange and transport of energy in the atmosphere. Ice, as sheets or
105 as sea ice, reflects a certain percentage of incoming solar radiation back into the atmosphere. The
106 albedo (reflectivity) of ice cover ranges from 80% when it is freshly snow covered to around
107 50% during the summer melt season (but lower in areas of ponded ice). This high reflectivity
108 contrasts with the dark ocean surface, which has an albedo of less than 10%. Ice’s high albedo
109 and its large surface area, coupled with the solar energy used to melt ice and to increase the
110 sensible heat content of the ocean, keep the Arctic atmosphere cool during summer. This cooler

111 polar atmosphere helps to maintain a steady poleward transport of atmospheric energy (heat)
112 from lower latitudes into the Arctic. During autumn and winter, energy derived from incoming
113 solar radiation is small or nonexistent in Polar areas. However, heat loss from the surface adds
114 heat to the atmosphere, and it reduces the requirements for atmospheric heat to be transported
115 poleward into the Arctic (Serreze et al., 2007a).

116 Model experiments have addressed potential changes in the regional and large-scale
117 aspects of atmospheric circulation that are associated with loss of sea ice. The models commonly
118 use ice conditions that have been projected through the 21st century (see following section).
119 Magnusdottir et al. (2004) found that a reduced area of winter sea ice in the North Atlantic
120 modified the modeled circulation in the same way as the North Atlantic Oscillation; declining ice
121 promotes a negative North Atlantic Oscillation response: storm tracks are weaker and shifted to
122 the south. Many observations show that sea ice in this region affects the development of mid-
123 and high-latitude cyclones because of the strong horizontal temperature gradients along the ice
124 margin (e.g., Tsukernik et al., 2007). Singarayer et al. (2006) forced a model by combining the
125 area of sea ice in 1980–2000 and projected reductions in sea ice until 2100. In one simulation,
126 mid-latitude storm tracks were intensified and they increased winter precipitation throughout
127 western and southern Europe. Sewall and Sloan (2004) found that reduced ice cover led to less
128 rainfall in the American west. In summary, although these and other simulations point to the
129 importance of sea ice on climate outside of the Arctic, different models may produce very
130 different results. Coordinated experiments that use a suite of models is needed to help to reduce
131 uncertainty.

132 Climate models also indicate that changes in the melting of and export of sea ice to the
133 North Atlantic can modify large-scale ocean circulation (e.g., Delworth et al., 1997; Mauritzen

134 and Hakkinen, 1997; Holland et al., 2001). In particular, exporting more freshwater from the
135 Arctic may alter the Atlantic meridional overturning circulation (MOC) it increases the stability
136 of the upper ocean and suppresses the formation of North Atlantic Deep Water. This suppression
137 may have far-reaching climate consequences. The considerable freshening of the North Atlantic
138 since the 1960s has an Arctic source (Peterson et al., 2006). Total Arctic freshwater output to the
139 North Atlantic is projected to increase through the 21st century, and decreases in the export of
140 sea ice will be more than balanced by the export of liquid freshwater (derived from the melting
141 of Arctic ice and increased net precipitation). However, less ice may melt in the Greenland-
142 Iceland-Norwegian (GIN) seas because less ice is moved through Fram Strait into those seas.
143 These changes may increase vertical instability in the ocean regions where deep water forms and
144 counteract the tendency of a warmer climate to increase ocean stability (Holland et al., 2006b).
145 However, this possible instability may be mitigated somewhat if less sea ice accumulates in the
146 Greenland-Iceland-Norwegian seas. Additionally, as discussed by Levermann et al. (2007), the
147 reduction in sea ice may help to stabilize the Atlantic meridional overturning circulation by
148 removing the insulating ice cover which, perhaps counterintuitively, limits the amount of heat
149 lost by the ocean to the atmosphere. Thus, sea ice may help to maintain the formation of deep
150 water in the Greenland-Iceland-Norwegian seas. Overall, a smaller area of sea ice influences the
151 Atlantic meridional overturning circulation in sometimes competing ways. How they will
152 ultimately affect future climate is not yet certain.

153

154 **8.2.3 Recent Changes and Projections for the Future**

155 On the basis of satellite records, the extent of sea ice has diminished in every month and
156 most obviously in September, for which the trend for the period 1979–2007 is 10% per decade

157 (Figure 8.2). (Satellite records originated in the National Snow and Ice Data Center
158 (http://nsidc.org/data/seaice_index/) and combine information from the Nimbus-7 Scanning
159 Multichannel Microwave Radiometer (October 1978–1987) and the Defense Meteorological
160 Satellite Program Special Sensor Microwave/Imager (1987–present.) Conditions in 2007 serve
161 as an exclamation point on this ice loss (Comiso et al., 2008; Stroeve et al., 2008). The average
162 September ice extent in 2007 of 4.28 million km² was not only the least ever recorded but also
163 23% lower than the previous September record low of 5.56 million km² set in 2005. The
164 difference in areas corresponds with an area roughly the size of Texas and California combined.
165 On the basis of an extended sea ice record, it appears that area of ice in September 2007 is only
166 half of its area in 1950–70 (estimated by use of the Hadley Centre sea ice and sea surface
167 temperature data set (HadISST) (Rayner et al., 2003)..

168

169 **FIGURE 8.2 NEAR HERE**

170

171 Many factors may have contributed to this ice loss (as reviewed by Serreze et al., 2007b),
172 such as general Arctic warming (Rothrock and Zhang, 2005), extended summer melt (Stroeve et
173 al., 2006), effects of the changing phase of the Northern Annular Mode and the North Atlantic
174 Oscillation. These and other atmospheric patterns have flushed some older, thicker ice out of the
175 Arctic and left thinner ice that is more easily melted out in summer (e.g., Rigor and Wallace,
176 2004; Rothrock and Zhang, 2005; Maslanik et al., 2007a), changed ocean heat transport
177 (Polyakov et al., 2005; Shimada et al., 2006), and increased recent spring cloud cover that
178 augments the longwave radiation flux to the surface (Francis and Hunter, 2006). Strong evidence
179 for a thinning ice cover comes from an ice-tracking algorithm applied to satellite and buoy data,

180 which suggests that the area of the Arctic Ocean covered by predominantly older (and hence
181 generally thicker) ice (ice 5 years old or older) decreased by 56% between 1982 and 2007.
182 Within the central Arctic Ocean, the coverage of old ice has declined by 88%, and ice that is at
183 least 9 years old (ice that tends to be sequestered in the Beaufort Gyre) has essentially
184 disappeared. Examination of the distribution of ice of various thickness suggests that this loss of
185 older ice translates to a decrease in mean thickness for the Arctic from 2.6 m in March 1987 to
186 2.0 m in 2007 (Maslanik et al., 2007b).

187 The role of greenhouse gas forcing on the observed ice loss finds strong support from the
188 study of Zhang and Walsh (2006). These authors show that for the period 1979–1999, the multi-
189 model mean trend projected by models discussed in the Intergovernmental Panel on Climate
190 Change Fourth Assessment Report (IPCC-AR4) is downward, as are trends from most individual
191 models. However, Stroeve et al. (2007) find that few or none (depending on the time period of
192 analysis) of the September trends from the IPCC-AR4 runs are as large as observed. If the multi-
193 model mean trend is assumed to be a reasonable representation of change forced by increased
194 concentrations of greenhouse gases, then 33–38% of the observed September trend from 1953 to
195 2006 is externally forced and that percentage increases to 47–57% from 1979 to 2006, when
196 both the model mean and observed trend are larger. Although this trend argues that natural
197 variability has strongly contributed to the observed trend, Stroeve et al. (2006) concluded that, as
198 a group, the models underestimate the sensitivity of sea ice cover to forcing by greenhouse gases.
199 Overly thick ice assumed by many of the models appears to provide at least a partial explanation.

200 The Intergovernmental Panel on Climate Change Fourth Assessment Report (IPCC-AR4)
201 models driven with the SRES A1B emissions scenario (in which CO₂ reaches 720 parts per
202 million (ppm), in comparison to the current value of 380 ppm, by the year 2100), point to

203 complete or nearly complete loss (less than 1×10^6 km²) of September sea ice anywhere from
204 year 2040 to well beyond the year 2100, depending on the model and particular run (ensemble
205 member) for that model. Even by the late 21st century, most models project a thin ice cover in
206 March (Serreze et al., 2007b). However, given the findings just discussed, the models as a group
207 may be too conservative—predict a later rather than earlier date—when the Arctic Ocean will be
208 ice-free in summer.

209 Abrupt change in future Arctic ice conditions is difficult to model. For instance, the
210 extent of end-of-summer ice is sensitive to ice thickness in spring (simulations based on the
211 Community Climate System Model, version 3 (Holland et al., 2006a)). If the ice is already thin
212 in the spring, then a “kick” associated with natural climate variability might make it melt rapidly
213 in the summer owing to ice-albedo feedback. In the Community Climate System Model, version
214 3 events, anomalous ocean heat transport acts as this trigger. In one ensemble member, the area
215 of September ice decreases from about 6×10^6 km² to 2×10^6 km² in 10 years, resulting in an
216 essentially ice-free September by 2040. This result is not just an artifact of Community Climate
217 System Model, version 3: a number of other climate models show similar rapid ice loss.

218 These recent reductions in the extent and thickness of ice cover and the projections for its
219 further shrinkage necessitate a comprehensive investigation of the longer term history of Arctic
220 sea ice. To interpret present changes we need to understand the Arctic’s natural variability. A
221 special emphasis should be placed on the times of change such as the initiation of seasonal and
222 then perennial ice and the periods of its later reductions.

223

224 **8.3 Types of Paleoclimate Archives and Proxies for the Sea-Ice Record**

225

226 The past distribution of sea ice is recorded in sediments preserved on the sea floor and in

227 deposits along many Arctic coasts. Indirect information on sea-ice extent can be derived from
228 cores drilled in glaciers and ice sheets such as the Greenland ice sheet. Ice cores record
229 atmospheric precipitation, which is linked with air-sea exchanges in surrounding oceanic areas.
230 Such paleoclimate information provides a context within which the patterns and effects of the
231 current and future ice-reduced state of the Arctic can be evaluated.

232

233 **8.3.1 Marine Sedimentary Records**

234 The most complete and spatially extensive records of past sea ice are provided by sea-
235 floor sediments from areas that are or have been covered by floating ice. Sea ice affects
236 deposition of such sediments directly or indirectly through physical, chemical, and biological
237 processes. These processes and, thus, ice characteristics can be reconstructed from a number of
238 sediment proxies outlined below.

239 Sediment cores that represent the long-term history of sea ice embracing several million
240 years are most likely to be found in the deep, central part of the Arctic Ocean where the sea floor
241 was not eroded during periods of lower sea-level (and larger ice sheets). On the other hand, rates
242 of sediment deposition in the central Arctic Ocean are generally low, on the order of centimeters
243 or even millimeters per thousand years (Backman et al., 2004; Darby et al., 2006), so that
244 sedimentary records from these areas may not capture short-term variations in
245 paleoenvironments. In contrast, cores from Arctic continental margins usually represent a much
246 shorter time interval, less than 20 thousand years (k.y.) since the last glacial maximum, but they
247 sometimes provide high-resolution records that capture events on century or even decadal time
248 scales. Therefore, investigators need sediment cores from both the central basin and continental
249 margins of the Arctic Ocean to fully characterize sea-ice history and its relation to climate

250 change.

251 Until recently, and for logistical reasons, most cores relevant to the history of sea ice
252 cover were collected from low-Arctic marginal seas, such as the Barents Sea and the Norwegian-
253 Greenland Sea. There, modern ice conditions allow for easier ship operation, whereas sampling
254 in the central Arctic Ocean requires the use of heavy icebreakers. Recent advances in drilling the
255 floor of the Arctic Ocean—notably the first deep-sea drilling in the central Arctic Ocean (ACEX:
256 Backman et al., 2006) and the 2005 Trans-Arctic Expedition (HOTRAX: Darby et al., 2005)—
257 provide new, high-quality material from the Arctic Ocean proper with which to characterize
258 variations in ice cover during the late Cenozoic (the last few million years). A number of
259 sediment proxies have been used to predict the presence or absence of sea ice in down-core
260 studies. The most direct proxies are derived from sediment that melts out or drops from ice
261 owing to the following sequence of processes: (1) sediment is entrained in sea ice, (2) this ice is
262 transported by wind and surface currents to the sites of interest, and (3) sediment is released and
263 deposited. The size of sediment grains is commonly analyzed to identify ice-rafted debris. The
264 entrainment of sediments in sea ice mostly occurs along the shallow continental margins during
265 periods of ice freeze-up and is largely restricted to silt and clay-size sediments and rarely
266 contains grains larger than 0.1 millimeters (mm) (Lisitzin, 2002; Darby, 2003). Coarser ice-
267 rafted debris is mostly transported by floating icebergs rather than by regular sea ice
268 (Dowdeswell et al., 1994; Andrews, 2000). A small volume of coarse grains are shed from steep
269 coastal cliffs onto land-fast ice. To link sediment with sea ice may require investigations other
270 than measurement of grain size: for example, examination of shapes and surface textures of
271 quartz grains will help distinguish sea-ice-rafted and iceberg-rafted material (Helland and
272 Holmes, 1997; Dunhill et al., 1998). Detailed grain-size distributions say something about ice

273 conditions. For example, massive accumulation of silt-size grains (mostly larger than 0.01 mm)
274 may indicate the position of an ice margin where melting ice is the source of most sediment
275 (Hebbeln, 2000).

276 Some indicators (sediment provenance indicators) help to establish the source of
277 sediment and thus help to track ice drift. Especially telling is sediment carrying some diagnostic
278 peculiarity that is foreign to the site of deposition and that can be explained only by ice
279 transport—such as the particular composition of iron-oxide sand grains, which can be matched
280 with an extensive data base of source areas around the Arctic Ocean (Darby, 2003). Bulk
281 sediment analyzed by quantitative methods such as X-ray diffraction can also be used in those
282 instances where minerals that are “exotic” relative to the composition of the nearest terrestrial
283 sources are deposited. Quartz in Iceland marine cores (Moros et al., 2006; Andrews and Eberl,
284 2007) and dolomite (limestone rich in magnesium), in sediments deposited along eastern Baffin
285 Island and Labrador are two examples (Andrews et al., 2006).

286 Sediment cores commonly contain microscopic organisms that bear skeletons (for
287 example foraminifers, diatoms, and dinocysts). These organisms are widely used for deciphering
288 the past environments in which these organisms lived. Some marine planktonic organisms live in
289 or on sea ice or are otherwise associated with ice. Skeletons of such organisms in bottom
290 sediments indicate the condition of ice cover above the study site. Other organisms that live in
291 open water can be used to identify intervals of diminished ice. Remnants of ice-related algae
292 such as diatoms and dinocysts have been used to infer changes in the length of the ice-cover
293 season (Koç and Jansen, 1994; de Vernal and Hillaire-Marcel, 2000; Mudie et al., 2006; Solignac
294 et al., 2006). To quantify the relationship between these organisms and paleoenvironment, three
295 major research steps are required. The first is to develop a database of the percent compositions

296 in a certain group of organisms from water-column or surficial sea-floor samples that span a
297 wide environmental range. Second, various statistical methods must be used to express the
298 relationship (usually called “transfer functions”) between these compositions and key
299 environmental parameters, such as sea-ice duration and summer surface temperatures. Finally,
300 after sediment cores are analyzed and transfer functions are developed on the modern data sets,
301 they are then applied to the temporal (i.e., down-core) data. The usefulness of the transfer
302 functions, however, depends upon the accuracy of the environmental data, which is commonly
303 quite limited in Arctic areas.

304 Bottom dwelling (benthic) organisms in polar seas are also affected by ice cover because
305 it controls what food can reach the sea floor. The particular suite of benthic organisms preserved
306 in sediments can help to identify ice-covered sites. For instance, environments within the pack
307 ice produce very little organic matter, whereas environments on the margin of the ice produce a
308 great deal. Accordingly, species of bottom-dwelling organisms that prefer high fluxes of fresh
309 organic matter can indicate, for the Arctic shelves, the location of the ice margin (Polyak et al.,
310 2002; Jennings et al., 2004). In the central Arctic Ocean, benthic foraminifers and ostracodes
311 also offer a good potential for identifying ice conditions (Cronin et al., 1995; Wollenburg and
312 Kuhnt, 2000; Polyak et al., 2004).

313 The composition of organic matter in sediment, including specific organic compounds
314 (biomarkers), can also be used to reconstruct the environment in which it formed. For instance, a
315 specific biomarker, IP25, can be associated with diatoms living in sea ice (Belt et al., 2007). The
316 method has been tested by the analysis of sea-floor samples from the Canadian Arctic and is
317 being further applied to down-core samples for characterization of past ice conditions.

318 It is important to understand that although all of the above proxies have a potential for

319 identifying the former presence of or the seasonal duration of sea-ice cover, each of them has
320 limitations that complicate interpretations based on a single proxy. For instance, by use of a
321 dinocyst transfer function from East Greenland, it was estimated that the sea-ice duration is
322 about 2–3 months (Solignac et al., 2006) when in reality it is closer to 9 months (Hastings,
323 1960). Agreement among many proxies is required for a confident inference about variations in
324 sea-ice conditions. A thorough understanding of sea-ice history depends on the refining of sea-
325 ice proxies in sediment taken from strategically selected sites in the Arctic Ocean and along its
326 continental margins.

327

328 **8.3.2 Coastal Records**

329 In many places along the Arctic and subarctic coasts, evidence of the extent of past sea
330 ice is recorded in coastal-plain sediments, marine terraces, ancient barrier island sequences, and
331 beaches. Deposits in all of these formerly marine environments are now above water owing to
332 relative changes in sea level caused by eustatic, glacioisostatic, or tectonic factors. Although
333 these coastal deposits represent a limited time span and geographic distribution, they provide
334 critical information that can be compared with marine sediment records. The primary difference
335 between coastal and sea-floor records is in the type of fossils recovered. Notably, the spacious
336 coastal exposures (as compared with sediment cores) enable large paleontological material such
337 as plant remains, driftwood, whalebone, and relatively large mollusks to be recovered. These
338 items contribute valuable information about past sea-surface and air temperatures, the northward
339 expansions of subarctic and more temperate species, and the seasonality of past sea-ice cover.
340 For example, fossils preserved in these sequences document the dispersals of coastal marine
341 biota between the Pacific, Arctic, and North Atlantic regions, and they commonly carry telling

342 evidence of ice conditions. Plant remains in their turn provide a much-needed link to
343 documented information about past vegetation on land throughout Arctic and subarctic regions.
344 The location of the northern tree line that is presently controlled by the July 7°C mean isotherm
345 is a critical paleobotanic indicator for understanding ice conditions in the Arctic. Nowhere in the
346 Arctic do trees exist near shores lined with perennial sea ice; they thrive only in southerly
347 reaches of regions of seasonal ice. The combination of spatial relationships between marine and
348 terrestrial data allows a comprehensive reconstruction of past climate.

349

350 **8.3.3 Coastal Plains and Raised Marine Sequences**

351 A number of coastal plains around the Arctic are blanketed by marine sediment
352 sequences laid down during high sea levels. Although these sequences lie inland of coastlines
353 that today are bordered by perennial or by seasonal sea ice, they commonly contain packages of
354 fossil-rich sediments that provide an exceptional record of earlier warm periods. The most well-
355 documented sections are those preserved along the eastern and northern coasts of Greenland
356 (Funder et al., 1985, 2001), the eastern Canadian Arctic (Miller et al., 1985), Ellesmere Island
357 (Fyles et al., 1998), Meighen Island (Matthews, 1987; Matthews and Overden, 1990; Fyles et al.,
358 1991), Banks Island (Vincent, 1990; Fyles et al., 1994), the North Slope of Alaska (Carter et al.,
359 1986; Brigham-Grette and Carter, 1992); the Bering Strait (Kaufman and Brigham-Grette, 1993;
360 Brigham-Grette and Hopkins, 1995), and in the western Eurasian Arctic (Funder et al., 2002)
361 (Figure 8.3). In nearly all cases the primary evidence used to estimate the extent of past sea ice is
362 *in situ* molluscan and microfossil assemblages. These assemblages, from many sites, coupled
363 with evidence for the northward expansion of tree line during interglacial intervals (e.g., Funder
364 et al., 1985; Repenning et al., 1987; Bennike and Böcher, 1990; CAPE, 2006), provide an

365 essential view of past sea-ice conditions with direct implications for sea surface temperatures,
366 sea ice extent, and seasonality.

367

368 FIGURE 8.3 NEAR HERE

369

370 **8.3.4 Driftwood**

371 The presence or absence of sea ice may be inferred from the distribution of tree logs,
372 mostly spruce and larch found in raised beaches along the coasts of Arctic Canada (Dyke et al.,
373 1997), Greenland (Bennike, 2004), Svalbard (Haggbloom, 1982), and Iceland (Eggertsson, 1993).
374 Coasts with the highest numbers of driftwood probably were once near a sea-ice margin, whereas
375 coasts hosting more modest amounts were near either too much ice or too open water—neither of
376 which deliver much driftwood. Most of the logs found are attributed to a northern Russian
377 source, although some can be traced to northwest Canada and Alaska. Logs can drift only about
378 1 year before they become waterlogged and sink (Haggbloom, 1982). The logs are probably
379 derived from rivers flooded by spring snowmelt, which bring sediment and trees onto **landfast**
380 **ice** around the margin of the Arctic Basin. In areas other than Iceland, the glacial isostatic uplift
381 of the land has led to a staircase of raised beaches hosting various numbers of logs with time. An
382 extensive database catalogs these variations in the beaching of logs during the present
383 interglacial (Holocene). These variations have been associated with the growth and
384 disappearance of landfast sea ice (which restricts the beaching of driftwood) and changes in
385 atmospheric circulation with resulting changes in ocean surface circulation (Dyke et al., 1997).

386

387 **8.3.5 Whalebone**

388 Reconstructions of sea-ice conditions in the Canadian Arctic Archipelago have to date
389 been derived mainly from the distribution in space and time of marine mammal bones in raised
390 marine deposits (Dyke et al., 1996, 1999; Fisher et al., 2006). Several large marine mammals
391 have strong affinities for sea ice: polar bear, several species of seal, walrus, narwhal, beluga
392 (white) whale, and bowhead (Greenland right) whale. Of these, the bowhead has left the most
393 abundant, hence most useful, fossil record, followed by the walrus and the narwhal. Radiocarbon
394 dating of these remains has yielded a large set of results, largely available through Harington
395 (2003) and Kaufman et al. (2004).

396 Former sea-ice conditions can be reconstructed from bowhead whale remains because
397 seasonal migrations of the whale are dictated by the oscillations of the sea-ice pack. The species
398 is thought to have had a strong preference for ice-edge environments since the Pliocene (2.6–5.3
399 million years ago (Ma)), perhaps because that environment allows it to escape from its only
400 natural predator, the killer whale. The Pacific population of bowheads spends winter and early
401 spring along the ice edge in the Bering Sea and advances northward in the summer ice into the
402 Canadian Beaufort Sea region along the western edge of the Canadian Arctic Archipelago. The
403 Atlantic population spends winter and early spring in the northern Labrador Sea between
404 southwest Greenland and northern Labrador and advances northward in summer into the eastern
405 channels of the Canadian Arctic Archipelago. In normal summers, the Pacific and Atlantic
406 bowheads are prevented from meeting by a large, persistent, plug of sea-ice that occupies the
407 central region of the Canadian Arctic Archipelago; i.e., the central part of the Northwest Passage
408 (Figure 8.4). Both populations retreat southward upon autumn freeze-up.

409

410

FIGURE 8.4 NEAR HERE

411

412 However, the ice-edge environment is hazardous, especially during freeze-up, and
413 individuals or pods may become entrapped (as has been observed today). Detailed measurements
414 of fossil bowhead skulls (a proxy of age) now found in raised marine deposits allow a
415 reconstruction of their lengths (Dyke et al., 1996; Savelle et al., 2000). The distribution of
416 lengths compares very closely with the length distribution of the modern Beaufort Sea bowhead
417 population (Figure 8.5), indicating that the cause of death of many bowheads in the past was a
418 catastrophic process that affected all ages indiscriminately. This process can be best interpreted
419 as ice entrapment.

420

421

FIGURE 8.5 NEAR HERE

422

423 **8.3.6 Ice Cores**

424 Among paleoenvironmental archives, ice cores from glaciers and ice sheets have a
425 particular strength as a direct recorder of atmospheric composition, especially in the polar
426 regions, at a fine time resolution. The main issue is whether ice cores contain any information
427 about the past extent of sea ice. Such information may be inferred indirectly: for example, one
428 can imagine that higher temperatures recorded in an ice core are associated with reduced sea ice.
429 However, the real goal is to find a chemical indicator whose concentration is mainly controlled
430 by past sea-ice extent (or by a combination of ice extent and other climate characteristics that can
431 be deduced independently). Any such indicator must be transported for relatively long distances,
432 as by wind, from the sea ice or the ocean beyond. Such an indicator frozen into ice cores would
433 then allow ice cores to give an integrated view throughout a region for some time average, but

434 the disadvantage is that atmospheric transport can then determine what is delivered to the ice.

435 The ice-core proxy that has most commonly been considered as a possible sea ice
436 indicator is sea salt, usually estimated by measuring a major ion in sea salt, sodium (Na). In most
437 of the world's oceans, salt in sea water becomes an aerosol in the atmosphere by means of a
438 bubble bursting at the ocean surface, and formation of the aerosol is related to wind speed at the
439 ocean surface (Guelle et al., 2001). Expanding sea ice moves the source region (open ocean)
440 further from ice core sites, so that a first assumption is that a more extensive sea ice cover should
441 lead to less sea salt in an ice core.

442 A statistically significant inverse relationship between annual average sea salt in the
443 Penny Ice Cap ice core (Baffin Island) and the spring sea ice coverage in Baffin Bay (Grumet et
444 al., 2001) was found for the 20th century, and it has been suggested that the extended record
445 could be used to assess the extent of past sea ice in this region. However, the correlation
446 coefficient in this study was low, indicating that only about 7% of the variability in the
447 abundance of sea salt was directly linked to variability in position of sea ice. The inverse
448 relationship between sea salt and sea-ice cover in Baffin Bay was also reported for a short core
449 from Devon Island (Kinnard et al., 2006). However, more geographically extensive work is
450 needed to show whether these records can reliably reconstruct past sea ice extent.

451 For Greenland, the use of sea salt in this way seems even more problematic. Sea salt in
452 aerosol and snow throughout the Greenland plateau tends to peak in concentration in the winter
453 months (Mosher et al., 1993; Whitlow et al., 1992), when sea ice extent is largest, which already
454 suggests that other factors are more important than the proximity of open ocean. Most authors
455 carrying out statistical analyses on sea salt in Greenland ice cores in recent years have found
456 relationships with aspects of atmospheric circulation patterns rather than with sea ice extent

457 (Fischer, 2001; Fischer and Mieding, 2005; Hutterli et al., 2007). Sea-salt records from
458 Greenland ice cores have therefore been used as general indicators of storminess (inducing
459 production of sea salt aerosol) and transport strength (Mayewski et al., 1994; O'Brien et al.,
460 1995), rather than as sea ice proxies.

461 An alternative interpretation has arisen from study of Antarctic aerosol and ice cores,
462 where the sea ice surface itself can be a source of large amounts of sea-salt aerosol in coastal
463 Antarctica (Rankin et al., 2002); this relationship between sea salt and sea ice might also be
464 applicable at some sites in the Arctic (Rankin et al., 2005). Current ideas about the source of sea-
465 ice relate it to the production of new, thin ice. In the regions around Greenland and the nearby
466 islands, much of the sea ice is old ice that has been advected, rather than new ice. It therefore
467 seems unlikely that the method can easily be applied under present conditions (Fischer et al.,
468 2007). The complicated geometry of the oceans around Greenland compared with the radial
469 symmetry of Antarctica also poses problems in any interpretation. It is possible that under the
470 colder conditions of the last glacial period, new ice produced around Greenland may have led to
471 a more dominant sea-ice source, opening up the possibility that there may be a sea ice record
472 available within this period. However, there is no published basis on which to rely at the moment
473 (2008), and the balance of importance between salt production and salt transport in the Arctic
474 needs further investigation.

475 One other chemical (methanesulfonic acid, MSA) has been used as a sea-ice proxy in the
476 Antarctic (e.g., Curran et al., 2003). However, studies of MSA in the Arctic do not yet support
477 any simple statistical relationship with sea ice there (Isaksson et al., 2005).

478 In summary, sea salt in ice cores has the potential to add a well-resolved and regionally
479 integrated picture of the past extent of sea ice extent. At one site weak statistical evidence

480 supports a relationship between sea ice extent and sea salt. However, the complexities of aerosol
481 production and transport mean that no firm basis yet exists for using sea salt in ice cores to
482 estimate past sea-ice extent in the Arctic. Further investigation is warranted to establish whether
483 such proxies might be usable: investigators need a better understanding of the sources of proxies
484 in the Arctic region, further statistical study of the modern controls on their distribution, and
485 modeling studies to assess proxies' sensitivity to major changes in sea-ice extent.

486

487 **8.3.7 Historical Records**

488 Historical records may describe recent paleoclimatic processes such as weather and ice
489 conditions. The longest historical records of ice cover exist from ice-marginal areas that are more
490 accessible for shipping, as exemplified by a compilation for the Barents Sea covering four
491 centuries in variable detail (Vinje, 1999, 2001). Systematic records of the position of sea-ice
492 margin around the Arctic Ocean have been compiled for the period since 1870 (Walsh, 1978;
493 Walsh and Chapman, 2001). These sources vary in quality and availability with time. More
494 reliable observational data on ice concentrations for the entire Arctic are available since 1953,
495 and the most accurate data from satellite imagery is available since 1972 (Cavalieri et al., 2003).

496 Seas around Iceland provide a rare opportunity to investigate the ice record in a more
497 distant past because Iceland has for 1200 years recorded observations of drift ice (i.e., sea ice and
498 icebergs) following the settlement of the island in approximately 870 CE (Koch, 1945;
499 Bergthorsson, 1969; Ogilvie, 1984; Ogilvie et al., 2000). This long record has facilitated efforts
500 to quantify the changes in the extent and duration of drift ice around the Iceland coasts during the
501 last 1200 years (Koch, 1945; Bergthorsson, 1969). During times of extreme drift-ice incursions,
502 ice wraps around Iceland in a clockwise motion. Ice commonly develops off the northwest and

503 north coasts and only occasionally extends into southwest Iceland waters (Ogilvie, 1996).
504 Historical sources have been used to construct a sea-ice index that compares well with
505 springtime temperatures at a climate station in northwest Iceland (Figure 8.6).

506

507 **FIGURE 8.6 NEAR HERE**

508

509 **8.4 History of Arctic Sea-Ice Extent and Circulation Patterns**

510

511 **8.4.1 Pre-Quaternary History (Prior to ~2.6 Ma ago)**

512 The shrinkage of the perennial ice cover in the Arctic and predictions that it may
513 completely disappear within the next 50 years or even sooner (Holland et al., 2006a; Stroeve et
514 al., 2008) are especially disturbing in light of recent discoveries that sea ice in the Arctic has
515 persisted for the past 2 million years and may have originated several million years earlier
516 (Darby, 2008; Krylov et al., 2008). Until recently, evidence of long-term (million-year scale)
517 climatic history of the north polar areas was limited to fragmentary records from the Arctic
518 periphery. The ACEX deep-sea drilling borehole in the central Arctic Ocean (Backman et al.,
519 2006) provides new information about its Cenozoic history for comparison with circum-Arctic
520 records. Drilling results confirmed that about 50 Ma, during the Eocene Optimum (Figure 4.8 in
521 Chapter 4), the Arctic Ocean was considerably warmer than it is today, as much as 24°C at least
522 in the summers, and fresh-water subtropical aquatic ferns grew in abundance (Moran et al.,
523 2006). This environment is consistent with forests of enormous metasequoia that stood at the
524 same time on shores of the Arctic Ocean—such as on Ellesmere Island across lowlying delta
525 floodplains riddled with lakes and swamps (Francis, 1988; McKenna, 1980) Coarse grains

526 occurring in ACEX sediment as old as about 46 Ma indicate the possible onset of drifting ice and
527 perhaps even some glaciers in the Arctic during the cooling that followed the thermal optimum
528 (Moran et al., 2006; St. John, 2008). This cooling matches the timing of a large-scale
529 reorganization of the continents, notably the oceanic separation of Antarctica and of a sharp
530 decrease in atmospheric CO₂ concentration of more than 1,000 parts per million (ppm) (Pearson
531 and Palmer, 2000; Lowenstein and Demicco, 2006; also see Figure 4.2). However, in the Eocene
532 the ACEX site was at the margin of rather than in the center of the Arctic Ocean (O'Regan et al.,
533 2008) and therefore coarse grains may have been delivered to this site by rivers rather than by
534 drifting ice. The circum-Arctic coasts at this time were still occupied by rich, high-biomass
535 forests of redwood and by wetlands characteristic of temperate conditions (LePage et al., 2005;
536 Williams et al., 2003). Continued cooling, punctuated by an abrupt temperature decrease at the
537 Eocene-Oligocene boundary about 34 Ma, triggered massive Antarctic glaciation. It may have
538 also led to the increase in winter ice in the Arctic. This inference cannot yet be verified in the
539 central Arctic Ocean because the ACEX record contains no sediment deposited between about
540 44 to 18 Ma. Mean annual temperatures at the Eocene-Oligocene transition (about 33.9 Ma)
541 dropped from nearly 11°C to 4°C in southern Alaska (Wolfe, 1980, 1997) at this time, whereas
542 fossil assemblages and isotopic data in marine sediments along the coasts of the Beaufort Sea
543 suggest waters with a seasonal range between 1°C and 9°C (Oleinik et al., 2007). The first
544 glaciers may have developed in Greenland about the same time, on the basis of coarse grains
545 interpreted as iceberg-rafted debris in the North Atlantic (Eldrett et al., 2007). Sustained,
546 relatively warm conditions lingered during the early Miocene (about 23–16 Ma) when cool-
547 temperate metasequoia dominated the forests of northeast Alaska and the Yukon (White and
548 Ager, 1994; White et al., 1997), and the central Canadian Arctic Islands were covered in mixed

549 conifer-hardwood forests similar to those of southern Maritime Canada and New England today.
550 Such forests and associated wildlife would have easily tolerated seasonal sea ice, but they would
551 not have survived the harshness of perennial ice cover on the adjacent ocean (Whitlock and
552 Dawson, 1990).

553 A large unconformity (a surface in a sequence of sediments that represents missing
554 deposits, and thus missing time) in the ACEX record prevents us from characterizing sea-ice
555 conditions between about 44–18 Ma (Backman et al., 2008). Sediments overlying the
556 unconformity contain little ice-rafted debris, and they indicate a smaller volume of sea ice in the
557 Arctic Ocean at that time (St. John, 2008). Marked changes in Arctic climate in the middle
558 Miocene were concurrent with global cooling and the onset of Antarctic reglaciation (Figure 4.8
559 in Chapter 4). These changes may have been promoted by the opening of the Fram Strait
560 between the Eurasian and Greenland margins about 17 Ma, which allowed the modern circulation
561 system in the Arctic Ocean to develop (Jakobsson et al., 2007). Resultant cooling led to a change
562 from pine-redwood-dominated to larch-spruce-dominated floodplains and swamps at the Arctic
563 periphery at about 16 Ma as recorded, for example, on Banks Island by extensive peats with
564 stumps in growth position (Fyles et al., 1994; Williams, 2006). A combination of cooling and
565 increased moisture from the North Atlantic caused ice masses on and around Svalbard to grow
566 and icebergs to discharge into the eastern Arctic Ocean and the Greenland Sea at about 15 Ma
567 (Knies and Gaina, 2008). The source of sediment in the central Arctic Ocean changed between
568 13–14 Ma and indicates the likelihood that sea ice was now perennial (Krylov et al., 2008),
569 although the ice’s geographic distribution and persistence is not yet understood. Evidence of
570 perennial ice can be found in even older sediments, starting from at least 14 Ma (Darby, 2008).
571 Several pulses of more-abundant-than-normal ice-rafted debris in the late Miocene ACEX record

572 indicate further growth of sea ice (St. John, 2008). This interpretation is consistent a cooling
573 climate indicated by the spread of pine-dominated forests in northern Alaska (White et al., 1997).
574 On the other hand, paleobotanical evidence also suggests that throughout the late Miocene and
575 most of the Pliocene in at least some intervals perennial ice was severely restricted or absent.
576 Thus, extensive braided-river deposits of the Beaufort Formation (early to middle Pliocene,
577 about 5.3–3 Ma) that blanket much of the western Canadian Arctic Islands enclose abundant logs
578 and other woody detritus representing more than 100 vascular plants such as pine (2 and 5
579 needles) and birch, and dominated at some locations by spruce and larch (Fyles, 1990; Devaney,
580 1991). Although these floral remains indicate overall boreal conditions cooler than in the
581 Miocene, extensive perennial sea ice is not likely to have existed in the adjacent Beaufort Sea
582 during this time. This inference is consistent with the presence of the bivalve Icelandic Cyprine
583 (*Arctica islandica*) in marine sediments capping the Beaufort Formation on Meighen Island at
584 80°N and dated to the peak of Pliocene warming, about 3.2 Ma (Fyles et al., 1991). Foraminifers
585 in Pliocene deposits in the Beaufort-Mackenzie area are also characteristic of boreal but not yet
586 high-Arctic waters (McNeil, 1990), whereas the only known pre-Quaternary foraminiferal
587 evidence from the central Arctic Ocean indicates seasonally ice-free conditions in the early
588 Pliocene about 700 km north of the Alaskan coast (Mullen and McNeil, 1995).

589 Cooling in the late Pliocene profoundly reorganized the Arctic system: tree line retreated
590 from the Arctic coasts (White et al., 1997; Matthews and Telka, 1997), permafrost formed (Sher
591 et al., 1979; Brigham-Grette and Carter, 1992), and continental ice masses grew around the
592 Arctic Ocean—for example, the Svalbard ice sheet advanced onto the outer shelf (Knies et al.,
593 2002) and between 2.9–2.6 Ma ice sheets began to grow in North America (Duk-Rodkin et al.,
594 2004). The ACEX cores record especially large volumes of high ice-rafted debris in the Arctic

595 Ocean around 2 Ma (St. John, 2008). Despite the overall cooling, extensive warm intervals
596 during the late Pliocene and the initial stages of the Quaternary (about 2.4–3 Ma) are repeatedly
597 documented at the Arctic periphery from northwest Alaska to northeastern Greenland (Feyling-
598 Hanssen et al., 1983; Funder et al., 1985, 2001; Carter et al., 1986; Bennike and Böcher, 1990;
599 Kaufman, 1991; Brigham-Grette and Carter, 1992). For example, beetle and plant macrofossils
600 in the nearshore high-energy sediments of the upper Kap København Formation on northeast
601 Greenland, dated about 2.4 Ma, mimic paleoenvironmental conditions similar to those of
602 southern Labrador today (Funder et al., 1985; 2001; Bennike and Böcher, 1990). At the same
603 time, marine conditions were distinctly Arctic but, analogous with present-day faunas along the
604 Russian coast, open water must have existed for 2 or 3 months in the summer. These results
605 imply that summer sea ice in the entire Arctic Ocean was probably much reduced.

606 A more complete history of perennial versus seasonal sea ice and ice-free intervals during
607 the past several million years requires additional sedimentary records distributed throughout the
608 Arctic Ocean and a synthesis of sediment and paleobiological evidence from both land and sea.
609 This history will provide new clues about the stability of the Arctic sea ice and about the
610 sensitivity of the Arctic Ocean to changing temperatures and other climatic features such as snow
611 and vegetation cover.

612

613 **8.4.2 Quaternary Variations (the past 2.6 Ma)**

614 The Quaternary period of Earth's history during the past 2.6 million years (m.y.) or so is
615 characterized by overall low temperatures and especially large swings in climate regime (Figure
616 4.9 in Chapter 4). These swings are related to changes in insolation (incoming solar radiation)
617 modulated by Earth's orbital parameters with periodicities of tens to hundreds of thousand years

618 (see Chapter 4 for more detail). During cold periods when large ice masses are formed, such as
619 during the Quaternary, these variations are amplified by powerful feedbacks due to changes in
620 the albedo (reflectivity) of Earth's surface and concentration of greenhouse gases in the
621 atmosphere. Quaternary climate history is composed of cold intervals (glacials) when very large
622 ice sheets formed in northern Eurasia and North America and of interspersed warm intervals
623 (interglacials), such as the present one, referred to as the Holocene (which began about 11.5
624 thousand years ago (ka). Temperatures at Earth's surface during some interglacials were similar
625 to or even somewhat warmer than those of today; therefore, climatic conditions during those
626 times can be used as approximate analogs for the conditions predicted by climate models for the
627 21st century (Otto-Bliesner et al., 2006; Goosse et al., 2007). One of the biggest questions in this
628 respect is to what degree sea-ice cover was reduced in the Arctic during those warm intervals.
629 This issue is insufficiently understood because interglacial deposits at the Arctic margins are
630 exposed only in fragments (CAPE, 2006) and because sedimentary records from the Arctic
631 Ocean generally have only low resolution. Even the age assigned to sediments that appear to be
632 interglacial is commonly problematic because of the poor preservation of fossils and various
633 stratigraphic complications (e.g., Backman et al., 2004). A better understanding has begun to
634 emerge from recent collections of sediment cores from strategic sites drilled in the Arctic Ocean
635 such as ACEX (Backman et al., 2006) and HOTRAX (Darby et al., 2005). The severity of ice
636 conditions (widespread, thick, perennial ice) during glacial stages is indicated by of the extreme
637 rarity of biological remains in cool-climate sediment layers and possible non-deposition intervals
638 due to especially solid ice (Polyak et al., 2004; Darby et al., 2006; Cronin et al., 2008). In
639 contrast, interglacials are characterized by higher marine productivity that indicates reduced ice
640 cover. In particular, planktonic foraminifers typical of subpolar, seasonally open water lived in

641 the area north of Greenland during the last interglacial (marine isotope stage 5e), 120–130 ka
642 (Figure 8.7, Nørgaard-Pedersen et al., 2007a,b). Given that this area is presently characterized by
643 especially thick and widespread ice, the entire Arctic Ocean may have been free of summer ice
644 cover in the interval 120–130 ka. Investigators need to carefully examine correlative sediments
645 throughout the Arctic Ocean to determine whether the observed low-ice or possibly ice-free
646 conditions north of Greenland were merely local or extended around the basin. Some intervals in
647 sediment cores from various sites in the central Arctic have been reported to contain subpolar
648 microfauna (e.g., Herman, 1974; Clark et al., 1990), but their age was not well constrained. New
649 sediment core studies are needed to place these intervals in the coherent stratigraphic context and
650 to reconstruct corresponding ancient ice conditions. This task is especially important as only
651 those records from the central Arctic Ocean can provide direct evidence for ocean-wide ice-free
652 water.

653

654 **FIGURE 8.7 NEAR HERE**

655

656 Some coastal exposures of interglacial deposits such as marine isotope stage 11 (about
657 400 ka) and 5e (about 120–130 ka) also indicate water temperatures warmer than present and,
658 thus, reduced ice. For example, deposits of the last interglacial on the Alaskan coast of the
659 Chukchi Sea (the so-called Pelukian transgression) contain some fossils of species that are
660 limited today to the northwest Pacific, whereas inter-tidal snails found near Nome, just slightly
661 south of the Bering Strait, suggest that the coast here may have been annually ice free (Brigham-
662 Grette and Hopkins, 1995; Brigham-Grette et al., 2001). On the Russian side of the Bering Strait,
663 foraminifer assemblages suggest that coastal waters were fairly warm, like those in the Sea of

664 Okhotsk and Sea of Japan (Brigham-Grette et al., 2001). Deposits of the same age along the
665 northern Arctic coastal plain show that at least eight mollusk species extended their distribution
666 ranges well into the Beaufort Sea (Brigham-Grette and Hopkins, 1995). Deposits near Barrow
667 include at least one mollusk and several ostracode species known now only from the North
668 Atlantic. Taken together, these findings suggest that during the peak of the last interglacial, about
669 120–130 ka, the winter limit of sea ice did not extend south of the Bering Strait and was located
670 perhaps 800 km north of historical limits (such as on Figure 8.1), whereas summer sea-surface
671 temperatures were warmer than present through the Bering Strait and into the Beaufort Sea.

672

673 **8.4.3 The Holocene (the most recent 11.5 ka)**

674 The present interglacial that has lasted approximately 11.5 k.y. is characterized by much
675 more paleoceanographic data than earlier warm periods, because Holocene deposits are
676 ubiquitous on continental shelves and along many coastlines. Owing to relatively high
677 sedimentation rates at continental margins, ice drift patterns can be constructed on sub-millennial
678 scales from some sedimentary records. Thus, the periodic influx of large numbers of iron oxide
679 grains from specific sources, as into the Siberian margin-to-sea-floor area north of Alaska, has
680 been linked to a certain mode of the atmospheric circulation pattern (Darby and Bischof, 2004).
681 If this link is proven, it will signify the existence of longer term atmospheric cycles in the Arctic
682 than the decadal Arctic Oscillation observed during the last century (Thompson and Wallace,
683 1998).

684 Many proxy records indicate that early Holocene temperatures were warmer than today
685 and that the Arctic contained less ice. This climate is consistent with a higher intensity of
686 insolation that peaked about 11 ka owing to Earth's orbital variations. Evidence of warmer

687 temperatures appears in many paleoclimatic records from the high Arctic—Svalbard and
688 northern Greenland, northwestern North America, and eastern Siberia (Kaufman et al., 2004;
689 Blake, 2006; Fisher et al., 2006; Funder and Kjær, 2007). Decreased sea-ice cover in the western
690 Arctic during the early Holocene has also been inferred from high sodium concentrations in the
691 Penny Ice Cap of Baffin Island (Fisher et al., 1998) and the Greenland ice sheet (Mayewski et
692 al., 1994), although the implications of salt concentration is yet to be defined. Areas that were
693 affected by the extended melting of the Laurentide ice sheet, especially the northeastern sites in
694 North America and the adjacent North Atlantic, show more complex patterns of temperature and
695 ice distribution (Kaufman et al., 2004).

696 An extensive record has been compiled from bowhead whale findings along the coasts of
697 the Canadian Arctic Archipelago straits (Dyke et al., 1996, 1999; Fisher et al., 2006).

698 Understanding the dynamics of ice conditions in this region is especially important for modern-
699 day considerations because ice-free, navigable straits through the Canadian Arctic Archipelago
700 will provide new opportunities for shipping lanes. The current set of radiocarbon dates on
701 bowheads from the Canadian Arctic Archipelago coasts is grouped into three regions: western,
702 central, and eastern (Figure 8.8). The central region today is the area of normally persistent
703 summer sea ice; the western region is within the summer range of the Pacific bowhead; the
704 eastern region is within the summer range of the Atlantic bowhead. These three graphs allow us
705 to draw the following conclusions:

- 706 1. Bowhead bones have been most commonly found in all three regions in early Holocene
707 (10–8 ka) deposits. At that time Pacific and Atlantic bowheads were able to intermingle
708 freely along the length of the Northwest Passage indicating at least periodically ice-free
709 summers.

- 710 2. Following an interval (8–5 ka) containing fewer bones, abundant bowhead bones have
711 been found in deposits in the eastern channels during the middle Holocene (5–3 ka). At
712 times, the Atlantic bowheads penetrated the central region, particularly 4.5–4.2 ka. The
713 Pacific bowhead apparently did not extend its range at this time.
- 714 3. A final peak of bowhead bones has been found about 1.5–0.75 ka in all three regions,
715 suggesting an open Northwest Passage during at least some summers. During this interval
716 the bowhead-hunting Thule Inuit (Eskimo) expanded eastward out of the Bering Sea
717 region and ultimately spread to Greenland and Labrador.
- 718 4. The decline of bowhead abundances during the last few centuries is evident in all three
719 graphs. Thule bowhead hunters abandoned the high Arctic of Canada and Greenland
720 during the Little Ice Age cooling (around 13th to 19th centuries) and Thule living in
721 more southern Arctic regions increasingly focused on alternate resources.

722
723 FIGURE 8.8 NEAR HERE
724

725 On the basis of the summer ice melt record of the Agassiz Ice Cap (Fisher et al., 2006),
726 summer temperatures that accompanied the early Holocene bowhead maximum are estimated at
727 about 3°C above mid-20th century conditions, when July mean daily temperatures along the
728 central Northwest Passage were about 5°C. Unless other processes, such as a different ocean
729 circulation pattern, were also forcing greater summer sea-ice clearance in the early Holocene, the
730 value of 3°C is an upper bound on the amount of warming necessary to clear the Northwest
731 Passage region of summer sea ice. At times during the middle and late Holocene (especially 4.5–
732 4.2 ka) the threshold condition was approached and, at least briefly, met, as indicated by Atlantic

756

FIGURE 8.10 NEAR HERE

757

758 Along the North Greenland coasts, isostatically raised staircases of wave-generated beach
759 ridges (Figure 8.11) document seasonally open water (Funder and Kjær, 2007). Large numbers
760 of striated boulders in and on the marine sediments also indicate that the ocean was open enough
761 for icebergs to drift along the shore and drop their loads. Presently the North Greenland coastline
762 is permanently surrounded by pack ice, and rare icebergs are locked up in sea ice. Radiocarbon-
763 dated mollusk shells from beach ridges show that the beach ridges were formed in the early
764 Holocene, within the interval from about 8.5–6 ka, which is progressively shorter from south to
765 north. These wave-generated shores and abundant iceberg-deposited boulders indicate the
766 possibility that the adjacent Arctic Ocean was free of sea ice in summer at this time.

767

768 A somewhat different history of ice extent in the Holocene emerges from the northern
769 North Atlantic and Nordic seas, exemplified by the Iceland margin. A 12,000 year record of
770 quartz content in shelf sediment, which is used in this area as a proxy for the presence of drift ice
771 (Eiriksson et al., 2000), has been produced for a core (MD99-2269) from the northern Iceland
772 shelf. The record has a resolution of 30 years per sample (Moros et al., 2006); these results are
773 consistent with data obtained from 16 cores across the northwestern Iceland shelf (Andrews,
774 2007). These data show a minimum in quartz and, thus, ice cover at the end of deglaciation,
775 whereas the early Holocene area of ice increased and then reached another minimum around 6
776 ka, after which the content of quartz steadily rose (Figure 8.12). The lagged Holocene optimum
777 in the North Atlantic in comparison with high Arctic records can be explained by the nature of
778 oceanic controls on ice distribution. In particular, the discharge of glacial meltwater from the
remains of the Laurentide ice sheet slowed the warming in the North Atlantic region in the early

779 Holocene (Kaufman et al., 2004). Additionally, oceanic circulation seesawed between the eastern
780 and western regions of the Nordic seas throughout much of the Holocene. For example, in the
781 Norwegian Sea the Holocene ice-rafting peaked in the mid-Holocene, 6.5–3.7 ka (Risebrobakken
782 et al., 2003), and changes in Earth’s orbit forced decreasing summer temperatures and decreased
783 seasonality (Moros et al., 2004). By contrast, the middle Holocene is a relatively warm period off
784 East Greenland, and it received a strong subsurface current of Atlantic Water around 6.5–4 ka,
785 while ice-rafted debris was low (Jennings et al., 2002). These patterns are consistent with
786 modern marine and atmospheric temperatures that commonly change in opposite directions on
787 the eastern and western side of the North Atlantic (“seesaw effect” of van Loon and Rogers,
788 1978).

789

790 **FIGURE 8.12 NEAR HERE**

791

792 The Neoglacial cooling of the last few thousand years is considered overall to be related
793 to decreasing summer insolation (Koç and Jansen, 1994). However, high-resolution climate
794 records reveal greater complexity in the system—changes in seasonality and links with
795 conditions in low latitudes and southern high latitudes (e.g., Moros et al., 2004). Variations in the
796 volumes of ice-rafted debris indicate several cooling and warming intervals during Neoglacial
797 time, similar to the so-called “Little Ice Age” and “Medieval Warm Period” cycles of greater and
798 lesser areas of sea ice (Jennings and Weiner, 1996; Jennings et al., 2002; Moros et al., 2006;
799 Bond et al., 1997). Polar Water excursions have been reconstructed as multi-century to decadal-
800 scale variations superimposed on the Neoglacial cooling at several sites in the subarctic North
801 Atlantic (Andersen et al., 2004; Giraudeau et al., 2004; Jennings et al., 2002). In contrast, a

802 decrease in drift ice during the Neoglacial is documented for areas influenced by the North
803 Atlantic Current, possibly indicating a warming in the eastern Nordic Seas (Moros et al., 2006).
804 A seesaw climate pattern has been evident between seas adjacent to West Greenland and Europe.
805 For instance, warm periods in Europe around 800–100 BC and 800–1300 AD (Roman and the
806 Medieval Warm Periods) were cold periods on West Greenland because little warm Atlantic
807 Water fed into the West Greenland Current. Moreover, a cooling interval in western Europe
808 (during the Dark Ages) correlated with increased meltwater —and thus warming—on West
809 Greenland (Seidenkrantz et al., 2007).

810 Bond et al. (1997, 2001) suggested that cool periods manifested as past expansions of
811 drift ice and ice-rafted debris (most notably, hematite-stained quartz grains) in the North Atlantic
812 punctuated deglacial and Holocene records at intervals of about 1500 years and that these drift
813 ice events were a result of climates that cycled independently of glacial influence. Bond et al.
814 (2001) concluded that peak volumes of Holocene drift ice resulted from southward expansions of
815 polar waters that correlated with times of reduced solar output. This conclusion suggests that
816 variations in the Sun’s output is linked to centennial- to millennial-scale variations in Holocene
817 climate through effects on production of North Atlantic Deep Water. However, continued
818 investigation of the drift ice signal indicates that although the variations reported by Bond et al.
819 (2001) may record a solar influence on climate, they likely do not pertain to a simple index of
820 drift ice (Andrews et al., 2006). In addition, those cooling events prior to the Neoglacial interval
821 may stem from deglacial meltwater forcing rather than from southward drift of Arctic ice
822 (Giraudeau et al., 2004; Jennings et al., 2002). In an effort to test the idea of solar forcing of
823 1500 year cycles in Holocene climate change, Turney et al. (2005) compared Irish tree-ring-
824 derived chronologies and radiocarbon activity, a proxy for solar activity, with the Holocene drift-

825 ice sequence of Bond et al. (2001). They found a dominant 800-year cycle in moisture, reflecting
826 atmospheric circulation changes during the Holocene but no link with solar activity.

827 Despite many records from the Arctic margins indicating considerably reduced ice
828 covering the early Holocene, no evidence of the decline of perennial ice cover has been found in
829 sediment cores from the central Arctic Ocean. Arctic Ocean sediments contain some ice-rafted
830 debris interpreted to arrive from distant shelves requiring more than 1 year of ice drift (Darby
831 and Bischof, 2004). One explanation is that the true record of low-ice conditions has not yet been
832 found because of low sedimentation rates and stratigraphic uncertainties. Additional
833 investigation of cores by use of many proxies with highest possible resolution is needed to verify
834 the distribution of ice in the Arctic during the warmest phase of the current interglacial.

835

836 **8.4.4 Historical Period**

837 Arctic paleoclimate records that contain proxies such as lake and marine sediments, trees,
838 and ice cores indicate that from the mid-19th to late 20th century the Arctic warmed to the
839 highest temperatures in at least four centuries (Overpeck et al., 1997). Subglacial material
840 exposed by retreating glaciers in the Canadian Arctic indicates that modern temperatures are
841 warmer than any time in at least the past 1600 years (Anderson et al., 2008). Paleoclimatic proxy
842 records of the last two centuries agree well with hemispheric and global data (including
843 instrumental measurements) (Mann et al., 1999; Jones et al., 2001). The composite record of ice
844 conditions for Arctic ice margins since 1870 shows a steady retreat of seasonal ice since 1900; in
845 addition, the retreat of both seasonal and annual ice has accelerated during the last 50 years
846 (Figure 8.13) (Kinnard et al., 2008). The latter observations are the most reliable for the entire
847 data set and are based on satellite imagery since 1972. Patterns of ice-margin retreat differ

848 between different periods and regions of the Arctic, but the overall trend in ice is down: the
849 current decline of the Arctic sea-ice cover is much larger than decadal-scale climatic and
850 hydrographic periodic variations (e.g., Polyakov et al., 2005; Steele et al., 2008). This
851 remarkable warming and associated ice shrinkage is especially anomalous because orbitally
852 driven insolation has been decreasing steadily since its maximum at 11 ka, and it is now near its
853 minimum in the 21 k.y. precession cycle (e.g., Berger and Loutre, 2004)—and which should lead
854 to climate cooling.

855

856 **FIGURE 8.13 NEAR HERE**

857

858 **8.5 Synopsis**

859

860 Geological data indicate that the history of Arctic sea ice is closely linked with
861 temperature changes. Sea ice in the Arctic Ocean may have appeared as early as 46 Ma, after the
862 onset of a long-term climatic cooling related to a reorganization of the continents and subsequent
863 formation of large ice sheets in polar areas. Year-round ice in the Arctic possibly developed as
864 early as 13–14 Ma, in relation to a further overall cooling in climate and the establishment of the
865 modern hydrographic circulation in the Arctic Ocean. Nevertheless, extended seasonally ice-free
866 periods were likely until the onset of large-scale Quaternary glaciations in the Northern
867 Hemisphere approximately 2.5 Ma. These glaciations were likely to have been accompanied by a
868 fundamental increase in the extent and duration of sea ice. Ice may have been less prevalent
869 during Quaternary interglacials, and the Arctic Ocean even may have been seasonally ice free
870 during the warmest interglacials (owing to changes in insolation modulated by variations in

871 Earth's orbit that operate on time scales of tens to hundred thousand years). Reduced-ice
872 conditions are inferred, for example, for the previous interglacial and the onset of the current
873 interglacial, about 130 and 10 ka. These low-ice periods can be used as ancient analogs for future
874 conditions expected from the marked ongoing loss of Arctic ice cover. On time scales of
875 thousands and hundreds of years, patterns of ice circulation vary somewhat; this feature is not yet
876 well understood, but large periodic reductions in ice cover at these time scales are unlikely.
877 Recent historical observations suggest that ice cover has consistently shrunk since the late 19th
878 century and that shrinking has accelerated during the last several decades to produce the largest
879 ice reduction in at least the last few thousand years. This ice loss appears to be unrelated to
880 natural climatic and hydrographic variability on decadal time scales and longer term orbital
881 insolation changes.

882 These conclusions underscore the immense magnitude and unprecedented nature of the
883 current ice loss and dictate the urgent need for a comprehensive investigation of links and the
884 development of models that will accurately predict the future state of the Arctic. The latter task
885 in its turn requires realistic boundary conditions verified by paleoclimatic data.

886 **Chapter 8 Figure Captions**

887

888 **Figure 8.1** Northern ocean currents and extent of sea ice extent. UNEP/GRID-Arendal
889 Maps and Graphics Library. Dec 97. UNEP/GRID-Arendal. 19 Feb 2008. Philippe Rekacewicz,
890 UNEP/GRID-Arendal) http://maps.grida.no/go/graphic/ocean_currents_and_sea_ice_extent.

891

892 **Figure 8.2** Extent of Arctic sea ice in September, 1979–2007. The linear trend (trend line
893 shown in blue) including 2007 shows a decline of 10% per decade (courtesy National Snow and
894 Ice Data Center, Boulder, Colorado).

895

896 **Figure 8.3** Key marine sedimentary sequences exposed at the coasts of Arctic North
897 America and Greenland.

898

899 **Figure 8.4** Typical late 20th century summer ice conditions in the Canadian Arctic
900 Archipelago.

901

902 **Figure 8.5** The reconstructed lengths of Holocene bowhead whales on the basis of skull
903 measurements (485 animals) and mandible measurements (an additional 4 animals) (Savelle, et
904 al., 2000). This distribution is very similar to the distribution of lengths in living Pacific bowhead
905 whales; thus, past whale strandings affected all age classes.

906

907 **Figure 8.6** The sea-ice index on the Iceland shelf plotted against springtime air

908 temperatures in northwest Iceland that are affected by the distribution of ice in this region (from
909 Ogilvie, 1996). The two correlate well.

910

911 **Figure 8.7** Planktonic foraminiferal record, core GreenICE-11, north of Greenland (from
912 Nørgaard-Pedersen et al., 2007b). Note high numbers of a subpolar planktonic foraminifer *T.*
913 *quinqueloba* during the last interglacial, marine isotopic stage (MIS) 5e; they indicate warm
914 temperatures or reduced-ice conditions (or both) north of Greenland at that time.

915

916 **Figure 8.8** Distribution of radiocarbon ages (in thousands of years) of bowhead whales
917 in three regions of the Canadian Arctic Archipelago (data from Dyke et al., 1996; Savelle et al.,
918 2000).

919

920 **Figure 8.9** Distribution of radiocarbon ages of Holocene driftwood on the shores of
921 Baffin Bay (from Dyke et al., 1997).

922

923 **Figure 8.10** Reconstruction of the duration of ice cover (months per year) in northern
924 Baffin Bay during the Holocene on the basis of dinocyst assemblages (from Levac et al., 2001).

925

926 **Figure 8.11** Aerial photo (left) of wave-generated beach ridges (BR) at Kap Ole
927 Chiewitz, 83°25'N., northeast Greenland. D1–D4 are raised deltas. The oldest, D1, is dated about
928 10 ka whereas D4 is the modern delta. Only D3 is associated with wave activity. Beach ridges

929 were formed about 8.5–6 ka. The photograph on the right shows the upper beach ridge.

930

931 **Figure 8.12** Variations in the percentage of quartz (a proxy for drift ice) in Holocene
932 sediments from the northern Iceland shelf (from Moros et al., 2006). BP, before present.

933

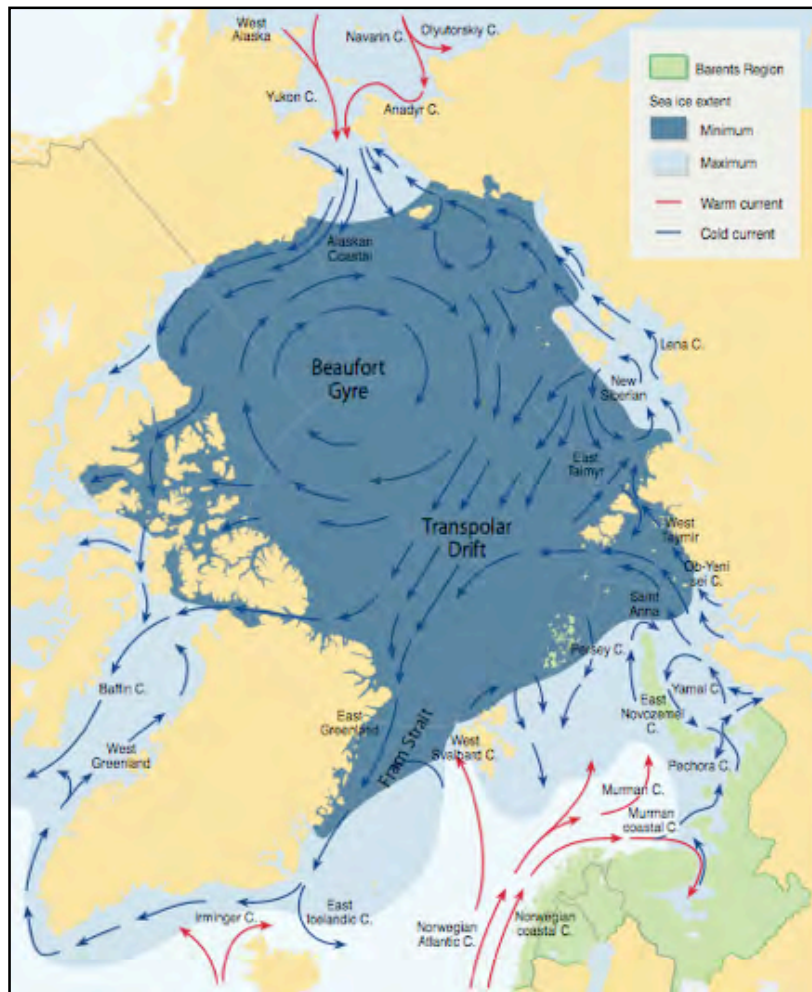
934 **Figure 8.13** Total sea-ice extent time series, 1870–2003 (from Kinnard et al., 2008).
935 Green lines: maximal extent. Blue lines: minimal extent. Thick lines are robust spline functions
936 that highlight low-frequency changes. Vertical dotted lines separate the three periods for which
937 data sources changed fundamentally: earliest, 1870–1952, observations of differing accuracy and
938 availability; intermediate, 1953–1971, generally accurate hemispheric observations; most recent,
939 1972–2003, satellite period, best accuracy and coverage.

940

941

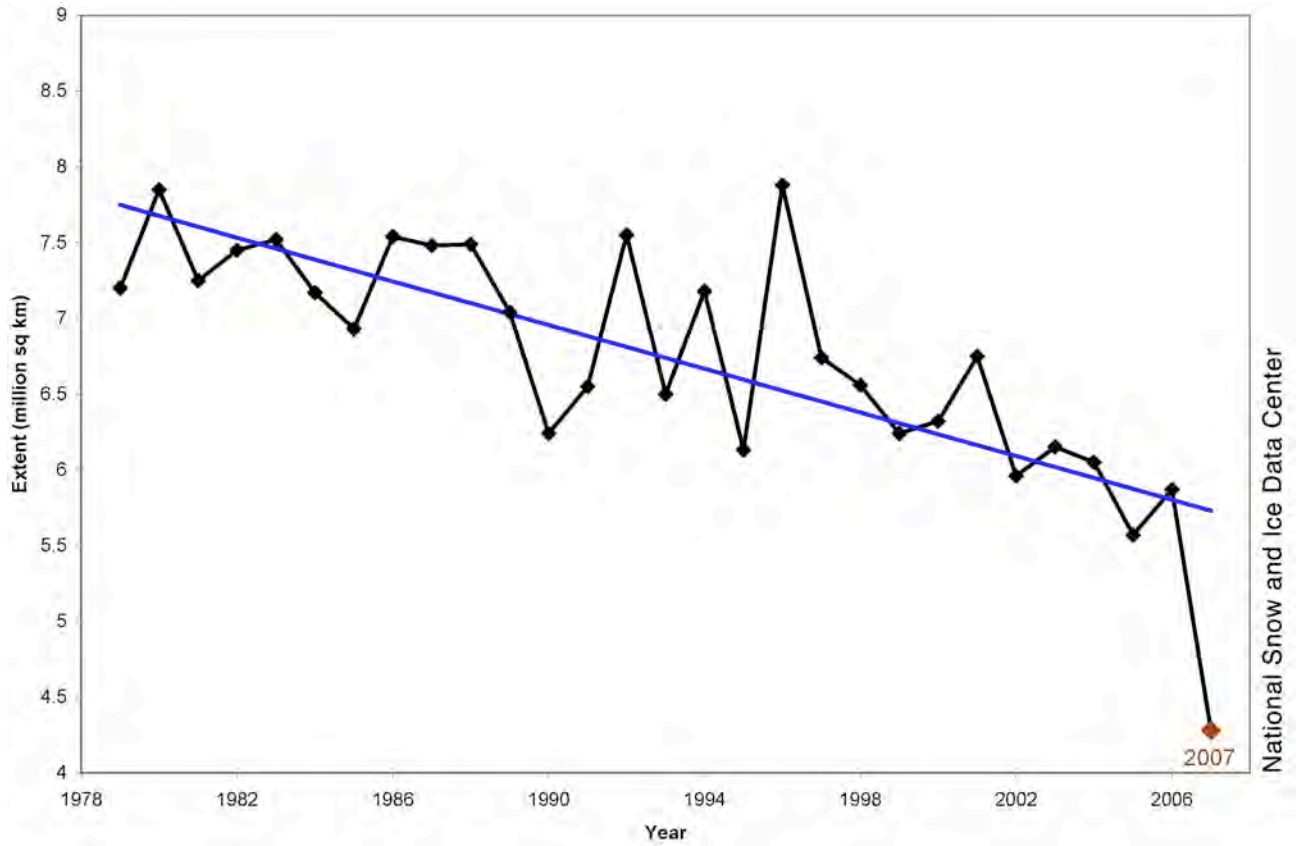
941

942



943 **Figure 8.1.** Northern ocean currents and extent of sea ice extent. UNEP/GRID-Arendal Maps
 944 and Graphics Library. Dec 97. UNEP/GRID-Arendal. 19 Feb 2008. Philippe Rekacewicz,
 945 UNEP/GRID-Arendal) http://maps.grida.no/go/graphic/ocean_currents_and_sea_ice_extent.

946



947

948 **Figure 8.2.** Extent of Arctic sea ice in September, 1979–2007. The linear trend (trend line shown
 949 in blue) including 2007 shows a decline of 10% per decade (courtesy National Snow and Ice
 950 Data Center, Boulder, Colorado).

951

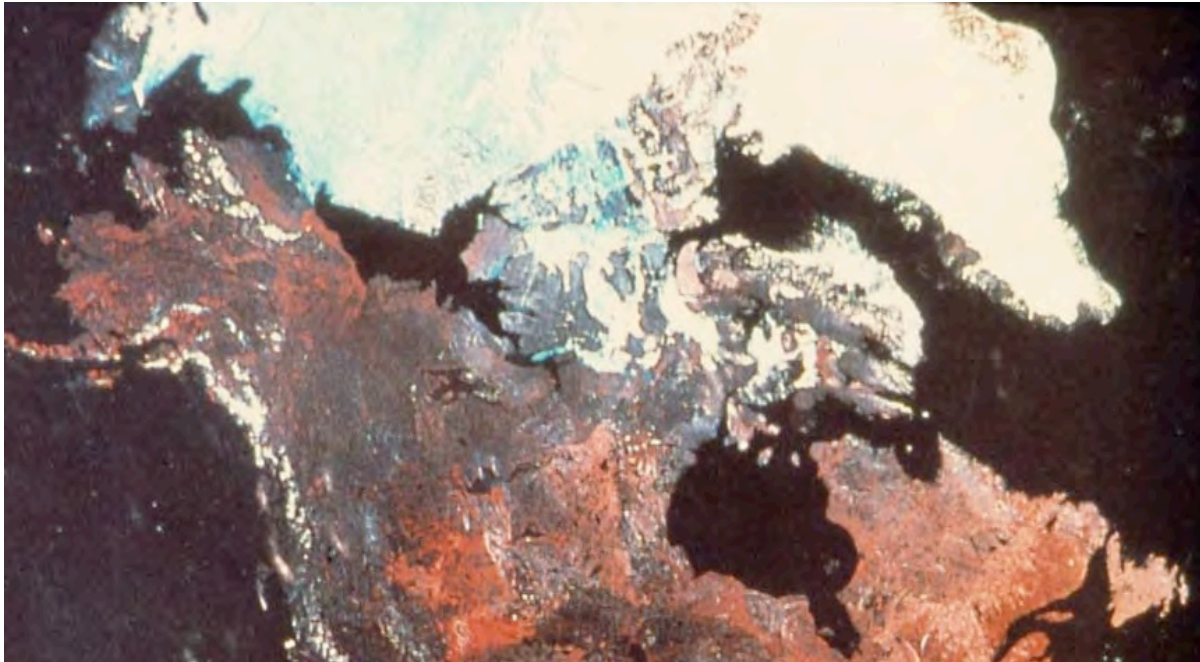
952



953 **Figure 8.3.** Key marine sedimentary sequences exposed at the coasts of Arctic North America
954 and Greenland.

955

955

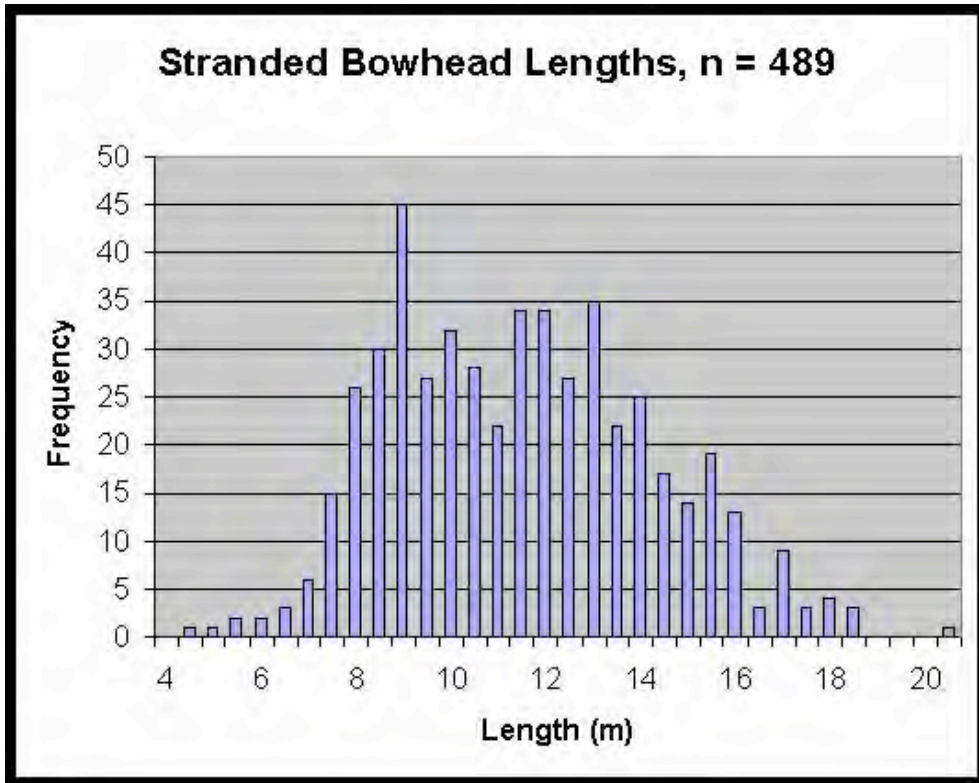


956

957 **Figure 8.4.** Typical late 20th century summer ice conditions in the Canadian Arctic Archipelago.

958

958

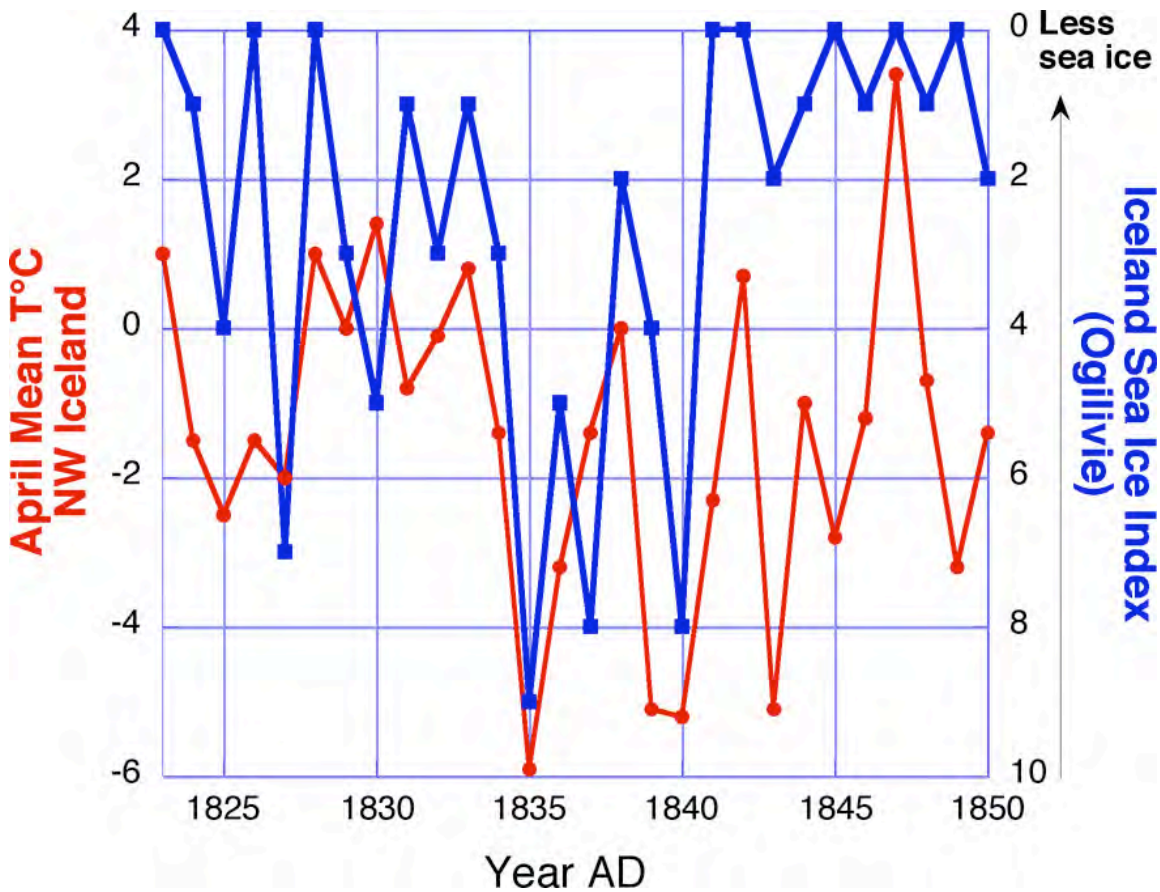


959

960 **Figure 8.5.** The reconstructed lengths of Holocene bowhead whales based on skull
 961 measurements (485 animals) and mandible measurements (an additional 4 animals) (Savelle, et
 962 al., 2000). This distribution is very similar to the lengths of living Pacific bowheads, indicating
 963 that past strandings affected all age classes.

964

964



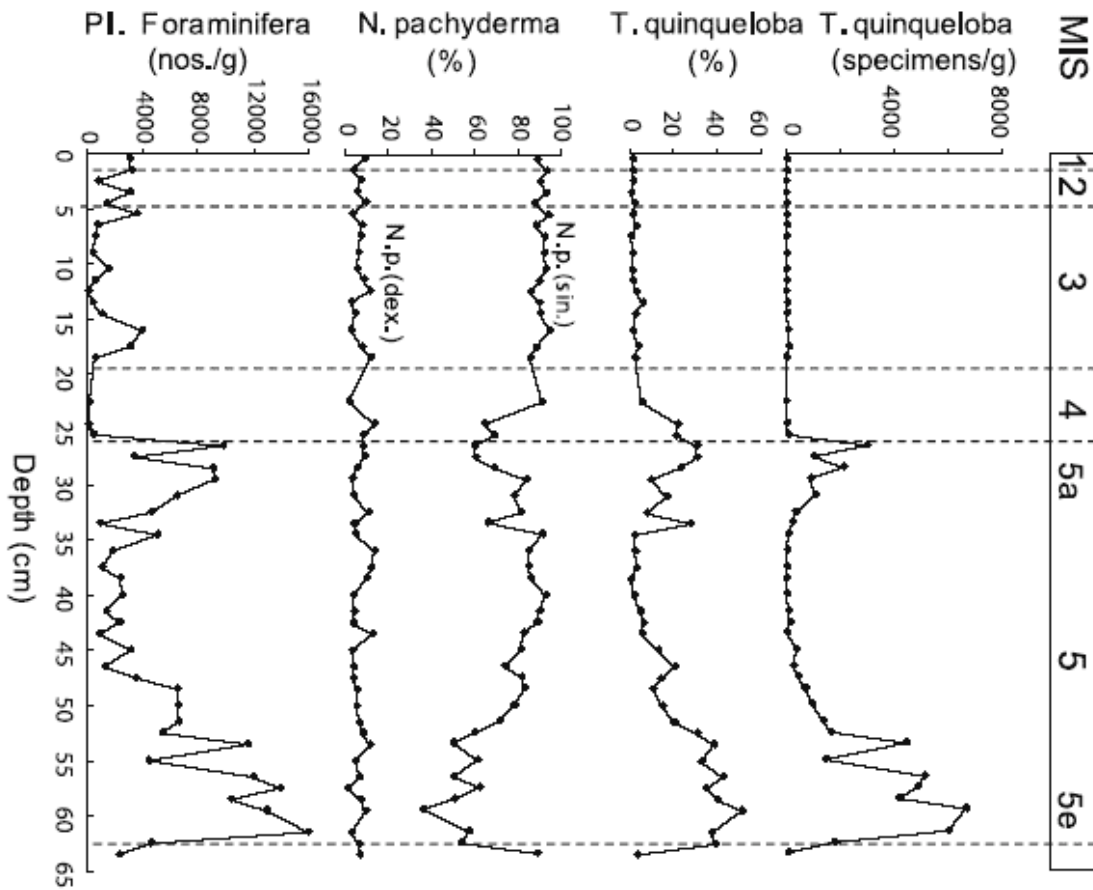
965

966 **Figure 8.6.** The sea-ice index on the Iceland shelf plotted against springtime air temperatures in
 967 northwest Iceland that are affected by the distribution of ice in this region (from Ogilvie, 1996).

968 The two correlate well.

969

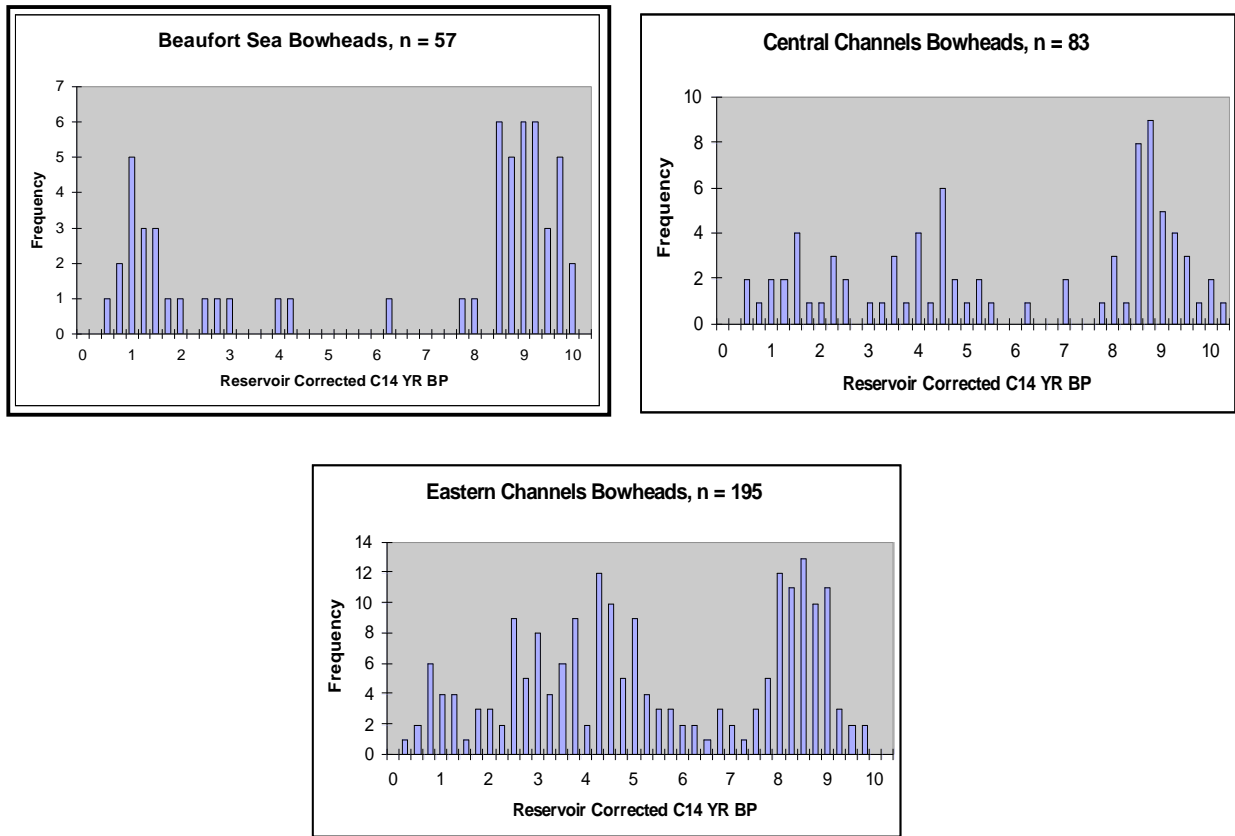
969



970

971 **Figure 8.7.** Planktonic foraminiferal record, core GreenICE-11, north of Greenland (from
 972 Nørgaard-Pedersen et al., 2007b). Note high numbers of a subpolar planktonic foraminifer *T.*
 973 *quinqueloba* during the last interglacial, marine isotopic stage (MIS) 5e; they indicate warm
 974 temperatures or reduced-ice conditions (or both) north of Greenland at that time.

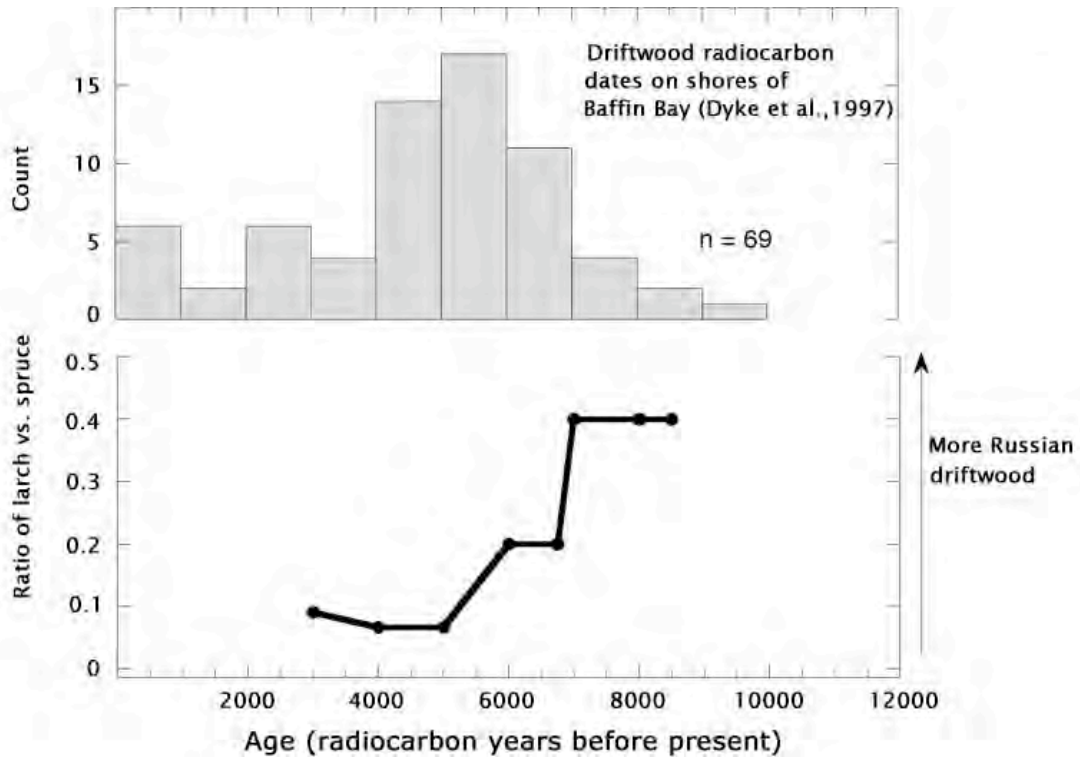
975



976

977

978 **Figure 8.8.** Distribution of radiocarbon ages (in thousands of years) of bowhead whales in three
 979 regions of the Canadian Arctic Archipelago (data from Dyke et al., 1996; Savelle et al., 2000).

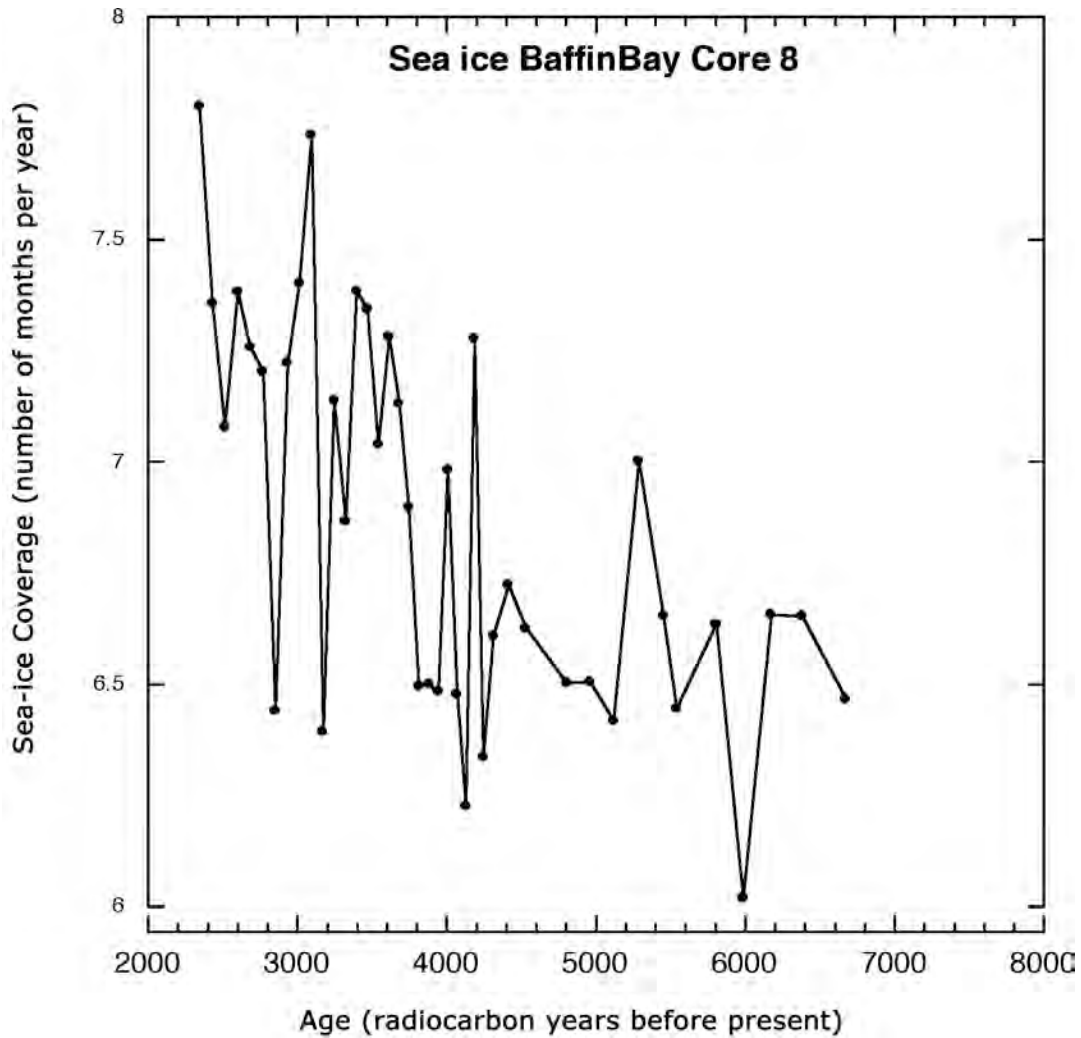


980

981

982 **Figure 8.9.** Distribution of radiocarbon ages of Holocene driftwood on the shores of Baffin Bay
 983 (from Dyke et al., 1997).

984

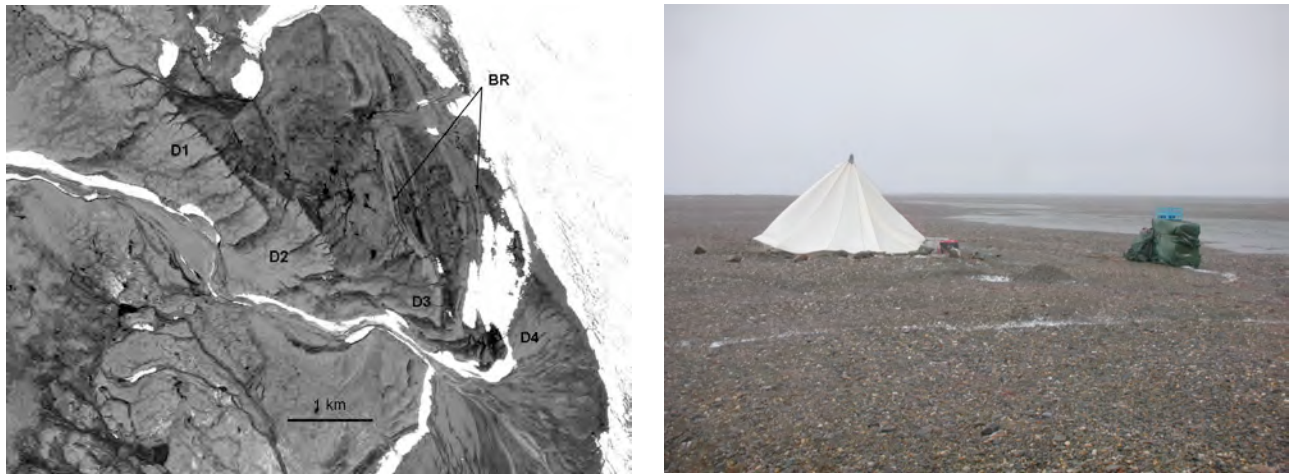


985

986 **Figure 8.10.** Reconstruction of the duration of ice cover (months per year) in northern Baffin
 987 Bay during the Holocene based on dinocyst assemblages (modified from Levac et al., 2001).

988

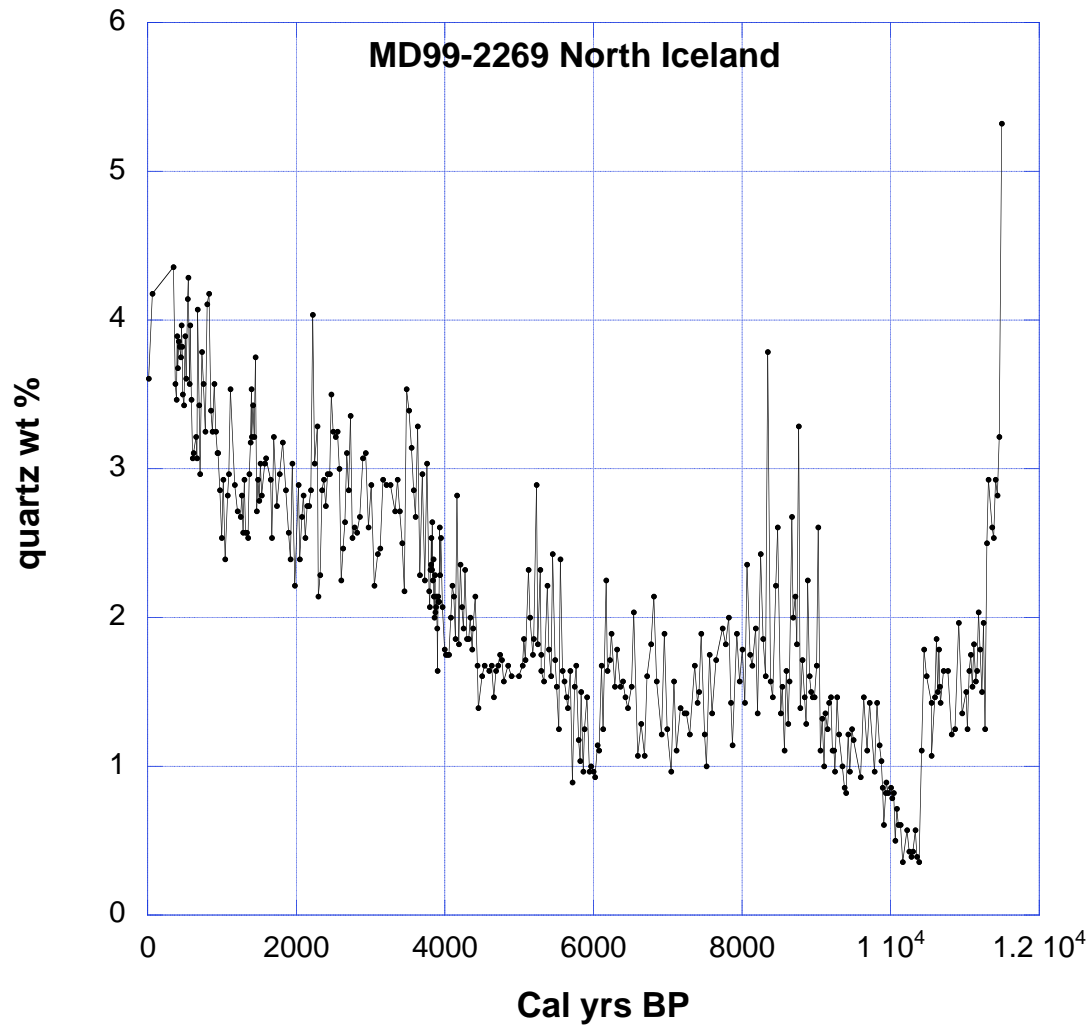
988



989

990 **Figure 8.11.** Aerial photo (left) of wave-generated beach ridges (BR) at Kap Ole Chiewitz,
991 83°25'N, northeast Greenland. D1-D4 are raised deltas. The oldest, D1, is dated to ~10 ka while
992 D4 is the modern delta. Only D3 is associated with wave activity. The period of beach ridge
993 formation is dated to ca. 8.5–6 ka. The photo on the right shows the upper beach ridge. (Funder,
994 S. and K. Kjær, 2007)

995

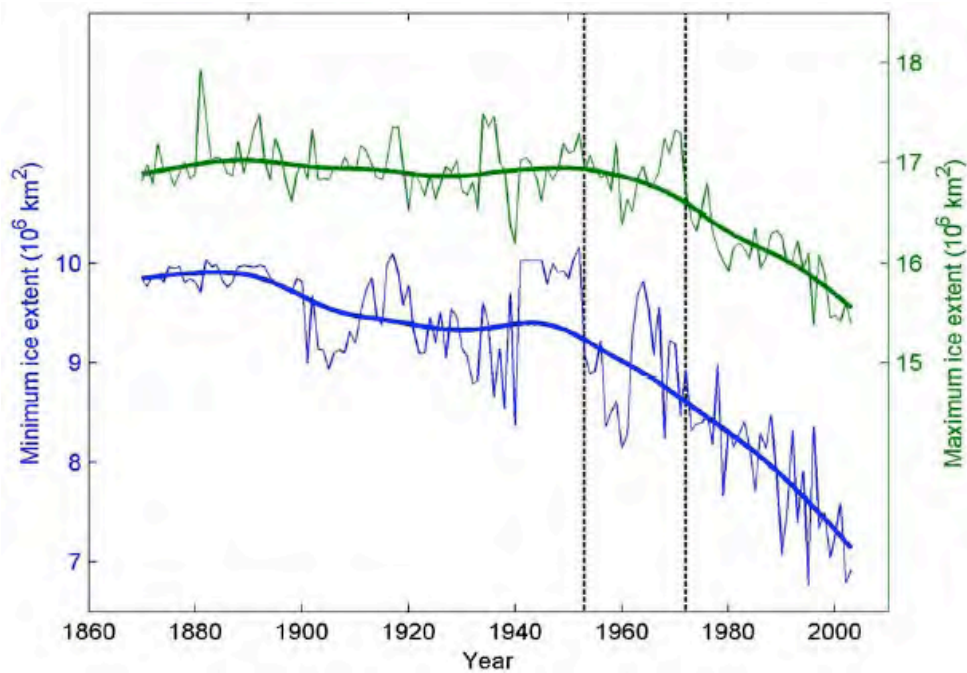


995

996

997 **Figure 8.12. Variations in the percentage of quartz (a proxy for drift ice) in Holocene**
998 **sediments from the northern Iceland shelf (from Moros et al., 2006). BP, before present.**

999



1000

1001 **Figure 8.13.** Total sea-ice extent time series, 1870–2003 (from Kinnard et al., 2008). Green
 1002 lines: maximal extent. Blue lines: minimal extent. Thick lines are robust spline functions that
 1003 highlight low-frequency changes. Vertical dotted lines separate the three periods for which data
 1004 sources changed fundamentally: earliest, 1870–1952, observations of differing accuracy and
 1005 availability; intermediate, 1953–1971, generally accurate hemispheric observations; most recent,
 1006 1972–2003, satellite period, best accuracy and coverage.

1007

1007

1008 **Chapter 8 References Cited**

1009

1010 **Andersen, C.**, N. Koç, and M. Moros, 2004: A highly unstable Holocene climate in the subpolar
1011 North Atlantic: evidence from diatoms. *Quaternary Science Reviews*, **23**, 2155-2166.

1012

1013 **Anderson, R.K.**, G.H. Miller, J.P. Briner, N.A. Lifton, and S.B. DeVogel, 2008: A millennial
1014 perspective on Arctic warming from 14C in quartz and plants emerging from beneath ice
1015 caps. *Geophysical Research Letters*, **35**, L01502, doi:10.1029/2007GL032057.

1016

1017 **Andrews, J.T.**, 2000: Icebergs and iceberg rafted detritus (IRD) in the North Atlantic—Facts and
1018 assumptions. *Oceanography*, **13**, 100-108.

1019

1020 **Andrews, J.T.**, 2007: A moderate resolution, definitive(?) record for Holocene variations in ice
1021 rafting around Iceland. *37th Arctic Workshop Program and Abstracts*, 34-35.

1022

1023 **Andrews, J.T.** and D.D. Eberl, 2007: Quantitative mineralogy of surface sediments on the
1024 Iceland shelf, and application to down-core studies of Holocene ice-rafted sediments.
1025 *Journal Sedimentary Research*, **77**, 469-479.

1026

1027 **Andrews, J.T.**, A.E. Jennings, M. Moros, C. Hillaire-Marcel, and D.D. Eberl, 2006: Is there a
1028 pervasive Holocene ice-rafted debris (IRD) signal in the northern North Atlantic? The
1029 answer appears to be either no, or it depends on the proxy! *PAGES Newsletter*, **14**, 7-9.

1030

1031 **Backman, J.**, M. Jakobsson, M. Frank, F. Sangiorgi, H. Brinkhuis, C. Stickley, M. O'Regan, R.
1032 Løvlie, H. Pälike, D. Spofforth, J. Gattacecca, K. Moran, J. King, and C. Heil, 2008: Age
1033 model and core-seismic integration for the Cenozoic Arctic Coring Expedition sediments
1034 from the Lomonosov Ridge. *Paleoceanography*, **23**, PA1S03,
1035 doi:10.1029/2007PA001476.

1036

1037 **Backman, J.**, M. Jakobsson, R. Løvlie, L. Polyak, and L.A. Febo, 2004: Is the central Arctic

- 1038 Ocean a sediment starved basin? *Quaternary Science Reviews*, **23**, 1435-1454.
- 1039 **Backman, J.**, K. Moran, D.B. McInroy, L.A. Mayer, and the Expedition 302 scientists, 2006:
1040 *Proceedings of IODP, 302*. Edinburgh (Integrated Ocean Drilling Program Management
1041 International, Inc.), doi:10.2204/iodp.proc.302.2006.
- 1042
- 1043 **Belt, S.T.**, G. Masse, S.J. Rowland, M. Poulin, C. Michel, and B. LeBlanc, 2007: A novel
1044 chemical fossil of palaeo sea ice: IP25. *Organic Geochemistry*, **38**, 16-27.
- 1045
- 1046 **Bennike, O.**, 2004: Holocene sea-ice variations in Greenland—Onshore evidence. *The*
1047 *Holocene*, **14**, 607-613.
- 1048
- 1049 **Bennike, O.** and J. Böcher, 1990: Forest-tundra neighboring the North Pole—Plant and insect
1050 remains from Plio-Pleistocene Kap Kobenhaven Formation, North Greenland. *Arctic*,
1051 **43(4)**, 331-338.
- 1052
- 1053 **Berger, A.** and M.F. Loutre, 2004: An exceptionally long interglacial ahead? *Science*,
1054 **297(5585)**, 1287-1288.
- 1055
- 1056 **Bergthorsson, P.**, 1969: An estimate of drift ice and temperature in Iceland in 1000 years.
1057 *Jokull*, **19**, 94-101.
- 1058
- 1059 **Blake, W., Jr.**, 1975: Radiocarbon age determination and postglacial emergence at Cape Storm,
1060 southern Ellesmere Island, Arctic Canada. *Geografiska Annaler*, **57**, 1-71.
- 1061
- 1062 **Blake, W., Jr.**, 2006: Occurrence of the *Mytilus edulis* complex on Nordaustlandet, Svalbard—
1063 Radiocarbon ages and climatic implications. *Polar Research*, **25(2)**, 123-137.
- 1064
- 1065 **Bond, G.**, B. Kromer, J. Beer, R. Muscheler, M.N. Evans, W. Showers, S. Hoffman, R. Lotti-
1066 Bond, I. Hajdas, G. Bonani, 2001: Persistent solar influence on North Atlantic climate
1067 during the Holocene. *Science*, **294**, 2130-2136.
- 1068

- 1069 **Bond, G., W. Showers, M. Cheseby, R. Lotti, P. Almasi, P. deMenocal, P. Priore, H. Cullen, I.**
1070 **Hajdas, and G. Bonani, 1997: A pervasive millennial-scale cycle in North Atlantic**
1071 **Holocene and glacial climates. *Science*, **278**, 1257-1265.**
1072
- 1073 **Brigham-Grette, J. and L.D. Carter, 1992: Pliocene marine transgressions of northern Alaska—**
1074 **Circumarctic correlations and paleoclimate. *Arctic*, **43(4)**, 74-89.**
1075
- 1076 **Brigham-Grette, J. and D.M. Hopkins, 1995: Emergent-marine record and paleoclimate of the**
1077 **last interglaciation along the northwest Alaskan coast. *Quaternary Research*, **43**, 154-**
1078 **173.**
1079
- 1080 **Brigham-Grette, J., D.M. Hopkins, V.F. Ivanov, A. Basilyan, S.L. Benson, P. Heiser, and V.**
1081 **Pushkar, 2001: Last interglacial (Isotope Stage 5) glacial and sea level history of coastal**
1082 **Chukotka Peninsula and St. Lawrence Island, western Beringia. *Quaternary Science***
1083 ***Reviews*, **20(1-3)** 419-436.**
1084
- 1085 **CircumArctic PaleoEnvironments (CAPE) Last Interglacial Project Members, 2006: Last**
1086 **Interglacial Arctic warmth confirms polar amplification of climate change. *Quaternary***
1087 ***Science Reviews*, **25**, 1383-1400.**
1088
- 1089 **Carter, L.D., J. Brigham-Grette, L. Marincovich, Jr., V.L. Pease, and U.S. Hillhouse, 1986: Late**
1090 **Cenozoic Arctic Ocean sea ice and terrestrial paleoclimate. *Geology*, **14**, 675-678.**
1091
- 1092 **Cavaliere, D.J., C.L. Parkinson, and K.Y. Vinnikov, 2003: 30-Year satellite record reveals**
1093 **contrasting Arctic and Antarctic sea ice variability, *Geophysical Research Letters*,**
1094 ****30(18)**, 1970, doi:10.1029/2003GL018031.**
1095
- 1096 **Clark, D.L., L.A. Chern, J.A. Hogler, C.M. Mennicke, and E.D. Atkins, 1990: Late Neogene**
1097 **climatic evolution of the central Arctic Ocean. *Marine Geology*, **93**, 69-94.**
1098
- 1099 **Comiso, J.C., C.L. Parkinson, R. Gersten, and L. Stock, 2008: Accelerated decline in the Arctic**

- 1100 sea ice cover. *Geophysical Research Letters*, **35**, L01703, doi:10.1029/2007GL031972.
- 1101
- 1102 **Cronin**, T.M., T.R. Holtz, Jr., R. Stein, R. Spielhagen, D. Fütterer, and J. Wollenburg, 1995:
- 1103 Late Quaternary paleoceanography of the Eurasian Basin, Arctic Ocean.
- 1104 *Paleoceanography*, **10**, 259-281.
- 1105
- 1106 **Cronin**, T.M., S.A. Smith, F. Eynaud, M. O'Regan, and J. King, 2008: Quaternary
- 1107 paleoceanography of the central Arctic based on IODP ACEX 302 foraminiferal
- 1108 assemblages. *Paleoceanography*, **23**, PA1S18, doi:10.1029/2007PA001484.
- 1109
- 1110 **Curran**, M.A.J., T. van Ommen, V. I. Morgan, K.L. Phillips, and A.S. Palmer, 2003: Ice core
- 1111 evidence for Antarctic sea ice decline since the 1950s. *Science*, **302**, 1203-1206.
- 1112
- 1113 **Darby**, D.A., 2003: Sources of sediment found in the sea ice from the western Arctic Ocean,
- 1114 new insights into processes of entrainment and drift patterns. *Journal of Geophysical*
- 1115 *Research*, **108**, 13-1 to 13-10, doi: 10, 1111029/1112002JC1001350, 1112003.
- 1116
- 1117 **Darby**, D.A., 2008: Arctic perennial ice cover over the last 14 million years. *Paleoceanography*,
- 1118 **23**, PA1S07, doi:10.1029/2007PA001479.
- 1119
- 1120 **Darby**, D.A. and J. Bischof, 2004: A Holocene record of changing Arctic Ocean ice drift
- 1121 analogous to the effects of the Arctic Oscillation. *Palaeoceanography*, **19(1 of 9)**,
- 1122 002004, doi:10.1029/2003PA000961.
- 1123
- 1124 **Darby**, D.A., M. Jakobsson, and L. Polyak, 2005: Icebreaker expedition collects key Arctic
- 1125 seafloor and ice data. *Eos, Transactions of the American Geophysical Union*, **86(52)**,
- 1126 549-556.
- 1127
- 1128 **Darby**, D.A., L. Polyak, and H. Bauch, 2006: Past glacial and interglacial conditions in the
- 1129 Arctic Ocean and marginal seas—A review. In: *Structure and function of contemporary*
- 1130 *food webs on Arctic shelves—A Pan-Arctic comparison*, [Wassman, P. (ed.)]. *Progress in*

1131 *Oceanography*, **71**, 129-144.

1132

1133 **de Vernal**, A. and C. Hillaire-Marcel, 2000: Sea-ice cover, sea-surface salinity and
1134 halo/thermocline structure of the northwest North Atlantic—Modern versus full glacial
1135 conditions. *Quaternary Science Reviews*, **19**, 65-85.

1136

1137 **Delworth**, T.L., S. Manabe, and R.J. Stouffer, 1997: Multidecadal climate variability in the
1138 Greenland Sea and surrounding regions: A coupled model simulation. *Geophysical*
1139 *Research Letters*, **24**, 257-260.

1140

1141 **Devaney**, J.R., 1991: Sedimentological highlights of the Lower Triassic Bjorne Formation,
1142 Ellesmere Island, Arctic Archipelago. In: *Current Research Part B, Geological Survey of*
1143 *Canada Paper 91-1B*, pp. 33-40.

1144

1145 **Dowdeswell**, J.A., R.J. Whittington, and P. Marienfeld, 1994: The origin of massive diamicton
1146 facies by iceberg rafting and scouring, Scorsby Sund, East Greenland. *Sedimentology*, **41**,
1147 21-35.

1148

1149 **Duk-Rodkin**, A., R.W. Barendregt, D.G. Froese, F. Weber, R.J. Enkin, I.R. Smith, G.D. Zazula,
1150 P. Waters, and R. Klassen, 2004: Timing and Extent of Plio-Pleistocene glaciations in
1151 North-Western Canada and East-Central Alaska. In: *Quaternary Glaciations-Extent and*
1152 *Chronology, Part II, North America*, [Ehlers, J. and P.L. Gibbard (eds.)]. Elsevier, New
1153 York, pp. 313-345.

1154

1155 **Dunhill**, G., 1998: *Comparison of Sea-Ice and Glacial-Ice Rafted Debris—Grain Size, Surface*
1156 *Features, and Grain Shape*. U.S. Geological Survey Open-File Report 98-0367, 74 pp.

1157

1158 **Dyke**, A.S., J. England, E. Reimnitz, and H. Jetté, 1997: Changes in driftwood delivery to the
1159 Canadian Arctic Archipelago—The hypothesis of postglacial oscillations of the
1160 Transpolar Drift. *Arctic*, **50**, 1-16.

1161

- 1162 **Dyke, A.S., J. Hooper, C.R. Harington, and J.M. Savelle, 1999:** The Late Wisconsinan and
1163 Holocene record of walrus (*Odobenus rosmarus*) from North America—A review with
1164 new data from Arctic and Atlantic Canada. *Arctic*, **52**, 160-181.
- 1165
- 1166 **Dyke, A.S., J. Hooper, and J.M. Savelle, 1996:** A history of sea ice in the Canadian Arctic
1167 Archipelago based on the postglacial remains of the bowhead whale (*Balaena*
1168 *mysticetus*). *Arctic*, **49**, 235-255.
- 1169
- 1170 **Eggertsson, O., 1993:** Origin of the driftwood on the coasts of Iceland—A dendrochronological
1171 study. *Jokull*, **43**, 15-32.
- 1172
- 1173 **Eiriksson, J., K.L. Knudsen, H. Hafliðason, and P. Henriksen, 2000:** Late-glacial and Holocene
1174 paleoceanography of the North Iceland Shelf. *Journal of Quaternary Science*, **15**, 23-42.
- 1175
- 1176 **Eldrett, J.S., I.C. Harding, P.A. Wilson, E. Butler, and A.P. Roberts, 2007:** Continental ice in
1177 Greenland during the Eocene and Oligocene. *Nature*, **446**, 176-179.
- 1178
- 1179 **Feyling-Hanssen, R.W., S. Funder, and K.S. Petersen, 1983:** The Lodin Elv Formation—A
1180 Plio/Pleistocene occurrence in Greenland. *Bulletin of the Geological Society of Denmark*,
1181 **31**, 81-106.
- 1182
- 1183 **Fischer, H., 2001:** Imprint of large-scale atmospheric transport patterns on sea-salt records in
1184 northern Greenland ice cores. *Journal of Geophysical Research*, **106**, 23977-23984.
- 1185
- 1186 **Fischer, H. and B. Mieding, 2005:** A 1,000-year ice core record of interannual to multidecadal
1187 variations in atmospheric circulation over the North Atlantic. *Climate Dynamics*, **25**, 65-
1188 74.
- 1189
- 1190 **Fischer, H., M.L. Siggaard-Andersen, U. Ruth, R. Rothlisberger, and E.W. Wolff, 2007:**
1191 Glacial-interglacial changes in mineral dust and sea salt records in polar ice cores—
1192 Sources, transport, deposition. *Reviews of Geophysics*, **45**, RG1002,

1193 doi:10.1029/2005RG000192.

1194

1195

1196 **Fisher**, D.A., R.M. Koerner, J.C. Bourgeois, G. Zielinski, C. Wake, C.U. Hammer, H.B.

1197 Clausen, N. Gundestrup, S. Johnsen, K. Goto-Azuma, T. Hondoh, E. Blake, and M.

1198 Gerasimoff, 1998: Penny Ice Cap cores, Baffin Island, Canada, and the Wisconsinan

1199 Foxe Dome connection—Two states of Hudson Bay ice cover. *Science*, **279**, 692–695.

1200

1201 **Francis**, J.A. and E. Hunter, 2006: New insight into the disappearing Arctic sea ice. *Eos*,

1202 *Transactions of the American Geophysical Union*, **87**, 509-511.

1203

1204 **Francis**, J.E., 1988: A 50-million-year-old fossil forest from Strathcona Fiord, Ellesmere Island,

1205 Arctic Canada—Evidence for a warm polar climate. *Arctic*, **41(4)**, 314-318.

1206

1207 **Funder**, S., N. Abrahamsen, O. Bennike, and R.W. Feyling-Hansen, 1985: Forested Arctic—

1208 Evidence from North Greenland, *Geology* 13, 542-546.

1209

1210 **Funder**, S., O. Bennike, J. Böcher, C. Israelson, K.S. Petersen, and L.A. Simonarson, 2001: Late

1211 Pliocene Greenland—The Kap København formation in North Greenland. *Bulletin of the*

1212 *Geological Society of Denmark*, **48**, 177-134.

1213

1214 **Funder**, S., I. Demidov, and Y. Yelovicheva, 2002: Hydrography and mollusc faunas of the

1215 Baltic and the White Sea-North Sea seaway in the Eemian. *Palaeogeography*,

1216 *Palaeoclimatology, Palaeoecology*, **184**, 275-304.

1217

1218 **Funder**, S. and K. Kjær, 2007: Ice free Arctic Ocean, an early Holocene analogue. *Eos*,

1219 *Transactions of the American Geophysical Union*, **88(52)**, Fall Meeting Supplement,

1220 Abstract PP11A-0203.

1221

1222 **Fyles**, J.G., 1990: Beaufort Formation (late Tertiary) as seen from Prince Patrick Island, arctic

1223 Canada. *Arctic*, **43**, 393-403.

- 1224
- 1225 **Fyles, J.G., L.V. Hills, J.V. Mathews, Jr., R.W. Barendregt, J. Baker, E. Irving, and H. Jetté,**
 1226 1994: Ballast Brook and Beaufort Formations (Late Tertiary) on northern Banks Island,
 1227 Arctic Canada, *Quaternary International*, **22/23**, 141-171.
- 1228
- 1229 **Fyles, J.G., L. Marinovich Jr., J.V. Mathews Jr., and R. Barendregt,** 1991: Unique mollusc find
 1230 in the Beaufort Formation (Pliocene) Meighen Island, Arctic Canada. In: *Current*
 1231 *Research, Part B, Geological Survey of Canada, Paper 91-1B*, pp. 461-468.
- 1232
- 1233 **Fyles, J.G., D.H. McNeil, , J.V. Matthews, R.W. Barendregt, L. Marinovich, Jr., E. Brouwers,**
 1234 J. Bednarski, J. Brigham-Grette, L.O. Ovsenden, J. Baker, and E. Irving, 1998: Geology
 1235 of the Hvitland Beds (Late Pliocene), White Point Lowland, Ellesmere Island, Arctic
 1236 Canada. *Geological Survey of Canada Bulletin*, **512**, 1-35.
- 1237
- 1238 **Giraudeau, J., A.E. Jennings, and J.T. Andrews,** 2004: Timing and mechanisms of surface and
 1239 intermediate water circulation changes in the Nordic Seas over the last 10,000 cal
 1240 years—A view from the North Iceland shelf. *Quaternary Science Reviews*, **23**, 2127-
 1241 2139.
- 1242
- 1243 **Goosse, H., E. Driesschaert, T. Fichefet, and M.-F. Loutre,** 2007: Information on the early
 1244 Holocene climate constrains the summer sea ice projections for the 21st century. *Climate*
 1245 *of the Past Discussions*, **2**, 999-1020.
- 1246
- 1247 **Gow, A.J. and W.B. Tucker III,** 1987: Physical properties of sea ice discharge from Fram Strait.
 1248 *Science*, **236**, 436-439.
- 1249
- 1250 **Grumet, N.S., C.P. Wake, P.A. Mayewski, G.A. Zielinski, S.I. Whitlow, R.M. Koerner, D.A.**
 1251 Fisher, and J.M. Woollett, 2001: Variability of sea-ice extent in Baffin Bay over the last
 1252 millennium. *Climatic Change*, **49**, 129-145.
- 1253
- 1254 **Guelle, W., M. Schulz, Y. Balkanski, and F. Dentener,** 2001: Influence of the source formulation

- 1255 on modeling the atmospheric global distribution of sea salt aerosol. *Journal of*
1256 *Geophysical Research*, **106**, 27509-27524.
- 1257
- 1258 **Hagblom**, A., 1982: Driftwood in Svalbard as an indicator of sea ice conditions. *Geografiska*
1259 *Annaler. Series A, Physical Geography*, **64A**, 81-94.
- 1260
- 1261 **Harrington**, C.R., 2003: *Annotated Bibliography of Quaternary Vertebrates of Northern North*
1262 *America With Radiocarbon Dates*. University of Toronto Press, 539 pp.
- 1263
- 1264 **Hastings**, A.D., 1960: Environment of Southeast Greenland. Quartermaster Research and
1265 Engineering Command U.S. Army Technical Report EP-140, 48 pp.
- 1266
- 1267 **Hebbeln**, D., 2000: Flux of ice-rafted detritus from sea ice in the Fram Strait. *Deep-Sea*
1268 *Research II*, **47**, 1773-1790.
- 1269
- 1270 **Helland**, P.E. and M.A. Holmes, 1997: Surface textural analysis of quartz sand grains from ODP
1271 Site 918 off the southeast coast of Greenland suggests glaciation of 24 southern
1272 Greenland at 11Ma. *Palaeogeography, Palaeoclimatology, Palaeoecology*, **135**, 109-
1273 121.
- 1274
- 1275 **Herman**, Y., 1974: Arctic Ocean sediments, microfauna, and the climatic record in late
1276 Cenozoic time. In: *Marine Geology and Oceanography of the Arctic Seas* [Herman, Y.
1277 (ed.)]. Springer-Verlag, Berlin, pp. 283-348.
- 1278
- 1279 **Holland**, M.M., C.M. Bitz, M. Eby, and A.J. Weaver, 2001: The role of ice-ocean interactions in
1280 the variability of the north Atlantic thermohaline circulation. *Journal of Climate*, **14**,
1281 656-675.
- 1282
- 1283 **Holland**, M.M., C.M. Bitz, and B. Tremblay, 2006a: Future abrupt reductions in the summer
1284 Arctic sea ice. *Geophysical Research Letters*, **33**, L23503, doi: 10.1029/2006GL028024.
- 1285

- 1286 **Holland, M.M.**, J. Finnis, and M.C. Serreze, 2006b: Simulated Arctic Ocean freshwater budgets
1287 in the 20th and 21st centuries. *Journal of Climate*, **19**, 6221-6242.
1288
- 1289 **Hutterli, M.A.**, T. Crueger, H. Fischer, K.K. Andersen, C.C. Raible, T.F. Stocker, M.L.
1290 Siggaard-Andersen, J.R. McConnell, R.C. Bales, and J. Burkhardt, 2007: The influence
1291 of regional circulation patterns on wet and dry mineral dust and sea salt deposition over
1292 Greenland. *Climate Dynamics*, **28**, 635-647.
1293
- 1294 **Isaksson, E.**, T. Kekonen, J.C. Moore, and R. Mulvaney, 2005: The methanesulfonic acid
1295 (MSA) record in a Svalbard ice core. *Annals of Glaciology*, **42**, 345-351.
1296
- 1297 **Jakobsson, M.**, J. Backman, B. Rudels, J. Nycander, M. Frank, L. Mayer, W. Jokat, F.
1298 Sangiorgi, M. O'Regan, H. Brinkhuis, J. King, and K. Moran, 2007: The Early Miocene
1299 onset of a ventilated circulation regime in the Arctic Ocean. *Nature*, **447(21)**, 986-990.
1300 doi:10.1038/nature05924.
1301
- 1302 **Jennings, A.E.**, K. Grönvold, R. Hilberman, M. Smith, and M. Hald, 2002: High-resolution
1303 study of Icelandic tephra in the Kangerlussuq Trough, Southeast Greenland, during the
1304 last deglaciation. *Journal of Quaternary Science*, **7**, 747-757.
1305
- 1306 **Jennings, A.E.** and N.J. Weiner, 1996: Environmental change in eastern Greenland during the
1307 last 1300 years—Evidence from foraminifera and lithofacies in Nansen Fjord, 68°N. *The*
1308 *Holocene*, **6**, 179-191.
1309
- 1310 **Jennings, A.E.**, N.J. Weiner, G. Helgadottir, and J.T. Andrews, 2004: Modern foraminiferal
1311 faunas of the Southwest to Northern Iceland shelf—Oceanographic and environmental
1312 controls. *Journal of Foraminiferal Research*, **34**, 180-207.
1313
- 1314 **Jones, P.D.**, T.J. Osborn, and K.R. Briffa, 2001: The evolution of climate over the last
1315 millennium. *Science*, **292**, 662-667.
1316

- 1317 **Kaufman, D.S.**, 1991: *Pliocene-Pleistocene chronostratigraphy, Nome, Alaska*. Ph.D.
 1318 dissertation, University of Colorado, Boulder, 297 pp.
 1319
- 1320 **Kaufman, D.S.**, T.A. Ager, N.J. Anderson, P.M. Anderson, J.T. Andrews, P.J. Bartlein, L.B.
 1321 Brubaker, L.L. Coats, L.C. Cwynar, M.L. Duvall, A.S. Dyke, M.E. Edwards, W.R.
 1322 Eisner, K. Gajewski, A. Geirsdóttir, F.S. Hu, A.E. Jennings, M.R. Kaplan, M.W. Kerwin,
 1323 A.V. Lozhkin, G.M. MacDonald, G.H. Miller, C.J. Mock, W.W. Oswald, B.L. Otto-
 1324 Bliesner, D.F. Porinchu, K. Rühland, J.P. Smol, E.J. Steig, and B.B. Wolfe, 2004.
 1325 Holocene thermal maximum in the western Arctic (0–180°W). *Quaternary Science*
 1326 *Reviews*, **23**, 529-560.
 1327
- 1328 **Kaufman, D.S.** and J. Brigham-Grette, 1993: Aminostratigraphic correlations and
 1329 paleotemperature implications, Pliocene-Pleistocene high sea level deposits,
 1330 northwestern Alaska. *Quaternary Science Reviews*, **12**, 21-33.
 1331
- 1332 **Kinnard, C.**, C.M. Zdanowicz, D.A. Fisher, and C.P. Wake, 2006: Calibration of an ice-core
 1333 glaciochemical (sea-salt) record with sea-ice variability in the Canadian Arctic. *Annals of*
 1334 *Glaciology*, **44**, 383-390.
 1335
- 1336 **Kinnard, C.**, C.M. Zdanowicz, R. Koerner, and D.A. Fisher, 2008: A changing Arctic seasonal
 1337 ice zone—Observations from 1870–2003 and possible oceanographic consequences,
 1338 *Geophysical Research Letters*, **35**, L02507, doi:10.1029/2007GL032507.
 1339
- 1340 **Knies, J.** and C. Gaina, 2008: Middle Miocene ice sheet expansion in the Arctic—Views from
 1341 the Barents Sea. *Geochemistry, Geophysics, Geosystems*, **9**, Q02015,
 1342 doi:10.1029/2007GC001824.
 1343
- 1344 **Knies, J.**, J. Matthiessen, C. Vogt, and R. Stein, 2002: Evidence of “mid-Pliocene (similar to 3
 1345 Ma) global warmth” in the eastern Arctic Ocean and implications for the
 1346 Svalbard/Barents Sea ice sheet during the late Pliocene and early Pleistocene (similar to
 1347 3 –1.7 Ma). *Boreas*, **31(1)**, 82-93.

1348

1349 **Koç**, N. and E. Jansen, 1994: Response of the high-latitude Northern Hemisphere to orbital
1350 climate forcing—Evidence from the Nordic Seas. *Geology*, **22**, 523-526.

1351

1352 **Koch**, L., 1945: The East Greenland Ice. *Meddelelser om Gronland*, **130(3)**, 1-375.

1353

1354 **Krylov**, A.A., I.A. Andreeva, C. Vogt, J. Backman, V.V. Krupskaya, G.E. Grikurov, K. Moran,
1355 and H. Shoji, 2008: A shift in heavy and clay mineral provenance indicates a middle
1356 Miocene onset of a perennial sea-ice cover in the Arctic Ocean. *Paleoceanography*, **23**,
1357 PA1S06, doi:10.1029/2007PA001497.

1358

1359 **LePage**, B.A., H. Yang, and M. Matsumoto, 2005: The evolution and biogeographic history of
1360 Metasequoia. In: *The Geobiology and Ecology of Metasequoia* [LePage, B.A., C.J.
1361 Williams, and H. Yang (eds.)]. Springer, New York, Chapter 1, pp. 4-81.

1362

1363 **Levac**, E., A. de Verna, and W.J. Blake, 2001: Sea-surface conditions in northernmost Baffin
1364 Bay during the Holocene—Palynological evidence. *Journal of Quaternary Science*, **16**,
1365 353-363.

1366

1367 **Levermann**, A., J. Mignot, S. Nawrath, and S. Rahmstorf, 2007: The role of Northern sea ice
1368 cover for the weakening of the thermohaline circulation under global warming. *Journal*
1369 *of Climate*, doi:10.1175/JCLI4232.1.

1370

1371 **Lisiecki**, L.E. and M.E. Raymo, 2005: A Pliocene-Pleistocene stack of 57 globally distributed
1372 benthic $\delta^{18}\text{O}$ records. *Paleoceanography*, **20**, doi:10.1029/2004PA001071.

1373

1374 **Lisitzin**, A.P., 2002: *Sea-Ice and Iceberg Sedimentation in the Ocean, Recent and Past*.
1375 Springer-Verlag, Berlin, 563 pp.

1376

1377 **Lowenstein**, T.K. and Demicco, R.V., 2006: Elevated Eocene atmospheric CO₂ and its
1378 subsequent decline. *Science*, **313**, 1928.

- 1379
- 1380 **Magnusdottir, G., C. Deser, and R. Saravanan, 2004:** The effects of North Atlantic SST and sea
1381 ice anomalies on the winter circulation in CCSM3, Part I—Main features and storm track
1382 characteristics of the response, *Journal of Climate*, **17**, 857-876.
- 1383
- 1384 **Mann, M.E., R.S. Bradley, and M.K. Hughes, 1999:** Northern Hemisphere temperatures during
1385 the millennium—Inferences, uncertainties, and limitations. *Geophysical Research*
1386 *Letters*, **26**, 759-764.
- 1387
- 1388 **Maslanik, J., S. Drobot, C. Fowler, W. Emery, and R. Barry, 2007a:** On the Arctic climate
1389 paradox and the continuing role of atmospheric circulation in affecting sea ice
1390 conditions. *Geophysical Research Letters*, 10.1029/2006GL028269.
- 1391
- 1392 **Maslanik, J.A, C. Fowler, J. Stroeve, S. Drobot, and J. Zwally, 2007b:** A younger, thinner Arctic
1393 ice cover—Increased potential for rapid, extensive ice loss, *Geophysical Research*
1394 *Letters*, **34**, L24501, doi:10.1029/2007GL032043.
- 1395
- 1396 **Matthews, J.V., Jr., 1987:** Plant macrofossils from the Neogene Beaufort Formation on Banks
1397 and Meighen islands, District of Franklin. In: *Current Research, Part A, Geological*
1398 *Survey of Canada Paper 87-1A*, pp. 73-87.
- 1399
- 1400 **Matthews, J.V., Jr. and L.E. Ovensen, 1990:** Late Tertiary plant macrofossils from localities in
1401 northern North America (Alaska, Yukon, and Northwest Territories). *Arctic*, **43(2)**, 364-
1402 392.
- 1403
- 1404 **Matthews, J.V., Jr., and A. Telka, , 1997.** Insect fossils from the Yukon. In: *Insects of the Yukon*
1405 [Danks, H.V. and J.A. Downes (eds.)]. Biological Survey of Canada (Terrestrial
1406 Arthropods), Ottawa, pp. 911-962.
- 1407
- 1408 **Mauritzen, C. and S. Hakkinen, 1997:** Influence of sea ice on the thermohaline circulation in the
1409 Arctic-North Atlantic Ocean. *Geophysical Research Letters*, **24**, 3257-3260.

1410

1411 **Mayewski, P.A.,** L.D. Meeker, S. Whitlow, M.S. Twickler, M.C. Morrison, P. Bloomfield, G.C.
1412 Bond, R.B. Alley, A.J. Gow, P.M. Grootes, D.A. Meese, M. Ram, K.C. Taylor, and W.
1413 Wumkes, 1994: Changes in atmospheric circulation and ocean ice cover over the North
1414 Atlantic during the last 41,000 years. *Science*, **263**, 1747-1751.

1415

1416 **McKenna, M.C.,** 1980. Eocene paleolatitude, climate and mammals of Ellesmere Island.
1417 *Paleogeography, Paleoclimatology and Paleoecology*, **30**, 349-362.

1418

1419 **McNeil, D.H.,** 1990: Tertiary marine events of the Beaufort-Mackenzie Basin and correlation of
1420 Oligocene to Pliocene marine outcrops in Arctic North America. *Arctic*, 1990, **43(4)**,
1421 301-313.

1422

1423 **Miller, G.H.,** 1985: Aminostratigraphy of Baffin Island shell-bearing deposits. In: *Late*
1424 *Quaternary Environments—Eastern Canadian Arctic, Baffin Bay and West Greenland*,
1425 [Andrews, J.T. (ed.)]. Allen and Unwin Publishers, Boston, pp. 394-427.

1426

1427 **Moran, K.,** J. Backman, H. Brinkhuis, S.C. Clemens, T. Cronin, G.R. Dickens, F. Eynaud, J.
1428 Gattacceca, M. Jakobsson, R.W. Jordan, M. Kaminski, J. King, N. Koç, A. Krylov, N.
1429 Martinez, J. Matthiessen, D. McInroy, T.C. Moore, J. Onodera, A.M. O'Regan, H.
1430 Pälike, B. Rea, D. Rio, T. Sakamoto, D.C. Smith, R. Stein, K. St. John, I. Suto, N.
1431 Suzuki, K. Takahashi, M. Watanabe, M. Yamamoto, J. Farrell, M. Frank, P. Kubik, W.
1432 Jokat, and Y. Kristoffersen, 2006: The Cenozoic palaeoenvironment of the Arctic Ocean.
1433 *Nature*, **441**, 601-605.

1434

1435 **Moros, M.,** J.T. Andrews, D.D. Eberl, and E. Jansen, 2006: The Holocene history of drift ice in
1436 the northern North Atlantic—Evidence for different spatial and temporal modes.
1437 *Palaeoceanography*, **21(1 of 10)**, doi:10.1029/2005PA001214.

1438

1439 **Moros, M.,** K. Emeis, B. Risebrobakken, I. Snowball, A. Kuijpers, J. McManus, E. Jansen,
1440 2004: Sea surface temperatures and ice rafting in the Holocene North Atlantic—Climate

- 1441 influences on northern Europe and Greenland. *Quaternary Science Reviews*, **23**, 2113-
1442 2126.
- 1443 **Mosher**, B.W., P. Winkler, and J.-L. Jaffrezo, 1993: Seasonal aerosol chemistry at Dye 3,
1444 Greenland. *Atmospheric Environment*, **27A**, 2761-2772.
- 1445
- 1446 **Mudie**, P.J., A. Rochon, M.A. Prins, D. Soenarjo, S.R. Troelstra, E. Levac, D.B. Scott, L.
1447 Roncaglia, and A. Kuijpers, 2006: Late Pleistocene-Holocene marine geology of Nares
1448 Strait region—Palaeoceanography from foraminifera and dinoflagellate cysts,
1449 sedimentology and stable isotopes. *Polarforschung*, **74**, 169-183.
- 1450
- 1451 **Mullen**, M.W. and D.H. McNeil, 1995: Biostratigraphic and paleoclimatic significance of a new
1452 Pliocene foraminiferal fauna from the central Arctic Ocean. *Marine Micropaleontology*,
1453 **26(1)**, 273-280.
- 1454
- 1455 **Nørgaard-Pedersen**, N., N. Mikkelsen, and Y. Kristoffersen, 2007a: Arctic Ocean record of last
1456 two glacial-interglacial cycles off North Greenland/Ellesmere Island—Implications for
1457 glacial history. *Marine Geology*, **244**, 93-108.
- 1458
- 1459 **Nørgaard-Pedersen**, N., N. Mikkelsen, S.J. Lassen, Y. Kristoffersen, and E. Sheldon, 2007b:
1460 Arctic Ocean sediment cores off northern Greenland reveal reduced sea ice
1461 concentrations during the last interglacial period. *Paleoceanography*, **22**, PA1218,
1462 doi:10.1029/2006PA001283.
- 1463
- 1464 **O'Brien**, S.R., P.A. Mayewski, L.D. Meeker, D.A. Meese, M.S. Twickler, and S.I. Whitlow,
1465 1995: Complexity of Holocene climate as reconstructed from a Greenland ice core.
1466 *Science*, **270**, 1962-1964.
- 1467
- 1468 **O'Regan**, M., K. Moran, J. Backman, M. Jakobsson, F. Sangiorgi, H., Brinkhuis, R. A.
1469 Pockalny, A. Skelton, C. Stickley, N. Koc, and H. Brumsack, 2008: Mid-Cenozoic
1470 tectonic and paleoenvironmental setting of the central Arctic Ocean, *Paleoceanography*,
1471 **23**, PA1S20, doi:10.1029/2007PA001559.

- 1472
- 1473 **Ogilvie, A.**, 1996: Sea-ice conditions off the coasts of Iceland A.D. 1601–1850 with special
1474 reference to part of the Maunder Minimum period (1675-1715). In: *North European*
1475 *climate data in the latter part of the Maunder Minimum period A.D. 1675-1715*.
1476 Stavanger Museum of Archaeology, Norway *AmS-Varia* 25, 9-12.
- 1477
- 1478 **Ogilvie, A.E., L.K. Barlow, and A.E. Jennings**, 2000: North Atlantic Climate c. A.D. 1000—
1479 Millennial reflections on the Viking discoveries of Iceland, Greenland and North
1480 America. *Weather*, **55**, 34-45.
- 1481
- 1482 **Ogilvie, A.E.J.**, 1984: The past climate and sea-ice record from Iceland, Part I—Data to A.D.
1483 1780. *Climatic Change*, **6**, 131-152.
- 1484
- 1485 **Oleinik, A., L. Marincovich, P. Swart, and R. Port**, 2007: Cold Late Oligocene Arctic Ocean—
1486 Faunal and stable isotopic evidence. *Eos, Transactions of the American Geophysical*
1487 *Union*, **88(52)**, Abstract PP43D-05.
- 1488
- 1489 **Otto-Bliesner, B.L., S.J. Marshall, J.T. Overpeck, G.H. Miller, A. Hu, and CAPE Last**
1490 **Interglacial Project members**, 2006, Simulating Arctic climate warmth and icefield
1491 retreat in the Last Interglaciation. *Science*, **311**, 1751-1753. doi:10.1126/science.1120808
- 1492
- 1493 **Overpeck, J., K. Hughen, D. Hardy, R. Bradley, R. Case, M. Douglas, B. Finney, K. Gajewski,**
1494 **G. Jacoby, A. Jennings, S. Lamoureux, A. Lasca, G. MacDonald, J. Moore, M. Retelle,**
1495 **S. Smith, A. Wolfe, and G. Zielinski**, 1997: Arctic environmental changes of the last four
1496 centuries. *Science*, **278**, 1251–1256.
- 1497
- 1498 **Pearson, P.N. and M.R. Palmer**, 2000: Atmospheric carbon dioxide concentrations over the past
1499 60 million years. *Nature*, **406**, 695-699.
- 1500
- 1501 **Peterson, B.J., J. McClelland, R. Curry, R.M. Holmes, J.E. Walsh, and K. Aagaard**, 2006:
1502 Trajectory shifts in the Arctic and Subarctic freshwater cycle. *Science*, **313**, 1061-1066.

1503

1504 **Petit, J.R., J. Jouzel, D. Raynaud, N.I. Barkov, J.-M. Barnola, I. Basile, M. Bender, J.**
1505 **Chappellaz, M. Davis, G. Delaygue, M. Delmotte, V.M. Kotlyakov, M. Legrand, V.Y.**
1506 **Lipenkov, C. Lorius, L. Pepin, C. Ritz, E. Saltzman, and M. Stievenard, 1999: Climate**
1507 **and atmospheric history of the past 420,000 years from the Vostok ice core, Antarctica.**
1508 ***Nature*, **399**, 429-436.**

1509

1510 **Polyak, L., W.B. Curry, D.A. Darby, J. Bischof, and T.M. Cronin, 2004: Contrasting**
1511 **glacial/interglacial regimes in the western Arctic Ocean as exemplified by a sedimentary**
1512 **record from the Mendeleev Ridge. *Paleogeography, Paleoclimatology and***
1513 ***Paleoecology*, **203**, 73-93.**

1514

1515 **Polyak, L., S. Korsun, L.A. Febo, V. Stanovoy, T. Khusid, M. Hald, B.E. Paulsen, and D.J.**
1516 **Lubinski, 2002: Benthic foraminiferal assemblages from the southern Kara Sea, a river**
1517 **influenced Arctic marine environment. *Journal of Foraminiferal Research*, **32**, 252-273.**

1518

1519 **Polyakov, I.V., A. Beszczynska, E.C. Carmack, I.A. Dmitrenko, E. Fahrbach, I.E. Frolov,**
1520 **R.Gerdes, E. Hansen, J. Holfort, V.V. Ivanov, M.A. Johnson, M. Karcher, F. Kauker, J.**
1521 **Morison, K.A. Orvik, U. Schauer, H.L. Simmons, Ø. Skagseth, V.T. Sokolov, M. Steele,**
1522 **L.A. Timokhov, D. Walsh, J.E. Walsh, 2005: One more step toward a warmer Arctic.**
1523 ***Geophysical Research Letters*, **32**, L17605, doi:10.1029/2005GL023740.**

1524

1525 **Rankin, A.M., E.W. Wolff, and S. Martin, 2002: Frost flowers—Implications for tropospheric**
1526 **chemistry and ice core interpretation. *Journal of Geophysical Research*, **107**, 4683,**
1527 **doi:10.1029/2002JD002492.**

1528

1529 **Rankin, A.M., E.W. Wolff, and R. Mulvaney, 2005: A reinterpretation of sea salt records in**
1530 **Greenland and Antarctic ice cores. *Annals of Glaciology*, **39**, 276-282.**

1531

1532 **Rayner, N.A., D.E. Parker, E.B. Horton, C.K. Folland, L.V. Alexander, D.P. Rowell, E.C. Kent,**
1533 **and A. Kaplan, 2003: Global analysis of sea surface temperature, sea ice, and night**

- 1534 marine air temperature since the late nineteenth century, *Journal of Geophysical*
 1535 *Research*, **108(D14)**, 4407. doi 4410.1029/2002JD002670.
- 1536
- 1537 **Repenning**, C.A., E.M. Brouwers, L.C. Carter, L. Marinovich, Jr., and T.A. Ager, 1987: *The*
 1538 *Beringian Ancestry of Phenacomys (Rodentia: Critetidae) and the Beginning of the*
 1539 *Modern Arctic Ocean Borderland Biota*. U.S. Geological Survey Bulletin 1687, 31 p.
- 1540
- 1541 **Rigor**, I.G. and J.M. Wallace, 2004: Variations in the age of Arctic sea-ice and summer sea-ice
 1542 extent. *Geophysical Research Letters*, **31**, L09401. doi:10.1029/2004GL019492
- 1543
- 1544 **Risebrobakken**, B., E. Jansen, C. Andersson, E. Mjelde, and K. Hevroy, 2003: A high-
 1545 resolution study of Holocene paleoclimatic and paleoceanographic changes in the Nordic
 1546 Seas. *Paleoceanography*, **18**, 1017-1031.
- 1547
- 1548 **Rothrock**, D.A. and J. Zhang, 2005: Arctic Ocean sea ice volume: What explains its recent
 1549 depletion? *Journal of Geophysical Research*, **110**, C01002, doi:10.1029/2004JC002282.
- 1550
- 1551 **Savelle**, J.M., A.A. Dyke, and A.P. McCartney, 2000: Holocene bowhead whale (*Balaena*
 1552 *mysticetus*) mortality patterns in the Canadian Arctic Archipelago. *Arctic*, **53(4)**, 414-
 1553 421.
- 1554
- 1555 **Seager**, R., D.S. Battisti, J. Yin, N. Gordon, N. Naik, A.C. Clement, M.A. Cane, 2002: Is the
 1556 Gulf Stream responsible for Europe's mild winters? *Quarterly Journal of the Royal*
 1557 *Meteorological Society*, **128B**, 2563-2586.
- 1558
- 1559 **Seidenkrantz**, M.-S., S. Aagaard-Sørensen, H. Sulsbrück, A. Kuijpers, K.G. Jensen, and H.
 1560 Kunzendorf, 2007: Hydrography and climate of the last 4400 years in a SW Greenland
 1561 fjord: implications for Labrador Sea palaeoceanography. *The Holocene*, **17**, 387-401.
- 1562
- 1563 **Serreze**, M.C., A.P. Barrett, A.J. Slater, M. Steele, J. Zhang, and K.E. Trenberth, 2007a: The
 1564 large-scale energy budget of the Arctic. *Journal of Geophysical Research*, **112**, D11122,

1565 doi:10.1029/2006JD008230.

1566

1567 **Serreze**, M.C., M.M. Holland, and J. Stroeve, 2007b: Perspectives on the Arctic's shrinking sea
1568 ice cover. *Science*, **315**, 1533-1536.

1569

1570 **Sewall**, J.O. and L.C. Sloan, 2004: Disappearing Arctic sea ice reduces available water in the
1571 American west, *Geophysical Research Letters*, **31**, doi:10.1029/2003GL019133.

1572

1573 **Sher**, A.V., T.N. Kaplina, Y.V. Kouznetsov, E.I. Virina, and V.S. Zazhigin, 1979: Late
1574 Cenozoic of the Kolyma Lowland. In: *XIV Pacific Science Congress. Tour Guide XI*.
1575 Academy of Sciences of USSR, Moscow, 115 pp.

1576

1577 **Shimada**, K., T. Kamoshida, M. Itoh, S. Nishino, E. Carmack, F. McLaughlin, S. Zimmermann,
1578 A. Proshutinsky, 2006: Pacific Ocean inflow—Influence on catastrophic reduction of sea
1579 ice cover in the Arctic Ocean. *Geophysical Research Letters*, **33**, L08605,
1580 doi:10.1029/2005GL025624.

1581

1582 **Singarayer**, J.S., J. Bamber, and P.J. Valdes, 2006: Twenty-first century climate impacts from a
1583 declining Arctic sea ice cover. *Journal of Climate*, **19**, 1109-1125.

1584

1585 **Smith**, L.M., G.H. Miller, B. Otto-Bliesner, and S.-I. Shin, 2003: Sensitivity of the Northern
1586 Hemisphere climate system to extreme changes in Arctic sea ice. *Quaternary Science*
1587 *Reviews*, **22**, 645-658.

1588

1589 **Solignac**, S., J. Giraudeau, and A. de Vernal, 2006: Holocene sea surface conditions in the
1590 western North Atlantic: Spatial and temporal heterogeneities. *Palaeoceanography*, **21**, 1-
1591 16.

1592

1593 **Steele**, M., W. Ermold, J. Zhang, 2008: Arctic Ocean surface warming trends over the past 100
1594 years. *Geophysical Research Letters*, **35**, L02614, doi:10.1029/2007GL031651.

1595

- 1596 **St. John, K.E.**, 2008: Cenozoic ice-rafting history of the central Arctic Ocean—Terrigenous
1597 sands on the Lomonosov Ridge. *Paleoceanography*, **23**, PA1S05,
1598 doi:10.1029/2007PA001483.
1599
- 1600 **Stroeve, J., M.M. Holland, W. Meier, T. Scambos, and M. Serreze**, 2007: Arctic sea ice decline:
1601 Faster than Forecast. *Geophysical Research Letters*, **34**, doi: 10.1029/2007GL029703.
1602
- 1603 **Stroeve, J.C., T. Markus, and W.N. Meier**, 2006: Recent changes in the Arctic melt season,
1604 *Annals of Glaciology*, **44**, 367-374.
1605
- 1606 **Stroeve, J., M. Serreze, S. Drobot, S. Gearheard, M. Holland, J. Maslanik, W. Meier, T.**
1607 **Scambos**, 2008: Arctic sea ice extent plummets in 2007. *Eos, Transactions of the*
1608 *American Geophysical Union*, **89**, 13-14.
1609
- 1610 **Thompson, D.W.J. and J.M. Wallace**, 1998: The Arctic Oscillation signature in the wintertime
1611 geopotential height and temperature fields. *Geophysical Research Letters*, **25(9)**, 1297-
1612 1300.
1613
- 1614 **Thorndike, A.S.**, 1986: Kinematics of sea ice. In: *The Geophysics of Sea Ice* [Untersteiner, N.
1615 (ed.)]. NATO ASI Series, Series B, Physics, Vol. 146, Plenum Press, New York, pp.
1616 489-549.
1617
- 1618 **Tremblay, L.B., L.A. Mysak, and A.S. Dyke**, 1997: Evidence from driftwood records for
1619 century-to-millennial scale variations of the high latitude atmospheric circulation during
1620 the Holocene. *Geophysical Research Letters*, **24**: 2027-2030.
1621
- 1622 **Tsukernik, M., D.N. Kindig, and M.C. Serreze**, 2007: Characteristics of winter cyclone activity
1623 in the northern North Atlantic: Insights from observations and regional modeling,
1624 *Journal of Geophysical Research*, **112**, D03101, doi:10.1029/2006JD007184.
1625
- 1626 **Turney, C., M. Baillie, S. Clemens, D. Brown, J. Palmer, J. Pilcher, P. Reimer, H.H. Leuschner,**

- 1627 2005: Testing solar forcing of pervasive Holocene climate cycles. *Journal of Quaternary*
1628 *Science*, **20**, 511-518.
- 1629
- 1630 **Van Loon**, H. and J.C. Rogers, 1978: The seesaw in winter temperature between Greenland and
1631 northern Europe. Part I—General Description. *Monthly Weather Review*, **106**, 296-310.
1632
- 1633 **Vincent**, J.-S., 1990: Late Tertiary and early Pleistocene deposits and history of Banks Island,
1634 southwestern Canadian Arctic Archipelago. *Arctic*, **43**, 339-363.
1635
- 1636 **Vinje**, T., 1999: Barents Sea ice edge variation over the past 400 years. *Extended Abstracts*,
1637 *Workshop on Sea-ice Charts of the Arctic*, Seattle, WA, World Meteorological
1638 Organization, WMO/TD, **949**, 4-6.
1639
- 1640 **Vinje**, T., 2001: Anomalies and Trends of Sea-Ice Extent and Atmospheric Circulation in the
1641 Nordic Seas during the Period 1864–1998. *Journal of Climate*, **14**, 255-67.
1642
- 1643 **Walsh**, J.E., 1978: A data set on Northern Hemisphere sea ice extent. World Data Center-A for
1644 Glaciology, Glaciological Data, Report GD-2 part 1, pp. 49-51.
1645
- 1646 **Walsh**, J.E. and W.L. Chapman, 2001: 20th-century sea-ice variations from observational data.
1647 *Annals of Glaciology*, **33**, 444-448.
1648
- 1649 **White**, J.M. and T.A. Ager, 1994: Palynology, paleoclimatology and correlation of middle
1650 Miocene beds from Porcupine River (Locality 90-1), Alaska. *Quaternary International*,
1651 **22/23**, 43-78.
1652
- 1653 **White**, J.M., T.A. Ager, D.P. Adam, E.B. Leopold, G. Liu, H. Jetté, and C.E. Schweger, 1997:
1654 An 18-million-year record of vegetation and climate change in northwestern Canada and
1655 Alaska: tectonic and global climatic correlates. *Palaeogeography, Paleoclimatology*,
1656 *Palaeoecology*, **130**, 293-306.
1657

- 1658 **Whitlock**, C. and M.R. Dawson, 1990: Pollen and vertebrates of the early Neogene Haughton
1659 Formation, Devon Island, Arctic Canada. *Arctic*, **43(4)**, 324-330.
1660
- 1661 **Whitlow**, S., P.A. Mayewski, and J.E. Dibb, 1992: A comparison of major chemical species
1662 seasonal concentration and accumulation at the South Pole and Summit, Greenland.
1663 *Atmospheric Environment*, **26A**, 2045-2054.
1664
- 1665 **Williams**, C.J. 2006. *Paleoenvironmental reconstruction of Polar Miocene and Pliocene Forests*
1666 *from the Western Canadian Arctic*. 19th Annual Keck Symposium;
1667 <http://keckgeology.org/publications>.
1668
- 1669 **Williams**, C.J., A.H. Johnson, B.A. LePage, D.R. Vann and T. Sweda, 2003: Reconstruction of
1670 Tertiary metasequoia forests II. Structure, biomass and productivity of Eocene floodplain
1671 forests in the Canadian Arctic. *Paleobiology*, **29(2)**, 238-274.
1672
- 1673 **Wolfe**, J.A., 1980: Tertiary climates and floristic relationships at high latitudes in the Northern
1674 Hemisphere. *Palaeogeography, Palaeoclimatology, and Palaeoecology*, **30**, 313-323.
1675
- 1676 **Wolfe**, J.A., 1997: Relations of environmental change to angiosperm evolution during the Late
1677 Cretaceous and Tertiary. In: *Evolution and diversification of land plants*, [Iwatsuki, K.
1678 and P.H. Raven (eds.)]. Springer-Verlag, Tokyo, pp. 269-290.
1679
- 1680 **Wollenburg**, J.E. and W. Kuhnt, 2000: The response of benthic foraminifers to carbon flux and
1681 primary production in the Arctic Ocean. *Marine Micropaleontology*, **40**, 189-231.
1682
- 1683 **Zachos**, J., M. Pagani, L. Sloan, E. Thomas, and K. Billups, 2001: Trends, rhythms, and
1684 aberrations in global climate 65 Ma to present. *Science*, **292(5517)**, 686-693.
1685
- 1686 **Zhang**, X., and J.E. Walsh, 2006: Toward a seasonally ice-covered Arctic Ocean: Scenarios
1687 from the IPCC AR4 model simulations. *Journal of Climate*, **19**, 1730-1747.

1 **Chapter 9 — Key Findings and Recommendations**

2

3

4 **Chapter Lead Authors**

5 **Richard B. Alley**, Pennsylvania State University, University Park, PA

6 **Julie Brigham-Grette**, University of Massachusetts, Amherst , MA

7 **Gifford Miller**, University of Colorado, Boulder, CO

8 **Leonid Polyak**, Ohio State University, Columbus, OH

9 **James White**, University of Colorado, Boulder, CO

10

10 **9.1 INTRODUCTION**

11 Paleoclimatic data provide a highly informative if incomplete history of Arctic climate.
12 Temperature history is especially well recorded, and it commonly allows researchers to
13 accurately reconstruct changes and rates of changes for particular seasons. Precipitation (rain or
14 snow) and the extent of ice on land and sea are some of the many other climate variables that
15 have also been reconstructed. The data also provide insight to the histories of many possible
16 causes of the climate changes and feedback processes that amplify or reduce the resulting
17 changes. Comparing climate with possible causes allows scientists to generate and test
18 hypotheses, and those hypotheses then become the basis for projections of future changes.

19 Arctic data show changes on numerous time scales and indicate many causes and
20 important feedback processes. Changes in greenhouse gases appear to have been especially
21 important in causing climate changes [sections 4.4; 5.4.1; 5.4.4, 6.4.1; 6.4.2]. Global climate
22 changes have been notably amplified in the Arctic [section 5.5.2], and warmer times have
23 melted ice on land and sea [chapter 8].¹

24

25 **9.2 SUMMARY OF KEY FINDINGS**

26 **Chapter 5 Temperature and Precipitation**

¹ Statistically valid confidence levels often can be attached to scientific findings, but commonly require many independent samples from a large population. Such a standard can be applied to paleoclimatic data in only some cases, whereas in other cases the necessary archives or interpretative tools are not available. However, expert judgment can also be used to assess confidence. The key findings here cannot all be evaluated rigorously using parametric statistics, but on the basis of assessment by the authors, all of the key findings are at least “likely” as used by the Intergovernmental Panel on Climate Change (more than 66% chance of being correct); the authors believe that the most of the findings are “very likely” (more than a 90% chance of being correct).

27 The Arctic of 65 million years ago (Ma) was much warmer than recently; forests grew in
28 all land regions and neither perennial sea ice nor the Greenland Ice Sheet were present. Gradual
29 but bumpy cooling has dominated since, with falling atmospheric CO₂ concentration apparently
30 the most important contributor to the cooling, although with possible additional contributions
31 from changing continental positions and their effect on atmospheric or oceanic circulation.
32 Warm “bumps” during the general cooling trend include the relatively abrupt Paleocene-Eocene
33 Thermal Maximum about 55 Ma, apparently caused by CO₂ release, and a more gradual
34 warming in the middle Pliocene (about 3 Ma) of uncertain cause.

35 Around 2.7 Ma cooling reached the threshold for extensive development of continental
36 ice sheets throughout the North American and Eurasian Arctic. Periodic growth and shrinkage
37 of the ice during tens of thousands of years were directly controlled by periodic changes in
38 northern hemisphere sunshine caused by features of Earth’s orbit. Recent work suggests that, in
39 the absence of human influence, the current interglacial would continue for a few tens of
40 thousands of years before the start of a new ice age. The large temperature differences between
41 glacial and interglacial periods, although driven by Earth’s orbital cycles and the globally
42 synchronous response, reflect the effects of strong positive feedbacks, such as changes in
43 atmospheric CO₂ and other greenhouse gases and in the extent of reflective snow and ice.

44 Interactions among the various orbital cycles have caused small differences between
45 successive interglacials. During the interglacial about 130–120 thousand years ago (ka), the
46 Arctic received more summer sunshine than in the current interglacial, and temperatures in
47 many places were consequently 4° to 6°C warmer than recently, which reduced ice on
48 Greenland (Chapter 7), raised sea level, and melted small glaciers and ice caps.

49 The cooling into and warming out of the most recent glacial were punctuated by
50 numerous abrupt climate changes, with millennial persistence of conditions between jumps
51 requiring years to decades. These events were very large around the North Atlantic but much
52 smaller elsewhere in the Arctic and beyond. Large changes in the extent of sea ice in the North
53 Atlantic were probably responsible, linked to changes in regional and global patterns of ocean
54 circulation. Freshening of the North Atlantic also favored formation of sea-ice.

55 These abrupt changes also occurred in the current interglacial (the Holocene), but they
56 ended as the Laurentide Ice Sheet on Canada melted away. Arctic temperatures in the
57 Holocene broadly responded to orbital changes with warmer temperatures during the early to
58 middle Holocene when there was more summer sunshine. Warming generally led to northward
59 migration of vegetation and to shrinkage of ice on land and sea. Small oscillations in climate
60 during the Holocene, such as the Medieval Climate Anomaly and the Little Ice Age, were
61 linked to variations in the sun-blocking effect of particles from explosive volcanoes and
62 perhaps to small variations in solar output or in ocean circulation or other factors. The warming
63 after the Little Ice Age began for largely natural reasons, but there is now high scientific
64 confidence that human contributions, and especially increasing concentrations of CO₂, have
65 come to dominate the warming (Jansen et al., 2007).

66 Comparison of summertime temperature anomalies for the Arctic and for lower
67 latitudes, averaged over at least millennia for key climatic intervals of the past, shows that
68 Arctic changes were threefold to fourfold larger than those in lower latitudes. This more
69 pronounced response applies to intervals that were both warmer and colder than in recent
70 decades. Arctic amplification of temperature changes thus appears to be a consistent feature of
71 the Earth system.

72

73 **Chapter 6 Rates of Change**

74 Climate changes have many causes and occur at different rates sustained for different
75 intervals. The changing atmospheric composition, and atmospheric and oceanic circulation
76 linked to tectonic processes during tens of millions of years have shifted the Arctic from ice-
77 free winters to icy summers. Features of Earth's orbit acting for tens of thousands of years have
78 rearranged sunshine on the planet and paced the growth and shrinkage of great ice-age ice
79 sheets. Anomalously cold single years have resulted from the influence of large, explosive
80 volcanoes, with slightly anomalous decades in response to the random variations in the
81 frequency of occurrence of such explosive volcanoes..

82 The local effects of these changes, as observed in Greenland or more generally around
83 the Arctic, yield trends such that more-persistent forcings have produced larger changes at a
84 lower average rate. Relative to these general trends, abrupt climate changes linked to shifts in
85 oceanic conditions of the North Atlantic produced anomalously large and rapid temperature
86 changes near the North Atlantic but relatively small average global temperature changes. And,
87 relative to these general trends, human-linked perturbations of the most recent decades do not
88 appear anomalously rapid or large, but changes projected as a part of the IPCC process can
89 become anomalously large and rapid.

90 Interpretation of these observations is complicated by lack of a generally accepted way
91 of formally assessing the effects or importance of size versus rate versus persistence of climate
92 change. The report here relied much more heavily on ice-core data from Greenland than would
93 be ideal in assessing Arctic-wide changes. Great opportunities exist for generation and synthesis
94 of other data sets to improve and extend the results here, using the techniques described in this

95 report. If widely applied, such research could remove the over-reliance on Greenland data.

96

97 **Chapter 7 The Greenland Ice Sheet**

98 Paleoclimate data show that the Greenland Ice Sheet has changed greatly with time and
99 has affected global sea level. Physical understanding indicates that many environmental factors
100 can force changes in ice-sheet size. Comparing histories of important forcings with ice-sheet
101 size implicates cooling as causing ice-sheet growth, warming as causing shrinkage, and
102 sufficiently large warming as causing loss. The evidence for temperature control is clearest for
103 temperatures similar to or warmer than those occurring in the last few millennia. The available
104 evidence shows less ice when snowfall was higher, indicating that snowfall rate is not the
105 leading control on ice-sheet size. Rising sea level tends to float marginal regions of ice sheets
106 and force their retreat, so the generally positive relation between sea level and temperature
107 means that, typically, both have pushed the ice sheet in the same direction. However, for some
108 small changes during the most recent millennia, marginal fluctuations in the ice sheet have been
109 opposed to those expected from local relative sea-level forcing but in the direction expected
110 from temperature forcing. This, plus the tendency for shrinkage to pull ice-sheet margins out of
111 the ocean, indicate that sea-level change has not been the dominant forcing at least for
112 temperatures similar to or greater than those of the last few millennia.

113 Histories of ice-sheet volume in fine time detail are not available, but the limited
114 paleoclimatic data at least agree that short-term and long-term response to temperature change
115 have been in the same direction. The best estimate from paleoclimatic data is thus that warming
116 shrinks the Greenland Ice Sheet, and warming of a few degrees is sufficient to cause ice-sheet
117 loss. Figure 7.13 shows a threshold for ice-sheet removal from sustained warming of 5°C, with

118 a range of uncertainties from 2° to 7°C, but tightly constrained numerical estimates are not
119 available, nor are rigorous error bounds, and the available data poorly constrain the rate of loss.
120 Numerous opportunities exist for additional data collection and analyses that would reduce the
121 uncertainties.

122

123 **Chapter 8 Arctic Sea Ice**

124 Geological data indicate that the history of Arctic sea ice is closely linked with
125 temperature changes. Sea ice in the Arctic Ocean may have appeared in response to long-term
126 cooling as early as 46 Ma. Year-round sea ice in the Arctic possibly developed as early as 13–
127 14 Ma, before the opening of the Bering Strait at 5.5 Ma. Nevertheless, extended seasonally ice-
128 free periods probably occurred until about 2.5 Ma. They ended with a large increase in the
129 extent and duration of sea-ice cover that more or less coincided with the onset of extensive
130 glaciation on land (within the considerable dating uncertainties). Some data suggest that ice
131 reductions marked subsequent interglacials and that the Arctic Ocean may have been seasonally
132 ice-free during the warmest events. For example, reduced-ice conditions are inferred for the last
133 interglacial and the onset of the current interglacial, about 130 and 10 ka .

134 Limited data suggest poorly understood variability in ice circulation for centuries to
135 millennia, but without strong periodic behavior on these time scales. Historical observations
136 suggest that ice cover has been shrinking since the late 19th century, and that the decline has
137 accelerated during the last several decades. This accelerated rate exceeds natural declines
138 typical of at least the most recent few millennia. This ice loss appears to be unrelated to natural
139 climatic and hydrographic variability on decadal time scales or to multi-millennial orbital
140 insolation changes.

141

142 **9.3 RECOMMENDATIONS**

143 Paleoclimatic data on the Arctic are generated by numerous international investigators
144 who study a great range of archives throughout the vast reaches of the Arctic. The value of this
145 diversity is evident in this report. Many of the key results of this report rest especially on the
146 outcomes of community-based syntheses, such as the CAPE Project, and on multiply replicated
147 and heavily sampled archives, such as the central Greenland deep ice cores. Results from the
148 ACEX deep coring in Arctic Ocean sediments were appearing as this report was being written;
149 these results were quite valuable and will become more so with synthesis and replication,
150 including comparison with land-based as well as marine records. The number of questions
151 answered, and raised, by this one new data set shows how sparse the data are on many aspects
152 of Arctic paleoclimate change. *We recommend that future research maintain and expand the*
153 *diversity of investigators, techniques, archives, and geographic locations, while promoting*
154 *development of community-based syntheses and multiply-replicated, heavily-sampled*
155 *archives; only through breadth and depth can the remaining uncertainties be reduced while*
156 *confidence in the results is improved.*

157

158 The questions asked of this study by the CCSP are relevant to public policy and require
159 answers. The answers provided here are, we hope, useful and informative. However, we
160 recognize that despite the contributions of numerous community members to this report, in
161 many cases a basis was not available in the refereed scientific literature to provide answers with
162 the accuracy and precision desired by policymakers. *We recommend that members of the*

163 *Arctic paleoclimatic community formulate future research activities to address in greater*
164 *detail the policy-relevant questions that motivated this report.*

165

166 Paleoclimatic data provide very clear evidence of past changes in important aspects of
167 the Arctic climate system. The ice of the Greenland ice sheet, smaller glaciers and ice caps, the
168 Arctic Ocean, and soils are shown to be vulnerable to warming, and Arctic ecosystems are
169 strongly affected by changing ice and climate. National and international studies generally
170 project rapid warming in the future. If this warming occurs, the paleoclimatic data indicate that
171 melting of ice and associated effects will follow, with implications for ecosystems and
172 economies. *We recommend that policymakers and science managers use the results presented*
173 *here in design of monitoring, process, and model-projection studies of Arctic change and*
174 *linked global responses.*

175

176 **Highlights of Key Findings**

177 • Arctic climate has changed greatly during the last 65 million years and
178 before, at highly varying rates and in response to many causes, with changing
179 atmospheric carbon-dioxide concentrations especially important in controlling
180 temperature.

181 • Arctic temperature changes have been larger than correlative globally
182 averaged changes, by approximately threefold to fourfold in both warmer and colder
183 times, in response to processes still active in the Arctic.

184 • Arctic temperatures have changed greatly but slowly in response to long-
185 lasting causes and by lesser amounts but more rapidly in response to other causes.

186 Human-forced changes of the most recent decades do not appear notably anomalous in
187 rate or size for their duration when they are compared with these natural changes, but
188 projections for future human-caused changes include the possibility of anomalously
189 large and rapid changes.

190 • The Greenland Ice Sheet has consistently grown with cooling and shrunk
191 with warming, and a warming of a few degrees (about 5°C, with uncertainties between
192 about 2° and 7°C) or more has been sufficient to completely or almost completely
193 remove the ice sheet if maintained long enough; the rate of that removal is poorly
194 known. Reduction in the size of the Greenland Ice Sheet in the past has resulted in sea
195 level rise.

196 • Warming has decreased sea ice, which in turn strongly magnifies
197 warming, and seasonally ice-free conditions and even year-round ice-free conditions
198 have occurred in response to sufficiently large but poorly quantified forcing.

199 • Although major climate changes have typically affected the whole Arctic,
200 important regional differences have been common; a full understanding of Arctic
201 climatology and paleoclimatology requires regionally-resolved studies.

202

202

203 **References Cited**

204 **Jansen, E., J. Overpeck, K.R. Briffa, J.-C. Duplessy, F. Joos, V. Masson-**
205 Delmotte, D. Olago, B. Otto-Bliesner, W.R. Peltier, S. Rahmstorf, R. Ramesh, D.
206 Raynaud, D. Rind, O. Solomina, R. Villalba, and D. Zhang, 2007: Palaeoclimate. In:
207 *Climate Change 2007—The Physical Science Basis. Contribution of Working Group I to*
208 *the Fourth Assessment Report of the Intergovernmental Panel on Climate Change*
209 [Solomon, S., D. Qin, M. Manning, Z. Chen, M. Marquis, K.B. Averyt, M. Tignor and
210 H.L. Miller (eds.)]. Cambridge University Press, Cambridge, United Kingdom, and New
211 York, pp. 434-497.